BIOCHEMICAL CHARACTERIZATION AND INDUSTRIAL APPLICATION OF α-AMYLASES FROM BACTERIA

A THESIS SUBMITTED IN PARTIAL FULFILLMENT OF THE REQUIREMENTS FOR THE DEGREE OF

Doctor of Philosophy

Jetendra Kumar Roy

Registration No.: 20 of 2009

School of Sciences

Department of Molecular Biology and Biotechnology

Tezpur University

December, 2013

DEDICATED TO MY BELOVED

PARENTS

Abstract

The starch hydrolytic enzymes consist of 30% of worldwide enzyme consumption and they represent the second most significant commercial enzyme. Among them amylases are the most important starch hydrolytic enzymes and comprise of 25% of total global enzyme market share. Amylolytic enzymes have diverse applications in starch processing, baking, automatic dishwashing detergents, textile desizing, medicine, pulp and paper, and brewing industry. However, requirements for each industry are very specific, mainly with reference to pH, oxidative stability, chelator resistance, and temperature behavior. Thus, a single enzyme cannot fulfill all the industrial demands. As a result, there is a constant demand for the search for novel enzymes having better thermostability, broad pH working range, surfactant stability and raw starch digesting properties to suit various industrial applications.

Mother Nature harbors a plethora of novel microorganisms that may produce novel enzymes suitable for various industrial applications. Soil biota consists of diverse microorganisms and its exploration is indispensable for isolating novel enzyme producing microbes. Considering the fact that Northeast India being present at the confluence of two major Eco-zones of the planet earth, has an immense biodiversity. Hence, an effort was made to isolate strains capable of producing high-titre of industrially important amylases from this bio-diverse region (Assam), which could retain their activity and stability under various industrial conditions. Taxonomic identification of these isolated strains was carried out by polyphasic approach, followed by optimization of culture conditions of such potent bacteria for maximizing their α-amylase yield. An effort was also made to isolate, purify and biochemically characterize the α-amylase(s) from the isolated promising microbial strains and to investigate their potential commercial applications. Subsequently, the gene for promising α-amylase was cloned and overexpressed in *E. coli* to produce commercially appreciable yields.

In wake of advances in industrial microbiological research, two α-amylase producing bacterial strains (AS01a & AS08E) were isolated from the soil sample of Assam On the basis of biochemical and morphological characterization, the isolated bacteria were categorized into *Bacillus* genus Molecular identification of strain AS01a by sequence analysis of 16S rDNA, 16S-23S rDNA ISR and other housekeeping genes such as *gyrA* and *rpoB*, showed up to 95-99% sequence similarity with the respective sequence from *Bacillus subtilis* group and thus the strain was identified as *Bacillus subtilis* strain AS01a. However, the analysis of these sequences from *Bacillus* sp strain AS08E showed up to 95-99% sequence similarity with the respective sequence from *Bacillus licheniformis* group and thus the strain was identified as the *Bacillus licheniformis* strain AS08E The influence of media components on α-amylase production from both the strains revealed that pH, carbon, and nitrogen sources play an important role in production of α-amylases Both the strains showed starch as the preferred carbon source for optimum α-amylase production, however, preference of nitrogen source by the bacterium varied in each case The *B subtilis* strain AS01a showed beef extract as the preferred nitrogen source while peptone was shown to be a preferred nitrogen source by *B licheniformis* strain AS08E The pH of the culture media also played a significant role in α-amylase production by both the strains The acidic environment (pH 6 0) was found to be best suited for optimum α-amylase production from *B subtilis* strain AS01a while an alkaline ambience (pH ~12 0) supported optimum α-amylase production from *B licheniformis* strain AS08E Three factors effecting α-amylase production from the aforementioned two bacterial strains (AS01a and AS08E) were further statistically optimized using response surface methodology, thereby investigating enhanced α-amylase production from these strains Statistical optimization studies yielded ~3-fold increase in α-amylase production from both the strains under optimized conditions as compared to non-optimized conditions

Present investigation also deals with physiochemical characterization of the enzyme A major α-amylase from the *B subtilis* strain AS01a (Amy-I) was purified, which yielded a protein of approx 21 0 kDa while from *B licheniformis* strain

AS08E, the major α-amylase (AmyBL-I) was found to be of ~ 55.0 kDa. Both the purified α-amylases were found to be active in alkaline condition (pH 8.0-12.0). The α-amylase purified from *B. subtilis* strain AS01a (Amy-I) showed optimum activity at pH 9.0 and temperature of 55°C, while that of α-amylase purified from *B. licheniformis* strain AS08E (AmyBL-I) demonstrated optimum activity at pH 10.0 and 80°C. Amy-I was also found to be Ca^{2+} independent enzyme and was thermostable up to 55°C, while AmyBL-I retained its activity up to 80°C in presence of 5 mM Ca^{2+} ion. Both the purified enzymes were found to be inhibited by 4-BPB suggesting presence of histidine in the active site of these enzymes. The end-product analysis of starch hydrolysis by Amy-I revealed that it forms high molecular weight oligosaccharides, maltose and small amount of glucose from starch, whereas AmyBL-I forms maltose and high molecular weight oligosaccharides from starch hydrolysis. The end-product determination studies revealed that both the amylases might be suitable for glucose/maltose syrup production in starch industries. The purified α-amylase also showed appreciable stability and compatibility with regard to various commercial laundry detergents suggesting their suitable candidature for inclusion in laundry detergent formulations for removing the starchy food stains from cloths.

From the commercial perspectives of these enzymes in starch processing and detergent industries, the gene encoding α-amylases from strain AS01a and strain AS08E were cloned and overexpressed in *E. coli*. Cloning of α-amylase genes was also considered for hyper-production of these enzymes and subsequently to study their structure-function relationship. Besides, it may also be helpful for enzyme engineering, where the enzyme could be engineered for harsh industrial processes as a part of future strategic research activity. An approximately, 2-kbp α-amylase gene from *B. subtilis* strain AS01a and 1.5-kbp from *B. licheniformis* strain AS08E (amplified using α-amylase gene specific primers) were successfully cloned into the pET28a expression vector and expressed in *E. coli* BL21 cells.

For targeting the extracellular expression of recombinant protein outside the *E. coli* cell membrane, the signal peptide of the native proteins was also cloned along with

the α-amylase gene sequence. However, the expression study of active recombinant enzyme in culture media revealed that its expression was very limited and thus, to maximize the extracellular expression of recombinant enzyme, culture condition was optimized using RSM. The optimization studies yielded ~7-8 fold increase in extracellular production of active recombinant α-amylase enzymes as compared to its production under non-optimized conditions. From the optimization studies, it was also observed that lower concentration of IPTG and temperature had positive effects on extracellular expression of recombinant α-amylase while higher concentration of EDTA and incubation time resulted in enhanced extracellular expression of recombinant protein in *E. coli*.

The recombinant enzymes were purified by the combination of HIC and gel-filtration column from the cell free supernatant (CFS) of *E. coli* cells harbouring the recombinant plasmids, containing amylase gene inserts. The purified recombinant enzyme (AmyBS-I) cloned from *B. subtilis* strain AS01a was purified up to 3.9-fold from *E. coli* CFS and its molecular weight was found to be ~69.0 kDa by SDS-PAGE analysis, while recombinant enzyme (Blamy-I) cloned from *B. licheniformis* strain AS08E was purified up to 16.6-fold from *E. coli* CFS with molecular weight of ~55.0 kDa. The recombinant α-amylase cloned from *B. subtilis* strain AS01a was found to be different from that of the purified wild type α-amylase (purified from the same parent strain), suggesting that the cloned α-amylase is an isoenzyme. Nevertheless, the recombinant α-amylase cloned from the *B. licheniformis* strain AS08E was very much similar to the wild type α-amylase purified from the same parent strain.

Cloned AmyBS-I was found to be different from the wild type α-amylase purified from the same parent strain, consequently, it was important to investigate its biochemical properties. The biochemical studies showed that it works optimally at pH 6.0 and temperature of 70°C. AmyBS-I was also found to be Ca^{2+} independent in nature, as it does not require Ca^{2+} for its thermostability or catalytic activity. The AmyBS-I showed thermostability up to 70°C and was found to be inhibited by 4-BPB (2 mM) which suggested presence of histidine in the active sites of this

enzyme. Considering the fact that AmyBS-I acts optimally under acidic condition and at high temperature, its applications in raw starch digestion and in baking industry were evaluated. The study showed that after six hours of incubation at 60°C, AmyBS-I could easily hydrolyze the raw wheat, potato, and rice starches up to 61%, 58%, and 44%, respectively. It also formed deep holes and eroded the smooth surfaces of all the tested starch granules, indicating its prospective usefulness in starch processing industries. The bread supplementation studies with the AmyBS-I and commercial α-amylase (Himedia) showed that the AmyBS-I supplemented bread had better bread amelioration quality as compared to the control and commercial enzyme supplemented ones. The partially purified α-amylase from *B. subtilis* strain AS01a was also used for immobilization studies on magnetic nanoparticles (MNP) and it was found that the immobilization of enzyme resulted in ~ 26-fold increase in specific activity as compared to free enzymes. The continuous starch hydrolysis experiment by MNP bound enzyme showed that there was significant increase in starch hydrolysis as compared to the free unbound enzyme.

Declaration

I hereby declare that "***Biochemical characterization and industrial application of amylases from bacteria***" has been submitted to the Tezpur University in the Department of Molecular Biology and Biotechnology under the School of Sciences for partial fulfillment for the award of the degree of Doctor of Philosophy in Molecular Biology and Biotechnology. This is an original work carried out by me. Further, I declare that no part of this has been reproduced elsewhere for award of any other degree.

Date: 20/12/2013

Place: Tezpur University, Tezpur

(Jetendra Kr. Roy)

Registration No.: 20 of 2009

TEZPUR UNIVERSITY
(A Central Govt. University)
DEPARTMENT OF MOLECULAR BIOLOGY AND BIOTECHNOLOGY
Tezpur, 784028, Assam, India

Dr. Ashis K. Mukherjee
Professor
E-mail: akm@tezu.ernet.in

Ph: 03712-267007/8/9 Ext.5405 (O)
Mobile: +917896003886
Fax: 03712-267005/6

CERTIFICATE OF THE PRINCIPAL SUPERVISOR

This is to certify that the thesis entitled "***Biochemical characterization and industrial application of amylases from bacteria***" submitted to the School of Sciences, Tezpur University in partial fulfillment for the award of the degree of Doctor of Philosophy in Molecular Biology and Biotechnology is a record of original research work carried out by Mr. Jetendra Kr. Roy under my personal supervision and guidance.

All helps received by him/her from various sources have been duly acknowledged. No part of this thesis has been reproduced elsewhere for award of any other degree.

Date: 20/12/2013
Place: Tezpur University

(A. K. Mukherjee)
Signature of Principal Supervisor
Professor, Dept. of MBBT
School of Sciences
Molecular Biology and Biotechnology

Professor A.K.Mukherjee,Ph.D.
Department of Molecular
Biology & Biotechnology
Tezpur University (Central)
Tezpur-784028, Assam

TEZPUR UNIVERSITY
(A Central Govt. University)
Tezpur-784028, Assam, India

CERTIFICATE OF THE EXTERNAL EXAMINAR

AND ODEC

This is to certify that the thesis entitled "***Biochemical characterization and industrial application of amylases from bacteria***" submitted by Mr. Jetendra Kr. Roy to Tezpur University in the Department of Molecular Biology and Biotechnology under the School of Sciences in partial fulfillment of the requirement for the award of the degree of Doctor of Philosophy in Molecular Biology and Biotechnology has been examined by us on _____and found to be satisfactory.

The Committee recommends for the award of the degree of Doctor of Philosophy.

Signature of:

Principal Supervisor **External examiner**

Date: **Date:**

Acknowledgement

First and foremost, I offer my gratitude to almighty God for bestowing me with the strength and courage to carry out my research work successfully.

I would like to express my sincere gratitude to my respected supervisor Prof. Ashis Kumar Mukherjee, Department of MBBT, for his enthusiastic guidance and inexhaustible inspiration, which enabled me to accomplish all my objectives. I greatly appreciate his constant support, encouragement, and constructive criticism, without which the present investigation would not have been possible.

I would also like to express my sincere thanks to Prof. M. K. Chaudhari, Vice chancellor, Tezpur University, Napaam, for giving me the opportunity to carry out my research work in this esteemed University.

I am very much obliged to my Doctoral Committee members: Prof. K. K. Baruah and Dr. S.K. Ray from Tezpur University for their sincere guidance and valuable suggestions to improve my research work.

I extend my deepest gratitude to the Head, all the faculties and staff members of Dept. of MBBT, specifically Dr. Kalyan Hazarika, Dr. Nabo K. Bordoloi, Mr. Pranab Mudoi, Mr. Samar Kakoti, Mr. Deepak and Mr. D. D. Bania for their intellectual and technical supports during the entire course of investigation.

The financial assistance in the form of a Senior Research Fellowship received from the CSIR, New Delhi is duly acknowledged.

I also express my special gratitude to my senior lab members, Dr. Sudhir K. Rai and Dr. Debashree Saikia for their help and support during the entire period of my research work. I am also grateful to my lab members (Rupamoni, Sourav, Bandana, Reena, Debananda, Sumita, Bhargab) for their support.

I thank all my seniors and juniors from the department of MBBT, especially Sonia-di, Clara-di, Ranjan-da and Nilu-di for being constant source of encouragement. I am thankful to Sapan, Barnali, Abdul, Pradip, Nima, and many others for their constant support.

I am equally thankful to all my friends from various other departments (specifically, Dept. of Energy, Chemical Science, FET & EFL) for their support throughout the work. I would like to thank Trisha for carefully editing my thesis.

Last but not the least, I would like to express my deep sense of gratitude to my family members –for their endless support, love and patience during my PhD work as well as in all stages of my life. I also thank my wife, Lucky for her love, support and motivation during the course of my research work.

Date: 20/12/2013

(Jetendra Kumar Roy)

Contents *Page No.*

List of Tables

Chapter 4: Results (*B. subtilis* strain AS01a)

Chapter 5: Results (*B. licheniformis* strain AS08E)

List of figures

Chapter 5: Results (*B. licheniformis* strain AS08E)

List of abbreviation

Abbreviations	Full form
Adj. R^2	Adjusted R^2
BLAST	Basic local alignment search tool
CFU	Colony forming unit
CV	Coefficient of variance
DF	Degree of freedom
DMSO	Dimethylsulphoxide
dNTPs	deoxynucleotide triphosphates
f-value	Fisher value
FTIR	Fourier transform infrared spectroscopy
Gm	Gram
G	Gravity
GFC	Gel-filtration chromatography
HIC	Hydrophobic interaction chromatography
IPTG	Isopropyl-thio-β-D-galactopyranoside
KBr	Potassium bromide
Kbp	Kilobase pair
kDa	Kilo Dalton
M	Molar
µg	Microgram
mM	Millimolar
mg /ml	Milligram / milliliter
ml	Milliliter
µl	Microlitre
min.	Minute
Na-EDTA	Disodium ethylene diamine tetra acetate
NH_4Cl	Ammonium chloride
NH_4NO_3	Ammonium nitrate
$(NH_4)_2SO_4$	Ammonium sulphate
$NaNO_3$	Sodium nitrate
N	Normality
NJ	Neighbor joining Method
OD	Optical density
ORF	Open reading frame
p-value	Probability value
Pred. R^2	Predicted R^2

PBD	Plackett- Burman design
PCR	Polymerase chain reaction
rRNA	Ribosomal ribonucleic acid
rDNA	Ribosomal deoxyribonucleic acid
RSM	Response surface methodology
rpm	Revolution per minute
S.D	Standard deviation
SOB	Super optimal broth
sec.	Second
t-test	Student's t-test
TAE	Tris/acetate/ethylenediamine tetra-acetic acid
TCA	Tri carboxylic acid
U	Units
v/v	Volume / volume
w/v	Weight / volume
w/w	Weight / Weight
X-Gal	5-bromo-4-chloro-3 indolyl-β-D-galactoside

Chapter I

INTRODUCTION

Chapter 1: Introduction

1.1. Introduction

Biotechnology is generally defined as "any technological application that uses biological systems, living organisms, or derivatives thereof, to make or modify products or processes for specific use" (UN Convention on Biological Diversity). Biotechnology is not a single field; it is rather a unified body of scientific knowledge domains [1]. Its multidisciplinary nature expands over diverse fields. It is an amalgamation of subjects, which includes chemistry, engineering, plant and animal biology, immunology, microbiology and lots more [1]. Biotechnology has applications in four major industrial areas, including health care (Red Biotechnology), crop and agriculture process improvement (Green Biotechnology), marine and aquatic applications (Blue Biotechnology), and industrial processes for improved product development (White Biotechnology) [2].

Industrial or white biotechnology is a major application of biotechnology for future economic development; it is an application of biotechnology to the eco-efficient production and processing of chemicals, materials, and bio-energy [3]. It uses the extraordinary capabilities of microbes and their enzymes with abundant diversity, efficiency and specificity, to make products useful in various industrial sectors such as chemicals, food, paper, textiles, detergent and bioenergy (such as biofuels or biogas) sectors. Biotechnology uses renewable raw materials in achieving these objectives and by doing so, it applies promising and innovative approaches towards cutting down greenhouse gas emissions [3]. Bio-catalysis or enzyme technology is one of the major parts of white biotechnology. Bio-catalysis processes mostly apply microbial enzymes to accelerate (catalyze) the conversion of substrate into a product(s). Though enzymes are born within the living cells to carry out specific cell process, they remain active outside the cells (*in vitro*) and retain their ability to perform very specific chemical transformations thereby making them progressively helpful in industrial processes [1].

1.2. Historical aspect of Industrial enzymes

The word 'biotechnology' may be relatively new, but its application has been around for many years. Microorganisms have been used for ages in the production of beer, wine, vinegar, yoghurt, and cheese [1]. In ancient Indian texts, there are mentions of 'soma' or 'sura', which were fermented alcoholic products [4]. The Egyptians, Sumerians, and Babylonians used to produce alcoholic beverages from barley, and the Greek epic poems (*The Iliad* and *The Odyssey*), written around 700 BC has references of the uses of calf and kid's stomachs (sources of rennet) for the production of cheese [1]. Sour dough bread appeared in Europe around 800 BC and even early Christian and Sanskrit writings describe various fermented dairy products [1]. Probably the first industrial application (in detergent) of cell free enzymes (proteases) was the use of pancreatic extract in 1913. Interestingly, the first enzyme produced industrially was an amylase from a fungal source in 1894, which was used as a pharmaceutical aid for the treatment of digestive disorders [5]. Application of enzymes in the starch industry is also not a new process. In the 1950s, fungal amylase was used to manufacture syrups that contained sugars, which could not be easily produced by conventional acid hydrolysis process [1]. The discovery of amyloglucosidase (which completely breaks down starch into glucose) in the 1960s revolutionized the syrup manufacturing industry and within a few years of its discovery, the enzyme process has completely replaced the chemical process of hydrolysis [1].

1.3. Current state of the Global Industrial Biotechnology

As per the reports of Global Industry Analysts, the global biotechnology industry is predicted to exceed $320 billion by 2015 [6]. Market growth is driven by economic recovery leading to increased R&D funding. Further, government initiatives and applications of biotechnology in agriculture and medical sciences have also strengthened the global biotechnology market. China, India, and many other developing nations have become major markets in the fields of agricultural and industrial biotechnology. Recent economic crisis in the US and the EU, because of limited capital inflows and the delay or cancellation of projects, have negatively

influenced the biotechnology market, and brought about a major revenue decline [6]. Nevertheless, the market is gradually entering a phase of recovery from the economic crisis. This has been made possible only due to new cost-saving and efficiency measures taken by government and many large biotechnological industries. Industrial funding depends upon favorable economic conditions and is limited to multinational companies, which are generally less in number. As such smaller industries are trying hard to raise their R&D funds. The situation is expected to improve as the smaller industries promise a more secure investment option to venture capitalists [6].

1.4. Current scenario of industrial biotechnology in India

The bio-industrial sector in India registered an 8% growth in its revenues with total sales of $142 million in the year 2011-12 [7]. The multinationals contribute about 65% of the market while the local companies meet the rest. However, the share of local companies has been increasing over the last 3-4 years as they have realized the huge potential of food enzymes. In addition to importing enzymes, India also exports enzymes for different purposes. The domestic consumption of enzymes generated about $110 million while its export generated about $32 million as revenues for the year 2011-12 [7].

The bio-industrial companies in India are headed by global leaders such as Novozymes South Asia followed by other domestic enzyme manufacturing industries, such as Advanced Enzymes, Lumis, Maps and Anthem (Table 1.1). In the last 10 years, the Indian industrial enzyme market has witnessed a growth of about 8-10 % and a similar growth rate is expected in the coming years. In Indian industrial enzyme market, textile and leather enzyme industries have shown considerable growth, while the detergent enzymes segment is still in its initial stage [7]. The industrial enzyme consumption in India is principally in the detergent markets (40%), followed by the starch markets (25%). Lately, enzymes have found wide applications in food, pharmaceutical, diagnostic, and chemical processing industries [8].

Table 1.1: Top five enzyme producing companies in India

Rank	Company	Region	Revenue in $ million			% Change over
			2011-12	2010-11	2009-10	2010-11
1	Novozymes South Asia*	South	61	51	44	20
2	Advanced Enzymes	West	37	32	24	14
3	Rossari Biotech*	West	16	15	11	7
4	Maps (India)	West	12	10	-	18
5	Titan Biotech	North	5	4	3	17

*Estimates *Biospectrum-ABLE-2012-survey*

1.5. Present scenario of microbial amylase research: Second largest enzyme in the enzyme market

The industrial enzyme companies produce enzymes for a wide variety of applications. The global market for industrial enzymes is estimated to be 3.0 billion USD [9], which is shared by food enzymes (29%), feed enzymes (15%), and general technical enzymes (56%) [10]. The world market for industrial enzymes is estimated to be even greater from the products obtained from these enzymes. Amylases are the second most widely used industrial enzyme after protease and they represent approximately 25-33% of the world enzyme production [11].

In view of the ever increasing demands of industrial enzymes, particularly amylases, it becomes essential to explore the vast exotic microbial diversity harbouring several novel enzymes which will be suitable for the harsh industrial process. Nature provides ample sources of amylases such as animals, plants, and microbes. However, the microbial enzymes have gained much preference for industrial production. The vast microbial diversity in nature is the major resource for the biotechnological products and processes. However, only 2% of this vast microbial diversity has been explored so far for enzyme sources [12, 13]. Considering the depth of this diversity, there is always a probability of discovering a promising microorganism with novel enzymes producing capabilities having better properties suitable for commercial exploitation [14]. An important source of enzyme is extremophiles whose specific properties are expected to bear novel products with novel applications. Further, 80% of the commercial enzymes are

produced using microorganisms isolated from different geographical regions. Northeastern zone of India, which is considered as one of the mega biodiversity zones of the world, may harbor several novel enzyme-producing microbes. However, a review of literature shows that limited attempts have been made so far to explore the industrially important microorganisms of this region.

1.6. Starch (Amylum): The energy storehouse

A major source of energy for non-photosynthetic organisms is starch, which also acts as a carbohydrate food reserve in plants. Besides, it also constitutes an important part of human diet and is processed both chemically and enzymatically into variety of products for their various uses such as in starch processing, food-feed, textile, detergent, and paper-pulp industries [15]. In addition, the starch hydrolysis products can also be fermented to produce ethanol. Regardless of the fact that a large number of plants are capable of producing starch, only a few plant sources are important for starch processing industries. The major industrial sources are maize, tapioca, potato, and wheat, but there are certain limitations in terms of their usage in some industrial food applications. This is due to low shear resistance, thermal decomposition, thermal resistance, and high tendency towards retrogradation of these starches [16]. Among various carbohydrate polymers, starch is of great demand due to its usefulness in different food products. Starch significantly improves the textural properties of food items and thus it is widely used in industrial applications as a thickener, gelling agent, colloidal stabilizer, bulking agent and water retention agent [17].

Plants produce starch by the process of photosynthesis and store it as granules in the form of tubers, seeds, and roots for long-term storage as a reserved energy source [18]. Starch is made up of two types of glucose polymers (amylose and amylopectin) which are linked together by glycosidic bonding through the C1 oxygen atom (Figure 1.1). These glycosidic bonds are highly stable at alkaline pH but can easily be hydrolyzed at low/acidic pH. Amylose is comprised of 6000 glucose units linked together by α, 1-4 glycosidic bonding and thus forms a linear polymer. Starch may contain amylose from 0-75%, but the usual content of amylose

is 20–25% of the total starch polymers. Amylopectin is made up of short linear chains of α, 1-4 glycosidic linkage of 10–60 glucose units and side chain of α, 1-6 linkage of 15–45 glucose units. The average number of branching points in amylopectin is usually 5%, but it may vary with different botanical origins [19, 20].

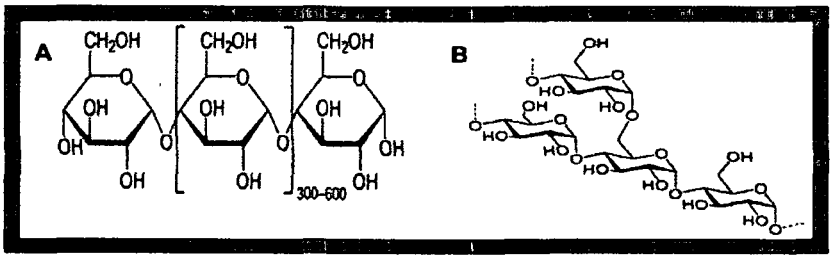

Figure 1.1: Glucose polymers present in starch molecules: (A) amylose and (B) amylopectin.

Starch granules are organized into two regions, namely, amorphous and crystalline. In case of tuber and root starches, the crystalline regions are mainly composed of amylopectin, while the amorphous regions are made up of amylose polymers [18]. In cereal starches, amylopectin forms the most important component of the crystalline region, however, the amyloses in cereal starches form complexes with lipid molecules that give rise to a weak crystalline structure, which further reinforces the granules [18]. Amylopectin is mostly soluble in water but amyloses, which are insoluble in cold water, make the starch granule insoluble as well. This property makes it relatively easier to extract starch granules from their plant source [18]. Again, retrogradation of starch is primarily due to amylose chain. In contrast, the highly branched amylopectin is less prone to retrogradation.

1.7.Starch-Digesting enzymes

A variety of bacteria produce extracellular or intracellular enzymes to convert starch or glycogen into simpler products, which can be used by them as energy and carbon sources. Starch digesting enzymes (amylases) are glycoside hydrolases (GHs), which mainly act upon α-(1, 4) and/or α-(1, 6) linkages of starch polymers. Most of the amylases are grouped into GH family 13 [also known as α-amylase family (EC 3.2.1.1)] [21], while β-amylases (EC 3.2.1.2) and

glucoamylases (EC 3.2.1.3) are grouped into GH14 and GH15 family, respectively [22]. There are mainly four groups of starch-converting enzymes namely (i) endoamylases, (ii) exoamylases, (iii) debranching enzymes, and (iv) transferases. The starch-converting enzymes falling in the above four groups, along with their sites of action on starch polymer, are shown below (Figure 1.2).

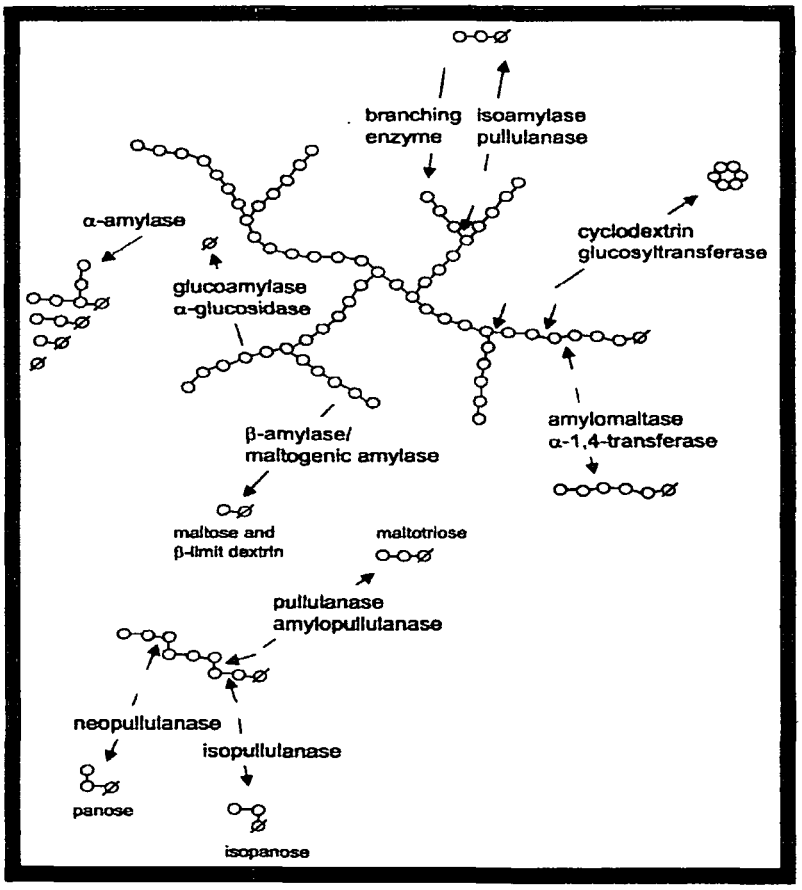

Figure 1.2: Schematic representation of the site of action on amylopectin molecules by various amylolytic enzymes. Glucose molecules are indicated by open circles while reducing ends are marked by a line through the open circle, Adapted from Turner et al., [23].

1.7.1. Endoamylases

Endoamylases are enzymes that randomly cleave α-1, 4 glycosidic bonds in amylose, amylopectin and related polysaccharides, and produce oligosaccharides

of varied chain lengths with α-configuration on the C1 of the reducing glucose unit produced [18, 24, 25]. This group of enzymes is the most widely distributed enzymes in nature and well-known example of this group is α-amylases (EC 3.2.1.1) [26]. Alpha-amylases are further classified into two groups – liquefying and saccharifying α-amylases. Liquefying α-amylase hydrolyses 30-40% of the glycosidic linkage in starch, while saccharifying hydrolyses 50-60% of the glycosidic linkage of starch molecules [27]. Majority of α-amylases are extracellular enzymes, however, few of them can be intracellular. Intracellular α-amylases enable the host cells to utilize maltodextrin/stored polysaccharides during the exponential growth phase [28]. The extracellular α-amylases are considered as one of the most thermostable proteins as they can work optimally at 130°C [29] and also show optimum pH activities from acidic to alkaline pH [28]. On the other hand, the cytoplasmic α-amylases are known to be active mostly around the neutral or acidic pH [28].

1.7.2. Exoamylases

The exoamylases act specifically on α-1, 4 glycosidic linkages of starch macromolecules from the non-reducing end and it results in production of low molecular weight oligosaccharides. Microbial exoamylases are of various types with respect to bond and substrate specificities as well as products that it forms. The enzymes that exclusively cleave α-1, 4 glycosidic bonds are known as β-amylase (EC 3.2.1.2) while enzymes that break both α-1, 4 and α-1, 6 glycosidic bonds are known as glucoamylase (EC 3.2.1.3) and α-glucosidase (EC 3.2.1.20) based on their substrate specificity [26]. The end-product obtained from both type of exoamylases are also different: glucoamylase and α-glucosidase produce only glucose, whereas β–amylase produces maltose and beta-limit dextrin as their end-products. Glucoamylase and β-amylase also convert the anomeric configuration of the end-product from one form to another (α→β) [5]. Glucoamylase and α-glucosidase differ from each other based on their substrate specificity. α-Glucosidase prefers short maltooligosaccharides and liberates glucose with an α-configuration, while glucoamylase acts best on long-chain polysaccharides [30].

Fungal glucoamylase is the most important class of industrial enzyme because of their suitability in a wide range of applications in the starch processing industry. They work optimally under acidic pH condition, which is the most desirable condition for the starch processing industry; however, they have lesser thermostability. Further, most of the reported glucoamylases are glycosylated and the carbohydrate moiety present in the enzyme is believed to play a significant role in maintaining the structural stability of the enzyme [31].

The other amylases in this class are cyclodextrin glycosyltransferase (EC 2.4.1.19) which has an additional transglycosylation activity, maltogenic α-amylase (glucan 1,4-α-glucanhydrolase, EC 3.2.1.133) which produces maltose exclusively [32], and maltotetraose (EC 3.2.1.60) [33] or maltohexaose (EC3.2.1.98) [34] amylases which form maltooligosaccharides exclusively.

1.7.3. Debranching enzyme

A third group of enzymes that hydrolyze starch polymer are the debranching enzymes that exclusively hydrolyze α, 1-6 glycosidic linkage as for example isoamylase (EC 3.2.1.68) and pullulanase type I (EC 3.2.1.41) [18]. The major difference between these debranching enzymes is their substrate preference towards pullulan (polymers of α, 1-6 linked maltotriose units) [35, 36]. Pullulanases are able to hydrolyze α, 1-6 glycosidic bond in both the pullulan and amylopectin molecules, whereas isoamylases are only capable of hydrolyzing α, 1-6 glycosidic linkage in amylopectin, yielding a long linear polysaccharides [18]. Besides, there is another type of pullulanase enzyme that can hydrolyze both α, 1-4 and α, 1-6 glycosidic linkage and thus can be categorized into group II pullulanase. These types of enzymes are also referred to as α-amylase – pullulanase or amylopullulanase and produce maltose and maltotriose as their main degradation products [18]. There also exists a special class of enzyme belonging to this group, which apart from debranching activity can perform transglycosylation with the formation of a new α, 1-4 or α,1-6 glycosidic bond and is called as neopullulanase (EC 3.2.1.135) [37].

1.7.4. Transferases

Transferases are the fourth group of starch-converting enzyme which cleave the α-1, 4 glycosidic bond of the donor molecule and form a new glycosidic bond by transferring a part of the donor molecule to a glycosidic acceptor [18]. Examples of this type of enzymes are amylomaltase (EC 2.4.1.25) and cyclodextrin glycosyltransferase (EC 2.4.1.19) which form a new α, 1-4 glycosidic bond, while branching enzymes (EC 2.4.1.18) form a new α, 1-6 glycosidic bond. Cyclodextrin glycosyltransferases make cyclic oligosaccharides with 6-8 glucose residues (cyclodextrins) via an intramolecular transglycosylation reaction while amylomaltases give rise to a linear product [18, 38, 39]. Further, amylomaltases are mainly found in microorganisms, which are involved in the utilization of maltose or the degradation of glycogen [38]. Glucan branching enzymes are another type of transferases enzymes, which are involved in the synthesis of glycogen in many microbes by forming α, 1-6 glycosidic bond in the side chains of glycogen [18].

1.8.The α-amylase family: Characteristics and Reaction mechanism

Enzymes that act on starch mostly belong to one family based on their amino acid sequence homology, i.e. α-amylase family or GH13 family as per the classification of Henrissat [40]. These enzymes have the following features:

(i) They attack α-glycosidic bonds and cleave this bond to produce α-anomeric mono or oligosaccharides (hydrolysis) and/or form α, 1-4 or 1-6 glycosidic linkages (transglycosylation).

(ii) They possess a $(\beta/\alpha)_8$ or TIM barrel (Figure 1.3) structure containing the catalytic site residues.

(iii)They possess four highly conserved regions in their primary sequence, which contain the amino acids that actively take part in catalysis or maintain the stability of the conserved TIM barrel topology [41].

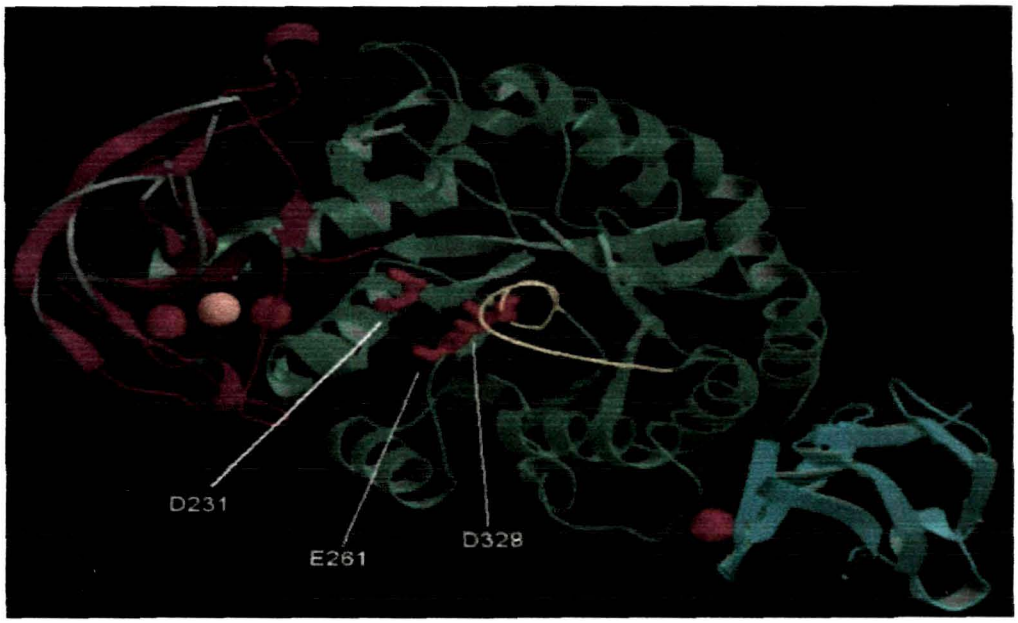

Figure 1.3: Domain organization of *B. licheniformis* α-amylase (BLA) enzyme (PDB code 1BLI). Domain A: green, domain B: magenta and domain C: cyan. Calcium ions (red spheres) and sodium ions (orange spheres) and the active site residues Asp231, Glu261 and Asp328 are shown in color (red). The loop connecting β7 to α7 is also shown in yellow color. Adapted from Nielsen & Borchert [42].

1.8.1. Conserved region/sequences

α-Amylase family contains four highly conserved sequences (I-IV), which are found within the TIM-barrel on β-strands 3, 4 and 5 and in the loop connecting β-strand 7 to α-helix 7 (Figure 1.4).

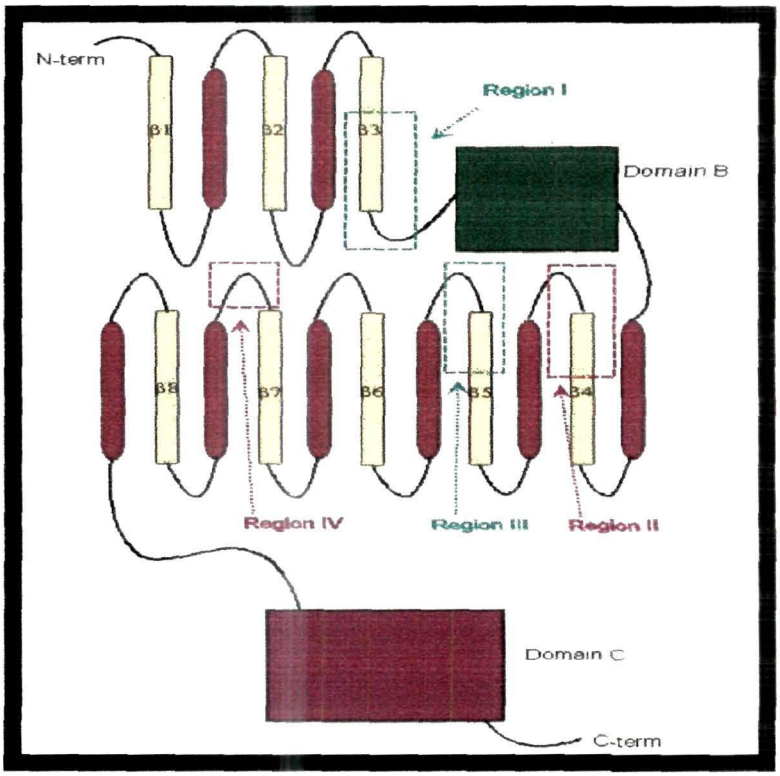

Figure 1.4: Topology illustration of α-amylase family. The four highly conserved sequences are indicated with dashed boxes, adapted from Nielsen & Borchert, [42].

The region I (Figure 1.4) comprises residues that are present in the C-terminal end of the third β-strand of the TIM barrel (β3). This region contains the three highly conserved amino acid residues (Figure 1.5) such as Asp100, Asn104, and His105 (BLA numbering) [42]. Further, there is always preference for Val at position 102 (BLA numbering), which is not explainable [42]. Asp100 plays an important role for the active site integrity of molecules, as it is hydrogen-bonded with Arg229, which is a fully conserved residue within hydrogen-bond distance of both the catalytic residues Asp231 and Glu261(BLA numbering). Nevertheless, Asn104 does not participate directly in the stabilization of the active site of enzyme, but it coordinates with the conserved calcium ion between the A and B domains [43]. Further the His105 residues interact with the C-terminal of β3 and the rest of the TIM-barrel by stabilizing hydrogen bonding between Asn104 and the backbone

oxygen of Tyr56 (BLA numbering) present in the loop connecting β2 to α2 strands [42].

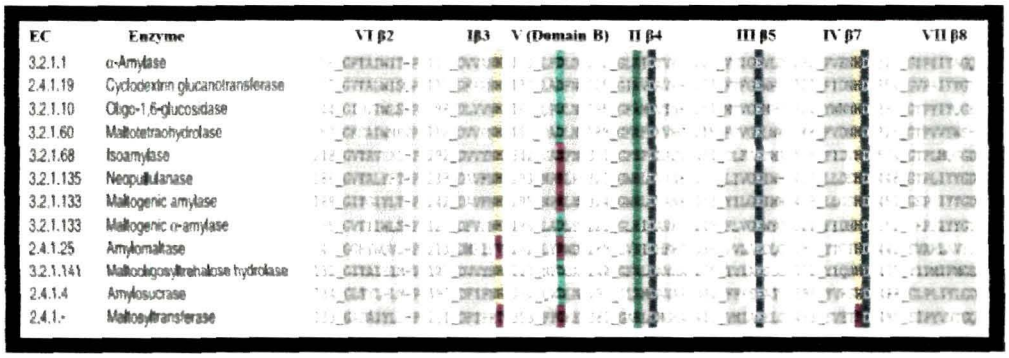

Figure 1.5: The seven conserved sequence regions found in the α-amylase family adapted from Janecek, [44]. The conserved sequence were compared with the following α-amylase family whose structure is known: α-amylase, *Aspergillus oryzae* [45]; cyclodextrin glucanotransferase, *Bacillus circulans* strain 8 [46]; oligo-1,6-glucosidase, *B. cereus* [47]; maltotetraohydrolase, *Pseudomonas stutzeri* [48]; isoamylase *P. amyloderamosa* [49]; neopullulanase, *Thermoactinomyces vulgaris* R-47 [50]; maltogenic amylase, *Thermus* sp. IM6501 [51]; maltogenic α-amylase, *B. stearothermophilus* [52]; amylomaltase, *Thermus aquaticus* [53]; maltooligosyltrehalose hydrolase, *Sulfolobus solfataricus* [54]; amylosucrase, *Neisseria polysaccharea* [55]; maltosyltransferase, *Thermotoga maritima* [56]. Blue color indicates: catalytic Asp & Glu; yellow: functional His; green: invariant Arg; turquoise: Ca^{2+}-binding Asp; while conserved residues are marked in grey and non-conserved residues in pink. The first column denotes the Enzyme Commission number of a given member and β2, β3, β4, β5, β7, and β8 indicate the β-sheet in which this conserved residues are present.

Region II (Figure 1.4 & 1.5) contains the catalytic nucleophile Asp231 and invariable Arg229 residues, located in the C-terminal of β4 strand [42]. These two residues are the highest conserved residues in almost all the α-amylases and indispensable for carrying out its catalytic activity [57]. The other two less conserved residues found in this region are Lys234 and His235 (BLA numbering),

which are believed to bind the reducing end of the glucose chain in the substrate-binding cleft [57].

Region III (Figure 1.4 & 1.5) contains only Glu261 as the most conserved residue that takes part in catalysis as a proton donor and is positioned in the fifth β-strand of the TIM-barrel at C-terminus [42].

Region IV (Figure 1.4) comprises residues present in the loop connecting β7 to α7 that protect the active site from the solvent [42]. This region contains the fully conserved residue Asp328 and strongly prefers His327, however, very often Phe, Val and Asn are seen at positions 323, 324 and 326, respectively. It has been observed that this loop is flexible, which allows substrate to bind and distort. It is believed that Asp328 is involved in substrate binding, distortion and in elevating the pKa of Glu261 [42].

In addition to the above four highly conserved regions, Janecek [58, 59] has proposed that there are also three more conserved regions in the α-amylase sequences (Figure 1.5). Out of these three regions, region V contains an invariable aspartic acid residue. This residue, present in the domain B, is believed to be involved in coordinating the conserved calcium ion and the hinge region of domain B.

1.8.2. The active site cleft

The active site cleft of α-amylase family is formed by the carboxyl end of β-sheets in the TIM barrel and is located at the interface between domain A and domain B. It has been found that the substrate-binding cleft can accommodate from four to ten glucose units (depending upon species). Certain amino acid residues bind each glucose unit, which constitute the binding subsite for that glucose unit. Davies et al. [60] have numbered the subsite according to the location of the scissile bond (cleavage point) with negative subsite numbers on the non-reducing side of the scissile bond (Figure 1.6). A typical α-amylase may have 2 to 3 subsites present on the reducing end (subsites +1, +2 and +3) while 2 to 7 on the non-reducing end of the scissile bond [61, 62].

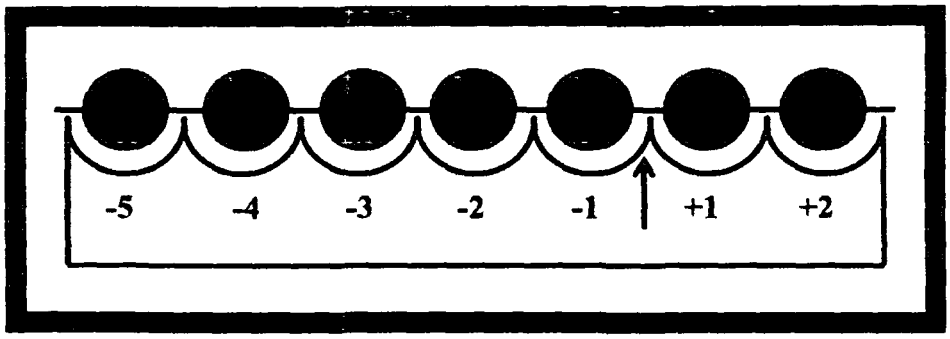

Figure 1.6: Nomenclature of active site cleft subsite for amylases family, the arrow indicates the point of enzymatic cleavage (scissile bond), adapted from Nielsen & Borchert [42].

1.8.3. The catalytic mechanism

The α-glycosidic linkage is the most stable chemical bond with $\sim 2\times10^{-15}s^{-1}$ spontaneous rate of hydrolysis at room temperature [63]. It has been observed that members of α-amylase family enhance this rate so immensely that they can be considered as the most efficient enzymes known to date. For example, cyclodextrin glycosyltransferase has a rate of hydrolysis of 3 s^{-1} and thereby increases the rate of hydrolysis by 10^{15} fold [39]. The most accepted catalytic mechanism of the α-amylase family is α-retaining double displacement methods. The catalysis mechanism involves the active site catalytic residues, glutamic acid as an acid/ base catalyst and an aspartate as the nucleophile (Figure 1.7). This process involves the following three major steps:

(i) The first step is the protonation of glycosidic oxygen by the glutamic acid (proton donor) and this is followed by nucleophilic attack by the catalytic aspartate on the C1 of sugar residue in the −1 subsite;

(ii) The second step is that the aglycon part of the substrate leaves the active site and a water molecule is activated presumably by deprotonated glutamate.

(iii) The final step is the hydrolysis of the covalent bond between the oxygen of the nucleophile and C1 of the sugar residue by the activated water molecules, thus completing the catalytic cycle.

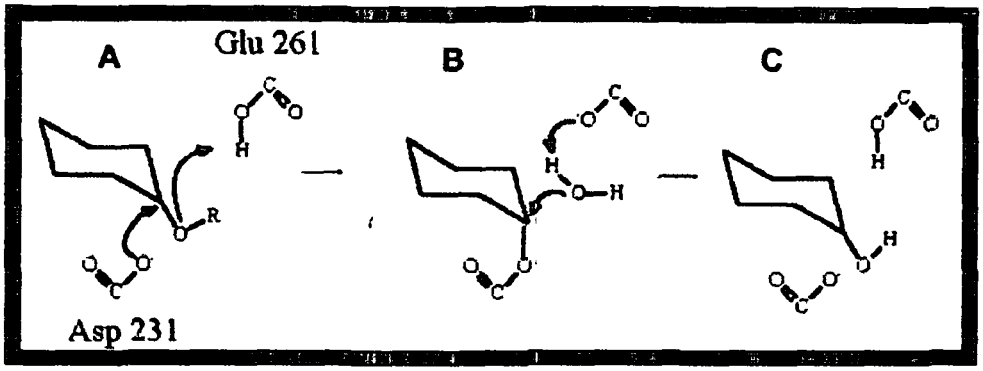

Figure 1.7: The double displacement mechanism of retaining glycosyl hydrolases. A: Protonation by Glu261 and nucleophilic attack on C1 glucose by Asp231, and departure of reduced substrate; B: activation of water molecules and cleavage of C1-Asp231 covalent bond; C: regeneration of initial protonation steps, adapted from Nielsen & Borchert [42].

Koshland [64] originally proposed the above double displacement mechanism; however, in the above catalysis process only two conserved catalytic residues take part directly. The third conserved catalytic residue, Asp 238 (BLA numbering), helps in the catalysis process indirectly, by binding to the OH-2 and OH-3 groups of the substrate through hydrogen bonding [65]. Asp238 also helps in the distortion of the substrate and elevation of pK_a of Glu261 by electrostatic interaction [65; 42]. The other possible conserved amino acid residues that take part in catalysis process are histidine, arginine, and tyrosine. They help the catalysis process by positioning the substrate and nucleophile into the correct orientation in the active site, by stabilizing the transition state, and by polarizing of the electronic structure of the substrate [65-68] Apart from these catalytic residues in the four conserved regions, an additional fifth conserved region exits This region contains aspartate, which is believed to take part in catalysis by acting as a calcium ligand [58, 59].

1.8.4. Calcium and sodium ions

α-Amylases contain a conserved calcium ion in between the domains A and B [43, 69], which is known for stabilizing the active enzyme [70]. The dissociation

constant for *Alteromona haloplanctis* α-amylase is 0.0050 nM [71], which suggests very strong affinity of calcium ion towards the enzyme molecules [42]. It is assumed that this conserved calcium ion mainly takes part in the structural stability of enzyme [43, 72, 73] as it is too distantly located from the active site to participate directly in catalysis. Besides, there is also evidence of the presence one or more calcium ions in several structures [43, 69, 74], and interestingly presence of linear Ca-Na-Ca triad in *B. licheniformis* amylase (BLA) [43, 62]. It has been observed that the mutations in this metal triad-binding site are highly detrimental to the thermostability in BLA [75].

1.8.5. Chloride ions

Various mammalian α-amylases are known to have a chloride ion in the active site, which enhances the catalytic efficiency of the enzyme, probably by elevating the p*K*a of the hydrogen-donating residue in the active site [42, 76]. However, it has also been reported in some of the psychrophilic α-amylase (AHA) from *Alteromonas haloplanctis* bacterium [77]. Further, it has been perceived that with binding of chloride ion there is dramatic increase in affinity for the conserved calcium ion [71], and thus it is believed that chloride ion also induces the conformational changes around the active site of enzyme. A mystifying feature of this type of α-amylases is the presence of a serine protease-like Glu-His-Ser triad in the interface between domains A and C, which is proposed to be capable of performing an auto-proteolytic cleavage [77].

1.8.6. Domain organization

Almost all the enzymes belonging to α-amylase family engage the α-retaining mechanism for catalysis but they vary widely in their substrate and product specificities. These alterations may be due to arrangement of different domains around the catalytic core (Table 1.2) or due to presence of extra sugar binding subsites [42]. The foremost conserved domain found invariably in all α-amylase family enzymes is the A-domain, which consists of eight parallel β-strands arranged in a barrel enclosed by eight α-helices [18]. The catalytic conserved active

site residues (Asp231, Glu261, and Asp328; BLA numbering) of the α-amylase family are found within this domain and form core of the molecule [18]. The $(\beta/\alpha)_8$ TIM barrel present in this domain was first observed in chicken muscle triose phosphate isomerase (TIM) [78].

The α-amylase family also contains the second most common conserved B-domain that protrudes between β3-sheet and α3-helix. It may range from 44 to 133 residues in length and play a pivotal role in substrate or Ca^{2+} binding [18]. Apart from the A and B-domains, there are also nine other domains that have been identified so far in the α-amylase family [18]. A number of enzymes belonging to this family, that hydrolyze interior α,1-6 glycosidic linkage, have a second protrusion of the A-domain (domain 2 or 7). All other domains (C to I) are present either in front or behind the A domain.

The C-domain consists of C-terminus of the BLA molecules and forms a Greek key motif structure. The function of this domain is unknown. However, the third calcium ion-binding site bridging between domain A and C, which is found exclusively in bacterial α-amylases, is responsible for the enhancement of BLA thermostability [43, 79]. Further, in cyclodextrin glycosyltransferase, this C-domain contains a maltose-binding site, which is involved in the binding of raw starch [67, 80]. In many maltogenic α-amylase and cyclodextrin glycosyltransferase, there exists a D-domain after the C-domain, whose function is still unknown.

Many of the raw starch binding α-amylase family have an E-domain that interacts with the substrate [80-82]. The other characteristic domains (F, H, and G-domain) of α-amylase family are found in the N-terminus of enzymes that have an endo-action/ α, 1-6 glycosidic bond hydrolytic activity of branched substrates [18].

Table 1.2: Domain organization of α-amylase family that acts on glucose-containing substrate, proposed by Maarel et al [18]

Enzyme	EC number	Domains	Main substrate
Amylosucrase	2 4 1 4		Sucrose
Sucrose phosphorylase	2 4 1 7		Sucrose
Glucan branching enzyme	2 4 1 18	A, B, F	Starch, glycogen
Cyclodextrin glycosyltransferase	2 4 1 19	A, B, C, D, E	Starch
Amylomaltase	2 4 1 25	A, B1, B2	Starch, glycogen
α-Amylase	3 2 1 1	A, B, C	Starch
Oligo-1,6-glucosidase	3 2 1 10	A, B	Amylopectin
α –Glucosidase	3 2 1 20		Starch
Amylopullulanase	3 2 1 41/3 2 1 1	A, B, H, G	Pullulan
Cyclomaltodextrinase	3 2 1 54	A, B	Cyclodextrins
Isopullulanase	3 2 1 57		Pullulan
Isoamylase	3 2 1 68	A, B, F	Amylopectin
Maltotetrose-forming amylase	3 2 1 60	A, B, C, E	Starch
Glucodextranase	3 2 1 70		Starch
Trehalose-6-phosphate hydrolase	3 2 1 93		Trehalose
Maltohexaose-forming amylase	3 2 1 98		Starch
Maltogenic amylase	3 2 1 133	A, B, C, D, E	Starch
Neopullulanase	3 2 1 135	A, B, G	Pullulan
Malto-oligosyl trehalase hydrolase	3 2 1 141		Trehalose
Malto-oligosyl trehalase synthase	5 4 99 15		Maltose

1.9. Microbial production of Alpha-amylase

α-Amylases are ubiquitous enzymes that are distributed thoroughly in the plant, animal and microbial kingdoms for their carbohydrate metabolism [26, 29] Amylases that are derived from plant and microbial sources have been used for centuries as food additives, for example barley amylases in brewing industry and fungal amylases in preparation of oriental foods [26] Even though amylases are distributed widely in nature, microbial sources, specifically fungal and bacterial amylases, have been explored immensely for the industrial production due to various advantages that it offers [26] The major advantages of using microbial amylases are that they are cost effective, economical in bulk production, and require

less time and space. Besides, microbes are easy to manipulate in order to obtain enzymes of desired characteristics [29, 83].

α-Amylase can be harvested from different species of microorganisms, however to meet most of the industrial needs, the α-amylase from the *Bacillus* genus have been widely used [26]. *B. subtilis, B. licheniformis, B. stearothermophilus,* and *B. amyloliquefaciens* are known to be good producers of α-amylase and have been widely explored for the application in a number of industrial processes such as in food, fermentation, textiles, and paper industries [5; 26]. The commercial fungal α-amylase production is limited to a few species of mesophilic fungi though they are the most preferred source over other microbial sources because of their GRAS (Generally Recognized As Safe) status [29]. Fungal sources are mostly confined to *Aspergillus* and *Penicillium* [84]. Among the array of extracellular enzymes produced by *Aspergillus* species, amylases are the most significant industrial enzymes [85].

1.10. Cloning of α-amylase genes and enzyme engineering

Cloning of α-amylase genes have been done extensively for the molecular study of proteins, their hyper-production, and protein engineering in order to achieve desirable characteristics [26]. α-Amylase was one of the first proteins adopted for genetic manipulation due to existence of an easy screening assay and the availability of amylase negative strains [9]. The purpose of cloning of α-amylase genes can be many but it is carried out most importantly for the expression of thermostable enzymes, higher enzyme productivity, co-expression of two enzymes by the same organism, and for the improvement of existing enzyme characteristics by enzyme engineering [5]. α-Amylase genes have been cloned from different bacterial and fungal sources in appropriate host organisms mostly in *Escherichia coli* or *Saccharomyces cerevisiae* using suitable vectors (Table 1.3).

Table 1.3: Cloning of some of the α-amylase genes from different source

Gene source	Recombinant host	Vector	Reference
Alteromonas haloplanktis	*Escherichia coli*	pUC12	[86]
Aspergillus kawachii IFO 4308	*S cerevisiae*	pYcDE1	[87]
Bacillus amyloliquefaciens	*Escherichia coli*	pETAM	[88]
B licheniformis	*Escherichia coli*	pBR322	[89]
B subtilis	*Escherichia coli*	pUC8	[90]
B subtilis	*S cerevisiae*	pPB-G, pPG/AB, pPG/MM	[91]
Halothermothrix orenii	*Escherichia coli*	pBluescript SK	[92]
Lipomyces starkeyi	*Escherichia coli*	pGEM-1	[93]
Thermococcus hydrothermalis	*Escherichia coli*	pBluescript II KS	[94]

Most of the starch processing industries, which utilize α-amylases, are carried out at higher temperature and pH [42] Thus, enzymes withstanding this extreme environment is a matter of great significance and has been addressed by many industries and academia. Very often α-amylases become inactive for industrial applications owing to the extreme environment and many more reasons The major detrimental factor is incubation at high temperatures that causes unfolding of amylases, incubation at extreme pH values and exposure to chelating and oxidizing agents can also result in denaturation of enzymes [95, 96] Thus, there is a persistent demand for improving the stability of this enzyme, so that they are better suited for this harsh industrial process

To address these issues, various approaches were applied One such approach was to screen novel microbial strains capable of producing α-amylase from extreme environments such as hydrothermal vents, salt and soda lakes, and brine pools [97-99] This has been applied successfully by various researchers and industrial groups in obtaining a highly thermostable enzyme such as a thermostable pullulanase from *Feridobacterium pennaorans* [100] or an α-amylase from *Pyrococcus woesei* [101] which led to a number of patent applications However, even being thermostable in nature, most of these amylases, if not all, do not meet all the industrial needs [18]

Another approach would be enzyme engineering, which is known to be a promising technique to achieve this goal by integrating desired properties in the appropriate gene [26]. In the case of the α-amylase family, these desired properties may include high thermostability, broad pH profile, Ca-independence, activity at high concentration of starch, protease resistance, raw starch digestibility, insensibility to catabolite repression and hyper-production (Table 1.4). The most important technique used in enzyme engineering is site-directed mutagenesis; which alters the properties of an existing enzyme based on its structural information [9]. Using this technique several achievements have been made. For example, Declerck [102] has introduced three mutations (Asn172 → Arg, His156 →Tyr and Ala181 → Thr) in the α-amylase from *B. licheniformis* which resulted in a 5-fold increase in thermostability. Similarly, stability at lower pH was attained by substitutions Met15→Thr/Asn188→Ser [103] and stabilization of the protein by insertion of prolines in loop regions of BLA [104]. Combination of error-prone PCR and gene shuffling of α-amylase gene resulted in a mutant showing broader range pH and 5-fold higher activity at pH-10 compared to that of the wild type enzyme [105]. Further, there are reports showing that incorporation of hydrophobic residues at the surface of *B. licheniformis* amylase resulted in increases in thermostability [106].

Table 1.4: Implication of some of the engineered amylases

Source of gene	Expression host	Types of genetic modification	Improvement	References
Bacillus stearothermophilus	*E coli* DH5α	Site-directed mutation (Asn331→Ser Glu332→val)	loss of activity towards substrate, thus it indicates substrate binding site	[107]
B licheniformis	*B subtilis* WB600	double substitutions (Leu134→Arg, Ser320→Ala)	acid-resistant capability of mutant was significantly enhanced	[108]
B subtilis BF768	*B subtilis* WB600	200 U/ml→723 U/ml	Hyper-production of moderate thermostable amylase	[109]
B licheniformis MTCC 6598	*E coli* BL21	site-directed mutagenesis of calcium-binding sites (N104→D104, D161→N161, D183→N183, D200→N200, D430→N430)	calcium binding site is sensitive to any modification	[110]
Bacillus sp US149	*E coli* DH5α	site-directed mutagenesis (Gly312→Ala, Lys436→Arg)	double mutant enhanced thermostability	[111]
B amyloliquefaciens	*B subtilis* 1A717	calcium-binding sites (Asp231→Asn, Asp233→Asn, Asp438→Gly)	substitution resulted in dramatic reduction in activity and thermostability	[112]
B stearothermophilus US100	*E coli* DH5α	double substitutions (Asn315 →Asp, Val450→Gly)	major end product shifts from maltopentaose/maltohexaose→maltose/maltotriose	[113]
Geobacillus stearothermophilus US100	*Escherichia coli* blueXL1-Blue	substitution (met 197 → ala)	thermostability & resistance to chelating agents	[114]

1.11. Amylase purification

Downstream processing for obtaining pure enzyme from bulk production is a tedious process and constitutes a major percentage of overall production cost if the purity requirement for final product is very stringent [26]. The industrial production of amylases requires little or no downstream processing even though it produces in bulk quantity; this is because the commercial use of enzyme usually does not require purified enzyme [29]. However, the enzyme used for applications in pharmaceutical and clinical sectors requires high purity amylases [29]. The purified form of enzyme is also a prerequisite in studies of structure-function relationships and biochemical property determination.

Purification strategies employed in downstream processing after fermentation are strongly dependent on the market demand, processing cost, purity requirement, and available technology [26]. The constant effort for the development of large-scale cost effective purification process has resulted in evolution of techniques that provide fast, efficient, consistent, and economical protocol for purification in fewer processing steps [26]. The conventional purification process of α-amylases from microbial sources involves the separation of culture from the fermentation broth and then selective precipitation by using ammonium sulphate or organic solvents (chilled acetone/ethanol) thereby to obtain concentrated amylases. The crude concentrated preparation is then subjected to various chromatography techniques, which usually include affinity, ion exchange, hydrophobicity interactions, gel filtration, and reverse phase chromatography [29]. The various strategies employed in the purification of α-amylase from various sources are listed below (Table 1.5).

Table 1.5: Various strategies employed for microbial α-amylases purification

Microorganism	Purification strategy	Purification fold/yield (%)	Reference
Fungi and yeast			
A. oryzae NRC 401013	DE52-Cellulose (pH 7 0), 70% $(NH_4)_2SO_4$, Sephacryl-S300	NI[1]	[115]
A. flavus LINK	50-90% $(NH_4)_2SO_4$, DEAE-Sephadex A50 (pH 6 5)	13 8/70	[116]
Cryptococcus sp S-2	Ultrafiltration, a-Cyclodextrin coupled with Sepharose 6B (pH 7 0)	140/78	[117]
Saccharomyces cerevisiae YPB-G	Ultrafiltration, b-Cyclodextrin linked Sepharose 6B (Epoxy activated, pH 4 5), Sephadex G-100 (pH 4 5)	5 0/2 0	[118]
Thermomonospora curvata	Ultrafiltration, 75% ethanol precipitation, Sephadex G-150 (pH 8 0), DEAE Cellulose, ultrafiltration	66/9	[119]
Bacteria			
Alicyclobacillus sp A4	Ultrafiltration, HiTrap SP XL column (Ion exchange)	-/21 8	[120]
Bacillus sp IMD434	Acetone precipitation, Resource Q, Phenyl Sepharose CL-4B	266/ -	[121]
Bacillus US147	Freeze drying, Q-Sepharose Cl 6B, Biogel P100	5/35	[122]
B licheniformis CUMC 305	65% $(NH_4)_2SO_4$, CM-Cellulose (pH 6 4)	212/42	[123]
B licheniformis NCIB 6346	DEAE-Cellulose DE52 (pH 5 3)	33/66	[124]
B megaterium VUMB109	80% $(NH_4)_2SO_4$, DEAE cellulose, Sephadex G-100	27/38	[125]
B subtilis	60% $(NH_4)_2SO_4$, Sephacryl-S200, 60% $(NH_4)_2SO_4$, S-Sepharose	17/9	[126]
B. subtilis 65	Sephacryl S-300, CM Sephadex C-50	30 85/24 8	[127]
Lactobacillus plantarum A6	Ultrafiltration, 50-80% $(NH_4)_2SO_4$, ultrafiltration, DEAE-Cellulose	20/35	[128]
Streptococcus bovis JB1	70% $(NH_4)_2SO_4$, Sephadex G-25 (pH 7 5), Mono Q	6 9/50	[129]

[1] No information

1.12. Amylase immobilization

Enzyme catalytic activity depends on its three dimensional structure and conformation; any disturbances in these, either temporary or permanent, by physical/chemical agent can affect its catalytic function [26]. Thus, it becomes essential to protect enzymes from destructive environments in order to maintain its catalytic activity [26]. Further, it becomes important to reuse the relatively expensive biocatalyst (enzyme) thereby to make an economically feasible process [130]. Therefore, immobilization of enzymes has become an important tool for protecting and stabilizing enzymes; it can enhance enzyme properties and makes them feasible for repetitive utilization either in batch or continuous mode [5]. Furthermore, immobilization of enzymes also increases thermostability and resistance to various physical and chemical denaturing/oxidizing agents. Thus, it enhances the operational stability of immobilized enzymes and circumvents product contamination by enzymes. Table 1.6 lists some of the immobilization techniques developed for α-amylases.

Table 1.6: Some of the immobilization techniques used for immobilizing α-amylase from different sources

Source	Immobilizing agent	% Activity retained (after immobilization)	References
A. oryzae	Cu^{2+} chelated poly(ethylene glycol dimethacrylate-n-vinyl imidazole) matrix via adsorption	70% after 20 cycles	[131]
Bacillus sp.	Copolymers of butyl acrylate and ethylene glycol dimethacrylate activated with glutaraldehyde	79.2% after 1 month's storage at 4°C	[132]
B. subtilis	Bis(2-ethylhexyl) sulfosuccinate sodium salt (AOT) coated a-amylase entrapped into butylacrylate-acrylic acid copolymer (BuA/AAc)	60% after 15 cycles	[133]
B. licheniformis	Poly(hydroxyethyl methacrylate-co-glycidyl methacrylate)	76%	[134]
B. subtilis	Ca-alginate gel capsules	90% after 20 cycles	[135]
α-amylase: glucoamylase (1:3)	(1) Hydrophilic silica gel	92.3% after 10 cycles	[136]
	(2) DEAE-cellulose entrapped in alginate beads	88.9% after 10 cycles	
Bacillus sp.	immobilized through NH_2- groups onto the epoxy rings of magnetic poly glycidyl methacrylate [m-poly (GMA)] beads.	80% after 80 days	[137]

1.13. Use of Alpha-amylase in biotechnology

Starch-based industries are the largest user of hydrolytic enzymes for hydrolysis and modification of this starch polymers into various useful products [138]. Among the various hydrolytic enzymes, amylases are the most important ones. Notably, amylase is the oldest commercialized enzyme, first used in 1984 as a pharmaceutical drug for the treatment of digestive disorders [29]. Ever since, amylase has found its application in various industrial processes such as in food, detergents, textiles, paper, and starch hydrolysis industry. Microbial amylases have completely replaced chemical hydrolysis in the starch processing industry, which is costly and hazardous [29]. Amylases can also find potential application in the pharmaceutical and fine chemical industries. However, the most widespread applications of α-amylases are in the starch industry where it is used for production of valuable fructose and glucose syrups from raw starch materials [139].

Table 1.7: List of industrial sectors where α-amylases are used for various biotechnological applications

Industries	Uses	Source of amylase used	References
Food	Production of glucose syrups, crystalline glucose;	*Anoxybacillus flavothermus*	[140]
	Production of high fructose corn syrups;	*Anoxybacillus contaminans*	[141]
	Production of maltose syrups;	*Bacillus acidicola*	[142]
	Reduction of haze formation in juices;	*Bacillus licheniformis*	[143]
	Solubilization and saccharification of starch for alcohol fermentation in brewing industries;	*Bacillus amyloliquefaciens*	[144]
	Retardation of staling in baking industry;	*Bacillus stearothermophilus*	[145]
	Reduction of viscosity of sugar syrups;	*Pseudomonas saccharophila*	[146]
Detergent	Used as an additive to remove starch based dirt's	*Bacillus licheniformis* NH1	[147]
Paper	Reduction of viscosity of starch from paper	*Bacillus amyloliquefaciens*	[148]
Textile	Warp sizing of textile fibers	*Bacillus* sp. KR-8104	[149]
Pharmaceutical	Used as a digestive aid	*A. oryzae*	[150]

1.13.1. Starch/syrup industry

Sugar syrup production such as glucose, maltose, maltotriose, dextrins sugar, and fructose from the starch conversion process is the major part of the starch processing industry. The hydrolysates produced are extensively used as a carbon source in fermentation as well as sweetening agents in food processing industries [25]. The age-old process of starch hydrolysis involves acid hydrolysis, however recently enzyme-based hydrolysis has totally replaced the acid conversion of starch due to various advantages that it offers such as specificity of the reaction, stability of the generated products, lower energy requirements, cost-effective, elimination of neutralization steps and more importantly its environmental friendliness [151].

Starch conversion in starch processing industries, is generally carried out by the synergistic action of a bacterial α-amylase and fungal glucoamylase. The enzymatic starch conversion involves the following three stages: gelatinization, which involves dissolution of starch granules; liquefaction, which partially hydrolyses and reduces viscosity; and final break down into glucose and maltose by saccharification [10]. The first two steps are carried out at higher temperature (70-80°C) and thus employ α-amylase, which is active at higher temperature. The α-amylases from *Bacillus* sp. is the most preferred enzyme for this application due to their remarkable thermostability [152]. Further, requirement of thermostable α-amylases is also crucial as their application minimizes contamination risk and saves energy by reducing the process reaction time [5]. Hydrolysis is also carried out at higher temperatures to minimize the polymerization of D-glucose into isomaltose [18]. The final step of saccharification is carried out by applying fungal glucoamylase to act on starch-sugar mixture thereby converting it into simple sugars. This glucose so obtained can be converted into high fructose containing syrups (HFCS, 42% fructose) by enzymatic isomerization of glucose into fructose by use of glucose isomerase. Due to the presence of higher sweetening property, the production of HFCS gets a major boost up for conversion of large quantities of corn and other botanical starches to this sweetening agent. HFCS finds major

application in beverage industries as a sweetener in soft drinks, besides being used in many food industries [153].

Moreover, the production of sweeteners from starchy food material by using enzymes provides a better alternative to food-processing industries by lessening the burden on sugar cane industries for demands of sweetening agents. Furthermore, bioconversions of starch into sweetener also offer an alternative use for highly perishable starchy materials that cannot be stored for longer period due to lack of proper preservation techniques, particularly in the tropical regions [154].

1.13.2. Food industries

The advent of modern biotechnology in food industries resulted in tremendous changes. There are many report which suggest that genetically engineered enzymes have been successfully and safely applied in the food industry. Amylases are widely used in processed-food industry such as in baking for improving bread or cakes quality, in beverages for clarification of haze formed in beer or fruit juices, or for the pretreatment of animal feed for improving digestibility [18]. The most widespread use of amylase in the food industry is in bread, where enzyme is added to the dough mixture of bread to degrade the starch into smaller dextrin, which in turn is used by yeast for fermentation [29]. With the addition of amylases in dough, the rate of fermentation is enhanced and viscosity of dough is reduced, which results in improvement in the volume and texture of bread [29]. Further, the additional sugars generated in the dough by the action of enzyme improves the taste, crust color, and toasting qualities of the bread. Besides generating fermentable compounds, α-amylases inclusion in bread also retards staling rate and thereby increases the retention of softness for longer period and increases the shelf-life of these products [29]. A thermostable maltogenic amylase obtained from *B. stearothermophilus* is commercially used in the baking industry [29].

1.13.3. Biofuel industries

The most utilized liquid biofuel is bioethanol. For bioethanol production, the most preferred substrate is starch, due to its low price and easily availability of raw materials in most parts of the world. The conventional process for bioethanol production from starch involves solubilization of starch by heating and subsequently treating it with enzymes such as glucoamylases and α-amylases to obtain fermentable sugar. This is further acted upon by yeast (*Saccharomyces cerevisiae*) thereby converting sugar into ethanol by fermentation [155]. Efforts have been made to obtain a new strain of yeast by protoplast fusion that can directly act upon starch to produce ethanol without the addition of saccharifying steps [156]. Amylases obtained from thermo-resistant bacteria of *Bacillus* strains have been commonly used during the first step of hydrolysis of starch suspensions [157]. A constant effort is made to engineer microbial strains that are capable of producing ethanol efficiently and can survive the higher concentration of ethanol (the major hindrance in bioethanol production). Due to genetic makeup, *S. cerevisiae* is the best suitable microbial strain for bioethanol production and thus efforts are made to isolate yeast mutant strains that are resistant to higher concentrations of ethanol [158].

1.13.4. Detergent industries

The detergent industry is one of the major consumers of enzymes as it accounts for about 40% of the total worldwide enzyme consumption and thus it represents one of the most successful applications of enzymes in biotechnological industries [159]. The main advantage of enzyme-supplemented detergent is that it is much milder than enzyme-free detergent and thus safe for skin and compatible for delicate china and wooden dishware [29]. Further, detergents supplemented with enzymes show enhancement in ability to remove tough stains and make the detergent more environmentally safe [147]. Amylases are the second largest enzymes used in the enzymatic detergent formulation, and 90% of all liquid detergents contain this enzyme [29]. Amylases are principally used in laundry and automatic dishwashing detergents to degrade the leftover residues of starchy foods

such as pasta, chocolate, baby food, barbecue sauce, potatoes, custard, and curry gravies to dextrin and smaller oligosaccharides [160, 161]. Besides removing starchy dirt from cloths, it also provides a whiteness benefit as starch tends to spread and act as a strong attractant for many types of particulate soils [159].

The successful application of amylases for inclusion in laundry and dishwashing detergent formulation is mainly dependent on its stability and compatibility with various detergent components [159]. Further, the use of amylases in detergent industries also requires that the enzyme must be stable and should show an optimal level of activity in commercially utilized formulations and in the presence of proteases used in detergent formulations [162]. Many alkaline amylases have been found to be suitable for inclusion in detergent formulation, but the chelating agent found in detergent restricts their uses, as their stability is dependent on Ca^{2+} ion. Therefore, there is constant search for Ca^{2+}independent amylases, which are stable in an oxidative environment and show optimum degree of activity in the presence of various detergent components. Most of the amylases which find application in detergent industry are derived from *Bacillus* or *Aspergillus* [159, 163]. Purafect OxAm® and Duramyl® are two engineered commercial detergent enzymes marketed by Genencore International and Novozyme respectively.

1.13.5. Textile industries

In the textile industry, the starch paste is applied to the thread/yarn to strengthen and prevent it from breaking during warp weaving. Starch is used as a sizing agent because it is cheap, easily available, and can be removed quite easily [29]. Sizing also prevents loss of string by friction, cutting and generation of static electricity on the string by giving softness to the surface of string due to laid down warp. Amylases are used for desizing process and they selectively remove the size and do not attack the fiber [29]. Desizing by amylases randomly cleaves the warp starch into water-soluble dextrins, which can be easily removed by washing and after desizing cloth goes to scouring and dyeing. Amylase from *Bacillus* sp. has been successfully employed in textile industries for quite a long time [164].

1.13.6. Paper industries

The pulp and paper industry uses α-amylases for the modification of starch of coated paper. The starch coating makes the surface of paper sufficiently smooth and strong, to improve the writing quality of the paper. However, the viscosity of natural starch is too high for paper sizing and therefore after sizing with starch, it is treated with the amylases to partially degrade the polymer [165]. Starch is also a good choice as sizing agent for the finishing of paper, improving the quality and erasebility, in addition to a good coating agent for the paper. The size also enhances the stiffness and strength of the paper [166]. The sizing of paper is generally done at 45-60°C and thus it requires mesophilic α-amylase [29]. A number of commercial amylases exist for the application in paper industry, which include Termamyl®, Fungamyl® and BAN® supplied by Novozymes, Denmark [29].

1.13.7. Clinical and medicinal applications

With the advancement of biotechnology, the application of amylases has expanded to various new emerging areas; one such area is in clinical and medicinal application. A decade ago, it was proposed that if amylases with suitable properties could be prepared then they would be possibly useful in the pharmaceutical and fine chemicals industries [167]. However, the application of amylases for medicinal purpose is not a completely new area. The first commercial production of enzyme was an amylase from a fungal source in 1894 for the treatment of digestive disorders, since then, it has expanded its horizon to various fields [5] The recent trends of using biodegradable polymers for controlled drug delivery have been a major focus of interest in pharmaceutical research.

Starch is a natural biodegradable polysaccharide in the human body and thus has a great potentiality for controlled drug delivery [168]. Therefore, efforts are targeted to produce hydrogels. Further, it has been reported that the addition of α-amylase to this hydrogel can modulate the release of drugs and thus addition of α-amylase to cross-link amylose (CLA) tablets has been started [169]. The other medical application of amylases is not direct but it can help in identifying natural

amylase inhibitors, which can be orally administrated thereby inhibiting α-amylase activity in saliva and pancreatic juice, and reducing digestion and absorption of starch. This can effectively cure or prevent obesity [170]. Besides, a process for the detection of higher oligosaccharides and a biosensor for process monitoring have also been developed, which involve the application of amylases [29].

1.13.8. Elimination of environmental pollutants

Starch polymers are ubiquitous in nature, as a reserve stored energy in many species of plant, and present extensively in the waste materials produced from processing of plant materials or food processing industries [171]. These starch wastes are produced in large quantities and thus are causing pollution problems. Therefore, treatment of this starch based effluent by amylolytic enzyme producing microbes may result in production of valuable product like microbial biomass protein for animal feed and may purify the effluent as well [172, 173].

1.13.9. Molecular applications

Reporter gene assay is the most essential molecular biology tool for the study of gene regulatory elements and gene expression [174]. In molecular biology, the amylase gene can serve as a reporter gene for selection of successful integration of a construct in addition to antibiotic resistance. Further, the screening of recombinant clones will be easier as insertion of foreign DNA into amylase gene will result in a loss of amylolytic activity in the host cell which can be easily assayed by using a simple and inexpensive iodine staining procedure [175].

1.14. Future prospects of amylase

It is evident from the above study that amylase is the most important industrial enzyme. Even though the starch processing industries have been prevalent for many decades and a number of microbial sources have been isolated and identified for the efficient production of amylases, only a few selected strains of fungi and bacteria meet the industrial demands. Therefore, there is a continuing search for new microorganisms that can be used for amylase production which can

suit industrial demands. Apart from ever-increasing demands in detergent, food and starch industries, amylases are also in great demand in various other industries such as paper and pulp, textile, etc. Further, to meet the ever-growing demand for fuel energy, the search for non-renewable energy source has become a focus of much research these days. Thus, bioethanol production from plant based starch material has gained immense importance, which in turn demands the search for efficient raw starch digesting amylolytic enzymes.

Environment-friendly processes are gaining ground all over the world, therefore, enzymes are often replacing the age old chemical process. Enzyme-based processes are not only ecofriendly but they also save lot of money by reducing water and energy consumption that ultimately reduce the cost of production. However, successful industrial application of enzyme requires efficient large-scale production and the structural and functional relationships of the enzymes have to be known in detail. This will eventually improve the stability of the existing enzymes and help in discovering many new ones, which are best suited for harsh industrial processes.

In spite of several years of extensive research on several aspects of amylases, there are still numerous gaps in our knowledge of these enzymes. There is ample scope for improving their properties to suit industrial demands. The natural biodiversity provides valuable resources for identification of novel microbes suitable for novel applications. A recent trend is identification of novel enzymes from exotic microorganisms that can withstand hot water, freezing arctic water, saline water, or extremely acidic or alkaline habitats. These exotic microbes may harbor amylases, which are likely to mimic some of the unnatural properties that are desirable for their commercial applications. Exploitation of biodiversity to identify microbes that produce amylases well suited for diverse applications is the most prospective alternative. However, application of extremophile amylases in industrial processes is hampered due to inability of growing these extremophiles in laboratory cultures. Therefore, with the help of enzyme engineering, cloning and

expression into mesophilic hosts could rationalize the use of enzymes from extremophiles.

Therefore, the present research is mostly focused on developing α-amylase from microbes that are thermo-tolerant and pH tolerant. Besides it is also undertaken for optimizing production cost, modifying them genetically, or applying site-directed mutagenesis to acquire desired properties in the enzyme. It is anticipated that amylases will continue to flourish into new applications such as biopharmaceutical sector and expand its horizon.

1.15. Aims and objective of the present study

The Northeastern zone of India, considered as one of the mega biodiversity zones of the world, may harbor several previously uncharacterized microbial species that may produce novel/potent enzymes suitable for commercial applications [159]. Bearing this in mind, the present investigation was initiated with an aim to isolate α-amylase secreting potent microbial strains from this region and to identify these strains by polyphasic approach. Furthermore, the overall cost of enzyme production is one of the major obstacles in successful industrial application of enzymes [176]; therefore, the optimization of fermentation medium through a statistical approach was undertaken in the present investigation for optimization of amylase production under submerged fermentation.

Highly purified enzyme is not obligatory for commercial industrial applications [29]; however, in the pharmaceutical-clinical sectors and before assessing the biotechnological/commercial potential of any enzyme, characterization of biochemical properties of purified enzyme is most important and advantageous. Thus, with an aim to investigate some biotechnological applications of the α-amylases purified in this study, the enzymes were biochemically characterized. Finally, in order to understand the structure-function relationship and to improve some biochemical properties (by enzyme engineering) better suited for industrial application (which may be considered for future studies),

the α-amylase genes from the above strains were cloned and overexpressed in *E. coli*.

The present study was undertaken with the following aims and objectives:

1. Screening, isolation, and identification of α-amylase producing promising bacteria from the environmental samples of North-East, India.
2. Optimization of culture conditions and nutritional requirements of the selected strain(s) by submerged fermentation in order to maximize the α-amylase production.
3. Purification of a major/promising α-amylase from a potential strain followed by characterization of some of its biochemical properties and assessment of its biotechnological potential.
4. Cloning and expression of a major and/or novel α-amylase gene(s) from a promising microbial strain.

Chapter II

REVIEW OF LITERATURE

Chapter 2: Review of Literature

2.1. Amylase producing organisms

Amongst the wide varieties of industrial enzymes, amylase constitutes a major share of the enzyme market due to its wide area of potential biotechnological applications Amylase represents approximately 30% of worldwide enzyme production out of the total estimated enzyme market of 5 1 billion US$ [9, 18, 177] The first commercially produced enzyme was an amylase from a fungal source in 1894 as a pharmaceutical aid for the treatment of digestive disorders [178] Since then, with the advent of modern biotechnology, the spectrum of amylase application has widened into many fields, such as clinical, medicinal, and analytical chemistry, besides being widely used in starch saccharification, food, fermentation, textiles, paper and detergent industries [5, 29] At present, commercially available microbial amylases have almost completely replaced the chemical hydrolysis of starch in starch processing industries [179]

Almost all living organism such as plants, animals and microbial kingdoms can produce amylases for their metabolism of carbon source [29, 159, 180] However, amylases from microorganisms have a broad spectrum of industrial applications, as they tend to be more stable than their plant and animal counterparts [181] The major advantages of using microbial sources for amylases production are that they can be grown economically in bulk quantity and can be manipulated easily to obtain enzymes of desired characteristics [29] α-Amylases can be obtained from several sources of micro-organism such as fungi, yeasts and bacteria, however, fungal and bacterial amylases have dominated applications in the industrial sector [29]

2.1.1. Bacterial amylase

α-Amylase can be derived from several genera of bacteria, but for commercial applications it is mainly obtained from the genus *Bacillus* [26, 139, 180] It is estimated that *Bacillus* spp enzymes alone comprise about 50% of the

total global enzyme market [10, 182]. Further, bacterial amylase is the most common choice over the fungal amylase for industrial application as it offers several characteristic advantages over the latter [5]. Bacterial amylases show some unique characteristics such as thermo-tolerant, halo-tolerant, alkalophilic, and acidophilic properties, which make them superior over the amylases from other sources [10, 183].

Additionally, most of the industrial processes are carried out at higher temperature and thus, thermostable enzymes are the most preferred characteristic for industrial application. One such requirement is in starch industry where the enzymatic liquefaction and saccharification of starch are performed at 100–110°C. Thus, starch-processing industries require amylolytic enzymes that are optimally active and stable at this temperature to produce valuable products like glucose, crystalline dextrose, dextrose syrup, maltose, and maltodextrins from starch [139, 184]. Thermostable enzymes isolated from thermophilic bacteria or archaea mostly fulfill these requirements of starch industries. Nevertheless, bacterial amylases are more easily grown and manipulated to obtain thermostable enzyme [138, 184]. Among the bacterial kingdom, *B. subtilis, B. stearothermophilus, B. licheniformis,* and *B. amyloliquifaciens* are known to be good producers of α-amylase suitable for various applications [5, 139, 170, 185, 186].

Enzymes produced by halophilic microorganisms are equally important for industrial application as they are optimally active at high salt concentration, which are employed in many industrial processes where many of the enzymatic conversions are inhibited due to high salinity [139, 187, 188]. Additionally, it has been observed that most of the halobacterial enzymes are significantly thermotolerant and remain stable at room temperature for long periods [139, 189]. Some of the halophilic bacteria from which halophilic amylases have been characterized belong to *Chromohalobacter* sp. [188], *Halobacillus* sp. [187], *Haloarcula hispanica* [190], *Halomonas meridiana* [191], and *Bacillus dipsosauri* [192].

2.1.2. *Fungal amylase*

Most of the reported amylases from fungal sources are mainly limited to terrestrial isolates, which grow at mesophilic conditions [29, 139]. The fungal amylases are mainly confined to *Aspergillus* species and a few others species from *Penicillium, Rhizopus*, etc. [84, 139]. Fortunately, the amylases produced by *Aspergillus* species are the most significant and industrially important enzymes from an array of extracellular enzymes [190]. The two most industrially important filamentous fungi are *Aspergillus oryzae* and *Aspergillus niger*. Together they produce most of the fungal enzymes that are used comprehensively in the industry [139]. *A. oryzae* serves as a promising host for the expression of heterologous proteins due to its ability to extracellularly secrete a large amount of industrial enzymes such as amylases [194], while *A. niger* has drawn attention due to its tolerance to grow and produce amylases in acidic (pH <3) conditions, which prevents bacterial contamination [195]. This group of fungi is the most suitable candidate for solid-state fermentation (SSF) due to their morphological makeup, which allows them to easily colonize and penetrate into the solid substrate [196]. Further, the fungal α-amylases have been granted GRAS (Generally Recognized As Safe) status, which makes them the most preferred over the amylases isolated from other microbial sources [29]. Reports also suggest the existence of thermophilic fungi such as *Thermomyces lanuginosus*, which are excellent producers of thermostable amylases [197, 198].

2.2. Types of α-amylases

A variety of bacteria, fungi, and yeasts produce extracellular amylases that can degrade starch in different physiochemical conditions. With the advent of modern biotechnology, the last few decades have seen an upsurge in polysaccharide hydrolyzing enzymes with novel properties that are suitable for various industrial applications [9]. As a result, the enzyme-based starch saccharification process has totally replaced the chemical method [9]. α-Amylase, which is the main hydrolytic enzyme, is broadly classified into acidic, neutral, or alkaline based on its optimal pH activity [9, 29]. The optimal pH for α-amylases activity ranges from 2.0 to 12.0,

however, most of the α-amylases show optimal activity around neutral pH [5, 9, 29]. Each α-amylase (acidic, neutral, and alkaline) is suited for different industrial applications, such as acidic and neutral amylases in starch saccharification and food industries, while alkaline amylase is the prerequisite for detergent industries [9, 29]. Apart from these classifications, α-amylases are also grouped into thermostable, halotolerant or raw starch digesting enzymes (RSDE). Therefore, there is a persistent demand for α-amylases with desired characteristics for diverse applications, which always encourages the researcher to look forward for improving the industrial process in terms of economics and feasibility [9, 199].

2.2.1. Alkaline amylase

Alkaliphiles are those microorganisms which exhibit growth and thrive well in extreme alkaline pH (pH ≥ 9.0) environments [200]. These extremophiles produce large numbers of industrially useful alkaliphilic enzymes, and the major consumer for these enzymes is the detergent industry, which represents approximately 40% of total worldwide enzyme consumption [114, 200]. Alkaliphilic bacteria alone do not produce all of these enzymes but they share the major portion of alkaliphilic enzymes [200]. Alkaline enzymes from alkaliphilic bacteria are selected due to their long-term stability in detergent components and additives such as bleach activators, softeners, and perfumes [201]. Alkaline amylases are in great demand as an additive in dishwashing and laundry detergent to remove starchy food residues from dishes and food stains from fabrics [202, 203]. Further, enzymes to be included in automatic dishwashing detergents are required to be fully thermostable at high pH, because automatic dishwasher operates at high pH and above 60°C [202]. Though many of the alkaline amylases have been isolated and characterized since their first isolation from *Bacillus* strain A-40-2 in 1971 [204] it still remains a challenging task to obtain completely stable alkaline amylase suitable for the detergent industry [201, 202]. Since then numerous alkaline amylases have been isolated and characterized for suitable applications in the detergent industry as shown in Table 2.1 but only a little success has been achieved so far. Nevertheless, there is ample scope for exploration. In Table 2.1, it can be seen that alkaline amylase production is mainly dominated by

Bacillus sp and some of the actinomycetes groups, because of their adaptability towards various harsh environments

Table 2.1: Alkaline amylase producing Bacterial strains of commercial value

Organism	Optimum pH	Optimum Temp. (°C)	References
Bacillus sp ANT-6	10 5	80 0	[83]
Bacillus sp NRRL B 3881	9 2	50 0	[200]
Bacillus subtilis	6 5	50 0	[29]
Bacillus sp L1711	9 5-10 0	45 0	[205]
Bacillus sp KSM-1378	8 0-8 5	55 0	[206]
Bacillus sp WN11	8 0-8 5	75 0-80 0	[207]
Bacillus sp GM8901	11 0-12 0	60 0	[208]
Bacillus KSM-K38	8 0-9 5	55 0-60 0	[209]
Bacillus sp 1S 23	9 0	70 0	[210]
Bacillus sp A-40-2	10 5	55 0	[211]
Bacillus sp 17 1	4 5-10 0	-	[211]
Bacillus sp 38-2	8 0-9 0	-	[211]
Bacillus sp PN5	10 0	90 0	[157]
Bacillus US147	9 0	70 0	[122]
Bacillus sp AAH-31	8 5	70 0	[202]
Halobacterium salinarum MMD047	9 0	40 0	[212]
Streptomyces gulbargensis	8 5-11 0	45 0	[213]

2.2.2. Acidic amylase

Acid-stable extracellular enzymes are mainly exploited for the degradation of polymeric carbon sources such as starch, glycogen, amylose, amylopectin etc , which naturally occurs at acidic pH ranging from 3 2 to 4 5 [214] Since the enzyme produced by microbes are growth associated [29], therefore the acid-stable amylases are produced mainly by microorganisms which grow at lower pH values Commercial demands for acid-stable α-amylases are largely fulfilled by *Bacillus* sp and *Aspergillus* sp , which grow at pH $\leq$ 6 0 [29] The most promising acid-stable amylases are from thermoacidophiles, which produce enzymes that are active at low pH and high temperature, and thus these enzymes can be applied in starch, textile, and fruit juice industries [9, 120] Further, the demand for this class of

enzyme from extreme thermoacidophiles may increase in near future, as they may prove beneficial for harsh industrial conditions [9, 120].

Presently the starch processing industries are employing α-amylases which are active at 95°C and pH 6.8 and they are stabilized by addition of Ca^{2+}, however, the natural pH of various native starches are much below (3.2 to 4.5) [9, 215]. Thus, to carry out liquefaction of starch, the pH of starch slurry needs to be raised from its native pH to 5.8-6.2 so that the enzyme can act optimally. In addition, Ca^{2+} ions also need to be added to enhance the activity and/or stability of this enzyme [9]. Further, the next step of starch processing (i.e. saccharification) also needs another round of pH adjustment from 5.8-6.2 to 4.2-4.5 [142, 217]. Therefore, there is a great demand for acidic amylase, which are active around the native pH of starch, so that the repeated process of pH adjustment can be avoided which is time consuming and escalates the cost of product formation [142, 216]. Exotic extremophiles are naturally gifted with the enzymes that are suitable for various industrial applications, thus extremophiles harboring novel enzymes are in great demand in the field of white biotechnology [9]. However, *Bacillus* or *Aspergillus* species and a few thermoacidophiles listed in Table 2.2 mostly fulfill the present industrial demands for acidic α-amylases.

Table 2.2: Acid-stable amylase producing microbes

Organism	Optimum pH	Optimum Temp. (°C)	References
Bacteria			
Alicyclobacillus sp A4	4 2	75 0	[120]
A acidocaldarius	3 0	75 0	[217]
Bacillus acidocaldarius	3 5	70 0	[218]
B caldolyticus	5 5	70 0	[219]
B circulans GRS 313	4 9	48 0	[220]
B licheniformis NH1	4 0-9 0	90 0	[221]
B stearothermophilus	4 6-5 1	55 0-70 0	[222]
B stearothermophilus US 100	5 6	80 0	[223]
Bacillus sp	4 5	70 0	[183]
Bacillus sp KR8104	4 0-6 0	75 0-80 0	[224]
Bacillus sp WN 11	5 5	75 0-80 0	[207]
Bacillus sp YX1	5 0	40 0-50 0	[225]
Bacillus sp US 100	5 6	82	[226]
Bacillus subtilis KCC 103	5 0-7 0	65 0-70 0	[227]
Geobacillus sp LH8	5 0-7 0	80 0	[228]
Lactobacillus manihotivorans	5 5	55 0	[229]
Pyrococcus furiosus	5 6	115 0	[230]
Fungi			
Aspergillus awamori ATCC 22342	4 8-5 0	50	[231]
A chevalieri NSPRI	5 5	40 0	[232]
A flavus LINK	6 0	55 0	[116]
A foetidus ATCC 10254	5 0	45 0	[233]
A fumigatus	6 0	50 0	[234]
A hennebergi	5 5	50 0	[235]
A niger	5 0	60 0	[236]
A oryzae M13	4 0	50 0	[237]
A orvzae	4 8	35 0-37 0	[238]
A usamii	3 0-5 5	60-70 0	[239]
Fusarium vasinfectum	4 4-5 0	45 0-50 0	[240]
Paecilomyces sp	4 0	45 0	[241]
Thermomyces lanuginosus	5 6	65 0	[242]
Trichoderma viride	5 5	60 0	[243]

Yeast			
Lipomyces kononenkoae CBS 5608	4.5-7.0	70 0	[244]
Cryptococcus flavus	5 5	50 0	[245]
Cryptococcus sp. S-2	6.0	37.0	[117]

2.2.3. Halo-tolerant amylase

Microbial biota is not limited to some specific environments; rather, it can be found in diverse environments, which include extreme salinity, pH, temperature, and pressure [246]. Notions that extremophiles can survive under non-standard condition in harsh environment led to the assumption that their enzymes may be adapted to extreme environments as well, which may prove suitable for some biotechnological application [246]. Various enzymes isolated from such extremophiles support this assumption. One such supporting example is halo-tolerant amylase isolated from halophiles, a group of microorganisms that can grow optimally under hypersaline environments by maintaining their osmatic balance [246] Halophiles are categorized into slight halophiles [3% (w/v) salt], moderate halophiles [3-15% (w/v) salt] and extreme halophiles [25% (w/v) salt] based on their salt tolerance level [247]. The majority of microorganisms inhabiting this environment comprise bacteria and archaea [248].

In the last few years, considerable interest has been drawn to explore these halophilic microorganisms or their enzymes for their potential biotechnological application in different fields [249]. Besides being intrinsically stable and active at high salt concentrations, halotolerant enzymes are also active at high temperature, over a broad range of pH and in organic solvents [250-252]. These properties make the halotolerant enzymes attractive for biotechnological applications, such as food processing, environmental bioremediation and biosynthetic processes where high salt concentration would inhibit the enzymatic conversion process [251, 253, 254]. Halotolerant α-amylases also show optimal activity in various salt concentrations (Table 2.3), which makes them potential candidates for industrial processes that commonly use high salt concentration [250]. Further, organic solvent tolerant halophilic amylases can also find application in bio-remediation of carbohydrate-

polluted salt marshes and industrial wastewaters contaminated with organic solvents [255]

Table 2.3: Some halo-tolerant amylases isolated from the different microbes

Organism	Salt-tolerance	Optimum pH	Optimum Temp. (°C)	References
Bacteria				
Bacillus sp TSCVKK	10% NaCl	7 5	55 0	[256]
Bacillus dipsosauri	1 0 M KCl	6 5	60 0	[192]
Chromohalobacter sp TVSP 101	0-20% NaCl	9 0	65 0	[188]
Halomonas meridian	10% NaCl	7 0	37 0	[199]
Halobacterium halobium	0 05% NaCl	6 4-6 6	55 0	[257]
Micrococcus halobius	0 25M NaCl	6 0-7 0	50 0-55 0	[258]
Nesterenkonia sp strain F	0 0–4 0M NaCl	7 5	45 0	[259]
Thalassobacillus sp LY18	10% NaCl	9 0	70 0	[260]
Archae				
Haloarcula hispanica	4 0-5 0M NaCl	6 5	50 0	[190]
Haloarcula sp strain S-1	4 3M NaCl	7 0	50 0	[261]
Haloferax mediterranei	3 0M NaCl	7 0-8 0	50 0-60 0	[262]
Natronococcus sp strain Ah-36	2 5M NaCl	8 7	55 0	[263]

2.2.4. Thermostable amylase

Most of the industrial processes are carried out at higher temperature and thus the enzyme used in these industries needs to be thermostable for its successful application [138, 139] Thermostable enzymes are mainly isolated from thermophilic organisms and they have found a wide range of industrial applications because of their inherent stability at higher temperature [138, 139, 264] These thermophiles are mostly isolated from the different exotic ecological zones of the earth The most successful application of thermostable enzyme is amylases in starch processing industries [138, 265], where enzymatic liquefaction and saccharification of starch are performed at high temperatures (100–110°C) to produce valuable products like glucose, crystalline dextrose, dextrose syrup, maltose and

maltodextrins from starch polymers [179, 184]. Applications of thermostable amylase are also desirable in starch processing industries due to various advantages, such as reduction in cooling costs, a better solubility of substrate, a lower viscosity which allows proper mixing and pumping of substrate, and less risk in microbial contamination where processes are run for longer periods [179, 266].

Thermostable α-amylases have been largely isolated from diversified sources of microorganisms that grow optimally above 45-122°C [267]. Although a thermostable amylase could be obtained from a variety of sources, it is a challenging task to obtain commercially acceptable yield. Thus, most of the thermostable amylases, isolated from thermophilic bacteria or archaea, are cloned and expressed in mesophilic host system for commercial production [266, 268]. To meet the industrial demands, *Bacillus* is the most widely used genus for the production of thermostable α-amylases (Table 2.4). Species of *Bacillus* such as *B. subtilis, B. stearothermophilus, B. licheniformis,* and *B. amyloliquefaciens* are considered as good sources for thermostable α-amylase production at commercial levels [152]. Archaeal α-amylases, on the other hand, have to compete with the *Bacillus* α-amylases that already have excellent thermophilic properties. Table 2.4 shows a list of some thermostable microbial α-amylases, which have been isolated and characterized.

Table 2.4 Some of the thermostable α-amylases produced by various microbes

Organisms	Optimum Temperature (°C)	Optimum pH	Ca^{2+} requirements[1]	References
Bacteria				
Alicyclobacillus sp A4	75	4 2	-	[120]
A acidocaldarius	75	3	-	[269]
Bacillus sp	70	4 5	+	[183]
B flavothermus	60	5 5-6 0	-	[270]
B lentus	70	6 1	+	[271]
B licheniformis NH1	90	4 0-9 0	-	[221]
B licheniformis	85-90	6 5-7 0	+	[272]
B stearothermophilus	55-70	4 6-5 1	+	[221]
B subtilis 65	60	6	+	[127]
Chloroflexus aurantiacus	71	7 5	+	[273]
Dictyoglomus thermophilum	90	5 5	NI	[274]
Geobacillus sp LH8	80	5 0-7 0	+	[228]
G thermoleovorans	100	8	-	[275]
Halothermothrix orenii	60	7	+	[276]
Lactobacillus amylovorus	60-65	5 5-6 0	NI	[277]
L plantarum	65	5 5	-	[128]
Rhodothermus marinus	85	6 5-7 0	NI	[184]
Thermotoga maritima	85-90	7	+	[278]
Thermus filiformis	95	5 5-6 0	+	[279]
Fungi				
Lipomyces kononenkoae	70	4 5-5 0	NI	[244]
Scytalidium thermophilum	60	6	-	[280]
Archaea				
Desulfurococcus mucosus	100	5 5	NI	[268]

[1] NI = No Information, + = positive effect, - = No effect

Pyrococcus furiosus	100	6.5-7.5	NI	[281]
P. furiosus	115	5.6	+	[230]
P. woesei	100	5.5	-	[282]
Pyrodyctium abyssi	100	5	NI	[98]
Thermococcus celer	90	5.5	NI	[268]
T. profundus DT5432	80	5.5	NI	[268]
T. aggregans	100	5.5	NI	[283]
T. fumicolans	95	4.0-6.3	NI	[284]
T. hydrothermalis	85	4.8-7.8	NI	[284]
T. profundus	80	5.5-6.0	+	[285]
T. lanuginosus	60	5.6	NI	[286]

Almost invariably all the thermostable α-amylases used in starch saccharification require Ca^{2+} for activity and/or stability. This added Ca^{2+} ion must be removed from the product stream before further processing by using ion exchangers [275, 287]. Otherwise, this may form a calcium oxalate that may block process pipes and heat exchangers [138]. Besides, its accumulation is also not desirable in some products like beer etc. However, its precipitation can be controlled by decrease in calcium ion requirement of enzymes and lowering pH of the production process. Nevertheless, researchers look forward to finding a better alternative for this, which led to the discovery of thermostable α-amylases that do not require Ca^{2+} ions for their activity or stability [209, 287, 289]. Since then only a few of them have been isolated and characterized and, thus, it opens a new avenue for the researcher to explore the thermostable α-amylases which are Ca^{2+} independent (Table 2.4).

2.2.5. Raw starch digesting amylase

Conventional conversion of starch macromolecules into useful products such as glucose requires an energy-intensive three-step process i.e., gelatinization liquefaction and saccharification of starch [16, 287, 290]. Each energy-intensive step escalates the production cost of starch-based products [16, 291]. Thus, to reduce the energy consumption during these processes for cost effective utilization of natural resources is the most desirable objective in starch processing industries.

In addition, the viscosity problem faced by the starch processing industries can be solved if the starch hydrolysis can be obtained below the gelatinization temperature of starch [16, 292]. This has engrossed the researcher globally to discover raw starch digesting/degrading enzymes (RSDE) which can act directly on raw starch granules below the gelatinization temperature and hydrolyze the raw starch in a single step [16, 290]. Therefore, RSDE can significantly reduce the energy consumption, which ultimately reduces the cost of the final products. It has been estimated that the use of RSDE in ethanol production can save up to 10–20% of total energy used during the process [290, 293].

Moreover, it is difficult to hydrolyze raw starch granules completely by a single enzyme and thus a synergy of multi-RSDE must be applied to hydrolyze raw starch completely [290]. Raw starch digesting α-amylase (RSDA) is a type of endoamylase, and thus it randomly hydrolyzes the α-1, 4 glycosidic linkages inside the starch macromolecules and destroys its structure quickly [290]. Earlier it was reported that most of the RSDA enzymes show strong correlation between the hydrolysis of raw starch and the adsorption to raw starch but now it has been found that it is not an obligatory requirement [294]. Since RSDA cannot completely hydrolyze starch macromolecules, therefore, it needs to be treated with glucoamylase for complete hydrolysis of raw starch. Further, it has been observed that when raw starch is heated to ~60°C, then RSDE can efficiently hydrolyze the macromolecules [16, 295, 296].

The RSDA producing microorganisms are widely distributed in nature, among which fungi, yeasts, and bacteria are the major producers of RSDA enzymes [290]. It has been reported that microbes, which grow well on rotting starchy material, soil, and air, are the most common producers of RSDA [290, 291]. Among them the potent producers of RSDA are fungi and yeast such as *Aspergillus* sp., *Rhizopus* sp., and *Cryptococcus* sp., and few of them from bacterial and actinomycetes strains belonging to *Bacillus* sp., *Cytophaga* sp., *Geobacillus* sp., and *Streptomyces* sp. have also been reported [16, 121, 225, 290, 297]. The recent trends for producing bioethanol from a range of starchy material due to global fossil

fuel crisis, made the RSDA enzymes even more demanding and thus RSDA capable of digesting various raw starch efficiently from different botanical origin are very attractive [120, 298]. The Table 2.5 shows various raw starch digesting enzymes, isolated and characterized from various microorganism and with their optimum pH and temperature.

Table 2.5: Raw starch digesting α-amylase producing microbes

Organisms	Raw starch digesting capabilities	Optimum pH/ Temperature	Reference
Fungi			
Aspergillus awamori KT-11	Corn	4.8/37 0	[299]
Aspergillus ficum	Corn	2.0/-	[300]
Cryptococcus sp. S-2	Wheat/corn/rice/ Sweet-potato	6.0/37.0	[301]
Thermomyces lanuginosus F1	NI	5.0/60.0	[302]
Bacteria			
Anoxybacillus contaminans	Wheat	4.5/60.0	[141]
Bacillus amyloliquefaciens	Rice/corn/wheat/potato/ Sweet potato	6.0/55.0	[88]
Bacillus amyloliquefaciens	Potato; corn; wheat; rice	5.0-/50.0	[303]
B. licheniformis ATCC 9945a	Triticale/wheat/potato/ Horseradish/corn	6.5/90 0	[298]
Bacillus sp. B1018	NI	5.8/55.0	[304]
Bacillus sp. MKCS6.2	Cassava/Corn	6.5/37.0	[305]
Bacillus sp. I-3	Potato	7.0/70.0	[16]
Bacillus sp. IMD 434	Rice/corn	6.0/65.0	[121]
Bacillus sp. IMD 435	Corn/rice	6.0/65.0	[306]
Bacillus sp. TS-23	Wheat/corn/rice/potato	9 0/70.0	[307]
Bacillus sp. WN11	Potato/corn	5.5/75.0-80.0	[207]
Bacillus sp. YX-1	Corn/wheat/potato	5.0/40.0-50 0	[225]
B. stearothermophilus	Corn/wheat/potato/ Sweet-potato	NI/70.0	[308]
B. subtilis 65	Corn/wheat/sweet-potato	6.0/60.0	[127]
B. subtilis JS-2004	NI	8.0/70.0	[179]
B. subtilis IFO 3108	Corn/waxy/wheat/potato	6.0/65.0	[294]

Clostridium butyricum T-7	Corn/wheat/potato/ Sweet-potato	5 0/37 0	[309]
Cytophaga sp	NI	4 0-6 0/50 0	[310]
Geobacillus thermodenitrificans HRO10	Potato/sorghum Cocoyam/cassava	5 5/75 0-80 0	[311]
Nesterenkonia, sp strain F	Wheat/corn	7 5/45 0	[259]
Streptomyces sp no 4	Cassava	5 5/50 0	[312]

2.3. *Microbial Identification of amylase producing bacteria*

The accurate and definitive identification of microorganisms based on phenotypic, genotypic, and biological characteristics is one of the cornerstones to differentiate it from other pathogenic or non-pathogenic microorganisms for the study in the field of microbiology and infectious diseases [313] Further, the microbes used for commercial enzyme production should be precisely identified so that the downstream product obtained from these microbes does not pose any threat to humankind or environment [314] The traditional method of microbial classification based on morphological, physiological, and biochemical data gives us a blurred taxonomic status and thus requires further clarification [315] Moreover, any single identification method cannot give the exact picture of bacterial identity, therefore, nowadays a polyphasic approach is considered for the identification of the bacteria

The polyphasic approach of bacterial identification may consist of various methods, which may include complete 16S rRNA gene sequencing, analyses of molecular markers, and signature pattern(s), biochemical assays, physiological and morphological tests [315] However, the choice of methods for microbial identification solely depends on its necessity, such as, in clinical laboratories phenotypic analysis can tell whether it is infectious/toxic while for food microbiology complete identification is mandatory [313] Further, strengths and weaknesses of each identification method should also be kept in mind while selecting a method, so that a conclusive and definite identification can be done [314] The methods commonly used in identification and substantiation of

taxonomic classification of amylase producing microorganisms are summarized below in details.

2.3.1. Phenotypic analysis

The phenotypic characterization of any strain is the first step towards its identification. The first and foremost step for bacterial identification is that it should start with a pure culture. Initial identification of a bacterium is usually carried out by studying its morphological, biochemical and metabolic properties by testing its growth requirements and enzymatic activities [316]. The biochemical tests usually comprise of growing bacteria in a specific growth media, nutrients, chemicals, or growth conditions to produce an observable or measurable biochemical response, thereby enabling its identification based on numerical method. These responses may be from utilization of different carbon and nitrogen sources, growth requirements (such as anaerobic/aerobic, range of optimum pH/temperature), products generated by fermentation/enzymes/ antimicrobial activity, as well as sensitivity to metabolic inhibitors and antibiotics [316].

One of the major disadvantages of phenotypic method is the conditional gene expression where same organism may show different phenotypes in different environment and thus it is not reliable and reproducible [315, 317]. Thus, phenotypic data should be compared with the known/related bacteria so that it is acceptable with a high level of confidence and can be distinguished from phylogenetically close relatives that potentially pose safety concerns. Phenotypic results should be considered as the preliminary identification process and thus, accurate identity can only be established by supporting data from other methods.

2.3.2. Molecular approach for bacterial identifications

In the last few years, the molecular approach has proven a useful tool for microbial identification [316]. With the rapid development of molecular methods, it has given the robustness, promptness, and accuracy of the molecular method to rapidly detect, identify, classify, and establish its taxonomic position among the closely related genera and species [318]. Bacterial identification using molecular

methods is mainly dependent on the comparison of nucleotide sequences (DNA, RNA) or protein profiles of bacteria with the documented reports of known organisms [318]. Molecular methods of bacterial identification are considered very sensitive as it can detect even low concentrations of viable or non-viable bacteria in both pure and complex samples.

The most widely used molecular approach for bacterial identification is based on the analysis of 16S rRNA gene [319, 320]. 16S rRNA gene is also considered as the phylogenetic marker or 'evolutionary chronometer' for the bacterial identification because it has an alternating conserved sequence region, which is usually preferred to characterize bacteria at genus or species level [316, 318]. However, sequence analysis of 16S rRNA gene alone may not discriminate closely related species because of the highly conserved nature of this region [14, 321]. Therefore, other genetic targets can be used instead of rRNA genes to accurately identify its phylogenetic position even discriminating closely related species [318]. Internally transcribed sequences of 16S-23S rDNA, and other housekeeping genes such as *groEL* [322], *rpoB* [323], *recA* [324], *gyrB* [325] and hsp 60 heat shock protein [326] may be used to differentiate among bacterial genus or species. The conserved nucleotide sequences in housekeeping genes are very low which makes them difficult in designing PCR primers, but if successfully designed then they have the capability to successfully discriminate even closely related species [318]. Table 2.6 shows the various methods utilized by various researchers for the bacterial identification of α-amylase-producing bacteria.

Table 2.6: Various methods used for identification of α-amylase-producing bacteria

Organism	Identification Method	Reference
Bacillus sp AAH-31	16S rDNA	[202]
Bacillus sp WPD616	16S rDNA	[327]
Bacillus sp GRE1	Biochemical (API 50CHB)II	[328]
Bacillus sp Ferdowsicous	Phenotypic, 16S rDNA	[183]
Bacillus acidicola	16S rDNA	[142]
Bacillus cohnii US147	Phenotypic, 16S rDNA	[122]
Bacillus clausii BT-21	16S rDNA	[329]
Bacillus subtilis US116	API 50 CHB, 16S rDNA, 16S–23S ISR	[330]
Geobacillus thermoleovorans NP54	16S rDNA	[275]
Halobacterium salinarum MMD047	Phenotypic, 16S rDNA	[212]
Pseudomonas stutzeri strain 7193	Phenotypic, 16S rDNA	[331]

2.4. Media components optimization

To meet the industrial demands, it is necessary to improve the product yield of a system without increasing the actual cost of production [332] Further, in the development of any fermentation process, media optimization is the prime objective for improving the productivity of microbial metabolite by manipulating the nutritional and physical parameters due to its impact on economy and feasibility of the process [195, 332, 333] However, the classical 'single variable at a time' method of media optimization of these parameters is quite laborious and time consuming This method is also unbefitting for a large number of variables as it is unable to determine the true optimum value resulted from interaction of variables [332-334] Several statistically factorial designs are available to identify optimum level of responses through factorial design and use of Response Surface Methodology (RSM) [297, 333, 335]

When numbers of parameters (media components) to be screened and optimized are larger in numbers then experiments based on multi-factorial design will be difficult to analyze [336] Hence, optimization of fermentation media is carried out in two-steps initially, large numbers of variables are screened using

Pareto's law to understand the significance of their effect on the product formation, and then significant variables are selected for further optimizations [336, 337].

The Plackett–Burman statistical method is a two-level design to screen n numbers of variables in n+1 experimental run for maximum response [336, 338]. This experimental design is available in multiples of four runs and requires less numbers of experimental runs, which ultimately save time, chemicals, glassware, and work force. Therefore, it proves to be an excellent screening method [336, 339]. Further, Plackett–Burman factorial design (PBD) is useful for screening of the main factors from a large number of process variables that can be fixed or eliminated in further optimization process [336].

RSM is a collection of statistical methods for designing experiments, constructing models, evaluating the effect of factors, and obtaining optimum conditions for desirable responses [335]. It combines fractional factorial design and a second-degree polynomial model to investigate complex processes, and thus, an efficient statistical technique for optimization of multiple variables with less experiments [340]. Several reports on the process optimization for amylase production using different models and designs are shown below (Table 6). Many researchers have reported the application of PBD for initial screening of factors influencing amylase production followed by interaction study using RSM.

Table 2.7: Various statistical methods applied for the optimization of amylase productions

Microorganisms	Optimization method	Reference
Aspergillus oryzae CBS 819.72	PBD; Box–Behnken design	[333]
Aspergillus niger ATCC 16404	PBD	[195]
Bacillus sp. RKY3	PBD; RSM	[337]
Bacillus acidicola	RSM	[341]
Bacillus amyloliquefaciens	PBD; RSM	[303]
Bacillus brevis MTCC 7521	RSM	[342]
Bacillus subtilis 168	PBD; RSM	[343]
Bacillus subtilis KCC103	RSM	[11]
Brevibacterium linens DSM 20158	PBD; RSM	[332]
Geobacillus thermoleovorans	RSM	[289]
Streptomyces erumpens MTCC 7317	RSM	[344]
Thermomyces lanuginosus	RSM	[345]

2.5. Purifications strategies and biochemical characterization of amylases from different organisms

Bacterial and fungal α-amylases that are produced extracellularly into the culture media are studied extensively, for the ease of production, manipulation, and optimization of production media [29]. Different strategies have been employed for purification of extracellular amylases isolated from these microorganisms for exploiting specific characteristics of these enzymes. Commercial use of amylases, normally, does not require the enzyme to be in purified form, but their application in the pharmaceutical and clinical sectors and in understanding structure-function relationships, demand high purity of the enzymes [29]. Laboratory scale purification for α-amylase includes combination of various chromatography techniques. The modern strategies used for the purification of amylases at laboratory scale are listed in Table 1.5 (Chapter 1). However, the often used purification techniques include selective concentration of cell free supernatant (crude enzyme) by precipitation using ammonium sulphate or chilled organic

solvents followed by affinity, ion exchange and/or gel filtration chromatography [29]. Different combinations of chromatography techniques yield different degrees of purified enzymes and the highest yield (78%) was achieved in case of α-amylase purified from *Cryptococcus* sp. S-2 (Table 1.5) [117]. The emerging technology made the cumbersome purification techniques into a fast, efficient, and economical process involving fewer steps [26].

The physicochemical properties of purified α-amylases from several microorganisms have been studied extensively and some of them are presented in Table 2.8. The pH optima for microbial α-amylases may vary from 2.0 to 12.0 [29, 346]. However, most of the α-amylases from bacteria and fungi have pH optima in the acidic to neutral range [5]. The lowest acidic pH optima of 3.0 was observed for the α-amylase obtained from *Alicyclobacillus acidocaldarius* [269], while extremely alkalophilic α-amylase with pH optima of 11-12 has been reported from *Bacillus* sp. GM8901 [347]. Most of the α-amylases reported are generally stable over a wide range of pH from 4.0 to 11.0 [29].

The working temperature for most of the microbial α-amylases is growth associated [346] and it was found to be the lowest (25-30 °C) in case of *F. oxysporum* amylase [348] and highest (115°C) in case of archaebacteria, *Pyrococcus furiosus* [230]. Thermo-stabilities of α-amylase isolated from *Bacillus licheniformis* CUMC 305 was reported to be as high as 4 h at 100 °C [123]. Thermostability of microbial α-amylases is affected by the presence of various factors such as calcium ion, substrate, and other stabilizers [346]. Starch has also shown the thermo-stabilization effect on α-amylase activity isolated from *B. licheniformis* CUMC 305 [123] and *Bacillus* sp. WN 11 [207] while stabilizing effect of calcium ion has been reported from many species as shown in Table 2.4.

The molecular weights of microbial α-amylases ranges from ~10 to 210 kDa. α-Amylase with the lowest weight (10 kDa) has been reported from *Bacillus caldolyticus* [349] and the one with the highest weight (210 kDa) from *Chloroflexus aurantiacus* [350]. However, most of the microbial α-amylases are usually around 50-60 kDa as calculated from cloned α-amylase genes and their deduced amino

acid sequences [346]. Glycosylation of bacterial amylases are very rare, however, few of them are from *L. kononenkoae* [244] and *B. stearothermophilus* [351].

Heavy metal ions, sulfhydryl group reagents, N-bromosuccinimide (NBS), p-hydroxy mercuribenzoic acid, iodoacetate, EDTA and EGTA are well known for inhibiting microbial α-amylases activity [9, 121]. Mercuric ions also known to inhibit several α-amylases [183], suggesting the presence of a carboxyl group in the enzyme molecules [220]. Additionally, mercuric ions is also known to oxidize indole rings and interacts with the aromatic rings present in tryptophan residues [9, 352]. Inhibition of amylase activity in the presence of NBS demonstrates the catalytic role of tryptophan residues in the enzyme molecules [9, 353], while inhibition in presence of dithiothreitol and β-mercaptoethanol suggests the role of –SH groups in the catalytic site of these enzymes [9]. There are also reports, which suggest that DTT has stimulated and inhibited the activities of α-amylases [28]. The kinetic behavior of the purified microbial amylases shows that it has varied degrees of affinity towards natural substrate as K_m value ranges from 0.05 mg/ml to 11.66 mg/ml for starch molecules (Table 2.8).

Table 2.8: Some of the α-amylases purified and characterized from different organisms in recent years (2000 A.D. onwards)

Organisms	Molecular wt. (kDa)	Opt. pH	Opt. Temp.	Inhibitors	Stabilizer	Additional properties	References
Fungi							
Aspergillus awamori KT-11	70	4.8	37	-	-	raw starch digesting enzymes	[299]
Cryptococcus flavus	75	5.5	50	Cu^{2+}, Fe^{2+}, Hg^{2+}	-	Km (0.056 mg/ml)	[245]
Scytalidium thermophilum	36	6	60	$HgCl_2$, $CuCl_2$	Starch	Ca^{2+} independent enzyme	[280]
Bacteria							
Alicyclobacillus sp. A4	64	4.2	75	Cr^{3+},Cu^{2+},Fe^{3+},Pb^{2+}, Hg^{2+},Ag^{+}, SDS		Ca^{2+} independent, digest raw starch	[120]
Bacillus licheniformis ATCC 9945a	31	6.5	90	EDTA, Hg^{2+}	Ca^{2+}	raw starch digesting enzymes	[298]
B. amyloliquefaciens	58	5.0-8.0	50.0-60.0	EDTA, SDS, Urea, K^{+}, Mn^{2+}	Ca^{2+} and Cu^{2+}	Km(3.076 mg), Vmax (4.11 mg/min) for starch	[303]
B. amyloliquefaciens	52	6	55	Hg^{2+}, Fe^{3+}, Zn^{2+}, Ag^{+}	Mg^{2+}, Ba^{2+}, Ca^{2+}, Cu^{2+}	Km(1.92 mg/ml), Vmax (351 U/ml)	[88]
B. dipsosauri	80	6.5	60	Zn^{2+}, Cd^{2+}	Na_2SO_4		[192]
B. circulans GRS 313	48	4.9	48	Hg^{2+}, Mn^{2+}, Fe^{3+},Cu^{2+}	Co^{2+} , Mg^{2+}	K_m (11.66 mg/ml), V_{max} (68.97 U)	[220]
B. licheniformis NH1	58	4.0-9.0	90	Hg^{2+}, Zn^{2+}, EDTA, Sodium perborate	-	No effect of Ca^{2+} ions	[221]
B. stearothermophilus US 100	59	5.6	80		Ca^{2+}	maltopentaose; maltohexaose as end product	[223]
B. sp. Ferdowsicous	53	4.5	70	Hg^{2+}	-	Ca^{2+}-independent	[183]
Bacillus sp. KR8104	59	3.5	75.0-80.0	-	-	Ca^{2+}-independent	[224]
Bacillus sp. YX1	56	5.0	40.0-50.0	-	-	raw starch digesting enzymes	[225]
Bacillus subtilis DM-03	42.8	9.0	55.0	PMSF, 4-BPB, EDTA, Ni^{2+}, Mn^{2+}	-	Km (1.2 mg/ml), glucose as major product	[354]
B. subtilis KCC 103	53	5.0-7.0	65.0-70.0	Hg^{2+},Ag^{2+}, p-hydroxymercurybenzoate	-	Km (2.6 mg/ml), Vmax (909 U/mg)	[227]
B. subtilis	48	6.5	50	Hg^{2+}, Fe^{3+}, Al^{3+}	Mn^{2+}, Co^{2+}	Km (3.845 mg/ml) Vmax (585.1mg)	[29]
Bacillus sp. ANT-6	94.5	10.5	80	Zn^{2+}, Na^{+}, Na-sulphide, EDTA,	Ca^{2+}	NI	[82]
Bacillus sp. L1711	51	9.5-10.0	45	Ca^{2+},Zn^{2+},Mg^{2+},Mn^{2+},Ba^{2+}, Cu^{2+}	Na^{+},Co^{2+}	Km (1.9 mg/ml), sp. activity (18.5 U/mg)	[205]

Bacillus KSM-K38	55	8 0-9 5	55 0-60 0	-	-	maltose as major end products	[209]
Bacillus sp PN5	-	10	90	sodium hypochlorite	-	(partially purified)	[157]
Bacillus US147	30	9	70	SDS, $NaBO_3$, H_2O_2, $ZnCl_2$, EDTA	-	Km (0 7 mg/ml), Vmax (2 2 U/ml)	[122]
Bacillus sp AAH-31	91	8 5	70	SDS	-		[202]
Chromohalobacter sp TVSP 101	72/62	9	65	-	-	Km(125 and 166 mM), Vmax (5 88 and 5 0 U/mg)	[188]
Geobacillus thermoleovorans	26	8	100	Sn^{2+}, Hg^{2+}, and Pb^{2+}, EDTA, PMSF, N-ethylmaleimide, DTT	Co^{2+}, Fe^{2+}	Km(1 11mg/ml), Vmax (500 µmol/mg/min) for starch	[275]
G thermodenitrificans HRO10	58	5 5	75 0-80 0	EGTA, EDTA, IAA, pCMB	Ca^{2+}	K_m (3 05 mg/ml), V_{max} (7 35 U/ml)	[311]
Geobacillus sp. LH8	52	5 0-7 0	80	Mg^{2+}, Ba^{2+}, Ni^{2+}, Zn^{2+}, Fe^{3+}, Cu^{2+}, EDTA		Km (3 mg/ml), Vmax (6 5 micromol/min)	[228]
Halomonas meridiana	49	7	37	-	10% NaCl	Maltose, maltotriose as end products	[191]
Lactobacillus manihotivorans	135	5 5	55	-	-	Km (3 4 mg/ml), Vmax (32 55 kJ/mol)	[229]
Nesterenkonia sp strain F	57	7 5	45	EDTA	Ca^{2+}	active at high salt concentrations (0–4 M)	[259]
Streptomyces gulbargensis	55	8 5-11 0	45	Co^{2+}, Ba^{2+}, Ag^{+}, Hg^{2+}	Ca^{2+}	Km (5 0 mg/ml), sp activity (1,341 3 U/mg)	[213]
Thalassobacillus sp LY18	31	9	70	EDTA, DEPC, β-mercaptoethanol	Ca^{2+}	organic solvent-tolerant	[260]
Archaea							
Haloarcula hispanica	50	6 5	50	EDTA	Ca^{2+}	active at high salt concentrations (4– 5M)	[190]
Haloarcula sp strain S-1	70	7	50	Rb^{+}, Fe^{2+}, Fe^{3+},Cu^{2+}, Co^{2+}, Zn^{2+}, Ni^{2+}, Al^{2+}, EDTA	-	Organic solvent tolerance of halophilic α-amylase	[261]
Haloferax mediterranei	58	7 0-8 0	50 0-60 0	-	-	active at high salt concentrations (2– 4M)	[262]
Halobacterium salinarum MMD047	56	9	40	Ca^{2+}, Cd^{2+}, Ni^{2+}, Hg^{2+}, Co^{2+}, Zn^{2+}, EDTA	Mn^{2+}		[212]
Pyrococcus furiosus	44(subunit)	5 6	115	-	-	Ca^{2+}-independent	[230]
Thermococcus profundus DT5432	42	5 5	80	IAA, N -bromosuccinic acid, SDS, guanidine-HCl	Ca^{2+}	Km (0 23%)	[268]

Chapter III

MATERIAL & METHODS

Chapter 3: Material & Methods

3.1. Materials

3.1.1. Consumables

The consumable materials like sterilized polystyrene tubes (15 ml and 50 ml), microfuge tubes (1.5 ml and 2.0 ml), PCR tubes, micropipettes tips (1.0 ml, 200 µl and 10 µl), and petri-dishes were purchased from Tarson, India; 100, 250, 500, and 1000 ml Erlenmeyer flask and test tubes were purchased from Borosil, Mumbai, India. Autoclavable polythene bags and paraffin roll were procured from Himedia lab, India.

3.1.2. Chemicals & media

Following solvents such as methanol, 2-propanol, n-hexane, ethanol, acetonitrile, and chemical such as Tween-20, Tween-80,Triton-X-100, glycine, sodium dodecyl sulphate (SDS), coomassie brilliant blue, starch, EDTA, acrylamide, bis-acrylamide, Folin-Ciocalteu's, and dinitrosalicylic acid (DNS) were procured either from Merck (India) or Himedia (India). For buffer preparation following salts such as Tris-HCl, sodium hydroxide, sodium carbonate, potassium dihydrogen phosphate, di-sodium hydrogen phosphate, and di-potassium hydrogen phosphate were obtained either from Merck (India) or Himedia (India). The various media components and metal ions used in the present study such as D-glucose, sucrose, maltose, cellulose, ammonium sulphate, ammonium nitrate, potassium nitrate, ammonium chloride, ferric/ferrous chloride, magnesium chloride, mercuric chloride, copper chloride, zinc sulphate, manganese chloride, calcium chloride, cadmium chloride, cobalt chloride, nickel chloride, sodium nitrate, sodium chloride, etc. were purchased either from Merck (India) or from Himedia (India).

DEAE Sephadex A-50 matrix, Sephacryl S-200 matrix, CM-Cellulose matrix, 3-(aminopropyl) triethoxy silane, carbodimide/cyanimide, ethidium bromide, phenylmethylsulfonyl fluoride (PMSF), iodo acetic acid (IAA), 4-

bromophenacyl bromide (4-BPB), dithiothreitol (DTT) were purchased from Sigma-Aldrich, USA. Nutrient agar, nutrient broth, starch agar, Luria broth, yeast extract, beef extract, microbiological grade agar, agarose, peptone, trypton, antibiotics (ampicillin and kanamycin), and HiIMVIC Biochemical test kits were purchased from Himedia, India. HiPrep 16/60 Sephacryl S-200 HR and HiPrep Phenyl FF 16/10 pre-packed columns, used for the purification of proteins, were procured from GE Healthcare Bio-Sciences Corporation (USA).

3.1.3. Microbial cultures and vectors

Escherichia coli DH5α and *E. coli* BL21a pLys cells were used for cloning and transformation, respectively. They were obtained from Novagen suppliers (Merck Millipore, India). pET series [28a (+) and pET32a (+)] vectors (Novagen, Darmstadt, Germany) for the expression studies were kindly donated by Dr. Robin Doley of Tezpur University.

3.1.4. Molecular biology reagents

The kits for genomic DNA isolation, PCR purification, gel extraction, plasmid Miniprep, TA Cloning kit, CloneJET PCR cloning kit, restriction enzymes, PCR master-mix, nuclease-free water and TransformAid™ Bacterial Transformation kit were obtained from Fermentas (USA). All other molecular biological grade chemicals were procured either from Merck (USA) or from Hi-media (India).

3.2. Methods

3.2.1. Isolation and screening of α-amylase producing bacterial isolates

Soil samples were collected from different locations of Assam, Northeast India. Topsoil from various locations was collected in a sterile container using sterile spatula and then kept under sterile condition at room temperature until used. Screening for the amylase-producing bacteria was done by serial dilution method. Concisely, 1.0 g of soil sample was mixed with 9.0 ml of 0.9% (w/v) sterile saline and serially diluted up to 10^{-6}. Then a 100 µl aliquot of each dilution was plated on

starch nutrient agar plates and incubated for 24-48 h at 45°C under static condition in an inverted position.

After the period of incubation, the plates were flooded with Logul's solution (Himedia, India) and a clear area (starch hydrolysis) surrounding the bacterial growth showed positive reaction for extracellular α-amylase secretion while absence of clear zone around bacterial colonies was considered as a non-secretion of α-amylase enzyme. The α-amylase-producing bacteria were counted on a Cubek colony counter and the zone of hydrolysis (in mm) around the colonies was measured. Colonies showing halo formation were selected and further streaked on nutrient starch agar plates so as to obtain pure colonies for bacterial identification and characterization.

Pure colonies were further screened for the isolation of acidic and alkaline amylase producing bacteria. Therefore, pure colonies of such bacteria were allowed to grow at different pH (6.0-12.0) for different time intervals (24–120 h) at 45°c in 100 ml Nutrient broth supplemented with 1.0 %, (w/v) starch, placed in a 250 ml Erlenmeyer flask with constant shaking (200 rev/min) on a rotary shaker. At a regular time interval, 5.0 ml aliquots were withdrawn aseptically and were centrifuged at 5000 rpm for 10 min at 4°C. Subsequently, cell pellets were taken for the determination of cell mass and culture supernatant was used for determination of α-amylase activity (Section 3.2.3) and protein concentration (Section 3.2.6).

3.2.2. Identification of the isolated strains

The taxonomic identifications of selected α-amylase producing bacterial strains were determined by following the polyphasic approach. Bacterial strains were initially identified by morphological and biochemical tests and finally by molecular biological approach.

3.2.2.1. Morphological and biochemical characterization of bacterial strains

Morphological characterization of the bacterial strains was done by simple staining, negative staining, Gram staining and spore staining methods. These were performed by streaking pure bacterial colonies on agar plates for 24 h at 45°C followed by spreading of a loop-full of bacterial colonies over a clean glass slide, air-drying for 5-10 min, and subsequently heat fixing. This was followed by differential staining procedure as described by Bergey's Manual of Systematic Bacteriology [355]. After the staining procedure, slides were then dried by gently tapping with tissue paper and the bacteria were observed under oil-immersion objective lens (1000 X) of a light microscope (Leica ATC 2000, Leica Microsystem).

Biochemical characterization of the bacterial isolates was performed using Rapid Biochemical Identification Test Kits (KBM001 & KB001) (Himedia Lab, India), following the instructions of the manufacturer. These kits consist of sterile media for Indole, Methyl red, Voges Proskauer's, Citrate Utilization, H_2S production test and fermentation test towards eight different carbohydrates (glucose, adonitol, lactose, arabinose, sorbitol, mannitol, rhamnose and sucrose). The bacterial isolates were then inoculated in each testplates well of the above kits aseptically either by using sterile loopful of bacteria directly from culture plates or by inoculating 50 µl of bacterial liquid culture. The bacterial inoculum for the broth culture was prepared by inoculating 5 ml of sterile nutrient broth media with a single colony of bacteria from master culture plates, followed by incubating them at 45°C for 8-12 h until inoculum turbidity is $\geq$ 1.0 at 600 nm.

3.2.2.2. Molecular characterization of bacterial isolates

The molecular taxonomic position of the bacterial isolates were determined by PCR amplification of 16S rDNA, 16S-23S inter spacer region and housekeeping (*gyrA*, and *rpoB*) genes, and then analyzing them with the reported sequence present in public database such as NCBI.

3.2.2.2.1. Chromosomal DNA isolation and purification

Chromosomal DNA of bacterial isolates was isolated and purified either by using alkaline lysis method [356] or by Genomic DNA extraction kit (Fermentas). Genomic DNA extraction by alkaline lysis method was done as described by Ausubel et al. [356]. The cell pellet was obtained from 5 ml of overnight culture by centrifugation at 10,000 rpm for 10 min at 4°C (Beckman Coulter, Inc., USA). The cell pellet was then re-suspended in a 0.8 ml of solution-I (Appendix I) and to this mixture 160 µl of lysozyme (10 mg/ml) was added and incubated at room temperature (24°C) for 20 min. Subsequently, 44.5 µl of 10% (w/v) SDS solution was added to the reaction mixture, which was then re-incubated for 10 min at 50°C. Thereafter, 53.3 µl of RNase A (10 mg/ml) was added and incubated at 37°C for 90 min. This was followed by addition of 45.3 µl of Na-EDTA (0.1 M, pH 8.0) and re-incubation at 50°C for 10 min. To in-activate the nuclease as well as to digest the proteins of the reaction mixture, 26.6 µl of proteinase K (5.0 mg/ml stock) was added and the mixture was incubated at 50°C for 16 h. Then, an equal volume of saturated phenol (saturated with 0.1 M Tris-HCl, pH 8.0) was added to the reaction mixture and it was mixed thoroughly.

The mixture was then centrifuged at 10,000 rpm for 10 min and the upper (aqueous) phase was aspirated into a sterile microfuge tube. Then 700 µl of (1:1) phenol and chloroform-isoamylalcohol (24:1) was added to the reaction mixture. After centrifugation at 10,000 rpm for 10 min, the upper phase was transferred into a sterile microfuge tube, and then an equal volume of chloroform-isoamylalcohol (24:1) was added and the mixture spun for another 10 min at 10,000 rpm. The upper phase was then transferred to a sterile microfuge tube and $1/10^{th}$ volume of 3 M Na-acetate, pH 7.0 solution was added. Subsequently, DNA was precipitated by adding two volumes of ice-cold absolute ethanol, and DNA was recovered by centrifugation. After removal of alcohol, DNA was re-suspended in 10 mM Tris HCl-1 mM EDTA buffer (pH 8.0) at a final concentration of 1 µg/ml and was stored at 4°C until it was further used.

Bacterial genomic DNA isolation using GeneJET genomic DNA purification kit (Fermentas, USA) was performed by harvesting 5 ml of overnight culture in a microfuge tube by centrifugation for 10 min at 5,000 rpm. This was followed by suspension of pellets in 180 µl of lysis buffer and further incubation for 30 min at 37°C. Later, 200 µl of Lysis solution and 20 µl of proteinase K were added and mixed uniformly. The reaction mixture was then incubated at 50°C for 30 min and after the period of incubation it was cooled and 20 µl of RNase A solution was added by vortexing. The mixture was then incubated for 10 min at room temperature and 400 µl of 50% ethanol was added and mixed by vortexing. The clear lysates were then transformed into a GeneJET™ Genomic DNA purification column, which was in turn inserted into a collection tube. The column was then centrifuged for 1 min at 6,000 rpm and the flow-through was discarded. Subsequently, the column was placed into a new 2 ml collection tube to which 500 µl of wash buffer-I (Ferments, USA) was added and after centrifugation at 8000 rpm for 1 min, the flow-through was discarded. Subsequently, 500 µl of wash buffer-II was added to the purification column and it was centrifuged at 12,000 rpm for 3 min. The flow-through so obtained was discarded and column was placed into sterile 1.5 ml microfuge tube. To elute the genomic DNA from the purification column, 200 µl of elution buffer was added to the center of the column and after incubation for 2 min at room temperature, the DNA was collected in a fresh microfuge tube by centrifugation at 10,000 rpm for 1 min. The purity of the preparation was then determined by taking optical density of the eluted DNA at 260 and 280 nm.

3.2.2.2.2. PCR primers designing for 16S rDNA, 16S-23S ISR and various housekeeping genes

For amplification of 16S rRNA gene of the bacterial strain, universal primers designed by Weisburg et al. [357] (shown in Table 3.1) were used. For 16S-23S rDNA intergenic spacer region (ISR) amplification, the complementary nucleotide sequence base position of 11128-11149 of 16S and base position 11988-12009 of 23S rRNA genes, (*B. subtilis*) were used as primer sequence (Table 3.1). For the specificity of ISR amplification, a second set of primers (nested PCR) was

designed to amplify specifically intergenic spacer region using the first set of PCR-product as template. The nested primers (Table 3.1) were designed to anneal at the position of 11334-11355 of the 16S rRNA and 11770-11790 of 23s rRNA genes.

To amplify the housekeeping genes viz. *gyrA* and *rpoB*, primers were designed based on the GyrA and RpoB coding sequences of *B. subtilis* 168 (GenBank Accession No: CP002468). The *gyrA* primers extended from position 7237 to position 7260 (Table 3.1) and from position 8261 to position 8238 (Table 3.1), yielding a 1,024-bp PCR segment. The *rpoB* primers extended from position 1102 to position 1125 (Table 3.1) and from position 1910 to position 1887 (Table 3.1), yielding an 808-bp PCR segment.

Table 3.1: Primers used for amplification of various genes for systematic identification of bacteria

Primer pair	Primer sequences (5'–3')	Location	Product size (Approx.)	Reference
16S rDNA	RTF: 5'-AGAGTTTGATCCTGGCTCAG-3'	27F	1500 bp	[159]
primers	RTR. 5'-AAGGAGGTGATCCAGCCGCA-3'	1525R		
gyrA primers	GYAF: 5'-CAGTCAGGAAATGCGTACGTCCTT-3'	7237-7260	1024 bp	[159, 358]
	GYAR 5'-CAAGGTAATGCTCCAGGCATTGCT-3'	8261-8238		
rpoB primers	RPBF: 5'- AGGTCAACTAGTTCAGTATGGAC-3'	1102-1124	808 bp	[159, 358]
	RPBR: 5'- AAGAACCATAACCGGCAACTT-3'	1910-1887		
16S-23S ISR	ISRP1. 5'-AGTCTGCAACTCGACTGCGTG-3'	11128-11149	880 bp	[159]
primers	ISRP2: 5'-CAACCCCAAGAGGCAAGCCTC-3'	11988-12009		
16S-23S ISR	ISRP3: 5'-GGAAGGTGCGGCTGGATCACC-3'	11334-11355	457 bp	[159]
primers	ISRP4: 5'-CCCGAAGCATATCGGTGTTCG-3'	11770-11790		
(Nested primers)				

3.2.2.2.3. *PCR amplification and purification of the amplified genes*

DNA amplification was performed with Genamp PCR system (Applied Biosystem, USA). A typical PCR reaction mixture contains 2.5 µl of 10 X PCR buffer (Fermentas, USA), 2.0 µl of 25 mM $MgCl_2$ and 2.5 µl of 2 mM deoxynucleotide triphosphate (dNTP) mix. To this reaction mixture, each primer at a final concentration of 20 pmoles, 2.5 U of Taq DNA polymerase (Fermentas, USA) and 5 µl (~1 µg) of genomic DNA were added and final volume was adjusted to 30 µl with sterile nuclease-free water (Fermentas, USA). Standardized PCR conditions with respect to each set of primers are shown in Table 3.2. PCR amplification of targeted genes was verified by DNA gel electrophoresis. For this, 5 µl of PCR products were loaded onto a 0.8% (w/v) agarose gel prepared in 1X TAE (Tris-acetate-EDTA) buffer and made to run for 45 min at a constant current of 60 mA and 80 V.

The PCR products obtained were purified using PCR purification/Gel-extraction kits (Fermentas, USA). PCR purification was performed by mixing 1:1 volume of binding buffer with the PCR mix and then by transforming the resultant mixture into the GeneJET™ Purification column. The column was then centrifuged at 10,000-14,000 rpm for 1 min and the flow-through so obtained was discarded. Then the column was washed twice with the 700 µl of washing buffer by centrifugation at 14,000 rpm for 1 min and the flow-through was discarded. Finally, purified DNA was eluted into a fresh sterile 1.5 ml microfuge tube from the column by adding 50 µl of elution buffer at the center of the column and centrifugation for 1 min at 12,000 rpm.

Purification of the PCR product by gel extraction method was performed by excising the desired band (pre-run in agarose gel) into a clean pre-weighed microfuge tube and then mixing it with the equal volume of binding buffer (1:1 ratio). The agarose gel was dissolved by incubating the gel-mixture at 50-60°C for 10 min with mixing in between. The remaining steps were followed as described above in the direct PCR purification methods (Section 3.2.2.2.3.).

Table 3.2: Standardized PCR conditions used for the amplification of various bacterial identification genes

Primers pair	Initial denaturation	PCR cycles (30)			Final Extension	Storage
		Denaturation	Annealing	Extension		
16S rDNA	94°C for 5 min	94°C for 1 min	58°C for 30 sec	72°C for 2 min	72°C for 7 min	4°C for ∞
gyrA	94°C for 5 min	94°C for 1 min	55°C for 30 sec	72°C for 2 min	72°C for 7 min	4°C for ∞
rpoB	94°C for 5 min	94°C for 1 min	50°C for 30 sec	72°C for 2 min	72°C for 7 min	4°C for ∞
16S-23S ISR	94°C for 5 min	94°C for 1 min	54°C for 30 sec	72°C for 1.5 min	72°C for 7 min	4°C for ∞
Nested ISR	94°C for 5 min	94°C for 1 min	54°C for 30 sec	72°C for 1.5 min	72°C for 7 min	4°C for ∞

3.2.2.2.4. DNA Sequencing

DNA sequencing was performed using 3130 Genetic Analyzer (Applied Biosystem, Switzerland). Before sequencing, sequencing PCR was performed by chain termination method using Big Dye Version 3.1 kit (Applied Biosystem, Switzerland). A standard sequencing PCR mix contains 1 µl of Big Dye, 1.5 µl of Big Dye buffer, 20.0 pmoles of primer and 50-100 ng of template DNA. Final volume of the reaction mixture was adjusted to 20 µl with nuclease-free sterile water and sequencing PCR was set with initial denaturation steps for 5 min at 95°C followed by 25 cycles consisting of denaturation steps at 95°C for 30 s, annealing at 54°C for 10 s and extension steps at 60°C for 4 min. Finally, after the 25th cycle of PCR amplification, PCR products were stored at 4°C until used.

The PCR products so obtained were purified before processing for sequencing to remove the excess dyes and reactants present in the reaction mix using ethanol precipitation methods. The reaction mixture was purified by transferring the PCR product into a clean 1.5 ml microfuge tubes followed by addition of 12 µl master mix-I (10 µl of nuclease free water and 2 µl of 125 mM EDTA solution). After proper mixing of the content, a master mix-II solution [2 µl of 3 M Na-acetate buffer (pH 4.6) and 50 µl of ethanol] was added by slight vortexing and then the sample was left at room temperature for 15 min. Subsequently, the reaction mixture was centrifuged at 12,000 rpm for 20 min and supernatant was decanted. Afterwards, 250 µl of 70% ethanol was added to the reaction tube and then it was centrifuged at 12,000 rpm for 10 min and the supernatant was discarded. Thereafter to each reaction tube, 15 µl of HiDi formamide solution was added and mixed by short vortexing. Finally, the sample was transferred into the sequencing plate for denaturation steps and for electrophoresis.

3.2.2.2.5. Phylogenetic tree construction

Quality of DNA sequences was verified manually with the help of BioEdit software (www.mbio.ncsu.edu/bioedit) and homology search of each sequence was

performed using the NCBI database (http://blast.ncbi.nlm.nih.gov). The 16S rDNA, 16S-23S ISR, GyrA, and RpoB gene sequences of bacteria under study were aligned with reference sequences showing sequence homology in NCBI database, using the multiple sequence alignment programme of MEGA 4 [359]. Phylogenetic trees were constructed by distance matrix-based cluster algorithms viz. unweighted pair group method with averages (UPGMA), neighbour-joining [360], maximum-likelihood [361] and maximum-parsimony [362] analyses. All positions containing gaps and missing data were eliminated from the dataset (complete deletion option). The stability of trees obtained from these cluster analyses was assessed by using BOOTSTRAP programme in sets of 1000 resampling (MEGA 4). Each tree was rooted using *E. coli* MG1655 (NCBI accession no. U00096) as an out-group. The gene sequences determined in the present study were deposited in GenBank database under different accession number with respect to each strain (http://www.ncbi.nlm.nih.gov/Genbank).

3.2.3. Amylase assay

Amylolytic activity of amylase enzyme was assayed by measuring the reducing sugars [363] released from 1.0% (w/v) of starch dissolved in buffer (with respect to enzyme). Briefly, in a test-tube, 1 ml of 1% starch solution with 1950 µl of respective buffer and 50 µl of enzyme solution (purified/crude) were added. The mixture was then incubated at 45°C/optimum temperature of enzyme for 30 min followed by stopping the reaction by adding 1 ml of DNS reagent. After the reaction was stopped, tubes were incubated in boiling water bath for 5 min and then cooled in running tap water. Subsequently, optical density was recorded at 540 nm (Themo Scientific Multiskan Go, USA) and the amount of reducing sugar thus liberated was determined using standard curve of D-glucose. One unit of enzyme activity was defined as the liberation of reducing sugars equivalent to 1 µmol of D-glucose liberated per min under the assay condition [159, 354].

3.2.4. Dextrinizing activity

Dextrinization activity of enzyme was determined using the iodometric method as described by Fuwa [364] with little modifications [162]. The reaction mixture consisting of 400 µl of soluble starch (1% w/v) dissolved in a suitable buffer, 390 µl of respective enzyme buffer and 10 µl of the test sample was incubated at 45°C/optimum temperature of enzyme for 30 min. The reaction was then stopped by adding 100 µl of acetic acid (1 M) and 100 µl of iodine reagent (1% iodine in ethanol/potassium iodide 10%/H_2O in 1:3:1 ratio). The reaction mixture was diluted with 4 ml of dH_2O and the color intensity produced by the iodine–starch mixture was measured at 660 nm. One unit of dextrinizing activity was defined as the quantity of enzyme that hydrolyzed 1 mg of starch per min under the assayed condition.

3.2.5. Total carbohydrate estimation

The amount of total soluble sugar/carbohydrate was estimated by phenol sulphuric method [365]. In a typical reaction mixture, 1.0 ml of test sample was mixed with 1.0 ml of 5% phenol and subsequently, 5.0 ml of 96% sulphuric acid was rapidly added to the reaction mixture. Each tube was gently agitated during the addition of the acid and then the sample was allowed to stand at room temperature for 20 min. The absorbance of the characteristic yellow orange color, thus developed, was measured at 490 nm against the reagent blank. Amount of sugar present in the test samples (in mg) was calculated using a standard curve prepared by known concentration of D-glucose.

3.2.6. Protein quantification

The protein content of the cell-free supernatant and the purified enzyme was assayed by using Folin-Lowry's method [366], which measures the blue color complex formation at 660 nm. Briefly, the reaction mixture containing 50-100 µl of protein was diluted with dH_2O to make the final volume of reaction mixture up to 250 µl. Thereafter, 2.5 ml of alkaline copper sulphate solution (Appendix I) was added, mixed well and incubated at room temperature for 10 min. After incubation

periods, 250 µl of diluted Folin-C (1:2) reagent was added to the reaction mixture and after 30 min of incubation at room condition, absorbance was measured at 660 nm. From a standard curve of bovine serum albumin (BSA), the protein content of the unknown sample was determined.

3.2.7. *Prescreening of culture conditions influencing bacterial growth and α-amylase production in submerged fermentation (SmF) condition*

Pre-screening of culture components influencing α-amylase production under SmF were done by "one variable at a time" methods for *B. subtilis* strain AS01a. Any one of the following carbon sources such as glycerol, glucose, galactose, lactose, sucrose, maltose, starch, and cellulose were added (1.0%, w/v, or v/v) in the M9 culture media to check the α-amylase production and bacterial growth. The effect of various organic or inorganic nitrogen sources on α-amylase production and bacterial growth was studied by supplementing M9 media with 1% (w/v) of any of the following nutrient beef extract, yeast extract, peptone, tryptone, casein, NH_4Cl, KNO_3, NH_4NO_3, $NaNO_3$, and $(NH_4)_2SO_4$.

Effects of pH and temperature on α-amylase production and bacterial growth were also investigated under SmF, by adjusting pH of the M9 medium from 5.0-12.0 and incubating the bacterial culture at various temperature (30-60°C), respectively. The impact of agitation on α-amylase production and bacterial growth was evaluated by agitating the culture at various speeds from 100-300 rpm in an incubator shaker at the optimum pH and temperature of growth. The effect of incubation time was evaluated by post-incubation of culture for 24-120 h, under optimized conditions. At various time intervals, a suitable volume of bacterial culture was withdrawn aseptically and the bacterial growth and α-amylase production were determined by following the standard procedure described above.

3.2.8. *Process optimization for enhancing the enzyme production*

From the initial screening results, the factors which induce the α-amylase production were selected and their individual effect was identified by PBD and interaction effect by RSM.

3.2.8.1. Plackett-Burman Design for selection of significant variables

Our preliminary screening of strain AS01a using the 'one variable at a time' approach showed that it was a time intensive and tedious process. Thus, for screening of most significant factor(s) influencing α-amylase production from *B. licheniformis* strain AS08E, the 'one variable at a time' approach was abandoned and PBD screening experiments was taken up. A total of eleven factors based on review of literature and screening results of factors influencing α-amylase production from *B. subtilis* strain AS01a, were subjected to PBD experiments for identifying the most significant factors effecting the α-amylase productions from strain AS08E (Table 3.3). Based on PBD, each parameter was examined at two different levels, higher (+1) and lower level (-1). Simultaneously, a center point was also run to evaluate the linear and curvature effects of the variables [367]. The PBD experimental design is based on the following first-order polynomial model:

$$Y = \beta_0 + \sum \beta_i X_i \ldots\ldots\ldots\ldots\ldots\ldots\ldots (1)$$

Where Y is the response (total α-amylase activity in U), β_o is the model intercepts, β_i is the linear coefficient, and X_i is the level of the independent variable. PBD assumes that there are no interactions between the different factors. The α-amylase activity assay was carried out in triplicate and the averages of these experimental values were taken as response Y. From the regression analysis of the variables, the significant factors ($P < 0.05$) influencing α-amylase production were selected and they were further optimized by using RSM.

Table 3.3: Range of different independent variables used in PBD for α-amylase productions from strain AS08E

Factors (AS08E strain)	Levels		
	+	0	-
$CaCl_2$ (% w/v)	0.1	0.075	0.05
Beef extract (%)	1.5	1	0.5
Glycerol (% w/v)	1.5	1	0.5
KNO_3 (% w/v)	0.2	0.15	0.1
Maltose (% w/v)	1.5	1	0.5
NaCl (%)	0.75	0.5	0.25
NH_4Cl (% w/v)	0.2	0.15	0.1
Peptone (%)	1.5	1	0.5
pH (H^+)	12.5	12.0	11.5
Starch (%)	2	1.25	0.5
Temperature (°C)	53	45	37

3.2.8.2. Response surface methodology for interaction study

RSM was used to estimate the interaction effects of various variables on the amylase yield (responses). A central composite design (CCD) was applied to understand the effect of three significant variables: (i) C_1, (ii) C_2, and (iii) C_3 for the augmentation of α-amylase production for each strain. The independent variables, which were capable of influencing the α-amylase production (Y) for each bacterium under SmF, are shown in Table 3.4. A conventional level for each factor was set to zero as a coded level. The three factors were studied at three levels consisting of 20 experimental runs, and were adopted to analyze the experimental data. The least and extreme ranges of the variables with their values in actual are shown in Table 3.4. The response value (Y) in each trial was the average of triplicate results. The data obtained from RSM on α-amylase production were subjected to analysis of variance (ANOVA). The resultant data were fitted as a second order polynomial regression equation including single and cross effect of each variable.

$$Y = a_0 + \sum_{i=1}^{3} a_i C_i + \sum_{i=1}^{3} a_{ii} C_i^2 + \sum_{i=1}^{2} \sum_{j=i+1}^{3} a_{ij} C_i C_j \ldots\ldots\ldots\ldots\ldots\ldots\ldots (2)$$

Where, Y= predicted response (total α-amylase activity in U/ml), a_0 intercept term, a_i = linear effect, a_{ii} = square effect, a_{ij} = interaction effect, and C_i and C_j = variables. The above equation was used to optimize the values of independent parameters for the response. The following equation was used for coding the variables:

$$C_i = \frac{C_i - C_0}{\Delta C_i}, where\ i = 1,2,3,\ldots\ldots,k \ldots\ldots\ldots\ldots\ldots\ldots (3)$$

Multiple regression analysis, response surface plots, and ANOVA were performed using Minitab 15 Statistical Software® (Minitab Inc, PA, USA). The statistical implication of the model equation and the model terms were evaluated via student's t-test. The quality of fitness of the second-order polynomial model equation was expressed via the coefficient of determination (R^2) and the adjusted R^2. The integration of different optimized variables yielding utmost response was attempted to validate the model.

Table 3.4: Range of values for the response surface methodology

Independent Variables	Levels				
	-2	-1	0	1	2
***Bacillus subtilis* strain AS01a**					
Starch (%)	0.58	0.75	1	1.25	1.42
Beef extract (%)	0.13	0.2	0.3	0.4	0.47
pH(H^+)	4.3	5.0	6.0	7.0	7.7
***Bacillus licheniformis* strain AS08E**					
Starch (%)	1 16	1 5	2.0	2 5	2.84
Peptone (%)	0.08	0.25	0.5	0.75	0.92
pH(H^+)	9.2	10.5	11.5	12.5	13.8

3.2.8.3. Validation of the model

The optimized fermentation conditions for α-amylase production as found by analysis of RSM was experimentally validated by culturing the bacterial strain in a 5-liters fermenter (New Brunswick Scientific, USA). In the fermenter, 3 liters of the statistically optimized M9 media [supplemented with the best carbon and nitrogen sources at a desired concentration (% w/v)] were inoculated with mid-logarithmic culture of bacteria and operated with foam/anti-foam probe system. The pH of medium and temperature were adjusted to their optimum values for each strain. The agitation speed was 200 rpm, provided by a centrifuge propeller. The O_2 and pH electrodes were used for controlling process conditions. The cells were harvested at different time periods (24, 48, 60, 72 and 96 h post inoculation), and the cell-free clear supernatant was used to determine the α-amylase yield.

3.2.9. Isolation and Purification of α-amylases

Purification of enzyme from different bacterial strains was performed by combination of various chromatographic techniques. Unless otherwise stated, all the fractionations were carried out either at 4°C while using FPLC or at room temperature (~24°C).

3.2.9.1. Purification of a major alkaline α-amylase from Bacillus subtilis strain AS01a

Purification of an alkaline α-amylase from *Bacillus subtilis* strain AS01a was performed by ammonium sulphate precipitation of cell-free culture supernatant followed by acetone precipitation and the final purification was achieved by gel-filtration method. At each purification step, enzyme activity and protein concentrations were determined by following standard assay protocols (Section 3.2.3. and Section 3.2.6., respectively).

3.2.9.1.1. Ammonium sulphate precipitation of culture supernatant

One liter of statistically optimized media was inoculated with mid-logarithmic culture of bacterial inoculum (*B. subtilis* strain AS01a) and cells were

allowed to grow for 60 h in a 5-litre fermenter (New Brunswick Scientific, USA) at an agitation speed of 200 rpm and at 45°C. After the period of incubation, cells were harvested by centrifugation at 5000 rpm for 10 min. To the cell-free supernatant (CFS), solid $(NH_4)_2SO_4$ was added gradually to make its final concentration up to 50% (w/v) and the mixture was allowed to stir slowly for another 4 h. The precipitated proteins were then recovered by centrifugation of the resultant mixture at 8000 rpm for 15 min and then they were dissolved in a minimum volume of 20 mM K-phosphate buffer, pH 7.0. The above fraction was then dialyzed extensively against the same buffer to remove the salt and the α-amylase activity of the dialyzed fraction was examined.

3.2.9.1.2. Acetone precipitation method

The volume of the $(NH_4)_2SO_4$ fraction was raised after dialyses steps; therefore, pre-chilled acetone was added to the protein solution (after dialysis) at a final ratio of 1:1.5, v/v and the solution was kept at −20°C for 12 h. Thereafter, precipitated proteins were recovered by centrifugation of mixture at 8000 rpm for 15 min and the resulting pellet so obtained was then dissolved in 1.5 ml of 20 mM K-phosphate buffer, pH 7.0.

3.2.9.1.3. Gel-filtrations

The above protein solution was then loaded onto a Sephadex G-50 gel-filtration column (1 cm × 64 cm) pre-equilibrated with 20 mM K-phosphate buffer, pH 7.0. Elution of the proteins was carried out with the equilibration buffer at a flow rate of 24 ml/h. One-ml fractions were collected and each fraction was checked for α-amylase activity and protein content. The fraction showing highest α-amylase activity was then analyzed by SDS-PAGE (Section 3.2.10.1)

3.2.9.2. Purification of a thermostable α-amylase from B. licheniformis strain AS08E

An extracellular thermostable α-amylase was purified from *B. licheniformis* strain AS08E's cell free supernatant (CFS) by hydrophobic interaction

chromatography (HIC) followed by fractionation of the HIC-bound proteins through gel-filtration chromatography. At each purification step, enzyme activity and protein concentration were determined by following standard assay protocols (Sections 3.2.3. and 3.2.6.).

3.2.9.2.1. Hydrophobic interaction chromatography

Purification of thermostable α-amylase was initiated by cultivating *B. licheniformis* strain AS08E in a 5-liter fermenter (New Brunswick Scientific, USA) containing 1-liter of the statistically optimized media at an agitation speed of 200 rpm for 60 h at 45°C. Solid $(NH_4)_2SO_4$ was gradually added to 1-liter CFS to attain 1 M solution then the mixture was stirred slowly for an additional 30 min at 4°C to mix uniformly. This solution was then applied to the pre-equilibrated Phenyl-Sepharose column (5 mm × 20 mm) attached to an AKTA FPLC purification system (Amersham biosciences, Uppsala, Sweden). The Phenyl-Sepharose column was pre-equilibrated with 50 mM K-phosphate buffer, pH 7.4 containing 1.0 M $(NH_4)_2SO_4$. The bound proteins were first washed and then eluted with the linear gradient of 1.0–0.0 M $(NH_4)_2SO_4$ in 50 mM K-phosphate buffer (pH 7.4) at a flow rate of 2 ml/min. Two-ml fractions were collected and elution of proteins was monitored at 280 nm. The fractions showing maximum α-amylase activity were pooled, dialyzed and concentrated by using ultrafiltration unit (50-kDa cutoff membrane) (Amicon, Beverly, MA, USA).

3.2.9.2.2. Gel-filtrations chromatography

The above concentrated pooled fraction was further fractionated using FPLC-Sephacryl S-200 gel filtration column (120 ml), pre-equilibrated with 50 mM K-phosphate buffer (pH 7.4). Elution of proteins was carried out with the equilibration buffer at a flow rate of 20 ml/h. One-ml fractions were collected and elution of protein was monitored at 280 nm. Each fraction was checked for α-amylase activity and protein content. The fraction showing highest α-amylase activity was analyzed by SDS-PAGE (Section 3.2.10.1).

3.2.10. Biochemical characterization of the purified enzymes from these strains

The purified enzymes were characterized for the determination of biochemical properties using the procedures described below.

3.2.10.1. Assessment of purity and molecular weight determinations

The homogeneity as well as molecular mass of the gel filtration fraction displaying highest α-amylase activity was checked by either 10% or 12.5% SDS-PAGE of protein(s) under reducing (treated with β-mercaptoethanol) as well as non-reducing conditions [368]. Briefly, 50 µg of crude enzyme and 15 µg of each purified enzyme were loaded into separate wells of loading gels. Preparation and casting of both separating and loading gels were done as described by Laemmli [368] and compositions of both the gels are given in Appendix I.

Electrophoresis was performed at a constant current of 20 mA until the dye front (bromophenol blue) reached the bottom of the gel. After electrophoresis, proteins in the gel were fixed by incubating the gel in 20% TCA for 30 min at room temperature followed by washing the gel several times in distilled water Subsequently, proteins were developed in the gel by staining with 0.1% Coomassie Brilliant Blue R-250 in methanol: acetic acid: water (4:1:5 v/v/v) solution. Protein bands were visualized by destaining the gel with the methanol: acetic acid: water (4:1:5 v/v/v) solution and subsequently, the gel was scanned in an image analyzer (Biospectrum® 500 Imaging system, India). Mobility of the purified protein was compared with the standard protein molecular markers ranging from 10-250 kDa (Fermentas, USA) Molecular weight of the unknown protein was measured by calculating its *Rf* value.

The N-terminal amino acid sequence of purified protein (AmyBL-I) was determined by electrophoretically transferring the purified AmyBL-I band from SDS-PAGE to a polyvinylidene difluoride (PVDF) membrane. Thereafter, the band was excised and sequence was determined by the automated Edman degradation method on an ABI Procise 494 protein sequencer (Applied Biosystems). The sequence so obtained was homology searched in NCBI database and then aligned using CLC Main Workbench 5 software (http://www.clcbio com).

3.2.10.2. Amylase zymographic study

For amylase zymography study, 1% (w/v) soluble starch was incorporated into the native PAGE (without reducing agents and SDS) prior to the addition of ammonium persulphate solution in pre-casting gel mixture. After casting, the gel was run at a constant current of 15 mA for about 5 h at 4°C and then it was washed with 50 mM K-phosphate buffer, pH 7.0, containing 1% (v/v) Triton-X-100. Thereafter, it was reacted overnight with a 1% (w/v) soluble starch dissolved in K-phosphate buffer, pH 7.0, containing 0.5% (v/v) Triton-X-100 and 0.6% NaN_3 at 45°C [159, 369]. The gel was then stained with iodine solution until clear band appeared.

3.2.10.3. Dose-dependent α-amylase activity

To determine the effect of enzyme concentration on starch hydrolysis activity, different amounts of enzyme (0.5 to 10.0 μg) were added to the one ml of 1% starch (w/v) solution and the final volume was adjusted to 2 ml. The starch hydrolytic activity was assayed by following the method as described in Section 3.2.3.

3.2.10.4. Determination of optimum time of incubation

To check the kinetics of enzyme-catalyzed reaction, an optimum concentration of α-amylase enzyme was incubated with 1% starch (w/v) solution reaction mixture for different time interval of 5, 10, 15, 30, and 60 min. After each interval of incubation, enzyme reaction was stopped by adding DNS solution (dinitrosalicylic acid) and α-amylase activity was assayed as described in Section 3.2.3.

3.2.10.5. Determination of optimum pH

To determine the optimum pH of the enzyme-catalyzed reaction, 10 μg of purified enzyme was incubated with different pH buffers (5.0, 6.0, 7.0, 8.0, 9.0, 10.0, 11.0, 12.0, and 13.0) and amylase activity in each buffer was determined. The following buffers (50 mM) were used for the optimum pH determination: Na-

citrate buffer (pH 4.0-5.0), K-phosphate buffer (pH 6.0-7.0), Tris-HCl (pH 8.0-9.0), and glycine-NaOH (pH 10.0-13.0). To study the stability of the purified enzyme as a function of pH, a fixed amount of purified enzyme was mixed with 2.0 ml of the above buffer and resultant mixture was incubated at 37°C for desired periods. Thereafter, amylase activity at each pH was determined as described in Section 3.2.3. The activity of enzyme at optimum pH is considered as 100% and other values were compared with that.

3.2.10.6. Determination of optimum temperature

To determine the optimum temperature for enzyme activity, 5-10 µg of purified enzyme was added to 1 ml of 1% starch (dissolved in 50 mM buffer at optimum pH) solution and the mixture was then incubated at different temperatures ranging from 40 to 100°C for optimum time of each enzyme. For each assay, a control was also run in parallel. After the desired period of incubation, enzyme reactions were terminated by adding DNS and subsequently amylase activity was measured by the method described in Section 3.2.3.

3.2.10.7. Thermostability determination

For determining the thermostability of catalytic activity, α-amylases were incubated at different temperatures ranging from 50 to 100 °C for 30 min either in the presence or in absence of 5 mM Ca^{2+} ions in appropriate buffer. Subsequently, the test samples were withdrawn after the incubation period and 1 ml of 1% (w/v) starch solution was added to each test samples and residual α-amylase activity was estimated against the control (100% activity) following the standard α-amylase activity assayed procedure as described in Section 3.2.3.

3.2.10.8. Kinetics study

The K_m and V_{max} values of the amylase enzymes were calculated by Lineweaver–Burk plot using 0.1-2% (w/v) soluble starch as a substrate [370]. The plots were drawn by plotting the reciprocal of substrate concentration (1/[S]) on x-axis vs. reciprocal of enzyme velocities (1/v) on y-axis. The turnover number (K_{cat})

of the enzyme was determined by dividing the value of V_{max} with the quantity of enzyme (E) used for driving the reaction [K_{cat} = (V_{max})/ (E)]. All the experiments were performed in triplicates and their mean values were used for plotting.

3.2.10.9. Effects of various Metal ions

To investigate the effects of different divalent metal ions on the α-amylase activity, the purified enzyme was pre-incubated with different divalent cations (5 mM) for 30 min at room temperature. The metal ions tested were Ni^{2+}, Co^{2+}, Mg^{2+}, Mo^{2+}, Fe^{2+}, Hg^{2+}, Cu^{2+}, Zn^{2+}, Mn^{2+}, Ca^{2+}, and Cd^{2+}. Subsequently, starch hydrolytic activity was determined under the optimized assay condition, following the enzyme assay protocol described in Section 3.2.3. The enzyme activity in absence of metal ions served as positive control (100% activity) and the percentage of α-amylase activity of the test samples (in presence of metal ions) was calculated against this value.

3.2.10.10. Effects of various inhibitors, oxidizing agents and surfactants

Chemical modulators, viz. 4-bromophenacyl bromide (4-BPB), iodoacetamide (IAA) and phenyl methyl sulfonyl fluoride (PMSF), were used to modify histidine, cysteine, and serine residues of purified enzyme respectively to investigate their role in the enzyme catalysis process. To carry out this, 10 μg of purified enzyme was incubated with the above effector molecules (2-5 mM final concentration) in an assay buffer for 30 min at room temperature. Thereafter, the residual amylase activity of each test sample (in presence of effector molecules) was estimated by following the standard amylase activity assayed protocol as described in Section 3.2.3. The amylase activity without any of above effectors molecules was considered as 100% activity (control) and other values were compared with that [354].

To investigate the effects of various surfactants (1% of SDS, Tween-20, Tween-80, and Trition–X 100), chelating (2 mM EDTA), denaturing (2-5 M urea), oxidizing (1% H_2O_2) and bleaching (2 mM sodium perborate) agents on α-amylase activity, 10 μg of purified enzyme was pre-incubated with these chemicals for 30

min at room temperature followed by assay of residual α-amylase activity (Section 3.2.3.). The α-amylase activity without any of the abovementioned reagents was considered as 100% activity (control) and other values were compared with that.

3.2.10.11. End-product determination by TLC

The end-products of starch hydrolysis were analyzed and identified by thin-layer chromatography (TLC) with a pre-coated silica gel plate (Merck 60 HPTLC plate, Darmstadt, Germany). The reaction was initiated by incubating 100 units of α-amylase with 2% (w/v) starch dissolved in 50 mM K-phosphate buffer (pH 7.0) at optimum temperature. After specific periods of incubation, 50 µl aliquots (starch-hydrolyzed products) were withdrawn from each reaction and analyzed by silica gel TLC as described by Kusuda et al. [371]. Briefly, the reaction products were loaded on TLC plates and were developed with a chloroform/acetic acid/water (5:7:1) solvent system. After developing the plates, spots were visualized by spraying the plate with 20% sulfuric acid/ethanol reagent, drying and baking in an oven at 180°C for 3 min. Standard solutions such as glucose and maltose were run side-by-side.

For quantitative analysis of the product formations, each spot from unstained plates corresponding to the developed region of the chromatogram (in another plate) was scraped into separate tubes and dissolved in minimum volume of water. The liberated sugar from each spot was then quantified using phenol-sulphuric method as described in Section 3.2.5.

3.2.11. Cloning of α-amylase gene from the bacteria under study

Considering the economic relevance and ever growing industrial demands for α-amylase enzymes in the market, the molecular cloning of the amylase genes from the isolated bacteria was initiated for the hyper-production and future enzyme engineering of the cloned enzymes. Alpha-amylase gene from the isolated strains were first cloned into a cloning vector (TA/pJET) for complete determination of its sequence and then it was expressed into *E coli* using the pET expression system.

Strategies used for the cloning of amylase gene from the strains AS01a and AS08E are illustrated below (Figure 3.1).

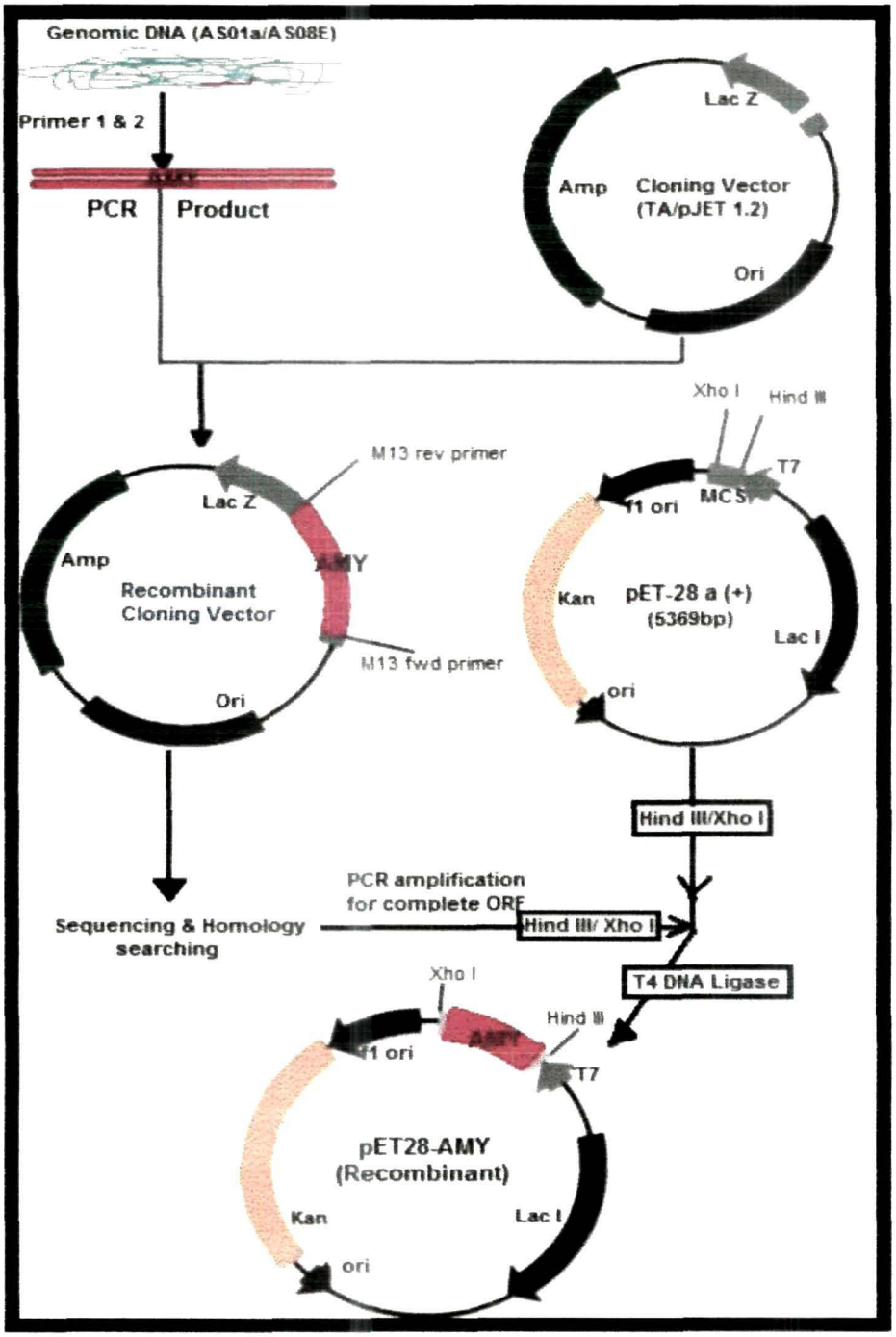

Figure 3.1: Schematic representation of cloning experiment for α-amylase genes in *E. coli*.

3.2.11.1. Isolation of α-amylase gene and cloning into TA/pJET cloning vector

3.2.11.1.1. Isolation of α-amylase encoding gene

Genes encoding α-amylase from *B. subtilis* strain AS01a and *B. licheniformis* strain AS08E were PCR amplified by designing species-specific primers based on α-amylase gene sequences from *B. subtilis* BF7658 (Genbank accession No. FJ463162) and *B. licheniformis* DSM13 (Genbank accession No. AE017333), respectively. Genomic DNA from *B. subtilis* strain AS01a and *B. licheniformis* strain AS08E cells were isolated and purified using Fermentas genomic DNA extraction kit as described in Section 3.2.2.2.1.

3.2.11.1.2. PCR amplification and purification of the amplified gene

PCR amplification of α-amylase genes from *B. subtilis* strain AS01a and *B. licheniformis* strain AS08E was done by using genomic DNA isolated (Section 3.2.11.1.1.) from these strains and PCR primers BSF1 & BSR2 and BLF1 & BLR2, respectively (Table 3.5).

Table 3.5: Primers used in cloning α-amylase gene from AS01a & AS08E.

Primer pair	Primer sequences (5'–3')*	Product size
B. subtilis strain AS01a	**BSF1:** 5'-CCC**AAGCTT**TTGCGCTTACAGCACCGTCGATCAA-3'	~1500 bp
	BSR2: 5'-CGC**GGATCC**TTGAAAGAATGTGTTACACCT-3'	
	BSF3: 5'-CCC**AAGCTT**CTATGTTTGCAAAACGATTCAA-3'	~1980 bp
	BSR4: 5'-CCG**CTCGAG**CTCAATGGGGAAGAGAACC-3'	
B. licheniformis strain AS08E	**BLF1:** 5'-CCC**AAGCTT**CTGCAAATCTTAAAGGGACGCTG-3'	~1480 bp
	BLR2: 5-CCG**CTCGAG**CCTATCTTTGAACATAAATTGAAAC-3'	
	BLF3: 5'-CCC**AAGCTT**CTATGAAACAACAAAAACGG-3'	~1560 bp
	BLR4: 5'-CCG**CTCGAG**CCTATCTTTGAACATAAATTG-3'	

*Green = *Hind* III, Yellow = *Xho* I and Blue = *Bam* H I restriction sites

PCR mixture was prepared as described in Section 3.2.2.2.3. For the PCR amplification, the following conditions were applied: initial denaturation for 5 min

at 95°C followed by 30 cycles consisting of 1 min denaturation at 95°C, 30 s of annealing at 59°C (for AS01a)/60°C (for AS08E) and elongation steps for 2 min at 72°C. After 30 cycles of amplification, a final extension for 7 min at 72°C was performed to fill up sticky ends, if there were any. Finally, the PCR products were stored at 4°C until further use. PCR products so obtained were gel purified using the procedure described in Section 3.2.2.3.3.

3.2.11.1.3. Ligation of PCR product into cloning vector

Ligation of PCR product into a cloning vector (TA/pJET1.2) was initiated by setting up a reaction mixture containing the following components in a microfuge tube kept on ice: 10 µl of ligase buffer (10X), 1 µl of gel purified PCR product (50-100 ng), 1 µl of cloning vector (50 ng/µl), 1 µl of T4 DNA Ligase (5 units/µl) with the final volume adjusted up to 20 µl with the nuclease-free sterile water. The reaction mixture was then vortexed for a short period, centrifuged for 10 s, and subsequently incubated at 16°C for overnight. However, in the case of pJET1.2 cloning vector, before the addition of ligase and vector to the reaction mixture, insert-blunting steps were performed by adding 1 µl of blunting enzyme following the instruction of the manufacturer.

3.2.11.1.4. Competent cell preparations

DH5α/BL21a competent cells were prepared by calcium chloride method. In brief, a single bacterial colony was inoculated into 5 ml of SOB (Super optimal broth) media (Appendix I) and the cells were allowed to grow for overnight at 37°C with shaking at 250 rpm. On the subsequent day, 100 ml of SOB medium was inoculated with the 1 ml of saturated overnight culture and the culture was allowed to grow at the above conditions until OD reached 0.4 at 600 nm (usually 2-3 h). Thereafter, the cells were chilled on ice for 10 min and suspensions were spun down at 5,000 rpm for 5 min at 4°C. After centrifugation steps, cell pellets were re-suspended in half the original volume of ice-cold 100 mM $MgCl_2$ and the sample was incubated on ice for another 15 min. After the incubation step, cell suspensions were spun down at 5,000 rpm for 5 min at 4°C and pellets were collected. Pellets

were re-dissolved in half the original volume of ice-cold 100 mM $CaCl_2$ solution. This was followed by re-incubation of cell suspension on ice bath for another 15 min. Cell pellets were harvested by centrifugation at 5,000 rpm for 5 min at 4°C. The pellets so obtained were re-suspended in 1 ml of ice-cold solution of 100 mM $CaCl_2$ containing 20% glycerol and subsequently, aliquots of 100 µl were aliquoted into pre-chilled microfuge tubes and stored at -70°C until further use.

3.2.11.1.5. Transformation of competent cells by heat shock method

For transformation experiments, competent cell aliquots were taken out from -70°C freezer and allowed to thaw on ice for 10 min. Then the cells were suspended evenly by mixing. 2 µl of ligation product was then added to the cells and they were mixed gently. After incubation of the reaction tube on ice for 30 min, the cells were heat-shocked for 90 s at 42°C in a water bath, followed by placement on ice for another 2 min. This was followed by addition of 600 µl of LB media to each tube and then the tubes were incubated at 37°C for 1 h. After the incubation period, about 350 µl of transformed cells were plated on the pre-made LB-agar (LBA) plates containing kanamycin (30 µg/ml) / ampicillin (100 µg/ml) antibiotics depending upon vector used. Cells were spread evenly on the plates, and then incubated in upside down position for 12-16 h at 37°C in a static incubator.

3.2.11.1.6. Blue white selection of recombinant clones

For screening of recombinant clones on transformation plates, a blue/white selection procedure was followed. Before plating of transformed cells to a LBA plates, 40 µl X-gal (5-bromo-4-chloro-3-indolyl-b-D-galactopyranoside) stock solution (20 mg/ml) and 40 µl IPTG (isopropyl-b-D-thiogalactopyranoside) stock solution (100 mM) were spread evenly on the surface of the plate. The plates were then left to dry for few minutes under a laminar hood and then the transformed cells were plated on this X-gal, IPTG, and antibiotics-containing LBA plates.

3.2.11.1.7. Plasmid isolation and sequencing of recombinant vector

To investigate successful ligation of the PCR product, recombinant plasmids need to be isolated from the recombinant clones (white colonies from blue-white selection). Therefore, recombinant plasmids were isolated by following alkaline lysis method as described by the miniprep plasmid isolation kit (Fermentas, USA). Briefly, 5 ml of overnight culture cells harboring plasmids were grown in appropriate antibiotics [kanamycin (30 µg/ml) /ampicillin (100 µg/ml)] and were harvested by centrifugation at 8,000 rpm for 5 min. Cell pellets were then re-suspended by vortexing into 250 µl of RNase-containing suspension buffer (P1). This was followed by mixing of cell suspension in 250 µl lysis buffer (P2) by inverting tubes 4-6 times. Then the reaction mixture was neutralized by the addition and mixing of 350 µl of neutralization buffer (P3) by inverting tubes 4-6 times. This was followed by centrifugation at 13,000 rpm for 10 min and subsequent transfer of supernatant into spin column and further centrifugation at same speed for 30 s. After centrifugation, the flow-through was discarded and the column was washed twice with the 0.75 ml of washing buffer (Fermentas, USA) by centrifuging at 13,000 rpm for 30 s. To remove any residual wash buffer, the spin column was centrifuged again at 13,000 rpm for 30 s. After the washing steps, DNA was eluted from the column in a clean microfuge tube (1.5 ml) by adding 50 µl of elution buffer (Fermentas, USA) to the center of the column. After incubating the spin column for 1 min it was eventually centrifuged at 13,000 rpm for 1 min.

Sequencing of recombinant plasmid was accomplished to ascertain successful ligation of PCR product by chain termination method using plasmid-specific primers (described in Section 3.2.2.2.4). Sequences so obtained were then blast searched using NCBI database for checking the completeness of the coding sequence. However, after sequence analysis it was found that both ligated PCR products (AS01a & AS08E amylase gene) did not cover the complete coding sequence (Open Reading Frame). Thus, a new set of primers (BSF3 & BSR4 for *B. subtilis* strain AS01a and BLF3 & BLR4 for *B. licheniformis* strain AS08E) was

designed for each strain to cover the complete ORF before cloning it into an expression vectors (Table 3.5).

3.2.11.2. Re-cloning of α-amylase gene into expression vector (pET28a)

In order to target the recombinant α-amylase outside the cell membrane into the *E. coli* culture media (extracellular secretion), primers were designed to cover the complete ORF, including the signal peptide (BSF3 & BSR4 for strain AS01a and BLF3 & BLR4 for strain AS08E). A restriction site was also introduced into each primer (Table 3.5) for the production of overhang products as it helps in direct cloning of PCR products into expression vector The complete coding sequence of the α-amylase genes from *B. subtilis* strain AS01a and *B. licheniformis* strain AS08E were PCR-amplified by using genomic DNA (isolated from above strains) and PCR primers BSF3 & BSR4 and BLF3 & BLR4, respectively (Table 3.5).

The PCR mixture was prepared as described in Section 3.2.2.2.3., and the PCR was performed as described in Section 3.2.11.1.2., with slight modification in annealing steps. Annealing for the BSF3 & BSR4 set of primers (strain AS01a) was carried out at 62°C for 30 s, while for BLF3 & BLR4 set of primers (strain AS08E), it was carried out at 58°C for 30 s. The PCR products so obtained after PCR amplification were gel purified by following the procedure described in Section 3.2.2.2.3.

Restriction digestion of PCR products and the expression vector (pET-28a) were carried out under similar conditions and with the same set of restriction enzymes (*Xho* I and *Hind* III). The restriction digestion experiment was set into a clean microfuge tube on ice, which contained 2 µl of 10X restriction buffer (R) (Fermentas, USA), 1.5 µl of each restriction enzyme (10 units), 2-5 µl of DNA [PCR products (~100 ng) /pET28a (~50 ng)] and the final volume of reaction mix was adjusted up to 20 µl with nuclease-free water. After mixing all components gently, they were spin down for a few seconds and subsequently incubated at 37°C for 1-16 h in water bath. After completion of digestion, restriction enzymes were

inactivated by incubating at 80°C for 20 min and the digested products were then gel purified as described in Section 3.2.2.2.3.

After digestion, restricted PCR fragment and pET-28a vector were ligated together (see Section 3.2.11.1.3.) and transformed into competent *E. coli* BL21a cells as described in Section 3.2.11.1.5. On successful transformation, recombinant clones were checked for the desired insert by restriction analysis of recombinant plasmids (isolated from recombinant clones) using the same set of restriction enzymes used for cloning.

3.2.11.3. Sequencing and primary structure determination

The recombinant plasmids were isolated from the *E. coli* cells [see Section 3.2.11.1.7.) and were sequenced (see Section 3.2.2.2.4.) by automated DNA sequencing units (3130 Genetic Analyzer, Applied Biosystem, Switzerland). The nucleotide sequences so obtained after sequencing as well as their deduced amino acid sequence were homology searched using NCBI-BLAST programme of NCBI database (http://www.ncbi.nlm.nih.gov). Further, with the help of primary structure analysis tools available at http://www.expasy.org, the amino acid sequences were analyzed and their primary structures were determined. The signal peptides were predicted using the neutral networks (NN) and Hidden Markov Models (HMM) competent on Gram-positive bacteria (SignalP 4–0 server, Technical University of Denmark) [372]. The multiple amino acid sequence alignment was accomplished using CLUSTAL W2 program [373] of EMBL–EBI online software (http://www.ebi.ac.uk) and the resulting alignment was illustrated through NCBI-conserved domain program (http://www.ncbi.nlm.nih.gov).

3.2.11.4. Expression and purification of the cloned amylase gene in E. coli

3.2.11.4.1. Induction and over expression of recombinant proteins

To induce and examine the expression of extracellular α-amylase secretion by the recombinant clones on solid media, individual clones were streaked cultured on LB agar plates supplemented with 0.5% (w/v) soluble starch, 30 μg/ml

kanamycin, and 40 µl of IPTG (100 mM) solution. The plates were then incubated at 37°C for 18 h in a static incubator. After the incubation period, the plates were stained with the KI_2 solution to visualize the zones of starch digestion (α-amylase production) around the colonies.

For induction and expression in broth culture, the cells containing the recombinant plasmids were then grown in 50 ml LB medium supplemented with 30 µg/ml kanamycin at 37°C and 200 rpm until the culture reached mid-log phase (0.3–0.4 OD at 600 nm). Cells were then induced by addition of 1 mM final concentration of IPTG solution for the expression of recombinant protein. The induced cells were then allowed to grow overnight at 30°C and 200 rpm for the expression of recombinant α-amylase into the culture media. The overnight cultures were subsequently centrifuged at 5000 rpm for 20 min at 4°C and the cell free supernatant (CFS) was used for the measurement of extracellular α-amylase production and SDS-PAGE analysis. The CFS from native *E. coli* cells was used as negative control. For the determination of intracellular α-amylase activity, if any, the cell pellets were re-suspended in Tris–HCl buffer (pH 8.0) and the cells were disrupted by combination of lysozyme (1 mg/g of cells) treatment followed by sonication for 3 min and then subjected to centrifugation at 12,000 rpm for 10 min at 4°C. The supernatant of clear lysate was then used for the measurement of intracellular α-amylase activity.

3.2.11.4.2. Statistical optimization of extracellular expression of recombinant proteins

With the help of signal peptides, recombinant amylases were able to be exported outside the cell, however, a large fraction remained inside the cell. Therefore, RSM [374] was applied to optimize the cultivation conditions for over-expression of recombinant α-amylase from *E. coli* into the culture media. The optimization was designed based on a rotatable central composite design (CCD) with 30 experimental trials involving 8 star points and 6 replicates at the central points. Design Expert (State-Ease, USA) was applied to analyze the obtained results. The cultivation conditions investigated were concentration of IPTG (C1),

post induction time (C2), post induction temperature (C3) and concentration of **EDTA (C4)**, while the α-amylase activity (Y) was collected as the responses. These parameters were selected, as they were believed to be the most crucial factors for the expression of recombinant protein and considered by various researchers for optimization of the expression of recombinant protein in *E. coli* [375-377]. Details of lower limit, central values, and the upper limit are shown in Table 3.6. For statistical calculations, the relationship between the coded values and actual value is as described in Eq. (4):

$$C_i = \frac{A_i - A_0}{\Delta A_i},\ i = 1,2,3,\ldots,k \qquad (4)$$

Where C_i is a coded value of the variable, A_i is the actual value, A_0 is the actual value of A_i at the center point, and the star point was set with α of 2.0 from the coded center point. The significance of the experimental data was analyzed using the ANOVA test. A *p*-value (Probability > F) less than 0.05 indicated that the model terms are significant. Adequacy of the model developed were further validated using numerical method optimization option of the Design-Expert (version 7.0.0, Stat-Ease, Inc.) software.

Table 3.6: Various levels of independent variables used for the optimization study for extracellular expression of recombinant α-amylases (cloned from strains AS01a and AS08E) in *E. coli*

Independent Variables	Levels				
	-2	-1	0	1	2
IPTG (μM) (C1)	0.0	0.2	0.6	1.0	1.4
Time of post Induction (h) (C2)	6	12	18	24	30
Temperature (°C) (C3)	15	20	25	30	35
EDTA (mM) (C4)	8.5	17	25.5	34	42.5

3.2.11.4.3. Purification and biochemical characterizations of recombinant proteins

For the purification of recombinant amylases, 100 ml of Terrific Broth (TB) supplemented with 30 µg/ml kanamycin was inoculated with the transformed colony (harboring recombinant plasmids) and was induced for the extracellular expression of recombinant enzymes as described in Section 3.2.11.4.1. After the period of induction (overnight culture), cells were harvested by centrifugation at 5000 rpm for 20 min at 4°C and the CFS were collected. Solid $(NH_4)_2SO_4$ was gradually added to the CFS at 4°C by slow mixing to attain a final concentration of 1.0 M. The solution was then stirred slowly for additional 30 min. After proper mixing of the CFS, recombinant α-amylase enzyme was purified by a combination of HIC and gel-filtration chromatography techniques as described in Section 3.2.9.2. Biochemical characterization of the purified recombinant proteins were performed as described in Section 3.2.10.

3.2.12. Industrial application of the purified enzyme

3.2.12.1. Detergent stability

To determine the potentiality of the purified α-amylases as a laundry detergent additive, a detergent stability test was performed. Commercial laundry detergents available in the local market such as Surf excel® and Wheel® (Hindustan Lever Ltd., India), Tide® and Ariel® (Procter & Gamble, India), Henko® (Henkel India Ltd.), Fena Ultra® (Fena Pvt. Ltd., India), Safed® (Safechem Industries Ltd., India) and Ujala® (Jyothy Laboratories Ltd., India) were undertaken for this studies [160]. Before the α-amylase stability assay, the detergent solutions (7 mg/ml to stimulate washing condition) were pre-heated at 100°C for 90 min to destroy the endogenous enzyme activity, if any (which was reconfirmed by α-amylase assay of heated detergents solutions). Then the purified enzyme was mixed to a final concentration of 1 µg of protein/ml of detergent solution. Subsequently, the reaction mixture was incubated at 37°C for 1 h and residual α-amylase activity was measured by standard assay procedure described in

Section 3.2.3., and compared with the control (enzyme in tap water without detergent). The relative activities of the purified α-amylases in the presence of laundry detergent were expressed in percentage, considering the activity of control (without detergent) as 100%.

To test the stability of purified α-amylases in presence of proteases (present in detergent formulations), the former enzymes were incubated with 2 U/ml of commercial protease preparation (proteinase K) for 1 h at 37°C, and thereafter, the residual amylase activity was determined against the control (α-amylase without protease treatment).

3.2.12.2. Wash performance analysis

With an aim to determine the efficacy of purified amylases to be used as a bio-detergent additive, their wash performance was evaluated. This was done by determining the chocolate stain releasing capacity of the purified α-amylases from cotton fabrics as described by Hmidet et al. [147] with the following modifications. Briefly, chocolate was heated at 70°C to liquefy it and 100 µl (10 mg/µl of total carbohydrate solution) of the liquefied chocolate was stained to cotton fabrics (5 cm × 5 cm), which was then dried overnight under hot air oven [147]. To test the wash performance, each piece of stained fabric was dipped in each of the following flasks containing: (a) 25 ml of tap water (control), (b) 20 ml of tap water and 5.0 ml of 500 U/ml of purified amylases, (c) 20 ml of tap water and 5 ml of heated detergent (7 mg/ml), and (d) 20 ml of tap water and 5 ml of heated detergent (7 mg/ml) containing 500 U/ml of purified α-amylases preparation. The flasks were then kept at 37°C for 60 min. After that, the fabric pieces were taken out of the flask and the leftover washes were used to determine the quantity of total carbohydrate released from chocolate stained fabric by phenol-sulphuric method as described in Section 3.2.5. Stain removal capacity of the purified enzymes was also determined by visual examination of whiteness of the tested pieces of dried fabric [147] against the untreated chocolate stained fabric, which was considered as a control.

3.2.12.3. Desizing activity

To ascertain the desizing efficiency of purified enzymes, each piece of cotton fabric (5 × 5 cm^2) was starched in liquid solution and oven dried. The cloth strips were then dipped into separate flasks containing (a) 25 ml of tap water (control), and (b) 20 ml of tap water and 5 ml of 500 U/ml of purified enzyme. The test flasks were kept at 75°C for 30 min followed by removal of the cloth strips. After drying, each cloth strip was stained with KI_2 solution. Visual examination of various pieces of dried cloth exhibited the desizing efficiency of the purified enzymes [147].

3.2.12.4. Raw starch digesting ability

The efficiency of purified enzymes to digest various raw starches (rice, wheat and potato starch) was determined by incubating α-amylase (10 μg /ml) with 5.0 mL of 2% (w/v) starch dissolved in 50 mM phosphate buffer (pH ~7.0), as starch liquefaction processes are mostly carried out this pH. The mixture was then incubated at 60-70°C (as most of starch gelatinized above this temperature) for 6 h. The extent of starch hydrolysis was determined by estimating the amount of reducing sugars released in each case and the percentage starch hydrolysis was expressed using the equation (5) shown below:

$$Raw\ starch\ hydrolysis\ (\%) = \frac{A_1}{A_0} \times 0.9 \times 100 \ldots\ldots\ldots\ldots\ldots\ldots\ldots\ldots (5)$$

Where A_1 was the amount of sugar (mg/ml) in the supernatant after the reaction and A_0 was the amount of raw starch before the reaction. The factor 0.9 (162/180) is the conversion factor due to the addition of water molecules to glycosyl moiety on hydrolysis [287].

3.2.12.5. Raw starch adsorption analysis

Affinity of purified amylases towards raw starch was studied by incubating 0.2 g of raw starch granules dissolved in 1 ml of K-phosphate buffer (pH 7.0) with 100 U of enzyme at 4°C for 30 min. After the incubation period, the reaction

mixture was centrifuged for 5000 rpm for 5 min. The enzyme activity in the supernatant was determined and its adsorbability percentage [16] was calculated as given by:

$$Adsorption\ (\%) = \frac{A-B}{A} \times 100 \ldots\ldots\ldots\ldots\ldots\ldots\ldots\ldots (6)$$

Where, A and B represent the α-amylase activity in supernatant before and after adsorption on raw starch granules, respectively.

Starch binding study of the purified α-amylase was also determined by monitoring the intrinsic fluorescence spectra of purified enzyme and soluble starch (dissolved in 20 mM K-phosphate buffer by slight warming) using Perkin Elmer LS55 fluorescence spectrophotometer. For binding study, the enzyme sample was incubated with the starch solution in a cell for 5 min at 25°C, and then excited at 295 nm. Consequently, the emission spectra were registered from 300 to 500 nm. The excitation and emission slit were both set to 5 nm [378]. A blank was also set up under similar conditions for determining any effect of the phosphate buffer solution.

3.2.12.6. SEM analysis of digested raw starch

Scanning Electron Microscopy (SEM) images of digested raw starch (enzyme treated) were compared with the undigested starch at 15 kV (JEOL model JSM-6390 LV). Hydrolyzed raw starch was prepared for the SEM analysis by collecting the un-dissolved raw starch from hydrolysis experiment (Section 3.2.12.4.) by centrifugation. The pellets so obtained were washed thrice with 70% ethanol and were dried in air before the SEM analysis was conducted [159, 299]. Controls for every raw starch material (without enzyme treatment) were also maintained and were treated under similar conditions for comparative study.

3.2.12.7. Bread supplementation as anti-staling agent

The application of purified acidic amylase as anti-staling agent on bread making was evaluated by the procedure described by Sharma and Satyanarayana

[341]. The dough mixture was supplemented either with the purified enzyme or with a commercial α-amylase preparation (Himedia, Mumbai) at a ratio of 0.03 g/100 g of dough (w/w) mixture. This was followed by mechanical blending with 60% (w/v) of water for 30 min to produce the dough. Control dough was also prepared where no enzyme was added. These were then kept for proofing followed by fermentation for 1 h at 33°C and 85% relative humidity. The proved doughs were baked in electric oven at 220°C for 60 min. Subsequently, bread loaves were cooled (1 h), packed in polythene bags, and stored for 5 days at room temperature.

To determine the reducing sugar content of the bread, 1.0 g of each bread sample was dissolved in 5 ml of 0.1 M Na-acetate buffer (pH 4.5), mixed well by vortexing, and centrifuged at 10,000 rpm for 15 min. Presence of reducing sugar in the supernatant was determined using DNS reagent [159]. Moisture content of the bread samples was estimated by drying the bread at 105°C to constant weight. To determine the bread color, a breadcrumb was attached to HunterLab (Ultra-scan VIS, USA) and average value of triplicate readings was recorded. The brownness index (*BI*) for the bread color was calculated [380] using the following equation:

$$BI = \frac{100\,(x - 0.31)}{0.17}, \qquad where\ x = \frac{(a + 1.75L)}{(5.645L + a - 3.012b)} \qquad (7)$$

Whereas L = lightness index (0-100 = black – white), a = redness and greenness [(+100) – (-80) = red – green] and b = yellowness and blueness [(+70) – (-80) = yellow – blue].

For assessing the shelf-life, bread samples kept at room temperature were visually inspected on alternate days for texture, softness, and staling. The crumb texture of the loaves (hardness, springiness, cohesiveness, and gumminess) was evaluated by texture profile analysis (TPA) using a texture analyzer (TA-HD-plus, Stable Micro Systems, UK.) having a 35-mm flat-end aluminum compression disk (probe P/35). Slices of 2 cm thickness were compressed to 40% of their original height in a TPA double compression test, at 1 mm/s speed test, with a 20 s delay between the 1st and 2nd compression [380]. A semi-trained panel did sensory

analysis for overall acceptability of the bread samples. All these experiments were performed in triplicate, and the average values were determined.

3.2.12.8. Immobilization of α-amylase on Magnetic Nano-particle

3.2.12.8.1. Preparation of iron-oxide magnetic nanoparticle (MNPs)

Iron-oxide MNPs were prepared as described by Rossi et al. [381]. Briefly, 1.0 M KOH solution was added drop wise to 25 ml of 0.1 N $FeCl_2$ [dissolved in MilliQ water (Millipore, Billerica, MA, USA)], with constant stirring at room temperature until pH 7.2 was achieved and a characteristic dark green color was observed. To this suspension, 250 µl of 3 % (v/v) H_2O_2 was added to turn dark green suspension into a black precipitate, which was attracted by a permanent magnet. After separating the particles by magnetic decantation, they were washed thrice with 20 ml of distilled water and a final washing with 20 ml of acetone. After overnight drying at room temperature, the yield of MNPs was determined.

3.2.12.8.2. Covalent Coupling of α-amylase onto Iron-oxide MNPs

Alpha-amylase was covalently attached to MNPs by following the protocol described by Mukherjee et al. [382]. Briefly, 25 mg (optimized value) of iron-oxide MNPs were suspended by sonication in 20 mM Tris-HCl, pH 8.0 buffer (optimized buffer). Subsequently, 500 µl of freshly prepared cyanamide solution (20 mg/ml in respective buffer) was added to the above suspension and it was mixed by further sonication for 15 min at room temperature. Then, 500 µl of α-amylase enzyme (2 mg/ml of protein concentration) was added to the cyanamide-treated MNP suspension and it was again sonicated for 30 min at 4°C (ice-bath). The enzyme-coupled with Fe_3O_4 MNPs was separated from the reaction mixture by magnetic decantation and was washed with distilled water several times until no protein was detected in the post washes. The washed enzyme-coupled MNPs were then re-suspended in 2.0 ml of the respective buffer containing 0.1 M NaCl (for flocculation of MNPs), and finally stored at 4°C until used.

The amount of protein immobilized onto iron-oxide MNPs was determined by measuring the total protein content (Section 3.2.6.) of the supernatant in post immobilization process as well as the pooled post washes, then subtracting this combined value of protein content from the total enzyme solution used for the binding study.

3.2.12.8.3. Biophysical characterization of free and α-amylase coupled MNPs

Size and morphology (free and enzyme bound) of iron-oxide MNPs were determined by SEM (JEOL model JSM-6390 LV) at 80 kV. Other biophysical characterizations such as magnetic behavior, binding affinity and Nano-crystallite size of free and enzyme bound MNPs were determined by using hysteresis loop tracer (Model HLT-III, Sestechno), FTIR (Fourier transform infrared) spectrophotometer (Nicolet, model Impact-410) and by measuring X-ray diffraction (XRD) on a X-ray diffractometer (Miniflex, Rigaku Corporation, Japan), respectively [382]. Thermal and storage stabilities as well as reusability of enzyme bound MNPs were determined by following the procedure described by Mukherjee et al. [382].

3.2.12.8.4. Application of MNP-bound α-amylase for continuous starch hydrolysis

For application of MNP-bound α-amylase for continuous starch hydrolysis, a glass column (10 x 25 mm) was packed with iron-oxide MNP-bound α-amylase and washed with 0.1 M Tris-HCl (pH 9.0) buffer several times. Then 2.0 ml of 1% (w/v) starch dissolved in 0.1 M Tris-HCl buffer (pH 9.0) was transferred to the column and incubated at 45°C for different time periods. The starch-hydrolysis efficiency of MNP-bound α-amylase was compared with starch hydrolysis by un-immobilized enzyme under identical condition. Two controls were set up where starch was kept at 45°C without enzyme and with free iron-oxide MNP particles.

Chapter IV

RESULTS

Chapter 4: Results

4.1. Screening of soil samples

The pH of the soil sample (AS01) collected from Golaghat district of Assam, India, was found to be ~6.5. Thus, with an aim to isolate novel acidic α-amylase producing bacterial strain from this soil sample, it was screened on a starch agar plate. By serial dilution methods, six colonies were found capable of producing extracellular amylases, as they were able to form a clear halo zone around the colonies. Among the six amylase-producing colonies, the strain AS01a showed the maximum zone of starch hydrolysis (19.0 mm) on starch agar plates and thus it was selected for further studies. Figure 4.1 illustrates the starch hydrolyzing activity by this strain on starch agar plates by streak plate methods.

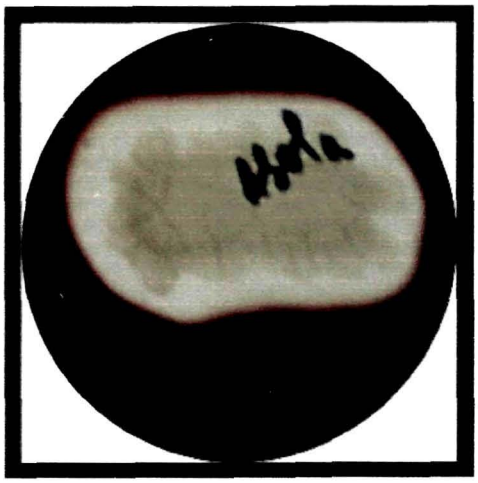

Figure 4.1: Plates showing halo zone formation on starch agar plates by extracellular α-amylase producing strain AS01a isolated from soil sample of Golaghat district of Assam, India.

4.2. Identification of bacteria

4.2.1. Morphological and biochemical identification

Gram staining revealed that strain AS01a is a gram-positive, non-motile, non-acid fast bacterium and shows the formation of round/oval shaped spores (Figure 4.2).

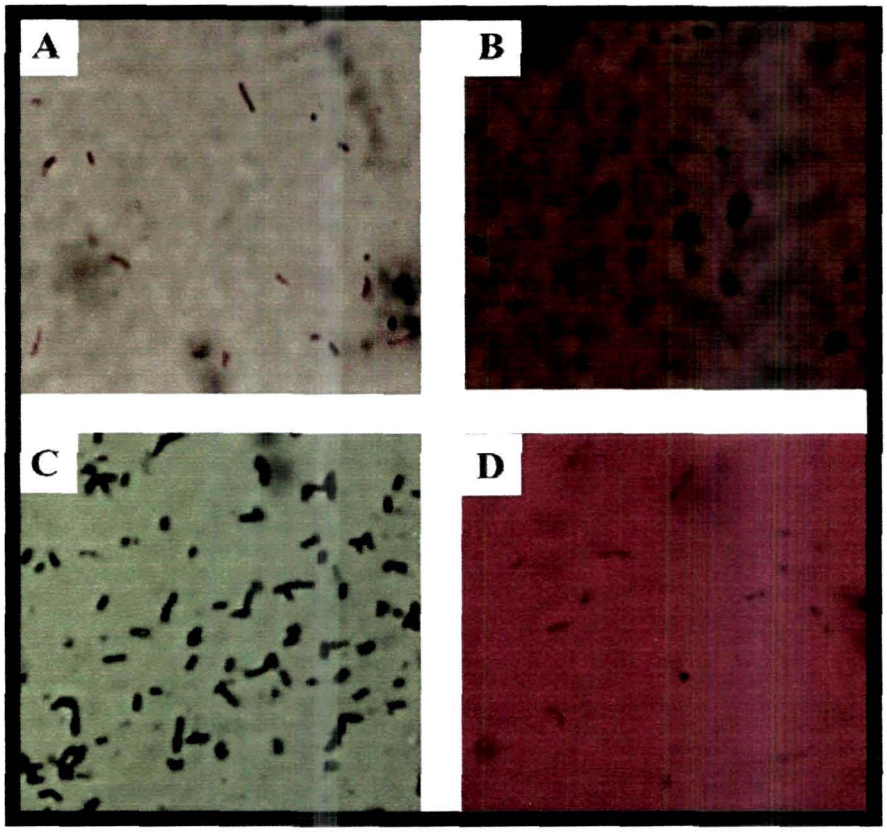

Figure 4.2: Differential staining of the extracellular amylase producing strain AS01a (A: Gram staining; B: spore staining; C: malachite staining; D: acid-fast staining).

Figure 4.3 shows that the AS01a strain is capable of hydrolyzing various carbon sources and it shows positive citrate, nitrate, and catalase results for tests. A summary result obtained after morphological and biochemical analysis of the isolated strain are shown in Table 4.1.

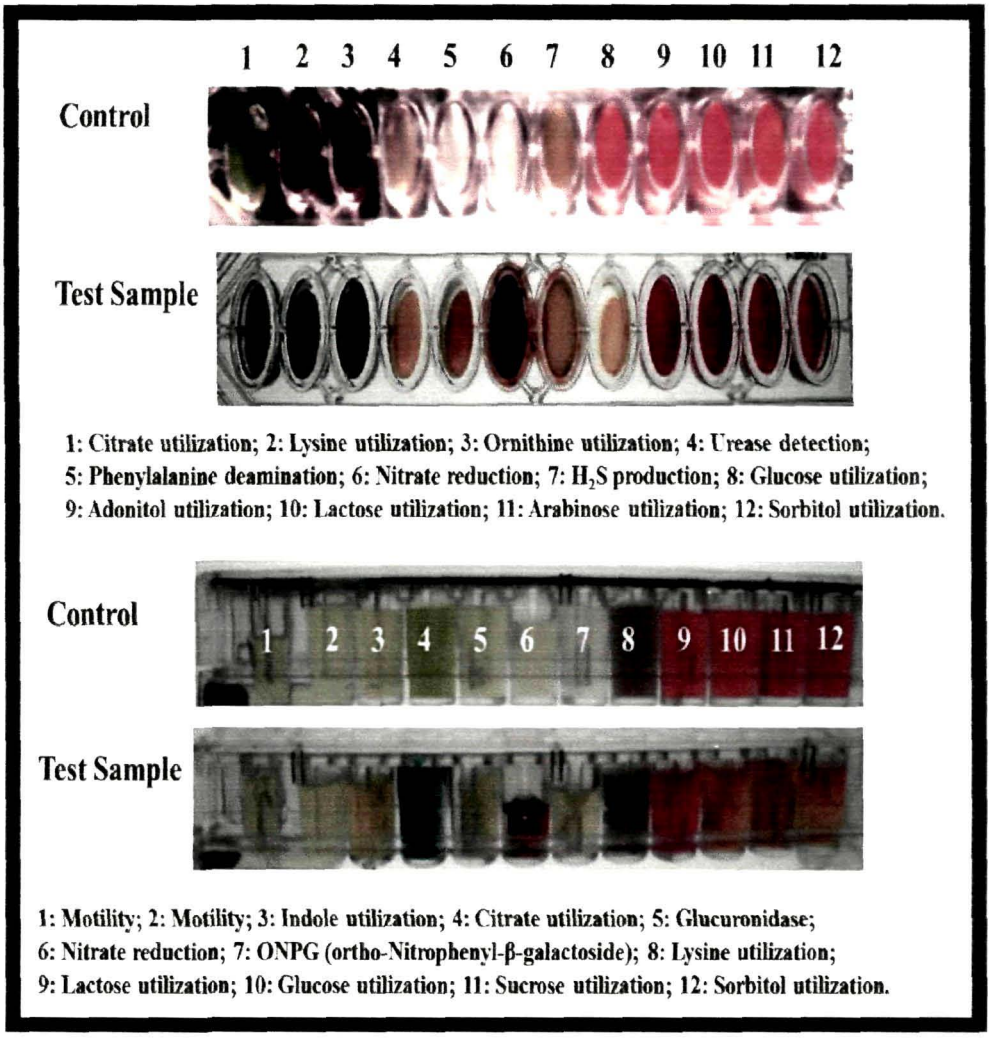

Figure 4.3: Biochemical characterization of the isolated strain AS01a

The analysis of morphological and biochemical properties of the bacterium (strain AS01a) according to the Bergey's manual of systematic bacteriology [316, 355] suggests that strain AS01a belongs to the *Bacillus* genus and thus it is designated as *Bacillus* sp. strain AS01a.

Table 4.1 A summary of biochemical and morphological characteristics of the strain AS01a The result represents the observation of triplicate experiments

Characteristics	Observation
Morphology	Rod shaped, motile negative, Gram positive, spores are round/oval
Growth pH	5.0 – 9.0, optimum at pH 6.0
Growth temperature	Growth range 30-55°C, optimum at 45 -50 °C
Growth in NaCl	0.5 – 5.0% (w/v)
Catalase	Positive
Voges-Proskauer Test	Negative
Methyl Red Test	Negative
Utilization of D- Glucose	Positive
Utilization of Lactose	Variable
Utilization of Adonitol	Variable
Utilization of Arabinose	Positive
Utilization of Sorbitol	Positive
Utilization of Sucrose	Positive
Gas from Glucose	Negative
Hydrolysis of casein	Variables
Hydrolysis of gelatin	Positive
Hydrolysis of starch	Positive
Urease activity	Negative
Citrate utilization	Positive
Indole formation	Variable
Nitrate reduction	Positive
Lysine utilization	Negative
H_2S production	Negative
Ornithine utilization	Positive
Phenylalanine deamination	Positive
Glucuronidase test	Negative
ONPG	Negative

4.2.2. Molecular identification

4.2.2.1. 16S rDNA based identification

Genomic DNA from *Bacillus* sp. strain AS01a was isolated and purified using genomic DNA extraction kit obtained from Fermentas (USA). From the agarose gel analysis, it can be seen that a PCR product of approximately 1500 bp was amplified from the *Bacillus* sp. strain AS01a by using the universal 16S rDNA primers (Table 3.1) and genomic DNA isolated from the above strain (Figure 4.4).

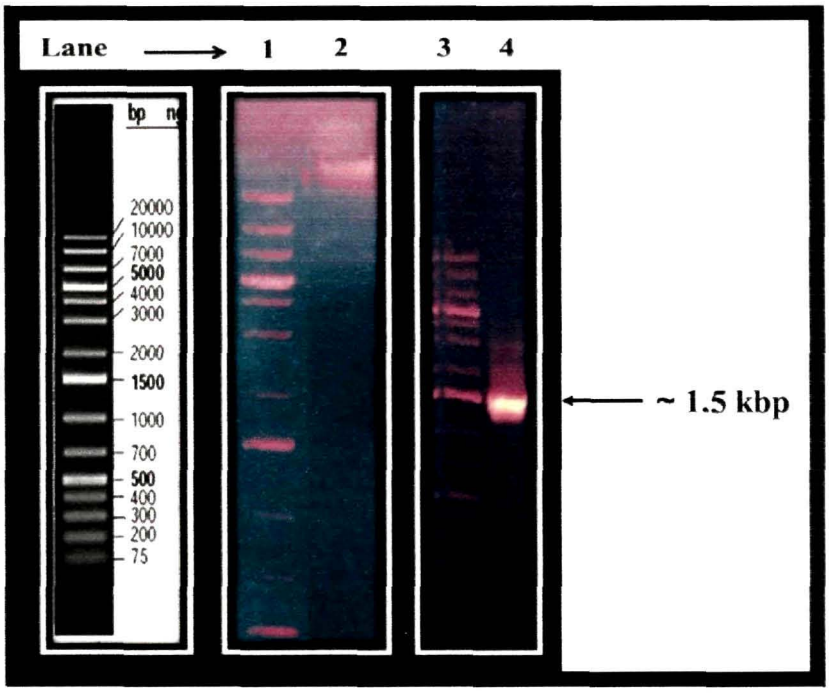

Figure 4.4: Agarose gel analysis of genomic DNA and PCR amplified 16S rDNA from strain AS01a (lanes 1 & 3: 1 kbp DNA ladder; lane 2: genomic DNA from strain AS01a and lane 4: PCR amplified 16S rDNA).

Sequencing of this purified PCR product by Big Dye 3.1 chain termination methods and blastn analysis of the 16S rDNA sequence shows that it has 99% sequence homology with various *Bacillus* species (Table 4.2). The 16S rDNA sequence of strain AS01a was deposited in the NCBI database (www.ncbi.nlm.nih.gov) with the accession number FJ887877 (Table 4.2).

Table 4.2: Percentage identity of 16S rDNA from *Bacillus* sp strain AS01a with other bacteria using blastn programme of NCBI database

Description	Query cover	Maximum identity	Accession
Bacillus sp AS-S01a 16S ribosomal RNA gene, partial sequence	100%	100%	FJ887877
B subtilis strain B215 16S ribosomal RNA gene, partial sequence	98%	99%	EU684952
B sp DC3158 16S ribosomal RNA gene, partial sequence	98%	99%	GU121479
B subtilis strain DYU1 16S ribosomal RNA gene, partial sequence	98%	99%	EF442670
B. subtilis strain CICC10153 16S ribosomal RNA gene, partial sequence	98%	99%	AY971359
B subtilis strain GTG-59 16S ribosomal RNA gene, partial sequence	98%	99%	JX845578
B. sp AB410d partial 16S rRNA gene, isolate AB410d	98%	99%	FR821120
B. subtilis strain TAT1-8 16S ribosomal RNA gene, partial sequence	98%	99%	HQ236066
B subtilis strain NB-01 16S ribosomal RNA gene, partial sequence	98%	99%	HM214542
B. subtilis WL-6 16S ribosomal RNA gene, partial sequence	98%	99%	DQ198162
B licheniformis strain KIBGE-IB1 16S ribosomal RNA gene	98%	99%	GU216258

Phylogenetic trees are constructed to understand the evolutionary history of the species. Based on 16S rRNA gene sequence of AS01a and related bacterial species, a phylogenetic tree was constructed by neighbor-joining method (Figure 4.5) using the MEGA 5.1 software. The phylogenetic tree so obtained based on 16S rDNA, shows that *Bacillus* sp. strain AS01a occupies a position among the cluster of *Bacillus subtilis* groups and shows close phylogenetic position with the *Bacillus* sp. DC3158 (Figure 4.5).

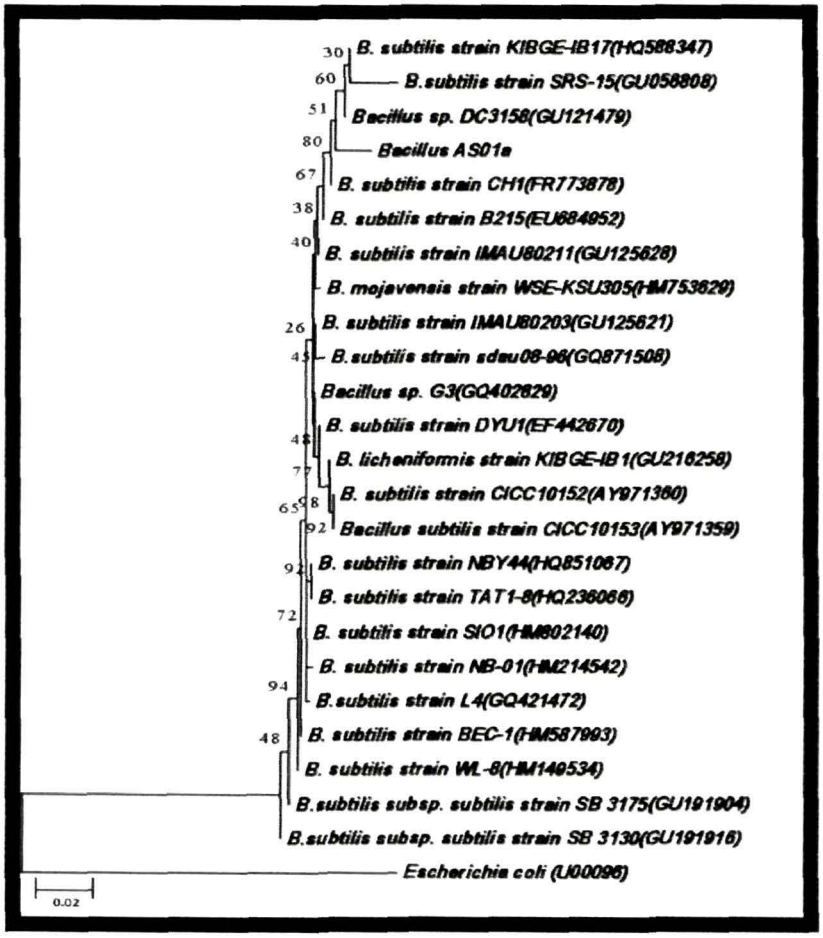

Figure 4.5: Phylogenetic relationships of strain AS01a and other closely related *Bacillus* species based on 16S rDNA sequencing. The tree was generated by considering the sequence from *Escherichia coli* strain K 12 MG1655 (accession number U00096) as out-group. The data set was resampled 1000 times by using the bootstrap option and percentage of bootstrap values are given at the nodes.

4.2.2.2. Gyrase A gene analysis

Gyrase A gene from *Bacillus* sp. strain AS01a was PCR amplified using its genomic DNA and primers designed based on the conserved region of gyrase A gene. By agarose gel electrophoresis, the PCR-amplified *gyr*A gene demonstrated a distinct band of approximately 1000 bp, which is in accordance with the expected gene size of gyrase A (Figure 4.6).

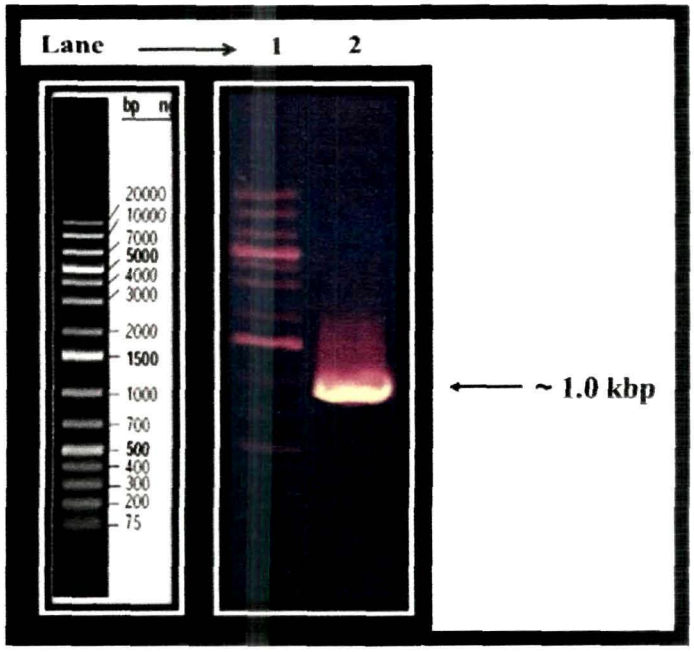

Figure 4.6: Agarose gel analysis of PCR-amplified gyrase A gene from *Bacillus* sp. strain AS01a (lane 1: 1 kbp ladder and lane 2: PCR-amplified product of GyrA gene).

The sequence of gyrase A gene from *Bacillus* sp. AS01a was then blastn searched in NCBI database, which revealed that it shares up to 97% of the *gyr*A gene sequence and shows maximum identity up to 99% with *B. subtilis* group (Table 4.3). Further, the sequence generated during the study is deposited in the public database (NCBI) under the accession number JN133844 (Table 4.3).

Table 4.3: Percentage identity of GyrA gene from AS01a with other bacteria using blastn programme of NCBI database.

Description	Query cover	Maximum identity	Accession
Bacillus sp. AS01a gyrase A (*gyrA*) gene, partial cds (coding sequence)	100%	100%	JN133844
B. subtilis strain NRRL B-23974 gyrase subunit A (*gyrA*) gene, partial cds	97%	99%	AY663691
B. subtilis strain NRRL BD-566 gyrase subunit alpha (*gyrA*) gene, partial cds	96%	100%	EU138629
B. subtilis strain NRRL BD-586 gyrase subunit alpha (*gyrA*) gene, partial cds	96%	100%	EU138636
B. subtilis strain NRRL BD-559 gyrase subunit alpha (*gyrA*) gene, partial cds	96%	99%	EU138628
B. subtilis strain NRRL B-23974 gyrase subunit alpha (*gyrA*) gene, partial cds	96%	99%	EU138618
B. subtilis strain NRRL BD-609 gyrase subunit alpha (*gyrA*) gene, partial cds	96%	99%	EU138647
B. subtilis strain NRRL B-23934 gyrase subunit A (*gyrA*) gene, partial cds	96%	98%	AY663690
B. subtilis KCTC 3494 DNA gyrase subunit A (*gyrA*) gene, partial cds	95%	99%	AF272022
B. subtilis gyrA gene for DNA gyrase subunit alpha, partial cds,	95%	99%	AB612174

A phylogram was built between the gyrase A gene sequence from *Bacillus* sp. strain AS01a and homologous sequences obtained from the other related bacterial strains by using neighbor-joining method (Figure 4.7). Phylogenetic analysis clustered the strain AS01a into *Bacillus* subtilis group and showed its close relatedness with the *Bacillus subtilis* strain NRRL BD-588 (Figure 4.7).

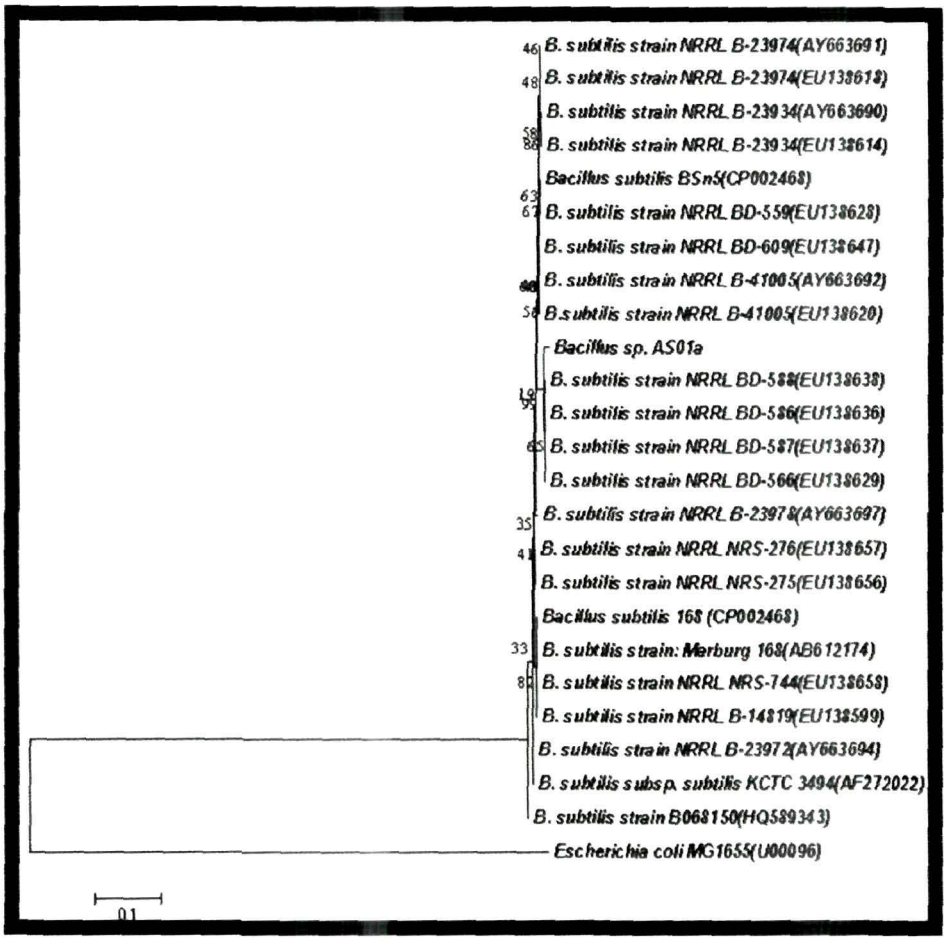

Figure 4.7: Evolutionary relationships of strain AS01a and other closely related *Bacillus* species based on gyrase A gene sequence. The tree was generated by considering the sequence from *Escherichia coli* strain K 12 MG1655 (accession no U00096) as out-group. The data set was resampled 1000 times by using the bootstrap option and percentage of bootstrap values are given at the nodes.

4.2.2.3.Rpo B gene analysis

The conserved gene of RNA polymerase B (*rpoB*) is also one of the potential candidates for the identification of a bacterium. The *rpoB* gene from the genomic DNA of the *Bacillus* sp. strain AS01a was amplified using primers based on conserved region of the above gene (Table 3.1). The agarose gel analysis of the PCR-amplified *rpoB* from *Bacillus* sp. strain AS01a resulted into the appearance of a band size of ~500 bp, which is in accordance with the expected size of the gene (Figure 4.8).

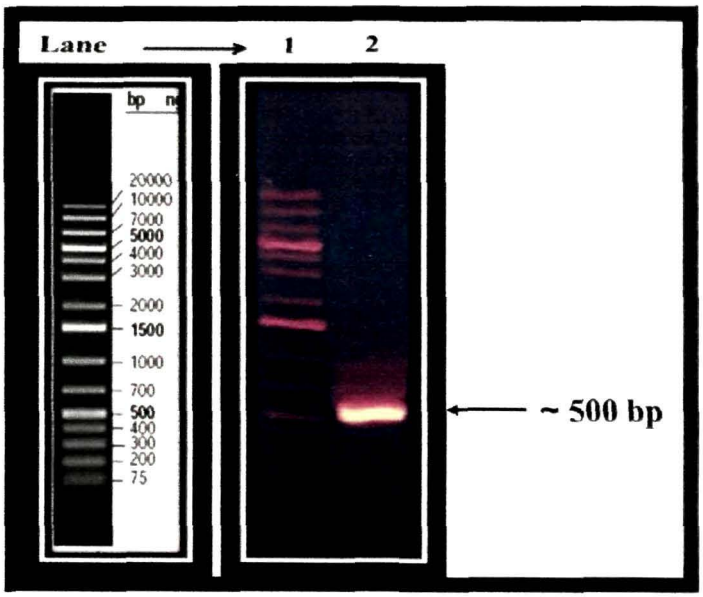

Figure 4.8: Agarose gel analysis of PCR-amplified Rpo B gene from the *Bacillus* sp. strain AS01a (lane 1: 1 kbp DNA ladder and lane 2: amplified *rpoB* product).

The Rpo B gene sequence was then homology searched using blastn programme of the NCBI database, which shows that the AS01a RpoB gene sequence is 99-100% similar with other RpoB gene sequences from the *Bacillus subtilis* group (Table 4.4). The Rpo-B gene sequence obtained from *Bacillus* sp. strain AS01a was deposited in the NCBI database under accession number JN133845 (Table 4.4).

Table 4.4: Percentage identity of RpoB gene from AS01a with other bacteria using blastn programme of NCBI database.

Description	Query cover	Maximum identity	Accession
Bacillus sp. AS01a RpoB (*rpoB*) gene, partial cds (coding sequence)	100%	100%	JN133845
B. subtilis BSn5, complete genome	99%	100%	CP002468
B. subtilis subsp. subtilis str. 168 complete genome	99%	100%	AL009126
B. subtilis strain SV 3-5 RpoB (*rpoB*) gene, partial cds	98%	99%	EU137650
B. subtilis strain SV 2-3 RpoB (*rpoB*) gene, partial cds	98%	99%	EU137646
B. subtilis strain SV 1-6 RpoB (*rpoB*) gene, partial cds	98%	100%	EU137645
B. subtilis strain SV 2-4 RpoB (*rpoB*) gene, partial cds	98%	99%	EU137647
B. subtilis subsp. subtilis strain 3EC4A17 RpoB (*rpoB*) gene, partial cds	96%	100%	EF015346
B. subtilis subsp. subtilis strain RO-OO-2 RpoB (*rpoB*) gene, partial cds	96%	99%	EF015384
B. subtilis subsp. spizizenii strain 3EC7A3 RpoB (*rpoB*) gene, partial cds	96%	99%	EF015374

A distance tree was constructed based on *rpoB* sequence from *B.* sp. AS01a and other closely related homologous gene sequences obtained from the blastn searched by using neighbor-joining method. The analysis of sequence alignment suggests that AS01a belongs to the *Bacillus subtilis* group and is closely related with *B. subtilis subsp.* strain 3EC4A17.

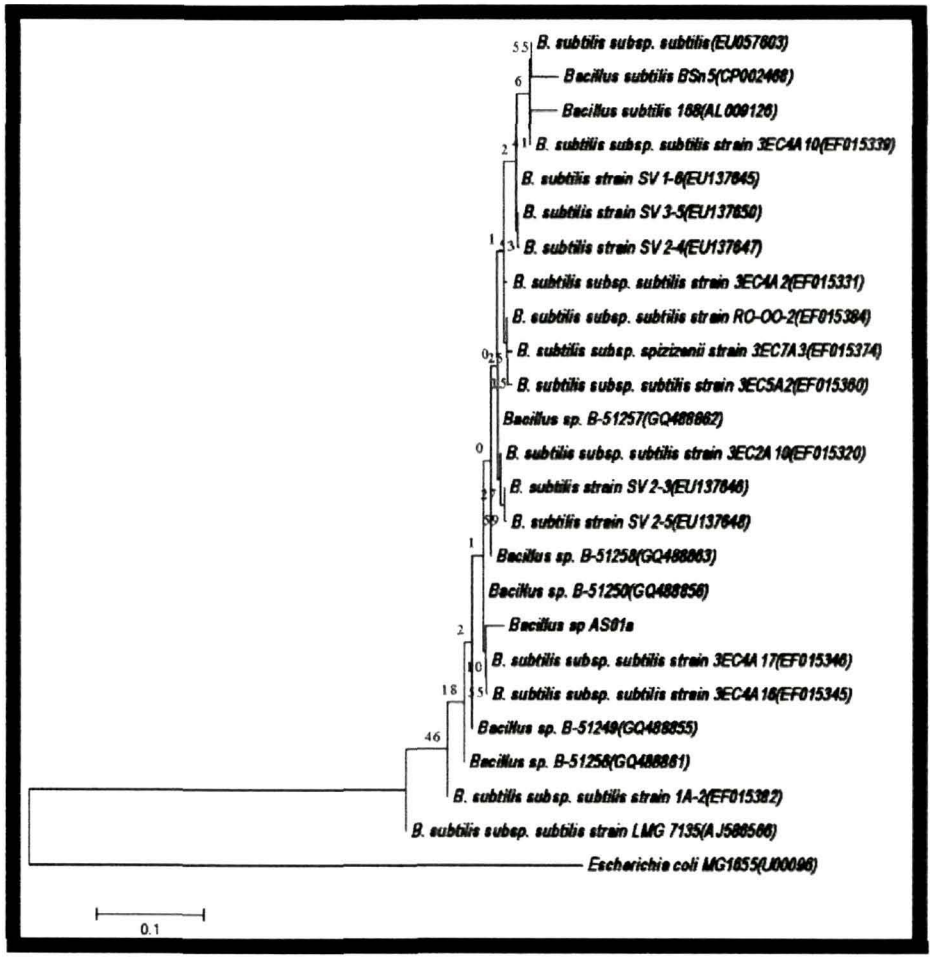

Figure 4.9: Evolutionary relationships of strain AS01a and other closely related *Bacillus* species based on RNA polymerase B gene sequences. The tree was generated by considering the Rpo-B gene sequence from *Escherichia coli* strain K 12 MG1655 (accession no U00096) as out-group. The data set was resampled 1000 times by using the bootstrap option and percentage of bootstrap values are given at the nodes.

4.2.2.4. Analysis of 16S-23S intergenic spacer region (ISR)

Intergenic spacer region between 16S-23S has a high degree of variation even between closely related species; therefore, it can be used to discriminate between species. The PCR amplification of ISR from *Bacillus* sp. strain AS01a and its analysis on agarose gel electrophoresis, showed three bands on the agarose gel (Figure 4.10). However, the band size of ~500 bp was selected for further studies as the expected band size of the spacer region is ~450 bp.

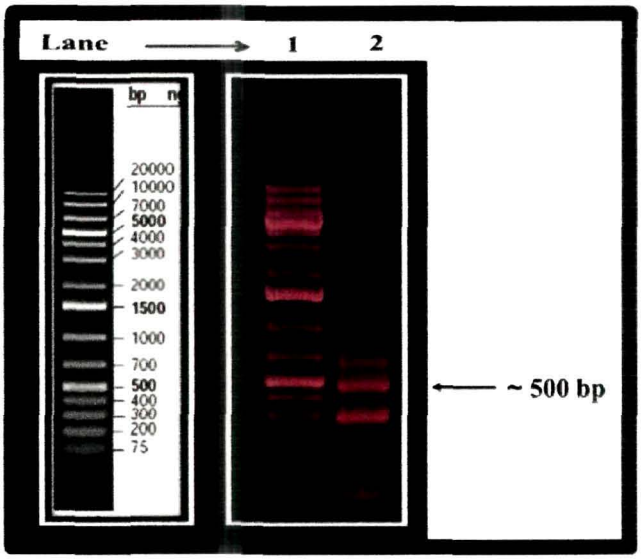

Figure 4.10: Agarose gel electrophoresis of PCR-amplified ISR region from the strain AS01a (Lane 1: 1 kbp DNA ladder and lane 2: PCR-amplified ISR region product).

The sequence of amplified 16S-23S ISR region from the strain AS01a was blastn searched using NCBI database. It showed 98% sequence coverage of ISR gene sequence from other *B. subtilis* strains. The 16S-23S ISR region sequence from *Bacillus* sp. strain AS01a has been deposited in the NCBI database (accession number JN118575).

Table 4.5: Percentage identity of ISR gene from AS01a with other bacteria using blastn programme of NCBI database.

Description	Query cover	Maximum identity	Accession
B. subtilis strain AS-01a 16S-23S ribosomal RNA-ISR, partial sequence	100%	100%	JN118575
B. subtilis strain Tpb55 16S-23S ribosomal RNA-ISR, partial sequence	98%	96%	DQ672263
B. subtilis strain IDCC 16S-23S ribosomal RNA-ISR, partial sequence	83%	97%	EF533983
B. mojavensis clone MOJ1F 16S-23S ribosomal RNA-ISR, partial sequence	85%	96%	AF478089
B. subtilis strain IDCC 1103 16S-23S ribosomal RNA-ISR, partial sequence	83%	96%	EF533985
B. subtilis strain 4428 16S-23S ribosomal RNA-ISR, partial sequence	76%	97%	GQ255891
B. subtilis strain BPB-10 16S-23S ribosomal RNA-ISR, partial sequence	95%	91%	AY157575
B. subtilis 16S rRNA gene, ITS1 and 23S rRNA gene (partial), strain US116	95%	91%	AJ544538
B. subtilis strain 4604 16S-23S ribosomal RNA-ISR, partial sequence	70%	98%	GQ255889
B. subtilis strain 4481 16S-23S ribosomal RNA-ISR, partial sequence	68%	98%	GQ255892

Phylogenetic tree based on the sequence 16S-23S ISR region of *Bacillus* sp. strain AS01a and other closely related bacteria was constructed with the help of sequence alignment software by using neighbor-joining method. The analysis of aligned sequences suggests that strain AS01a belongs to the *B. subtilis* group and it shows close relatedness with *Bacillus subtilis* strain Tpb55.

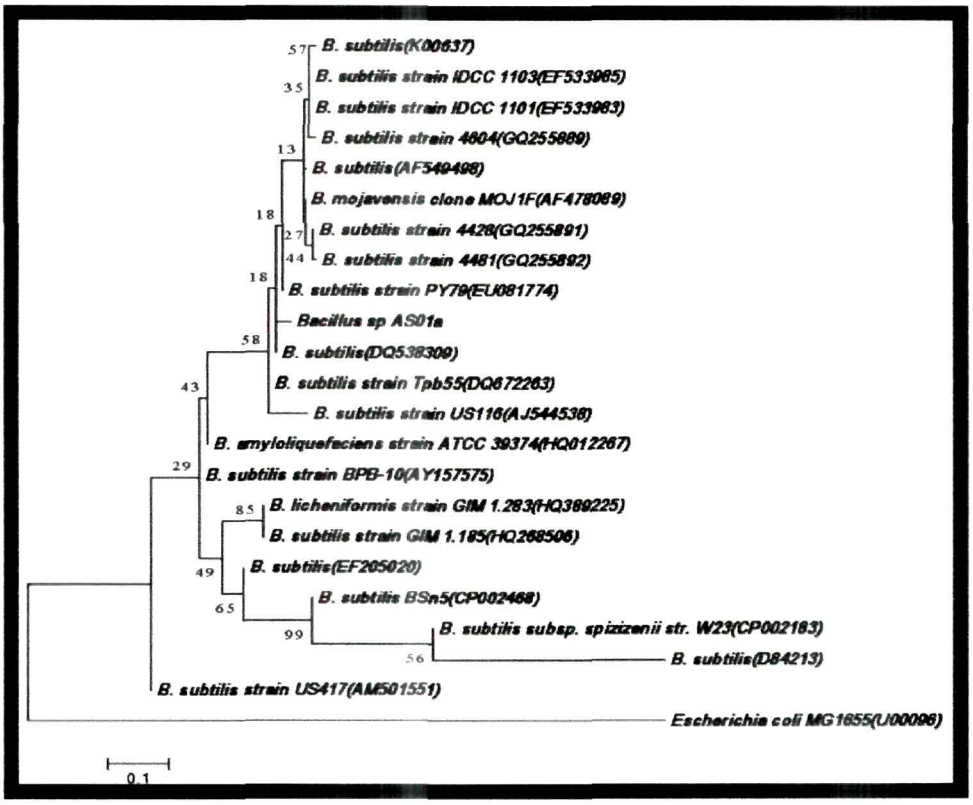

Figure 4.11: Evolutionary relationships of strain AS01a and other closely related *Bacillus* species based on 16S-23S ISR sequence by NJ method. The tree was generated by considering the sequence from *Escherichia coli* strain K 12 MG1655 (accession no U00096) as out-group. The data set was resampled 1000 times by using the bootstrap option and percentage of bootstrap values are given at the nodes.

By following various method of bacterial identification, including morphological, biochemical and molecular approach the isolated bacterial strain AS01a was identified as *Bacillus subtilis* and named as *B. subtilis* strain AS01a.

4.3. Screening of significant factors influencing α-amylase production from *B. subtilis* strain AS01a

4.3.1. Effect of carbon source on α-amylase production

Various carbon sources were screened to see the effect on bacterial growth and α-amylase production by *B. subtilis* strain AS01a. Among the tested sources of carbon, starch was found to be the most preferred carbon source for both α-amylase production and bacterial growth followed by galactose, and then lactose (Figure 4.12). Although, from figure 4.12, it can be seen that the α-amylase/dry mass ratio is higher in case of galactose, however, maximum α-amylase production (428 U/ml) was achieved only in the presence of 1% (w/v) starch as a sole carbon source rather than in case of galactose as a sole carbon source. This implies that bacterium could easily metabolizes the simplest sugar galactose and can induce the basal level expression of α-amylase production, however, α-amylase production can only be maximized in the presence of its natural inducer i.e. starch [29].

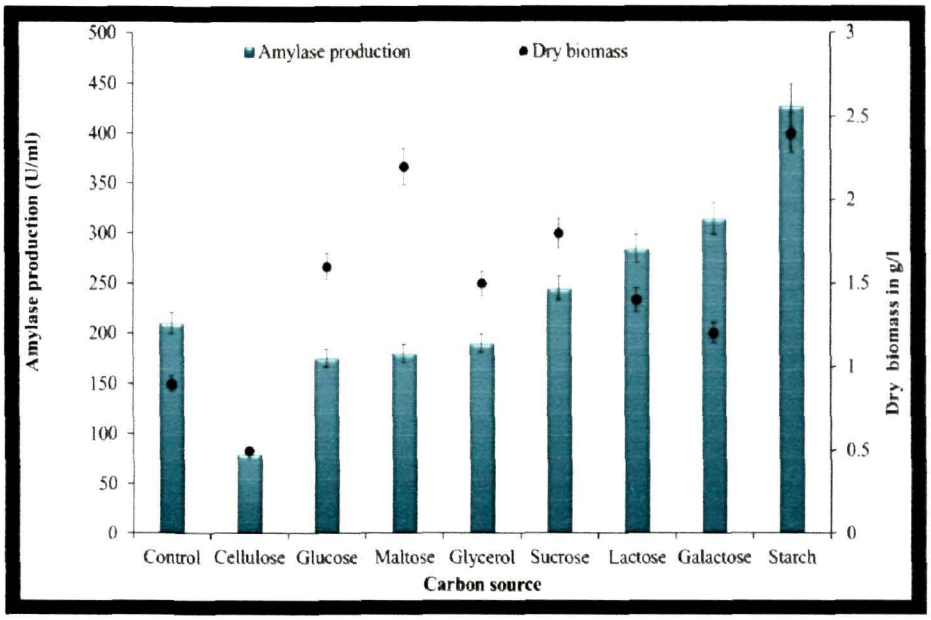

Figure 4.12: Influence of various sources of carbon on growth of and α-amylase production by *B. subtilis* strain AS01a. Values are mean ± S.D. of triplicates. The values vary significantly at p-value ≤ 0.05, w.r.t. control (non-supplemented media).

4.3.2. Effect of nitrogen source on α-amylase production

Among the various nitrogen sources tested for the α-amylase production, beef extract was found to be most influential followed by peptone and then NH_4Cl (Figure 4.13). Optimum levels of α-amylase production as well as bacterial growth were achieved in presence of beef extract supplementation as a nitrogen source (Figure 4.13).

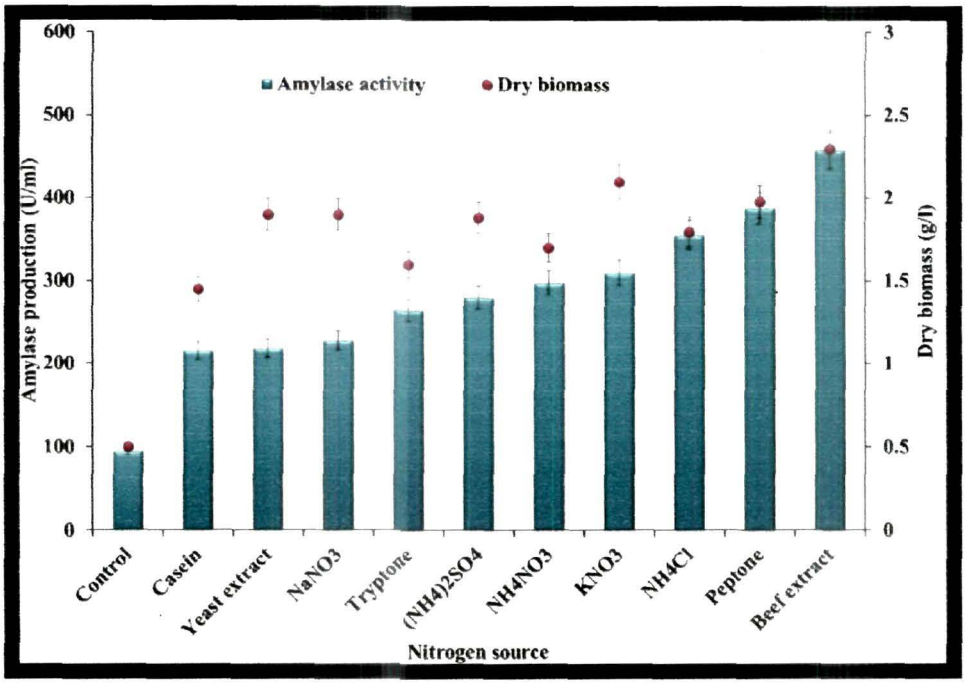

Figure 4.13: Influence of various sources of nitrogen on the growth and production of α-amylase by *B. subtilis* strain AS01a. Values are mean ± S.D. of triplicate determinations. The values vary significantly w.r.t. control (non-supplemented media) at p-value ≤ 0.001.

4.3.3. Effect of pH on α-amylase production

To see the effect of pH on growth and production of enzyme, the bacterium was grown in the production media at different pH ranging from 5.0–12.0 and it was found that maximum α-amylase production (430 U/ml) was achieved when the bacterium was grown at pH 6.0 (Figure 4.14). Since the bacterium was isolated from an acidic environment, it can grow and produce amylases optimally in acidic

pH environment; however, in the alkaline environment there is sharp decline in both α-amylase production and growth of the bacteria (Figure 4.14). Therefore, in further studies, pH of the culture media was maintained at pH 6.0 for optimum growth and α-amylase production by the bacterium *B. subtilis* strain AS01a.

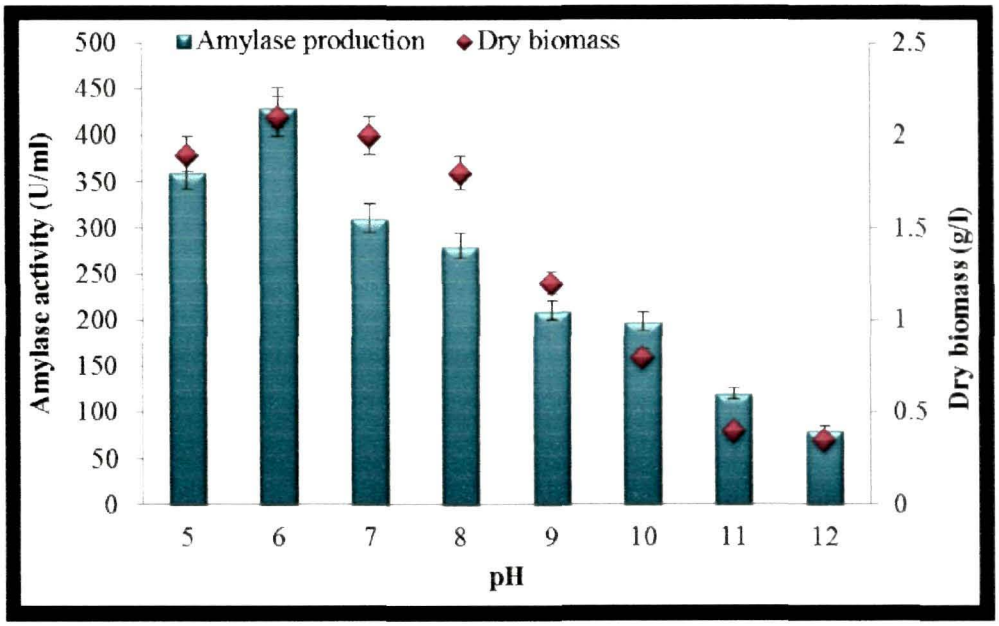

Figure 4.14: Effect of pH of the media on growth of, and α-amylase production by, *B. subtilis* strain AS01a. Values are mean ± S.D. of triplicate determinations and they are significant at p-value ≤ 0.001.

4.3.4. Effect of temperature on α-amylase production

In Figure 4.15, we can see that, with increase in temperature from 30 to 45°C of culture media, there was significant increased in α-amylase production; however, beyond this temperature there was sharp decrease in production of α-amylase as well as growth of the bacteria (Figure 4.15). The maximum α-amylase production (380 U/ml) by *B. subtilis* strain AS01a was achieved at 45°C and thus it was considered as the optimum temperature for amylase production by this bacterium. The bacterial dry biomass (1.8 g/l) was also maximal at this optimum temperature (Figure 4.15). Therefore, for other studies the bacterium growth was maintained at 45°C for α-amylase production.

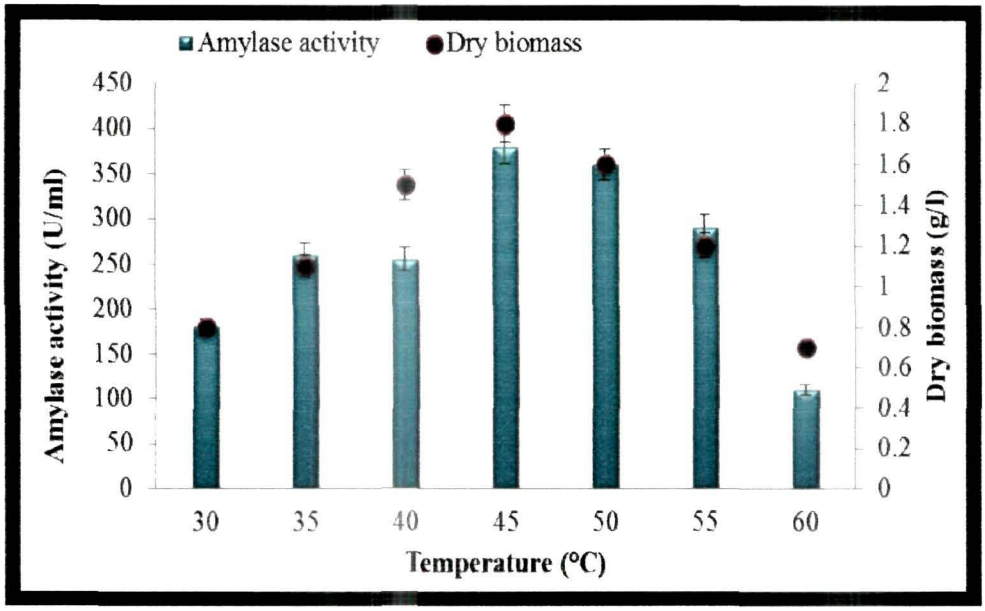

Figure 4.15: Effect of temperature on growth of, and α-amylase production by, *B. subtilis* strain AS01a. Values are mean ± S.D. of triplicate determinations having level of significant at p-value ≤ 0.001.

4.3.5. Effect of incubation time on α-amylase production

Kinetics of α-amylase production by *B. subtilis* strain AS01a showed that the α-amylase production increased with time and it reached maximum after 60 h of incubation at 45°C and pH 6.0. Further incubation at aforesaid condition resulted in a decrease in α-amylase production (Figure 4.16). Thus, the kinetics of α-amylase production suggest that the optimum time of incubation for α-amylase production is 60 h even though the saturation of bacterial growth is reached much before that (48 h of incubation). These also suggest that there is a lag between induction of gene expression and production of enzyme as the maximum α-amylase production was only achieved during the stationary phase of bacterial growth (Figure 4.16).

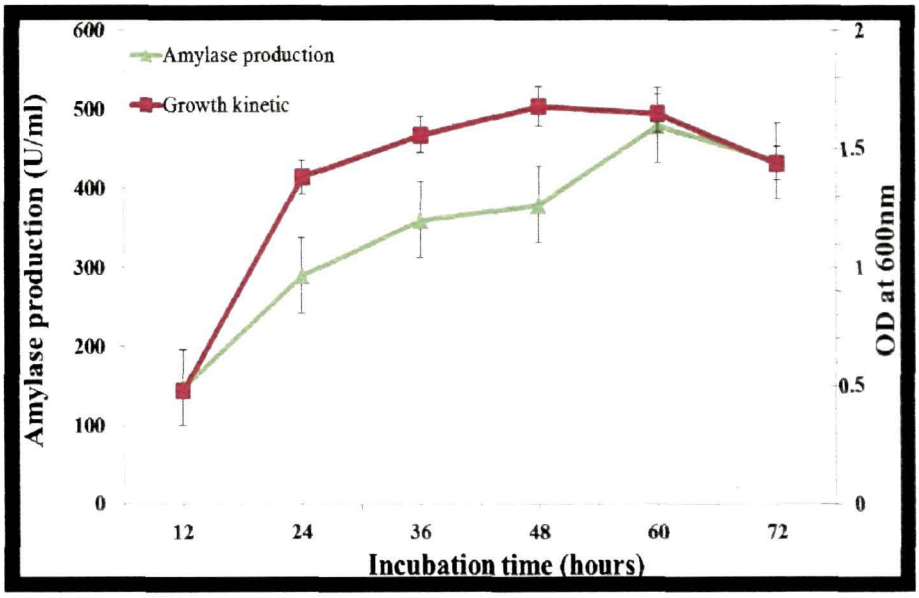

Figure 4.16: Kinetics of growth ( ) and α-amylase production (▲) by *Bacillus subtilis* strain AS01a on M9 medium containing (1% w/v) starch and beef-extract (3 g/l), pH 6.0. Values are mean ± S.D. of triplicate determinations with p-value ≤ 0.001.

4.4. Statistical optimization of significant factors influencing α-amylase production by Response Surface Methodology (RSM)

Among the various factors screened, carbon (starch) and nitrogen (beef extract) sources and pH of the media were found to be the most significant factors influencing α-amylase production by *B. subtilis* strain AS01a. Therefore, these factors were considered for further optimization to evaluate the interaction effect among the variables to maximize α-amylase production from this strain using RSM.

The central value/concentration of the different factors was selected based on the initial screening experiments. The design matrix showing different levels of variables (calculated based on central composite designs) are shown with their predicted and observed responses (yield of α-amylase) in Table 4.6.

Table 4.6: Observed responses and predicted values of α-amylase production by *B. subtilis* strain AS01a using RSM. The observed values are mean ± S.D. of triplicate determinations having *p*-value ≤ 0.001.

Run no.	Independent Variables			Y Response (α-amylase yield in Units)	
	C_1	C_2	C_3	Observed value	Predicted value
1	-1(0.75)	-1(0.2)	-1(5)	234.0 ± 11.7	266.30
2	1(1.25)	-1(0.2)	-1(5)	518.5 ± 25.9	516.00
3	-1(0.75)	1(0.4)	-1(5)	286.5 ± 14.3	316.02
4	1(1.25)	1(0.4)	-1(5)	243.5 ± 12.2	256.46
5	-1(0.75)	-1(0.2)	1(7)	10.5 ± 1.0	18.16
6	1(1.25)	-1(0.2)	1(7)	525.0 ± 26.0	516.61
7	-1(0.75)	1(0.4)	1(7)	263.5 ± 13.2	287.12
8	1(1.25)	1(0.4)	1(7)	487.5 ± 24.4	476.32
9	-α(0.58)	0(0.3)	0(6)	228.5 ± 11.0	183.03
10	+α(1.42)	0(0.3)	0(6)	536.5 ± 27.0	552.09
11	0(1)	-α(0.13)	0(6)	445.0 ± 22.3	437.60
12	0(1)	+α(0.47)	0(6)	468.0 ± 23.4	445.53
13	0(1)	0(0.3)	-α(4.3)	246.0 ± 12.3	213.21
14	0(1)	0(0.3)	+α(7.7)	186.5 ± 9.3	189.42
15	0(1)	0(0.3)	0(6)	418.5 ± 20.9	452.98
16	0(1)	0(0.3)	0(6)	423.0 ± 21.1	452.98
17	0(1)	0(0.3)	0(6)	416.0 ± 21.0	452.98
18	0(1)	0(0.3)	0(6)	426.0 ± 21.0	452.98
19	0(1)	0(0.3)	0(6)	424.0 ± 21.0	452.98
20	0(1)	0(0.3)	0(6)	423.0 ± 21.0	452.98

An actual model was developed to predict the optimum cultivation condition for maximum α-amylase production and the model equation was fitted by regression analysis, which is given by the following equation:

$$Y = -1492.03 + 494.04C_1 - 580.17C_2 + 517.54C_3 - 309.94C_1^2 + 679.94C_1^2 - 78.15C_1^2 - 3092.5C_1C_2 + 248.75C_1C_3 + 548.13C_2C_3 \ldots\ldots\ldots\ldots (4.1)$$

Where, Y refers to the response i.e. enzyme activity (U/ml), C_1 is starch concentration (% w/v), C_2 is beef extract concentration (% w/v) and C_3 is pH of the media. The coefficient of the model including the significance of each coefficient

was determined by *t*-test and *p*-values Table 4 7 shows that all the terms of the model except the linear effects of C_1 (starch content), C_2 (beef extract) and square effect of C_2 (beef-extract) were significant (P<0 05) The negative coefficient observed in case of beef extract indicates that a lower concentration of it can increase the alkaline α-amylase production

Table 4.7: Model coefficients estimated by multiple linear regressions (significance of regression coefficients) for amylase production by *Bacillus subtilis* strain AS01a under shake-flask study

Factor	Coefficient	SE coefficient	Computed *t*-value	*p*-value
Constant	-1492 03	421 466	-3 540	0 005
C_1	494 04	335 572	1 472	0 172
C_2	-580 17	793 519	-0 731	0 481
C_3	517 54	95 687	5 409	0 000
C_1^2	-309 94	111 043	-2 791	0 019
C_2^2	679 14	694 020	0 979	0 351
C_3^2	-78 15	6 940	-11 260	0 000
$C_1 C_2$	-3092 50	372 596	-8 300	0 000
$C_1 C_3$	248 75	37 260	6 676	0 000
$C_2 C_3$	548 13	93 149	5 884	0 000

The analysis of variance (ANOVA) by Fisher's statistical test was conducted for the second-order response surface model and it is presented in Table 4 8 The ANOVA of the quadratic regression model demonstrated that the model is highly significant, as evident from the Fisher's *F*-test value (57 87) and with a very low probability value [(P-model > F) = 0 001] The significance of the quadratic model was also evident from the coefficient of determination (R^2) value The R^2 and adjusted R^2 values were determined as 98 12% and 96 42%, respectively (Table 4 8) The observed values of R^2 suggest that the fitted model could explain 98 12% of the total variation and hence vouches for adequacy of the model The adjusted R^2 value (96 42%) also advocates for a high significance of the model

Table 4.8: ANOVA for the α-amylase produced by *B. subtilis* strain AS01a

Source	DF	Seq SS	Adj SS	Adj MS	*F*-value	Prob > *F*
Regression	9	361520	361520	40168 9	57 87	0 000
Linear	3	165180	23539	7846 3	11 30	0 001
Square	3	93549	93549	31183 0	44 92	0 000
Interaction	3	102791	102791	34263 8	49 36	0 000
Residual Error	10	6941	6941	694 1		
Lack-of-Fit	5	6868	6868	1373 6	93 44	0 000
Pure Error	5	74	74	14 7		
Total	19	368462				

R^2 = 98 12% R^2(pred) = 85 77% R^2(adj) = 96.42%

The three-dimensional response surface plots and two dimensional contour plots are the graphical representations of the regression equation and are drawn as a function of two factors at a time while maintaining the other factor at the minimum or zero level. Figures 4.17 and 4.18 depict the response surface plots and contour plots obtained after solving the regression equation, respectively. It can be seen from Figure 4.17(c) that a lower concentration of beef extract and higher concentration of starch could induce α-amylase production. In Figure 4.17(a-b), it can be perceived that the culture media with acidic pH can also favor the maximum α-amylase production. The contour plots (Figure 4 18) show the significant interaction amongst the variables. Figure 4.18(b) demonstrates that the higher concentration of starch and acidic pH of the media can enhance the α-amylase production. In Figure 4.18(c) it can be seen that a lower concentration of beef extract and a higher concentration of starch enhance α-amylase production from *B. subtilis* strain AS01a under submerged fermentation.

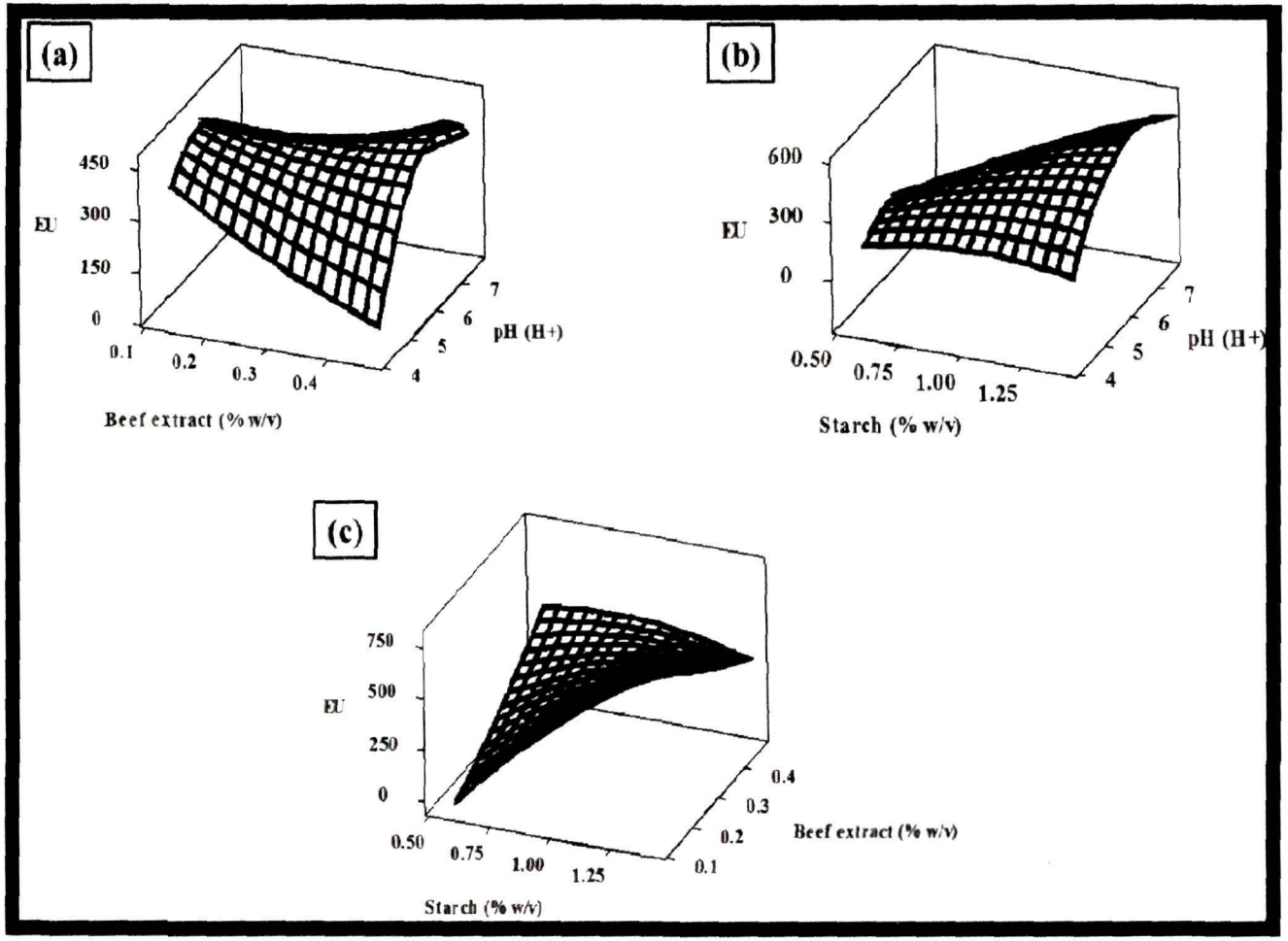

Figure 4.17: Response surface plots for α-amylase production by *B. subtilis* strain AS01a. The interactions between (A) pH vs beef extract (% w/v) (B) pH vs starch (% w/v) (C) starch (% w/v) vs beef extract (% w/v).

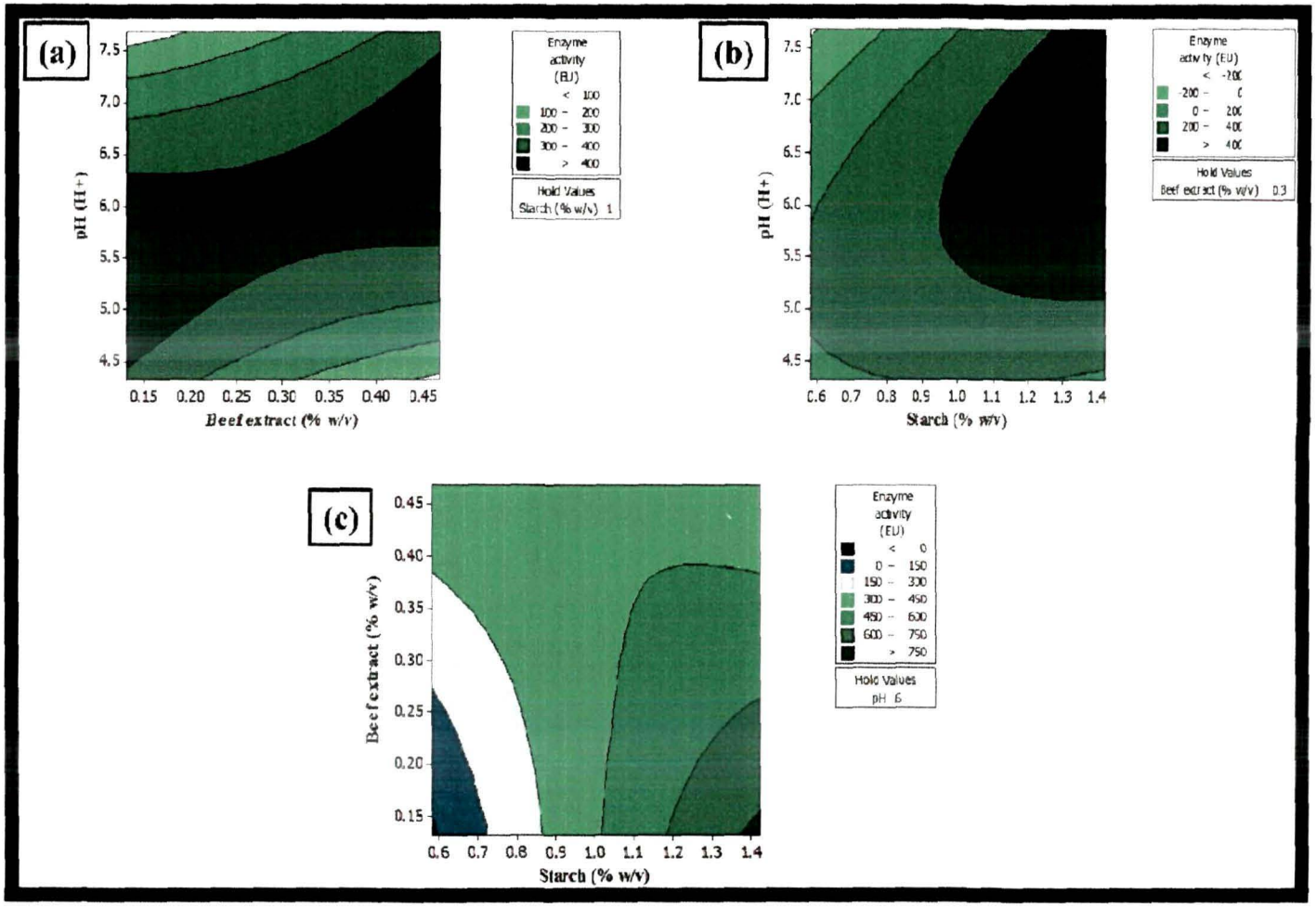

Figure 4.18: Contour plots showing interaction effect of test variables on α-amylase production from *B. subtilis* strain AS01a. (A) pH vs beef extract (% w/v) (B) pH vs starch (% w/v) (C) starch (% w/v) vs beef extract (% w/v).

By solving the regression Equation 4.1, the optimum levels of test variables for maximum α-amylase yield (785.8 Units) were predicted by using the predict programme (Minitab 15 Statistical Software®) as 1.421 % (w/v) of starch, 0.131 % (w/v) of beef-extract and at 6.1 pH of the medium (Figure 4.19).

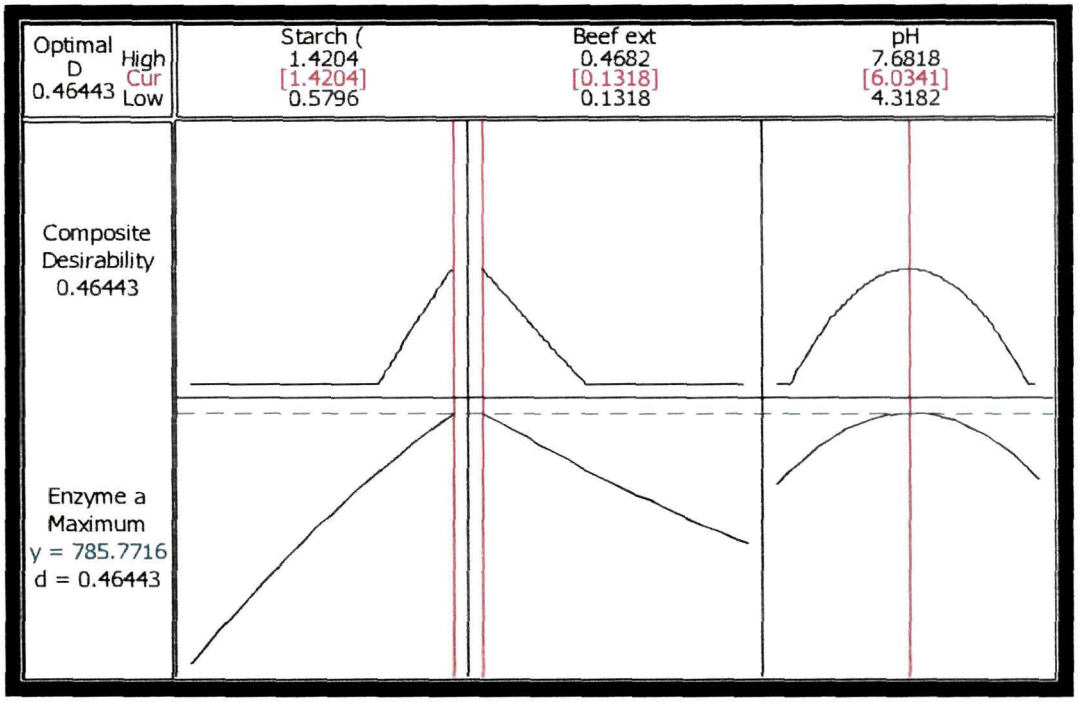

Figure 4.19: Optimization plot showing the optimum value for maximum α-amylase production from *B. subtilis* strain AS01a.

The predicted response for α-amylase yield was 785.77 units (Figure 4.19), while the actual experimental value for α-amylase production in a process-controlled fermenter was obtained as 799.0 ± 39.95 units (mean ± S.D., n=3, *p*-value = <0.001) post 72 h of incubation, which established the validity of the model (Table 4.9).

Table 4.9: Optimized conditions with predicted and observed response achieved after RSM implementation.

Factors	Optimized values	Predicted response	Observed response	Fold increase in production
Starch (%)	1.421	786.0 U/ml	799.0 ± 39.95 U/ml	~2.8-fold from initial productions
Beef extract (%)	0.131			
pH(H^+)	6.1			

4.5. Isolation and purification of α-amylase from *B. subtilis* strain AS01a

The α-amylase enzyme was isolated from optimized culture media of *B. subtilis* strain AS01a by $(NH_4)_2SO_4$ precipitation method followed by concentrating the dialyzed fraction using acetone. The acetone-concentrated protein was fractionated through a gel-filtration column (GFC) which resulted in elution of proteins into three major peaks. However, GF-II peak shows the major α-amylase activity (Figure 4.20).

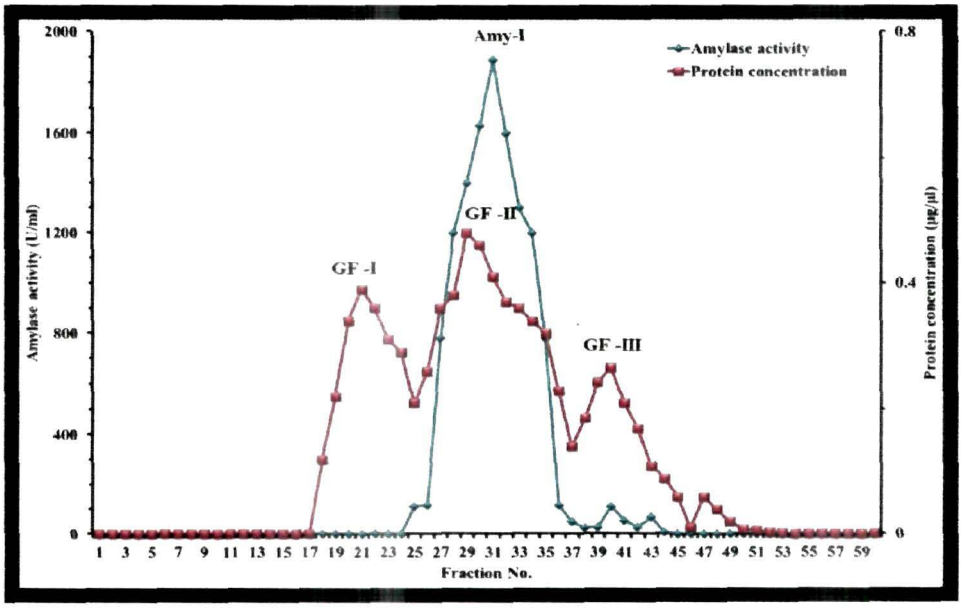

Figure 4.20: Gel-filtration profile of acetone-precipitated fraction of α-amylase from *B. subtilis* strain AS01a through Sephadex G-50 column.

Homogeneity as well as molecular mass of the GF II peak was analyzed by the SDS-PAGE (Figure 4.21). The purified enzyme shows a distinct single band of ~21.0 kDa under reducing conditions (Figure 4.21) and analysis of this protein under native conditions (i.e. zymographic study) also yielded a single clear zone of starch hydrolysis around 21.0 kDa (Figure 4.21). Both these studies suggest that the purified enzyme is monomeric in nature and that it has an approximate molecular mass of 21.0 kDa.

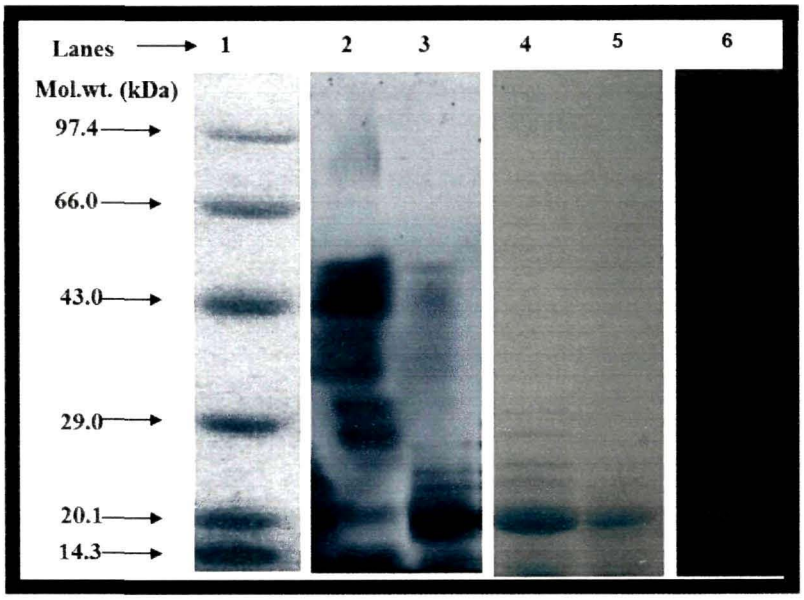

Figure 4.21: SDS-PAGE analysis of purified α-amylase from *B. subtilis* strain AS01a; lane 1: protein molecular weight markers; lane 2: crude enzyme (30 µg); lane 3: $(NH_4)_2SO_4$ precipitated protein (30 µg); lane 4: acetone-precipitated fraction (25 µg); lane 5: gel-filtration fraction (15 µg) and lane 6: zymogram of purified amylase (10 µg).

With three steps of purification using ammonium sulphate, acetone, and gel filtration chromatography, the α-amylase enzyme from *B. subtilis* strain AS01a was purified up to 7.5-fold purification with 0.3% of total enzyme recovery (Table 4.10).

Table 4.10: Summary of purification of α-amylase from *B. subtilis* strain AS01a. Values represent a typical experiment.

Purification step	Total protein (mg)	Total activity (U)	Enzyme recovery (%)	Sp. Activity (U /mg)	Purification (fold)
Crude extract	3160.0	635000.0	100	201.0	1.0
$(NH_4)_2SO_4$ precipitation	160.8	42500.0	6.7	264.0	1.3
Acetone precipitation	10.2	3120.0	0.5	305.0	1.5
Sephadex G-50	1.3	1890.0	0.3	1500.0	7.5

4.6. Biochemical characterization of purified protein

4.6.1. Determination of optimum dose and time of incubation

To investigate the optimum dose for the purified enzyme from the *B. subtilis* strain AS01a, 1% starch solution was incubated with the purified enzyme in various doses ranging from 5-30 µg/ml (Figure 4.22). The enzyme activity was found to increase in a linear pattern as the concentration of enzyme increased. However, at concentration of 15 µg/ml of protein, the enzyme activity reached its optimum value and a further increase in enzyme concentration did not enhance the enzyme activity (Figure 4.22).

Figure 4.23 shows the effect of incubation time on α-amylase activity by incubating the purified enzyme for various time-periods ranging from 5-60 min (Figure 4.23). The graph shows that enzyme activity increases with respect to incubation time but after 30 min of incubation, no further increase in enzyme activity was noticed suggesting that the optimum time required for α-amylase activity was 30 min (Figure 4.23).

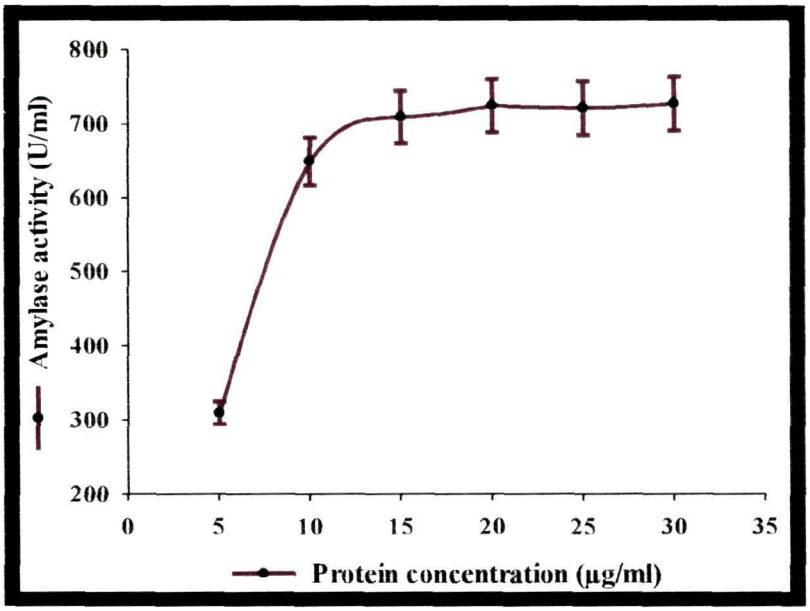

Figure 4.22: Graph showing optimum dose determination of the purified enzyme from *B. subtilis* strain AS01a. Values are mean ± S.D., n = 3 with *p*-value ≤ 0.001.

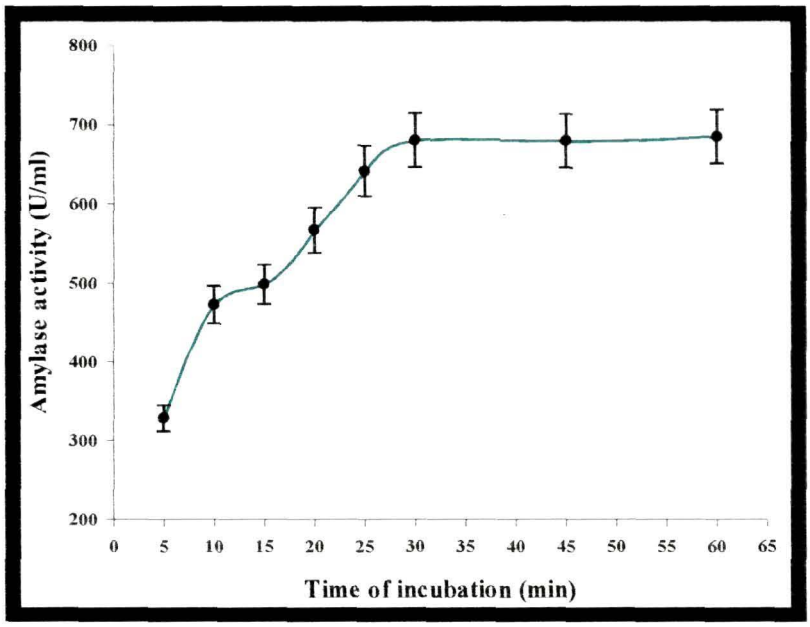

Figure 4.23: Determination of optimum time of incubation for the purified α-amylase from *B. subtilis* strain AS01a. Values are mean ± S.D., n = 3 having level of significant at *p*-value ≤ 0.001.

4.6.2. Optimum temperature and pH

To determine the optimum pH and temperature of the purified enzyme from *B. subtilis* strain AS01a, the purified α-amylase was incubated at various pH values from 6.0-12.0 (Figure 4.24) and at various temperature ranging from 35-75°C (Figure 4.25), respectively. Figure 4.24 shows that the optimum pH for the purified enzyme is 9.0, whereas the optimum temperature for enzyme activity was found to be 55°C (Figure 4.25).

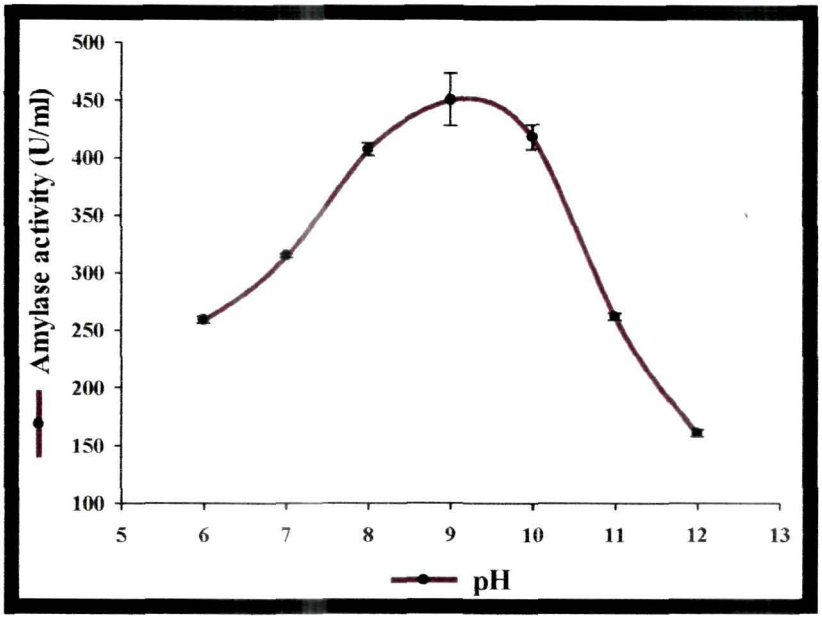

Figure 4.24: Graph showing pH dependence of the activity of the purified enzyme from *B. subtilis* strain AS01a. Values are mean ± S.D. of triplicate determinations with p-value ≤ 0.001.

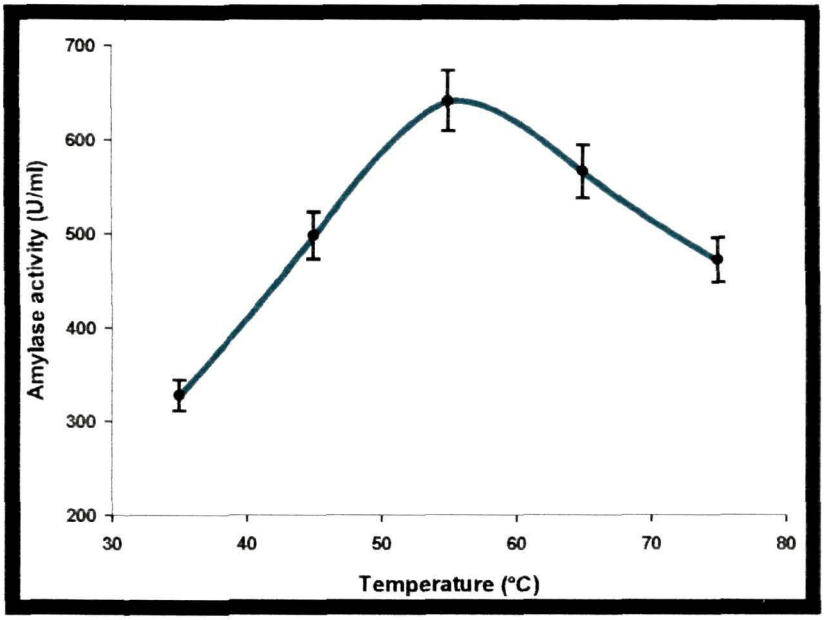

Figure 4.25: Plot showing temperature dependence of the activity of the purified enzyme from *B. subtilis* strain AS01a. Values are mean ± S.D. (n=3) with *p*-value of ≤ 0.001.

4.6.3. Thermostability of the purified enzyme

Thermostability study revealed that heating the purified α-amylase for 30 min at 45 °C had no effect on enzyme activity, but heating beyond this temperature resulted in a gradual loss of enzyme activity, indicating moderate thermostable nature of the purified α-amylase (Figure 4.26). Further, 5 mM Ca^{2+} ions did not improve the thermostability of purified α-amylase suggesting that it is a Ca^{2+} independent enzyme (Figure 4.26).

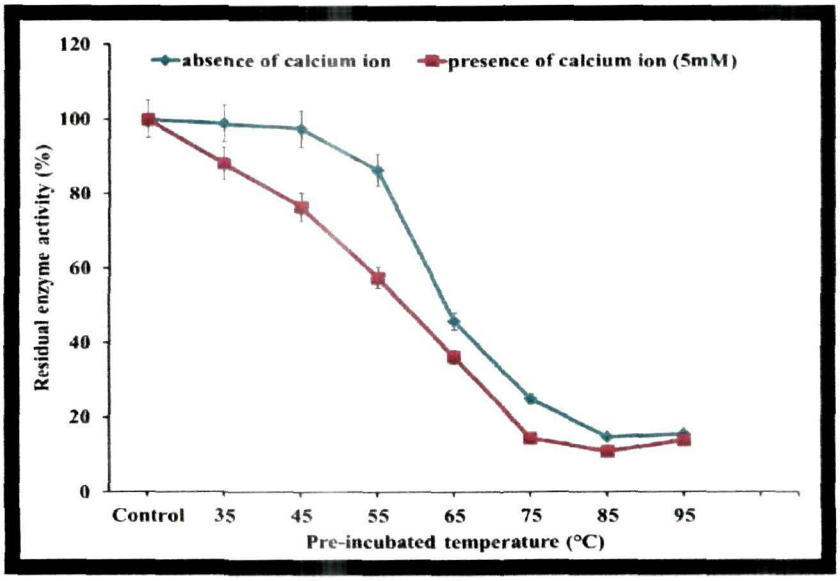

Figure 4.26: Effect of temperature on stability of purified α-amylase from *B. subtilis* strain AS01a in presence (■) and absence (◆) of (5 mM) Ca^{2+} ion.

4.6.4. Kinetics study of the purified α-amylase from B. subtilis strain AS01a

The K_m and V_{max} values for the purified α-amylase towards starch were determined as 1.9 ± 0.1 mg/ml and 198.21 ± 4.9 µmol/min/mg, respectively (Figure 4.27).

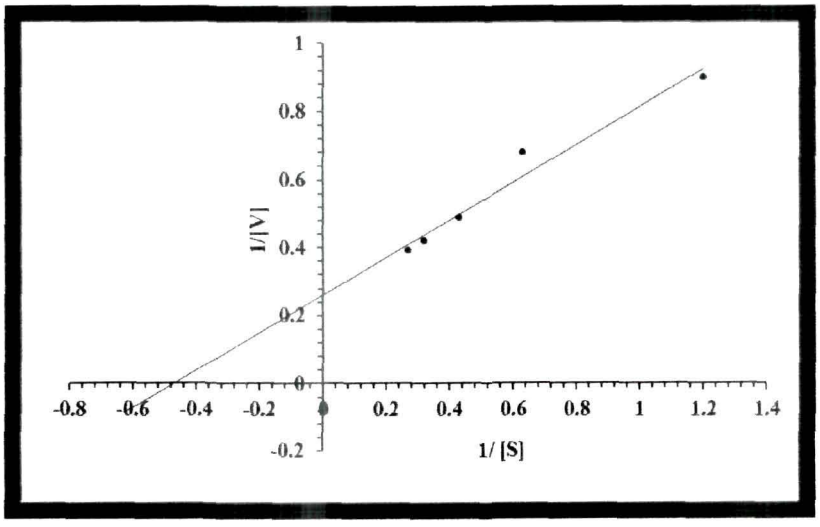

Figure 4.27: Lineweaver-Burk plot to determine K_m and V_{max} values of the purified α-amylase from *B. subtilis* strain AS01a. Each data point is a mean of triplicate determinations.

4.6.5. TLC analysis for end-product determination

TLC analysis of starch hydrolysis end-product by the purified enzyme shows production of high molecular weight oligosaccharides as the main hydrolytic products and very small amount of glucose post 60 min of incubation of soluble starch with purified α-amylase (Figure 4.28). This confirmed that the purified enzyme is an α-amylase and a good candidate for application in the food processing industry.

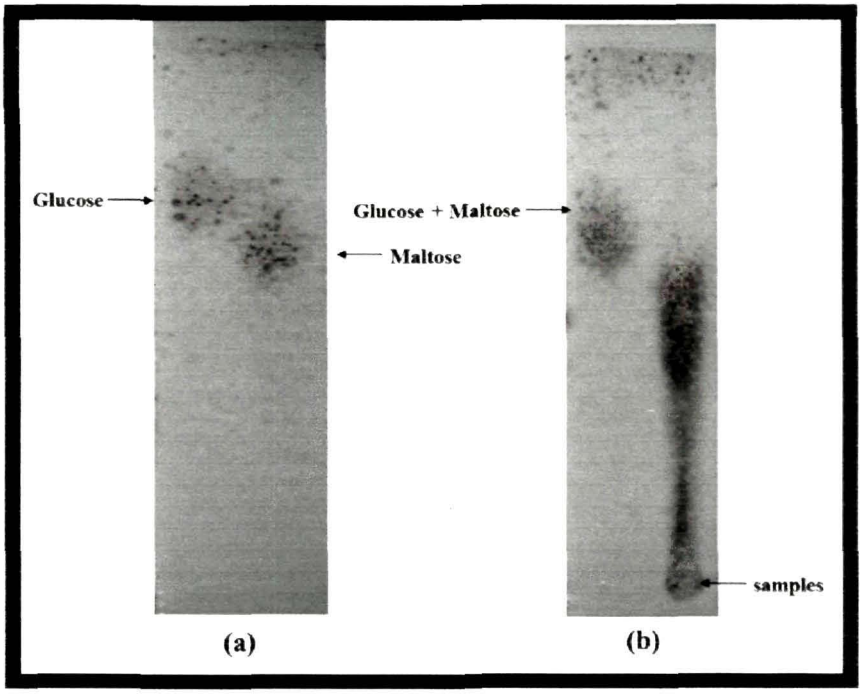

Figure 4.28: Thin layer chromatogram of digested product obtained from hydrolysis of (1% w/v) soluble starch by purified α-amylase. (a) TLC of standard sugar (glucose and maltose) and (b) separation of starch digested products.

4.6.6. Effects of inhibitors, surfactant, denaturing and oxidizing agent on activity of α-amylase

The effect of various effectors/modifying reagents on enzyme activity is shown in Table 4.11. In Table 4.11 we can see that EDTA does not show any adverse effect on enzyme activity suggesting that the enzyme is a metal independent one. Further, when the enzyme was incubated in the presence of

inhibitors like PMSF and 4-BPB the enzyme activity was reduced to 38.8 and 32.8% of its original activity suggesting a role for serine and histidine residues in the catalysis process (Table 4.11). Oxidizing agent such as sodium perborate and denaturing agent such as urea demonstrated slight reduction in enzyme activity while surfactants showed marginal or no effect on the enzymatic activity suggesting a potential application of the present enzyme in the laundry detergent industry.

Table 4.11: Effects of chemicals and group modifying reagents on the purified α-amylase enzyme from *B. subtilis* strain AS01a. The data represent mean ± S.D. ($n = 3$, p-value ≤ 0.001). The value with the same superscript did not vary significantly w.r.t. control (p-value > 0.05).

Effectors	Enzyme activity (%)
Control (without effector)	100[a]
EDTA (2mM)	101.0 ± 5.5[a]
PMSF (2mM)	38.8 ± 1.9
4-BPB (2mM)	32.8 ± 1.6
$NaBO_3$ (5mM)	73.2 ± 3.6
Urea (2M)	79.6 ± 3.9
SDS (1% w/v)	103.3 ± 5.6[a]
Triton-x 100 (1% v/v)	103.4 ± 5.2[a]
Tween-20 (1% v/v)	105.0 ± 5.3[a]
Tween-80 (1% v/v)	106.0 ± 5.3[a]

4.7. Industrial application of the purified enzyme

4.7.1. Starch digestibility by the action of purified enzyme

The SEM photographs of starch granules before and after the degradation with α-amylase at 55°C for 60 min show the formation of pits and holes on the starch granules (Figure 4.29), which demonstrate the raw starch digesting ability of the purified enzyme.

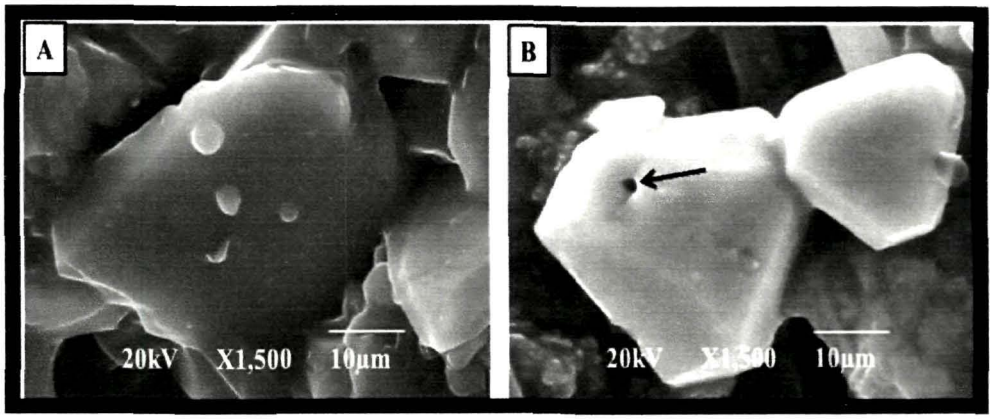

Figure 4.29: Scanning electron microscopic (SEM) photographs of starch granules (Himedia); (A) before and (B) after 60 min of incubation with the purified α-amylase (20 µg/ml) at 55°C. Arrows show formation of pits and holes on treated starch granules.

4.7.2. Detergent stability of the purified enzyme

The α-amylase from *B. subtilis* strain AS01a exhibited a significant stability and compatibility with all the tested commercial laundry detergents (Figure 4.30). The α-amylase retained 69.0% to 100.0% and 100.0% to 153.0% of its original activity in presence of detergents at 30 and 37°C, respectively (Figure 4.30). The partial loss/gain of the enzyme activity in some of the laundry detergents may be attributed to inhibitory/stimulatory effect(s) of the detergent component(s) [14]. In Figure 4.30, we can see that Fena ultra® laundry detergent component(s) is the most compatible detergent for the purified enzyme isolated from *B. subtilis* strain AS01a.

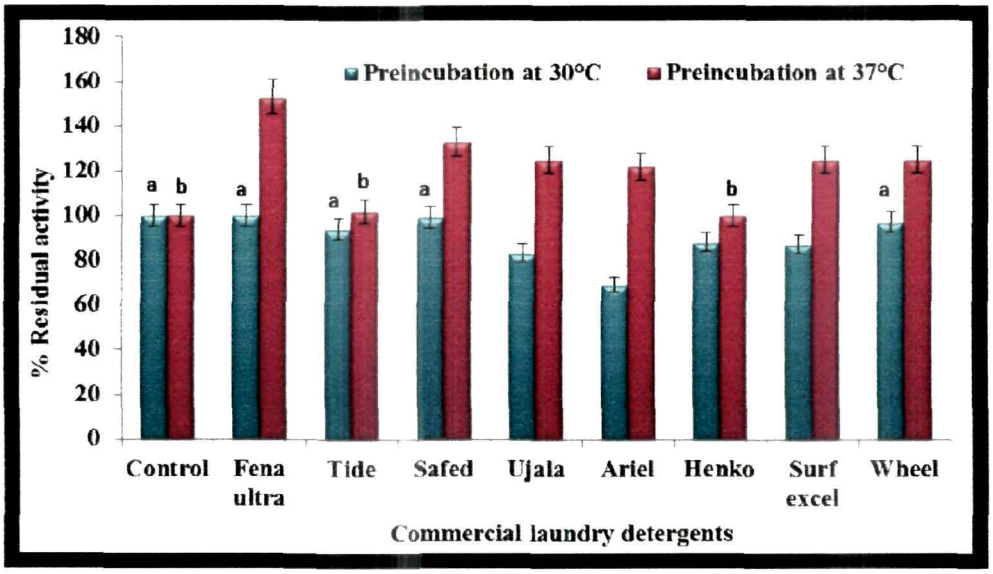

Figure 4.30: Detergent stability and compatibility of purified α-amylase (0.7 mg/ml) from *B. subtilis* strain AS01a at 30°C (■) and 37°C (■). Values are mean ± S.D. of triplicate determinations. Each bar represent mean ± S.D. (n = 3) with *p*-value ≤ 0.001. The bar with the same superscript did not vary siginificantly w.r.t. control (*p*-value > 0.05).

4.7.3. Wash performance on chocolate stain

Stain removal ability of the purified α-amylase was assessed using cotton fabric, pre-stained with chocolate. The treatment of chocolate stain by (Fena®) detergent (7 mg/ml) supplemented with the purified α-amylase (500 U/ml) resulted in better stain removal from the cotton fabrics as compared to stain removal properties of the detergent/enzyme alone (Figure 4.31). The estimation of total carbohydrate release in the leftover washes suggests a 2.8-fold increase in case of α-amylase supplemented with detergent as compared to release of carbohydrate by detergent/enzyme alone [Figure 4.31(e)].

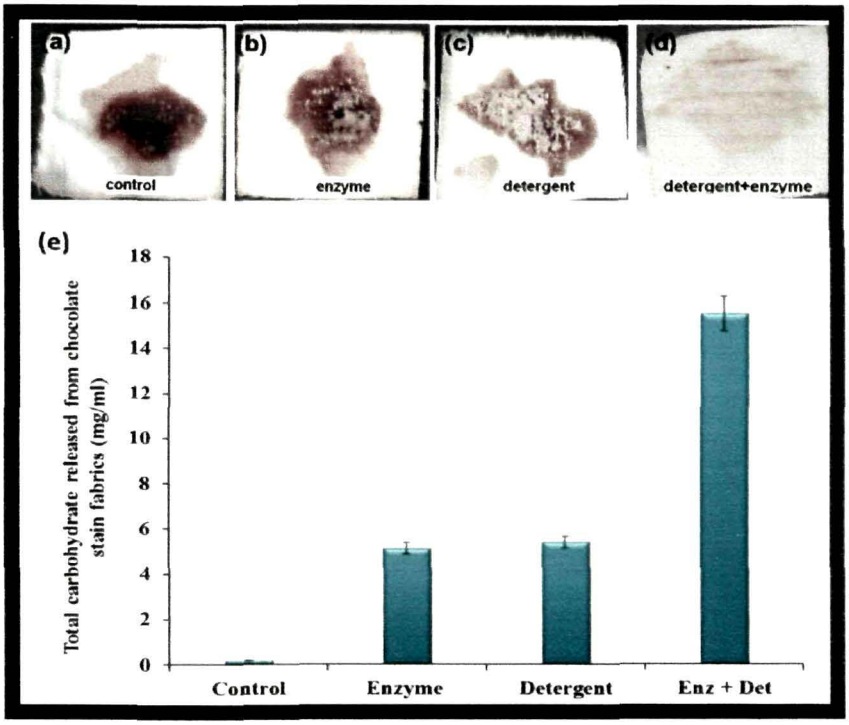

Figure 4.31: Wash performance analysis of chocolate-stained cloth pieces washed with (a) Control: tap water, (b) detergent (7 mg/ml), (c) purified α-amylase (500 U/ml) and (d) purified α-amylase (500 U/ml) + detergent (7 mg/ml). (e) Quantitative estimation of total carbohydrate release from the chocolate stained fabrics after 1 h incubation at 37°C with detergent, α-amylase, or detergent supplemented with α-amylase. Each bar graph represent mean ± S.D. (n = 3) and they vary significantly w.r.t. control (p-value ≤ 0.001).

4.8. Cloning and expression of another α-amylase (AmyBS-I) gene from *B. subtilis* strain AS01a

4.8.1. PCR amplification of α-amylase gene from B. subtilis strain AS01a and cloning it into a TA cloning vector

The PCR amplification of α-amylase gene from *B. subtilis* strain AS01a using species-specific primers resulted in amplification of approximately 1500 bp products (Figure 4.32).

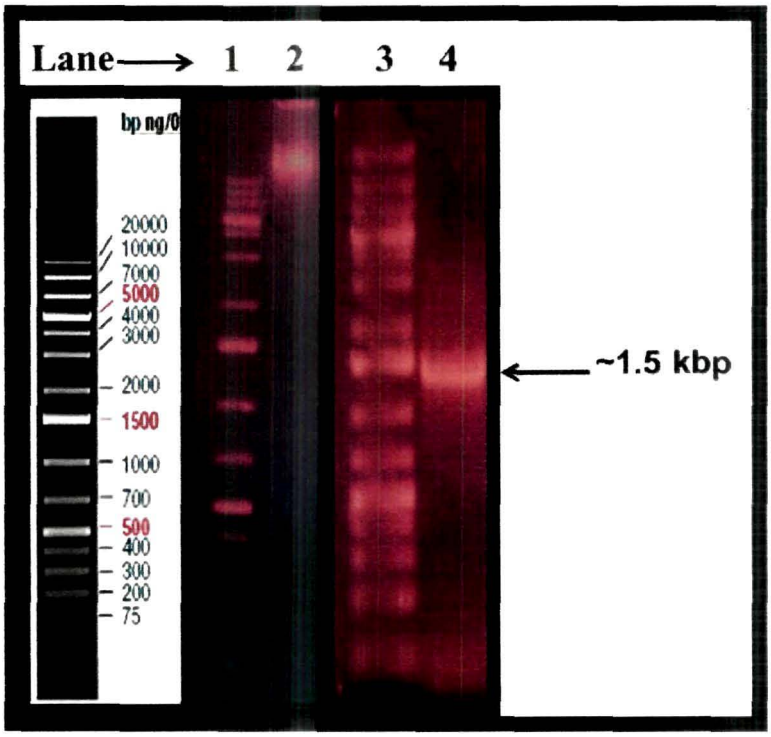

Figure 4.32: Agarose gel analysis of genomic DNA from *B. subtilis* strain AS01a and PCR-amplified α-amylase gene from its genomic DNA using BSF1 and BSR2 set of primers. Lanes 1 & 3; 1 kbp DNA ladder, lanes 2; genomic DNA from strain AS01a, lane 4; amplified PCR product (α-amylase gene)

The purified PCR-amplified product was then ligated into TA cloning vector and transformed into a competent *E. coli* DH5α cells, which resulted into appearance of a single white colony on the transformation plate containing IPTG and X-gal solution [Figure 4.33(a)]. The white colony was then screened for confirmation of the successful ligation of the insert by colony PCR, restriction digestion, and PCR amplification of ligated product by using recombinant TA vector. Restriction digestion of the recombinant TA vector with *Hind* III restriction enzymes yielded a single band of ~ 4500 bp on agarose gel, which is the expected size of recombinant TA vector (~3000 bp+1500 bp) [Figure 4.33 (b)].

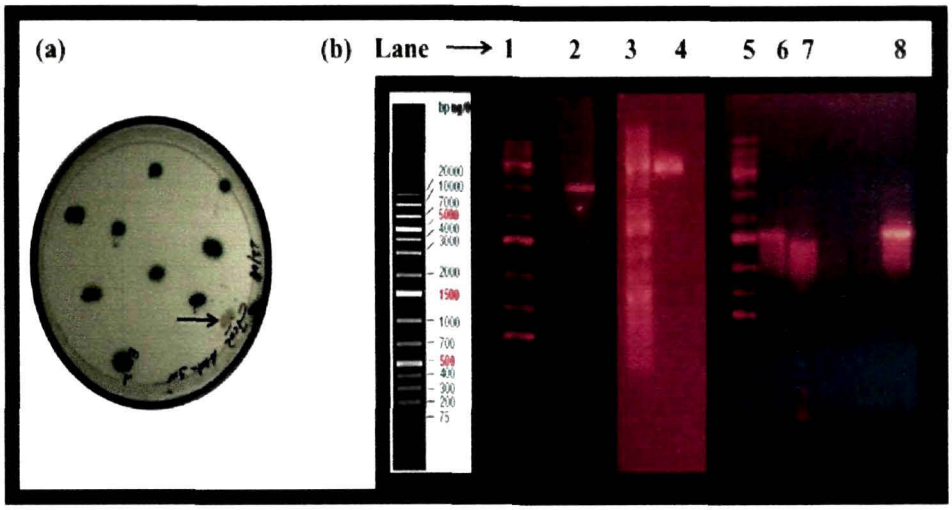

Figure 4.33: (a) Transformation plate containing recombinant TA vector (recombinant clone is marked with an arrow). (b) Agarose gel analysis of the recombinant clone lanes 1, 3 and 5, 1 kbp DNA ladder; lane 2, control plasmid; lane 4, *Hind* III-digested recombinant TA plasmid; lanes 6 and 7, colony PCR of recombinant clone; lane 8, amplified insert from recombinant TA plasmid using BSF1-BSR2 set of primers.

Colony PCR of recombinant clone and PCR amplification of ligated product in recombinant TA vector using BSF1-BSR2 set of primers resulted into appearance of 1500 bp amplified product on agarose gel [Figure 4.33 (b)]. The sequence analysis of the recombinant vector showed that the ligated product (α-amylase gene) is 94 to 97% identical with the other *Bacillus subtilis* α-amylase gene (Table 4.12). However, it was found that the cloned insert did not cover the complete open reading frame (ORF) of α-amylase gene.

Table 4.12: Sequence homology of cloned α-amylase gene from *B. subtilis* strain AS01a in TA cloning vector with the other bacterial α-amylase gene using blastn programme of NCBI database.

Description	Query cover	Maximum identity	Accession No.
B. subtilis strain OI1085 alpha-amylase (amyE) gene	100%	97%	FJ643607
B. subtilis amylase gene, a starch degrading enzyme	100%	97%	V00101
B. sp. HYC-1-3 amylase gene, complete cds	100%	97%	GU979526
B. amyloliquefaciens strain DL-3-4-1 amylase gene	100%	97%	GU979524
B. subtilis alpha-amylase gene	100%	97%	K00563
B. subtilis strain XL15 alpha-amylase gene	100%	96%	EF051632
B. subtilis strain BF7658 amylase precursor (amyE) gene	96%	97%	FJ463162
B. subtilis alpha-amylase gene	96%	96%	M79444
B. subtilis strain FS321 alpha-amylase gene	100%	95%	EU195860
B. subtilis strain A28 alpha-amylase gene	100%	94%	JX163316

4.8.2. Re-cloning of α-amylase gene into pET28a expression vector

Sequence analysis of the cloned insert showed that it did not cover the complete ORF of the α-amylase gene; therefore, a new set of primers was designed based on closely related α-amylase gene sequence (Table 4.12). Using the new set of primers and genomic DNA from stain AS01a, PCR was performed to amplify the complete ORF of α-amylase gene from *B. subtilis* strain AS01a. Agarose gel analysis of PCR-amplified products showed a band of ~2000 bp, which is in accordance with the expected gene size (Figure 4.34).

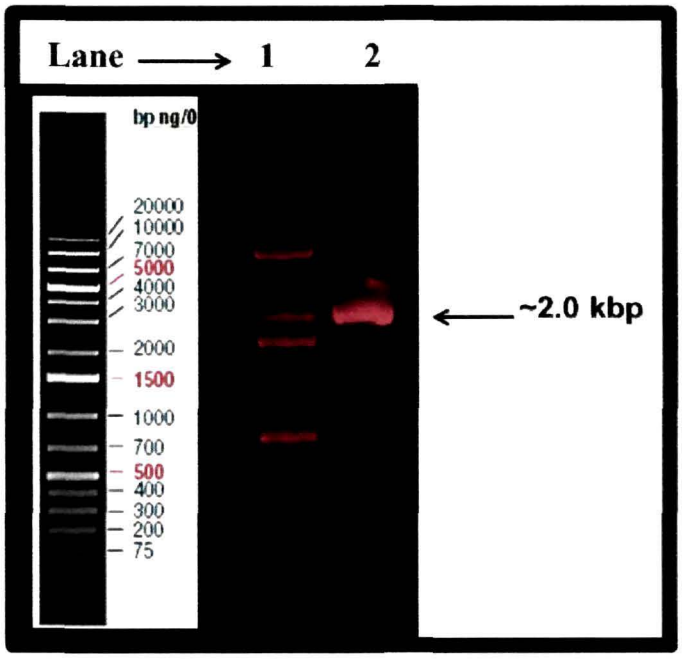

Figure 4.34: Agarose gel analysis of amplified α-amylase gene from strain AS01a using new set of primers (BSF3 and BSR4). Lane 1, 1 kb DNA ladder; lane 2, PCR amplified product.

Ligation of amplified PCR product into pET28a (+) expression vector and its subsequent transformation into competent *E. coli* BL21a cells resulted into numbers of white recombinant colonies on X-gal plate as seen in Figure 4.35(b).

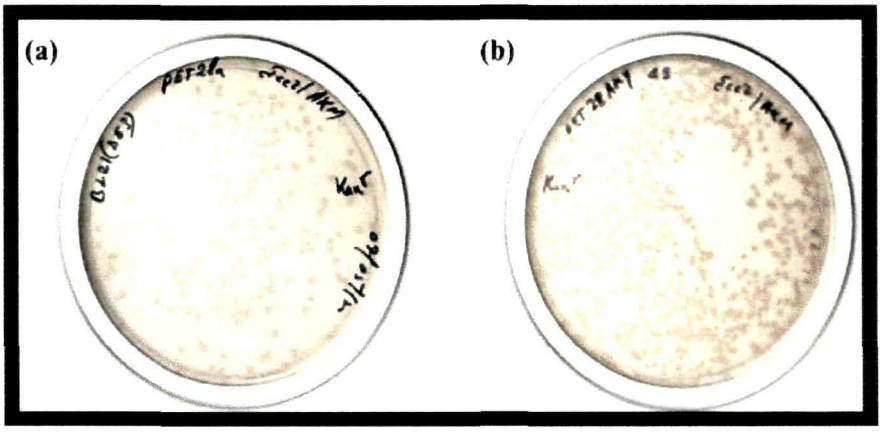

Figure 4.35: Transformed *E. coli* BL21a cells containing pET28a (a) and recombinant pET28a vector containing amylase gene insert from AS01a (b).

The double digestion of recombinant plasmid (pET28-BSAMY) obtained from transformed colonies resulted into separation of two bands on agarose gel according to the vector and the ligated insert size (Figure 4.36). The PCR amplification of pET28-BSAMY using T7 and gene (α-amylase) specific primers resulted in appearance of a PCR product of ~2 kbp on agarose gel, which was in accordance with the expected ligated products (Figure 4.36).

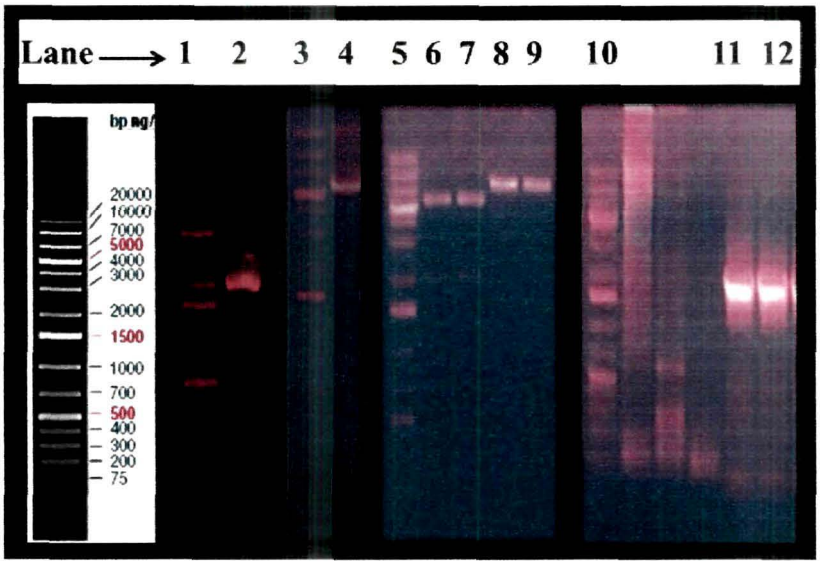

Figure 4.36: Agarose gel analysis of pET28-BSAMY vector by restriction digestion and PCR amplification. Lanes 1, 3, 5 and 10, 1 kb DNA ladder; lane 2, PCR amplified product (α-amylase gene); lane 4, *Hind* III-digested pET28a; lanes 6 and 7, double digestion of pET28-BSAMY with *Hind* III and *Xho* I; lanes 8 and 9, single digestion of pET28-BSAMY with *Xho* I; lane 11, PCR amplification of pET28-BSAMY using T7 primer; and lane 12, PCR amplification of pET28-BSAMY using gene specific primers.

The sequence analysis of the ligated insert in recombinant vector (pET28-BSAMY) shows that it was 97-99% similar to the *B. subtilis* α-amylase gene (Table 4.13). The cloned α-amylase gene from strain AS01a shows close relatedness (99% similarity) with the α-amylase gene from *B. subtilis* strain OI1085 (Table 4.13). Further, sequence analysis of the cloned insert also revealed that it covered the complete ORF. The nucleotide sequence generated from the cloned insert was

deposited in the public NCBI database under the Genbank accession number KC113313.

Table 4.13: Sequence homology of cloned α-amylase gene from strain AS01a in pET28a vector (pET28-BSAMY) with other bacteria using blastn programme of NCBI database

Description	Query cover	Maximum identity	Accession No.
Bacillus subtilis strain AS01a alpha amylase gene	100%	100%	KC113313
B. subtilis strain OI1085 alpha-amylase (amyE) gene	100%	99%	FJ643607
B. subtilis amylase gene, a starch degrading enzyme	100%	99%	V00101
B. sp. HYC-1-3 amylase gene, complete cds	99%	99%	GU979526
B. amyloliquefaciens strain DL-3-4-1 amylase gene	100%	99%	GU979524
B. subtilis subsp. *subtilis* str. 168 amylase gene	100%	99%	AL009126
B. subtilis strain HLSSK-3 amylase gene, complete cds	99%	99%	GU979525
B. subtilis strain XL15 alpha-amylase gene	100%	98%	EF051632
B. subtilis strain I527 amylase gene, complete cds	100%	97%	GU979529
B. subtilis strain BF7658 amylase precursor (amyE) gene	71%	99%	FJ463162

The deduced amino acid sequence obtained from the cloned α-amylase insert sequence shows that it contains a signal peptide sequence (SPS) at its N-terminus, which can facilitate the extracellular expression of recombinant protein (AmyBS-I) into the culture media (Figure 4.37). The amino acid sequence analysis of AmyBS-I also suggests that it is 99% similar to the *B. subtilis* HLSSK-3 (ADH93704), and *B. subtilis* strain OI1085 (ACM91731), whereas it showed 98% similarity with *B. amyloliquefaciens* DL 341(ADH93703) and *B. subtilis* (ABW75769) (Figure 4.37). The AmyBS-I was also found to contain the four most conserved regions including the catalytic and Ca^{2+} binding site of α-amylase enzyme (Figure 4.37). The calculated pI/Mw of the AmyBS-I was estimated to be 5.8/72387 Dalton and 5.53/68875.6 Dalton for the precursor (containing SPS) and for the mature protein, respectively.

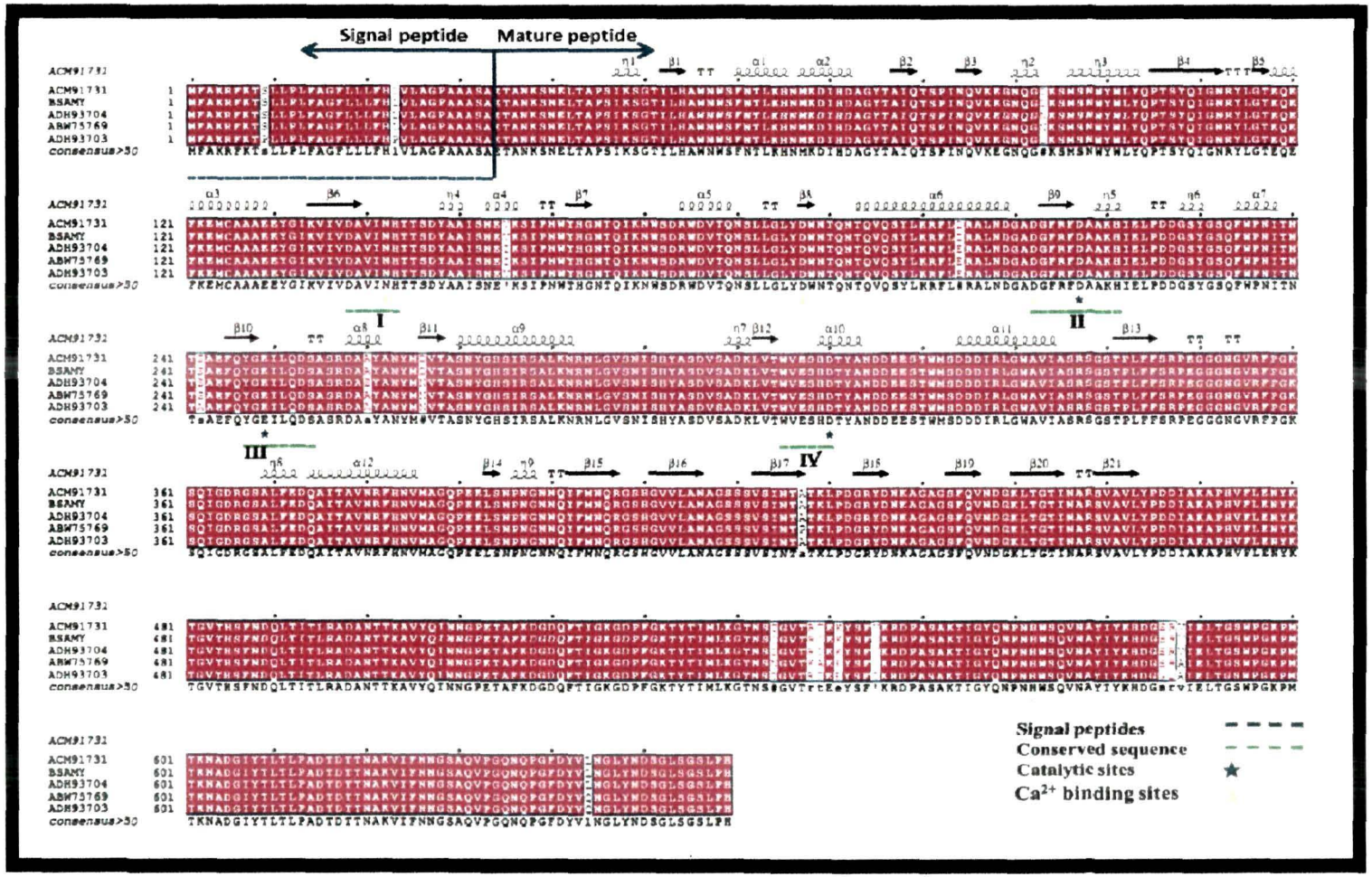

Figure 4.37: Multiple sequence alignment of deduced amino acid sequence of amyBS-I with homologous α-amylases. The secondary structure assignments of the AmyBS-I is indicated at the top of the alignment. The TTT and TT letters represent strict alpha and beta turns, respectively.

4.8.3. Expression analysis of recombinant protein

Considering the importance of targeting recombinant protein outside the cell membrane, primers were designed to clone the α-amylase gene along with its signal peptide for expression of recombinant protein outside the cell membrane. To check the expression of active recombinant protein outside the cell membrane into the surrounding medium, the recombinant cells were induced on starch agar plates and as well as in liquid broth. In Figure 4.38 (a), we can see that the four recombinant clones screened on starch agar plates show formation of zone of starch hydrolysis around the colonies. This suggests that the recombinant clones are capable of expression and secretion of active recombinant protein outside the cell membrane. Further, the broth culture study also showed that recombinant clones effectively extracellularly express the recombinant protein into the culture media (Figure 4.38b). Therefore, the recombinant clones containing the AmyBS-I gene can successfully express recombinant protein into active form outside the cell membrane using its own (*Bacillus*) signal peptide.

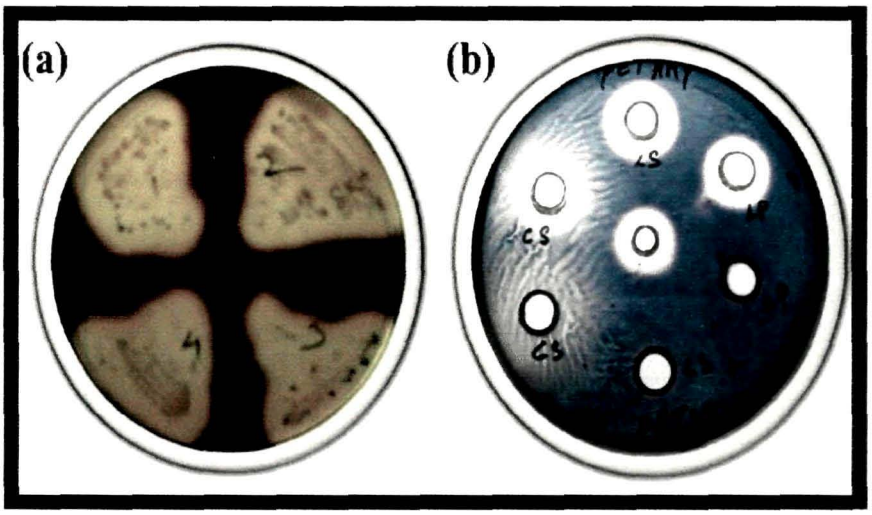

Figure 4.38: Starch agar plate analysis of extracellular expression of recombinant amylase from *B. subtilis* AS01a in *E. coli*. (a) Streak plate method (b) culture broth analysis (CS: culture supernatant; LP: lysed cell pellets and LS: lysed cells culture supernatant).

4.8.4. Statistical optimization of culture conditions for extracellular expression of AmyBS-I

With the help of its native *B. subtilis* signal peptide, AmyBS-I was successfully expressed outside the cell membrane, however, SDS-PAGE analysis of expressed AmyBS-I showed that majority of the target protein was accumulated as inclusion bodies in the *E. coli* cytoplasm (Figure 4.39). Therefore, in order to reduce the formation of inclusion bodies and for efficient secretion of functionally active AmyBS-I into the culture medium, the *E. coli* culture condition was optimized using RSM.

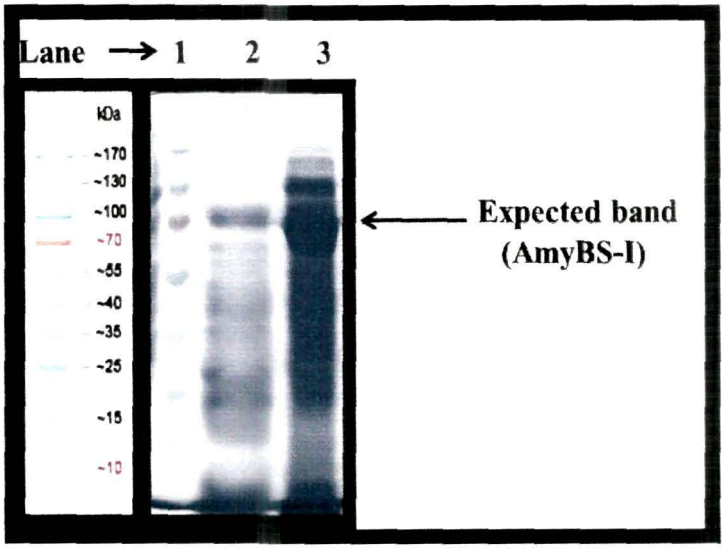

Figure 4.39: SDS-PAGE analysis of overexpressed AmyBS-I in *E. coli*. Lane 1, pre-stained protein marker; lane 2, cell free supernatant; lane 3, cell pellet extract.

Based on review of literature, the four significant factors such IPTG concentration, induction-temperature, post-induction period and EDTA concentration were found to be most crucial factors for the expression of recombinant protein outside the cell membrane [375-377]. Therefore, these four factors were optimized using RSM for the efficient expression of recombinant α-amylase from *E. coli* into the culture media. The design matrix (based on central composite design) showing different levels of experimental run with their outmost responses of both predicted and observed values are presented in the Table 4.14 below.

Table 4.14: Design matrix in both coded and actual (in bracket) values with their corresponding experimental and predicted responses (enzyme activity) for the extracellular expression of AmyBS-I in *E. coli* culture media. The actual values represent mean ± S. D. (n = 3), p-value ≤ 0.001.

Run Order	IPTG (mM) (C1)	Time of post Induction (h) (C2)	Temperature (°C) (C3)	EDTA (mM) (C4)	Enzyme activity (U/ml)	
					Predicted values	Actual values
1.	-1.0 (0.2)	-1.0 (12)	-1.0 (20)	-1.0 (17)	95.28	101.67 ± 5.0
2.	1.0 (1)	-1.0 (12)	-1.0 (20)	-1.0 (17)	111.61	116.79 ± 5.8
3.	-1.0 (0.2)	1.0 (24)	-1 0 (20)	-1.0 (17)	172.45	186 83 ± 9.3
4.	1.0 (1)	1.0 (24)	-1.0 (20)	-1.0 (17)	131.6	136 51 ± 6.8
5.	-1.0 (0.2)	-1.0 (12)	1.0 (30)	-1.0 (17)	124.08	123 56 ± 6.2
6.	1.0 (1)	-1.0 (12)	1.0 (30)	-1.0 (17)	154.31	159.73 ± 7.9
7.	-1.0 (0.2)	1.0 (24)	1.0 (30)	-1.0 (17)	151.37	159.35 ± 7.9
8.	1.0 (1)	1.0 (24)	1.0 (30)	-1.0 (17)	124.41	124 98 ± 6.2
9.	-1.0 (0.2)	-1.0 (12)	-1.0 (20)	1.0 (34)	117.25	129 ± 6.4
10.	1.0 (1)	-1.0 (12)	-1.0 (20)	1.0 (34)	121.11	120.3 ± 6.0
11.	-1.0 (0.2)	1.0 (24)	-1.0 (20)	1.0 (34)	215.59	217.34 ± 10.8
12.	1.0 (1)	1.0 (24)	-1.0 (20)	1.0 (34)	162.26	175.11 ± 8.7
13.	-1.0 (0.2)	-1.0 (12)	1 0 (30)	1.0 (34)	92.24	94.5 ± 4.7
14.	1.0 (1)	-1.0 (12)	1.0 (30)	1.0 (34)	109.99	107.93 ± 5.4
15.	-1.0 (0.2)	1.0 (24)	1.0 (30)	1.0 (34)	140.69	147.84 ± 7.4
16.	1.0 (1)	1.0 (24)	1.0 (30)	1.0 (34)	101.26	102.04 ± 5.1
17.	-2.0 (0)	0.0 (18)	0.0 (25)	0.0 (25.5)	122.35	98.255 ± 4.9
18.	2.0 (1.4)	0.0 (18)	0.0 (25)	0.0 (25.5)	150.74	144 82 ± 7.2
19.	0.0 (0.6)	-2.0 (6)	0.0 (25)	0.0 (25.5)	109.46	105 414 ± 5.3
20.	0.0 (0.6)	2.0 (30)	0.0 (25)	0.0 (25.5)	177.9	162.482 ± 8.1
21.	0.0 (0.6)	0.0 (18)	-2.0 (15)	0.0 (25.5)	114.18	95 735 ± 4.7
22.	0.0 (0.6)	0.0 (18)	2.0 (35)	0.0 (25.5)	81.98	80.95 ± 4.0
23.	0.0 (0.6)	0.0 (18)	0.0 (25)	-2.0 (8.5)	127.92	115.519 ± 5.8
24.	0.0 (0.6)	0.0 (18)	0.0 (25)	2.0 (42.5)	126.74	119.657 ± 5.9
25.	0.0 (0.6)	0.0 (18)	0.0 (25)	0.0 (25.5)	51.21	51.86 ± 2.5
26.	0.0 (0.6)	0.0 (18)	0.0 (25)	0.0 (25.5)	51.21	54.28 ± 2.7
27.	0.0 (0.6)	0.0 (18)	0.0 (25)	0.0 (25.5)	51.21	52.26 ± 2.6
28.	0.0 (0.6)	0.0 (18)	0.0 (25)	0.0 (25.5)	51.21	56 28 ± 2.8
29.	0.0 (0.6)	0.0 (18)	0.0 (25)	0.0 (25.5)	51.21	50.86 ± 2.5
30.	0.0 (0.6)	0.0 (18)	0.0 (25)	0.0 (25.5)	51.21	52.26 ± 2.6

By processing the above variables, a mathematical model that represents the second order polynomial was obtained as shown in Eq. (4.2). The model term was evaluated by multiple regression analysis to predict the optimum cultivation conditions for maximizing the extracellular expression of recombinant AmyBS-I. All the terms regardless of their significance are included in the following equation:

$$Y = 390.89 - 135.51C_1 - 8.95C_2 - 10.5C_3 - 23.36C_4 + 173.57C_1^2 + 0.64C_2^2 + 0.46C_3^2 + 3.04C_4^2 - 5.95C_1C_2 + 1.74C_1C_3 - 3.12C_1C_4 - 0.42C_2C_3 + 0.35C_2C_4 - 1.08C_3C_4 \quad (3)$$

Where Y is the response i.e. enzyme activity (U/ml) and C_1-C_4 are the actual values of the test variables where C_1 represents IPTG concentration (mM); C_2 time of post induction (h); C_3 temperature of induction (°C) and C_4 represents EDTA concentration (mM).

The coefficient of the model including the significance of each coefficient was determined by *p*-values, the model terms with the *p*-value (*Probability*> *F*) less than 0.05 are considered to be significant. In Table 4.15, we can see that C_1, C_2, C_3, C_1^2, C_2^2, C_3^2, C_4^2, C_1C_2, C_2C_3, and C_3C_4 are significant model terms. The analysis of variance (ANOVA) by Fisher's statistical test was conducted for the quadratic model and the results demonstrated that the computed *F*-value for the model was 25.14, which implies that the model was significant (Table 4.15) There was only a 0.01% chance that a "Model *F*-Value" could occur due to noise. The model's fitness accuracy can also be checked by determining the coefficient of correlation ($R^2 = 0.959$). It was obvious from the value of R^2 that the deduced model could not explain only 4.1% of the total variation (Table 4.15). The value of adjusted R^2 (0.92) also supported the significance of the model (Table 4.15).

Table 4.15: ANOVA for the response surface quadratic model for the extracellular expression of recombinant α-amylase from the *E. coli*

Source	Sum of Squares	Degrees of freedom	Mean Squares	*F*-value	Prob. *(P)*> *F*
Model	51933.7	14	3709.5	25.14	< 0.0001
IPTG (C_1)	901.9	1	901.9	6.1	0.0259
Time (C_2)	799.5	1	799.5	5.4	0.0343
Temperature (C_3)	564.8	1	564.8	3.8	0.0693
EDTA (C_4)	946.3	1	946.3	6.4	0.0230
$(C_1)^2$	14921.9	1	14921.9	101.1	< 0.0001
$(C_2)^2$	14833.2	1	14833.2	100.5	< 0.0001
$(C_3)^2$	3810.6	1	3810.6	25.8	0.0001
$(C_4)^2$	10049.2	1	10049.2	68.1	< 0.0001
C_1* C_2	3270.1	1	3270.1	22.2	0.0003
C_1* C_3	192.9	1	192.9	1.3	0.2707
C_1* C_4	155.6	1	155.6	1.0	0.3207
C_2* C_3	2488.5	1	2488.5	16.9	0.0009
C_2* C_4	448.2	1	448.2	3.0	0.1018
C_3* C_4	2896.0	1	2896.0	19.6	0.0005
Residual (error)	2213.0	15	147.5		
Lack of fit	2193.6	10	219.4	56.64	0.0002
Pure error	19.4	5	3.9		
Total	54146.7	29			

R^2 = 0.959, Adj. R^2 = 0.92, Pred. R^2 = 0.79 and CV= 10.58%

The three-dimensional response surface plot and two-dimensional contour plot are the graphical representations for the regression equation and are used to investigate the interaction amongst the variables. Figure 4.40 shows the response surface curves, and contour plots for variations in extracellular amylase activity as a function of two variables at a time, while the other variables were maintained at their respective zero level. From Figures 4.40 (A-B), we can conclude that lowering the IPTG concentration as well as temperature has a positive effect on high-level secretion of recombinant α-amylase into the culture medium. On the other hand, increased EDTA concentration as well as increased incubation time result in better

expression and secretion of recombinant α-amylase into the culture medium (Figure 4.40).

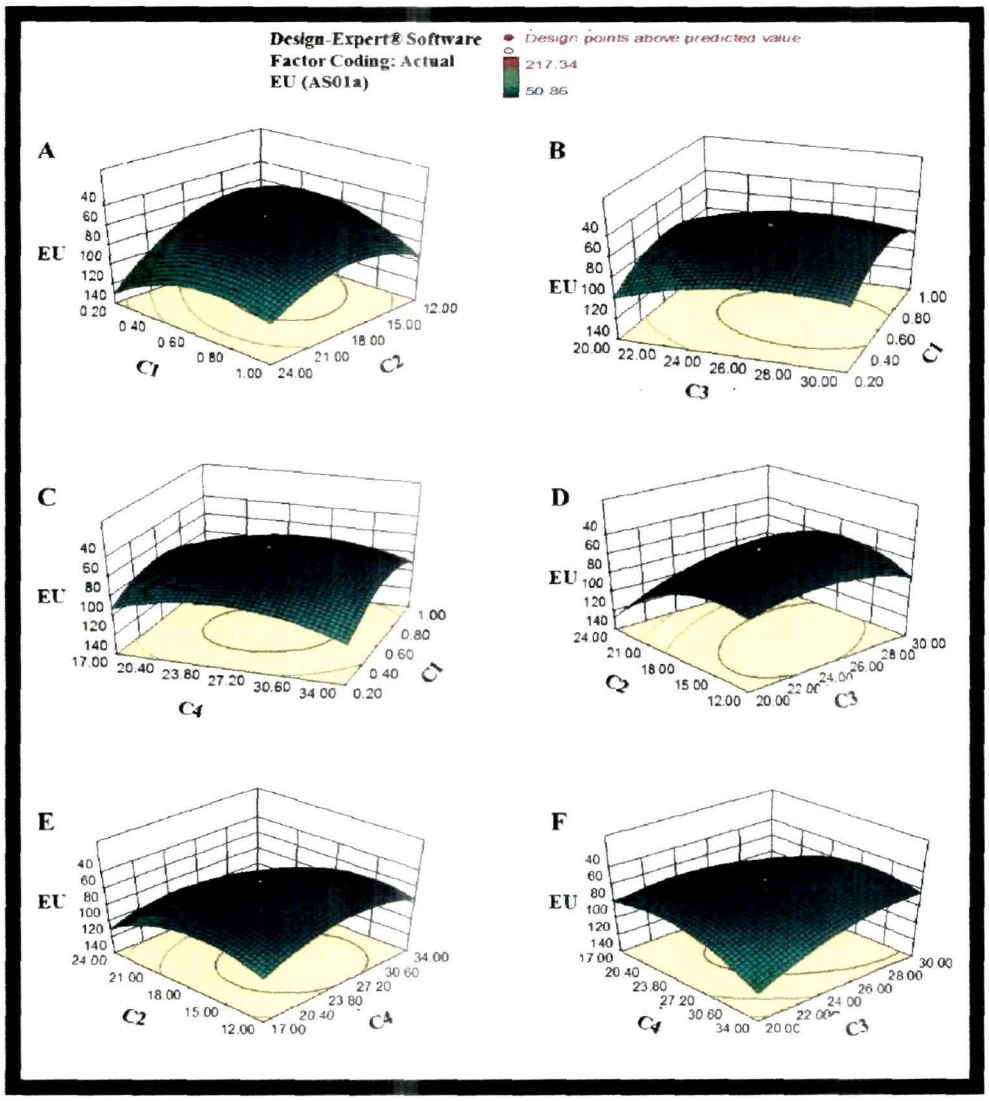

Figure 4.40: Response surface plots showing interaction effect of test variables on extracellular overexpression of AmyBS-I from *E. coli* BL21 cells. (A) C_1 vs C_2, (B) C_1 vs C_3, (C) C_1 vs C_4, (D) C_2 vs C_3, (E) C_2 vs C_4 and (F) C_3 vs C_4.

The four optimized test variables obtained from regression Eq. 4.2 using numerical method, were IPTG concentration = 0.15 mM, post induction time = 30 h, temperature of incubation = 15°C and EDTA concentration = 42.5 mM. The predicted value for the extracellular AmyBS-I activity at optimized conditions was

calculated as 530.01 U/ml (Figure 4.41). The actual experimental value was 478.24 ± 23.9 U/ml (mean ± S.D., n=3, P = <0.001), which was in close agreement with the predicted value, thus justifying the suitability of the RSM model applied in the present study for enhancing the extracellular secretion of AmyBS-I. The model exhibited a significant improvement in the extracellular expression of recombinant α-amylase (approx. 9-fold) under optimized conditions as compared to non-optimized conditions. Our study showed that the culture conditions such as low IPTG concentration, low temperature, and increase in post-induction time play a critical role in the heterologous extracellular expression of recombinant protein.

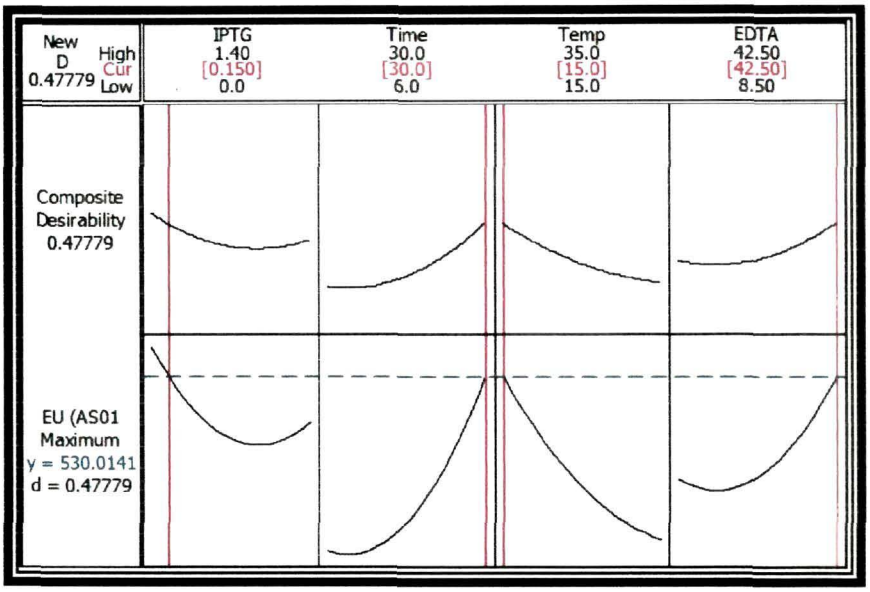

Figure 4.41: Optimization plot showing the optimum value for maximum extracellular amylase (AmyBS-I) production from *E. coli* BL21 cells.

4.8.5. Isolation and purification of recombinant protein (AmyBS-I)

Isolation and purification of AmyBS-I were carried out by growing the recombinant clones in optimized culture conditions. The fractionation of cell free culture supernatant through hydrophobic interaction column (HIC) resulted into elution of bound recombinant protein (AmyBS-I) into a single peak with 0% salt gradient (Figure 4.42).

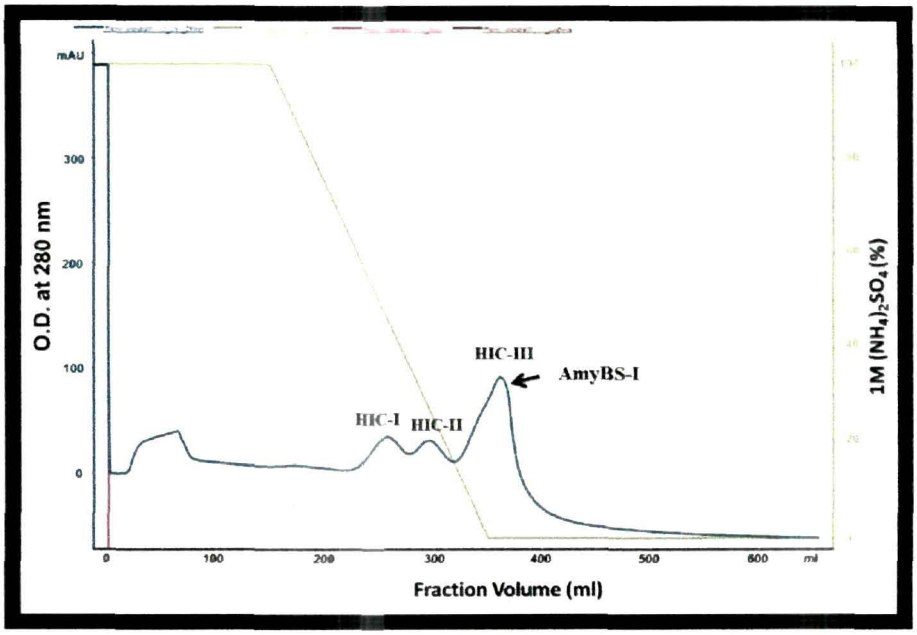

Figure 4.42: Elution profile of recombinant α-amylase (AmyBS-I) from *E. coli* BL21 cells on phenyl-sepharose column. The active peak that exhibits α-amylase activity is marked with an arrow on the chromatogram.

Further fractionation of AmyBS-I through gel-filtration column resulted into separation of protein into three peaks (Figure 4.43). However, only GF-II peak showed the amylolytic activity (Figure 4.43).

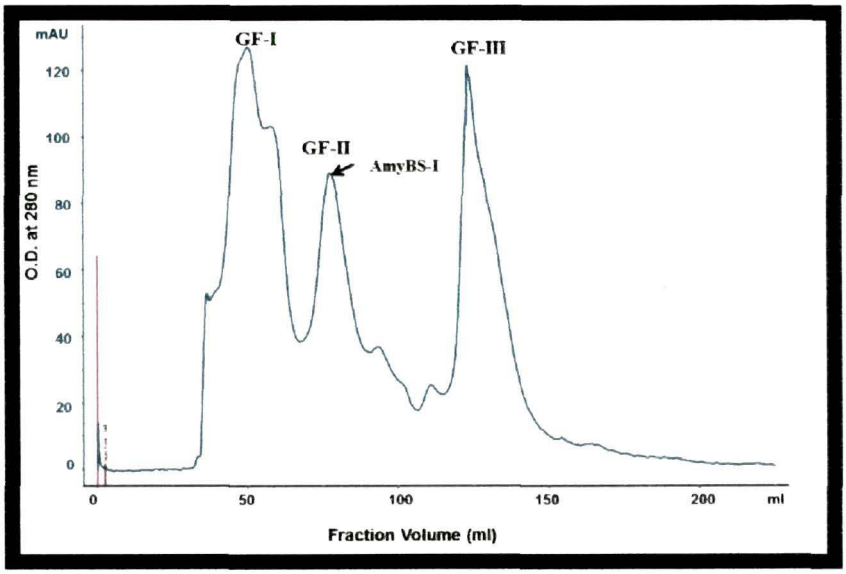

Figure 4.43: Elution profile of recombinant α-amylase (AmyBS-I) on Sephacryl S-200 column. The active peak that exhibits amylase activity is marked with an arrow on the chromatogram.

Homogeneity analysis of purified active GF-II fraction by SDS-PAGE analysis showed a single band of approximately 69.0 kDa under reduced condition, which is in accordance with the gene size (Figure 4.44). Zymographic analysis of the purified recombinant protein showed a single clear zone of starch hydrolysis corresponding to a protein of 69.0 kDa (Figure 4.44). This purified enzyme was named AmyBS-I. The study also suggests that the presence of isoform of recombinant α-amylase (AmyBS-I), as the molecular mass of AmyBS-I differs from the wild type α-amylase (Amy-I) purified from the same parent strain (*B. subtilis* strain AS01a).

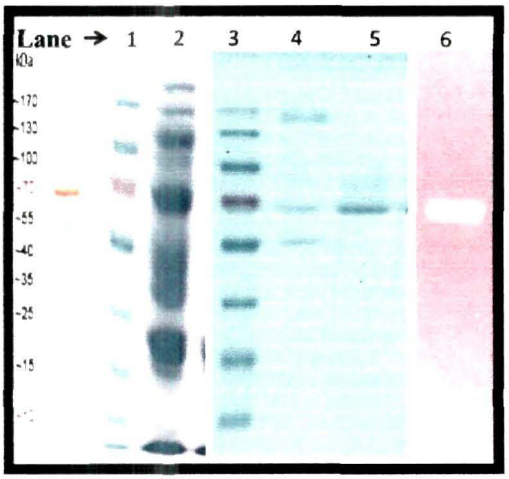

Figure 4.44: SDS-PAGE analysis of purified AmyBS-I. Lanes 1 and 3, Fermentas pre-stained protein markers; lane 2, crude culture supernatant (30 µg); lane 4, phenyl-sepharose pooled fraction (25 µg); lane 5, purified gel filtration fraction (GF-II, 25 µg); lane 6, zymograph of purified AmyBS-I (20 µg).

Summary of purification of the recombinant α-amylase AmyBS-I is shown in Table 4.16. The purification chart shows that AmyBS-I was purified 3.9-fold with 19.5% of recovery of the total α-amylase by the two-step purification process (Table 4.16).

Table 4.16: Summary of purification of AmyBS-I, data represent a typical experiment.

Purification steps	Total protein (mg)	Total activity (Units)	Specific activity (U/mg)	Enzyme recovery (%)	Purification fold
Culture supernatant	120.0	15625.0	130	100	1.0
Phenyl-sepharose	80.0	11400.0	142.5	72.9	1.1
Sephacryl S-200	6.0	3040.0	506.7	19.5	3.9

4.8.6. Biochemical characterization of recombinant α-amylase

4.8.6.1. Determination of optimum pH and temperature

The plotting of enzyme activity against pH of the assay medium revealed that the enzyme activity increases in parallel with pH from 4.0 to 6.0 but beyond pH 6.0, activity started declining (Figure 4.45). However, AmyBS-I retains ~80 % of its original activity (activity at pH 6.0) at pH 8.0 (Figure 4.45).

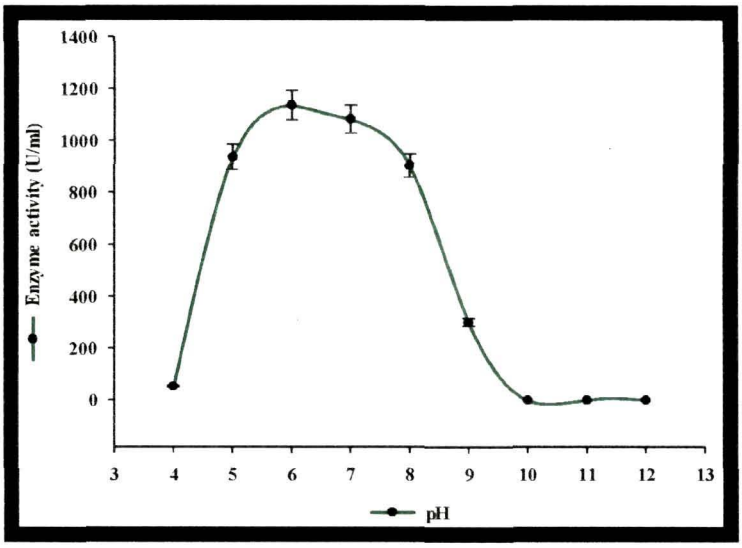

Figure 4.45: Graphs showing pH dependence of α-amylase activity of AmyBS-I. Each value represents mean ± S.D. of triplicate determinations having *p*-value ≤ 0.001 compared to control.

With the rise in temperature from 30°C to 70°C, there was increase in enzyme activity but after 70°C, a sharp fall in enzyme activity was noticed, suggesting that AmyBS-I has optimal activity at 70°C (Figure 4.46).

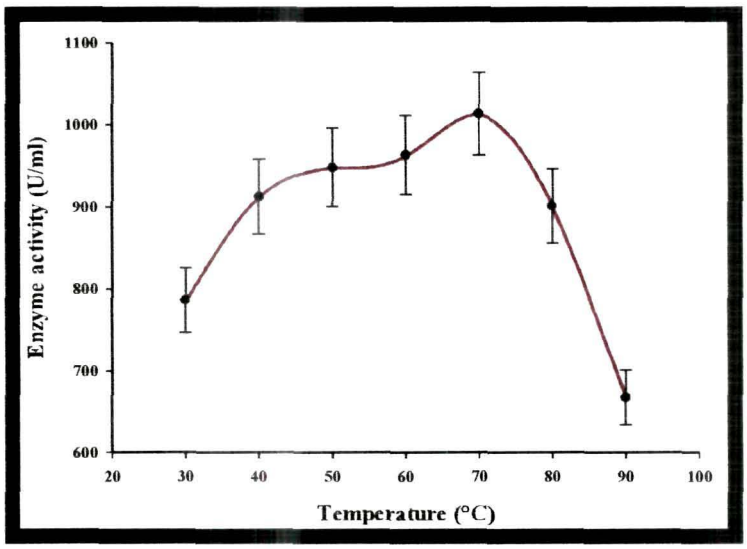

Figure 4.46: Graphs showing temperature profile for the amylase activity of recombinant enzyme AmyBS-I. Each data represents mean ± S.D. (n =3), with *p*-value ≤ 0.001 compared to control.

4.8.6.2. Thermostability of AmyBS-I

From thermostability study (Figure 4.47), we can conclude that the enzyme is stable upto 70°C both in presence and in absence of Ca^{2+}. However, the enzyme lost 80% of its original activity at 80°C (Figure 4.47). Further, Ca^{2+} ion does not contribute any significant stability to the purified enzyme, which suggests that AmyBS-I is a Ca^{2+} independent α-amylase enzyme (Figure 4.47) suggesting its potential candidature for starch industry due to various advantages.

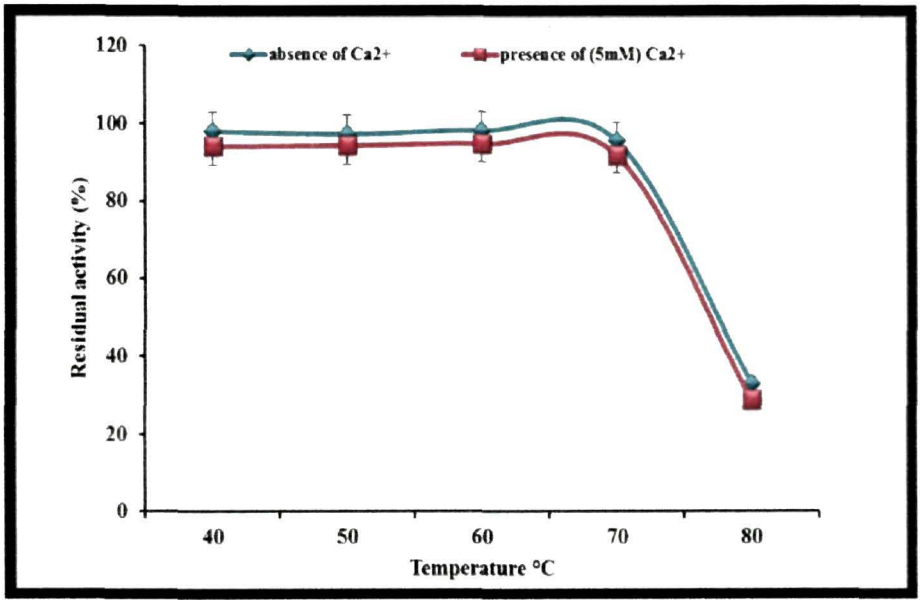

Figure 4.47: Effect of temperature on stability of purified recombinant enzyme (AmyBS-I) both in presence (■) and in absence (◆) of (5 mM) Ca^{2+} ion.

4.8.6.3. Kinetics of starch hydrolysis by AmyBS-I

From Lineweaver-Burk plot, the K_m and V_{max} values of AmyBS-I were calculated as 2.7 ± 0.14 mg/ml and 454.0 ± 22.7 µmol/min/mg of starch, respectively (Figure 4.48).

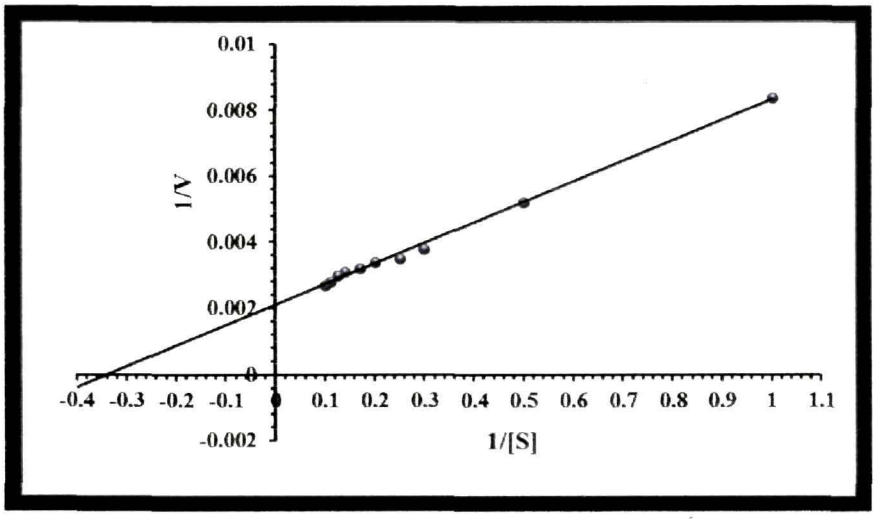

Figure 4.48: Lineweaver-Burk plot to determine K_m and V_{max} values of AmyBS-I. Each data point is a mean of triplicate determinations.

4.8.6.4. Effects of various metal ions, inhibitors, metal chelators and oxidizing agents on AmyBS-I activity

The starch hydrolysis of AmyBS-I was greatly influenced by the presence of metal ions by either activating or inhibiting the enzyme activity (Table 4.17). For example, enzyme activity in presence of Fe^{2+}, Cu^{2+}, Zn^{2+}, and Hg^{2+} was inhibited upto 70.5 to 94.5% as compared to control (Table 4.17). In contrast, other metal ions such as Co^{2+}, Ni^{2+}, Mn^{2+}, and Mg^{2+} were found to activate the enzyme beyond control levels (Table 4.17). Further, EDTA, a metal chelating agent did not show any adverse effect on the enzyme activity suggesting that the AmyBS-I is a metal independent enzyme (Table 4.17). However, in the presence of PMSF, AmyBS-I lost around 22% of its original activity suggesting the presence of serine in the active site, which is also evident from the AmyBS-I sequence analysis. The purified enzyme was also inhibited by oxidizing agent such as sodium perborate and surfactants such as SDS, Tween 20/80; however, the activity of AmyBS-I was slightly enhanced in presence of organic solvents such as acetonitrile and methanol (Table 4.17).

Table 4.17: Effects of various chemical/group modifying agents on activity of AmyBS-I. Values are mean ± SD of triplicate determinations (n=3). The values with same superscript do not differ significantly w.r.t. control group (p-value > 0.05).

Effectors	% Activity
Control (without effectors)	**100[a]**
Cu^{2+}	20.8 ± 1.1
Fe^{2+}	29.5 ± 1.5
Co^{2+}	114 ± 5.7
Hg^{2+}	5.5 ± 0.3
Ca^{2+}	98.2 ± 4.9[a]
Zn^{2+}	15.4 ± 0.8
Ni^{2+}	114.97 ± 5.7
Mn^{2+}	115.52 ± 5.7
Mg^{2+}	117.82 ± 5.9
EDTA (2mM)	119.68 ± 5.9
PMSF(2mM)	68.8 ± 3.4
NaCl	98.05 ± 4.9[a]
$NaBO_3$(5mM)	43.4 ± 2.1
Urea(2M)	115.42 ± 5.8
SDS (1% w/v)	83.4 ± 4.2
Tween-20 (1% v/v)	67.64 ± 3.4
Tween-80 (1% v/v)	34.48 ± 1.7
Acetonitrile (30%)	115.49 ± 5.7
Methanol (30%)	118.89 ± 5.9

4.8.6.5. TLC analysis of the end-product of starch hydrolysis by AmyBS-I

TLC analysis of end-product from starch hydrolysis by AmyBS-I demonstrates the formation of oligosaccharide mixtures after 1 h of treatment while after 3 h of treatment, maltose and glucose were observed as the major end-product (Figure 4.49). However, after 12 h of treatment of soluble starch with AmyBS-I, formation of glucose (82.5%), surpassed the maltose production (17.5%) (Figure 4.45 and Table 4.18). This result proves that AmyBS-I is an endo-acting α-amylase enzyme.

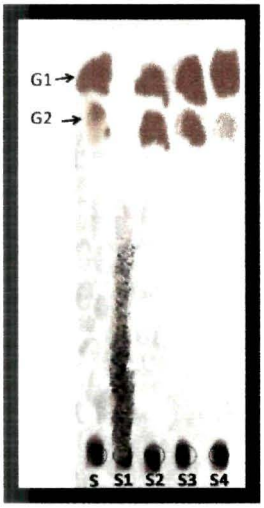

Figure 4.49: TLC analysis of end product of starch hydrolysis by AmyBS-I. S = standard sugar (G1: maltose and G2: glucose), S1, S2, S3 and S4 are starch hydrolyzed products after 1, 3, 6 and 12 h treatment with AmyBS-I respectively.

Table 4.18: Densitometer analysis of total starch hydrolyzed end-products by AmyBS-I at different time interval. Values are mean ± SD, where n = 3. The values differ significantly w.r.t. control (p-value ≤ 0.001).

Sugar	Percentage of different hydrolyzed end products			
	1h	3h	6h	12h
G1 (Glucose)	0	66.5±3.3	71.6±3.5	82.5±4.1
G2 (Maltose)	0	33.4±1.6	28.4±1.4	17.5±1.0

4.8.7. Possible industrial application of AmyBS-I

4.8.7.1. Raw starch digestion capabilities of AmyBS-I

The raw starch digestion capacity of AmyBS-I showed that after 6 h of incubation, it could hydrolyze wheat, potato, and rice raw starches up to 61 ± 3.0%, 58 ± 2.9% and 44 ± 2.2% (mean ± S.D., p-value ≤ 0.05), respectively. Further, SEM analysis of these digested raw starches showed that AmyBS-I forms pits and deep holes on the surfaces of all the tested raw starches (Figure 4.50).

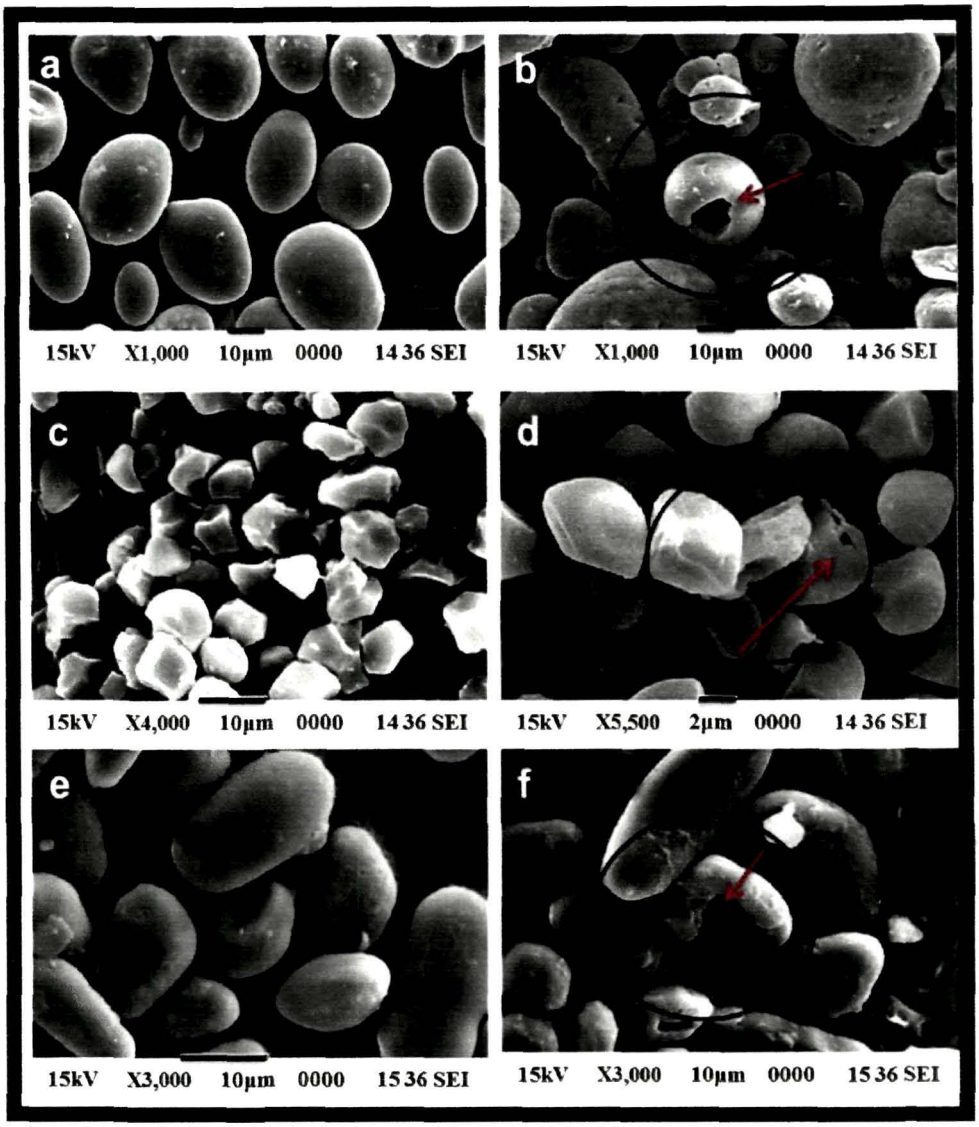

Figure 4.50: SEM images of raw starch granules before and after hydrolysis with AmyBS-I for 6h. (a) Untreated potato starch, (b) AmyBS-I treated potato starch, (c) untreated rice starch, (d) AmyBS-I treated rice starch, (e) untreated wheat starch; and (f) AmyBS-I treated wheat starch. Arrow indicates hole and pit formation on treated starch granules.

4.8.7.2. Application of AmyBS-I in bread amelioration

Supplementation of recombinant AmyBS-I and commercial α-amylase to wheat dough resulted in increase in shelf-life of bread; however, AmyBS-I

supplementation resulted in a considerably higher anti-staling effect as compared to control ones. It was also found that the AmyBS-I supplemented bread has a better loaf volume as compared to bread supplemented with commercial amylase (Figure 4.51).

Figure 4.51: Crumb structure of loaf prepared without supplementation (control) or supplementation with Himedia or AmyBS-I enzyme.

Further, bread supplementation with AmyBS-I resulted in better crumb color, softness, sugar and moisture content as compared to the commercial α-amylase supplemented or control bread (Table 4.19). The moisture content of AmyBS-I supplemented bread was found within the range of 35-40%, suggesting adequate softness. Sugar content of bread that improves the taste, crust color, and toasting qualities of bread was also found to be higher in case of AmyBS-I supplemented bread as compared to commercial amylase supplemented bread or control (Table 4.19). The brownness index (BI) of AmyBS-I supplemented bread was also found comparable with the commercial α-amylase supplemented bread (Table 4.19).

Table 4.19: Comparisons and properties of bread supplemented with commercial amylase and AmyBS-I.

Parameter	Control	Amylase (Himedia)	AmyBS-I
Weight of dough (g)	100 ± 5.0	100 ± 5.0	100 ± 5.0
Weight of bread (g)	87.5 ± 4.4[a]	76.5 ± 3.8[a]	77 ± 3.8[a]
Dough rise (cm)	2.2 ± 0.1[a]	2.9 ± 0.2[a]	3.4 ± 0.2[a]
Shelf-life (days)	4	5	5
Bread moisture (%)	42.1 ± 2.1[a]	39.8 ± 1.9[a]	39.1 ± 1.9[a]
Reducing sugars (mg/g of bread)	37.6 ± 1.8[a]	42.4 ± 2.1[a]	44.0 ± 2.2[a]
Overall acceptability[b]	++	+++	++++
Bread Color[c]			
***L*-value**	49.3	48.1	50.9
***a*-value**	1.2	2.5	2.9
***b*-value**	12.7	14.0	14.9

Control bread was made without supplementation of amylase to the dough.

[a]Each value is expressed as mean ± standard error (n =3). Means followed by a different letter within the same row are significantly different (p-value < 0.05).

[b]Sensory evaluation (+ =average, ++ = good, +++ = very good, ++++ = the best)

[c]L = lightness index (0-100 = black – white), a = redness and greenness [(+100) – (-80) = red – green] while, b = yellowness and blueness [(+70) – (-80) = yellow – blue]

Texture profile analysis (TPA) of bread before and after its storage may directly correlate with the staling rate of bread. Therefore, the effect of AmyBS-I supplementation on bread softness was assessed by TPA evaluation and it was found that AmyBS-I supplementation of bread decreased the hardness of bread as compared to control or commercial α-amylase supplemented bread (Figure 4.52). However, springiness, cohesiveness and gumminess of bread after AmyBS-I addition were unaffected (Table 4.20). Although the hardness of all the breads (supplemented with AmyBS-I, commercial amylase and control) increased with time, nevertheless, AmyBS-I supplemented bread showed the slowest staling rate (Figure 4.52).

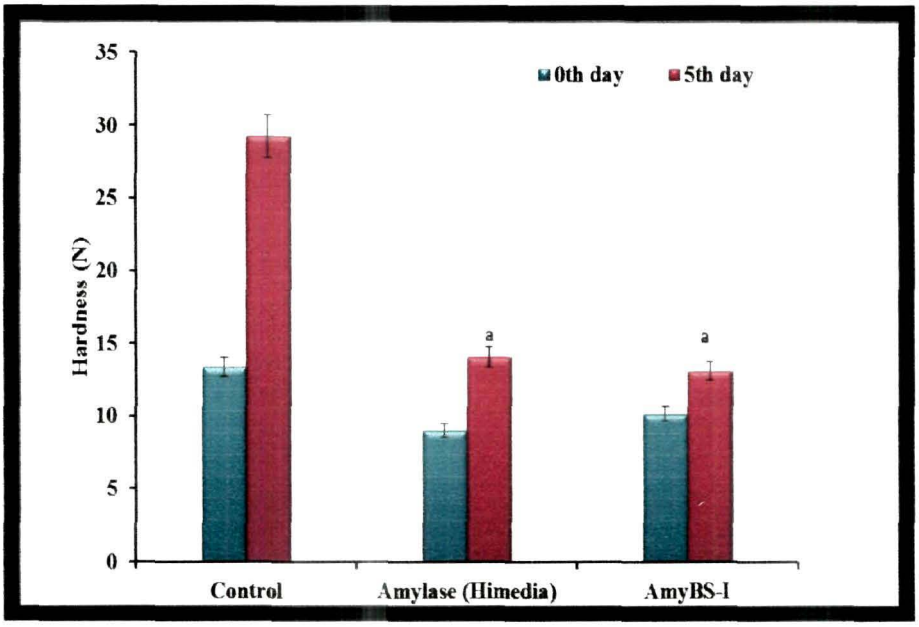

Figure 4.52: Effect of commercial enzyme (Himedia) and AmyBS-I supplementation on bread staling. Values are mean ± S.D. of triplicate determinations having p-value ≤ 0.001. The bars with same superscript do not differ each other significantly (p-value > 0.05).

Table 4.20: Difference in texture profile (between 0^{th} day and 5^{th} day) on storage of various bread samples supplemented with AmyBS-I and a commercial α-amylase. Each value is mean ± S.D. of triplicate determinations having p-value ≤ 0.05. The value with same superscript within raw do not differ each other significantly (p-value > 0.05).

Parameters	Control	Bread supplemented with	
		Commercial α-amylase	AmyBS-I
Increase in Hardness (N)	15.83 ± 0.79	4.05 ± 0.2	2.96 ± 0.14
Increase in Gumminess (N)	1.7 ± 0.08	0.58 ± 0.029	0.45 ± 0.02
Decrease in Springiness	0.12 ± 0.006[a]	0.12 ± 0.006[a]	0.15 ± 0.007
Decrease in Cohesiveness	0.18 ± 0.009	0.12 ± 0.006	0.14± 0.007

4.9. Immobilization of α-amylase onto magnetic nanoparticles

Considering the ever-increasing demand for thermostable, raw starch digesting microbial α-amylases in starch processing industries, in the present study a partially purified α-amylase from *B. subtilis* strain AS01a was immobilized on the iron-oxide MNP. Figure 4.53 shows that the iron oxide magnetic nanoparticles prepared by selective precipitation of $FeCl_2$, were strongly attracted towards a permanent magnet (Figure 4.53).

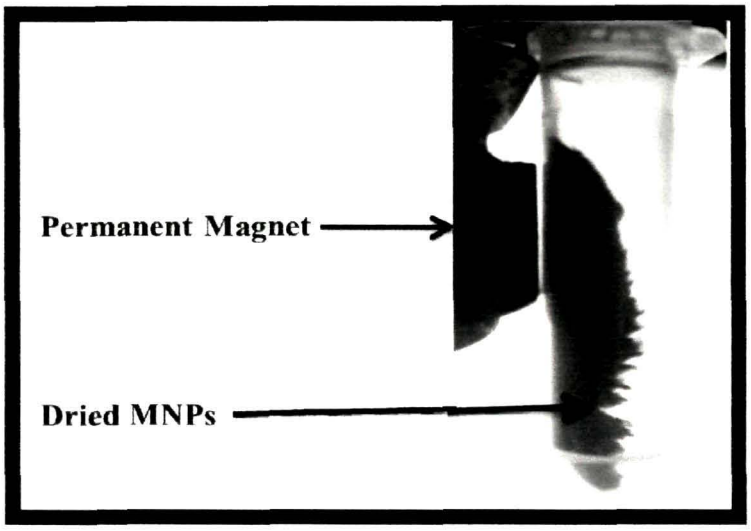

Figure 4.53: Magnetic properties of the MNPs towards the permanent magnet

4.9.1. Covalent immobilization of α-amylase onto iron oxide MNPs and its biophysical characterization

The XRD pattern of the synthesized iron oxide MNPs (Figure 4.54) shows the characteristic peaks for maghemite at 26.1°, 30.1°, 35.8°, 43.1°, 57.1° and 62.6° [382]. Using the X-PERT software, the nanocrystallite size for the bare MNPs was found to be ~38.2 nm. Further, the α-amylase bound MNPs showed almost similar crystallite size of ~38.4 nm suggesting that enzyme immobilization on MNPs does not alter nanocrystallite size.

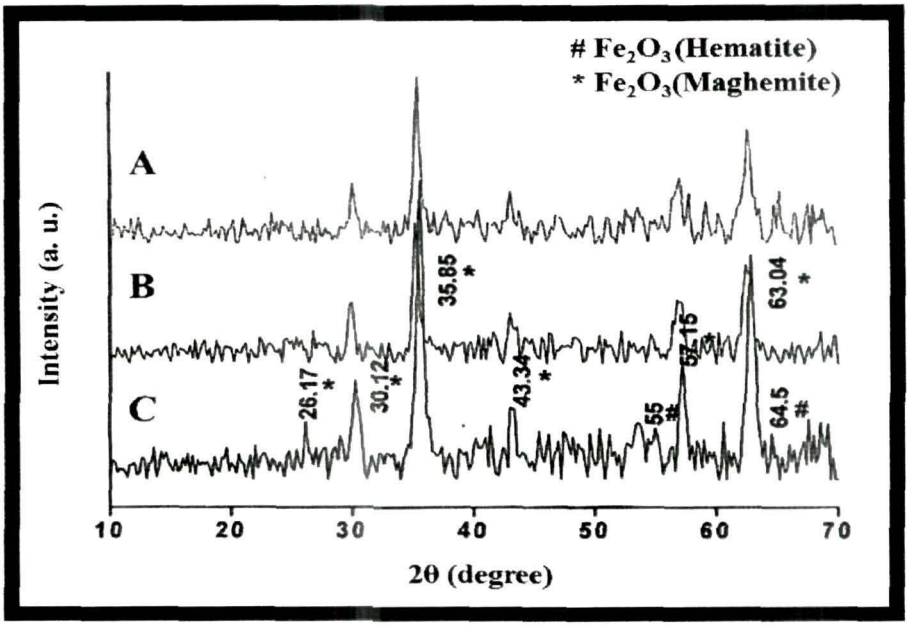

Figure 4.54: XRD spectra of (A) enzyme bound on functionalized MNPs (B) functionalized MNPs and (C) non-functionalized MNPs

Figures 4.55 and 4.56 show the FTIR spectra of the bare MNP and MNP bound amylase, respectively. The characteristic band of metal oxygen interaction at around 584.57 cm^{-1} was typical for the synthesized iron-oxide magnetic nanoparticles (Figure 4.55). Wavenumbers 1467.36, 1516.86 and 1629.30 cm^{-1} as seen in MNP-bound amylase spectra are assignable to the symmetric stretching of the dissociated carboxylic group originating from the amino acid, amide I and amide II (Figure 4.56). There was band shifting from 1627 cm^{-1} to 1629 cm^{-1} post MNP functionalization with cyanamide and enzyme coupling process. Band 2923.90 cm^{-1} shown in Figure 4.55 disappeared in the spectrum of MNP-bound amylase and a new high intensity band at 2950.28 cm^{-1} (Figure 4.56) was assigned to the C-H bond stretching vibration post treatment with cyanamid. A very broad band of O-H stretching was observed in 3000-3600 cm^{-1} region during MNP KOH treatment.

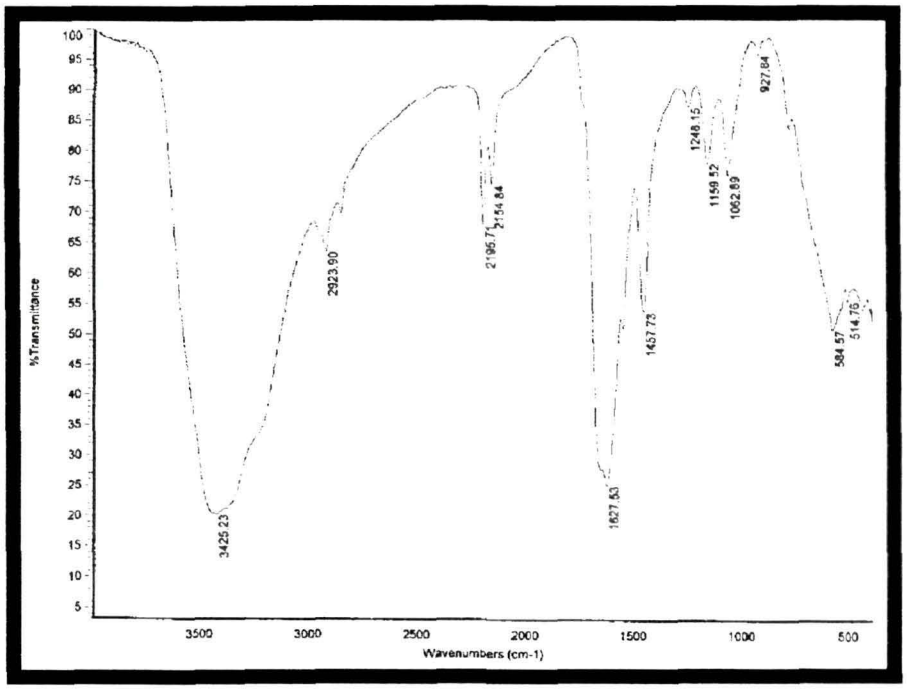

Figure 4.55: FT-IR spectra of functionalized magnetic nano particles.

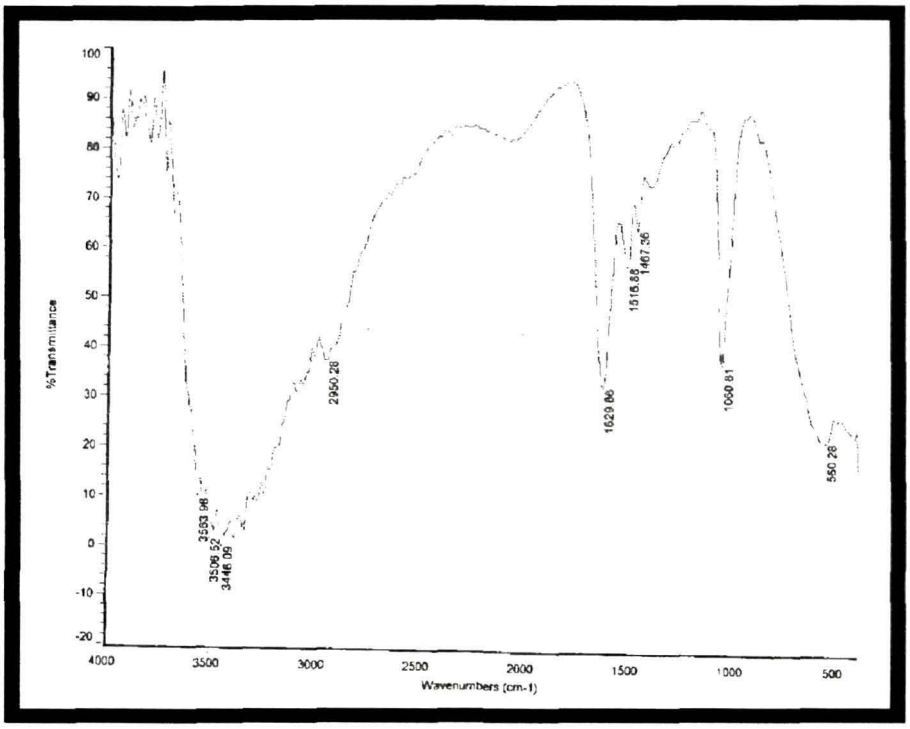

Figure 4.56: FT-IR spectra of functionalized MNPs-bound α-amylase

Magnetic properties of iron oxide MNP demonstrated low field (178G) hysteresis loop and the magnetization at this field remained constant for bare as well as enzyme bound MNPs. The saturation magnetization (μs), remnant magnetization (μr) and coercivity (Hc) values for free iron-oxide MNP were determined as 4.648 emu cm^{-3}, 2.703 emu cm^{-3} and 9.28 G, respectively and for α-amylase coupled MNP, these values were estimated as 4.589 emu cm^{-3}, 2.711 emu cm^{-3}, and 9.6 G, respectively. The magnetic susceptibility ($\lambda = 0.366$), remained the same for both bare and enzyme immobilized MNPs.

4.9.2. Starch hydrolysis efficiency of iron-oxide MNP bioconjugate

Packed-column study by MNP coupled α-amylase showed that the degree of starch hydrolysis increased with an increase in incubation time up to 60 min (Fig 4.57). However, incubation beyond this time showed no significant increase in starch hydrolysis with respect to time (Figure 4.53). Moreover, the percentage of starch hydrolysis by MNP-bound α-amylase was significantly higher (p-value < 0.01) as compared to free (native) enzyme as well as MNP alone (Figure 4.57).

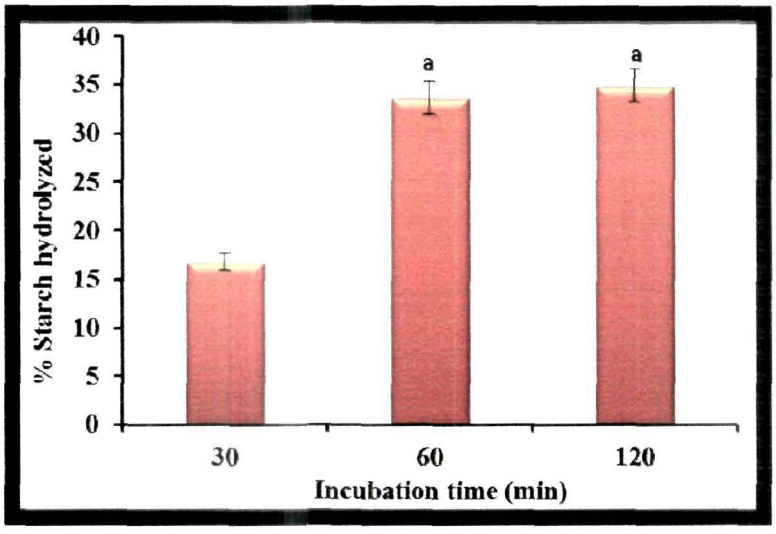

Figure 4.57: Starch hydrolysis by iron oxide MNP-bound α-amylase at different time intervals. Values are mean ± S.D. (n = 3), having p-value ≤ 0.001. The bars with same superscript do not vary each other significantly (p-value > 0.05).

Chapter V

RESULTS

Chapter 5: Results

5.1. Screening of soil samples

The soil sample (AS08) collected from the Sivasagar district of Assam, India, was estimated to have soil pH of ~8.1. Using the serial dilution method, five strains capable of producing extracellular alkaline α-amylase on alkaline starch agar media (pH 12.0) were found. Amongst the five strains, the strain AS08E showed the largest zone of starch hydrolysis around the colonies (0.66 ± 0.04 cm^2) and, thus, it was selected for further studies. Figure 5.1 shows the halo zone formation by the selected strain on alkaline starch agar plate.

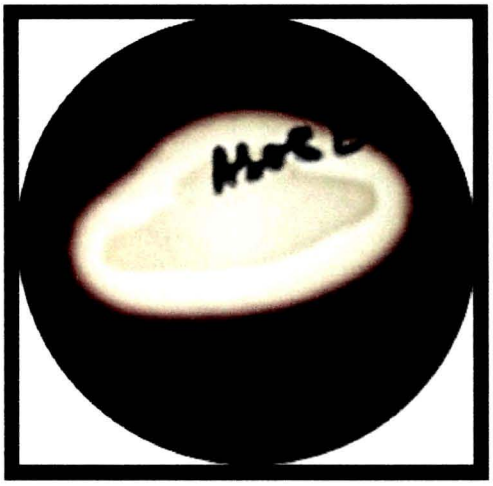

Figure 5.1: Plates showing halo zone formation on starch agar plates by extracellular α-amylase producing strain AS08E isolated from soil sample obtained from Sivasagar district of Assam, India.

5.2. Identification of bacteria

5.2.1. Morphological and biochemical identification of the isolates AS08E

By differential staining of strain AS08E, it was found to be rod-shaped, Gram-positive, non-motile, non-acid fast bacterium and showed the formation of round/oval shaped spores (Figure 5.2).

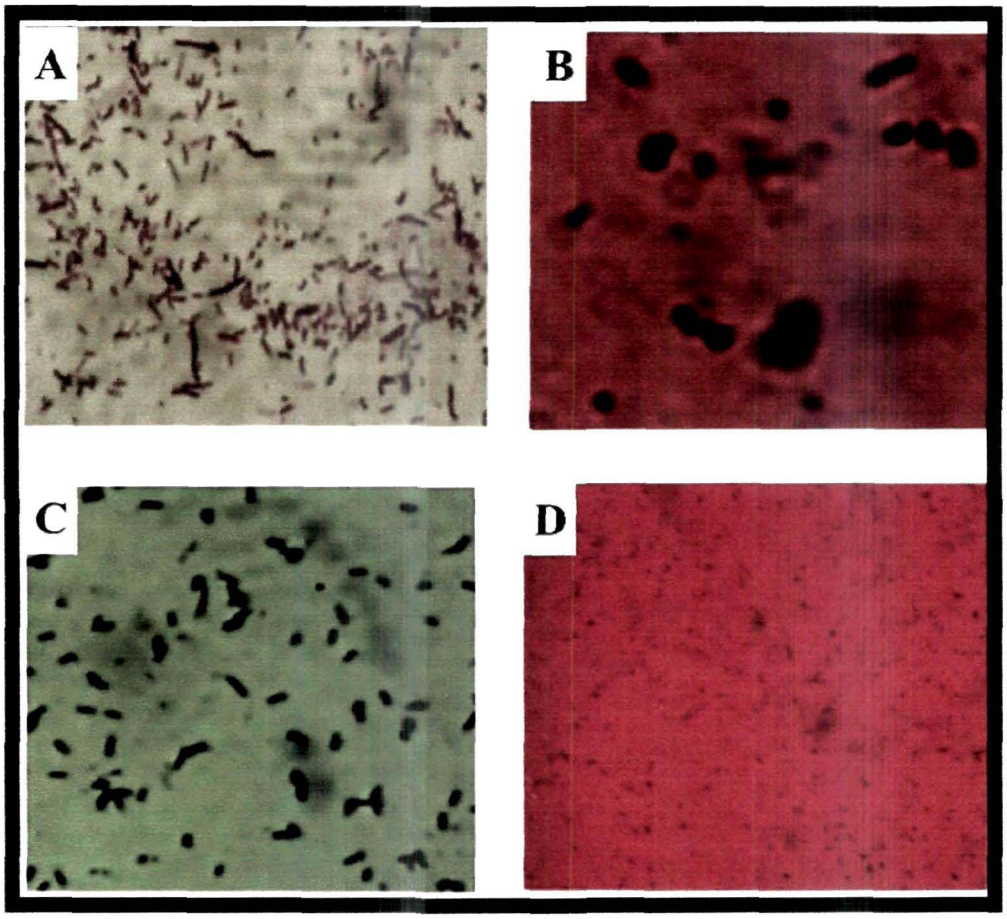

Figure 5.2: Differential staining of the extracellular α-amylase producing strain AS08E (A: Gram staining; B: spore staining; C: malachite staining; D: acid-fast staining).

Biochemical characterization revealed that among the tested carbon source, bacterium AS08E could utilize sucrose, lactose, adonitol, and arabinose as seen from the biochemical test plates (Figure 5.3). The strain AS08E also showed utilization of citrate, nitrate, and phenylalanine deamination positive tests although it was unable to produce indole from tryptophan or gas from glucose (Figure 5.3). The starch hydrolysis experiment clearly demonstrated that the isolated strain was capable of hydrolyzing starch by virtue of producing α-amylase into the culture medium.

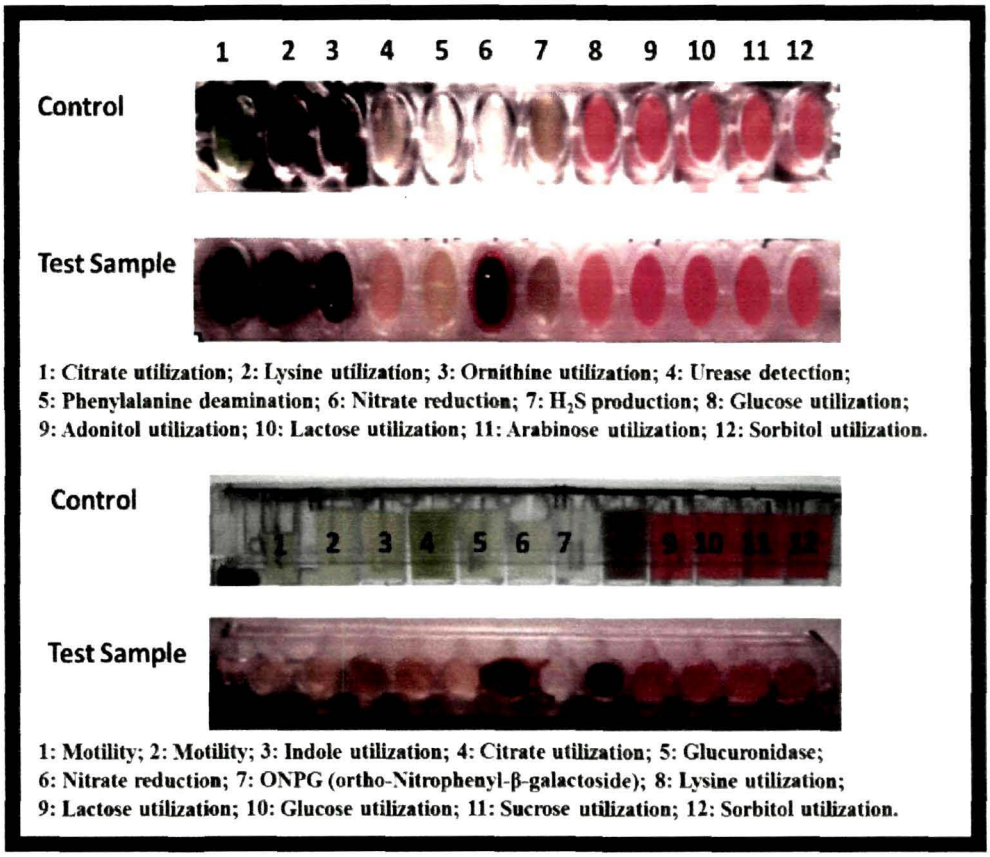

Figure 5.3: Biochemical characterization of the isolated strain AS08E

The data obtained after analysis of various morphological and biochemical properties of the strain AS08E are listed in Table 5.1. Analysis of these data according to the Bergey's manual of systematic bacteriology [316, 355], suggested that the isolated bacterium belongs to *Bacillus* genus and therefore it is named *Bacillus* sp. strain AS08E.

Table 5.1: A summary of biochemical and morphological characteristics of strain AS08E. The result represents the observation of three experiments.

Characteristics	Observation
Morphology	Rod shaped, motile negative, Gram positive, spores are round/oval
Growth pH	6.0 – 13, optimum at pH 11.0
Growth temperature	Growth range 30-60°C, optimum at 45°C
Growth in NaCl	0.5 – 4.0% (w/v)
Catalase	Positive
Voges-Proskauer Test	Negative
Methyl Red Test	Negative
Different sugar utilization test	
D- Glucose	Negative
Lactose	Variable
Adonitol	Positive
Arabinose	Variable
Sorbitol	Negative
Sucrose	Positive
Gas from Glucose	Negative
Hydrolysis of casein	N.D.
Hydrolysis of gelatin	N.D.
Hydrolysis of starch	Positive
Urease activity	Negative
Citrate utilization	Positive
Indole formation	Negative
Nitrate reduction	Positive
Lysine utilization	Negative
H_2S production	Negative
Ornithine utilization	Negative
Phenylalanine deamination	Positive
Glucuronidase test	Negative
ONPG (ortho-Nitrophenyl-β-galactoside)	Negative

N.D.: Not determined

5.2.2. Molecular identification

5.2.2.1. 16S rDNA based identification

Figure 5.4 shows the agarose gel analysis of genomic DNA isolated and purified from the *Bacillus* sp. strain AS08E. The 16S ribosomal RNA gene amplification from the *Bacillus* sp. strain AS08E using universal primers (Table 3.1) and its genomic DNA resulted into appearance of ~1500 bp product, which was in accordance with the expected 16S rDNA size (Figure 5.4).

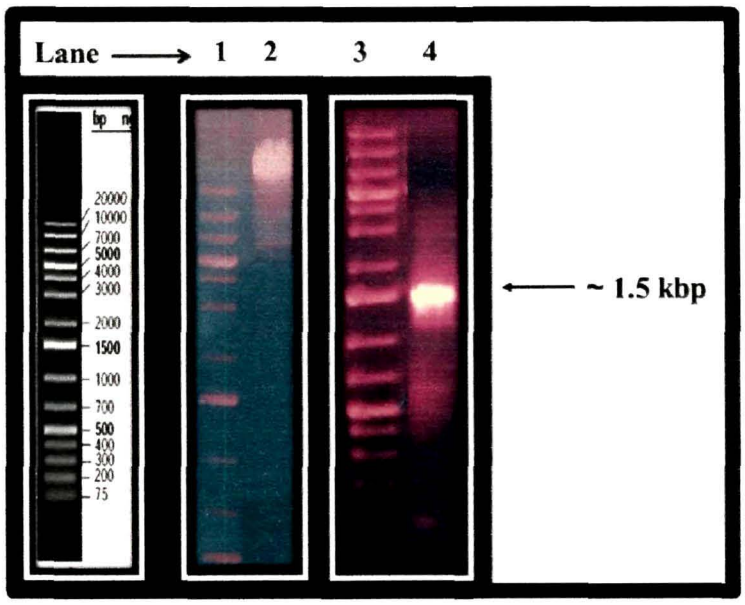

Figure 5.4: Agarose gel analysis of genomic DNA and PCR amplified 16S rDNA from strain AS08E (lane 1 & 3: 1 kbp DNA ladder; lane 2: genomic DNA from AS01a and lane 4: PCR-amplified 16S rDNA).

Sequencing of the PCR-amplified product from strain AS08E followed by blastn analysis of this sequence showed that it has 99-100% sequence homology with the reported 16S rDNA sequence of *Bacillus* species (Table 5.2). The 16S rDNA sequence of strain AS08E was deposited in the NCBI database with the accession number JN118574 (Table 5.2).

Table 5.2: Results of sequence homology analysis of 16S rDNA from *Bacillus* sp. strain AS08E with 16S rDNA of other bacteria using blastn programme of NCBI database

Description	Query cover	Maximum identity	Accession No.
Bacillus licheniformis strain AS08E 16S ribosomal RNA gene, partial sequence	100%	100%	JN118574
B. licheniformis strain BPRIST039 16S ribosomal RNA gene, partial sequence	99%	100%	JF700489
B. licheniformis strain BPRIST038 16S ribosomal RNA gene, partial sequence	99%	100%	JF700488
B. licheniformis strain BPRIST006 16S ribosomal RNA gene, partial sequence	99%	100%	JF414759
B. licheniformis strain CICC 10087 16S ribosomal RNA gene, partial sequence	99%	100%	DQ082995
B. licheniformis strain MML2501 16S ribosomal RNA gene, partial sequence	99%	100%	EU344793
B. licheniformis strain CICC 10100 16S ribosomal RNA gene, partial sequence	99%	100%	DQ082996
B. licheniformis strain AIS72 16S ribosomal RNA gene, partial sequence	99%	99%	GU967452
B. licheniformis strain AIS03 16S ribosomal RNA gene, partial sequence	99%	99%	GU967445
Bacillus sp. D6 16S ribosomal RNA gene, partial sequence	99%	99%	EU281636

In order to understand the phylogenetic position of the isolated strain the phylogenetic tree was constructed based on 16S rDNA sequences of AS08E and other related bacterial species by neighbor-joining method (Figure 5.5). The phylogenetic tree so obtained showed that *Bacillus* sp. strain AS08E clustered among the *Bacillus licheniformis* groups and showed close phylogenetic relationship with *Bacillus licheniformis* strain M27 (Figure 5.5).

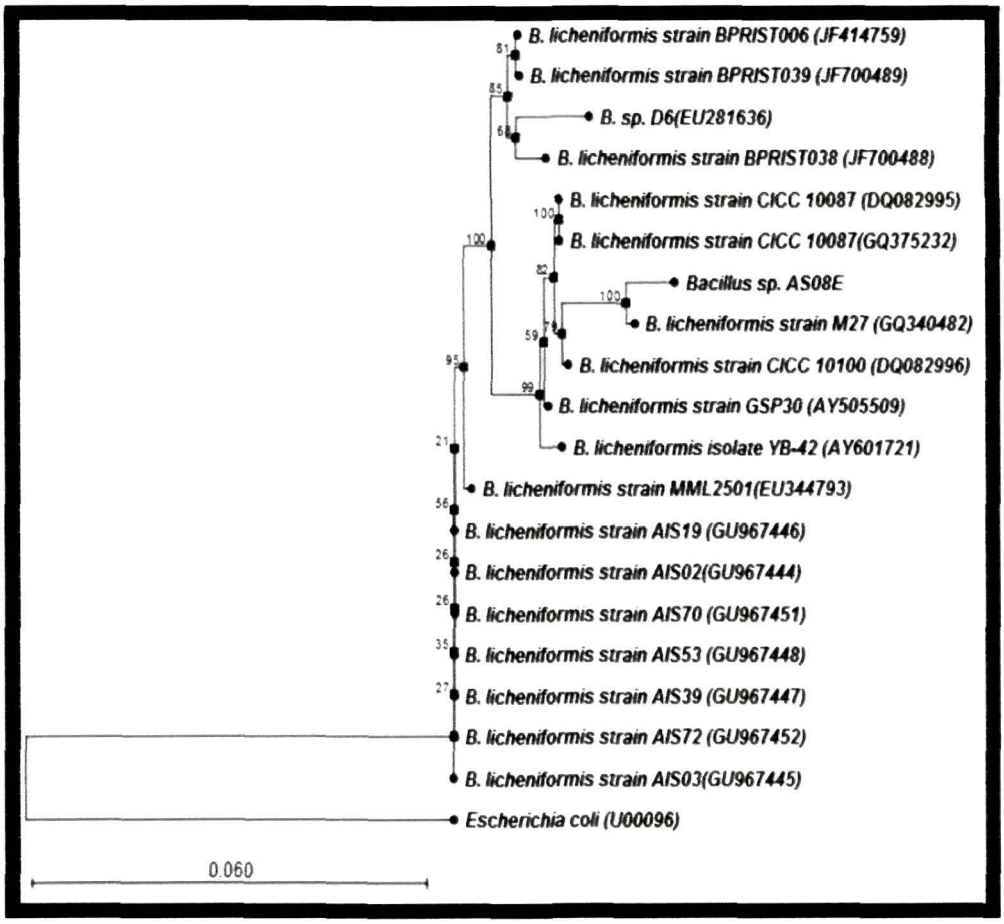

Figure 5.5: Phylogenetic relationships of strain AS08E and other closely related *Bacillus* species based on 16S rDNA sequencing. The tree was generated by considering the sequence from *Escherichia coli* strain K 12 MG1655 (accession no U00096) as out-group. The data set was resampled 1000 times by using the bootstrap option and percentage of bootstrap values are given at the nodes.

5.2.2.2. Gyrase A gene analysis

The PCR amplification of the GyrA gene from strain AS08E resulted into appearance of ~1000 bp gene product on agarose gel (Figure 5.6), which was in accordance with the expected size of the gene encoding the bacterial gyrase subunit A.

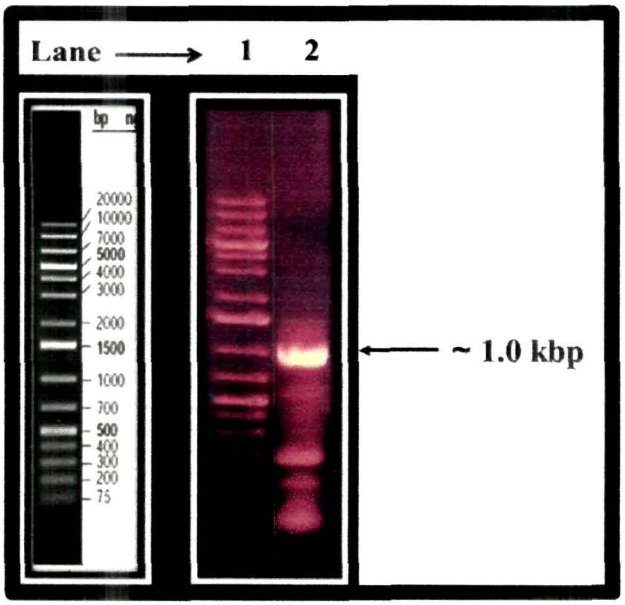

Figure 5.6: Agarose gel analysis of PCR-amplified gyrase A gene from *Bacillus* sp. strain AS08E (lane 1: 1 kbp ladder and lane 2: PCR-amplified product of GyrA gene).

The sequencing and analysis of GyrA gene from *Bacillus* sp. strain AS08E, using blastn programme of NCBI database (www.ncbi.nlm.nih.gov.in), showed that it was 99% homologous with other *B. licheniformis* GyrA gene sequences present in the NCBI database (Table 5.3). The partial sequence of GyrA gene from strain AS08E was deposited in the NCBI database under accession number JN133841 (Table 5.3).

Table 5.3: Percentage homology of GyrA gene from strain AS08E with GyrA gene sequence of other bacteria using blastn programme of NCBI database

Description	Query cover	Maximum identity	Accession No.
Bacillus licheniformis strain AS08E gyrase A (*gyrA*) gene, partial cds (coding sequence)	100%	100%	JN133841
B. licheniformis ATCC 14580, complete genome	100%	99%	CP000002
B. licheniformis DSM 13 = ATCC 14580, complete genome	100%	99%	AE017333
B. licheniformis KCTC 2215 DNA gyrase subunit A (*gyrA*) gene, partial cds	96%	100%	AF272018
B. licheniformis KCTC 1918T DNA gyrase subunit A (*gyrA*) gene, partial cds	90%	100%	AF272017
B. licheniformis strain RS-1 DNA gyrase subunit A (*gyrA*) gene, partial cds	100%	97%	DQ995270
B. licheniformis strain CICC 10085 gyrase subunit A (*gyrA*) gene, partial cds	81%	100%	GQ355995
B. licheniformis partial GyrA gene for DNA gyrase A subunit, strain LMG 12363T	71%	100%	AJ579786
B. licheniformis strain 3EC5C4 DNA gyrase subunit A (*gyrA*) gene, partial cds	70%	100%	EF026687

The phylogenetic position of the strain AS08E was determined by the multiple sequence alignment of its GyrA gene sequence and other similar sequences obtained from the NCBI database, using MEGA 5.1 software. The phylogram constructed by neighbor-joining method of MEGA 5.1 software revealed that strain AS08E was clustered among the *B. licheniformis* groups and was found to be closely related with the *B. licheniformis* strain KCTC 2215 (Figure 5.7).

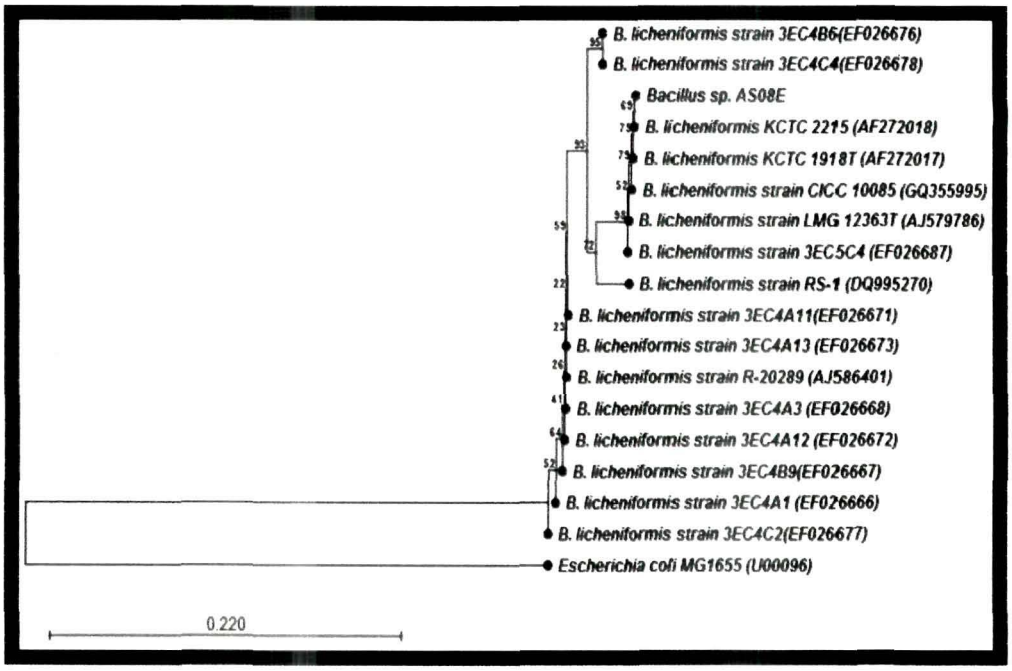

Figure 5.7: Evolutionary relationships of strain AS08E and other closely related *Bacillus licheniformis* based on gyrase A gene sequence considering *E. coli* as an out-group. The data set was resampled 1000 times by using the bootstrap option and percentage of bootstrap values are given at the nodes.

5.2.2.3. Rpo B gene analysis

Among the core genome sequencing for bacterial identification, *rpo*B is one of the potential candidates for bacterial phylogenetic analysis and identification. The PCR amplification of this gene from the strain AS08E using gene-specific primers (Table 3.1) and its genomic DNA resulted into appearance of ~500 bp PCR product on agarose gel analysis (Figure 5.8).

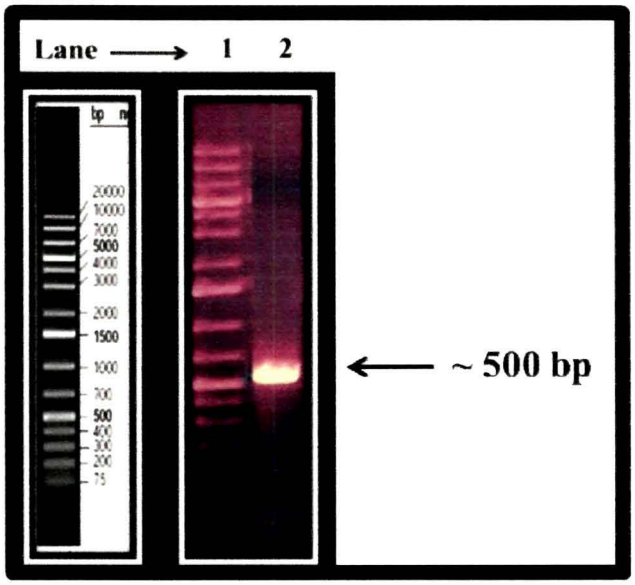

Figure 5.8: Agarose gel analysis of PCR-amplified RpoB gene from the *Bacillus* sp. strain AS08E (lane 1: 1 kbp DNA ladder and lane 2: amplified *rpoB* product).

The PCR-amplified product was then subjected to sequencing and the analysis of this sequence so obtained by blastn searched in NCBI database showed that it was up to 100% homologous with the known RpoB gene sequence from *B. licheniformis* reported in the database (Table 5.4). The sequence of RpoB gene obtained in the present study was deposited in the NCBI database with the accession number JN133842.

Table 5.4: Percentage identity of RpoB gene from strain AS08E with the same gene from other bacteria using blastn programme of NCBI database

Description	Query cover	Maximum identity	Accession No.
Bacillus licheniformis strain AS08E, RpoB (rpoB) gene, partial cds	100%	100%	JN133842
B. licheniformis strain NRS-1264 RpoB (rpoB) gene, partial cds	100%	100%	EF015395
B. licheniformis strain 3EC4A9 RpoB (rpoB) gene, partial cds	100%	100%	EF015338
B. licheniformis DSM 13 = ATCC 14580, complete genome	100%	100%	AE017333
B. licheniformis partial RpoB gene for RNA polymerase beta subunit, strain LMG 12363T	100%	100%	AJ579782
B. licheniformis strain 3EC4A4 RpoB (rpoB) gene, partial cds	100%	99%	EF015333
B. licheniformis strain 3EC4C3 RpoB (rpoB) gene, partial cds	100%	99%	EF015357
B. licheniformis partial RpoB gene for RNA polymerase beta subunit, strain LMG 17659	99%	99%	AJ579783
B. licheniformis partial RpoB gene for RNA polymerase beta subunit, strain LMG 7559	99%	98%	AJ579781
B. licheniformis RpoB gene for RNA polymerase beta subunit, strain IFO 12195	100%	99%	AB089340

The evolutionary tree was constructed based on multiple sequence alignment of the RpoB gene sequence from strain AS08E and other homologous sequences retrieved from NCBI database. The phylogram obtained by neighbor-joining method revealed that the isolated strain AS08E was clustered among the *B. licheniformis* group and showed close relatedness with the *B. licheniformis* strain IFO 12201 (Figure 5.9).

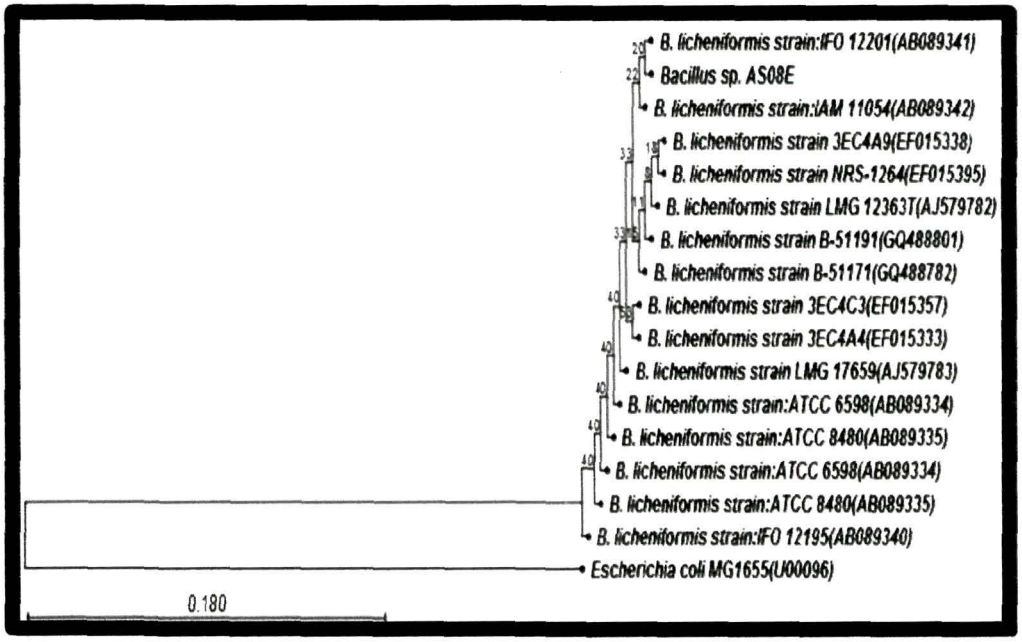

Figure 5.9: Evolutionary relationships of strain AS08E and other closely related *Bacillus* species based on RNA polymerase B gene sequencing. The tree was generated by considering the sequence from *Escherichia coli* strain K 12 MG1655 (accession no U00096) as out-group. The data set was resampled 1000 times by using the bootstrap option and percentage of bootstrap values are given at the nodes.

5.2.2.4. Analysis of 16S-23S Intergenic spacer region (ISR)

PCR amplification of 16S-23S ISR from the strain AS08E using ISR-specific primers (P3 and P4) listed in Table 3.1 resulted into appearance of three major bands on agarose gel analysis (Figure 5.10).

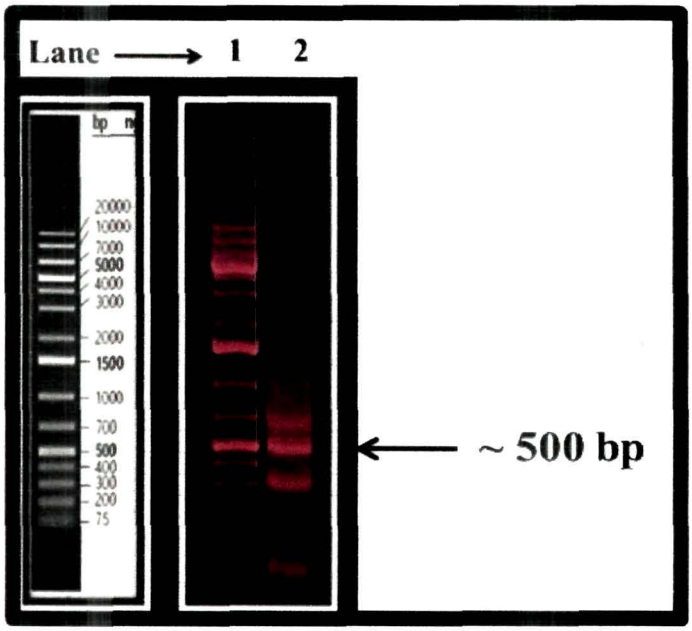

Figure 5.10: Agarose gel analysis of PCR-amplified 16S-23S ISR region from strain AS08E (Lane 1: 1 kbp DNA ladder and lane 2: PCR-amplified ISR gene product).

Among the three amplified bands, only the band corresponding to the expected gene size (~500 bp) was excised and gel purified for sequencing. Sequencing and analysis of this ISR sequence revealed that it was up to 98% homologous with the other 16S-23S ISR gene sequences reported in the Genbank database (www.ncbi.nlm.nih.gov). The gene sequence so obtained in this study was deposited in the NCBI database under the accession number JN133843.

Table 5.5: Comparison of percentage identity of 16S-23S ISR gene from strain AS08E with similar region of other bacteria using blastn programme of NCBI database

Description	Query cover	Maximum identity	Accession No.
Bacillus licheniformis strain AS08E 16S-23S ribosomal RNA ISR, partial sequence	100%	100%	JN133843
B. subtilis strain IDCC 1101 16S-23S ribosomal RNA ISR, partial sequence	91%	94%	EF533983
B. mojavensis clone MOJ1F 16S-23S ribosomal RNA ISR, partial sequence	91%	94%	AF478089
B. subtilis strain PY79 16S-23S ribosomal RNA ISR, partial sequence	91%	94%	EU081774
B. subtilis strain 4428 16S-23S ribosomal RNA ISR, partial sequence	91%	93%	GQ255891
B. subtilis strain Tpb55 16S-23S ribosomal RNA ISR, partial sequence	83%	93%	DQ672263
B. licheniformis strain AIS72 16S-23S ribosomal RNA ISR, partial sequence	55%	100%	GU967461
B. licheniformis strain AIS68 16S-23S ribosomal RNA ISR, partial sequence	55%	100%	GU967459
B. licheniformis strain AIS64 16S-23S ribosomal RNA ISR, partial sequence	55%	100%	GU967458

Phylogenetic tree was constructed based on multiple sequence alignment of 16S-23S ISR sequence of *Bacillus* sp. strain AS08E and other homologous sequences obtained from NCBI database. The aligned DNA sequences were then used for phylogram construction by neighbor-joining method. The analysis of this phylogram suggested that the strain AS08E belonged to the *Bacillus licheniformis* group and showed its close similarity with *B. licheniformis* strain EI-3N_F (Figure 5.11).

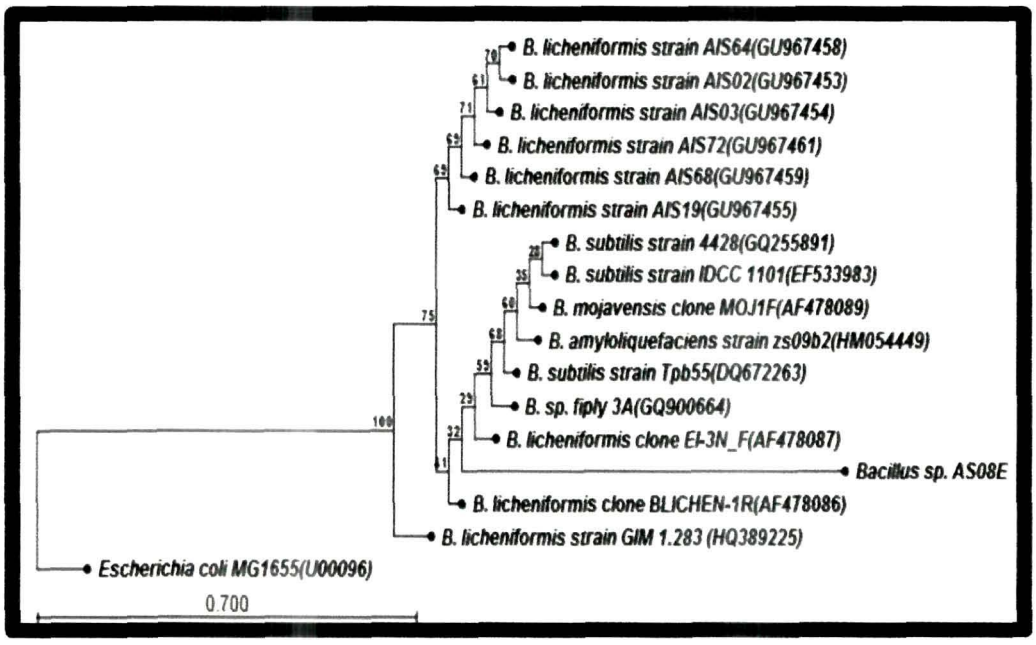

Figure 5.11: Evolutionary relationships of strain AS08E and other closely related *Bacillus* species based on 16S-23S ISR sequence by neighbor-joining method. The tree was generated by considering the sequence from *E. coli* strain K 12 MG1655 (accession no U00096) as out-group. The data set was resampled 1000 times by using the bootstrap option and percentage of bootstrap values are given at the nodes.

Based on polyphasic approach (morphological, biochemical and molecular methods) of bacterial identification, the isolated bacterium strain AS08E was identified as *Bacillus licheniformis* and was named *B. licheniformis* strain AS08E.

5.3. α-Amylase production from alkalophilic *B. licheniformis* strain AS08E under submerged fermentation.

5.3.1. Determination of growth kinetics

Figure 5.12 shows that the bacterial cell biomass increases with an increase in time up to 72 h. However, with further increase in incubation time, the growth starts declining, suggesting that the optimal growth of bacteria was at 72 h. Further, from Figure 5.12, it can also be concluded that the α-amylase production from *B. licheniformis* strain AS08E is growth associated and shows maximum enzyme production within 48-72 h of incubation under submerged fermentation (SmF) conditions.

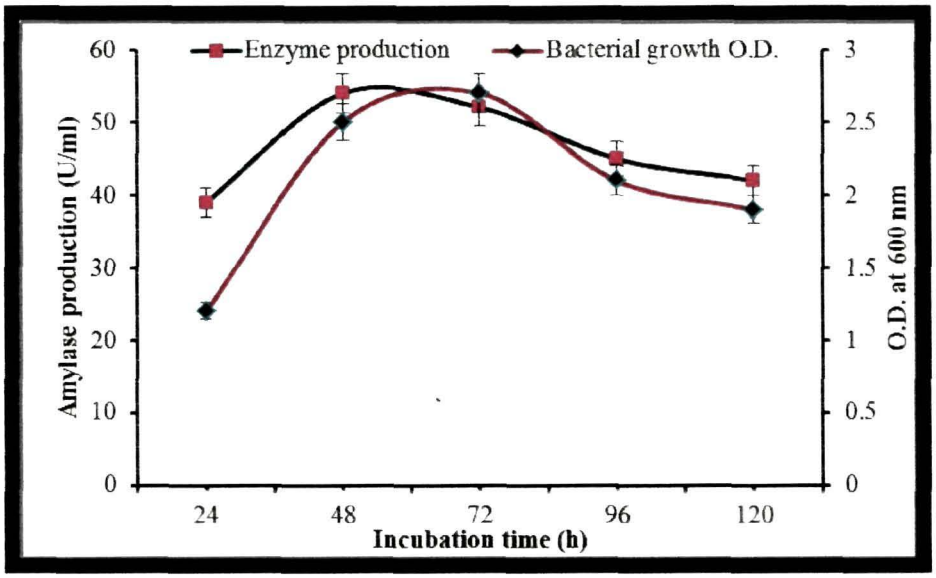

Figure 5.12: Growth kinetics and enzyme production of *B. licheniformis* strain AS08E under SmF. Data represents mean ± S.D. (where n = 3) with *p*-value ≤ 0.001.

5.3.2.Screening of significant factors influencing α-amylase production from Bacillus licheniformis strain AS08E using Plackett-Burman

For the selection of significant factors influencing the alkaline α-amylase production from *B. licheniformis* strain AS08E, a total of eleven variables were analyzed with regard to their effects on alkaline α-amylase production from this strain using a Plackett–Burman design (Table 5.6). These variables were considered for the study because of their important role in the alkaline α-amylase production by bacteria. The design matrix selected for the screening of significant variables for alkaline α-amylase production and the corresponding responses are shown in Table 5.6.

Pareto chart (Figure 5.13) shows that among the eleven tested variables influencing the alkaline α-amylase production, only three of them were found to be significant (p-value < 0.05) and are beyond the statistical reference line which determines the magnitude and the importance of an effect [336, 337]. The normality plot (Figure 5.14), implies that starch has a positive effect whereas peptone and pH of the media has a negative effect on alkaline α-amylase production from *B. licheniformis* strain AS08E. The model equation for the alkaline α-amylase production by neglecting the non-significant terms (p-value > 0.05) can be fitted in linear equation as

$$y = 335.01 + 45.73A - 31.93B - 29.32C \ldots\ldots\ldots\ldots\ldots\ldots (5.1)$$

Where y = α-amylase activity (U/ml), A = starch concentration (% w/v), B = peptone concentration (% w/v) and C = pH of the medium, respectively.

Table 5.6: Observed and predicted values of alkaline α-amylase production by *B. licheniformis* strain AS08E using Plackett - Burman design. The observed values represent mean ± S. D. (n = 3), p-value ≤ 0.001.

Run order	Starch (% w/v)	Beef extract (% w/v)	Peptone (% w/v)	NaCl (% w/v)	Temp. (°c)	pH (H+)	NH_4Cl (% w/v)	Glycerol (% w/v)	KNO_3 (% w/v)	Maltose (% w/v)	$CaCl_2$ (% w/v)	Enzyme activity (U/ml)	
												Observed	Predicted
1.	2(+)	0.5(-)	1.5(+)	0.25(-)	37(-)	11.5(-)	0.2(+)	1.5(+)	0.2(+)	0.5(-)	0.1(+)	69.53 ± 3.4	67.1
2.	2(+)	1.5(+)	0.5(-)	0.75(+)	37(-)	11.5(-)	0.1(-)	1.5(+)	0.2(+)	1.5(+)	0.05(-)	115.43 ± 5.7	112.9
3.	0.5(-)	1.5(+)	1.5(+)	0.25(-)	53(+)	11.5(-)	0.1(-)	0.5(-)	0.2(+)	1.5(+)	0.1(+)	14.45 ± 0.7	12.0
4.	2(+)	0.5(-)	1.5(+)	0.75(+)	37(-)	12.5(+)	0.1(-)	0.5(-)	0.1(-)	1.5(+)	0.1(+)	63.24 ± 3.1	60.8
5.	2(+)	1.5(+)	0.5(-)	0.75(+)	53(+)	11.5(-)	0.2(+)	0.5(-)	0.1(-)	0.5(-)	0.1(+)	146.54 ± 7.3	144.1
6.	2(+)	1.5(+)	1.5(+)	0.25(-)	53(+)	12.5(+)	0.1(-)	1.5(+)	0.1(-)	0.5(-)	0.05(-)	36.89 ± 1.8	34.4
7.	0.5(-)	1.5(+)	1.5(+)	0.75(+)	37(-)	12.5(+)	0.2(+)	0.5(-)	0.2(+)	0.5(-)	0.05(-)	15.13 ± 0.7	12.7
8.	0.5(-)	0.5(-)	1.5(+)	0.75(+)	53(+)	11.5(-)	0.2(+)	1.5(+)	0.1(-)	1.5(+)	0.05(-)	35.87 ± 1.8	33.4
9.	0.5(-)	0.5(-)	0.5(-)	0.75(+)	53(+)	12.5(+)	0.1(-)	1.5(+)	0.2(+)	0.5(-)	0.1(+)	7.31 ± 0.4	4.8
10.	2(+)	0.5(-)	0.5(-)	0.25(-)	53(+)	12.5(+)	0.2(+)	0.5(-)	0.2(+)	1.5(+)	0.05(-)	105.06 ± 5.2	102.6
11.	0.5(-)	1.5(+)	0.5(-)	0.25(-)	37(-)	12.5(+)	0.2(+)	1.5(+)	0.1(-)	1.5(+)	0.1(+)	15.3 ± 0.7	12.8
12.	0.5(-)	0.5(-)	0.5(-)	0.25(-)	37(-)	11.5(-)	0.1(-)	0.5(-)	0.1(-)	0.5(-)	0.05(-)	37.06 ± 1.8	34.6
13.	1.25(0)	1(0)	1(0)	0.5(0)	45(0)	12(0)	0.15(0)	1(0)	0.15(0)	1(0)	0.075(0)	42.17 ± 2.1	52.7
14.	1.25(0)	1(0)	1(0)	0.5(0)	45(0)	12(0)	0.15(0)	1(0)	0.15(0)	1(0)	0.075(0)	39.45 ± 1.9	52.7
15.	1.25(0)	1(0)	1(0)	0.5(0)	45(0)	12(0)	0.15(0)	1(0)	0.15(0)	1(0)	0.075(0)	47.26 ± 2.3	52.7

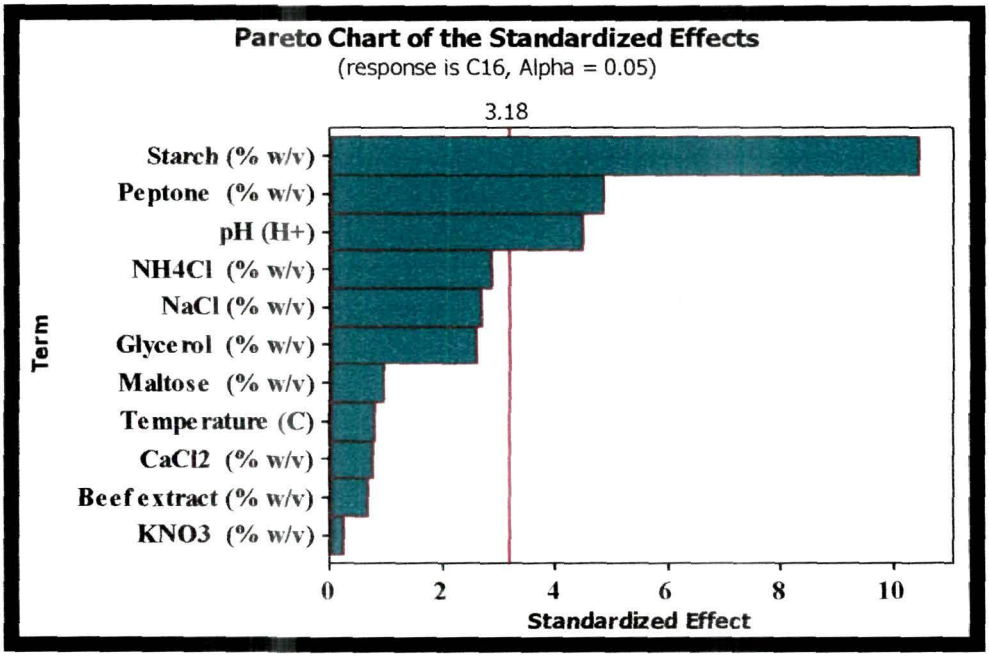

Figure 5.13: Pareto plot showing the significant factors influencing alkaline α-amylase production by *B. licheniformis* strain AS08E.

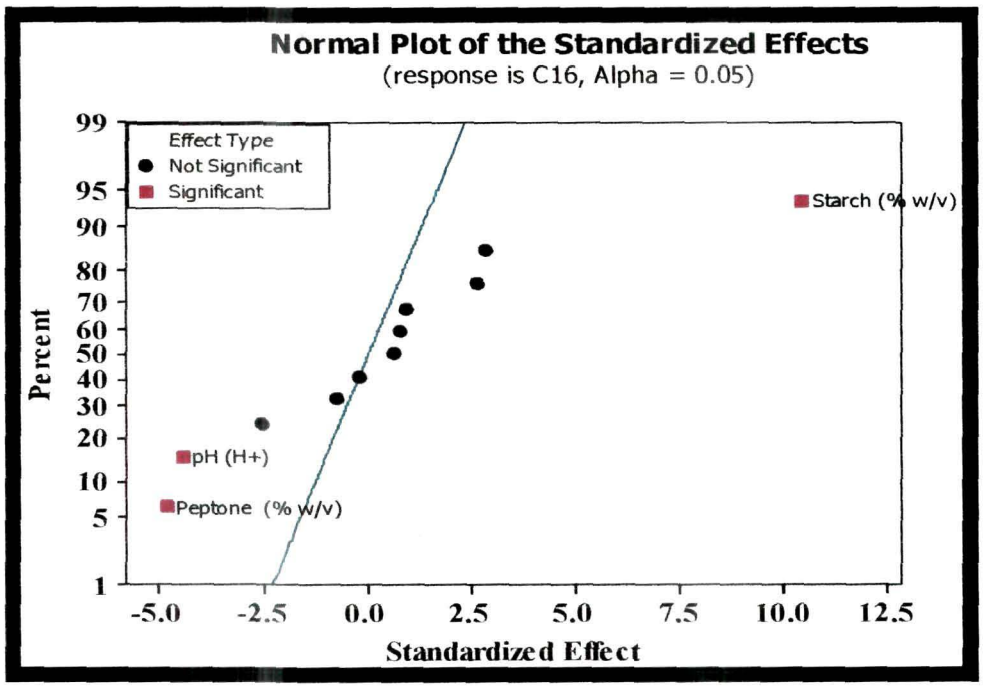

Figure 5.14: Normal plot showing the significant factors influencing alkaline α-amylase production by *B. licheniformis* strain AS08E.

Further statistical analysis of the model terms of the Plackett-Burman design for the alkaline α-amylase production from *B. licheniformis* strain AS08E showed that the terms were significant (Table 5.7). Significance of the model and quality of fit of the polynomial model equation were expressed by the coefficient of determination (R^2) which was 98.33% (Table 5.7). In other words, the model could explain 98.33% of the variability in the response. The value of the adjusted determination coefficient (adjusted R^2 = 92.23%) was also found to be very high which advocates for the significance of the model. This result showed that the response equation so obtained was a suitable model for the Plackett–Burman design experiments

Table 5.7: Statistical analysis of the model using Plackett-Burman design

Source	SS-	DF	MS-	*F*-value	Prob (*P*)> *F*
Model	22916 2	11	2083 29	16 10	0 021
Residual Error	388.1	3	129.37		
Lack of Fit	356 7	1	356.68	22 69	0.041
Pure Error	31 4	2	15 72		
Total	23304.3	14			

R^2 = 98.33%, Adj R^2 = 92 23%, SS: sum of squares; DF: degree of freedom, MS mean square

The adequacy of the model was calculated, and the variables evidencing statistically significant effects were screened, via Student's *t*-test for ANOVA (Table 5 8). Factors evidencing *p*-values of less than 0.05 were considered to have significant effects on the response, and were therefore selected for further optimization studies. As has been shown in the ANOVA Table (Table 5.8), starch with *p*-value = 0.002, was considered as the most significant factor influencing alkaline α-amylase production from *B. licheniformis* strain AS08E. This was followed by peptone with a *p*-value of 0.017 and then pH of medium with a *p*-value = 0.021

Tables 5.8: Estimated effect, regression coefficient and corresponding *t*-value and *p*-values for α-amylase activity in eleven variable PBD experiment

Variables	Effect	Coefficient	Standard error	*t*- value	*p*-value
Starch(% w/v)	68 6	34.3	11 28	10 45	0 002[a]
Maltose (% w/v)	6 15	3 07	11.28	0 94	0 418
Glycerol (% w/v)	-16 86	-8 43	11 28	-2.57	0.083
Beef extract(% w/v)	4 28	2 14	11 28	0.65	0:561
Peptone(% w/v)	-31 93	-15.97	11.28	-4 86	0 017[b]
NH_4Cl (% w/v)	18.84	9 42	11.28	2 87	0 064
KNO_3 (% w/v)	-1 33	-0 67	11 28	-0 20	0 852
NaCl(% w/v)	17.54	8 77	11.28	2 67	0.076
$CaCl_2$ (% w/v)	-4 85	-2 42	11 28	-0 74	0 514
Temperature(°c)	5.07	2.54	11.28	0.77	0.496
pH	-29 32	-14 66	11 28	-4 47	0 021[b]

[a]Significant positive effect, [b] Significant negative effect

From the ANOVA Table we can also conclude that the higher concentration of starch has a positive effect while the lower concentration of peptone and the lower pH value of the medium could increase the extracellular alkaline α-amylase production from *B. licheniformis* strain AS08E. Therefore, in further media optimization experiment, starch was kept at higher range of values while peptone and pH value of the medium were kept at lower ranges of values and all other terms were either eliminated or kept at a middle/central value.

5.3.3. Statistical optimization of significant factors by RSM

Three factors (starch, peptone, and pH of the medium) were identified to play a significant role in alkaline α-amylase production by *B. licheniformis* strain AS08E using Plackett-Burman design. To optimize these significant variables and to study their interaction effects on alkaline α-amylase production, experiment was conducted by RSM. The experiments were targeted toward the construction of a quadratic model consisting of twenty trials The design matrix and the corresponding results of RSM experiments to determine the effects of three independent variables (starch, peptone, and pH of the medium), along with the

mean predicted values, are shown in Table 5.9. Multiple regression analysis was used to analyze the data. The polynomial equation (equation 5.2) derived from regression analysis is given below:

$$y = 3358.84 + 370.63C_1 - 270.01C_2 + 549.37C_3 - 87.26C_1^2 - 272.91C_2^2 - 25.17C_3^2 + 60.63C_1C_2 + 2.01C_1C_3 + 37.63C_2C_3 \quad \ldots\ldots\ldots\ldots\ldots\ldots\ldots\ldots \quad (5.2)$$

Where y = responses (enzyme activity in U/ml), C_1 = starch conc. (% w/v), C_2 = peptone conc. (% w/v) and C_3 = pH of the media, respectively.

Table 5.9: Observed responses and predicted values of alkaline α-amylase production by *B. licheniformis* strain AS08E using RSM. The observed values are mean ± S. D. (n = 3) with p-value ≤ 0.001.

Run no.	Independent Variables			Y Response (α-amylase yield in U/ml)	
	C_1	C_2	C_3	Observed value	Predicted value
1	-1(1.5)	-1 (0.25)	-1(10.5)	75 14 ± 3 7	62 37
2	1(2 5)	-1 (0.25)	-1(10.5)	128.18 ± 6.4	120.26
3	-1(1.5)	1(0 75)	-1(10 5)	39.61 ± 1 9	33.44
4	1(2.5)	1(0.75)	-1(10.5)	117.47 ± 5.8	121.64
5	-1(1.5)	-1 (0 25)	1(12 5)	32.47 ± 1 6	28.12
6	1(2.5)	-1 (0.25)	1(12 5)	84.04 ± 4.2	90.02
7	-1(1.5)	1(0.75)	1(12.5)	29.07 ± 1.4	36.81
8	1(2.5)	1(0.75)	1(12.5)	116.45 ± 5 8	129.03
9	-α(1.16)	0(0.5)	0(11 5)	7 82 ± 0.4	16.95
10	+α(2.84)	0(0.5)	0(11.5)	152.04 ± 7.6	143 17
11	0(2.0)	-α(0.08)	0(11 5)	78.09 ± 3.9	89.29
12	0(2.0)	+α(0.92)	0(11.5)	108.69 ± 5 4	97.75
13	0(2.0)	0(0 5)	-α(9 8)	60.52 ± 3.0	81.83
14	0(2.0)	0(0.5)	+α(13.2)	72.36 ± 3.6	59.25
15	0(2.0)	0(0.5)	0(11.5)	136 11 ± 6.8	141.72
16	0(2 0)	0(0.5)	0(11 5)	148.75 ± 7 4	141.72
17	0(2.0)	0(0.5)	0(11.5)	141 68 ± 7.1	141.72
18	0(2 0)	0(0.5)	0(11 5)	140 55 ± 7.0	141 72
19	0(2.0)	0(0.5)	0(11.5)	138.95 ± 6.9	141.72
20	0(2 0)	0(0.5)	0(11.5)	144.56 ± 7 2	141.72

The adequacy of the model was checked via ANOVA, which was tested using Fisher's statistical analysis (Table 5.10) The model F value of 30 04 implies the significance of the proposed model The fit of the model equation was further evaluated by determining the R^2 value The observed values of R^2 (Table 5 10) explained that the fitted model could explain 96 43% of the total variation and hence vouched for adequacy of the model The adjusted R^2 value (93 22%) also advocated for a high significance of the model

Table 5.10: ANOVA for the alkaline α-amylase produced by *B licheniformis* strain AS08E

Source	SS	DF	MS	F-value	Prob (P)> F
Regression	38075 4	9	4230 61	30 04	0 000
Linear	19929 3	3	2930 99	20 81	0 000
Square	19929 3	3	5656 91	40 17	0 000
Interaction	1175 4	3	391 81	2 78	0 096
Residual Error	1408 3	10	140 83		
Lack-of-Fit	1310 3	5	262 06	13 37	0 006
Pure Error	98 0	5	19 60		
Total	39483 7	19			

R^2 = 96 43%, R^2 (adj) = 93 22%, SS, sum of squares, DF, degree of freedom, MS, mean square

The p-value denotes the significance of the coefficient and is an important factor in understanding the pattern of the mutual interactions among the variables (Table 5 11) The p-values suggested that among the three variables studied, C_2 (peptone concentration) and C_3 (pH of the media) showed maximum interaction between the two variables Among the tested variables viz, starch concentration and pH of the medium demonstrated positive coefficient suggesting that they act as inducers for alkaline α-amylase production The negative coefficient observed for the peptone (linear and square effect) suggested that a decrease in the concentration of this complex organic source of nitrogen could improve the alkaline α-amylase yield from *B licheniformis* strain AS08E

Table 5.11: Estimated model coefficients by multiple linear regressions (significance of regression coefficients) for alkaline α-amylase production by *B licheniformis* strain AS08E under SmF study

Factor	Coefficient	SE coefficient	Computed *t*-value	*p*-value
Constant	-3358 84	475 05	-7 07	0
C_1	370 63	110 167	3 364	0 007
C_2	-271 01	210 765	-1 286	0 227
C_3	549 37	74 376	7 386	0
C_1^2	-87 26	12 504	-6 979	0
C_2^2	-272 91	50 016	-5 456	0
C_3^2	-25 17	3 126	-8 052	0
$C_1 C_2$	60 63	33 565	1 806	0.101
$C_1 C_3$	2 01	8 391	0 24	0 815
$C_2 C_3$	37 63	16 783	2 242	0 049

The three-dimensional response surface plots and contour plots as a function of two factors at a time, maintaining the third factor at the minimum (zero) level, are shown in Figure 5.15 and Figure 5.16, respectively These plots are graphical representations of the regression equation and used to investigate the interaction amongst the variables and to determine optimum conditions for alkaline α-amylase production From Figures 5 15A & C, it can be concluded that a higher concentration of starch (up to 2.5% w/v) and lower concentration of peptone (0.5-0.7% w/v) could induce the optimum alkaline α-amylase production from *B. licheniformis* strain AS08E. Similarly, the contour plot (Figure 5.16) indicates significant interaction between the peptone concentration and pH of the medium for optimum alkaline α-amylase production from *B licheniformis* strain AS08E

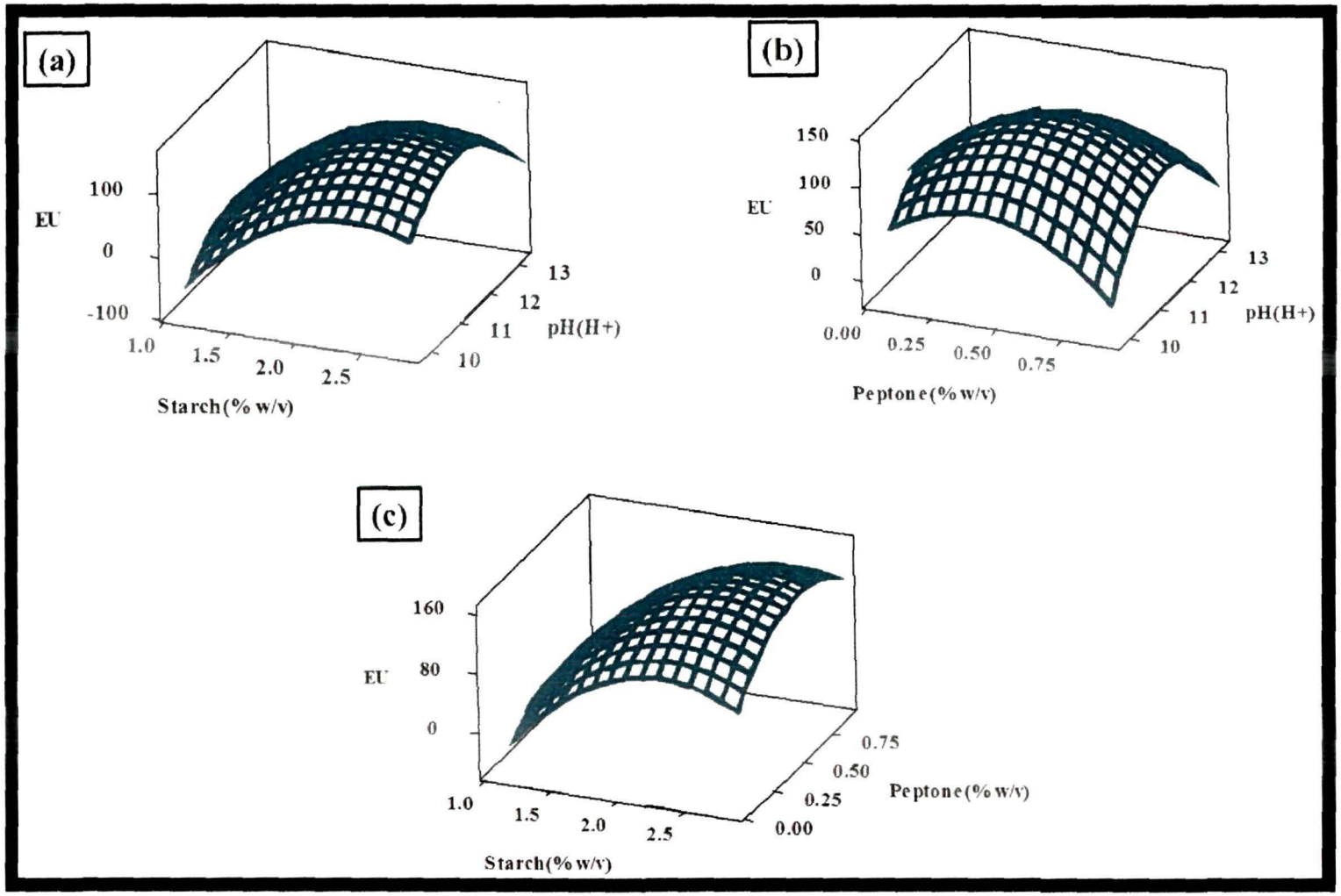

Figure 5.15: Response surface plots for alkaline α-amylase production by *B. licheniformis* strain AS08E. The interactions between (A) pH vs starch (% w/v); (B) pH vs peptone (% w/v) and (C) starch (% w/v) vs peptone (% w/v).

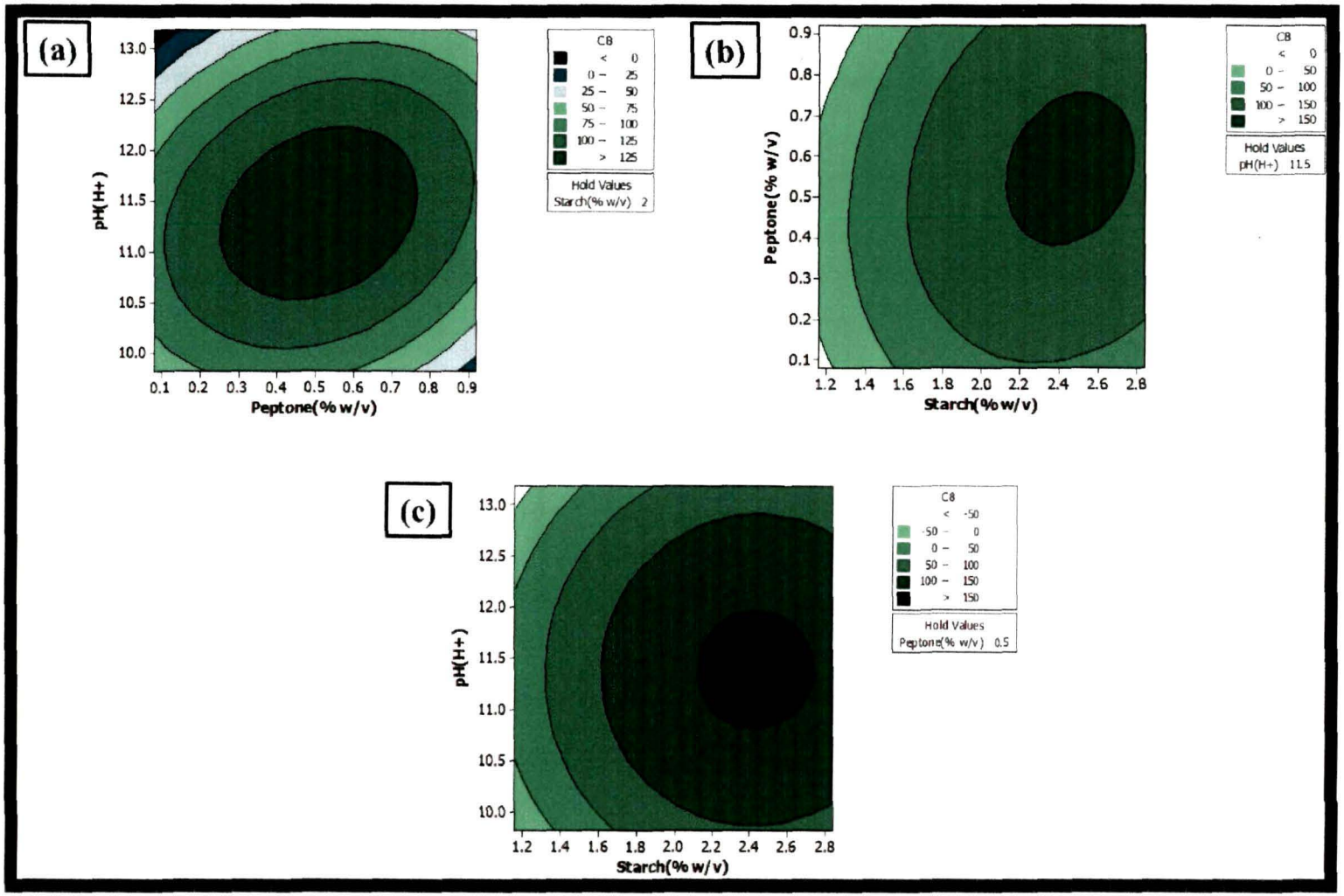

Figure 5.16: Contour plots showing interaction effect of test variables on alkaline α-amylase production from *B. licheniformis* strain AS08E. (A) pH vs peptone (% w/v) (B) peptone vs starch (% w/v) (C) starch (% w/v) vs pH (% w/v).

5.3.4. Validation of the model for the optimum alkaline α-amylase production

The optimum levels of test variables for maximum alkaline α-amylase production from *B. licheniformis* strain AS08E were obtained by solving the regression Equation 5.2. Using the predict programme of Minitab 15 Statistical Software®, the predicted values for each variable was determined as 2.40 % (w/v) of starch, 0.56 % (w/v) of peptone and at pH 11.4 of the medium for achieving the maximal response (Figure 5.17).

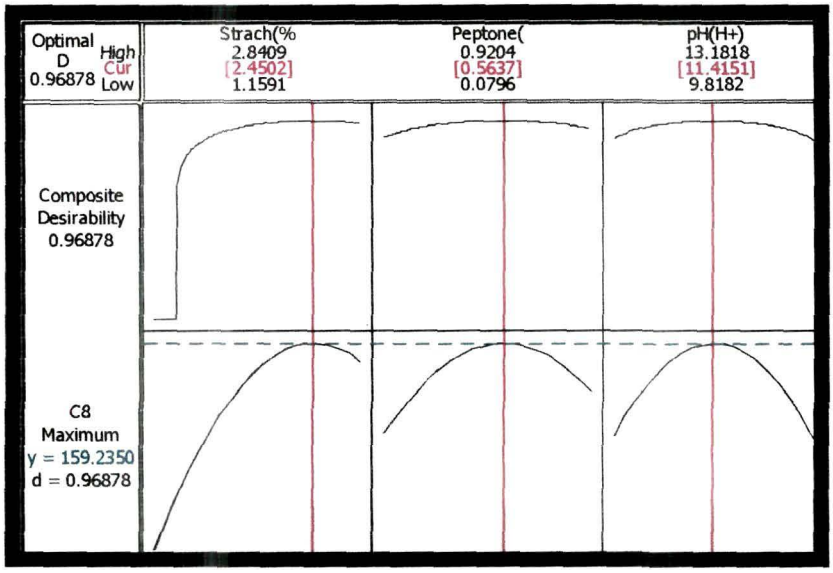

Figure 5.17: Optimization plot showing the optimum value for maximum thermostable α-amylase production from *Bacillus licheniformis* strain AS08E.

The alkaline α-amylase yield under the optimized conditions was 162.9 ± 8.1 U/ml (mean ± S.D., n=3, *p*-value = <0.001) in a process control bioreactor as compared to the predicted response of 159.2 U/ml for the maximum alkaline α-amylase production from *B. licheniformis* strain AS08E (Table 5.12). This shows that there is an excellent correlation between predicted and observed values, which justifies the validity of the response model, and the existence of an optimum point. With the use of optimized media, there is approximately 3-fold improvement in alkaline α-amylase production compared to production of the same enzyme under non-optimized conditions.

Table 5.12: Optimized conditions with predicted and observed response achieved after RSM implementation

Factors	Optimized values	Predicted response	Observed response	Fold increase in production
Starch (%)	2.4	159.2 x 10^3 U/l	162.9 x 10^3 U/l	~3-fold from initial productions
Peptone (%)	0.56			
pH(H^+)	11.4			

5.4. Isolation and purification of α-amylase from *B. licheniformis* strain AS08E

Fractionation of cell free supernatant (CFS) from *B. licheniformis* strain AS08E using a hydrophobic interaction column (HIC) resulted in elution of bound proteins in a single peak (HIC-I) with 0% salt [$(NH_4)_2SO_4$] concentration (Figure 5.18). Enzyme activity analysis of this peak showed that it retained the α-amylase activity and thus it was pulled out for further fractionation through gel-filtration chromatography

Further fractionation of the HIC-bound fraction on a gel filtration (Sephacryl S-200) column resulted in separation of proteins into four peaks, however, analysis of enzyme activity of each peak revealed that α-amylase activity was confined to the third (GF-III) peak (Figure 5.19). The protein in this peak was assessed for purity of preparation.

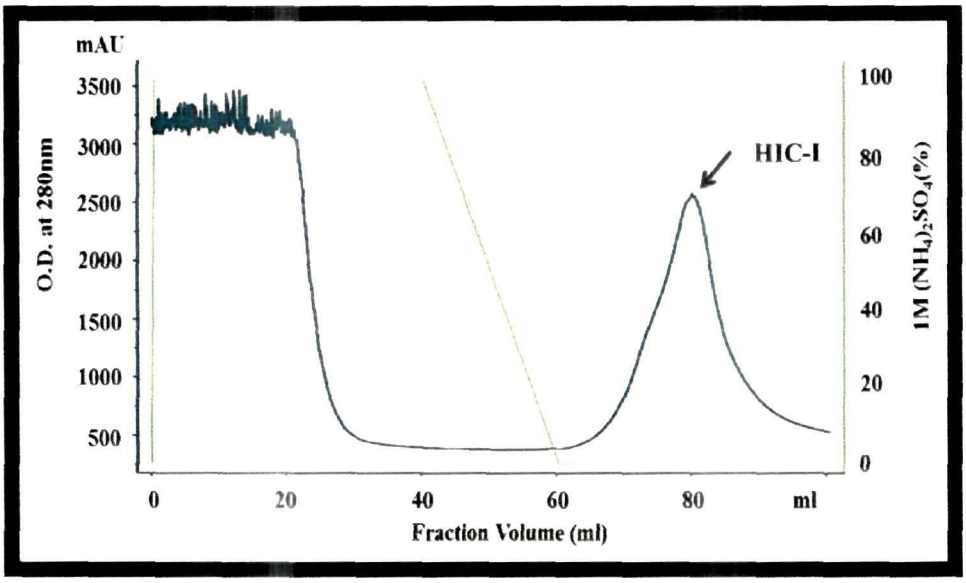

Figure 5.18: Elution profile of alkaline α-amylase from *B. licheniformis* strain AS08E cells on phenyl-sepharose column. The active peak exhibiting α-amylase activity is marked with an arrow on the chromatogram.

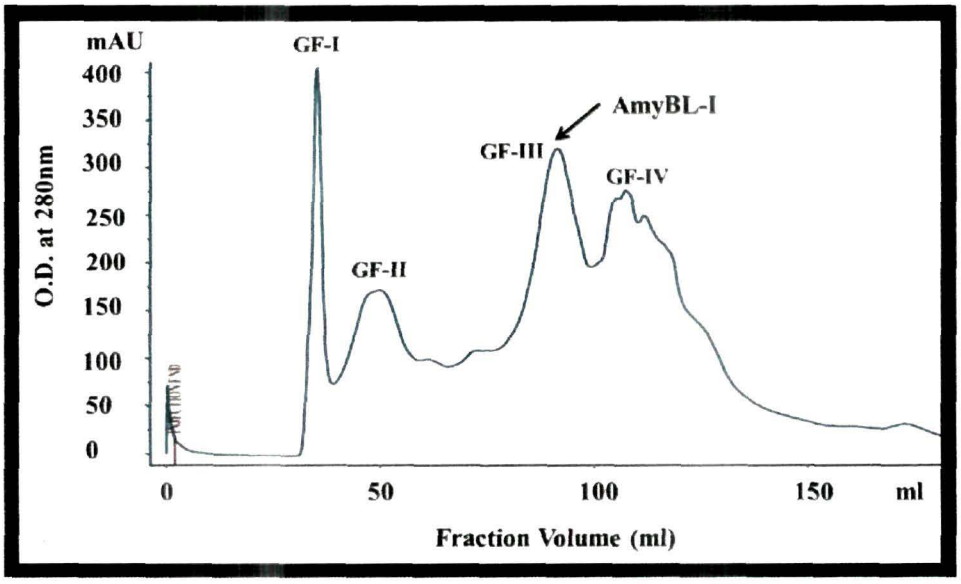

Figure 5.19: Elution profile of alkaline α-amylase (AmyBL-I) from *B. licheniformis* strain AS08E cells on Sephacryl S-200 column. The active peak exhibiting α-amylase activity is marked with an arrow on the chromatogram.

The gel filtration fraction showed a single band of ~55.0 kDa on a 10% SDS-PAGE gel run under reducing conditions (Figure 5.20). Analysis of purified AmyBL-I under native condition (zymographic analysis), also revealed a clear zone of starch hydrolysis at around ~55.0 kDa (Figure 5.20). Thus, it can be concluded that the purified enzyme has a molecular mass of ~55.0 kDa and it is monomeric in nature. This enzyme was named AmyBL-I.

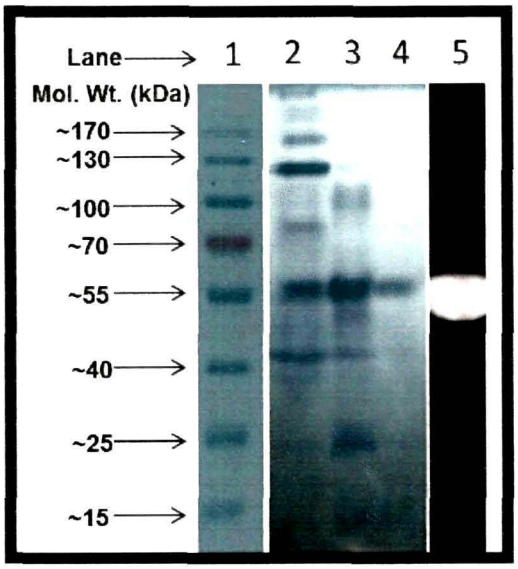

Figure 5.20: SDS-PAGE analysis of purified α-amylase from *B. licheniformis* strain AS08E; lane 1: protein molecular weight markers, lane 2: crude enzyme (concentrated), lane 3: HIC fraction (25 µg), lane 4: purified α-amylase (GF-III, 15 µg), and lane 5: zymogram of purified α-amylase (20 µg).

Following the two steps of purification (phenyl-sepharose and gel-filtration), AmyBL-I was purified up to 14.5-fold from the culture supernatant of *B. licheniformis* strain AS08E with 6.9% α-amylase yield (Table 5.13).

Table 5.13: A summary of purification of AmyBL-I from *B. licheniformis* strain AS08E, data represent a typical experiment.

Purification step	Total protein (mg)	Total Activity (U)	Specific Activity (U/mg)	Purification (fold)	Enzyme Yield (%)
Crude extract	2390	172000	71.9	1	100.00
Phenyl-Sepharose	134	36000	268.6	3.7	20.93
Sephacryl S-200	11.4	11900	1043.8	14.5	6.9

5.5. Biochemical characterization of purified protein AmyBL-I

5.5.1. Optimum temperature and pH determination of purified enzyme AmyBL-I

Analysis of the purified AmyBL-I at various temperatures ranging from 40-90°C for 30 min showed that the enzyme was active over a wide range of temperatures but could act optimally at 80°C (Figure 5.21). The purified enzyme was also active over broad range of pH values from 6.0-12.0, however, it acted optimally at pH 10.0 (Figure 5.21). Thus, from these studies we can conclude that the purified enzyme from *B. licheniformis* strain AS08E works optimally at pH 10.0 and 80°C.

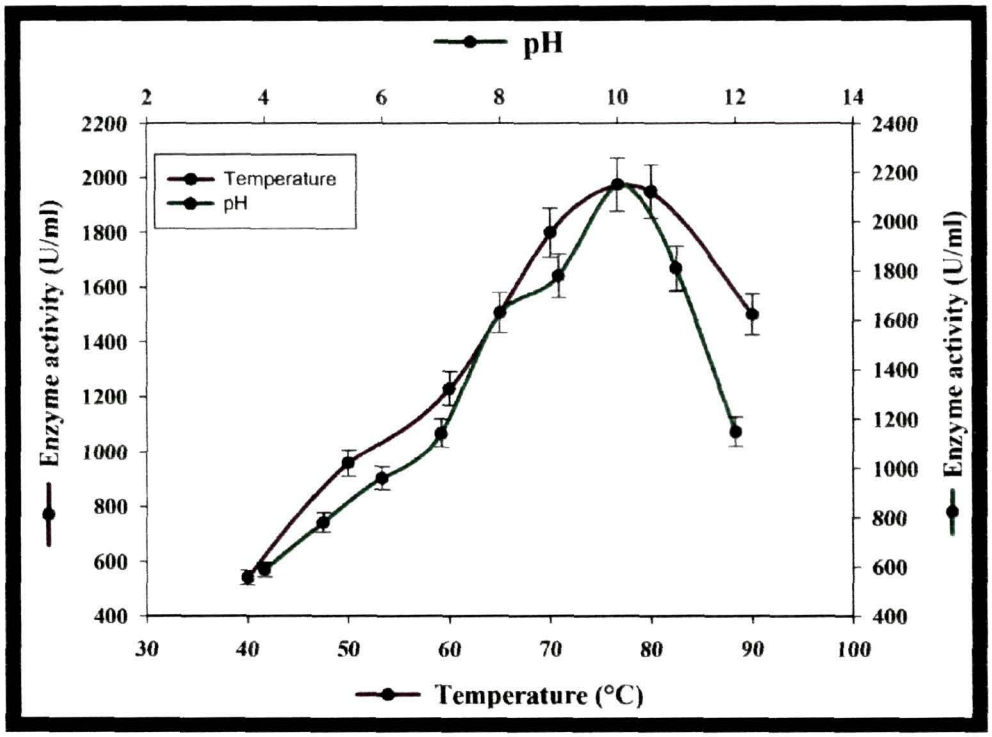

Figure 5.21: Determination of optimum pH and temperature for activity of AmyBL-I from *B. licheniformis* strain AS08E. Values are mean ± S.D. (n = 3), having p-value ≤ 0.05.

5.5.2. Thermostability study of AmyBL-I

The thermostability of AmyBL-I was investigated by incubating the enzyme at 40-100°C for 30 min either in presence or in absence of 5 mM Ca^{2+} ions. Enzyme incubated at 60°C for 60 min without Ca^{2+} ions did not show a change in enzyme activity as compared to non-heated enzyme. However, heating beyond this temperature resulted in a gradual loss of enzyme activity (Figure 5.22). Further, in the presence of 5 mM Ca^{2+} ions, the thermostability of AmyBL-I reached up to 80°C.

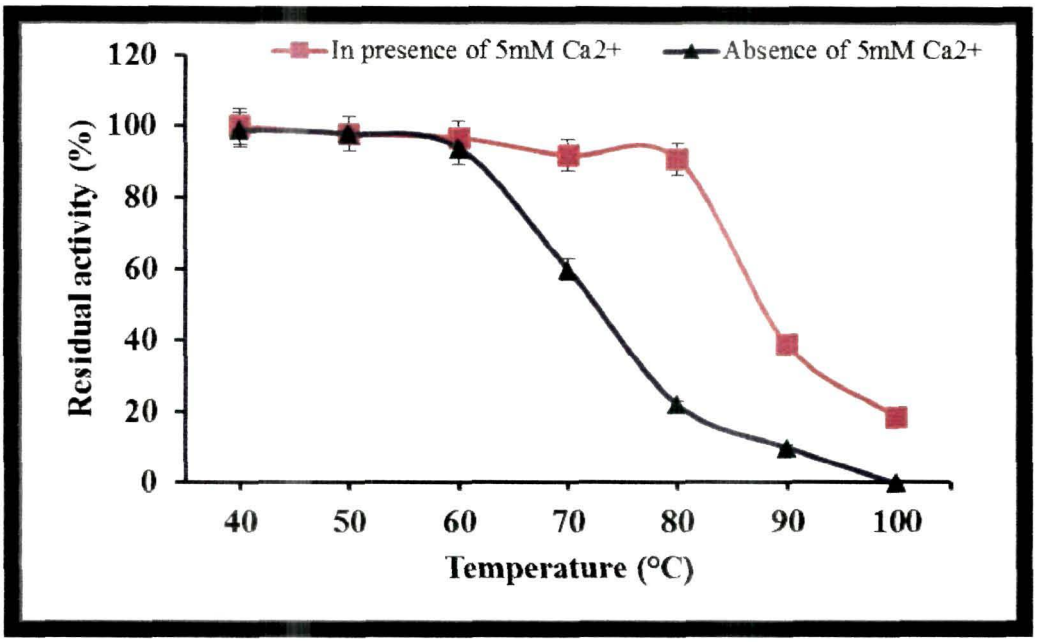

Figure 5.22: Effect of temperature on stability of AmyBL-I in the presence (■) and absence (▲) of Ca^{2+} ion (5 mM final conc.).

5.5.3. Kinetics study of AmyBL-I

The K_m and V_{max} values of AmyBL-I towards soluble starch were determined as 4.5 ± 0.2 mg/ml and 416.67 ± 20.8 µmol/min/mg, respectively (Figure 5.23).

5.5.4. Effects of various metal ions on purified enzyme AmyBL-I

The effect of different divalent cations (final conc. 5 mM) on enzyme activity of AmyBL-I showed that most of the tested divalent metal ions inhibited the enzyme activity by only 5-10%. However, in the presence of mercury ions, AmyBL-I lost approx. 95% of its original α-amylase activity (Figure 5.24).

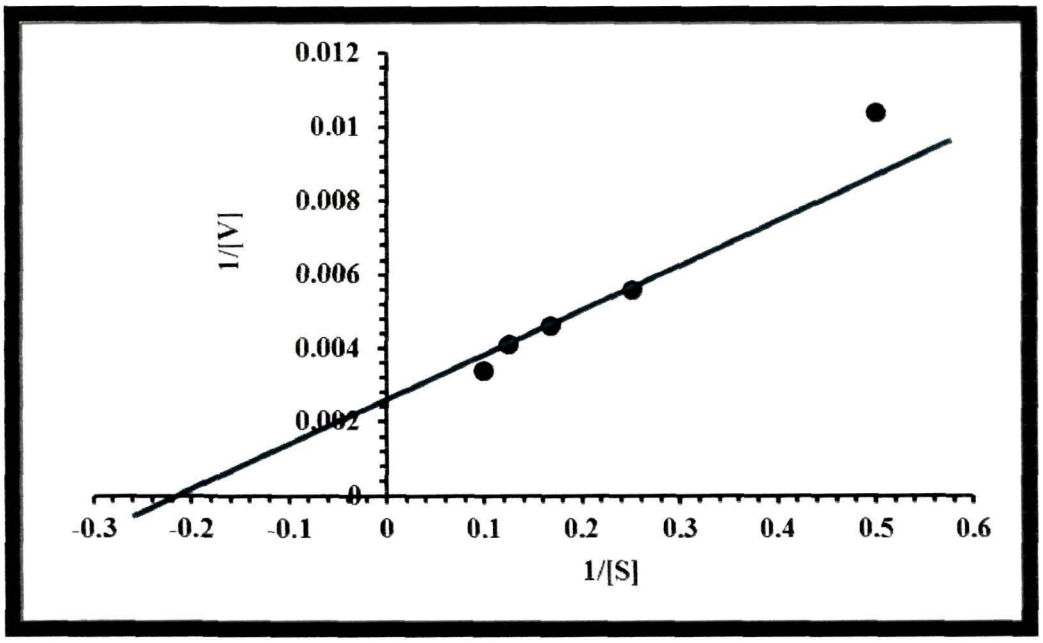

Figure 5.23: Lineweaver-Burk plot used to determination of K_m and V_{max} values for hydrolysis of starch by AmyBL-I. Each data point is a mean of triplicate determinations.

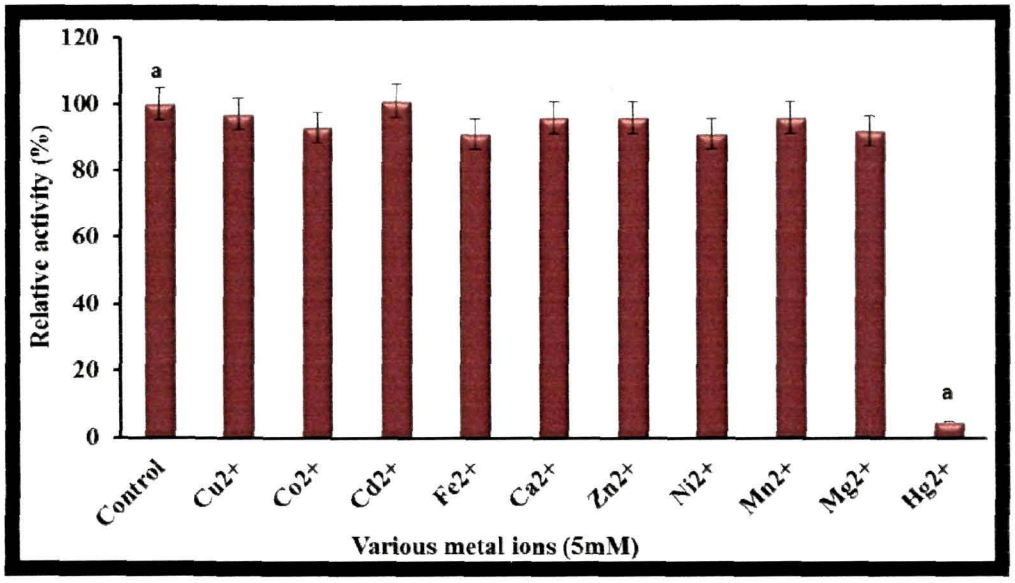

Figure 5.24: Effect of various metal ions on α-amylase activity of AmyBL-I. Values are mean ± S.D. of triplicate determinations with p-value ≤ 0.001. The bar with same superscript differ significantly w.r.t. control ($p < 0.05$).

5.5.5. *N-terminal amino acid sequence of AmyBL-I*

The N-terminal amino acid sequence of AmyBL-I by automated Edman degradation method was found to be **ANLNGTLMQYFEWYMPNDGQ** (Figure 5.25), which is identical to the N-terminal sequence of *B. licheniformis* α-amylase entries in the PDB (NCBI) database.

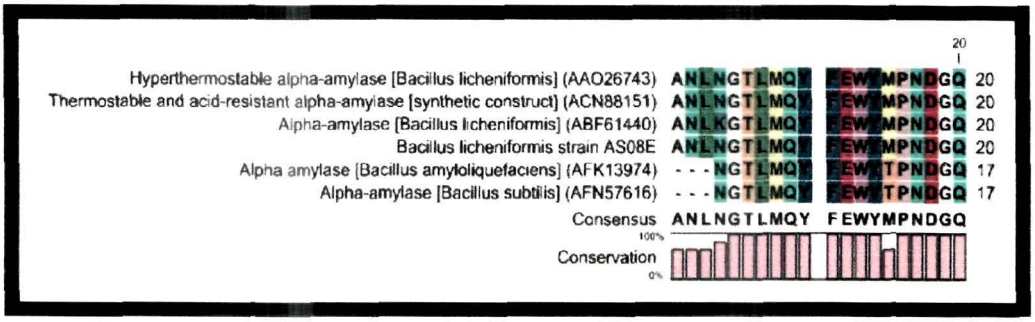

Figure 5.25: Multiple sequence alignment of the AmyBL-I N-terminal sequence and other closely related α-amylase sequences from NCBI database.

5.5.6. *Starch binding affinity of the purified α-amylase*

The interaction of soluble starch and AmyBL-I was studied by monitoring the change in intrinsic fluorescence of the enzyme (Figure 5.26). The characteristic emission spectrum for the enzyme was observed at 341 nm, while for the dissolved starch, it was 340 nm. Further, the fluorescence spectra of dissolved starch in the presence of AmyBL-I showed a clear shift in the band intensity and slight red shifting (342 nm) effect was noticed due to interaction effect between the two molecules (Figure 5.26).

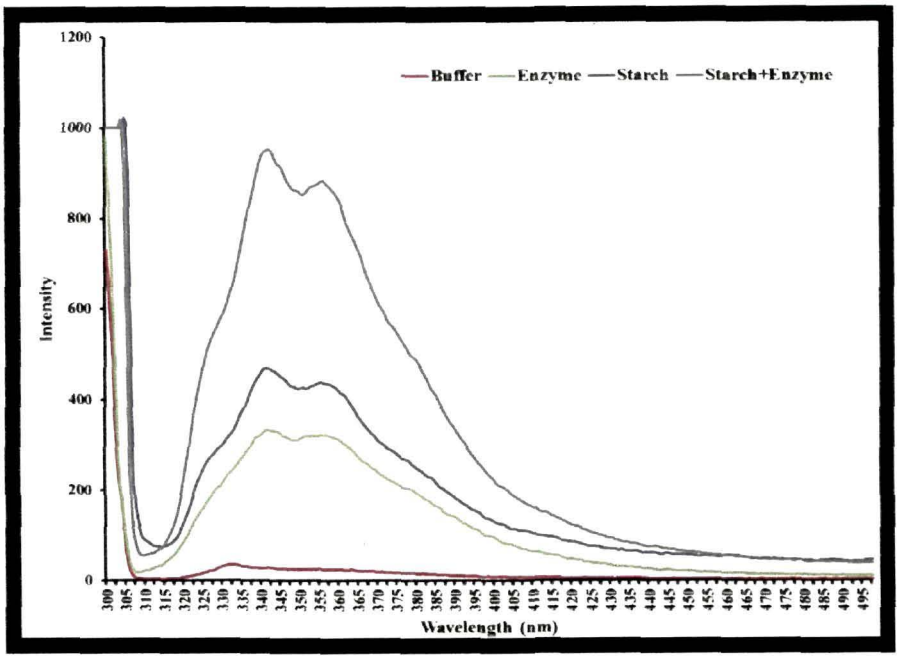

Figure 5.26: Starch binding by of AmyBL-I monitored using fluorescence spectroscopy.

5.5.7. Effects of various inhibitors on the α-amylase activity of AmyBL-I

AmyBL-I was tested for its stability and compatibility with various effectors/group modifying molecules to understand its biochemical properties. In the presence of PMSF and 4-BPB (2 mM final concentration) AmyBL-I showed a significant reduction in enzyme activity, thereby implying the presence of serine and histidine residues in the active site (Table 5.14). Further, incubation of AmyBL-I with 2 mM EDTA showed 52% reduction in enzyme activity as compared to control (Table 5.14) suggesting it to be a metalloenzyme. However, AmyBL-I demonstrated significant stability and compatibility in the presence of surfactants, oxidizing agents and organic solvents, implying its excellent candidature for inclusion in laundry detergent formulations. AmyBL-I also showed considerable stability in the presence of proteases such as proteinase K, thereby suggesting that AmyBL-I can also be used in laundry detergent formulations containing proteases (Table 5.14).

Table 5.14: Effects of various effectors/group modifying reagents on the catalytic activity of AmyBL-I. Each value represent mean ± S.D., where n = 3 with *p*-value ≤ 0.001. The value with same superscript do not differ significantly w.r.t. control (*p*-value > 0.05).

Effector	Residual activity (%)
Control (without effectors)	100[a]
EDTA (2 mM)	48.0 ± 2.4
PMSF(2 mM)	36.0 ± 1.8
4-BPB(2 mM)	43.0 ± 2.1
H_2O_2 (2 mM)	84.8 ± 4.2
SDS (1 mM)	88.0 ± 4.4
Triton-x 100 (1% v/v)	80.0 ± 4.0
Tween-80 (1% v/v)	86.0 ± 4.3
Methanol (30% v/v)	99.0 ± 4.9[a]
Ethanol(30% v/v)	97.0 ± 4.8[a]
Acetonitrile (30% v/v)	88.0 ± 4.4
Acetone(30% v/v)	98.0 ± 4.8[a]
Proteinase K (2 U/ml)	66.0 ± 3.3

5.6. Industrial application of AmyBL-I

5.6.1. Detergent stability

AmyBL-I exhibited significant stability and compatibility with all the tested commercial laundry detergents (Figure 5.27). It was observed that AmyBL-I retained up to 49.0-88.0% and 44.0-82.0% of its original activity in the presence of detergents at 30 and 37°C, respectively (Figure 4.27). The commercial α-amylase (Himedia) retained 37% to 55% and 32% to 51% of its activity under identical experimental conditions. Besides, it was also observed that among the tested detergents, Safed® laundry detergent component(s) may be the most compatible detergent for AmyBL-I (Fig: 5.27).

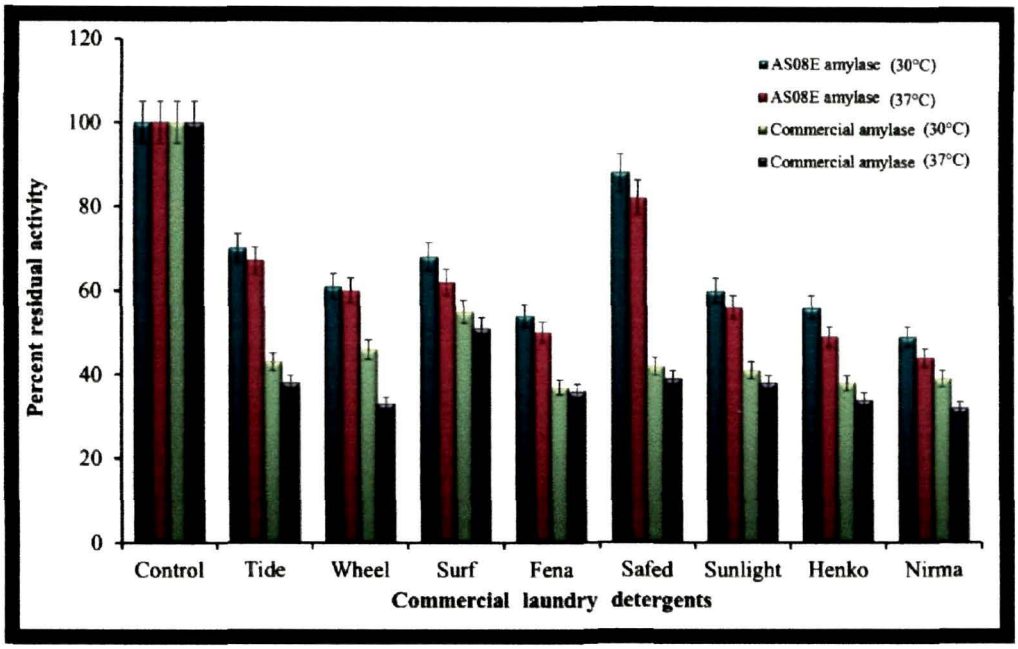

Figure 5.27: A comparison of detergent stability and compatibility of alkaline AmyBL-I with commercial α-amylases. Values are mean ± S.D. of triplicate determinations having p-value ≤ 0.05. Each value differ significant w.r.t. control (p-value < 0.05).

5.6.2. Wash performance test

As the detergent stability of AmyBL-I was found to be most compatible with the Safed® laundry detergent (see section 5.6.1), AmyBL-I supplemented Safed® detergent was tested for chocolate stain removal capabilities from stained fabrics. The visual examination of treated stained cotton fabrics showed that the enzyme (AmyBL-I) supplemented with Safed® detergent has better stain removal capabilities as compared to detergent/enzyme alone (Figure 5.28). The estimation of total carbohydrate released in the wash suggest that Safed® detergent supplemented with α-amylase (AmyBL-I) showed more than two-fold increase in carbohydrate release as compared to detergent/enzyme alone [Figure 5.28 (f)].

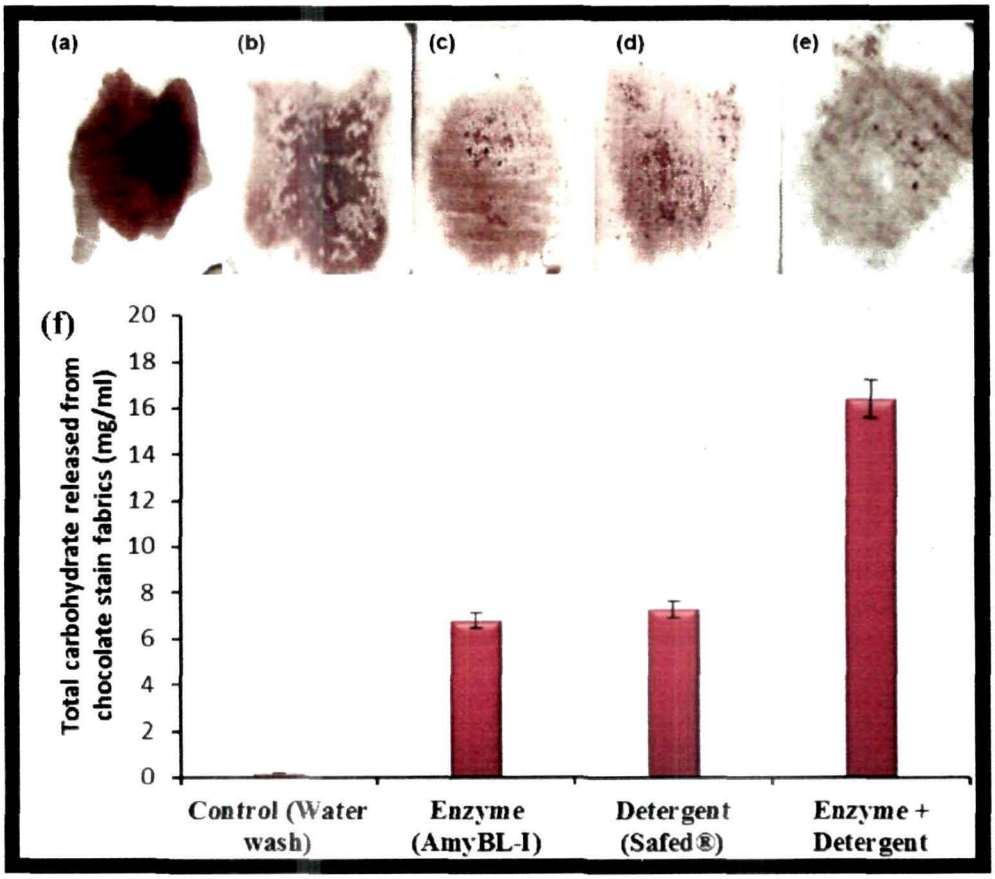

Figure 5.28: Wash performance analysis of AmyBL-I on chocolate-stained fabrics. (a) stained cloth, (b) washed with tap water, (c) washed with detergent solution (7 mg/ml), (d) washed with AmyBL-I (500 U/ml), and (e) washed with AmyBL-I (500 U/ml) supplemented detergent solution (7 mg/ml). (f) Quantitative estimation of total carbohydrate release from the wash performance tests stained fabrics. Values represent mean ± S.D. (n = 3) having p-value ≤ 0.001. The values vary significantly w.r.t. control (p-value < 0.05).

5.6.3. Desizing efficiency of the purified AmyBL-I

Starch removal or desizing efficiency of AmyBL-I was determined on starchy cotton fabrics. Visual examination of the enzyme-treated starchy cloths revealed that the enzyme has better starch removal activity as compared to the cloths washed in tap water, thus suggesting the potential candidature of AmyBL-I for desizing application in textile industry (Figure 5.29).

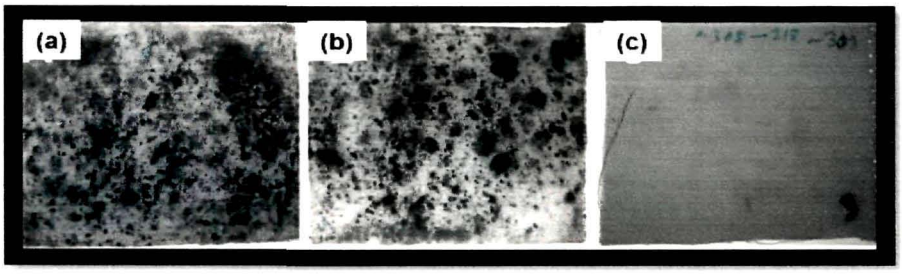

Figure 5.29: Desizing activity of AmyBL-I on starchy cloths (a) control without treatment, (b) washed in tap water, and (c) treated with alkaline α-amylase.

5.6.4. Raw starch adsorption and digestibility by the AmyBL-I

An adsorption study of AmyBL-I revealed that it has varied degrees of adsorption towards various raw starches. It showed 95% adsorbability towards raw potato starch, and 86% towards the raw wheat starch. The raw starch digestibility pattern showed that after 3 h of incubation with potato and wheat starch, AmyBL-I resulted in release of maltose and high molecular weight oligosaccharides as the major hydrolytic products (Figure 5.30). The quantitative analysis showed that after 3 h of incubation, the major product formed were disaccharides (maltose) 30-40%, followed by tri-saccharides (25-35%) and higher oligosaccharides (20-30%). Glucose comprised only 10-15% of total product formed.

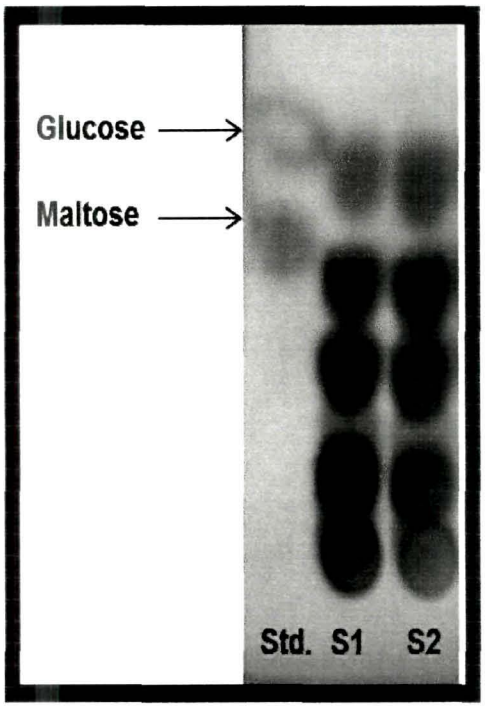

Figure 5.30: TLC analysis of raw potato and wheat starch hydrolysis by AmyBL-I; Std.: standard (Glucose & Maltose), S1 = hydrolyzed sample of potato starch after 3 h of treatment, S2 = hydrolyzed sample of wheat starch after 3 h of treatment at 60°C.

SEM analysis of the residual raw potato and wheat starch samples treated with AmyBL-I suggested that AmyBL-I could efficiently digest various raw starches as it formed holes and pits on the smooth surfaces of the raw starch granules (Figure 5.31).

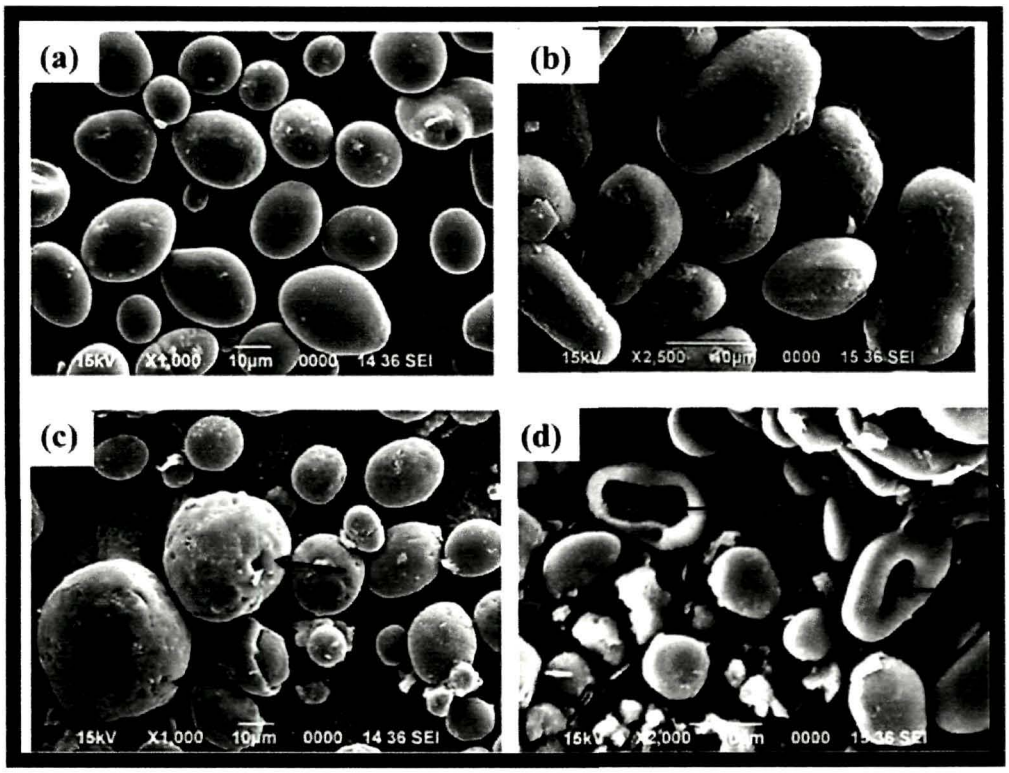

Figure 5.31: Scanning electron microscopic (SEM) photographs of AmyBL-I treated and untreated raw potato and wheat starches. **(a)** Untreated potato starch; **(b)** untreated wheat starch; **(c)** potato starch treated with AmyBL-I and **(d)** wheat starch treated with AmyBL-I for 3 h at 60°C (holes and pits are marked with an arrow on treated starch granules).

5.7. Cloning and expression of an α-amylase gene from *B. licheniformis* strain AS08E

5.7.1. PCR amplification of an α-amylase gene from B. licheniformis strain AS08E and cloning it into a pJET 1.2 cloning vector

From the total genomic DNA of *B. licheniformis* strain AS08E, a gene encoding an α-amylase enzyme was PCR-amplified using gene-specific primers. This resulted in the appearance of a band of ~1500 bp on agarose gel, which was also in accordance with the expected gene size of α-amylase from the bacteria (Figure 5.32).

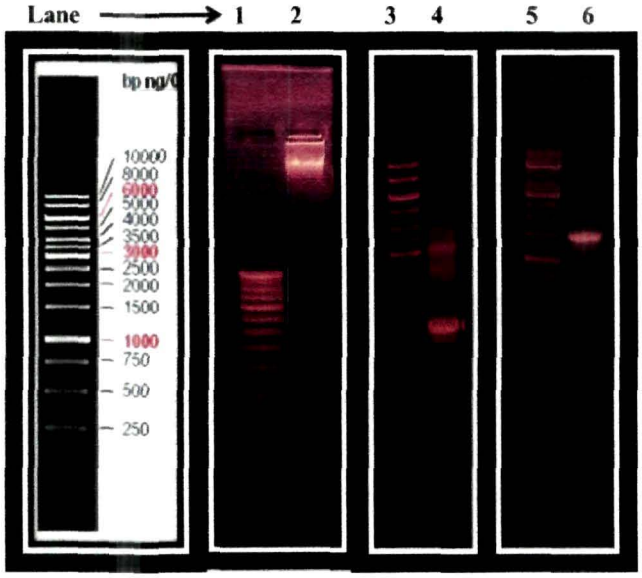

Figure 5.32: Agarose gel electrophoresis analysis of genomic DNA from *B. licheniformis* strain AS08E and amplification of its α-amylase gene using the primers BLF1 and BLR2. Lane 1, 3 & 5: 1 kb ladder; lane 2: purified genomic DNA from strain AS08E; lane 4: PCR-amplified product of α-amylase gene from strain AS08E and lane 6: purified DNA (PCR amplified product).

Transformation of recombinant pJET 1.2 cloning vector (containing amplified α-amylase gene fragment) into competent *E. coli* DH5α cells resulted into appearance of a single white colony on the transformed plate (Figure 5.33a). Screening of this clone by isolation of recombinant plasmid and then double digestion of the recombinant plasmid resulted into appearance of two bands (~3000 bp for plasmid and ~1500 bp for insert) on the agarose gel (Figure 5.33b). The ligation of PCR-amplified α-amylase gene product from *B. licheniformis* strain AS08E was also confirmed by PCR amplification of the insert from both the recombinant clone and recombinant plasmid (Figure 5.33b).

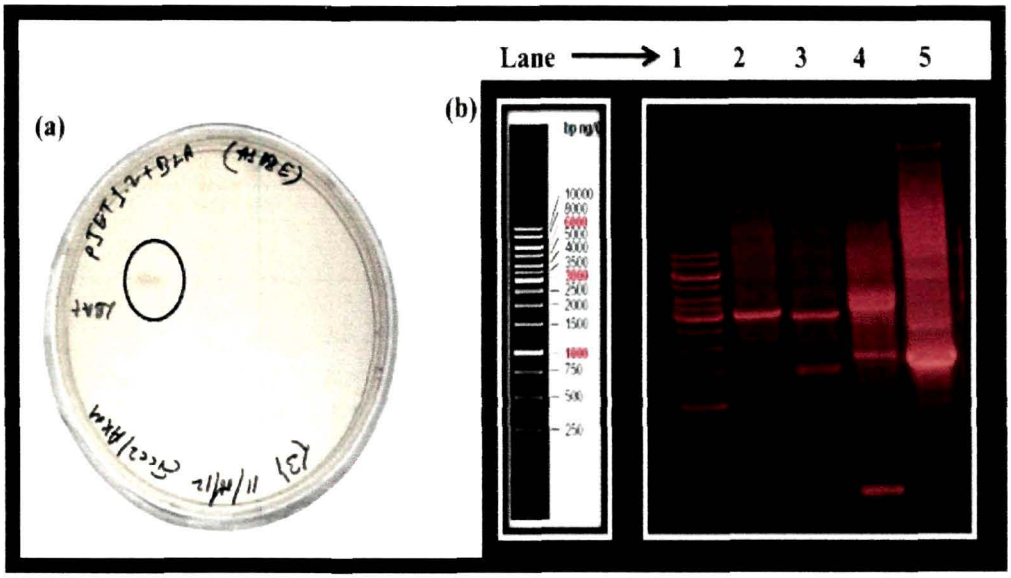

Figure 5.33: Cloning of PCR-amplified α-amylase gene from *B. licheniformis* strain AS08E into pJET1.2 cloning vector. **(a)** Transformed plate containing recombinant pJET 1.2 vector, **(b)** agarose gel analysis of transformed colony [lane 1: 1 kbp DNA ladder; lane 2: control plasmid (pJET 1.2); lane 3: double digested (*Xho* I & *Nco* I) pJETBLA vector; lane 4: colony PCR of recombinant clone and lane 5: PCR amplification of pJETBLA vector).

Sequence analysis of the cloned insert from recombinant plasmid (pJETBLA) revealed that it matches up to 99% with the *B. licheniformis* α-amylase gene coding sequence and showed highest similarity with the α-amylase gene from *B. licheniformis* ATCC 14580 (Table 5.15). However, sequence analysis of the cloned insert showed that it did not cover the complete α-amylase gene coding sequence. Therefore, a new set of primers was designed to cover the complete coding sequence based on the most similar sequence obtained after the sequence alignment (Table 5.15).

Table 5.15: Percentage identity of cloned α-amylase gene from strain AS08E in pJET 1.2 PCR cloning vector with other related bacterial α-amylase gene sequences.

Description	Query cover	Maximum identity	Accession No.
B. licheniformis ATCC 14580 α-amylase gene	100%	99%	CP000002
B. licheniformis DSM 13 = ATCC 14580, α-amylase gene	100%	99%	AE017333
B. licheniformis strain ATCC 27811 α-amylase (amyA) gene	100%	99%	AY630336
B. licheniformis strain AMP13 α-amylase (amyL) gene,	100%	99%	KC176797
Bacillus sp. 1-15 α-amylase gene, partial cds	99%	99%	JX090594
Synthetic construct thermostable and acid-resistant α-amylase precursor, gene	100%	99%	FJ792701
B. licheniformis strain TCCC11052 α-amylase gene	100%	99%	EU231641
B. licheniformis thermostable α-amylase precursor gene	100%	99%	FJ792700
B. licheniformis strain NH1 α-amylase gene	100%	94%	EF125542
B. licheniformis from Iran hyperthermostable α-amylase gene	100%	94%	AF438149

5.7.2. Re-cloning of α-amylase gene into pET28a expression vector

PCR amplification of α-amylase gene using new set of primers BLF3 and BLR4 (see Section 3.2.11.1.2) from genomic DNA from *B. licheniformis* strain AS08E resulted in appearance of a ~1540 bp PCR product on agarose gel (Figure 5.34), which was of expected α-amylase gene size. Ligation of this amplified product into pET28a expression vector followed by its transformation into competent *E. coli* BL21a cells (Figure 5.35) resulted into appearance of four transformed colonies on the transformed plate (Figure 5.35b).

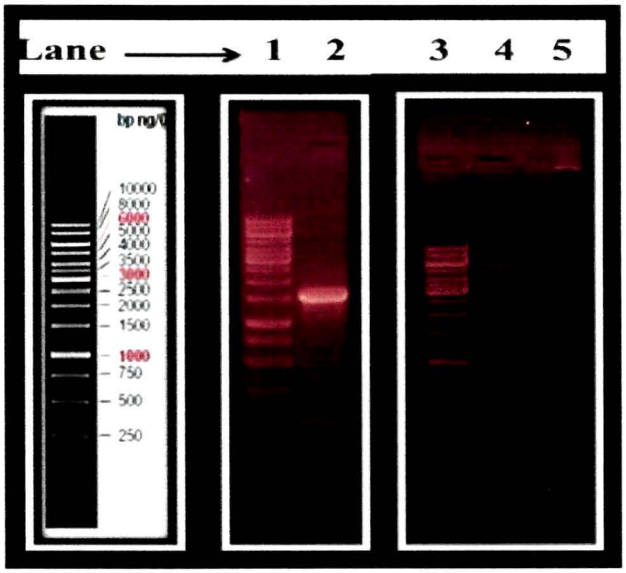

Figure 5.34: Agarose gel electrophoresis analysis of amplified α-amylase gene from strain AS08E using primers BLF3 and BLR4. Lane 1 and 3: 1 kbp DNA ladder; lane 2: amplified PCR product; lane 4: digested pET28a vector and lane 5: purified PCR product.

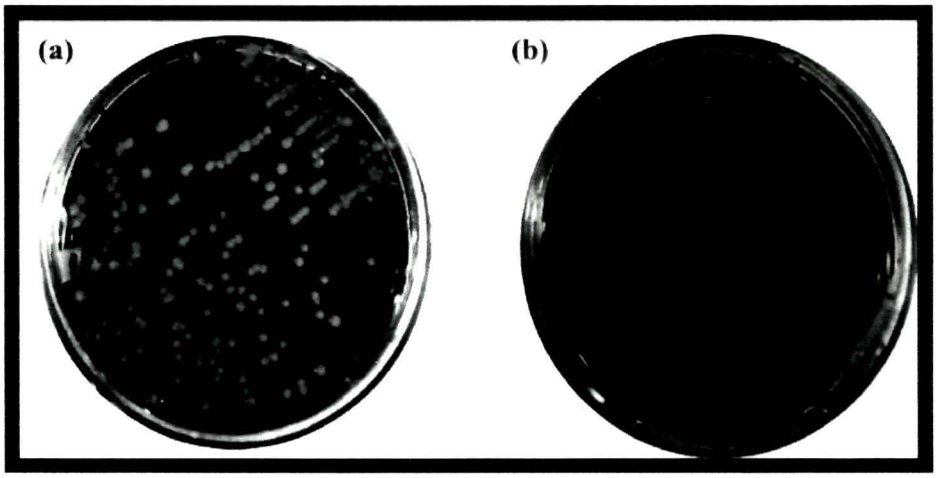

Figure 5.35: Transformed *E. coli* BL21a cells containing pET28a alone **(a)** and recombinant pET28a vector **(b)** containing α-amylase gene insert from AS08E.

Confirmation of ligation of α-amylase gene into pET28a was ascertained by digestion of recombinant plasmids (pETBLA2) isolated from recombinant clones. The single digestion of pETBLA2 with *Xho* I yielded a single band of ~7 kbp, while double digestion of pETBLA2 with *Hind* III and *Xho* I, yielded two bands of ~1500

bp and ~5500 bp, corresponding to the length of α-amylase gene and cloning vector (Figure 5.36), respectively. The PCR amplification of recombinant vector (pETBLA2) with T7 primers yielded a single band of ~1500 bp, which was also in accordance with the size of ligated gene insert (Figure 5.36).

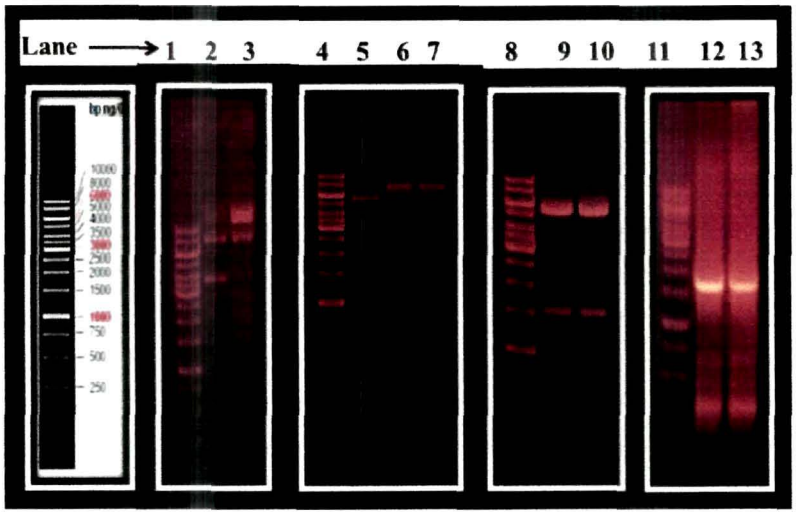

Figure 5.36: Agarose gel electrophoresis analysis of recombinant plasmid (pETBLA2) by restriction digestion and PCR amplification. Lanes 1, 4, 8 and 11: 1 kbp DNA ladder; lanes 2 and 3: pETBLA2 from clone 1 and 2, respectively; lane 5: pET28a (restriction digested with *Hind* III and *Xho* I); lanes 6 and 7: single digestion of pETBLA2; lanes 9 and 10: double digestion of pETBLA2, and lanes 12 and 13: PCR amplification of pETBLA2 using T7 primers.

Sequencing of the cloned insert revealed that it was 99% homologous with the α-amylase gene from *B. licheniformis* bacteria (Table 5.16). The analysis also revealed that the cloned α-amylase gene covered the complete open reading frame including the signal peptide sequence of α-amylase gene for efficient expression of recombinant protein outside the cell membrane. The sequence so obtained in this experiment was deposited in NCBI database under accession number KC802019.

Table 5.16: Sequence homology of cloned α-amylase gene from *B. licheniformis* strain AS08E and other α-amylase genes from closely related bacteria

Description	Query cover	Maximum identity	Accession No.
B. licheniformis strain AS08E α-amylase gen	100%	100%	KC802019
B. licheniformis ATCC 14580 α-amylase gene	100%	99%	CP000002
B. licheniformis DSM 13 = ATCC 14580, α-amylase gene	100%	99%	AE017333
B. licheniformis strain ATCC 27811 α-amylase (amyA) gene	100%	99%	AY630336
B. licheniformis strain AMP13 α-amylase (amyL) gene,	100%	99%	KC176797
Synthetic thermostable and acid-resistant α-amylase gene	100%	99%	FJ792701
B. licheniformis strain B0204 thermotolerant α-amylase (amyL)	100%	99%	DQ407266
B. licheniformis thermostable α-amylase precursor gene	100%	99%	FJ792700
B. licheniformis strain NH1 α-amylase gene	100%	94%	EF125542
B. licheniformis from Iran hyperthermostable α-amylase gene	100%	94%	AF438149

The deduced amino acid sequence (Blamy-I) from pETBLA2 insert showed presence of a prokaryotic signal peptide sequence at its N-terminus (Figure 5.37). The amino acid sequence analysis of Blamy-I showed 99% similarity with the α-amylase from *B. licheniformis* strain CICC 10181 (ACN88150) and *B. licheniformis* DSM 13 (YP077883), 98% similarity with *B. licheniformis* strain RH 101(ABF61440), and 96% similarity with the hyper-thermostable α-amylase from *B. licheniformis* (AAO26743) (Figure 5.37). Blamy-I sequence analysis also showed existence of the four most conserved sequences along with the conserved catalytic sites within these domains (Figure 5.37). In addition, amino acid analysis of Blamy-I illustrated the presence of three Ca^{2+} ion-binding sites at BLAMY133, BLAMY221 and BLAMY229 position of α-amylase primary structure (Figure 5.37). The calculated pI/Mw of Blamy-I was estimated to be 6.33/58549 Da. and 6.05/55268 Da for the precursor protein (containing SPS) and for the mature peptide, respectively.

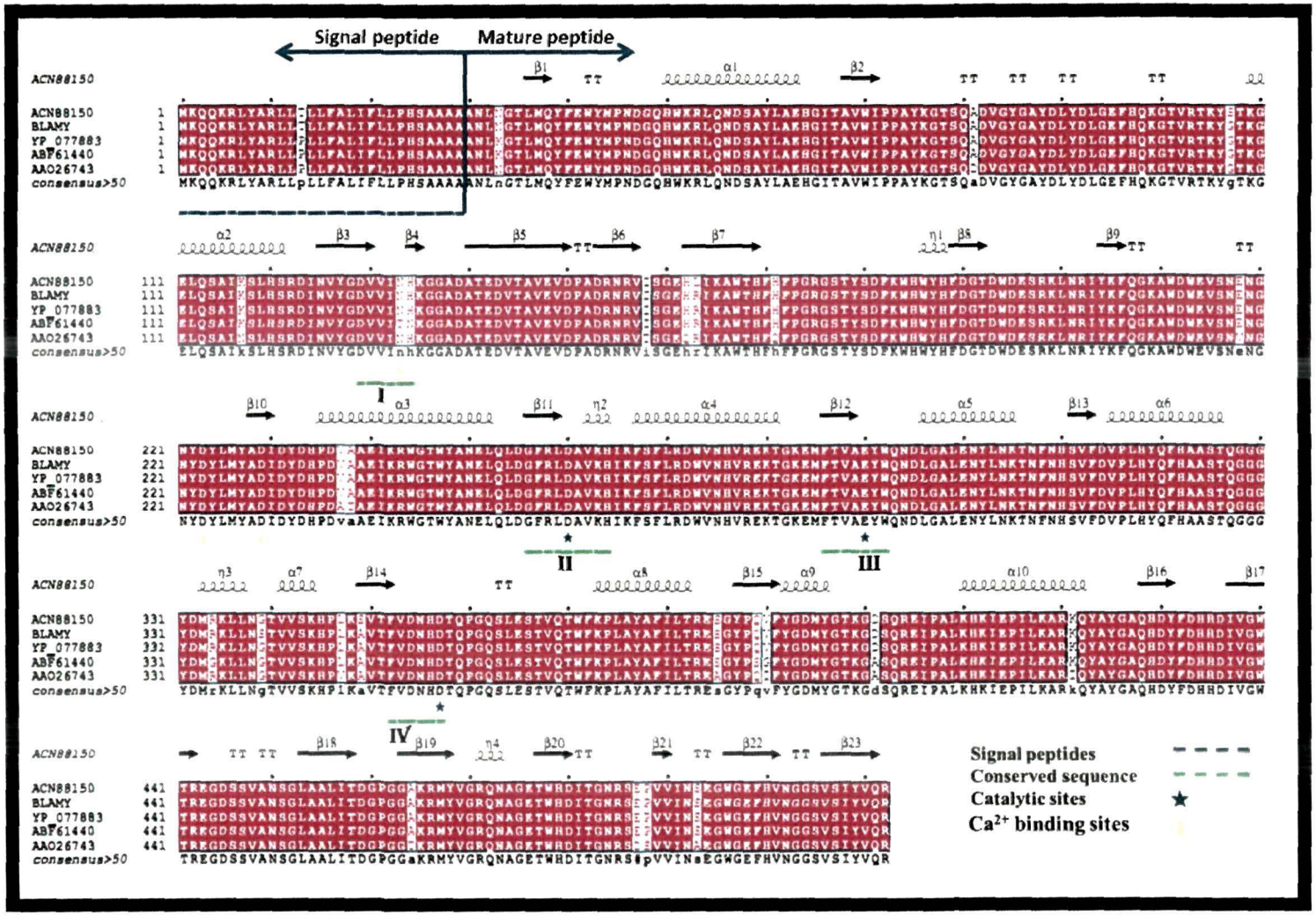

Figure 5.37: Multiple sequence alignment of Blamy-I with homologous α-amylase sequences. Secondary structure assignments are indicated at the top of the alignment. The TTT and TT letters represent strict alpha and beta turns, respectively.

5.7.3. Expression analysis of recombinant Blamy-I cloned from strain AS08E

Expression of recombinant protein outside the *E. coli* BL21 cell membrane was successfully achieved by cloning the α-amylase gene along with native signal peptide sequence from parent *B. licheniformis* strain AS08E (Figure 5.38). Analysis of recombinant clones harboring pETBLA2 plasmids on 1% starch-supplemented LBA plates showed halo zone formations around the induced colonies [Figure 5.38 (a)]. Similarly, analysis of culture broth also indicated that the induced cell could export the recombinant protein into the culture media through the *E. coli* cell membrane [Figure 5.38 (c)]. Thus, with the help of its indigenous signal peptide sequence, the recombinant protein (Blamy-I) could be easily targeted outside the *E. coli* cell membrane in its catalytically active form.

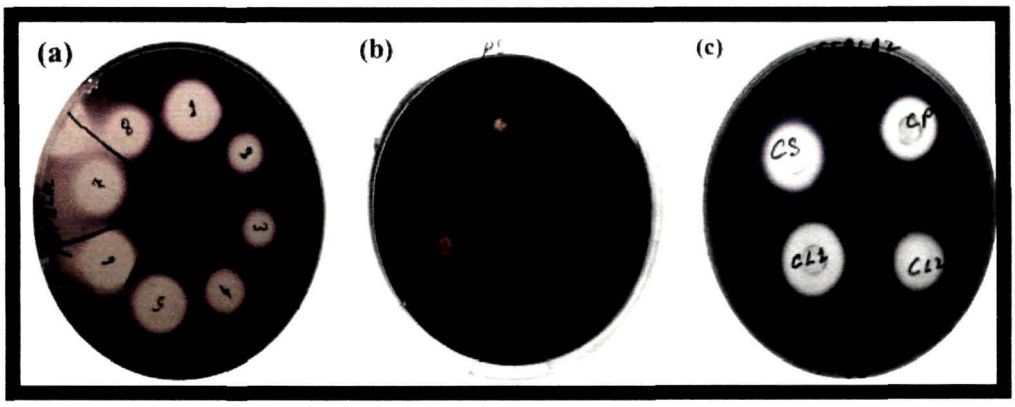

Figure 5.38: Analysis of extracellular expression of Blamy-I *E. coli*. **(a)** Recombinant clones spotted on starch agar plate, **(b)** broth analysis of control sample (pET28a vector containing cells) and **(c)** culture broth analysis of recombinant clone (CS: culture supernatant; CP: culture pallets and CL: lysed cells culture supernatant).

5.7.4. Statistical optimization of culture condition for extracellular expression of Blamy-I

With the help of the *Bacillus* signal peptide, Blamy-I was successfully targeted into the *E. coli* culture media. However, SDS-PAGE analysis of cell-free supernatant of culture media and total cell pellets displayed accumulation of the majority of the expressed protein inside the *E. coli* cytoplasm (Figure 5.39). Thus, to target this accumulated protein outside the cell membrane in their active form, the culture conditions of the host *E. coli* cell were optimized using RSM.

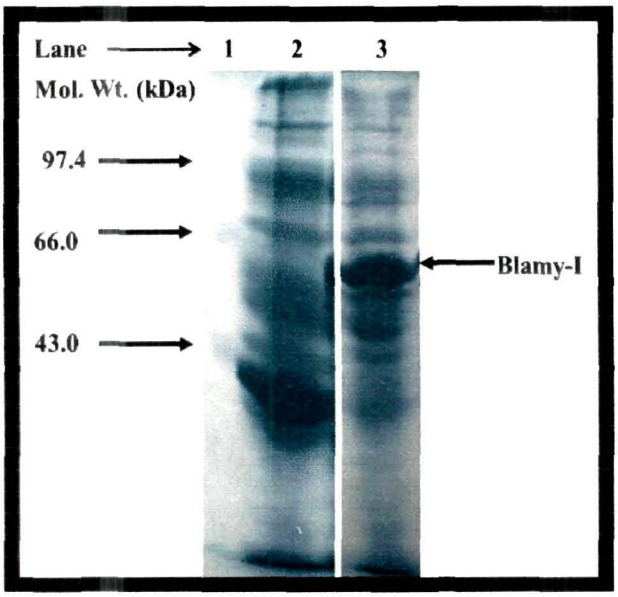

Figure 5.39: SDS-PAGE analysis of extracellular expression of recombinant Blamy-I in *E. coli*. Lane 1: protein marker; lane 2: CFS and lane 3: cell pellets.

Based on literature survey, four parameters (temperature of post-induction, IPTG concentration, post-induction incubation periods, and EDTA concentration) were identified as crucial factors for the successful expression of the recombinant proteins outside the cell membrane. These parameters were optimized using RSM. A full factorial central composite design (CCD) matrix with different levels of experimental run and their outmost responses (predicted and observed) is shown in Table 5.17.

Table 5.17: Design matrix in both coded and actual (in bracket) values with their corresponding experimental and predicted values for the extracellular expression of Blamy-I in *E. coli* culture media The observed values are mean ± S. D. (n = 3) with p-value ≤ 0.001

Run Order	IPTG (mM) (C_1)	Time of post Induction (h) (C_2)	Temperature (°C) (C_3)	EDTA (mM) (C_4)	Enzyme activity (U/ml)	
					Actual value	Predicted value
1.	-1 0 (0 2)	-1 0 (12)	-1 0 (20)	-1 0 (17)	98 26 ± 4 9	90 22
2.	1 0 (1)	-1 0 (12)	-1 0 (20)	-1 0 (17)	112 7 ± 5 6	108 34
3.	-1 0 (0 2)	1 0 (24)	-1 0 (20)	-1 0 (17)	179 81 ± 8 9	169 09
4.	1 0 (1)	1 0 (24)	-1 0 (20)	-1 0 (17)	140 81 ± 7 0	134 65
5.	-1 0 (0 2)	-1 0 (12)	1 0 (30)	-1 0 (17)	119 75 ± 5 9	122 44
6.	1 0 (1)	-1 0 (12)	1 0 (30)	-1 0 (17)	164 31 ± 8 2	157 67
7.	-1 0 (0 2)	1 0 (24)	1 0 (30)	-1 0 (17)	157 61 ± 7 8	147 54
8.	1 0 (1)	1 0 (24)	1 0 (30)	-1 0 (17)	126 89 ± 6 3	130 19
9.	-1 0 (0 2)	-1 0 (12)	-1 0 (20)	1 0 (34)	127 87 ± 6 3	118 12
10.	1 0 (1)	-1 0 (12)	-1 0 (20)	1 0 (34)	119 64 ± 5 9	117 43
11.	-1 0 (0 2)	1 0 (24)	-1 0 (20)	1 0 (34)	222 47 ± 11 1	216 83
12.	1 0 (1)	1 0 (24)	-1 0 (20)	1 0 (34)	172 72 ± 8 6	163 57
13.	-1 0 (0 2)	-1 0 (12)	1 0 (30)	1 0 (34)	98 95 ± 4 9	92 82
14.	1 0 (1)	-1 0 (12)	1 0 (30)	1 0 (34)	104 97 ± 5 2	109 23
15.	-1 0 (0 2)	1 0 (24)	1 0 (30)	1 0 (34)	139 86 ± 6 9	137 76
16.	1 0 (1)	1 0 (24)	1 0 (30)	1 0 (34)	105 88 ± 5 2	101 60
17.	-2 0 (0)	0 0 (18)	0 0 (25)	0 0 (25 5)	92 92 ± 4 6	116 55
18.	2 0 (1 4)	0 0 (18)	0 0 (25)	0 0 (25 5)	140 95 ± 7 0	146 40
19.	0 0 (0 6)	-2 0 (6)	0 0 (25)	0 0 (25 5)	103 74 ± 5 2	109 45
20.	0 0 (0 6)	2 0 (30)	0 0 (25)	0 0 (25 5)	167 67 ± 8 4	180 69
21.	0 0 (0 6)	0 0 (18)	-2 0 (15)	0 0 (25 5)	94 90 ± 4 7	113 54
22.	0 0 (0 6)	0 0 (18)	2 0 (35)	0 0 (25 5)	83 70 ± 4 2	83 79
23.	0 0 (0 6)	0 0 (18)	0 0 (25)	-2 0 (8 5)	119 95 ± 5 9	130 57
24.	0 0 (0 6)	0 0 (18)	0 0 (25)	2 0 (42 5)	121 74 ± 6 1	129 87
25.	0 0 (0 6)	0 0 (18)	0 0 (25)	0 0 (25 5)	52 93 ± 2 6	51 11
26.	0 0 (0 6)	0 0 (18)	0 0 (25)	0 0 (25 5)	53 99 ± 2 6	51 11
27.	0 0 (0 6)	0 0 (18)	0 0 (25)	0 0 (25 5)	50 59 ± 2 5	51 11
28.	0 0 (0 6)	0 0 (18)	0 0 (25)	0 0 (25 5)	52 51 ± 2 6	51 11
29.	0 0 (0 6)	0 0 (18)	0 0 (25)	0 0 (25 5)	51 19 ± 2 5	51 11
30.	0 0 (0 6)	0 0 (18)	0 0 (25)	0 0 (25 5)	54 45 ± 2 7	51 11

A mathematical model was developed by processing the above variables as shown in Eq. (5.3). The model terms were evaluated by multiple regression analysis to predict the optimum cultivation conditions to maximize the extracellular expression of Blamy-I. All terms regardless of their significance are included in the following equation:

$$Y = 368.75 - 126.95C_1 - 8.56C_2 - 9.96C_3 - 6.48C_4 + 163.38C_1^2 + 0.65C_2^2 + 0.48C_3^2 + 0.27C_4^2 - 5.47C_1C_2 + 2.14C_1C_3 - 1.38C_1C_4 - 0.44C_2C_3 + 0.09C_2C_4 - 0.34C_3C_4 \quad (5.3)$$

Where Y is the response, i.e. the enzyme activity (U/ml) and C_1–C_4 are the actual values of the test variables. The term C_1 represents IPTG concentration (mM); C_2 time of post induction (h); C_3 temperature of induction (°C) and C_4 represents EDTA concentration (mM).

The significance of the model and its coefficients were evaluated by their *p*-values and the model terms with the *p*-value (*Probability*> *F*) less than 0.05 were considered to be significant. The results showed that C_1, C_2, C_4, C_1^2, C_2^2, C_3^2, C_4^2, C_1C_2, C_2C_3, and C_3C_4 were significant model terms. The Fisher's statistical test was conducted for the quadratic model and the results demonstrated that the computed *F*-value for the model was 27.66, implying that the model terms were significant (Table 5.18). There was only a 0.01% chance that a "Model F-Value" could occur due to noise. The model's fitness can also be evaluated by determining coefficient of correlation (R^2) and adjusted R^2 values of regression equation and these values were found to be 0.9627 and 0.9279 respectively. This indicated that the deduced model could explain 96.27% of the variability in response (Table 5.18) and the significance of the model was also supported by the adjusted R^2 (92.79%) value (Table 5.18).

Table 5.18: ANOVA for the response surface quadratic model for the extracellular expression of Blamy-I from *E. coli* BL21a cells

Source	Sum of Squares	Degrees of freedom	Mean Squares	*F*-value	Prob. *(P)*> *F*
Model	52528.39	14	3752.028146	27.66	< 0.0001
IPTG (C_1)	791.66	1	791.66	5.84	0.0289
Time (C_2)	732.80	1	732.80	5.40	0.0346
Temperature (C_3)	505.08	1	505.08	3.72	0.0728
EDTA (C_4)	841.95	1	841.95	6.20	0.0249
$(C_1)^2$	13221.52	1	13221.52	97.46	< 0.0001
$(C_2)^2$	15381.08	1	15381.08	113.38	< 0.0001
$(C_3)^2$	3957.54	1	3957.54	29.17	< 0.0001
$(C_4)^2$	10911.51	1	10911.51	80.44	< 0.0001
C_1*C_2	2763.29	1	2763.29	20.37	0.0004
C_1*C_3	292.48	1	292.48	2.15	0.1627
C_1*C_4	353.89	1	353.89	2.61	0.1271
C_2*C_3	2892.02	1	2892.01	21.32	0.0003
C_2*C_4	393.76	1	393.76	2.90	0.1091
C_3*C_4	3307.57	1	3307.57	24.38	0.0002
Residual (error)	2034.81	15	135.65		
Lack of fit	2023.30	10	202.33	87.94	< 0.0001
Pure error	11.50	5	2.30		
Total	54563.20	29			

R^2 = 0.96, Adj. R^2 = 0.92, Pred R^2 = 0.81 and CV= 10.18%

Figure 5.40 (A-F) shows the response surface and contour plots for the extracellular α-amylase activity as a function of two variables while the other variable was maintained at its respective zero level. Figure 5.40 (A) demonstrates that lowering the IPTG concentration had a positive effect on extracellular secretion of α-amylase. Further, in Figure 5.40 (D), it can be seen that an increase in post-induction time and lowering of incubation temperature had positive effects on the extracellular expression of recombinant α-amylase. Moreover, EDTA concentration, which effects the cell permeability, also had a positive effect [Figure 5.40 (F)] and thus increases in these variables had direct impact on the increase in extracellular expression of Blamy-I.

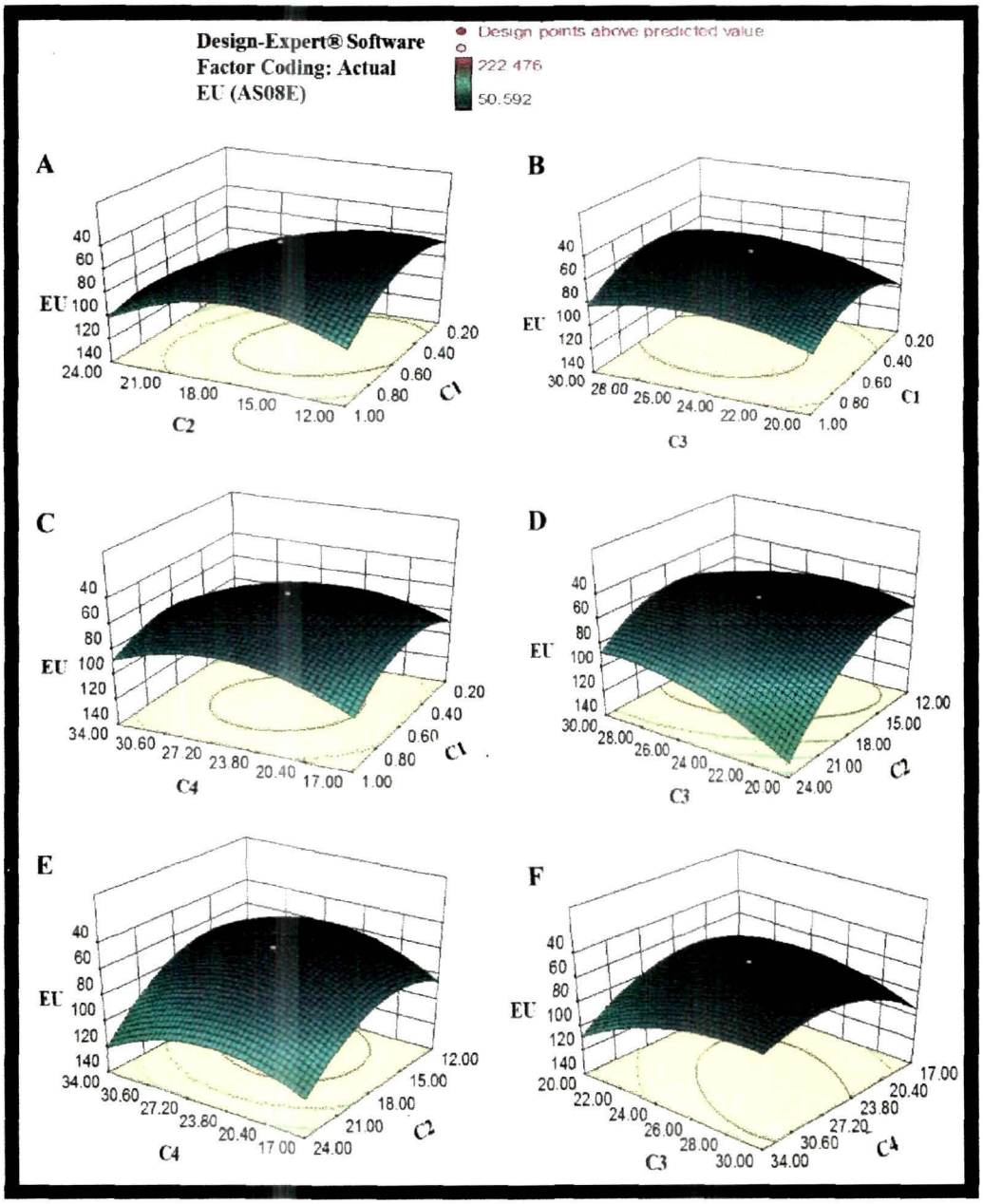

Figure 5.40: Response surface plots showing interaction effects of test variables on extracellular overexpression of Blamy-I from *E. coli* BL21 cells. (A) C_1 vs C_2, (B) C_1 vs C_3, (C) C_1 vs C_4, (D) C_2 vs C_3, (E) C_2 vs C_4 and (F) C_3 vs C_4.

By solving the regression Eq. 5.3, the optimum level of each tested parameter for the maximum extracellular expression of Blamy-I was determined as IPTG concentration = 0.1 mM, post induction time = 24 h, temperature of post-

induction = 20°C and EDTA concentration = 49.84 mM (Table 5.19). At these optimized values the predicted value for the extracellular Blamy-I activity was 427.62 U/ml, while the experimental value was found to be 409.5 ± 20.4U/ml (mean ± S.D.), which was in close agreement with the model prediction. The model demonstrated a significant improvement in the extracellular expression of Blamy-I (approx. 8-fold) under optimized culture conditions as compared to non-optimized conditions. Thus, this study vouches that the culture conditions such as low IPTG concentration, low temperature, and increase in post-induction time play a crucial role in the heterologous extracellular expression of recombinant protein such as Blamy-I.

Table 5.19: Optimized value for maximum extracellular expression of recombinant α-amylase (Blamy-I) production from *E. coli* BL21 cells.

IPTG (mM/ml)	Time of post Induction (h)	Temp. (°C)	EDTA (mM/ml)	Pred. values (EU)	Exp. values (EU)	Fold increase in extracellular expression
0.1	24	20	49.8	427.62	409.5	~8.0

5.7.5. Isolation and purification of recombinant protein (Blamy-I)

Blamy-I was isolated and purified from cell-free culture supernatant (CFS) of recombinant *E. coli* (harbouring pETBLA2) grown under optimized culture conditions. The fractionation of CFS using a phenyl-sepharose column resulted in separation of recombinant protein into two peaks, however, α-amylase activity was eluted in single peak (HIC-I) only (Figure 5.41).

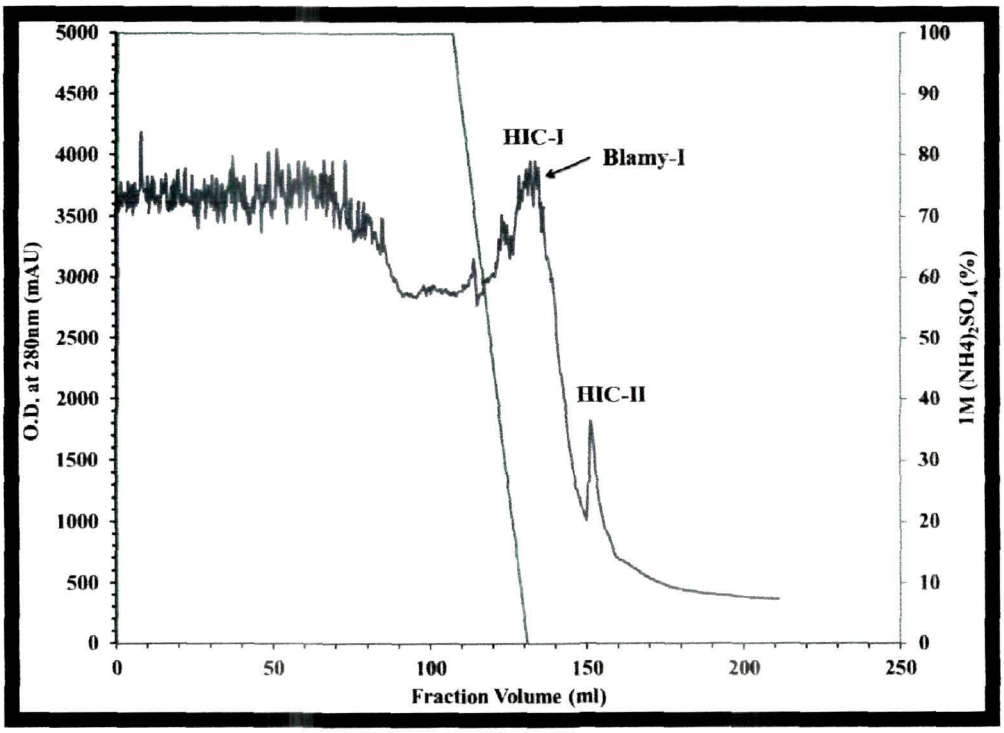

Figure 5.41: Chromatogram resulting from fractionation of recombinant Blamy-I on a phenyl-sepharose column.

Further fractionation of the pooled HIC-I fractions on a Sephacryl S-200 gel-filtration column resulted into separation of proteins into three different peaks. Nevertheless, enzyme activity analysis of each peak showed that only the GF-II peak retained α-amylase activity (Figure 5.42).

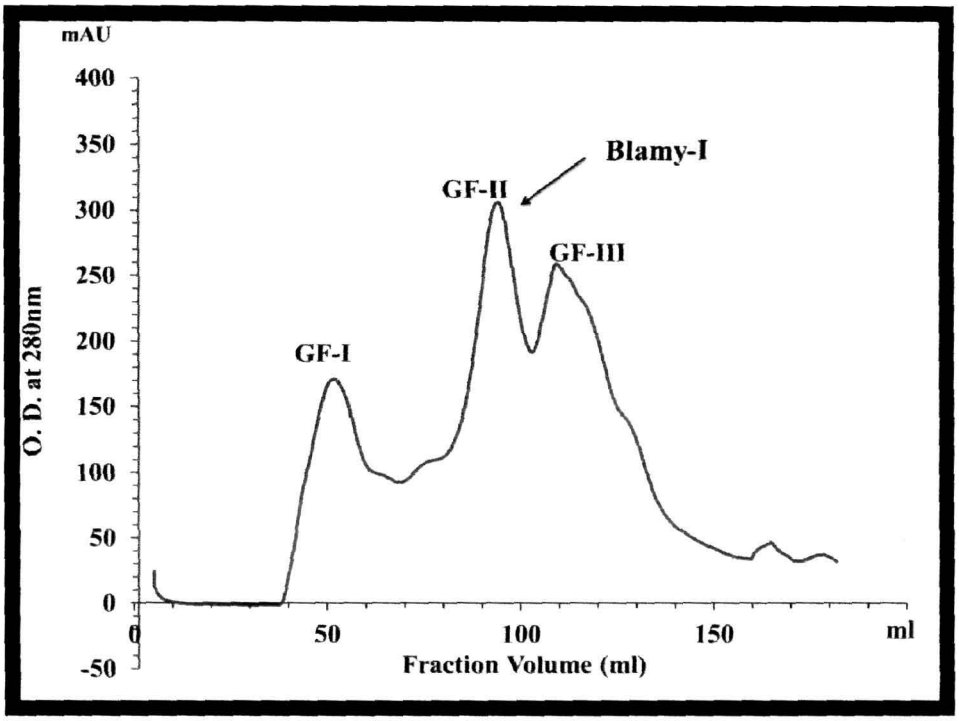

Figure 5.42: Chromatogram resulting from fractionation of recombinant α-amylase (Blamy-I) on a Sephacryl S-200 column. The peak exhibiting α-amylase activity is marked with an arrow on the chromatogram.

SDS-PAGE analysis of the active GF-II fraction showed the homogeneity of the purified protein and yielded a single band of approx. 55.0 kDa, under both reducing and non-reducing conditions (Figure 5.43). The SDS-PAGE analysis also revealed that the purified recombinant enzyme is a monomeric enzyme (Figure 5.43). Zymographic analysis of the purified recombinant Blamy-I also demonstrated the appearance of a single clear zone of starch hydrolysis on native PAGE corresponding to ~55.0 kDa (Figure 5.43).

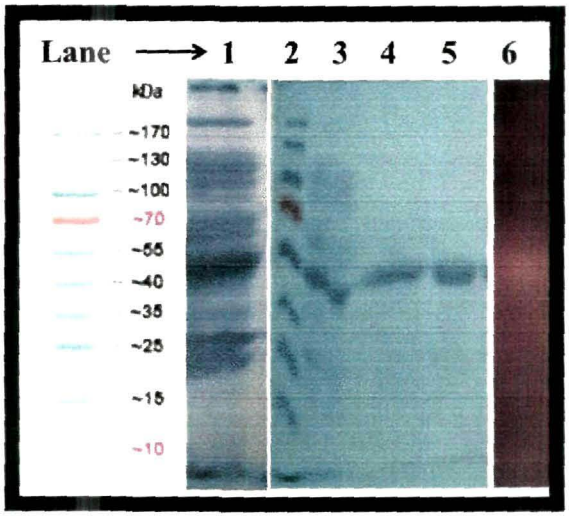

Figure 5.43: SDS-PAGE analysis of purified Blamy-I. Lane 1: crude culture supernatant (20 µg); lanes 2: Fermentas pre-stained protein markers, lane 3: phenyl-sepharose pooled fraction (20 µg), lane 4: purified reduced gel filtration fraction (15 µg); lane 5: purified non-reduced gel filtration fraction (15 µg); and lane 6: zymograph of purified Blamy-I (20 µg).

The purified recombinant α-amylase was named Blamy-I and a summary of purification of Blamy-I from recombinant *E. coli* BL21 (DE3) cells is shown in Table 5.20. With two steps of purification, Blamy-I was purified up to 16.6 fold with 19% of recovery of the total recombinant α-amylase produced by *E. coli* BL21 cells (Table 5.20).

Table 5.20: A summary of the purification of Blamy-I from the optimized CFS of recombinant *E. coli* BL21 cells, data represent a typical experiments.

Purification steps	Total protein (mg)	Total activity (Units)	Specific activity (U/mg)	Enzyme recovery (%)	Purification fold
Culture supernatant	525.0	39150.0	74.57	100	1.0
Phenyl-sepharose	50.0	12000.0	240.0	30.6	3.2
Sephacryl S-200	6.0	7440.0	1240	19.0	16.6

5.7.6. Biochemical characterization of Blamy-I

The SDS-PAGE analysis suggests Blamy-I is the same wild type α-amylase (AmyBL-I) Even so, it is essential to ascertain whether the cloned α-amylase (Blamy-I) is an identical or a different enzyme and to investigate if there is any change in some of the biochemical properties due to cloning As such, some of their biochemical properties have been investigated and presented in the table below

Table 5.21: Comparison of biochemical properties of the purified wild type α-amylase (AmyBL-I) and recombinant α-amylase (Blamy-I) from *B licheniformis* strain AS08E

Biochemical properties	Wild type α-amylase (AmyBL-I)	Recombinant α-Amylase (Blamy-I)
Molecular wt of the protein (kDa)	~55 0	~55 0
Optimum pH	10 0	10 0
Optimum Temperature (°C)	80 0	80 0
pH stability	6 0-12 0	6 0-12 0
Thermostability (°C) in presence of Ca^{2+} ions	Up to 80 0	Up to 80 0
Km	4 5 ± 0 2 mg/ml	5 56 ± 0 3 mg/ml
Ca^{2+} requirement	Ca^{2+}-dependent	Ca^{2+}-dependent
Inhibitors	EDTA, 4-BPB, Hg^{2+}	EDTA, 4-BPB, Hg^{2+}
End product of starch hydrolysis	Maltose and high molecular oligosaccharides detected as main hydrolytic product	Maltose and high molecular oligosaccharides detected as main hydrolytic product

From Table 5 21, it is evident that the purified recombinant enzyme is the same wild type α-amylase purified from *B licheniformis* strain AS08E, thus its biotechnological application has not been determined further

Chapter VI

DISCUSSION

Chapter 6: Discussion

Microorganisms, which are the storehouses for various useful industrial enzymes, are bread and butter for industrial biotechnology. In the microbial kingdom, bacteria represent the largest domain of prokaryotic microorganisms From the dawn of civilization, bacteria have been explored for the production of various useful industrial products, as they are easiest to grow, to manipulate, and to obtain desired properties of secondary metabolites [29]. α-Amylase, which represents the second most used industrial enzyme, has been isolated from various sources such as plants, animals, and microbes. However, industrial production of α-amylases mostly comes from microorganisms owing to the above stated advantages [29].

Recently, there has been a great upsurge in characterization of α-amylase producing microbes isolated from diverse sources for various industrial applications. Different industries have different demands regarding the applications of α-amylases. For example, the starch industry requires enzymes to be active under acidic pH conditions, as the natural pH of starch slurry is around 4.5 [225], whereas the laundry detergent industries require α-amylases to be active at alkaline conditions [202]. There are several reports available on α-amylase production from microbes but very few examples of its successful application in industries. Therefore, there is a constant search for novel α-amylase producing microbes to meet the specific industrial demands.

The Northeastern zone of India, considered as one of the mega biodiversity zones of the world, harbors several previously uncharacterized microbial species and many of them may produce novel/potent enzymes suitable for commercial applications [159]. Therefore, the present investigation was started with an aim to isolate potential α-amylases of bacterial origin from the soil sample of Northeast, India, and to explore some of the biotechnological applications of the purified enzymes from the isolated strain(s) In addition, the α-amylase genes from the

isolated bacterial strains were also intended to be cloned and extracellularly overexpressed in *E. coli* cells.

6.1. Isolation of α-amylase producing bacteria

α-Amylase is ubiquitous in nature, however, commercial production of α-amylase is mainly preferred from a microbial source [139]. Soil biota is the home to a large proportion of the world biodiversity; there are typically ~4 x 10^8 bacteria in one gram of soil. Therefore, isolation of novel α-amylase producing bacteria from soil sample is most desirable. Thus, in the present study soil samples from two different locations of Northeast India (Assam) were screened to isolate novel α-amylase producing bacteria. Two different soil samples were selected based on soil pH (acidic and alkaline), with an aim to identify and isolate novel acidic and alkaline α-amylase producing bacteria. By screening these soil samples, two distinct halo-zone-forming bacteria (acidic strain AS01a and alkaline strain AS08E) were isolated on starch agar plates by serial dilution methods. These strains were then used for further studies to isolate, purify, and characterize novel alkaline/acidic α-amylases.

6.2. Polyphasic approaches for bacterial identification

The phenotypic characterization of any strain is the first step towards bacterial identification. Gram staining is considered as invariably the first step towards any bacterial identification followed by various staining and biochemical identification [383]. The morphological analysis of both the bacteria revealed that they were Gram positive, rod-shaped, non-motile and spore forming bacteria, whereas biochemical studies showed that both of them are capable of hydrolyzing starch macromolecules (Table 4.1 and 5.1). Based on phenotypic characteristics and following the Bergey's manual of systematic bacteriology [355, 384] both the bacteria were categorized as member of the *Bacillus* genus. However, species level identification could only be established by genotypic studies since the genus *Bacillus* contains several phylogenetically diverse species with overlapping phenotypic characteristics [159].

The most common method for phylogenetic identification of bacteria up to species level is based on 16S rDNA analysis Thus, this approach was adopted for identification of the isolated strains The 16S rDNA sequence analysis from strain AS01a demonstrated up to 99 0% sequence similarity with other species of *B subtilis* group (Table 4 2), while strain AS08E, showed up to 99% sequence similarity with *B licheniformis* group (Table 5 2) The sequencing of 16S rRNA gene may not be sufficient to discriminate closely related bacterial species because of the highly conserved nature of this region Consequently, additional information was obtained by sequencing of the genes encoding the 'core genome' of conserved proteins [385]

Gyrase subunit A, which is an important DNA replication enzyme, has a higher rate of molecular evolution than 16S rDNA, thus it was considered as a suitable phylogenetic marker for the study of the species level [386] GyrA gene analysis of the bacterium strain AS01a showed 99% similarity with the *B subtilis* group (Table 4 3) while strain AS08E showed 99% similarity with the *B licheniformis* group (Table 4 3) Thus, based on GyrA gene sequence and phylogenetic analysis, the strain AS01a was found to belong to the *B subtilis* group while the strain AS08E was found to belong to the *B licheniformis* group of bacteria

RNA polymerase is a ubiquitous enzyme, which controls/regulates gene expression in all living organisms In bacteria, it consists of five subunits The catalytic subunit "β" (encoded by RpoB gene) is found to be universal and evolutionarily ancient in origin, which suggests that it is a powerful molecular chronometer [387] Thus, among the core genome sequencing for bacterial identification, *rpoB* is one of the potential candidates for bacterial phylogenetic analyses and identification Thus, RpoB gene was amplified from both the strains (AS01a & AS08E) to identify the isolated bacterial strain up to species level The RpoB gene from strain AS01a showed 100% similarity with known *rpoB* sequences from the *B subtilis* group (Table 4 4) while the RpoB gene from strain AS08E showed 100% similarity with known *rpoB* sequences from *B licheniformis* group

(Table 5 4) Therefore, based on sequence similarity and phylogenetic analysis of RpoB gene sequences, strains AS01a and AS08E were categorized into *B subtilis* and *B licheniformis* group, respectively

Molecular approach of phylogenetic identification of bacteria also includes 16S-23S rRNA intergenic spacer region (ISR) sequencing besides most widely used 16S rRNA and "core genome" protein genes sequencings [388] ISR is widely recognized for its sequence hyper-variation, which proves helpful for distinguishing between species [388] Based on ISR sequencing and analysis, strain AS01a showed 96% similarity with known ISR sequence from *B subtilis* group (Table 4 5) while the ISR from strain AS08E showed 94% similarity with the *B licheniformis* group (Table 5 5) Thus, ISR analysis from strain AS01a and strain AS08E reinforced that the strain AS01a belongs to *B subtilis* group while strain AS08E belongs to *B licheniformis* group, however due to their lower sequence similarity with the neighbor strains in the phylogenetic tree, both the strains demand a distinct position

Polyphasic approach of bacterial identification proves beneficial for the identification of the isolated bacterial strains up to species level The isolated strain AS01a was identified and named *B subtilis* strain AS01a [159] while strain AS08E was identified and named *B licheniformis* strain AS08E [389] using polyphasic approach Most of the α-amylase-producing bacterial strains have been characterized using a combination of 16S rDNA and few other using core genomes sequences However, the strategies used in present study may prove to be very useful for distinguishing bacteria up to strain level

6.3. Screening of process parameters influencing α-amylase production in SmF

Several physicochemical factors affect microbial enzyme production However, among these factors, composition of growth media, pH of the media, aeration, temperature, inoculum age, nitrogen source, and carbon source are believed to play a significant role [29] Moreover, approximately 90% of industrial

enzyme manufacturers produces enzyme using submerged fermentation (SmF) technique [390] SmF offers various advantages, such as proper agitation and mixing of substrate, easy to control moisture level, pH level, aeration level, and proper monitoring of microbial growth and dissolved oxygen [391-393] However, enzyme productions in SmF are influenced by various parameters as such, and therefore, it becomes important to screen and optimize various factors in order to obtain maximum product recovery As 30–40% of the total cost of industrial enzyme production is accounted for by the microbial growth media [394], in order to meet the industrial demands it becomes indispensable to increase the production without escalating the production cost Hence, optimization of media components and culture parameters are of prime objectives in the biological process of microbial enzyme production [195] The classical method of optimization involves optimizing a single variable at a time, which is time-consuming and fails to detect the true optimum values due to interactions between the variables. On the other hand, the statistical optimization technique not only allows quick screening of a large range of parameters but also reflects the role of each component in enzyme productions [395]

Various physiochemical components such as pH, temperature, incubation time, and carbon-nitrogen source were screened for enhancing α-amylase production by *B subtilis* strain AS01a The screening experiment showed that soluble starch was the most preferred carbon source for maximum growth as well as α-amylase production by strain AS01a. This phenomenon has been observed in several α-amylase-secreting *Bacillus* strains [159] Further, when glucose was supplied as a sole carbon source, it caused a catabolic repression for enzyme production [14, 29, 159] Among the tested nitrogen sources, beef extract was found to be the best nitrogen source followed by peptone, NH_4Cl, and KNO_3, which suggest that each bacterium has its own choice of either inorganic or organic nitrogen source for growth as well as α-amylase or other enzyme production [26, 29, 159, 396].

Nevertheless, among the various factors influencing α-amylase production, pH was found to be more influential, as diminutive change in pH can effect drastic change in both growth and enzyme production by the bacterium Thus, these three factors (concentration of starch, concentration of beef extract and pH of the media) were selected for statistical optimization studies for maximizing α-amylase production from *B subtilis* strain AS01a

Similarly, media components influencing α-amylase production from *B licheniformis* strain AS08E were evaluated by Plackett Burman design, eleven parameters consisting of various carbon-nitrogen sources, and biophysical parameters of media were studied Each factor was selected based on its role in bacterial α-amylase production and evaluated based on their *p*-values ($p < 0.05$ were considered as significant parameters) Starch with *p*-value of 0.002 was determined to be the most significant factor influencing α-amylase production from *B licheniformis* strain AS08E, followed by peptone ($p < 0.017$), and then by pH of the medium ($p < 0.021$) Significance of these factors was also evident from the Pareto charts and Normality plots, which suggest that α-amylase production was greatly influenced by these factors Thus, these three factors (concentration of starch, concentration of peptone and pH of the media) were selected for further optimization studies to attain optimum α-amylase production by *B licheniformis* strain AS08E Further, screening of media components also revealed that the bacterial strain AS08E could grow and produce α-amylase at a highly alkaline pH (12.5), which is probably the first report on production of alkaline α-amylase by any species of *Bacillus* at such a high pH [122, 139]

6.4. Statistical optimization of culture conditions for maximum α-amylase production using RSM

Since media components play an important role in enzyme production by bacteria [160], designing an appropriate fermentation medium for maximum enzyme yield is the prime objective of industrial enzyme production processes [303] Conventional media optimization experiments require a large set of experiments to study the influence of each factor of the media on enzyme

productions and are quite time consuming Conversely, statistical optimization of media components can handle large set of variables with lesser experiments and can generate responses based on interactions of the variables [397]. During the initial screening study of media components in both the cases (strain AS01a and strain AS08E), it was found that pH of the medium, concentration of carbon (starch) and nitrogen (beef extract/peptone) sources play a significant role in enzyme production. Thus, these parameters were further optimized by using RSM for maximum yield.

The results obtained from the RSM study in case of *B. subtilis* strain AS01a showed that all the terms of the model except the linear effects of starch and beef-extract content and square effect of beef-extract were significant ($P < 0.05$). The negative coefficient observed in case of beef extract indicates that lowering the concentration of this factor can increase α-amylase production. Similarly, in case of *B. licheniformis* strain AS08E, media optimization by RSM revealed that starch concentration and pH of the medium demonstrate a positive effect on α-amylase production. This suggests that an increase in the concentration of these factors might lead to an enhancement of α-amylase production. In contrast, the negative coefficient observed for peptone (linear and quadratic) suggests an inverse relationship between the concentration of this complex organic source of nitrogen and the production of α-amylase. Therefore, an increase in nitrogen content of the media may lead to a decrease in α-amylase production.

The coefficient of determination (R^2) which determines the fitness of the model was found to be 98.12% and 96.4% in case of media optimization through RSM from *B. subtilis* strain AS01a and *B. licheniformis* strain AS08E, respectively This suggests higher significance of both the models, as higher this value (R^2 closer to 1) stronger is the model and better can it predict the responses [398].

The three-dimensional (3D) response surface plots and two-dimensional (2D) contour plots are the graphical representations of the regression equation. These are used to investigate the interaction amongst the test variables and to determine the optimum concentration of each factor for maximum yield. In the case

of *B subtilis* strain AS01a, the 3D and 2D plots indicate that the lower concentration of beef-extract, higher concentration of starch and pH value of medium in acidic range induce optimum extracellular α-amylase production by this strain Similarly, in the case of *B licheniformis* strain AS08E, the 3D and 2D plots suggest that a lower concentration of peptone (nitrogen source) and higher concentration of starch (carbon source) are required for optimum α-amylase production by this strain Thus, the present study suggests that starch acts as an inducer whereas high concentrations of complex nitrogen sources such as peptone have an antagonistic effect on extracellular α-amylase production from the bacterial strains under study

The initial screening experiments as well as optimization of process parameters were carried out in shake-flasks study, however, the final validation of the response surface model was carried out in a process-controlled bioreactor This is because industrial enzyme production is unvaryingly carried out in such bioreactors The validation studies showed that for both the bacteria under study, there was a slight increase in production of α-amylase in a process-controlled bioreactor as compared to the model predicted responses Such disparity occurs due to constant maintenance of dissolved oxygen as well as pH of the medium at a desired level in a process-controlled bioreactor, which is not possible in shake-flask study [399, 400] Further, the close relationship between the predicted and experimental values also vouches for the validity and acceptability of both the statistical models for maximum α-amylase yield by the selected bacterial species

Culturing of bacteria under optimized conditions resulted in approximately three-fold increase in α-amylase production as compared to culturing of bacteria under a non-optimized medium suggesting successful application of the process optimization technique Under the optimized conditions, extracellular α-amylase production from *B subtilis* strain AS01a was significantly higher than some of the reported yield of α-amylase from other wild-type *B subtilis* strains such as *B subtilis* (639 1 U/ml) [343] and *B subtilis* KCC103 (144 5 U/ml) [11] under optimized conditions Although α-amylase production from the highly alkalophilic

strain *B licheniformis* strain AS08E was comparatively lower than the production from *B subtilis* strain AS01a, it was comparable with α-amylase production from some *Bacillus* strains such as *Bacillus* sp (76 14 U/ml) [401] and *B subtilis* KCC103 (144 5 U/ml) [11] under optimized conditions The optimum yield of α-amylase from *B licheniformis* strain AS08E was also significantly higher than obtained from *B licheniformis* NH1 (9 7 U/ml) under non-optimized conditions [147]

6.5. Purification of α-amylase from isolated bacterial strain

Industrial enzymes categorized under commodity enzymes, are generally produced in bulk quantities, and may require relatively little downstream processing [29] Moreover, for commercial application of α-amylase, generally a highly purified enzyme may not be required However, enzyme applications in the pharmaceutical and clinical sectors (specialized enzymes) require high purity amylases [29] Further, the purification strategies employed for industrial purposes should be inexpensive, rapid, high yielding, and acceptable to large-scale operations A highly purified form of enzyme is also a prerequisite for studying structure-function relationships and in assessing biochemical properties [29]

A monomeric α-amylase (Amy-I) of 21 0 kDa was purified to 7 7-fold homogeneity with three steps of purification from the culture supernatant of *B subtilis* strain AS01a In general, the molecular mass of α-amylases from bacteria particularly from *Bacillus* sp is reported between 50-60 kDa [29] and there is a dearth of report on such a low molecular mass α-amylase from bacteria. The α-amylase purified from *B licheniformis* strain AS08E was found to be a monomeric protein of molecular mass approximately 55-kDa.

6.6. Biochemical characterization of purified protein

Prior to any biotechnological application of an enzyme, the determination of its biochemical properties relevant to industrial application is of utmost importance The properties of microbial enzymes are mainly growth associated [29], however, there are reports which suggest that the secreted enzyme are much

more active/stable at a temperature and pH values far above those required for their optimal growth [138, 402] Considering all these facts it becomes important to investigate the biochemical properties of purified α-amylases from *B subtilis* strain AS01a (Amy-I) and *B licheniformis* strain AS08E (AmyBL-I) to determine their biotechnological applicability

6.6.1. Effect of pH and temperature on purified α-amylase activity

Amy-I showed optimum activity under alkaline pH (pH 9 0) which is in close agreement with the optimum pH required by various alkaline α-amylases from *Bacillus* US147 [122], *Bacillus* sp TS-23 [122], *H salinarum* MMD047 [212] and *S gulbargensis* [403] However, Amy-I showed better range of pH (8 0-12 0) stability compared to the above α-amylases Further, the pH optima displayed by AmyBL-I was similar with α-amylase of *Bacillus* L1711 [122] and *Bacillus* sp PN5 [157] but it showed a broader range of pH stability (6 0-12 0) compared to them Amy-I worked optimally at moderately thermophilic conditions of 55°C, which was higher than some of the reported alkaline α-amylases from strains like *Bacillus* sp isolate L1711 [122], *S gulbargensis* [403], and *Bacillus* sp NRRL B 3881 [403] However, the temperature optimum shown by AmyBL-I was much higher compared to the above stated alkaline α-amylases and Amy-I

Optimum temperature and pH study suggests that both the purified enzymes (Amy-I and AmyBL-I) are suitable for inclusion in automatic dishwashers and laundry detergent formulations The purified alkaline α-amylases may also serve as model proteins for understanding the molecular basis of the alkalophilicity of the enzymes, which may be of great value in enzyme tailoring [212]

6.6.2. Effect of Ca^{2+} ion on thermostability of the purified α-amylases

The affinity of Ca^{2+} ion towards α-amylases is much stronger than any other metal ions α-Amylases generally contain a minimum of one Ca^{2+} ion in their core, however this number may vary from one to ten [29] Amylases are much more thermostable in the presence of this Ca^{2+} ion than in its absence [29] However,

there are reports on the existence of Ca-independent amylases, which have more demands in starch processing industries. Generally α-amylases used in starch processing industries requires Ca^{2+} ion for their thermostability and in successive steps this ion must be removed from the product stream, consequently adding an extra cost to the final product [142, 275, 287]. In view of this, the thermostability of both the purified α-amylases (Amy-I and AmyBL-I) in presence and absence of Ca^{2+} ions were evaluated. Our study suggests that Amy-I is a Ca-independent and moderately thermostable enzyme which may have great demands in starch saccharification industry as it eliminates the addition of Ca^{2+} for improving the stability of α-amylases. Thus, the industrial use of this enzyme can be considered as a cost-effective one [289].

Similarly, study of purified AmyBL-I showed that it is stable up to 60 °C in absence of any additive, however, the temperature optimum for the same enzyme is enhanced to 80°C in the presence of starch. This indicates that substrate (starch) acts as a protective agent against the thermal denaturation of this enzyme by forming enzyme–substrate complex, which is more heat-stable than the enzyme alone [404]. However, in the presence of Ca^{2+} ions, the thermostability of AmyBL-I (absence of starch) can reach up to 80°C, suggesting that it is a metalloenzyme. This stabilizing effect of Ca^{2+} ions is presumably due to the presence of Ca^{2+} binding site in the enzyme that stabilizes it when Ca^{2+} is bound [26, 29]. The thermostable α-amylases isolated from *Anoxybacillus* sp. show optimum activity at 60°C [405] whereas those α-amylases isolated from *B. subtilis* JS-2004 [179] and *Bacillus* sp. I-3 [16] show optimum activity at 70°C. However, the stability of these enzymes can reach upto 70°C-80°C in the presence of Ca^{2+} ions suggesting that it plays a significant role in enhancing the thermostability of α-amylases. Therefore, the thermostability of AmyBL-I vouches for its application in starch processing industries where high temperature (80-90°C) is employed to achieve the liquefaction of starch [406].

6.6.3. *Effects of various enzyme modulating molecules on purified amylases*

Effector molecules such as metal chelators and chemical compounds (inhibitors) may help to study the characteristics of enzymes Enzyme inhibition by metal chelators such as EDTA indicate the requirement of certain metal ions for enzyme activity [26] while inhibition by chemical reagents (inhibitors) gives insight into the mechanism of enzyme action and presence of active residues in its catalytic site [407] Most of the α-amylases are inhibited by the presence of heavy metal ions, sulfhydryl group reagents, N-bromosuccinimide (NBS), p-hydroxy mercuribenzoic acid, iodoacetate, EDTA and EGTA [9, 29]

Amy-I and AmyBL-I were both significantly inhibited by chemical compounds such as PMSF and 4-BPB, suggesting the role of serine and histidine residues in the catalysis process (Table 6 1) A similar observation was reported for the α-amylase purified from *B subtilis* DM-03 [354] The catalytic activity of Amy-I is not inhibited in the presence of EDTA, suggesting that Amy-I is a metal independent enzyme Many researchers have reported metal chelator-resistant microbial α-amylases and these enzymes have high demand in the laundry detergent industry [205] Since AmyBL-I can lose upto 52% of its original enzyme activity in presence of EDTA, it suggests that it is a metal-dependent enzyme and requires Ca^{2+} ions for its stability, which is also evident from its thermostability study in presence/absence of Ca^{2+} ion

Since the purified enzymes in the present study are active at highly alkaline (pH 8 0-12 0) conditions, they may be suitable for application in laundry detergent formulations as well as for understanding the molecular basis of the alkalophilicity of the enzyme that may be useful for protein engineering [212] The presence of different types of surfactants in any heavy-duty laundry detergent hinders the task of incorporating enzymes in detergent manufacturing industries [408] Besides, detergent industries also demand that the added enzyme should be stable in the presence of bleach, surfactant, and denaturing agent Therefore, it is important to investigate the surfactant stability of any enzyme including α-amylases under study prior to their inclusion in commercial laundry detergent formulations Hence, the

stability of both the enzymes in presence of various surfactants, oxidizing and denaturing agents (SDS, Triton X-100, Tween-20, Tween-80, $NaBO_3$, and urea) was investigated. Both the purified enzymes showed considerable stability in presence of above chemicals and surfactants, which supports their candidature for inclusion in laundry detergent formulations Besides, Amy-I also has an added advantage for inclusion in liquid detergent used in hospitals as the working temperature employed to clean instruments in hospitals is around 50-55°C [162]. Further, AmyBL-I also showed considerable stability in presence of various organic solvents, which also supports its use in detergents containing organic solvents employed for washing colored stains from crocking and cutlery [122].

6.6.4. Effects of various metal ions on α-amylase activity

Divalent cations and transition metal ions are incorporated within many enzyme structures to stabilize the folded conformation of the protein or to facilitate direct participation in the catalysis process [409]. Even though most of the α-amylases are metal-activated enzymes having a strong affinity towards Ca^{2+} ion, most of the heavy metal ions are known to inhibit α-amylase activity [29]. Further, Ca^{2+} ions are also known to protect the enzyme from thermal denaturation [29]. The most common heavy metal ion inhibition is by mercuric poisoning, because it oxidizes indole rings and interacts with the aromatic rings present in tryptophan residues of the enzyme [9] In the present study, it was observed that mercuric ion (Hg^{2+}) inhibited amylase activity completely while other metal ions have little or no effects; similar observation were made in the case of α-amylases purified from *B. licheniformis* ATCC 9954a [298] and *B. subtilis* JS-2004 [179]. Only AmyBL-I requires Ca^{2+} for its stability and thermostability. Amy-I is Ca^{2+} independent, suggesting its usefulness in starch industries.

6.6.5. Kinetic studies of purified α-amylases

The K_m and V_{max} values, which indicate the affinity and efficiency of the enzyme towards its substrate (starch), were determined for each of the α-amylases under study. The kinetic studies for α-amylase (Amy-I) isolated from *B. subtilis*

strain AS01a, showed that its substrate (starch) specificity was much higher than the substrate (starch) specificity of α-amylase (AmyBL-I) purified from *B. licheniformis* strain AS08E. However, the substrate specificity of AmyBL-I towards soluble starch was found to be much superior as compared to the same property displayed by α-amylases from other bacterial species such as *B. circulans* GRS 313 [220], *B. stearothermophilus* ATCC 12980 [29], and *Geobacillus* sp. IIPTN [410].

6.7. Some of the industrial application of purified α-amylase

Amylases are the oldest commercialized enzymes, first used in 1984. They are the most important hydrolytic enzymes among all the starch-based industries [29]. Presently, they share the major enzyme world market (25%) and find application in almost all starch processing industries such as in food, detergents, textiles, and paper industry [29]. Thus, based on biochemical properties of purified amylases, we have explored some of the possible industrial applications of α-amylases under study in laundry detergent, raw starch digestion, and food industry.

6.7.1. Industrial application of amylases in laundry detergents

Nowadays, almost all laundry detergents contain hydrolytic enzymes as one of the major ingredients and detergent enzymes account for about 40% of the total worldwide enzyme consumption [114]. Detergent formulations containing enzymes have better ability to fight tough stains and make the detergent environmentally safe [14, 139, 159]. Amylases are the second most sought enzymes after proteases for use in laundry and automatic dishwashing detergent formulations to degrade the residues of starchy foods such as potatoes, gravies, custard, chocolate, etc. to dextrin and other smaller oligosaccharides, which can easily be removed by water wash [161]. Further, inclusion of α-amylases in laundry detergent is also important from the point of view of removal of starch stained from cloth surfaces, thereby giving whiteness benefit, as starch tends to attract various dirt particles [139].

The most important criteria for α-amylases used in detergent industries are that it should be active under alkaline pH conditions (because the pH of detergent is alkaline) and must resist the oxidizing environments of the detergents components [411] Another criterion associated with the use of α-amylases in the present-day detergent formulation is that the α-amylases should offer optimal activity and stability in the presence of proteases used in detergent formulations [162]. Although, many microbial alkaline α-amylases have been purified and characterized to date, very few of them have found application in the detergent industry due to harsh environment stability requirement [200]. Therefore, isolating and characterizing novel α-alkaline amylases suitable for application in detergent industries are always welcomed by the scientific community as well as by industries.

6.7.1.1. Compatibility studies of purified α-amylases with commercial laundry detergents

The biochemical properties of both the purified α-amylases (Amy-I and AmyBL-I) revealed that they offer remarkable stability against surfactant, oxidizing, bleaching and denaturing agents, and further, they can work at broad range of temperature and pH. This suggests their candidature for incorporation in detergent formulations for automatic dishwashers and laundries. The purified α-amylases from *B. subtilis* strain AS01a and *B. licheniformis* strain AS08E exhibited a significant stability and compatibility with all the tested commercial laundry detergents. In fact, in some cases the enzyme activity was found to be higher than the control (enzyme activity in absence of detergent), which may be attributed to some of the stimulatory effects of detergent component(s) such as ethoxylated surfactants, non-ionic copolymeric builders, and sucrose [14, 159, 412]. However, the partial loss in enzyme activity observed in some cases may result from inhibitory effect(s) of some of the detergent component(s) such as anionic surfactants, bleaching agents and water softening builders etc [14, 159, 412]. Further, in the presence of protease (proteinase K) both the purified α-amylases lost activity partially (20-30%), suggesting limited proteolytic attack on the enzyme

activity. Thus, it advocates the successful application of both the purified α-amylases in laundry detergent formulations containing protease enzymes and other enzymes, for enhancing the wash performance of detergents.

6.7.1.2. Wash performance analysis of purified α-amylases on chocolate stain

Detergent compatibility and stability of an enzyme does not determine its acceptability in detergent industries unless it is supported by wash performance analysis, which is more conclusive. Thus, the stain removal ability of both the purified enzymes was evaluated with the most suitable and compatible detergents (Amy-I with Fena® and AmyBL-I with Safed®) on chocolate-stained cotton fabrics. The treatment of chocolate stain by detergent supplemented with the purified α-amylase resulted in better stain removal from cotton fabrics compared to stain removal by detergent alone. The total carbohydrate release by the action of enzyme (Amy-I and AmyBL-I) supplemented with detergent showed more than two-fold increase compared to detergent/enzyme alone. Thus, this study reinforces the likely successful application of both the purified enzymes in detergent industries.

6.7.2. Application of purified α-amylase in desizing of textiles

Modern textile production processes introduce considerable strain on the warp during weaving, thus thread yarn must be prevented from breaking [29]. As such, sizing of these threads is done with the starch, which can be easily removed during desizing. Decent desizing of starch-sized textiles can only be achieved by the action of α-amylases, which selectively remove the size and do not attack the fibers [29]. Therefore, the application of AmyBL-I in textile desizing was investigated and it was found that the purified α-amylase can successfully remove starch from cotton fabrics, thereby preventing the warp thread from breaking off during the weaving process [139]. This reinforces the potential application of α-amylase in desizing activity in textile industries. Since most of the desizing activities are carried out at 60-100°C [149], and as the optimal temperature for Amy-I was much below (~55°C), it was inapt to investigate the desizing activity of Amy-I.

6.7.3. Application of purified α-amylases in food industries

Maltose, maltotriose, maltotetraose, and other oligosaccharides derived from starch hydrolysis have a great demand in food industries for their superior properties as base material for food production, sweetening agent and nutrient food productions for infants and aged persons [29, 212] Further, there is also a constant demand for purified maltose as an ingredient of transfusion liquids compared to conventionally used glucose. Besides, the high maltose forming enzymes also find their application in bioconversion of starch and in the baking industry [111, 289] The end-product determination of starch hydrolysis by Amy-I revealed that it could form high molecular weight oligosaccharides as the main hydrolytic products after 60 min of incubation. While maltose and high molecular weight oligosaccharides were detected as the main hydrolytic products after 180 min incubation of purified AmyBL-I with potato or wheat starch. Thus, these studies confirmed that both the purified enzymes (Amy-I and AmyBL-I) were indeed α-amylases and good candidates for application in the food processing industry. Starch degrading property of both the purified enzymes (under study) also revealed that they have different mode of action, which resulted in different end product formations. It also showed that the purified Amy-I belongs to liquefying class of α-amylases whereas AmyBL-I belongs to saccharifying class of α-amylase activity [9].

6.7.4. Industrial application of purified α-amylases in raw starch digestion

Conventional starch hydrolysis is an energy intensive process, which ultimately increases the production cost of starch-based products [290]. However, in the recent years' raw-starch digesting enzymes that hydrolyze raw starch much below the gelatinization temperatures have gained more importance [26]. This is because of the fact that this group of enzymes can significantly reduce the energy requirement and simplify the process in the starch industry [290]. It has been estimated that with the use of raw-starch digesting enzymes up to 10-20% reduction in energy consumption can be achieved in bioethanol production [293]. The other potential application of raw-starch digesting enzymes is to produce porous starch, a kind of environmentally friendly sorbent, which can find wide applications in the

food, drug, animal feed, and cosmetic industries [290] Considering the above advantages of raw starch digesting enzymes, the purified α-amylases in the present study were also investigated for their application in raw starch hydrolysis

6.7.4.1. Raw starch adsorbability and starch binding affinity

The raw starch digesting enzyme shows a strong correlation between hydrolysis of raw starch and adsorption on raw starch, therefore it was considered as one of the methods to determine the efficiency of raw starch digesting enzyme but now it is well proven that it is not an obligatory requirement [16] Various raw starch digesting enzymes show varied degrees of raw starch adsorbability In our study, the purified enzyme (AmyBL-I) showed 95% adsorbability towards raw potato starch and 86% towards raw wheat starch [389] Goyal et al [16] also observed similar degrees of adsorbability in their studies In contrary, Amy-I purified from the *B subtilis* strain AS01a did not show any adsorbability on any starch molecules

In order to investigate the interaction between raw amylum and the purified enzyme (AmyBL-I), the change in intrinsic fluorescence emissions of the enzyme was monitored with the help of fluorescence spectroscopy Maxima were observed for the enzyme and the dissolved starch at 341 nm [413] and 340 nm [414], respectively The fluorescence spectra obtained from the α-amylase enzyme incubated with starch showed that the α-amylase binds to the soluble starch, as there was a clear shift in the band intensity and slight red shifting (342 nm) effect due to interaction This result also suggests that binding of starch molecules to the tryptophan residues of enzyme protects it from quenching effects

6.7.4.2. Raw starch digestion efficiency

The raw starch digestion efficiency of both the purified α-amylase enzymes was assessed primarily by SEM The SEM analysis of starch granules before and after degradation with purified Amy-I from *B subtilis* strain AS01a revealed formation of holes on starch granules, which corroborate well with the report of Matsubara et al [299] The purified α-amylase from *B licheniformis* strain AS08E

also formed holes and pits on treated raw potato and wheat starches. This study, therefore, suggests the potential application of both the purified enzymes in raw starch digestion process, which may bring down the cost of starch-based products due to the use of less energy intensive process in starch industries.

6.8. Cloning and expression of α-amylase genes from the isolated strains

Molecular cloning of the α-amylase genes are extensively done for the molecular study of these proteins, their hyper-production and protein engineering [26]. Different industrial processes require α-amylases to be active at different physiological and biochemical conditions, which creates a constant search for enzymes with novel properties [26]. Thus, to fulfill this industrial requirement, one of the approaches adopted is screening of diverse members of the microbial environment. The other promising technique to achieve this goal is by enzyme engineering of the existing microbial enzymes for successful industrial application [29]. Engineering of α-amylase is mainly performed with an aim to integrate desired properties in the amylase genes These properties may include thermostability, broad pH profile, calcium independence, raw starch degrading ability, activity at high concentration of starch, protease resistance, resistance to catabolite repression and hyper-production [26] Considering the above advantages of cloning and bearing in mind the promising properties of the presently purified enzymes, we were prompted to clone the α-amylase genes from the isolated strains under study.

6.8.1. Cloning of α-amylase genes into an expression vector

The calcium independence, surfactant stability, broader pH applicability, and raw starch digesting efficiency of both the purified α-amylase enzymes in the present study led us to clone and express these enzymes in *E coli* for hyper-production and to study their structure-function relationships. Besides, cloning also helped in reducing energy consumption, as both the wild-type strains under present study needed to be cultivated at 45°C, whereas *E. coli* required much less time and temperature for production of cloned enzymes. Initially, approximately 1 5 kbp

amylase genes were amplified from both the isolated strains by using species-specific α-amylase primers These amplified products were found to contain incomplete ORF and thus a new sets of primers was designed to target complete amplification of ORF With the use of new sets of primers, α-amylase genes of size 1980 bp from strain AS01a and 1540 bp from AS08E were amplified These amplified products were then ligated into the pET-28a expression vector and successively transformed into competent *E coli* BL21 cells

Comparison of nucleotide sequences and deduced amino acid sequences obtained from sequencing of cloned α-amylase genes isolated from *B subtilis* strain AS01a (AmyBS-I) and *B licheniformis* strain AS08E (Blamy-I), showed significant similarity with reported α-amylase sequences isolated from respective species This suggests that the cloned gene from *B subtilis* strain AS01a (AmyBS-I) and *B licheniformis* strain AS08E (Blamy-I) were indeed α-amylase genes Further, analysis of the amino acid sequence of AmyBS-I and Blamy-I using conserved domain NCBI tools (www ncbi nlm nih gov) suggested that they belong to the glycosyl hydrolase family 13 of the α-amylase family [18]

6.8.2. Extracellular expression of recombinant proteins

For the extracellular expression of recombinant protein into the culture media, the signal peptide sequence of both the amylases genes were kept intact while cloning The screening of recombinant cells on starch agar plates showed the formation of halo zones around the recombinant bacterial colonies when flooded with iodine solution, which confirmed the successful extracellular expression of both the recombinant enzymes However, α-amylase assay as well as SDS-PAGE analysis suggested that the majority of the target proteins were accumulated as inclusion bodies in *E coli* Therefore, in order to reduce the formation of inclusion bodies and enhance secretion of functionally active recombinant α-amylase into the culture medium, the *E coli* culture parameters were optimized using response surface methodology

Media component and cultivation parameters are known to play an important role in extracellular expression of recombinant protein by *E. coli* [375, 377]. Moreover, targeting recombinant protein outside the cell membrane into the culture media or periplasmic space simplifies the downstream processing, folding and *in vivo* stability of the recombinant protein. Thus, it enables cost-effective production of soluble and biologically active recombinant proteins [415]. Therefore, four significant parameters (IPTG concentration, temperature, time of post-induction and EDTA concentration), which are believed to play significant role in extracellular expression of recombinant protein were optimized using RSM.

The RSM models in both the cases were evaluated and their fitness accuracy was checked by determining the coefficient of correlation (R^2) in each case. The R^2 value of each model for the extracellular expression of AmyBS-I and Blamy-I was found to be 95.9% and 96.3%, respectively, which indicates high significance of these models. Response surface and contour plots, which graphically represent the regression equation, investigate the interaction amongst the test variables and determine the optimum levels of variables, were evaluated in each case. Both the studies (AmyBS-I and Blamy-I) demonstrated that lowering of IPTG concentration as well as temperature had a positive effect, while increase in EDTA concentration as well as enhancing the incubation time resulted in better extracellular expression of recombinant α-amylases into the culture media. Ayadi et al. [2011] also reported that lower EDTA concentration and lower temperature have a positive effect on *Paenibacillus* CGTase production in *E. coli*. On the other hand, Lo et al. [377] also observed time-dependent enhancement of *Bacillus* CGTase enzyme production in *E. coli*, suggesting that prolongation of incubation time at a lower incubation temperature had a positive effect on production, proper folding, as well as extracellular secretion of recombinant proteins.

The extracellular expression of AmyBS-I and Blamy-I from recombinant *E. coli* showed that the lower temperature and lesser IPTG concentration maintained *E. coli* at less induced state, and thus it could efficiently express the correctly folded active recombinant protein outside the cell membrane [376, 416]. Further, a longer

induction period also provides sufficient time for correct folding of mature peptide that subsequently helps in extracellular expression of enzymatically active recombinant protein [377, 416]. On the other hand, EDTA improves the extracellular secretion of recombinant enzyme by permeabilizing the outer cell membrane of *E. coli* [416, 417]. Therefore, with the use of native α-amylase signal peptide sequence from parent bacterium and optimization of culture conditions, recombinant α-amylases (AmyBS-I and Blamy-I) were significantly expressed and secreted into the *E. coli* culture media.

6.8.3. Purification of recombinant enzyme from recombinant E. coli

Both the recombinant enzyme (AmyBS-I and Blamy-I) were purified using a combination of HIC and gel-filtration chromatography from the culture supernatant of recombinant *E. coli* cells. SDS-PAGE analysis of the purified AmyBS-I and Blamy-I showed a single band of approximately 69.0 kDa and 55.0 kDa, respectively, under both native and denatured conditions. This study suggests that AmyBS-I was in accordance with the predicted size of the amino acid sequence; however, it was different from the wild-type α-amylase (Amy-I) purified from the same parent strain. This suggests the presence of isoenzyme in *B. subtilis* strain AS01a, which is a common phenomenon, as bacteria need different enzymes for different environments [14]. However, the SDS-PAGE analysis revealed that Blamy-I was identical to its predicted mass based on its gene size as well as to wild-type α-amylase (AmyBL-I) purified from the parent strain. Thus, this study suggests that both the recombinant enzymes are indeed from their parent strains and they are not artifacts or contaminants.

The purification profile of both the recombinant enzymes showed that their yields were higher after two steps of purification from the recombinant *E. coli* cells as compared to the yield obtained from wild-type amylases from their parent strain. Thus, it may be anticipated that the major secreted protein in cell free supernatant was the recombinant enzyme and it was less contaminated with other proteins of *E. coli*. Further, the study also evidenced the successful extracellular overexpression of recombinant enzymes in *E. coli*. Additionally, zymographic study revealed that

both the recombinant enzymes were produced in an enzymatically active form. Thus, the approach applied in the current study may prove useful for the extracellular expression of other catalytically active recombinant enzymes in *E. coli*, as the expression of catalytically active recombinant enzyme in extracellular environment is the major concern in protein expression study [376].

6.8.4. Biochemical characterization of recombinant enzyme

Biochemical characterization of a recombinant enzyme and comparison of its properties with native enzyme purified from the wild-type strain was important in order to establish the functional similarity of the recombinant enzyme with its wild-type counterpart from which it was cloned. The comparative biochemical characterization of wild-type α-amylases purified from *B. subtilis* strain AS01a (Amy-I), *B. licheniformis* strain AS08E (AmyBL-I), and the recombinant α-amylases (AmyBS-I and Blamy-I) cloned from these strains revealed that Blamy-I was biochemically identical to its wild-type counterpart (AmyBL-I) purified from the parent strain. In contrast, AmyBS-I was very much different from the wild-type α-amylase (Amy-I) purified from same parent strain. The biochemical characterization of AmyBS-I also revealed that it has potential to be used in the starch saccharification industry as it was found to be thermostable (70°C), Ca^{2+} independent and an acidophilic (pH 6.0) enzyme, which are the most desirable characteristics in starch processing industries [287, 328]. AmyBS-I also showed higher temperature optima than many of the α-amylases purified from *Bacillus* sp. KSM 1378 [122], *Bacillus* sp. GM 8901 [122], and *Bacillus* sp. YX1 [183].

AmyBS-I lost up to 22% of its original activity in the presence of PMSF, suggesting presence of serine in the active site, which was also revealed by AmyBS-I sequence analysis (fourth conserved active site domain, S308). The K_m value of AmyBS-I towards soluble starch was higher than the alkaline α-amylase purified from the same parent strain, however, it was comparable with the substrate specificity of α-amylases from *B. subtilis* (3.85 mg/ml) [29] and *Bacillus* sp. TM1(4 mg/ml) [418]. Further, end-product analysis of starch hydrolysis by AmyBS-I

suggests that it was an endo-acting type α-amylase enzyme, which may be useful for the food and starch industry [159].

6.8.5. Some industrial application of recombinant AmyBS-I

The biochemical properties of AmyBS-I suggest that it is an acidic, Ca-independent and thermostable α-amylase, and is more suitable for application in the food and starch industries. Thus, its application in raw starch digestion and in baking industries as an anti-staling agent was investigated.

6.8.5.1. Raw starch hydrolysis by recombinant AmyBS-I

Conventional starch processing involves repeated steps of cooling and heating which is energy intensive [120, 287]. Since AmyBS-I can digest various raw-starches at 60-70°C, which is also the working range of glucoamylase (second step of starch saccharification), its application may eliminate the unnecessary repeated cooling and heating steps in the starch saccharification process [120]. AmyBS-I was able to hydrolyze wheat, potato and rice raw starches to various extents. This suggests its potential application in potato starch hydrolysis as only a few bacterial α-amylases are reported to digest this starch to such an extent [419]. Further, the raw starch digestibility of AmyBS-I was also supported by SEM analysis that showed the formation of pit and deep holes on the surface of all the tested raw starches, likewise the α-amylase purified from same parent strain [159]. Further, with the increase in demands of various raw starch digesting α-amylases in starch processing industries [303], AmyBS-I can prove to be more suitable candidate as it can efficiently hydrolyze various raw starches. Raw starch digesting study also suggests that AmyBS-I can find a wide range of applications in food and fermentation industries [225].

6.8.5.2. Anti-staling effects of AmyBS-I on bread

The amylases used in the baking industry to improve the shelf life of breads need to be moderately thermostable and should be active under acidic conditions. Additionally, they should also be able to produce fermentable sugars and dextrin as

end-products of hydrolysis, so that the yeast can act upon these in the next steps of bread making [341]. Dough supplementation showed that AmyBS-I and commercial α-amylases increased the shelf-life of bread; however, AmyBS-I had better anti-staling effects than the commercial enzyme (Himedia). Further, it was found that the AmyBS-I supplemented bread had a better loaf volume and crumb color compared to the commercial amylase supplemented or unsupplemented (control) bread The moisture content of the fresh bread has a direct correlation with the softness of the baked products and its ideal level should be around 35-40% [341]. Although the lower moisture content of bread is desirable to prevent microbial growth, it cannot be kept less than 30% because bread having moisture contents lower than this cannot be refreshed even after heating [420]. The moisture content of AmyBS-I supplemented bread was within the acceptable range and least among the tested samples which advocate adequate softness of the bread and least susceptible to the microbial attack. Sharma and Satyanarayana [341] have also found that the addition of α-amylase in the bread-making process increases the shelf-life of bread. The higher sugar content that gives a better taste, crust color, and toasting quality of bread was also found to be higher in the case of AmyBS-I supplemented bread as compared to other test samples [341].

Texture profile analysis (TPA) determines the staling rate of bread by physical examination of four parameters such as hardness, gumminess, cohesiveness, and springiness, which can be correlated with the sensory perception of bread and can define bread quality [380]. In general, the rate of increase in hardness and gumminess and decrease in cohesiveness and springiness with respect to time, determines the quality of bread [421]. In the present study, significant changes were observed in all the tested parameters of bread samples stored for five days. However, the bread supplemented with AmyBS-I had significant resistance to hardness and gumminess changes over the time as compared to control as well as commercial enzyme supplemented bread Thus, breads supplemented with AmyBS-I have adequate softness and low staling rate over time as compared to other tested samples (control & commercial amylase supplemented bread). Gambaro et al. [421] also observed that the addition of α-amylase retarded bread

starch retrograding, which maintains the freshness of the bread for a relatively longer period

6.9. Immobilization of α-amylase on magnetic nano-particle

Reusability of pricey enzyme is only possible through enzyme immobilization Enzyme immobilization on Magnetic Nano-particle (MNP) is found to be an effective and efficient method Covalent attachment is an important immobilization method (for enzymes), which has been demonstrated to induce higher resistance to temperature, denaturants, and organic solvents in several cases [422, 423] Considering the immense importance of the α-amylase isolated from *B subtilis* strain AS01a, we covalently attached the partially purified enzyme to MNPs [382]

The covalent immobilization of α-amylase on MNPs resulted in an increase in specific activity from 170 Units/mg (initial) to 4435 Units/mg post immobilization which indicates more than 26-fold increase in specific activity of the enzyme post binding onto MNP This increase in specific activity might be attributed to either increase in the surface area available to the enzyme moieties and/or a change in the conformation of catalytic site of α-amylase leading to higher catalytic efficiency [424] It also suggests that a very low amount of immobilized enzyme would be required to catalyze a reaction as compared to a free enzyme Therefore, immobilization of α-amylase on MNPs may be considered as a cost-effective process where cost of enzyme is a defining factor in industrial product development [382] This improvement of catalytic activity of α-amylase post binding onto iron-oxide MNPs was significantly higher compared to reported enhancement of catalytic activity of other enzymes for example lipase [424], yeast alcohol dehydrogenase [425] and alkaline phosphatase [426] immobilized onto iron-oxide MNPs

The heating experiment also demonstrated an increase in thermal stability of immobilized α-amylase compared to free enzyme which may be attributed to the restricted conformational mobility of the molecules post immobilization, [382,

422]. Further, starch hydrolysis by MNP-bound enzyme was more efficient than for the free enzyme [382]. Thus, the starch degrading efficiency, reusability and storage stability of MNP bound α-amylase compared to free α-amylase highlights the potential industrial application of the former in starch processing industries.

6.10. Conclusions

To sum up the present investigation, it can be stated that two potent α-amylase producing bacteria were isolated, characterized, and taxonomically identified as *Bacillus subtilis* strain AS01a and *Bacillus licheniformis* strain AS08E from the soil samples of Assam, Northeast India. The polyphasic approach followed for the identification of isolated bacterial strains proved to be the best option to discriminate even between the closely related species. Thus, the present study validates the use of universal 16S rDNA and intergenic spacer region (ISR) along with the other housekeeping genes for bacterial identifications up to species level.

Since the culture conditions of a bacterium influences the overall production level of enzyme (α-amylase), which in turn affects the cost of the end-product, it becomes necessary to identify and optimize these conditions properly. Considering this fact, statistical optimization of media components for maximum α-amylase production was undertaken for both the bacteria and with the use of optimized conditions, approximately three-fold increase in α-amylase production was achieved compared to non-optimized conditions. The response surface methodology applied in the present study also revealed that starch acts as an inducer whereas the nitrogen source showed a negative correlation on α-amylase productions from the bacteria under study. Thus, the statistical method of media optimization proved to be a useful tool for quick identification of media components and allowed us to determine the optimum conditions for maximum enzyme (product) yield from microbes.

The ever-increasing market demand for EDTA resistance, protease, surfactant, and oxidant-stable alkaline amylases in the detergent industries led us to isolate, purify, and characterize Amy-I from *B. subtilis* strain AS01, which is

well suited for working under these harsh conditions Furthermore, in order to cater to the need for starch and food processing industries, a raw starch digesting, high maltose forming and thermostable α-amylase (AmyBL-I) from *B licheniformis* strain AS08E was purified and characterized, which fulfills most of the demands of these industries Thus, the two purified enzymes in the present study have definite biotechnological applications in diverse industrial processes Besides, the bacterial strain (strain AS08E) isolated in the present study is probably the first example of a *Bacillus* which can grow and produce α-amylase in such a high alkaline pH (12 5) Therefore, the bacterium (strain AS08E) under study may be used as a model organism for understanding the molecular basis of the alkalophilicity of various enzymes

Considering the diverse applications of the purified enzymes from presently isolated bacteria, it became essential to investigate the future possibility of enzyme engineering for better α-amylase production, which would be suitable for harsh industrial process However, during our investigation we also encountered a prominent problem of inclusion bodies formation (enzymatically inactive) in *E coli*, which generally occurred during heterologous overexpression of recombinant protein in *E coli* [416] In order to solve this problem we targeted the recombinant protein to the culture media using the native signal peptide sequence of the enzyme from parent strain Further, we maximized the extracellular expression of recombinant enzymes using RSM Thus, by amalgamations of both the approaches, we efficiently targeted the catalytically active recombinant enzymes outside the cell membrane and obtained an approximately eight-fold increase in extracellular expression of recombinant enzyme in culture media compared to non-optimized conditions This bears the implication that this technique may be applied for efficient extracellular expression of other recombinant proteins in *E coli*

Further, the biochemical properties of α-amylase cloned from *B subtilis* strain AS01a (AmyBS-I) were found to be different from that of the wild-type enzyme purified from the same parent Thus, biotechnological applications of AmyBS-I was investigated and the biochemical properties suggested its suitability

for application in the starch and baking industries. AmyBS-I was found to be capable of digesting raw starches from various sources and can ameliorate crumb structure and shelf life bread, which is an added advantage for the baking industry. Further, immobilization of partially purified enzyme from *B. subtilis* strain AS01a on magnetic nanoparticles resulted into a significant improvement in the catalytic activity, thermal and storage stability, which enhanced the biotechnological potentiality of the enzyme in the starch processing industry. Therefore, it opened a new avenue of application of iron oxide magnetic nanoparticles for enzyme immobilization in a cost-effective manner to improve the catalytic efficiency as well as stability of an enzyme for its better application in different industrial sectors and can be taken up for the future course of study for the presently purified recombinant enzymes.

6.11. Future prospects

With the advent of new frontiers in biotechnology, the applications of amylases have extended in diverse fields of clinical, medicinal, and analytical chemistries, besides being in demand in the food, detergent and starch based industries. Thus, there is constant demand for more efficient α-amylases suitable for various industrial sectors, which can only be achieved either by chemical modification of the existing enzymes or through protein engineering. Therefore, the future work in this direction can be undertaken to improve the efficiency of presently cloned enzymes through enzyme engineering, either to improve the raw starch digestion efficiency, calcium independency, oxidative, surfactant, pH or temperature stability by identifying amino acid sequence responsible for these characteristics. The other task that may be undertaken is to make hybrid enzymes having broad applicability in industries. In addition, identifying the most potent natural α-amylase inhibitors (using docking studies) and testing their efficacy on the presently cloned α-amylases may help in identifying drug molecules for curing and preventing obesity [170]. As both the bacterial and mammalian amylases share a common structural, functional and catalytical features [42, 57], thus, bacterial α-amylase inhibitor may inhibit α-amylase activity in saliva and pancreatic juice, and

thereby reduce the digestion and absorption of starch (reduction of the calorie taken from meals) [170].

References

References

1. Saul D. J., Gibbs M. D., & Bergquist P. L. Biocatalysis: Industrial Enzymes and the Exploitation of Microorganisms in *Chemical Processes in New Zealand*, 2nd ed., New Zealand Institute of Chemistry, New Zealand, 1998. (www.nzic.org.nz/ChemProcesses/biotech/12H.pdf)
2. DaSilva, E. The Colours of Biotechnology: Science, Development and Humankind. *Electronic Journal of Biotechnology* 7(3), 2012. Retrieved on 22-11-2013 from http://158.251.16.30/index.php/ejbiotechnology/article/view/1114/1496.
3. OECD, *Future Prospects for Industrial Biotechnology*, OECD Publishing, 2011. (http://dx.doi.org/10.1787/9789264126633-en)
4. Oort, M. S. Surā in the Paippalāda Saṃhitā of the Atharvaveda, *J. Am. Orient. Soc.* **122**, 355-360, 2002.
5. Pandey, A., et al. Advances in microbial amylases, *Biotechnol. Appl. Biochem.* **31**, 135–52, 2000.
6. GIA, *Biotechnology – A Global Outlook*, Global Industry Analysts Inc., 2012, retrieved on 23-11-2013 from http://www.strategyr.com/pressGOS-093.asp.
7. Biospectrum India, *Industrial Biotechnology witness: 11.2% growth*, July, 2012, retrieved on 23-11-2013 from http://www.biospectrumindia.com/biospecindia/news/156450/industrial-biotechnology-witnesses-112-growth.
8. Khurana, G., Chauhan, A., & Hans, A. *Overview of Indian Biotech Market Associated with Climate change*, European Business and Technology Center, New Delhi, India, 2011. (http://www.ebtc.eu/pdf/110429_Overview-of-Indian-Biotech-Market-associated-with-climate-change.pdf)
9. Sharma, A., & Satyanarayana, T. Microbial acid-stable α-amylases: Characteristics, genetic engineering and applications, *Process Biochem.* **48**, 201–211, 2013.
10. Mobini-dehkordi, M. & Javan, F. A. Application of alpha-amylase in biotechnology, J. Biol. World **1**, 39–50, 2012.

11. Rajagopalan, G., & Krishnan, C. α-Amylase production from catabolite derepressed *Bacillus subtilis* KCC103 utilizing sugarcane bagasse hydrolysate. *Bioresour. Technol.* **99**, 3044–3050, 2008.

12. Wiseman, A. *Handbook of enzyme biotechnology*. Ellis Horwood Ltd., New York, 1985

13. Hasan, F. et al. Industrial applications of microbial lipases, *Enzyme Microb. Technol.* **39**, 235-251, 2006.

14. Rai, S.K. et al Characterisation of a detergent-stable alkaline protease from a novel thermophilic strain *Paenibacillus tezpurensis* sp. nov. AS-S24-II, *Appl. Microbiol. Biotechnol.* **85**, 1437–1450, 2010.

15. Cherry, J. R. & Fidantsef, A. L. Directed evolution of industrial enzymes: an update, *Curr. Opin. Biotechnol.* **14**, 438–443, 2003.

16. Goyal, N., Gupta, J.K., & Soni, S.K. A novel raw starch digesting thermostable α-amylase from *Bacillus* sp I-3 and its use in the direct hydrolysis of raw potato starch, *Enzyme Microb. Technol.* **37**, 723–734, 2005.

17. Singha, J., Kaurb, L., & McCarthy, O.J. Factors influencing the physico-chemical, morphological, thermal and rheological properties of some chemically modified starches for food applications—A review, *Food Hydrocolloids* **21**, 1–22, 2007.

18. van der Maarel, M. J. E. C., et al. Properties and applications of starch-converting enzymes of the α-amylase family, *J. Biotechnol.* **94**, 137–155, 2002.

19. Buleon, A., et al. Starch granules: structure and biosynthesis, *Int. J. Biol. Macromol.* **23**, 85–112, 1988.

20. Myers, A.M., et al. Recent progress towards understanding biosynthesis of the amylopectin crystal, *Plant Physiol.* **122**, 989–997, 2000.

21. Macgregor, E A , Janecek, S & Svensson, B Relationship of sequence and structure to specificity in the α-amylase family of enzymes, *Biochim. Biophys. Acta* **1546**, 1–20, 2001.

22. Coutinho, P.M., & Henrissat, B. Carbohydrate-active enzymes, 1999. (URL: http://www.cazy.org)

23. Turner, P., Mamo, G., & Karlsson, E.N. Potential and utilization of thermophiles and thermostable enzymes in biorefining, *Microb. Cell Fact.* **6,** 1-23, 2007.

24. Guzman-Maldonado, H., & Paredes-Lopez, O. Amylolytic enzymes and products derived from starch: a review, *Crit. Rev. Food Sci. Nutr.* **35**, 373–403, 1995.

25. Reddy, N. S., Nimmagadda, A., & Rao, K. R. S. S. An overview of the microbial α -amylase family, *African J. Biotechnol.* **2**, 645–648, 2003.

26. Sivaramakrishnan, S., et al. α-Amylases from microbial sources – An overview on recent developments, *Food Technol. Biotechnol.* **44**, 173–184, 2006.

27. Leveque, E., et al., Thermophilic archaeal amylolytic enzymes, *Enzyme Microb. Technol.* **26**, 3–14, 2000.

28. Ballschmiter, M., Futterer, O., & Liebl, W. Identification and characterization of a novel intracellular alkaline alpha-amylase from the hyperther- mophilic bacterium *Thermotoga maritima* MSB8, *Appl. Environ. Microbiol.* **72**, 2206–11, 2006.

29. Gupta, R., et al. Microbial α-amylases: a biotechnological perspective, *Process Biochem.* **00**, 1–18, 2003.

30. Fogarty, W.M. & Kelly, C.Y. Recent advances in microbial amylases, in *Microbial Enzymes and Biotechnology*, 2nd ed., Elsevier Science Publishers London, UK, 1990, 71–132.

31. Shenoy, B C., et al. Fungal Glucoamylase, *Biosci.* 7, 399 – 419, 1985.

32. Diderichsen, B. & Christiansen, L. Cloning of a maltogenic alpha-amylase from *Bacillus stearothermophilus*, *FEMS Microbiol. Lett.* **56**, 53-60, 1988.

33. Robyt, J.F. & Ackerman, R.J. Isolation, purification, and characterization of a maltotetraose-producing amylase from *Pseudomonas stuzeri, Arch. Biochem. Biophys.* **145**, 105–114, 1971.

34. Momma, M. Cloning and sequencing of the maltohexaose-producing amylase gene of *Klebsiella pneumonia, Biosci. Biotechnol. Biochem.* **64**, 428–431, 2000.

35 Bender, H , Lehman, J , & Wallenfels, K. Pullulan, ein extracellulares glucan von *Pullularia pullulans*, *Bioch. Biophys. Acta* **36**, 309–316, 1959.

36. Israilides, C., et al. Pullulan from agro-industrial wastes, *Biotechnol. Genet. Eng. Rev.* **16**, 309–324, 1999.

37. Takata, H., et al. Action of neopullulanase. Neopullulanase catalyzes both hydrolysis and transglycosylation at alpha-(1,4) and alpha-(1,6) glucosidic linkages, *J. Biol. Chem.* **267**, 18447–18452, 1992

38. Takaha, T. & Smith, S.M. The functions of 4-α-glucanotransferases and their use for the production of cyclic glucans, *Biotechnol Genet. Eng. Rev.* **16**, 257–280, 1999.

39. Van der Veen, B.A., et al. Engineering of cyclodextrin glycosyltransferase reaction and product specificity, *Biochem. Biophys. Acta* **1543**, 336–360, 2000.

40. Henrissat, B. A classification of glycosyl hydrolases based on amino acid sequence similarities, *Biochem. J.* **280**, 309–316, 1991.

41. Kuriki, T. & Imanaka, T. The concept of the α-amylase family: structural similarity and common catalytic mechanism, *J. Biosci. Bioeng.* **87**, 557–565, 1999.

42. Nielsen, J E. & Borchert, T.V. Protein engineering of bacterialα-amylases, *Biochim. Biophys. Acta* **1543**, 253–274, 2000.

43. Machius, M., et al. Activation of *Bacillus licheniformis* α-amylase through a disorder→order transition of the substrate-binding site mediated by a calcium-sodium-calcium metal triad, *Structure* **6**, 281–292, 1998.

44. Janecek, S How many conserved sequence regions are there in the α-amylase family?, *Biologia* **57**, 29–41, 2002.

45. Matsuura, Y., et al. Structure of possible catalytic residues of Taka-amylase A, *J. Biochem.* **95**, 697–702, 1984.

46. Klein, C., & Schulz, G.E. Structure of cyclodextrin glycosyltransferase refined at 2.0 A resolution, *J. Mol. Biol.* **217**, 737–750, 1991.

47. Kizaki H., et al. Polypeptide folding of *Bacillus cereus* ATCC7064 oligo-1,6-glucosidase revealed by 3 0 °A resolution X-ray analysis, *J. Biochem.* **113**, 646—649, 1993

48. Morishita Y., et al. Crystal structure of a maltotetraose-forming exo-amylase from *Pseudomonas stutzeri*, *J. Mol. Biol.* **267**, 661—672, 1997.

49. Katsuya Y., et al. Three-dimensional structure of *Pseudomonas* isoamylase at 2.2 °A resolution, *J. Mol. Biol.* **281**, 885—897, 1998.

50. Kamitori S., et al. Crystal structure of *Thermoactinomyces vulgaris* R-47 α-amylase II (TVAII) hydrolyzing cyclodextrins and pullulan at 2.6 °A resolution, *J. Mol. Biol* **287**, 907—921, 1999.

51. Kim J. S., et al. Crystal structure of a maltogenic amylase provides insights into a catalytic versatility, *J. Biol. Chem.* **274**, 26279—26286, 1999.

52. Dauter Z., et al. X-ray structure of Novamyl, the five-domain "maltogenic" α-amylase from *Bacillus stearothermophilus*: maltose and acarbose complexes at 1.7 °A resolution, *Biochemistry* **38**, 8385—8392, 1999.

53. Przylas I., et al. Crystal structure of amylomaltase from *Thermus aquaticus*, a glycosyltransferase catalysing the production of large cyclic glucans, *J. Mol. Biol.* **296**, 873—886, 2000.

54. Feese M. D., et al. Crystal structure of glycosyltrehalose trehalohydrolase from the hyperthermophilic archaeum *Sulfolobus solfataricus*, *J. Mol. Biol.* **301**, 451—464, 2000.

55. Skov, L.K., et al. Amylosucrase, a glucansynthesizing enzyme from the α-amylase family, *J. Biol. Chem.* **276**, 5273–5278, 2001.

56. Roujeinikova, A., et al Crystal structure of *Thermotoga maritima* 4-α-glucanotransferase and its acarbose complex: implications for substrate specificity and catalysis, *J. Mol. Biol.* **321**, 149–162, 2002.

57. Svensson, B. Protein engineering in the α-amylase family: catalytic mechanism, substrate specificity, and stability, *Plant Mol. Biol.* **25**, 141–157, 1994

58 Janecek, S New conserved amino acid region of α–amylases in the third loop of their $(\beta/\alpha)_8$-barrel domains, *Biochem. J.* **288**, 1069-1070, 1992.

59. Janecek, S., MacGregor, E.A., & Svensson, B. Characteristic differences in the primary structure allow discrimination of cyclodextrin glucanotransferases from α-amylases, *Biochem. J.* **305,** 685-686, 1995.

60. Davies, G.J., Wilson, K.S., & Henrissat, B. Nomenclature for sugar-binding subsites in glycosyl hydrolases, *Biochem. J.* **321,** 557-559, 1997.

61. MacGregor, E.A. α-amylase structure and activity, *J. Protein Chem.* **7,** 399-415, 1988.

62. Brzozowski, A.M., et al. Structural analysis of a chimeric bacterial α-amylase High resolution analysis of native and ligand complexes, *Biochemistry* **39,** 9099-9107, 2000.

63. Wolfenden, R., Lu, X., & Young, G. Spontaneous hydrolysis of glycosides, *J. Am. Chem. Soc.* **120,** 6814–6815, 1998.

64 Koshland, D.E Stereochemistry and the mechanism of enzymatic reactions, *Biol. Rev.* **28,** 416–436, 1953.

65. Uitdehaag, J.C.M., et al. X-ray structures along the reaction pathway of cyclodextrin glycosyltransferase elucidate catalysis in the α-amylase family, *Nature Struct. Biol.* **6,** 432–436, 1999.

66. Nakamura, A., Haga, K., & Yamane, K. Three histidine residues in the active center of cyclodextrin gluconotransferase from alkalophilic *Bacillus* sp. 1011 effects replacement on pH dependence and transiotion-state stabilization, *Biochemistry* **32,** 6624–6631, 1993.

67. Lawson, C.L., et al Nucleotide sequence and X-ray structure of cyclodextrin glycosyltransferase from *Bacillus circulans* strain 251 in a maltose-dependent crystal form, *J. Mol. Biol.* **236,** 590–600, 1994.

68. Strokopytov, B, et al. Structure of cyclodextrin glycosyltransferase complexed with a maltononaose inhibitor at 2.6 Å resolution. Implications for product specificity, *Biochemistry* **35,** 4241–4249, 1996.

69. Boel, E., et al. Calcium binding in α-amylases: an X-ray diffraction study at 2.1-Å resolution of two enzymes from *Aspergillus*, *Biochemistry* **29,** 6244-6249, 1990.

70 Vallee, B.L , et al. Metal content of α-amylases of various origins, *J Biol Chem* **234,** 2901-2905, 1959

71 Levitsky, A. & Steer, M L The allosteric activation of mammalian α-amylase by chloride, *Eur. J. Biochem.* **41,** 171-180, 1974.

72. Larson, S.B., et al Refined molecular structure of pig pancreatic α-amylase at 2 1 Å resolution, *J Mol Biol* **235**, 1560-1584, 1994

73 Buisson, G., et al. Three dimensional structure of porcine pancreatic α-amylase at 2 9Å resolution. Role of calcium in structure and activity, *EMBO J.* **6,** 3909-3916, 1987

74. Kadziola, A., et al Molecular structure of a barley α-amylase-inhibitor complex. implications for starch binding and catalysis, *J. Mol Biol* **278,** 205-217, 1998

75. Declerck, N., et al. Probing structural determinants specifying high thermostability in *Bacillus licheniformis* alpha-amylase, *J. Mol Biol.* **301**, 1041–1057, 2000

76 Feller, G., et al Structural and functional aspects of chloride binding to *Alteromonas haloplanctis* α-amylase, *J. Biol. Chem.* **271**, 23836-23841, 1996.

77. Aghajari, N , et al. Crystal structures of the psychrophilic α-amylase from *Alteromonas haloplanctis* in its native form and complexed with an inhibitor, *Protein Sci* 7, 564-572, 1998

78 Banner, D W. et al Structure of chicken muscle triose phosphate isomerase determined by crystallography at 2.5Å resolution using amino acid sequence data, *Nature* **255**, 609–614, 1975

79 Holm, L , et al Random mutagenesis used to probe the structure and function of *Bacillus stearothermophilus* alpha-amylase, *Protein Eng* **3**, 181–191, 1990.

80. Penninga, D , et al The raw starch-binding domain of cyclodextrin glycosyltransferase from *Bacillus circulans* strain 251, *J. Biol. Chem.* **271**, 32777–32784, 1996

81. Dalmia, B.K., Schutte, K., & Nikolov, Z.L. Domain E of *Bacillus macèrans* cyclodextrin gluconotransferase. an independent starch-binding domain, *Biotechnol. Bioeng.* **47**, 575–584, 1995.

82. Knegtel, R.M.A., et al. Crystallographic studies of the interaction of cyclodextrin glycosyltransferase from *Bacillus circulans* strain 251 with natural substrates and products, *J. Biol. Chem* **270**, 29256–29264, 1995.

83. Burhan, A. Enzymatic properties of a novel thermostable, thermophilic, alkaline and chelator resistant amylase from an alkaliphilic *Bacillus* sp. isolate ANT-6, *Process Biochem.* **38**, 1397–1403, 2003.

84. Kathiresan, K. & Manivannan, S. α-Amylase production by *Penicillium fellutanum* isolated from mangrove rhizosphere soil, *African J. Biotechnol.* **5**, 829-832, 2006.

85. Hernández, M.S., et al. Amylase production by *Aspergillus niger* in submerged cultivation on two wastes from food industries, *J. Food Process Eng.* **73**, 93–100, 2006.

86 Feller, G., Bussy, O. Le, & Gerday, C. Expression of psychrophilic genes in mesophilic hosts: Assessment of the folding state of a recombinant α – amylase, *Appl. Environ. Microbiol.* **64**, 1163–1165, 1998.

87. Kaneko, A. et al. Molecular cloning and determination of the nucleotide sequence of a gene encoding an acid-stable α-amylase from *Aspergillus kawachii* , *J. Ferment. Bioeng.* **81**, 292–296, 1996.

88. Demirkan, E.S., et al. α-Amylase from *B. amyloliquefaciens*: Purification, characterization, raw starch degradation and expression in *E. coli*, *Process Biochem.* **40**, 2629–2636, 2005.

89. Kim, I. C., et al. Catalytic properties of the cloned amylase from *Bacillus licheniformis*, *J Biol. Chem.* **267**, 22108–22114, 1992

90. Marco, J. L., et al. Purification and characterization of a truncated *Bacillus subtilis* α-amylase produced by *Escherichia coli, Appl Microbiol. Biotechnol.* **44**, 746–752, 1996.

91. Birol, G. et al. Ethanol production and fermentation characteristics of recombinant *Saccharomyces cerevisiae* strains grown on starch, *Enzyme Microb. Technol.* **22**, 672–677, 1998.

92. Mijts, B.N. & Patel, B.K.C. Cloning, sequencing and expression of an α-amylase gene (amyA, from the thermophilic halophile *Halothermothrix orenii* and purification and biochemical characterization of the recombinant enzyme, *Microbiol.* **148,** 2343–2349, 2002.

93. Kang, H.K., et al. Cloning and expression of *Lipomyces starkeyi* α-amylase in *Escherichia coli* and determination of some of its properties, *FEMS Microbiol. Lett.* **233**, 53–64, 2004.

94. Leveque, E., Haye, B., & Belarbi, A. Cloning and expression of an α-amylase encoding gene from the hyperthermophilic archaebacterium *Thermococcus hydrothermalis* and biochemical characterization of the recombinant enzyme, *FEMS Microbiol. Lett.* **186,** 67–71, 2000.

95. Bisgaard-Frantzen, H., et al. Development of industrially important α-amylases, *J. Appl. Glycosci.* **46**, 199-206, 1999.

96. Lecker, D.N. & Khan, A. Model for inactivation of α–amylase in the presence of salts: theoretical and experimental studies, *Biotechnol. Prog.* **14**, 621-625, 1998.

97. Sunna, A., et al. Glycosyl hydrolases from hyperthermophiles, *Extremophiles* **1**, 2 – 13, 1997.

98. Niehaus, F., et al. Extremophiles as a source of novel enzymes for industrial application, *Appl. Microbiol. Biotechnol.* **51**, 711–729, 1999.

99. Veille, C. & Zeikus, G.J. Hyperthermophilic enzymes: sources, use, and molecular mechanisms for thermostability, *Microbiol. Mol. Biol. Rev.* **65**, 1–43, 2001.

100. Bertoldo, C., et al. Pullulanase type I from *Feridobacterium pennaorans* Ven5: cloning, sequencing, and expression of the gene and biochemical characterization of the recombinant enzyme, *Appl. Environ. Microbiol.* **65**, 2084 – 2091, 1999.

101. Antranikian, G., Koch, R., & Spreinat, A. Novel hyper-thermostable alpha-amylase, Patent application WO 90/ 11352, 1990.

102. Declerck, N. et al. Hyperthermostabilisation of *Bacillus licheniformis* α-amylase and modulation of its stability over a 50°C temperature range, *Protein Eng.* **16**, 287–293, 2003.

103. Shaw, A. Bott, R., & Day, A.G. Protein engineering of α-amylase for low pH performance, *Curr. Opin. Biotechnol.* **10**, 349–352, 1999.

104. Matthews, B.W., Nicholson, H., & Bechtel, W.J. Enhanced protein thermostability from site-directed mutations that decrease the entropy of unfolding, *Proc. Natl. Acad. Sci. USA*, **84**, 6663–6667, 1987.

105. Bessler, C., et al. Directed evolution of a bacterial α-amylase: Toward enhanced pH performance and higher specific activity, *Protein Sci.* **12**, 2141–2149, 2003.

106. Machius, M., et al. Kinetic stabilization of *Bacillus licheniformis* α-amylase through introduction of hydrophobic residues at the surface, *J. Biol. Chem.* **278**, 11546–11553, 2003.

107. Cha, H., et al. Molecular and enzymatic characterization of a maltogenic amylase that hydrolyzes and transglycosylates acarbose, *Eur. J. Biochem.* **253**, 251–162, 1998.

108. Liu, Y., et al. Acid stabilization of *Bacillus licheniformis* alpha amylase through introduction of mutations, *Appl. Microbiol. Biotechnol.* **80**, 795–803, 2008.

109. Liu, Y., et al. High-level expression, purification and characterization of a recombinant medium-temperature alpha-amylase from *Bacillus subtilis*, *Biotechnol. Lett.* **32**, 119–124, 2010.

110. Priyadharshini, R., & Gunasekaran, P. Site-directed mutagenesis of the calcium-binding site of α-amylase of *Bacillus licheniformis*, *Biotechnol. Lett.* **29**, 1493–1499, 2007.

111. Ben, S., et al. Enhancement of the thermostability of the maltogenic amylase MAUS149 by Gly312Ala and Lys436Arg substitutions, *Bioresour. Technol.* **102**, 1740–1746, 2010.

112. Liu, Y., et al. Role of the calcium-binding residues Asp231, Asp233, and Asp438 in alpha-amylase of *Bacillus amyloliquefaciens* as revealed by mutational analysis, *Curr Microbiol.* **60**, 162–166, 2010

113. Ali, M.B , et al. Thermostability enhancement and change in starch hydrolysis profile of the maltohexaose-forming amylase of *Bacillus stearothermophilus* US100 strain, *Biochem. J* **394**, 51–56, 2006.

114. Khemakhem, B., et al. Engineering of the alpha-amylase from *Geobacillus stearothermophilus* US100 for detergent incorporation, *Biotechnol. Bioeng.* **102**, 380–389, 2009

115. Eratt, J.A., et al. The induction of α-amylase by starch in *Aspergillus oryzae*: evidence for controlled mRNA expression, *Can J. Biochem. Cell. Biol.* **62**, 678–90, 1984.

116. Khoo, S.L. et al. Purification and characterization of alpha-amylase from *Aspergillus flavus, Folia Microbiol.* **39**, 392-398, 1994.

117. Iefuji, P., et al. Raw-starch-digesting and thermostable α-amylase from the yeast *Cryptococcus* sp. S-2: purification, characterization, cloning and sequencing, *Biochem. J.* **318,** 989-96, 1996.

118. Moraes, L M.P. Filho, S.A., & Ulhoa, C.J. Purification and some properties of an α-amylase glucoamylase fusion protein from *Saccharomyces cerevisiae*, *World J. Microbiol. Biotechnol.* **15**, 561-564, 1999.

119 Glymph, J.L. & Stutzenberger, F J Production, purification and characterization of α-amylase from *Thermomonospora curvata, Appl. Environ. Microbiol.* **34**, 391-7, 1977.

120. Bai, Y , et al. Identification of an acidic α-amylase from *Alicyclobacillus* sp. A4 and assessment of its application in the starch industry, *Food Chem.* **131**, 1473–1478, 2012.

121 Hamilton, L.M , Kelly, C T., & Fogarty, W.M. Production and properties of the raw starch digesting α-amylase of *Bacillus* sp IMD 435, *Process Biochem.* **35**, 27-31, 1999

122. Ghorbel, R.E., et al. New thermostable amylase from *Bacillus cohnii* US147 with a broad pH applicability, *Appl. Biochem. Biotechnol.* **157,** 50–60, 2009.

123. Krishnan, T. & Chandra, A.K. Purification and characterization of α-amylase from *Bacillus licheniformis* CUMC305, *Appl Environ. Microbiol.* **46**, 430-7, 1983.

124. Morgan, F.J. & Priest, F.G. Characterization of a thermostable α-amylase from *Bacillus licheniformis* NCIB 6346, *J. Appl. Bacteriol.* **50,** 107–14, 1981.

125. Jana, M., et al. Salt-independent thermophilic α-amylase from *Bacillus megaterium* VUMB109: An efficacy testing for preparation of maltooligosaccharides, Ind. Crops Prod. **41**, 386–391, 2013.

126. Marco, J. L., et al. Purification and characterization of a truncated *Bacillus subtilis* α-amylase produced by *Escherichia coli, Appl. Microbiol. Biotechnol.* **44**, 746–752, 1996.

127. Hayashida, S., Teramoto, Y., & Inoue, T. Production and characteristics of raw-potato-starch-digesting α-amylase from *Bacillus subtilis* 65, *Appl. Environ. Microbiol.* **54**, 1516-1522, 1988.

128 Giraud, E., et al. Purification and characterization of an extracellular amylase from *Lactobacillus plantarum* strain A6, *J. Appl. Bacteriol.* **75,** 276-82, 1993.

129. Freer, S.N. Purification and characterization of the extracellular α-amylase from *Streptococcus bovis* JB 1, *Appl. Environ. Microbiol.* **59,** 1398-1402, 1993.

130. Mateo, C., et al. Improvement of enzyme activity, stability and selectivity via immobilization techniques, *Enzyme Microb Technol.* **40**, 1451–1463, 2007.

131. Kara, A., et al. Immobilization of α-amylase on Cu^{2+} chelated poly(ethylene glycol dimethacrylate-n-vinyl imidazole) matrix via adsorption, *React. Funct. Polym.* **62,** 61–68, 2005.

132. Bryjak, J. Glucoamylase, α-amylase and β-amylase immobilization on acrylic carriers, *Biochem. Eng. J.* **16**, 347–355, 2003.

133. El-Batal, A.I., Atia, K.S., & Eid, M. Stabilization of α-amylase by using anionic surfactant during the immobilization process, *Radiat. Phys. Chem.* **74**, 96–101, 2005.

134. Bayramoglu, G, Yilmaz, M. & Arica, M Y. Immobilization of a-thermostable α-amylase onto reactive membranes: Kinetics characterization

and application to continuous starch hydrolysis, *Food Chem.* **84**, 591–599, 2004.

135. Konsoula, Z. & Liakopoulou-Kyriakides, M. Starch hydrolysis by the action of an entrapped in alginate capsules α-amylase from *Bacillus subtilis*, *Process Biochem.* **41**, 343–349, 2006.

136. Park, D., et al. Immobilization of starch-converting enzymes on surface modified carriers using single and co-immobilized systems: Properties and application to starch hydrolysis, *Process Biochem.* **40,** 53–61, 2005.

137. Akkaya, B., Fazil, A., & Akkaya, R. Production and immobilization of a novel thermoalkalophilic extracellular amylase from *Bacilli* isolate, *Int. J. Biol. Macromol.* **50**, 991–995, 2012.

138. Haki, G. D. & Rakshit, S. K. Developments in industrially important thermostable enzymes: a review, *Bioresour Technol.* **89**, 17-34, 2003.

139. Souza, P.M. & Magalhães, P.O. Application of microbial α-amylase in industry – a review, *Brazilian J Microbiol.* **41**, 850–861, 2010.

140. Tawil, G., et al. Hydrolysis of concentrated raw starch: A new very efficient α-amylase from *Anoxybacillus flavothermus, Carbohydr. Polym.* **87**, 46–52, 2012.

141. Viksø-nielsen, A., et al. Development of new α-amylases for raw starch hydrolysis, *Biocatal. Biotransformation* **24**, 121–127, 2006.

142. Sharma, A. & Satyanarayana, T., High maltose-forming, Ca^{2+}-independent and acid stable α-amylase from a novel acidophilic bacterium, *Bacillus acidicola, Biotechnol. Lett.* **32**, 1503–1507, 2010.

143. Whitelabs, *Commercial Distilling Applications*, retrieved on 11-23-2013 from www.whitelabs.com/files/WhiteLabsEnzymeSolutions_Distilling.pdf.

144. Jamai, L., et al. Production of ethanol from starch by free and immobilized *Candida tropicalis* in the presence of alpha-amylase, *Bioresour. Technol.* **98**, 2765–70, 2007.

145. Błaszczak, W., et al. Structural changes in the wheat dough and bread with the addition of alpha-amylases, *Eur. Food Res. Technol.* **219**, 348–354, 2004.

146. Medhekar, R., et al., Reduced sugar syrups and methods of making reduced sugar syrups, In: United States Patent Application no. US 2013/0197104-A1; 2013.

147. Hmidet, N., et al. Alkaline proteases and thermostable alpha-amylase co-produced by *Bacillus licheniformis* NH1: Characterization and potential application as detergent additive, *Biochem. Eng. J.* **47**, 71–79, 2009.

148. Bruinenberg, P.M., et al. A process for surface sizing or coating of paper, In: European Patent Application no. EP0690170A1, 1996.

149. Chand, N., et al. Enzymatic desizing of cotton fabric using a Ca^{2+}-independent α-amylase with acidic pH profile, *J. Mol. Catal. B Enzym.* **83,** 46–50, 2012.

150. Becks, S., et al. Application of a liquid stable amylase reagent on the Ciba Corning Express clinical chemistry system, *Clin. Chem.* **41**, 186, 1995.

151. Satyanarayana, T., Rao, J.L.U M, & Ezhilvannan, M. α-Amylases, in *Enzyme Technology*, A. Pandey et al., eds Asiatech Publishers Inc, New-Delhi, 2005, 189–220

152. Prakash, O & Jaiswal, N. α-Amylase: An ideal representative of thermostable enzymes, *Appl. Biochem Biotechnol.* **160**, 2401–2414, 2010

153. Ramachandran, S., et al. Alpha amylase from a fungal culture grown on oil cakes and its properties, *Braz. Arch. Biol. Technol.* **47**, 309-317, 2004.

154 Hyum, H.H. & Zeirkus, J.G. Simultaneous and enhanced production of thermostable amylases and ethanol from starch by co-cultures of *Clostridium thermosulfurogenes* and *Clostridium thermohydrosulfuricum*, *Appl. Environ. Microbiol.* **49,** 1174 -1181, 1985.

155. Öner, E.T. Optimization of ethanol production from starch by an amylolytic nuclear petite *Saccharomyces cerevisiae* strain, *Yeast* **23**, 849-856, 2006.

156. Chi, Z. et al. *Saccharomycopsis fibuligera* and its applications in biotechnology, *Biotechnol. Adv.* **27**, 423-43, 2009.

157. Saxena, R K et al. A highly thermostable and alkaline amylase from a *Bacillus* sp. PN5, *Bioresour. Technol.* **98**, 260-265, 2007.

158 Mobini-Dehkordi, M., et al. Isolation of a novel mutant strain of *Saccharomyces cerevisiae* by ethyl methyl sulfonate mutagenesis approach as a high producer of bioethanol, *J. Biosci. Bioengin.* **105**, 403-408, 2008.

159. Roy, J.K., Rai, S.K., & Mukherjee, A.K. Characterization and application of a detergent-stable alkaline α-amylase from *Bacillus subtilis* strain AS-S01a, *Int J. Biol. Macromol* **50**, 219–29, 2012.

160. Mukherjee, A. K., Borah, M., & Rai, S. K. To study the influence of different components of fermentable substrates on induction of extracellular α-amylase synthesis by *Bacillus subtilis* DM-03 in solid-state fermentation and exploration of feasibility for inclusion of α-amylase in laundry detergent formulations, *Biochem. Eng. J.* **43,** 149–156, 2009.

161 Olsen, H S & Falholt, P The role of enzymes in modern detergency, *J. Surfactant Deterg.* **1**, 555–567, 1998.

162. Mitidieri, S., et al. Enzymatic detergent formulation containing amylase from *Aspergillus niger*: A comparative study with commercial detergent formulations, *Biores. Technol.* **97**, 1217–24, 2006.

163. Ramasesh, N., et al. Purification and characterization of thermophilic alpha-amylase of *Aspergillus niger*, *Starke* **34**, 274–279, 1982.

164. Haq, I. et al. Production of alpha amylase from a randomly induced mutant strain of *Bacillus amyloliqefaciens* and its application as a desizer in textile industry, *Pak. J. Bot.* **42,** 473-484, 2010.

165. Fryer, P.J. & Asteriadou, K.A. Prototype cleaning map: a classification of industrial cleaning processes, *Trends Food Sci. Technol* **20**, 255-262, 2009.

166 Kuddus, M. Microbial cold-active α-amylases: from fundamentals to recent developments, in *Current research, technology, and education topics in applied microbiology and microbial biotechnology*, A M. Vilas, eds., Formatex Research Center, Spain, 2010, 1265-1276.

167. Fogarty, W.M & Kelly, C T Microbial Enzymes and Bioconversions, in *Economic Microbiology*, A. H. Rose, eds., Academic Press, London, 1980, 115–170.

168. Kost, J. & Shefer, S. Chemically-modified polysaccharides for enzymatically controlled oral drug delivery, *Biomaterials* **11**, 695–698, 1990.

169. Dumoulina, Y., Cartiliera, L., & Mateescub, M. Cross-linked amylose tablets containing α-amylase: an enzymatically controlled drug release system, *J. Control. Release* **60**,161–167, 1999.

170. Benjamin, S., et al. A monograph on amylases from *Bacillus* spp., *Adv. Biosci. Biotechnol.* **4**, 227–241, 2013.

171. Barbesgard, P., Heldt-halsen, H., & Diterichsen, B. On the safety of the *Aspergillus oryzae*-A review, *Appl. Microbiol. Biotechnol.* **36**, 569-572, 1992.

172. Kingspohn, K., et al. Utilization of potato pulp from potato starch processing, *Process Biochem.* **28**, 91-98, 1993.

173. Wu, H., Mulchandani, A., & Chen, W. Versatile microbial surface-display for environmental remediation and biofuels production, *Trends Microbiol.* **14**, 181-188, 2008.

174. Aubel, D., et al. Design of a novel mammalian screening system for the detection of bioavailable, non-cytotoxic streptogramin antibiotics, *J. Antibiot.* **54**, 44–54, 2001.

175. Ikuta, N., et al. The alpha-amylase gene as a marker for gene cloning: direct screening for recombinant colonies, *Nature Biotechnol.* **8**, 241-242, 1990.

176. Chen, H.C. Optimizing the concentrations of carbon, nitrogen and phosphorus in a citric acid fermentation with response surface method, *Food Biotechnol.* **10**, 13–27, 1996.

177. Sanchez, S. & Demain, A.L. Enzymes and bioconversions of industrial, pharmaceutical and biotechnological significance, *Org. Process. Res. Dev.* **15**, 224–30, 2010.

178. Crueger, W. & Crueger, A. Industrial Microbiology (eds.), Sinauer Associates, Sunderland, MA, 1989, 189–218.

179. Asgher, M., et al. A thermostable α-amylase from a moderately thermophilic *Bacillus subtilis* strain for starch processing, *J. Food Eng.* **79**, 950–955, 2007.

180. Mojsov, K. Microbial α-amylases and their industrial Applications: a review, *Int. J. Manag. IT Eng.* **2**, 583-609, 2012.

181. Tanyildizi, M.S., Ozer, D., & Elibol, M., Optimization of α-amylase production by *Bacillus* sp. using response surface methodology, *Process Biochem.* **40**, 2291–2296, 2005.

182. Schallmey, M., Singh, A., & Ward, O.P. Developments in the use of *Bacillus* species for industrial production, *Can. J. Microbiol.* **50,** 1-17, 2004.

183. Asoodeh, A., Chamani, J., & Lagzian, M. A novel thermostable, acidophilic α-amylase from a new thermophilic "*Bacillus* sp. *Ferdowsicous*" isolated from Ferdows hot mineral spring in Iran: purification and biochemical characterization, *Int. J. Biol. Macromol.* **46,** 289–297, 2010.

184. Gomes, I., Gomes, J., & Steiner, W. Highly thermostable amylase and pullulanase of the extreme thermophilic eubacterium *Rhodothermus marinus*: production and partial characterization, *Bioresour. Technol.* **90**, 207-214, 2003.

185. Konsoula, Z. & Liakopoulou-Kyriakides, M. Co-production of alpha-amylase and beta-galactosidase by *Bacillus subtilis* in complex organic substrates, *Bioresour. Technol.* **98**, 150-157, 2007.

186. Tomazic, S.J. & Klibanov, A.M. Why is one *Bacillus* alpha-amylase more resistant against irreversible thermoinactivation than another?, *J. Biol. Chem.* **263**, 3092-3096, 2003.

187. Amoozegar, M.A., Malekzadeh, F., & Malik, K.A. Production of amylase by newly isolated moderate halophile, *Halobacillus* sp. strain MA-2, *J. Microbiol. Methods* **52**, 353-359, 2003.

188. Prakash, B., et al. Production, purification, and characterization of two extremely halotolerant, thermostable, and alkali-stable α-amylases from *Chromohalobacter* sp. TVSP 101, *Process Biochem.* **44**, 210–215, 2009.

189. Mohapatra, B.R., Bapuji, M., & Sree, A. Production of industrial enzymes (amylase, carboxymethylcellulase and protease) by bacteria isolated from marine sedentary organisms, *Acta Biotechnol.* **23**, 75–84, 2003.

190. Hutcheon, G.W., Vasisht, N., & Bolhuis, A. Characterisation of a highly stable alpha-amylase from the halophilic archaeon *Haloarcula hispanica*. *Extremophiles* **9**, 487-495, 2005.

191. Coronado, M., et al. Production and biochemical characterization of an alpha-amylase from the moderate halophile *Halomonas meridian, FEMS Microbiol. Lett.* **183**, 67-71, 2000.

192. Deutch, C.E. Characterization of a salt-tolerant extracellular α-amylase from *Bacillus dipsosauri*, Lett. Appl. Microbiol. 35, 78-84, 2002.

193. Kathiresan, K. & Manivannan, S. α-Amylase production by *Penicillium fellutanum* isolated from mangrove rhizosphere soil, *African J. Biotechnol.* **5**, 829-832, 2006.

194. Jin, B., et al. Utilisation of starch processing wastewater for production of microbial biomass protein and fungal α-amylase by *Aspergillus oryzae*, *Bioresour. Technol.* **66**, 201–206, 1998.

195. Djekrif-Dakhmouche, S., et al. Application of a statistical design to the optimization of culture medium for α-amylase production by *Aspergillus niger* ATCC 16404 grown on orange waste powder, *J. Food Process Eng.* **73**, 190–197, 2006.

196. Rahardjo, Y.S.P., et al. Aerial mycelia of *Aspergillus oryzae* accelerate α-amylase production in a model solid-state fermentation system, *Enzyme Microb. Technol.* **36**, 900–902, 2005.

197. Kunamneni, A., Permaul, K., & Singh, S. Amylase production in solid-state fermentation by the thermophilic fungus *Thermomyces lanuginosus*, *J. Biosci. Bioeng.* **100**, 168-171, 2005.

198. Jensen, B., et al. Enzyme production in continuous cultivation by the thermophilic fungus, *Thermomyces lanuginosus*, *Biotechnol. Lett.* 24, 41–45, 2002.

199. Martin, M L., & Hoseney, R.C. A mechanism of bread firming. II: role of starch hydrolyzing enzymes, *Cereal Chem.* **68,** 503–507, 1991.

200. Horikoshi, K. Alkaliphiles: some applications of their products for biotechnology, *Microbiol. Mol. Biol. Rev.* **63**, 735–750, 1999.

201. Kaur, P. & Vyas, A. Characterization and optimal production of alkaline α-amylase from *Bacillus* sp. DLB 9, *African J. Biotechnol.* **6**, 2674–2681, 2012.

202. Kim, D., et al. Purification and characterization of a liquefying α-amylase from alkalophilic thermophilic *Bacillus* sp. AAH-31, *Biosci. Biotechnol. Biochem.* **76**, 1–6, 2012.

203. Ito, S., et al. Alkaline detergent enzymes from alkaliphiles: enzymatic properties, genetic, and structures, *Extremophiles* **2**, 185–190, 1998.

204. Horikoshi, K. Production of alkaline enzymes by alkalophilic microorganisms, *Agric. Biol. Chem.* **35**, 1783-1791, 1971.

205. Bernhardsdotter, E.C.M.J., et al., Enzymic properties of an alkaline chelator-resistant α-amylase from an alkaliphilic *Bacillus* sp. isolate L1711, *Process Biochem.* **40**, 2401–2408, 2005.

206. Igarashi, K., et al. Enzymatic properties of a novel liquefying α-amylase from an alkaliphilic *Bacillus* isolate and entire nucleotide and amino acid sequence, *Appl. Environ. Microbiol.* **64**, 3282–3289, 1998.

207. Mamo, G. & Gessesse, A. Purification and characterization of two raw-starch-digesting thermostable α-amylases from a thermophilic *Bacillus*, *Enzyme Microb. Technol.* **25**, 433-438, 1999.

208. Kim, T.U., et al., Purification and characterization of a maltotetraose forming alkaline α-amylase from an alkalophilic *Bacillus* sp. GM8901, *Appl. Environ. Microbiol.* **61**, 3105-12, 1995.

209. Hagihara, H., et al. Novel that is highly resistant to chelating reagents and chemical oxidants from the alkaliphilic *Bacillus* isolate KSM-K38, *Appl. Environ. Microbiol.* **67**, 1744–1750, 2001.

210. Lin, L.L., Chyau, C.C., & Hsu, W.H. Production and properties of a raw starch-degrading amylase from the thermophilic and alkaliphilic *Bacillus* sp. TS-23, *Biotechnol. Appl. Biochem.* **28**, 61–68, 1996.

211. Horikoshi, K. Alkaliphiles—from an industrial point of view, *FEMS Microbiol. Rev.* **18**, 259–270, 1996.

212. Shanmughapriya, S., Optimization, production, and partial characterization of an alkalophilic amylase produced by sponge associated marine bacterium *Halobacterium salinarum* MMD047, *Biotechnol. Bioprocess Eng.* **14**, 67–75, 2009.

213. Dastager, G.S., Agasar, D., & Pandey, A. Production and partial purification of α-amylase from a novel isolate *Streptomyces gulbargensis*, *J. Ind. Microbiol. Biotechnol.* **36,**189–194, 2009.

214. Futterer, O., et al. Engineering of a *Bacillus* α-amylase with improved thermostability and calcium independency. *Appl. Biochem. Biotechnol.* **162**, 444–459, 2010.

215. Shivaramakrishnan, S., et al. α-Amylases from microbial sources–an overview on recent developments, *Food Technol. Biotechnol.* **44**, 173-184, 2006.

216. Antranikian, G. Microbial degradation of starch, in *Microbial degradation of natural products*, G. Winkelmann, eds., Weinheim VCH, Germany, 1992, 27-56.

217. Matzke, J., Schwermann, B., & Baker, E.P. Acidostable and acidophilic proteins: the example of the α-amylase from *Alicyclobacillus acidocaldarius*, *Comp. Biochem. Physiol.* **118**, 475-479, 1997.

218. Kanno, M. α-Amylase production by *Bacillus acidocaldarius, Bacillus stearothermophilus* and their D-cycloserine resistant mutants, *Agri. Biol. Chem.***50**, 2633-2635, 1986.

219. Koch, R., Zablowski, P., & Antranikian, G. Highly active and thermostable amylases and pullulanases from various anaerobic thermophiles, *Appl. Microbiol. Biotechnol.* **27,** 192-198, 1987.

220. Dey, G., et al. Purification and characterization of maltooligosaccharide-forming amylase from *Bacillus circulans* GRS 313, *J. Indust. Microbiol. Biotechnol.* **28,** 193-200, 2002.

221. Hmidet, N., et al. Purification and biochemical characterization of a novel α-amylase from *Bacillus licheniformis* NH1: Cloning, nucleotide sequence and expression of amyN gene in *Escherichia coli*, *Process Biochem.* **43**, 499–510, 2008.

222. Manning, B.G. & Campbell, L.L. Thermostable α–amylase of *Bacillus stearothermophilus, J. Biol. Chem.* **236**, 2952–2955, 1961.

223 Ali, M B, et al Purification and sequence analysis of the atypical maltohexaose-forming α-amylase of the *B stearothermophilus* US100, *Enzyme Microb Technol* **28,** 537–542, 2001

224 Sajedi, R H, et al A calcium independent α-amylase that is active and stable at low pH from the *Bacillus* sp KR-8104, *Enzyme Microb Technol* **36,** 666-671, 2005

225 Liu, X D & Xu, Y A novel raw starch digesting α-amylase from a newly isolated *Bacillus* sp YX-1 purification and characterization, *Biores Technol* **99,** 4315–20, 2008

226 Ali, M B, Mezghani, M, & Bejar, S A thermostable alpha amylase producing maltohexose from a newly isolated *Bacillus* sp US100 study of activity and molecular cloning of the corresponding gene, *Enzyme Microb Technol* **24,** 584-589, 1999

227 Nagarajan, D R, Rajagopalan, G, & Krishnan, C Purification and characterization of a maltooligosaccharide-forming alpha-amylase from a new *Bacillus subtilis* KCC103, *Appl Microbiol Biotechnol* **73,** 591-597, 2006

228 Mollania, N, et al Purification and characterization of a thermostable phytate resistant α-amylase from *Geobacillus* sp LH8, *Int J Biol Macromol* **46,** 27–36, 2010

229 Aguilar, G, et al Purification and characterization of an extracellular α-amylase produced by *Lactobacillus manihotivorans* LMG 18010T, an amylolytic lactic acid bacterium, *Enzyme Microb Technol* **27,** 406-413, 2000

230 Savchenko, A, et al *Pyrococcus furiosus* α-amylase is stabilized by calcium and zinc, *Biochemistry* **41,** 6193-6201, 2002

231 Bhella, R S & Altosaar, I Purification and some properties of the extracellular α-amylase from *Aspergillus awamori, Can J Microbiol* **31,** 149-155, 1985

232 Olutiola, P O α-Amylolytic activity of *Aspergillus chevalieri* from mouldy maize seeds, *Indian Phytopathol* **35,** 428-433, 1982

233. Michelena, V.V. & Castillo, F.J Production of amylase by *Aspergillus foetidus* on rice flour medium and characterization of the enzyme, *J. Appl. Bacteriol.* **56**, 395- 400, 1984.

234. Domingues, C.M. & Peralta, R.M. Production of amylase by soil fungi and partial biochemical characterization of amylase of a selected strain (*Aspergillus fumigatus fresenius*), *Can. J. Microbiol.* **39**, 681-5, 1993.

235. Alazard, D. & Baldensperger, J.F. Amylolytic enzymes from *Aspergillus hennebergi* (*A. niger* group): purification and characterization of amylases from solid and liquid cultures, *Carbohydr. Res.* **107**, 231-237, 1982

236. Ramachandran, N., Skreekantiah, K.R., & Murthy, V.S. Studies on the thermophilic amylolytic enzymes of a strain of *Aspergillus Aspergillus niger*, *Starch* **30**, 272-275, 1978

237. Yabuki, M., et al. Rapid induction of α-amylase by non-growing mycelia of *Aspergillus oryzae*, *Appl. Environ. Microbiol.* **34**:1-6, 1977

238. Jodal, I., et al. Hydrolysis of cyclodextrin by *Aspergillus oryzae* α-amylase, *Starch* **36**, 140-143, 1984

239. Suganuma, T., et al. N-terminal sequence of amino acids and some properties of an acid stable α-amylase from citric acid Koji (*Aspergillus usamii* var.), *Biosci Biotech. Biochem.* **60**, 177 -9, 1996.

240 Narayanan, A.S & Shanmugasundaram, E.R.B Studies on amylase of *Fusarium vasinfectum*, *Arch. Biochem. Biophys.* **118**, 317-322, 1967.

241. Zenin, C T & Park, Y K. Purification and characterization of acid α-amylase from *Paecilomyces* sp., *J. Ferment. Technol.* **61**, 109-14, 1983.

242. Mishra, R.S. & Maheshwari, R. Amylases of the thermophilic fungus *Thermomyces lanuginosus*: their purification, properties, action on starch and response to heat, *J. Biosci.* **21**, 653-72, 1996.

243. Schellart, J.A , et al. Starch degradation by the mold *Trichoderma viride* I, the mechanism of degradation, *Antonie Van Leeuwenhoek J. Microbiol. Serol.* **42**, 229-238, 1976

244 Prieto, J A., et al Purification and characterization of a new α-amylase of intermediate thermal stability from the yeast *Lipomyces kononenkoae*, *Biochem Cell Biol* **73**, 41-49, 1995

245 Wanderley, K J , et al Biochemical characterization of α-amylase from the yeast *Cryptococcus flavus*, *FEMS Microb Lett* **231,** 165-169, 2004

246 Van den Burg, B Extremophiles as a source for novel enzymes, Curr Opin Microbiol **6**, 213–218, 2003

247 Ventosa, A , Nieto, J J , & Oren, A Biology of moderately halophilic aerobic bacteria, *Microbiol Mol Biol Rev* **62**, 504– 544, 1998

248 Ventosa, A Unusual microorganisms from unusual habitats hypersaline environments. in *Prokaryotic Diversity-Mechanism and Significance*. N A Logan, et al , eds , Cambridge University Press, Cambridge, UK, 2006, 223-253

249 Mellado, E & Ventosa, A Biotechnological potential of moderately and extremely halophilic microorganisms, in *Microorganisms for Health Care, Food and Enzyme Production,* J L Barredo, ed , Research Signpost, Kerala, India, 2003, 233-256

250 Li, X , & Yu, H , Extracellular production of beta-amylase by a halophilic isolate, *Halobacillus* sp LY9, *J Ind Microbiol Biotechnol* **38**, 1837–1843, 2011

251 Gómez, J & Steiner, W The biocatalytic potential of extremophiles and extremozymes, *Food Technol Biotechnol* **2**, 223-235, 2004

252 Oren, A Industrial and environmental applications of halophilic microorganisms, *Environ Technol* **31**, 825-834, 2010

253 Ventosa, A & Nieto, J J Biotechnological applications and potentialities of halophilic microorganisms, *World J Microbiol Biotechnol* **11,** 85–94, 1995

254 Moreno, M L , et al Halophilic bacteria as a source of novel hydrolytic enzymes, *Life* **3**, 38–51, 2013

255 Shafiei, M , Ziaee, A , & Amoozegar, M A Purification and characterization of an organic-solvent-tolerant halophilic α-amylase from the moderately

halophilic *Nesterenkonia* sp strain F *J. Ind. Microbiol. Biotechnol.* **38**, 275–281, 2011.

256. Kiran, K.K. & Chandra, T S Production of surfactant and detergent-stable, halophilic, and alkalitolerant alpha-amylase by a moderately halophilic *Bacillus* sp. strain TSCVKK, *Appl Microbiol. Biotechnol.* **77**, 1023–1031, 2008.

257. Good, W M. & Hartman, P.A. Properties of amylase from *Halobacterium halobium*, *J. Bacteriol.* **104,** 601–3, 1970.

258. Onishi, H. & Sonoda, K. Purification and some properties of an extracellular amylase from a moderate halophile, *Micrococcus halobius*, *Appl. Environ. Microbiol.* **38**, 616–620, 1979

259 Shafiei, M., Ziaee, A., & Amoozegar, M. Purification and biochemical characterization of a novel SDS and surfactant stable, raw starch digesting, and halophilic α-amylase from a moderately halophilic bacterium, *Nesterenkonia* sp. strain F. *Process Biochem.* **45**, 694–699, 2010.

260. Li, X. & Yu, H. Characterization of an organic solvent-tolerant α-amylase from a halophilic isolate, *Thalassobacillus* sp. LY18, *Folia Microbiol.* **57**, 447–453, 2012.

261. Fukushima, T., et al. Organic solvent tolerance of halophilic α-amylase from a haloarchaeon, *Haloarcula* sp. strain S-1, *Extremophiles* **9,** 85–90, 2005.

262. Perez-Pomares, F., et al α-Amylase activity from the halophilic archaeon *Haloferax mediterranei*, *Extremophiles* **7**, 299–306, 2003.

263 Kobayashi, T., et al. Haloalkaliphilic maltotriose-forming α-amylase from the archaebacterium, *Natronococcus* sp. strains Ah-36, *J. Bacteriol.* **174**, 3439–44, 1992.

264. Demirijan, D., Moris-varas, F., & Cassidy, C. Enzymes from extremophiles, *Curr. Opin. Chem. Biol.* **5,** 144-151, 2001.

265. Sarikaya, E., et al. Comparison of degradation abilities of α- and β-amylases on raw starch granules, *Process Biochem.* **35**, 711-715, 2000.

266. Synowiecki, J., Grzybowska, B. & Zdzieblo, A. Sources, properties and suitability of new thermostable enzymes, *Crit. Rev. Food Sci. Nutr.* **46**, 197–205, 2006.

267. Madigan, M.T. & Martino, J.M. *Brock Biology of Micro-organism,* 11th ed., Pearson Publication, 2006.

268. Bertoldo, C. & Antranikian, G. Starch hydrolyzing enzymes from thermophilic archaea and bacteria, *Curr. Opin. Chem. Biol.* **6,** 151–160, 2002.

269. Schwermann, B., et al. Purification, properties and structural aspects of a thermoacidophilic α-amylase from *Alicyclobacillus acidocaldarius* ATCC 27009, Insight into acidostability of proteins, *Eur. J. Biochem.* **226**, 981-91, 1994.

270. Bolton, D.J., Kelly, C.T., & Fogarty, W.M. Effect of medium composition on formation of amylase, *Enzyme Microbial. Technol.* **20**, 340-343, 1997.

271. El-Aassar, S. A., et al. Purification of alpha-amylase from *Bacillus lentus* cultures, *Appl. Microbiol. Biotechnol.* **38**, 312–314, 1992.

272. Ramesh, M.V. & Lonsane, B.K. Characteristics and novel features of thermostable α-amylase produced by *Bacillus licheniformis* M-27 under solid-state fermentation, *Starch* **42,** 233-238, 1990.

273. Ratnakhanokchai, K., et al. Purification and properties of a maltotetraose- and maltotriose-producing amylase from *Chloroflexus aurantiacus*, *Appl. Environ. Microbiol.* **58**, 2490–2494, 1992.

274. Fukusumi, S., et al. Cloning and nucleotide sequence of a heat-stable amylase gene from an anaerobic thermophile, *Dictyoglomus thermophilum, Eur. J. Biochem.* **174,** 15–21, 1988.

275. Rao, J.L.U.M. & Satyanarayana, T. Purification and characterization of a hyperthermostable and high maltogenic α-amylase of an extreme thermophile *Geobacillus thermoleovorans*, *Appl. Biochem. Biotechnol.* **142**, 179–193, 2007.

276. Tan, T C., et al. Crystal structure of the polyextremophilic α-amylase AmyB from *Halothermothrix orenii*: details of a productive enzyme-substrate

complex and an N domain with a role in binding raw starch, *J. Mol. Biol.* **378**, 852–870, 2008.

277. Burgess-Cassler, A , & Imam, S. Partial purification and comparative characterization of α-amylase secreted by *Lactobacillus amylovorus*, *Curr. Microbiol.* **23**, 207 –21, 1991.

278. Liebl, W , Stemplinger, I , & Ruile, P. Properties and gene structure of the *Thermotoga maritima* α-amylase AmyA, a putative lipoprotein of a hyperthermophilic bacterium, *J. Bacteriol.* **179**, 941—948, 1997.

279. Egas, M. C., et al. Extracellular alpha-amylase from *Thermus filiformis* Ork A2 Purification and biochemical characterization, *Extremophiles* **2**, 23–32, 1998

280. Aquino, A.C M.M., et al. Studies on a thermostable α-amylase from the thermophilic fungus *Scytalidium thermophilum, Appl Microbiol. Biotechnol.* **61**, 323-328, 2003.

281. Landerman, K., et al. Alpha amylase from the hyper- thermophilic archaebacterium *Pyrococcus furious*. Cloning and sequencing of the gene and expression in *E. coli, J. Biol Chem* **268**, 24402–24407, 1993.

282. Koch, R., et al. Purification and properties of a hyperthermoactive α-amylase from the archaeobacterium *Pyrococcus woesei*, *Arch. Microbiol.* **155**, 572–578, 1991.

283. Canganella, F., Andrade, C. M., & Antranikian, G. Characterization of amylolytic and pullulytic enzymes from thermophilic archaea and from a new *Fervidobacterium* species, *Appl Microbiol. Biotechnol.* **42**, 239–245, 1994.

284 Estelle, L., et al. Thermostable amylolytic enzymes of thermophilic microorganisms from deep-sea hydrothermal vents, *CR Acad. Sci. Paris* **320**, 893–898, 1997.

285. Chung, Y C., et al. Purification and properties of extracellular amylase from the hyperthermophilic archeon *Thermococcus profundus* DT5432, *Appl. Environ. Microbiol.* **61**, 1502–1506, 1995

286 Jensen, B & Olsen, J Physicochemical properties of a purified alpha amylase from the thermophilic fungus *Thermomyces lanuginosus*, *Enzyme Microb Technol* **14,** 112–116, 1992

287 Mehta, D & Satyanarayana, T Biochemical and molecular characterization of recombinant acidic and thermostable raw-starch hydrolysing alpha-amylase from an extreme thermophile *Geobacillus thermoleovorans, J Mol Catal B Enzym* **85-86**, 229–238, 2013

288 Malhotra, R , Noorwez, S M & Satyanarayana, T Production and partial characterization of thermostable and calcium–independent α-amylase of an extreme thermophile *Bacillus thermoleovorans* NP54, *Lett Appl Microbiol* **31**, 378–384, 2000

289 Rao, J L U M & Satyanarayana, T Statistical optimization of a high maltose-forming, hyperthermostable and Ca^{2+}-independent α-amylase production by an extreme thermophile *Geobacillus thermoleovorans* using response surface methodology, *J Appl Microbiol* **95**, 712–718, 2003

290 Sun, H , et al Recent advances in microbial raw starch degrading enzymes, *Appl Biochem Biotechnol* **160**, 988–1003, 2010

291 Sun, H , et al Microbial production of raw starch digesting enzymes, *African J Biotechnol,* **8**, 1734–1739, 2009

292 Kelly, C T , et al The raw starch-degrading alkaline amylase of *Bacillus* sp IMD 370, J Ind Microbiol **15,** 446–448, 1995

293 Robertson, G H , et al Native or raw starch digestion A key step in energy efficient biorefining of grain, *J Agric Food Chem* **54**, 353–365, 2006

294 Mitsuiki, S , et al Comparative characterization of raw starch hydrolyzing α-amylases from various *Bacillus* strains *Enzyme Microb Technol* **37**, 410–416, 2005

295 Campus, B , Priest, F , & Stark, J Hydrolysis of starch granules by the amylase from *Bacillus stearothermophillus* NCA 26, *Process Biochem* **27**, 17–21, 1992

296 Qates, C G Towards an understanding of starch granule structure and hydrolysis, *Trends Food Sci Technol* **8**, 375–382, 1997

297. Soni, S K, et al Enhanced production of α-amylase from *Bacillus subtilis* subsp. *spizizenii* in solid state fermentation by response surface methodology and its evaluation in the hydrolysis of raw potato starch, *Starch* **64**, 64–77, 2012.

298. Bozic, N., et al. Production and properties of the highly efficient raw starch digesting α-amylase from a *Bacillus licheniformis* ATCC 9945a, *Biochem. Eng. J.* **53**, 203–209, 2011.

299. Matsubara, T., et al., Degradation of raw starch granules by α-amylase purified from culture of *Aspergillus awamori* KT-11, *J. Biochem. Mol. Biol.* **37**, 422–428, 2004.

300. Hayashida, S & Teramoto, Y Production and characteristics of raw-starch-digesting α-amylase from a protease-negative *Aspergillus ficum* mutant, *Appl. Environ. Microbiol.* **52**, 1068-1073, 1986.

301. Lefuji, H., et al. Raw-starch-digesting and thermostable α-amylase from the yeast *Cryptococcus* sp. S-2: purification, characterization, cloning and sequencing, *J Biochem.* **318**, 989-996, 1996.

302. Odibo, F.J.C., & Ulbrich-Hofmann, R. Thermostable α-amylase and glucoamylase from *Thermomyces lanuginosus* F1, *Acta. Biotechnol.* **21**, 141-153, 2001.

303. Gangadharan, D., et al. Response surface methodology for the optimization of alpha amylase production by *Bacillus amyloliquefaciens*, *Bioresour. Technol.* **99**, 4597–602, 2008.

304. Itkor, P., Tsukagoshi, N., & Udaka, S. Purification and properties of divalent cation-dependent raw-starch-digesting α-amylase from *Bacillus* sp. B1018, *J. Ferment. Bioeng.* **68**, 247–251, 1989

305. Puspasari, F., et al. Raw starch–degrading α-amylase from *Bacillus* aquimaris MKSC 6.2: isolation and expression of the gene, bioinformatics and biochemical characterization of the recombinant enzyme, *J. Appl. Microbiol* **114**, 108-120, 2013

306 Hamilton, L M , Kelly, C T , & Fogarty, W M Purification and properties of the raw starch degrading α-amylase of *Bacillus* sp IMD434, *Biotechol Lett* **21**,111-115, 1999

307 Lin, L L , Chyau, C C , & Hsu, W H Production and properties of a raw-starch-degrading α-amylase from thermophilic and alkaliphilic *Bacillus* sp TS-23, *Biotech Appl Biochem* **28**, 61–68, 1998

308 Kim, J , Nanmori, T , & Shinke, R Thermostable, raw-starch-digesting amylase from *Bacillus stearothermophilus, Appl Environ Microbiol* **55**, 1638–1639, 1989

309 Tanaka, T , et al Purification and some properties of raw starch-binding amylase of *Clostridium butyricum* T-7 isolated from mesophilic methane sludge, *Agric Biol Chem* **51**, 399-405, 1987

310 Jeang. C L , et al Cloning of a gene encoding raw-starch-digesting amylase from a *Cytophaga* sp and its expression in *Escherichia coli*, *Appl Environ Microbiol* **68**, 3651- 3654, 2002

311 Ezeji, T C & Bahl, H Production of raw-starch-hydrolysing α- amylase from the newly isolated *Geobacillus thermodenitrificans* HRO10, *World J Microbiol Biotechnol* **23**, 1311-1315, 2007

312 Primarini, D , & Ohta, Y Some enzyme properties of raw starch digesting amylases from *Streptomyces* sp No 4, *Starch* **52**, 28–32, 2000

313 Janda, J M & Abbott, S L Bacterial Identification for Publication When Is Enough Enough?, *J Clin Microbiol* **40**, 1887–1891, 2002

314 OECD *Guidance document on the use of taxonomy in risk assessment of microorganisms bacteria*, OECD Series on Harmonisation of Regulatory Oversight in Biotechnology 2003
(http //www oecd org/science/biotrack/46815778 pdf)

315 Prakash, O et al Polyphasic approach of bacterial classification – An overview of recent advances, *Indian J Microbiol* 47, 98–108 (2007)

316 Bergey, D H *Bergey's Manual of Systematic Bacteriology*, Springer Press, New York, 2005

317. On, S.L.W. & Holmes, B. Reproducibility of tolerance tests that are useful in the identification of compylobacteria, *J. Clin. Microbiol.* **29**, 1785–1788, 1991.

318. Unsal, B. *Phylogenetic analysis of bacterial communities in kefir by metagenomics*, Master Thesis, İzmir Institute of Technology, Izmir, 2008.

319. Mincer, T J., Fenical, W., & Jensen, P.R. Culture-dependent and culture-independent diversity within the obligate marine actinomycete genus *Salinispora*, *Appl. Environ. Microbiol.* **71**, 7019–7028, 2005.

320. Bosshard, P.P , et al. Ribosomal DNA sequencing for identification of aerobic gram-positive rods in the clinical laboratory, *J. Clin. Microbiol.* **43**, 4134–4140, 2003

321. Devulder, G., Montclos, M. P., & Flandrois, J. P. A multigene approach to phylogenetic analysis using the genus *Mycobacterium* as a model, *Int. J. Syst. Evol. Microbiol.* **55**, 293–302, 2005.

322. Tsai, J., et al. Identification of clinically relevant *Enterococcus* species by direct sequencing of groES and spacer region, *J. Clin. Microbiol.* **43**, 235-241, 2005.

323. Drancourt, M., & Raoult, D rpoB gene sequence-based identification of *Staphylococcus species*, *J. Clin. Microbiol.* 40(4):1333-8, 2002.

324. Blackwood, K.S., et al. Evaluation of recA sequences for identification of *Mycobacterium* species, *J. Clin. Microbiol.* **38**, 2846-2852, 2000.

325. Dauendorffer, J.N., et al. Identification of *Mycobacterial* species by PCR sequencing of quinolone resistance-determining regions of DNA Gyrase genes, *J. Clin. Microbiol.* **41**, 1311–1315, 2003.

326. Goh, S.H., et al. HSP60 gene sequences as universal targets for microbial species identification studies with coagulase-negative *staphylococci*, *J. Clin. Microbiol.* **34**, 818–823, 1996.

327 Liu, B , Wang, Y., & Zhang, X Characterization of a recombinant maltogenic amylase from deep-sea thermophilic *Bacillus* sp. WPD616, *Enzyme Microb. Technol.* **39**, 805–810, 2006

328 Haki, G D , Anceno, A J & Rakshit, S K A typical Ca^{2+}-independent, raw-starch hydrolysing α-amylase from *Bacillus* sp GRE1 characterization and gene isolation, *World J Microbiol Biotechnol* **24**, 2517-2524, 2008

329 Duedahl-olesen, L , Kragh, K M , & Zimmermann, W Purification and characterisation of a malto-oligosaccharide-forming amylase active at high pH from *Bacillus clausii* BT-21, *Carbohydr Res* **329**, 97–107, 2000

330 Messaoud, E Ben, et al Purification and properties of a maltoheptaose- and maltohexaose-forming amylase produced by *Bacillus subtilis* US116, *Enzyme Microb Technol* **34**, 662–666, 2004

331 Zhang, J & Zeng, R Molecular cloning and expression of an extracellular α-amylase gene from an Antarctic deep sea psychrotolerant *Pseudomonas stutzeri* strain 7193, *World J Microbiol Biotechnol.* **27**, 841–850, 2011

332 Shabbir, K , et al , Optimized production , purification and characterization of alpha amylase by *Brevibacterium linens* DSM 20158, using bio-statistical approach, *Ann Microbiol* **62**, 523–532, 2012

333 Kammoun, R , Naili, B , & Bejar, S Application of a statistical design to the optimization of parameters and culture medium for alpha- amylase production by *Aspergillus oryzae* CBS 819 72 grown on gruel (wheat grinding by-product), *Bioresour Technol* **99**, 5602-5609, 2008

334 Sifour, M , et al Enhanced production of lipase by the thermophilic *Geobacillus stearothermophilus* strain-5 using statistical experimental designs, *N Biotechnol* **27**, 330–336, 2010

335 Rairakhwada, D , et al Gene cloning, characterization, and heterologous expression of levansucrase from *Bacillus amyloliquefaciens*, *J Ind Microbiol Biotechnol* **37**, 195–204, 2010

336 Naveena, B J , Bhadriah, K , & Reddy, G Selection of medium components by Plackett – Burman design for production of L(+) lactic acid by *Lactobacillus amylophilus* GV6 in SSF using wheat bran, *Biores Technol* **96**, 485–490, 2005

337. Reddy, L.V.A., et al. Optimization of alkaline protease production by batch culture of *Bacillus* sp. RKY3 through Plackett – Burman and response surface methodological approaches, *Biores. Technol.* **99**, 2242–2249, 2008.

338. Vellanki, R. N., Potumarthi, R., & Mangamoori, L. N. Constitutive expression and optimization of nutrients for streptokinase production by *Pichia pastoris* using statistical methods, *Appl. Biochem. Biotechnol.* **158**, 25–40, 2009.

339. Carvalho, C.M.L., et al. Application of factorial design to the study of transesterification reactions using cutinase in AOT-reversed micelles, *Enzyme Microb. Technol.* **27**, 117–123, 1997.

340. Vohra, A. & Satyanarayana, T. Statistical optimization of medium components by response surface methodology to enhance phytase production by *Pichia anomala*, *Process Biochem.* **37**, 999–1004, 2002.

341. Sharma, A. & Satyanarayana, T. Production of acid-stable and high-maltose-forming α-amylase of *Bacillus acidicola* by solid-state fermentation and immobilized cells and its applicability in baking, *Appl. Biochem. Biotechnol.* **168**, 1025-34, 2012.

342. Ray, R.C. & Kar, S., Statistical optimization of α-amylase production by *Bacillus brevis* MTCC 7521 in solid-state fermentation using cassava bagasse, *Biologia* **65**, 864–870, 2009.

343. Sumrin, A., et al. Purification and medium optimization of α-amylase from *Bacillus subtilis* 168, *African J. Biotechnol.* **10**, 2119–2129, 2011.

344. Kar, S., Swain, M.R., & Ray, R.C. Statistical optimization of alpha-Amylase production with immobilized cells of *Streptomyces erumpens* MTCC 7317 in *Luffa cylindrica* L. sponge discs, *Appl. Biochem. Biotechnol.* **152**, 177-88, 2009.

345. Nguyen, Q.D., et al. Purification and characterisation of amylolytic enzymes from thermophilic fungus *Thermomyces lanuginosus* strain ATCC 34626, *Enzyme Microb. Technol.* **31**, 345–352, 2002.

346. Vihinen, M. & Mantsala, P. Microbial amylolytic enzymes, *Crit. Rev. Biochem. Mol. Biol.* **24**, 329-418, 1989.

347 Kim, T U , et al Purification and characterization of a maltotetraose forming alkaline α-amylase from an alkalophilic *Bacillus* sp GM8901, *Appl Environ Microbiol* **61,** 3105-12, 1995

348 Chary, S J & Reddy, S M Starch degrading enzymes of two species of *Fusarium*, *Folia Microbiol* **30**, 452-477, 1985

349 Grootegoed, J A , Lauwers, A M , & Heinen, W Separation and partial purification of extracellular amylase and protease from *Bacillus caldolyticus, Arch Microbiol* **90,** 223-232, 1973

350 Ratanakhanokchai, K , et al Purification and properties of a maltotetraose- and maltotriose-producing amylase from *Chloroflexus aurantiacus, Appl Environ Microbiol* **58**. 2490–2494. 1992

351 Srivastava, R A K Studies on extracellular and intracellular purified amylases from a thermophilic *Bacillus stearothermophilus*, *Enzyme Microb Technol* **6,** 422–426, 1984

352 Liu, W , et al Gene cloning, over-expression, and characterization of a xylanase from *Penicillium* sp CGMCC 1699, *Appl Biochem Biotechnol* **162,** 1–12, 2010

353 Sharma, A & Satyanarayana, T Cloning and expression of acidstable, high maltose-forming, Ca^{2+}-independent α-amylase from an acidophile *Bacillus acidicola* and its applicability in starch hydrolysis, *Extremophiles* **16**, 515–22, 2012

354 Das, K , Doley, R , & Mukherjee, A Purification and biochemical characterization of a thermostable, alkaliphilic, extracellular α-amylase from *Bacillus subtilis* DM-03, a strain isolated from the traditional fermented food of India, *Biotechnol Appl Biochem* **40**, 291–298, 2004

355 Garrity, G M *Bergey's manual of systematic bacteriology*, 2nd ed , Springer, 2005

356 Ausubel, F M , Brent, R , Kinston, R E , Moorse, D D , Seidman, J D , Smith, J A , Struhl, K *Short protocols in molecular biology,* Wiley, New York, 1995

357 Weisburg, W G , et al 16S ribosomal DNA amplification for phylogenetic study, *J Bacteriol* , **173**, 697–703, 1991

358. Roberts, M.S., Nakamura, L.K., & Cohan, F.M. *Bacillus mojavensis* sp.nov., distinguishable from *Bacillus subtilis* by sexual isolation, divergence in DNA sequence, and differences in fatty acid composition, *Int. J. Syst. Bacteriol.* **44,** 256–264, 1994.

359. Tamura, K., et al. MEGA4: Molecular Evolutionary Genetics Analysis (MEGA) software version 4.0, *Mol. Biol. Evol.* **24,** 1596–1599, 2007.

360. Saitou, N. & Nei, M. The neighbor-joining method: a new method for reconstructing phylogenetic trees, *Mol. Biol. Evol.* **4,** 406– 425, 1987

361. Felsenstein, J Evolutionary trees from DNA sequences: a maximum likelihood approach, *J. Mol. Evol.* **17,** 368 – 376, 1981.

362. Kluge, A.G. & Farris, J.S. Quantitative phyletics and the evolution of anurans, *Syst. Zool.* **18,** 1 –32, 1969

363. Miller, G. L. Use of dinitrosalicylic acid reagent for determination of reducing sugar, *Anal. Chem.* **31,** 426–428, 1969.

364. Fuwa, H. A new method for microdetermination of amylase activity by use of amylose as the substrate, *J. Biochem.* **41,** 583–603, 1954.

365. Dubios, M.K., et al. Calorimetric determination of sugar and related substance, *Analyt. Chem.* **26,** 351-356, 1951

366. Lowry, O.H. et al Protein measurement with the folin phenol reagent, *J. Biol. Chem* **193,** 265-275, 1951.

367. Plackett, R.L. & Burman, J.P. The design of optimum multifactorial experiments, *Biometrika* **33,** 305–325, 1946.

368. Laemmli, UK. Cleavage of structural proteins during the assembly of the head of Bacteriophage T4, *Nature* **277,** 680–685, 1970.

369. Upadhyay, M.K., et al. An improved zymographic method for detection of amylolytic enzymes of fungi on polyacrylamide gels, *Mycol* **19,** 138-140, 2005

370. Lineweaver, H. & Burk, D. The determination of enzyme dissociation constants, *J Am Chem. Soc.* **56,** 658–666, 1934

371. Kusuda, M., et al. Purification and some properties of α-amylase from an ectomycorrhizal fungus; *Tricholoma matsutake*. *Mycoscience* **44**, 311–317, 2003.

372. Mabrouk, S.B., et al. Cloning and sequencing of an original gene encoding a maltogenic amylase from *Bacillus* sp. US149 strain and characterization of the recombinant activity, *Mol. Biotechnol.* **38**, 211–219, 2008.

373. Thompson, J.D., Higgins, D.G., & Gibson, T.J. CLUSTAL-W improving the sensitivity of progressive multiple sequence alignment through sequence weighting, position-specific gap penalties and weight matrix choice, *Nucleic Acids Res.* **22**, 4673–4680, 1994.

374. Myers, R.H., & Montgomery, D.C. *Response surface methodology; process and product optimization using designed experiments*, 2nd ed., A Wiley-Interscience Publication, New York, 2002.

375. Ayadi, D.Z., et al. Excretory overexpression of *Paenibacillus pabuli* US132 cyclodextrin glucanotransferase (CGTase) in *Escherichia coli*: Gene cloning and optimization of the culture conditions using experimental design, *Biologia, 66*, 945—953, 2011.

376. Liu, S., et al. Effective approach to greatly enhancing selective secretion and expression of three cytoplasmic enzymes in *Escherichia coli* through synergistic effect of EDTA and lysozyme, *J. Ind. Microbiol. Biotechnol.* **39,** 1301–1307, 2012.

377. Lo, P.K., et al. Excretory over-expression of *Bacillus sp.*G1 cyclodextrin glucanotransferase (CGTase) in *Escherichia coli*: optimization of the cultivation conditions by response surface methodology, *Enzyme Microb. Technol.* **40**, 1256–1263, 2007.

378. Dabirmanesh, B., et al. Effect of ionic liquids on the structure, stability and activity of two related amylases, *Int. J. Biol. Macromol.* **48**, 93–97, 2011.

379. Zhu, H., et al. Rheofermentometer fermentation and bread making characteristics of dough containing xylo-oligosaccharide hydrolyzate from wheat bran, *J. Agric. Food Chem.* **58**, 1878–83, 2010.

380. Mnif, I., et al. Improvement of bread quality and bread shelf-life by *Bacillus subtilis* biosurfactant addition, *Food Sci. Biotechnol.* **21**, 1105–1112, 2012.

381. Rossi, L. M., Quach, A. D., & Rosenzweig Z. Glucose oxidase-magnetite nanoparticle bioconjugate for glucose sensing, *Ana. Bioanal. Chem.* **380**, 606-613, 2004.

382. Mukherjee, A.K., et al. Statistical optimization of α-amylase immobilization on iron-oxide magnetic nanoparticles, *Biotechnol. Bioprocess Eng.* **15**, 984–992, 2010.

383. Popescu, A. & Doyle R.J. The Gram stain after more than a century, *Biotech Histochem.* **71**, 145-51, 1996.

384. Cappuccino, J.G. & Sherman, N *Microbiology—A Laboratory Manual,* Addison- Wesley Longman, Inc., 1999.

385. Parkinson, N., et al Phylogenetic analysis of *Xanthomonas* species by comparison of partial gyrase B gene sequences, *Int J. Syst. Evol. Microbiol.* **57**, 2881–7, 2007.

386. Wang, L., et al. Comparison of gyrB gene sequences, 16S rRNA gene sequences and DNA–DNA hybridization in the *Bacillus subtilis* group, *Int. J. Syst. Evol. Microbiol.* **57**, 1846–1850, 2007.

387 Adekambi, T., Drancourt, M., & Raoult, D The rpo B gene as a tool for clinical microbiologists, *Trends Microbiol.* **17**, 37–45, 2008

388. Houpikian, P. & Raoult, D. 16S-23S rRNA Intergenic spacer regions for phylogenetic analysis, identification, and subtyping of *Bartonella* species, *J. Clin. Microbiol.* **39**, 2768–2778, 2001.

389. Roy, J.K. & Mukherjee, A.K. Applications of a high maltose forming, thermo-stable α-amylase from an extremely alkalophilic *Bacillus licheniformis* strain AS08E in food and laundry detergent industries, *Biochem Eng. J* 77, 220–230, 2013

390. Aguilar, C.N., et al. Culture conditions dictate protease and tannase production in submerged and solid-state cultures *Aspergillus niger* Aa-20, *Appl. Biochem. Biotechnol.* **102-103**, 407-414, 2002.

391. Krishna, C. Solid-state fermentation systems-án overview, *Crit. Rev. Biotechnol.* **25**, 1-30, 2005.

392. Singhania, R.R., et al. Recent advances in solid-state fermentation, *Biochem. Eng. J.* **44**, 13–18, 2009.

393. Couto, S. R. & Sanroman, M. A. Application of solid-state fermentation to food industry - A review, *J. Food. Eng.* **76**, 291-302, 2006.

394. Joo, H.S. & Chang, C.S. Production of protease from a new alkalophilic *Bacillus* sp. I-312 grown on soybean meal: optimization and some properties, *Process Biochem.* **40**, 1263–1270, 2005.

395. Wenster-Botz D (2000) Experimental design for fermentation media development: Statistical design or global random search? J Biosci Bioeng 90:473–483.

396. Rai, S.K., Konwarh, R., & Mukherjee, A.K. Purification , characterization and biotechnological application of an alkaline keratinase produced by *Bacillus subtilis* RM-01 in solid-state fermentation using chicken-feather as substrate, *Biochem. Eng. J.* **45**, 218–255, 2009.

397. Haaland, P.D. Statistical problem solving, in *Experimental Design in Biotechnology*, P.D. Haaland, eds., Marcel Dekker Inc., New York, 1989.

398. Daniel, W.W. A foundation for analysis in the health sciences. Hypothesis testing, in: *Biostatistics*, W.W. Daniel, eds., John Wiley and Sons, Inc., New York, 2000, 166–167.

399. Calik, P., Calik, G., & Ozdamar, T.H. Oxygen transfer effects in serine alkaline protease fermentation by *Bacillus licheniformis*: Use of citric acid as the carbon source, *Enzyme Microb. Technol.* **23**, 451–461, 1998.

400. Mukherjee, A.K. & Rai, S.K. A statistical approach for the enhanced production of alkaline protease showing fibrinolytic activity from a newly isolated Gram-negative *Bacillus* sp. strain AS-S20-I, *N. Biotechnol.* **28**, 182–189, 2011.

401. Dey, G. et al. Enhanced production of amylase by optimization of nutritional constituents using response surface methodology, *Biochem. Eng. J.* **7**, 227–231, 2001.

402. Saboto, D., et al. The β-glycosidase from the hyperthermophilic archaeon *Sulfolobus solfataricus*: enzyme activity and conformational dynamics at temperatures above 100°C, *Biophys. Chem.* **81**, 23–31, 1999.

403. Syed, D.G., Agasar, D. & Pandey, A. Production and partial purification of *alpha-amylase* from a novel isolate *Streptomyces gulbargensis*, *J. Ind. Microbiol. Biotechnol.* **36,** 189–194, 2009.

404. Michelin, M., et al. Purification and characterization of a thermostable α-amylase produced by the fungus *Paecilomyces variotii*, *Carbohydra. Res.* **345,** 2348–2353, 2010.

405. Chai, Y.Y., et al. Cloning and characterization of two new thermostable and alkalitolerant α-amylases from the *Anoxybacillus* species that produce high levels of maltose, *J. Ind. Microbiol. Biotechnol.* **39,** 731–741, 2012.

406. Arikan, B. Highly thermostable, thermophilic, alkaline, SDS and chelator resistant amylase from a thermophilic *Bacillus* sp. isolate A3-15, *Bioresour. Technol.* **99,** 3071–3076, 2008.

407. Sigma, D.S. & Moser, G. Chemical studies of enzyme active sites, *Ann. Rev. Biochem.* **44**, 889–931, 1975.

408. Kumar, C. G. & Takagi, H. Microbial alkaline proteases: from a bioindustrial viewpoint, *Biotechnol. Adv.* **17**, 561–94, 1999.

409. Copeland, R.A. *Enzymes: a practical introduction to structure, mechanism, and data analysis*, John Wiley & Sons, 2004.

410. Dheeran, P., et al. Characterization of hyperthermostable α-amylase from *Geobacillus* sp. IIPTN, *Appl. Microbiol. Biotechnol.* **86,** 1857–1866, 2010.

411. Kirk, O., Borchert, T.V., & Fuglsang, C.C. Industrial enzyme applications, *Curr. Opin. Biotechnol.* **13**, 345-351, 2002.

412. Maurer, K. Detergent proteases, *Curr. Opin. Biotechnol.* **15**, 330–334, 2004.

413. Burstein, E.A., Vedenkina, N.S., & Ivkova, M.N. Fluorescence and the location of tryptophan residues in protein molecules, *Photochem. Photobiol.* **18,** 263–279, 1973.

414. He, H.J., et al. Study of fluorescence spectra of starch suspension, *Guang pu xue yu guang pu fen xi Guang pu*, **26**, 1636-9, 2006. (PMID: 17112035).

415 Mergulhao F J M , Summers D K , & Monteiro G A Recombinant protein secretion in *Escherichia coli, Biotechnol Adv* **23**, 177–202, 2005

416 Roy, J K , et al Cloning and overexpression of raw starch digesting α-amylase gene from *Bacillus subtilis* strain AS01a in *Escherichia coli* and application of the purified recombinant α-amylase (AmyBS-I) in raw starch digestion and baking industry, *J Mol Catal B Enzym* **97**, 118–129, 2013

417 Falconer, R J , O Neill, B K., Middelberg, A P J Chemical treatment of *Escherichia coli* Extraction of intracellular protein from uninduced cells, *Biotechnol Bioeng* **53**, 453–458, 1997

418 Sajedi, R H , et al Purification, characterization and structural investigation of a new moderately thermophilic and partially calcium-independent extracellular amylase from *Bacillus* sp TM1, *Appl Biochem Biotechnol* **119**, 41–50, 2004

419 Li, H , et al Purification and characterization of extracellular amylase from the marine yeast *Aureobasidium pullulans* N13d and its raw potato starch digestion, *Enzyme Microb Technol* **40**, 1006–1012, 2007

420 Pyler, E J , in *Baking Science and Technology*, E J Pyler, eds , Vol 2, Sosland Publisher, Kansas, USA, 1988, 815–849

421 Gambaro, A , et al Influence of enzymes on the texture of brown pan bread *J Texture Stud* **37**, 300-314, 2006

422 Bayramoglu, G , Yılmaz, M , & Arica, M Y Immobilization of a thermostable α-amylase onto reactive membranes kinetics characterization and application to continuous starch hydrolysis, *Food Chem* **84**, 591–599, 2004

423 Turunc, O , et al Immobilization of α-amylase onto cyclic carbonate bearing hybrid material, *Food Chem* **112**, 992–997, 2009

424 Huang, S H , Liao, M H & Chen, D H Direct binding and characterization of lipase onto magnetic nanoparticles, *Biotechnol Prog* **19**, 1095-1100, 2003

425. Liao, M.H. & Chen, D. H. Immobilization of yeast alcohol dehydrogenase on magnetic nanoparticles for improving its stability, *Biotechnol. Lett.* **23,** 1723-1727, 2001.

426. Saiyed, Z. M., et al. Activity and stability of alkaline phosphatase (ALP) immobilized onto magnetic nanoparticles (Fe_3O_4), *J. Biotechnol.* **131,** 240-244, 2007.

Appendix-I

1. Media composition

a. Screening media for amylase producing bacteria

Composition	Concentration (gm/l)
Starch	10.0
Yeast extract	1.5
Beef extract	1.5
Peptone	5.0
NaCl	5.0
Agar	20.0
pH	6.0-12.0
Distilled water	1000 ml

b. Composition of M9 Media for amylase production

(I) M9 Medium composition	Concentration (gm/l)
Na_2HPO_4	6.0
KH_2PO_4	3.0
NH_4Cl	1.0
NaCl	0.5
$MgSO_4.H_2O$	0.246
$CaCl_2.7H_2O$	0.014
Carbon source	1.0

(II) Macro-nutrient composition	
$FeSO_4.7H_2O$	1.0 mg l^{-1}
$CuSO_4.5H_2O$	50.0 µg l^{-1}
H_3BO_3	10.0 µg l^{-1}
$MgSO_4.5H_2O$	10.0 µg l^{-1}
$ZnSO_4.7H_2O$	70.0 µg l^{-1}
MoO_3	10.0 µg l^{-1}

Add 1ml of macro –nutrient in 1000 ml of M9 production medium

c. Other microbiological media

(I) Nutrient Broth	Concentration (gm/l)
Yeast extract	1.5
Beef extract	1.5
Peptone	5.0

(II) Luria Broth	Concentration (gm/l)
Bacto-tryptone	10.0
Bacto-yeast extract	5.0
NaCl	5.0

(III) SOB	Concentration (gm/l)
Casein enzymic hydrolysate	20.0
Yeast extract 5.000	5.0
NaCl	5.0
Magnesium sulphate	2.4
Potassium chloride	0.19

(IV) TB	**Concentration (gm/l)**
Trypton	12.0
Yeast extract	12.0
Glycerol	4.0
KH_2PO_4	2 31
K_2HPO_4	12 54

2. Reagents, Buffers and Solutions

(A) Buffer and Reagents

(i) 50X TAE electrophoresis buffer	**Concentration (gm/l)**
Tris base	242
Na_2EDTA	37.2
Glacial acetic acid	57.1ml

Note: Final volume was adjusted to 1 liter with deionized water

(ii) Ethidium bromide stock solution	**Concentration (mg/ml)**
Ethidium Bromide	10

Note: Mixed well in deionized water and stored at room temperature in dark

(iii) 2x Gel loading dye (DNA)	**10ml stock (ml)**
2% Bromophenol blue	0.25
2% Xylene cyanol	0.25
Glycerol (100%)	7 0
Water	2.5

(iv) Antibiotics (Stock)	**Concentration (mg/ml)**
Ampicillin (sodium salt)	25.0
Kanamycin (sulfate)	30.0

Note: working solution: Ampicillin (50µg/ml) and Kanamycin (30µg/ml)

(v) X-gal (Stock) **Concentration (20mg/ml)**

Dissolve 200mg of X-gal in 10ml DMSO and store at -20°C

(vi) IPTG (stock) **Concentration (100mM)**

Dissolve 1.2g of IPTG in 50ml of deionized water and stored in aliquots at -20°C

(vii) Proteinase K (stock) **Concentration (10mg/ml)**

Dissolve 10mg of Proteinase K in 1ml of 10 mM Tris, 1mM Sodium-EDTA buffer and store at -20°C

(viii) RNase A **Concentration (10mg/ml)**

Dissolve 100 mg of RNase A in 10 mL of 10 mM Tris, 15 mM NaCl buffer and store at -20°C

(ix) DNS reagent	**Concentration (g/l)**
DNS	10.0
Phenol	2.0
Sodium sulphite	0 5
Sodium potassium tartrate	200 0
Sodium hydroxide	10 0

(x) Alkaline sodium carbonate	**Concentration (g/l)**
Sodium carbonate	20 0
Sodium hydroxide	4 0

(xi) Copper sulphate solution	**Concentration (g/l)**
Copper sulphate	5 0
Sodium potassium tartrate	10 0

(B) SDS-PAGE gel electrophoresis composition

(i) Resolving buffer (8X)	**Concentration (gm/l)**
1 5 M Tris-Cl (pH 8 8)	18 17

(ii) Stacking buffer (4X)	**Concentration (gm/l)**
0 5M Tris-Cl (pH 6 8)	6 06

Note Adjust the pH 8 8 with 6N HCl Make up the final volume to 100 ml with distilled water

(iii) Acrylamide mixture	**Concentration (gm/l)**
30 % acrylamide	30 0
0 8% bis-acrylamide	0 8

Note Dissolve in 100ml of warm deionized water to facilitate dissolution of bis-acrylamide Store in amber colour bottle at 4°C

(iv) Reservoir buffer (pH 8.3, 1X)	**Concentration (gm/l)**
Tris-Cl	3 0
Glycine	14 4
10% SDS	10 0

Note Dissolve in 1000ml of distilled water adjusted to pH to 8 3

(v) Sodium dodecyl sulfate (SDS)	**Concentration (gm/l)**
10 % SDS	10 0

(vi) Ammonium per sulphate (APS)	**Concentration (gm/l)**
10% APS	0 2

(vii) Staining solution	**Volume (ml / concentration)**
Methanol	40 0
Glacial acetic acid	10 0
Distilled water	50 0
Commassie brilliant blue	0 4 (gm/ ml)

(viii) Destaining solution

Composition	**Volume (ml)**
Methanol	40
Glacial acetic acid	10
Distilled water	50

(ix) Loading buffer (50 ml , 3X)

Composition	**Amount / volume**
Tris-Cl (pH 6 8)	1 296
SDS	3 0
Glycerol	1 5 ml
Bromophenol blue	3 0

Note 1ml of loading buffer mixed with 30µl of 2-mercaptoethanol (3%)

(x) Resolving gel composition (12.5%) for 20ml preparation

Components	Volume (ml)
Distilled water	4 2
1 5 M Tris-Cl (pH 8 8)	5 0
Acrylamide mixture	8 3
10% SDS	0 2
1o % APS	1 5
Glycerol	0 8
TEMED	0 025

(xi) Resolving gel composition (10%) for 20ml preparation

Components	Volume (ml)
Distilled water	5 7
1 5 M Tris-Cl (pH 8 8)	5 0
Acrylamide mixture	6 7
10% SDS	0 2
1 % APS	1 5
Glycerol	0 9
TEMED	0 02

(xii) Stacking gel (4X)

Components	Volume (ml)
Distilled water	5 4
0 5M Tris-Cl (pH 6 8)	2 5
10% SDS	0 1
Acrylamide mixture	1 3
1 % APS	0 7
Glycerol	0 4
TEMED	0 015

(C) Chemicals composition for chromosomal DNA isolation

(i) Solution I	Concentration (gm %)
50mM glucose	0 9
25mM Tris-Cl	0 30
10mM EDTA	0 37

(ii) Solution II	Concentration (gm %)
0 2N NaOH	0 0079
SDS	1 0

(iii) Solution III	Volume (ml)
5M Potassium acetate	60 0
Glacial acetic acid	11 5
Distilled water	28 5

Publications from present investigation

1. **Roy, J.K.,** Borah, A., Mahanta, C.L., Mukherjee, A.K. Cloning and overexpression of raw starch digesting α-amylase gene from *Bacillus subtilis* strain AS01a in *Escherichia coli* and application of the purified recombinant α-amylase (AmyBS-I) in raw starch digestion and baking industry, *J. Mol. Catal. B Enzym.* **97**, 118–129, 2013.

2. **Roy, J.K.** & Mukherjee, A.K. Applications of a high maltose forming, thermo-stable α-amylase from an extremely alkalophilic *Bacillus licheniformis* strain AS08E in food and laundry detergent industries, *Biochem. Eng. J.* 77, 220–230, 2013.

3. **Roy, J.K.**, Rai, S.K., & Mukherjee, A.K. Characterization and application of a detergent-stable alkaline α-amylase from *Bacillus subtilis* strain AS-S01a, *Int. J. Biol. Macromol.* **50**, 219–29, 2012.

4. Mukherjee, A.K., Kumar, T.S., Rai, S.K., **Roy, J.K.** Statistical optimization of α-amylase immobilization on iron-oxide magnetic nanoparticles, *Biotechnol. Bioprocess Eng.* **15**, 984–992, 2010.

Communicated manuscript

1. **Roy, J.K.** & Mukherjee, A.K. Cloning and extracellular expression of an α-amylase gene from a highly alkaline *Bacillus licheniformis* strain AS08E in *E. coli*: application of recombinant enzyme in digesting the raw starch from jackfruit (*Artocarpus heterophyllus*) seeds, a non-conventional source of starch.

Conferences/Seminar presentations

Roy, J.K., Mukherjee, A.K. Efficient extracellular expression of α-amylase from *Bacillus subtilis* AS01a in *E. coli* using *Bacillus* signal peptide. Presented at National seminar on "*Recent Advances in Microbial Biotechnology and Molecular Evolution,*" held at Tezpur University, Tezpur-2013.

Roy, J.K., Mukherjee, A.K. Optimization of thermostable amylase production from *Geobacillus thermodenitrificans* strain AS02a using Plackett–Burman and response surface methodology (RSM). Poster presented at *100th Indian Science Congress* held at Kolkata-2013.

Roy, J.K., Rai, S.K., Mukherjee, A.K. Partial purification and characterization of alkaline α-amylase from *Bacillus* sp. AS01a. Poster presented at *96th Indian Science Congress* held at NEHU, Shillong-2009.

PUBLICATIONS

Journal of Molecular Catalysis B: Enzymatic 97 (2013) 118–125

Contents lists available at ScienceDirect

Journal of Molecular Catalysis B: Enzymatic

journal homepage: www.elsevier.com/locate/molcatb

Cloning and overexpression of raw starch digesting α-amylase gene from *Bacillus subtilis* strain AS01a in *Escherichia coli* and application of the purified recombinant α-amylase (AmyBS-I) in raw starch digestion and baking industry

Jetendra K. Roy[a], Anjan Borah[b], Charu Lata Mahanta[b], Ashis K. Mukherjee[a,*]

[a] *Microbial Biotechnology and Protein Research Laboratory, Department of Molecular Biology and Biotechnology, School of Science, Tezpur 784 028, Assam, India*

[b] *Department of Food Engineering and Technology, School of Engineering, Tezpur University, Tezpur 784 028, Assam, India*

ARTICLE INFO

Article history:
Received 25 May 2013
Received in revised form 30 July 2013
Accepted 31 July 2013
Available online xxx

Keywords:
Protein expression
α-Amylase
Response surface method
Bacillus
Anti-staling

ABSTRACT

Considering the economic and industrial relevance of α-amylases used in food and starch industries, a raw starch digesting α-amylase gene (*amyBS-I*) from *Bacillus subtilis* strain AS01a was cloned and expressed in *Escherichia coli* BL21 cells. The gene also includes its signal peptide sequence (SPS) for facilitating the efficient extracellular expression of recombinant α-amylase (AmyBS-I) in correctly folded (enzymatically active) form. The native AmyBS-I consists of 659 amino acids with a molecular mass and pI of 72,387 Da and 5.8, respectively. The extracellular secretion of AmyBS-I after response surface optimization of culture conditions was found to be 7-fold higher as compared to its production under non-optimized conditions. Purified AmyBS-I demonstrated optimum activity at 70 °C and pH 6.0. It shows K_m and V_{max} values toward soluble starch as 2.7 mg/ml and 454 U/ml, respectively. Further, it does not require Ca^{2+} ion for its α-amylase activity/thermo-stability, which is an added advantage for its use in the starch industry. The AmyBS-I also hydrolyzed a wide variety of raw starches and produced maltose and glucose as main hydrolyzed products. The bread dough supplemented with AmyBS-I showed better amelioration of the bread quality as compared to the bread supplemented with commercial α-amylase.

1. Introduction

Alpha-amylases (1,4-α-D-glucan glucanohydrolase, [E.C. 3.2.1.1]) are extracellular starch hydrolytic enzymes that randomly cleave the 1,4-α-D-glucosidic linkages between adjacent glucose units in the linear amylose chain. This results in the formation of soluble maltodextrins, maltose, and glucose as end products of starch hydrolysis. Alpha-amylases comprise 30% of world's enzyme market [1,2] and are applied in many industrial processes such as starch liquefaction, textile, paper, brewing, baking, detergent, distilling industries, preparation of digestive aids, production of cakes, fruit juices, starch syrups, and pharmaceuticals [3]. Amylases, which show optimum activity in acidic pH, are primarily used in glucose syrup and baking industries, whereas those showing activities at alkaline pH have found applications in laundry detergent formulations [4].

Since starch is the second most abundant source of carbon and energy, therefore, a worldwide interest has been engrossed to use this economic carbon source in food processing industry to produce valuable products, like glucose, fructose and maltose syrups [5]. In addition, starch may also be converted to bio-ethanol [5]. However, the conventional way of starch processing requires a high input of energy, which in turn escalates the price of starch-based products [6]. Therefore, considerable efforts have been made to produce raw starch-digesting amylases capable of acting at acidic pH and at a moderate temperature much below the gelatinization temperature, which would be economical for the starch processing industries [6,7].

Recently we have reported the purification, characterization, and industrial application of an alkaline α-amylase from a high titer α-amylase producing *Bacillus subtilis* strain AS01a isolated from the soil sample of Assam, India [2]. In the present study, an attempt has been made to clone an α-amylase gene from the above strain and its expression in a mesophilic host (*Escherichia coli*). Interestingly, this recombinant enzyme (AmyBS-I) was found to have distinct properties from the previously reported alkaline α-amylase from the same bacterium [2]. However, the expression of heterologous proteins in

* Corresponding author. Tel.: +91 9957184351; fax: +91 3712 267005/267006.
E-mail address: akm@tezu.ernet.in (A.K. Mukherjee).

1381-1177/$ - see front matter © 2013 Elsevier B.V. All rights reserved.
http://dx.doi.org/10.1016/j.molcatb.2013.07.019

E coli has some limitations [8] For example, most of the recombinant proteins synthesized in the cytoplasm of *E coli* are not secreted out of the cell because of the complex arrangement of cell wall [8] Moreover, it occasionally accumulates as 'inclusion bodies' in the cytoplasm which does not show any enzymatic or biological activity and become lethal to the cell [9] From an industrial perspective, extracellular secretion of significant amount of recombinant protein in its enzymatically active form is highly appreciable for ease of downstream processing as well as application of this enzyme [8]

Recovery of biological active form of recombinant protein from inclusion bodies is a complicated and costly process Therefore, various strategies have been developed for the periplasmic and extracellular production of recombinant proteins in *E coli* [10] Several prokaryotic SPS, including PelB, OmpA, PhoA, endoxylanase, and StII [10] have been used for the efficient, extracellular production of heterologous recombinant proteins in *E coli* The present study shows the efficient, extracellular expression of an α-amylase gene that contains its SPS from *B subtilis* AS01a in *E coli* [2] Furthermore, the secretion of the recombinant enzyme was enhanced through response surface optimization of production conditions Here we also put forth the purification, biochemical characterization and raw starch digestion potential of this recombinant enzyme (AmyBS-I) as well as its application in baking industry

2. Materials and methods

2 1 Bacterial strains, chemicals and reagents

The genomic DNA of *B subtilis* strain AS01a was isolated and purified by using GeneJET genomic DNA purification kit procured from Fermentas (USA) *E coli* strains, DH5α was used for transformation studies while BL21 (DE3) (Novagen, Inc , CA, USA) was used for the over expression studies The TA cloning vector (Fermentas, USA) and pET28a (Invitrogen, CA, USA) were used for cloning and expression of the amylase gene, respectively The gel extraction kits, restriction enzymes, T4 DNA ligase, and DNA polymerase were procured from Fermentas (USA) All other molecular biology grade chemicals used in the present study were procured from either Merck (USA) or Hi-media (India)

2 2 Cloning of α-amylase gene in pTZ57R/T and pET 28a vectors

Cloning of the amylase gene from *B subtilis* strain AS01a was carried out as illustrated in Fig 1 Briefly, based on the available data of α-amylase gene sequence from *B subtilis* in NCBI database (www ncbi nlm nih gov), the α-amylase gene sequence of *B subtilis* BF7658 (Genbank accession No FJ463162) was retrieved randomly from NCBI database for designing primers Using the above retrieved sequence and freely available CloneAssistant 1 0 software (www bis zju edu cn/clone), the forward (5′-CCCAAGCTTTTGCGCTTACAGCA CCGTCGATCAA-3′) and reverse (5′-CGCGGATCCTTGAAAGAATGTGTTACACCT-3′) primers were designed to amplify α-amylase gene sequence (*amyBS-I*) from the genomic DNA of *B subtilis* strain AS01a [2] The amplified product (1 5 kb) so obtained was then inserted into a pTZ57R/T vector using InsTAclone PCR Cloning Kit (Fermentas, USA), following the instruction of the manufacturer The recombinant vector was then transformed into *E coli* DH5α competent cells However, after sequencing of recombinant vector, the α-amylase gene was found to be incomplete Therefore, the entire open reading frame (ORF) including SPS of the α-amylase of highest similar strain was taken to design the new set of primers

A unique *Hind* III restriction site (indicated in bold) was introduced in the forward primer (5′-CCC**AAGCTT**CTATGTTT-CCAAAACGATTCAA-3′) whereas *Xho* I restriction site (indicated in bold) was inserted in the reverse primer (5′-CCG**CTCGAG** CTCAATGGGGAAGAGAACC-3′) These primers were used to amplify the complete ORF of the α-amylase gene from *B subtilis* strain AS01a The PCR amplified product (~2 kb) was then double digested with the *Hind* III and *Xho* I and inserted into the *Hind* III and *Xho* I restriction sites of the pET-28a (+) vector Subsequently the recombinant plasmid (pETAMY) was transformed into *E coli* BL21 (DE3) competent cells, it was then plated on LBA plates containing kanamycin (30 μg/ml) The recombinant clones so obtained were further examined for extracellular secretion of α-amylase by culturing the individual clone on LBA plate supplemented with 0 5% (w/v) soluble starch, 30 μg/ml kanamycin and 40 μl of IPTG (isopropyl β-D-1-thiogalactopyranoside) (100 mM) After incubating the plates for 18 h at 37 °C, they were stained with the iodine solution to visualize the zones of starch hydrolysis (indicator of α-amylase production) surrounding the colonies

2 3 Induction and overexpression of B subtilis AS01a α-amylase gene in E coli BL21 (DE3)

The *E coli* BL21 (DE3) transformant harboring the pETAMY was grown in LB medium containing kanamycin (30 μg/ml) at 37 C 200 rpm until the culture reached the mid-logarithmic phase (~0 6 absorbance at 600 nm) The expression of recombinant protein was then induced by the addition of 1 0 mM IPTG After the different period of induction, cells were harvested by centrifugation (6000 rpm for 10 min at 4 °C) and the cell-free culture supernatant was used for the measurement of extracellular α-amylase production and SDS-PAGE analysis The cell-free culture supernatant from native (non-recombinant) *E coli* cells was used as negative control For the determination of intracellular α-amylase activity, if any, the cell pellets were re-suspended in Tris–HCl buffer (pH 8 0) and the cells were disrupted by lysozyme treatment followed by sonication The cell lysate was then subjected to centrifugation at 12,000 rpm for 10 min at 4 °C The supernatant of clear lysate was used for the measurement of intracellular α-amylase activity

2 4 Amino acid analysis and structure determination of recombinant enzyme

The recombinant plasmid containing α-amylase gene was isolated from the *E coli* cells and then sequenced using automated DNA sequencer (3130 Genetic Analyzer Applied Biosystem Switzerland) From the gene sequence, primary structure of the recombinant α-amylase was deduced using the Gene Runner software (www generunner net) The nucleotides and the deduced amino acid sequence homology searches were performed using BLAST program of NCBI database (http //www ncbi nlm nih gov) The signal peptide sequence was predicted using SignalP 4 0 server online program (http //www cbs dtu dk/services/SignalP) The multiple amino acid sequence alignment was accomplished using CLUSTAL W2 program [11] of EMBL-EBI online software (www ebi ac uk) The resulted aligned sequences were then investigated for the conserved domain searched in NCBI database (www ncbi nlm nih gov) Subsequently, the secondary structure of the recombinant protein was then predicted and superimposed using the ESPript online programme (www espript ibcp fr/ESPript/ESPript)

2 5 Alpha-amylase assay

The amylolytic activity was assayed by measuring the amounts of reducing sugar released by the action of enzyme from 1% (w/v) of soluble starch dissolved in 50 mM K-phosphate buffer (pH – 6 0) at 60 °C The amounts of reducing sugar released were estimated

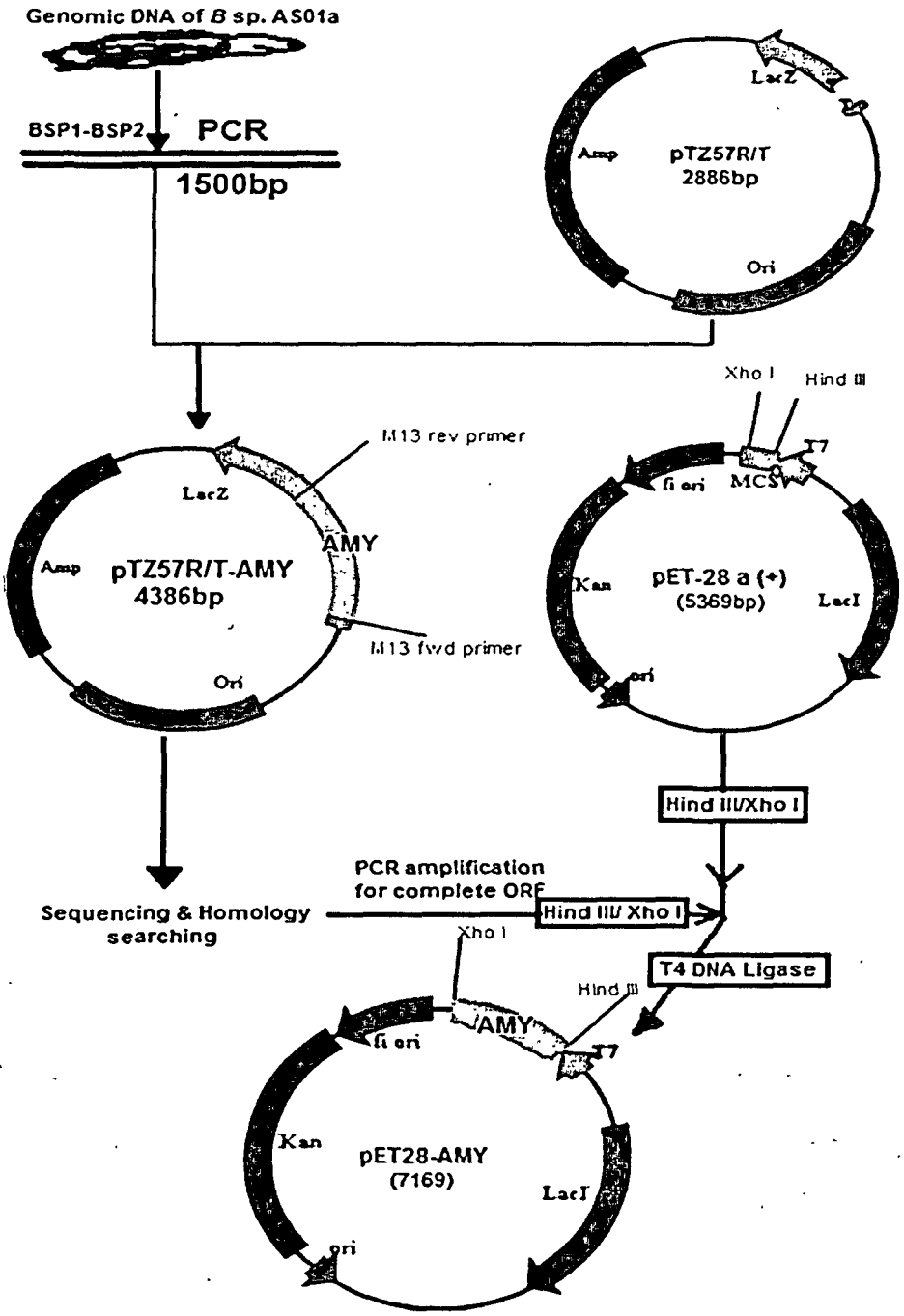

Fig. 1. Strategy used for the cloning of *amyBS-1* from *B. subtilis* strain AS01a into cloning and expression vectors.

by our previous illustrated method [12]. One unit of enzyme activity was defined as the liberation of reducing sugars equivalent to 1 μmol of D-glucose/min under the assay conditions [12].

2.6. Enhancement of extracellular expression of α-amylase into the expression media using response surface methodology

Response surface methodology [13] was applied to optimize the cultivation conditions for the over-expression of recombinant α-amylase in *E. coli*. The optimization was designed based on a rotatable central composite design (CCD) with 30 experimental trials involving 8 star points and 6 replicates at the central points. The CCD results were analyzed using DESIGN EXPERT (State-Ease, USA). The following four parameters viz. concentrations of IPTG (C_1), post-induction time (C_2), temperature (C_3), and concentrations of EDTA (C_4), were optimized through RSM. The rationale for selection of the above parameters was based on studies showing their crucial role in the extracellular expression of recombinant proteins in *E. coli* [8,14,15]. Details of lower limit, central values, and the upper limit are shown in Table 1. For statistical calculations, the relation between the coded values and actual values is described by Eq. (1):

$$C_i = \frac{A_i - A_0}{\Delta A_i}, \quad i = 1, 2, 3, \ldots, k \tag{1}$$

Table 1
Design matrix in both coded and actual (in bracket) values with their corresponding experimental and predicted activities of the recombinant AmyBS-I

Run order	IPTG (mM) (C_1)	Time of post Induction (h) (C_2)	Temperature (°C) (C_3)	EDTA (mM) (C_4)	Enzyme activity (U/ml)	Predicted values
1	−1 0 (0 2)	−1 0 (12)	−1 0 (20)	−1 0 (17)	101 67	95 28
2	1 0 (1)	−1 0 (12)	−1 0 (20)	−1 0 (17)	116 79	111 61
3	−1 0 (0 2)	1 0 (24)	−1 0 (20)	−1 0 (17)	186 83	172 45
4	1 0 (1)	1 0 (24)	−1 0 (20)	−1 0 (17)	136 51	131 6
5	−1 0 (0 2)	−1 0 (12)	1 0 (30)	−1 0 (17)	123 56	124 08
6	1 0 (1)	−1 0 (12)	1 0 (30)	−1 0 (17)	159 73	154 31
7	−1 0 (0 2)	1 0 (24)	1 0 (30)	−1 0 (17)	159 35	151 37
8	1 0 (1)	1 0 (24)	1 0 (30)	−1 0 (17)	124 98	124 41
9	−1 0 (0 2)	−1 0 (12)	−1 0 (20)	1 0 (34)	129 00	117 25
10	1 0 (1)	−1 0 (12)	−1 0 (20)	1 0 (34)	120 30	121 11
11	−1 0 (0 2)	1 0 (24)	−1 0 (20)	1 0 (34)	217 34	215 59
12	1 0 (1)	1 0 (24)	−1 0 (20)	1 0 (34)	175 11	162 26
13	−1 0 (0 2)	−1 0 (12)	1 0 (30)	1 0 (34)	94 50	92 24
14	1 0 (1)	−1 0 (12)	1 0 (30)	1 0 (34)	107 93	109 99
15	−1 0 (0 2)	1 0 (24)	1 0 (30)	1 0 (34)	147 84	140 69
16	1 0 (1)	1 0 (24)	1 0 (30)	1 0 (34)	102 04	101 26
17	−2 0 (0)	0 0 (18)	0 0 (25)	0 0 (25 5)	98 26	122 35
18	2 0 (1 4)	0 0 (18)	0 0 (25)	0 0 (25 5)	144 82	150 74
19	0 0 (0 6)	−2 0 (6)	0 0 (25)	0 0 (25 5)	105 42	109 46
20	0 0 (0 6)	2 0 (30)	0 0 (25)	0 0 (25 5)	162 48	177 90
21	0 0 (0 6)	0 0 (18)	−2 0 (15)	0 0 (25 5)	95 74	114 18
22	0 0 (0 6)	0 0 (18)	2 0 (35)	0 0 (25 5)	80 95	81 98
23	0 0 (0 6)	0 0 (18)	0 0 (25)	−2 0 (8 5)	115 52	127 92
24	0 0 (0 6)	0 0 (18)	0 0 (25)	2 0 (42 5)	119 66	126 74
25	0 0 (0 6)	0 0 (18)	0 0 (25)	0 0 (25 5)	51 86	51 21
26	0 0 (0 6)	0 0 (18)	0 0 (25)	0 0 (25 5)	54 28	51 21
27	0 0 (0 6)	0 0 (18)	0 0 (25)	0 0 (25 5)	52 26	51 21
28	0 0 (0 6)	0 0 (18)	0 0 (25)	0 0 (25 5)	56 28	51 21
29	0 0 (0 6)	0 0 (18)	0 0 (25)	0 0 (25 5)	50 86	51 21
30	0 0 (0 6)	0 0 (18)	0 0 (25)	0 0 (25 5)	52 26	51 21

where C_i is a coded value of the variable A_i is the actual value A_0 is the actual value of A_i at the center point, and the star point was set with α of 2 0 from the coded center point A mathematical model was developed using Design-Expert and the experiments were conducted according to design matrix (Table 1) arranged by the statistical software The significance of difference among the same sets of experimental data was analyzed using the ANOVA test A P-value (probability > F) of less than 0 05 indicated that the model terms were significant Adequacy of the developed model was further validated using numerical method optimization option of the Design-Expert (version 7 0 Stat-Ease, Inc) software

2 7 Isolation and purification of α-amylase from recombinant E coli strain

Solid ammonium sulphate [$(NH_4)_2SO_4$] was gradually added to the cell-free culture supernatant (obtained after 24 h of incubation) at 4 °C to attain 1 0 M solution The solution was then stirred slowly for additional 30 min at 4 °C It was then applied to a FPLC (AKTApurifier GE Healthcare, Uppsala, Sweden) coupled Phenyl-Sepharose column (5 mm × 20 mm) previously equilibrated with 50 mM Na-phosphate buffer pH 7 4 containing 1 0 M $(NH_4)_2SO_4$ The column was washed with a linear gradient of 1 0–0 0 M $(NH_4)_2SO_4$ in the same buffer at a flow rate of 1 ml/min, and 2 0 ml fraction was collected in each tube The active fractions were pooled and then dialyzed to remove the salt and subsequently it was concentrated by ultrafiltration unit (50-kDa cutoff membrane) (Amicon, Beverly, MA USA) This was followed by fractionation of the concentrated solution through HiPrep 16/60 Sephacryl S-200 HR (GE Healthcare Bio-Sciences Corp , USA) gel filtration column coupled with a FPLC system The column was then equilibrated with 50 mM Na-phosphate pH 7 4, and elution of protein(s) was carried out with the same buffer at a flow rate of 30 ml/h One milliliter fraction was collected in each tube and each fraction was checked for α-amylase activity and protein content

2 8 Determination of purity and molecular mass of recombinant protein

The homogeneity as well as molecular mass of the pooled gel-filtration fractions displaying α-amylase activity was checked by 10% SDS-PAGE analysis of the protein(s) [16] Amylase zymography analysis was done as described by Roy et al [2] The purified enzyme so obtained was named as AmyBS-I, and was used for characterizing its biochemical properties and application in starch processing industry

2 9 Biochemical characterization of purified AmyBS-I

The optimum pH and temperature for recombinant α-amylase (AmyBS-I) was determined by incubating 10 μg of enzyme with 1% (w/v) starch dissolved in different buffers (pH 4 0–12 0), or at different temperatures (30–90 °C) at optimum pH 6 0 In order to determine its thermostability, purified α-amylase (10 μg/ml) was incubated at different temperatures ranging from 40 to 100 °C for 30 min, in both presence and absence of 5 mM Ca^{2+} ions This was followed by assaying its residual activity against control

To investigate the effects of divalent metal ions, inhibitors and metal chelator on enzymatic activity of AmyBS-I, it was treated with divalent cations (5 mM) (Cu^{2+}, Fe^{2+}, Co^{2+}, Hg^{2+} Ca^{2+} Zn^{2+} Ni^{2+}, Mn^{2+}, Mg^{2+}), phenyl methyl sulfonyl fluoride (2 mM) and EDTA (2 mM) for 30 min at room temperature [12] The enzyme activity without any of the above-mentioned metal ions/inhibitors was considered as 100% activity and other values were compared with that [2,12] The kinetic properties viz K_m and V_{max} values of the purified AmyBS-I toward soluble starch were determined using Lineweaver–Burk double reciprocal plot [2]

2.10 Reaction end product determination by thin layer chromatography (TLC)

To determine the end product of starch hydrolysis, a reaction mixture containing 5.0 ml of 1% (w/v) soluble starch (Hi-media, India) dissolved in 50 mM Na-phosphate buffer (pH 6.0), was incubated with AmyBS-I at a concentration of 10 μg/ml of starch solution at 70 °C. An aliquot of reaction mixture was withdrawn at an interval of 1, 3, 6 and 12 h after the incubation, and starch hydrolysis products were analyzed by Slica gel G thin layer chromatography [17]. The product formation was quantitated by densitometry scanning of TLC plates followed by analysis with ImageJ software (www.rsbweb.nih.gov/ij).

2.11 Raw starch hydrolysis by the AmyBS-I

The efficiency of AmyBS-I to digest the raw starch obtained from various sources (rice, wheat, and potato) was determined by incubating 5.0 ml of 2% (w/v) starch dissolved in 50 mM Na-phosphate buffer (pH 6.0) with AmyBS-I at a concentration of 10 μg/ml at 60 °C for 6 h. The extent of starch hydrolysis was determined by estimating the amount of reducing sugars released from various starch by the action of AmyBS-I. The raw starch hydrolysis (R_h) potential of AmyBS-I was calculated using the formula R_h (%) = $(A_1/A_0) \times 0.9 \times 100$, where A_1 was the amount of sugar (mg/ml) in the supernatant after the reaction and A_0 was the amount of raw starch (mg/ml) before the reaction. The factor 0.9 (162/180) is the conversion factor due to the addition of water molecules to glycosyl moiety on hydrolysis [18]. After 6 h of hydrolysis, all starch grains were washed twice with pure ethanol and examined under scanning electron microscope at 15 kV (JEOL model JSM-6390 LV) as described previously [2].

2.12 Anti-staling effect of AmyBS-I on bread preparation

The application of AmyBS-I as anti-staling agent on bread making was evaluated by the procedure described by Sharma and Satyanarayana [19]. The dough mixture was supplemented with the enzyme preparation [AmyBS-I or commercial α-amylase (Hi-media, Mumbai)] in a ratio of 10 U/g of dough, followed by mechanical blending with 60% (w/v) water for 30 min to produce the dough. Control dough was also prepared where no enzyme was added. These were then kept for proofing followed by fermentation for 1 h at 33 °C and 85% relative humidity. The proved doughs were baked in electric oven at 220 °C for 60 min. Subsequently, bread loaves were cooled (60 min), packed in polythene bags, and stored for five days at room temperature.

To determine the reducing sugar content of the breads, 1 g of each bread sample was dissolved in 5 ml of 0.1 M Na-acetate buffer (pH 4.5), mixed well by vortexing, and centrifuged at 10,000 rpm for 15 min. Presence of reducing sugar in the supernatant was determined using DNS reagent [2]. Moisture content of the bread sample was estimated by drying the bread at 105 °C to constant weight. To determine the bread color, a breadcrumb was attached to HunterLab (Ultra-scan VIS, USA) then three readings were taken and average value was recorded. The brownness index (*BI*) for the bread color was calculated [20] using the following equation:

$$BI = \frac{100(x - 0.31)}{0.17}, \quad \text{where } x = \frac{(a + 1.75L)}{(5.645L + a - 3.012b)} \tag{2}$$

For assessing the self-life, bread samples kept at room temperature were visually inspected on alternate days for texture, softness, and staling. The crumb texture of the loaves (hardness, springiness, cohesiveness, and gumminess) was evaluated by texture profile analysis (TPA) method using a texture analyzer (TA-HD-plus, Stable Micro Systems, UK) having a 35-mm flat-end aluminum compression disk (probe P/35). Slices of 2 cm thickness were compressed to 40% of their original height in a TPA double compression test, at 1 mm/s speed test, with a 20 s delay between the 1st and 2nd compression [21]. A semi-trained panel did sensory analysis for overall acceptability of the bread samples. All these experiments were performed in triplicates, and the average values are presented.

3. Results and discussion

3.1 Cloning and sequencing of the gene encoding α-amylase from B. subtilis AS01a

The molecular cloning of the α-amylase from *B. subtilis* strain AS01a would be helpful for hyper-production of this enzyme, thereby to meet industrial needs and for the development of novel properties with enzyme engineering such as pH profile and thermostability. Overexpression of recombinant protein would also be helpful to understand its structure-function relationships and development of a better enzyme by site-directed mutagenesis (enzyme engineering) [22]. Furthermore, the expression of this α-amylase in *E. coli* system would be of great value to reduce the energy consumption during the enzyme production process because the parent strain *B. subtilis* AS01a needs to be cultivated at 45 °C [2]. Approximately 2 kb fragment containing complete ORF of α-amylase gene (*amyBS-I*) was amplified by PCR using *B. subtilis* strain AS01a genomic DNA as the template (Supplementary Fig. S1A). The PCR amplified product was successfully cloned first into pTZ57R/T vector, then into pET-28a expression vector for sequencing and expression of α-amylase gene, respectively (Fig. 1). The *amyBS-I* sequence contained a complete ORF with a length of 1980 bp, which encoded a polypeptide of 659 amino acid residues (including the SPS) with a calculated molecular mass of 72.4 kDa (Fig. 2).

The nucleotide sequence of *amyBS-I* from *B. subtilis* AS01a reported here has been deposited into GenBank database under accession number (KC113313). The homology search revealed a significant similarity of *amyBS-I* with α-amylases from *B. subtilis* strains (Fig. 2). The deduced amino acid sequence of *amyBS-I* was found to contain a prokaryotic SPS (Fig. 2). The analysis of deduced amino acid sequence of mature protein (AmyBS-I) using conserved domain search of NCBI (www.ncbi.nlm.nih.gov) suggested that it belongs to GH 13 family of glycoside hydrolase (GH) [1]. The calculated pI/M_w of the AmyBS-I was estimated to be 5.8/72,387 and 5.5/68,875.6 for the native protein (containing SPS) and for the mature peptide, respectively.

3.2 Expression of B. subtilis AS01a α-amylase gene in E. coli BL21 (DE3)

A recombinant plasmid, pETAMY, containing *B. subtilis* AS01a α-amylase gene into pET-28a vector was constructed for the extracellular expression of the AmyBS-I. Since the SPS helps in the extracellular expression of a recombinant protein, therefore complete ORF of α-amylase gene including its SPS from the *B. subtilis* strain AS01a was amplified and cloned into the expression vector. The formation of halo zones around the recombinant bacterial colonies on the starch agar plate after flooding with Gram's iodine re-confirmed the successful extracellular over-expression of AmyBS-I (Supplementary Fig. S1). The SDS-PAGE analysis of the cell extract as well as culture supernatant from *E. coli* BL21 harboring pETAMY showed a prominent protein band with an apparent

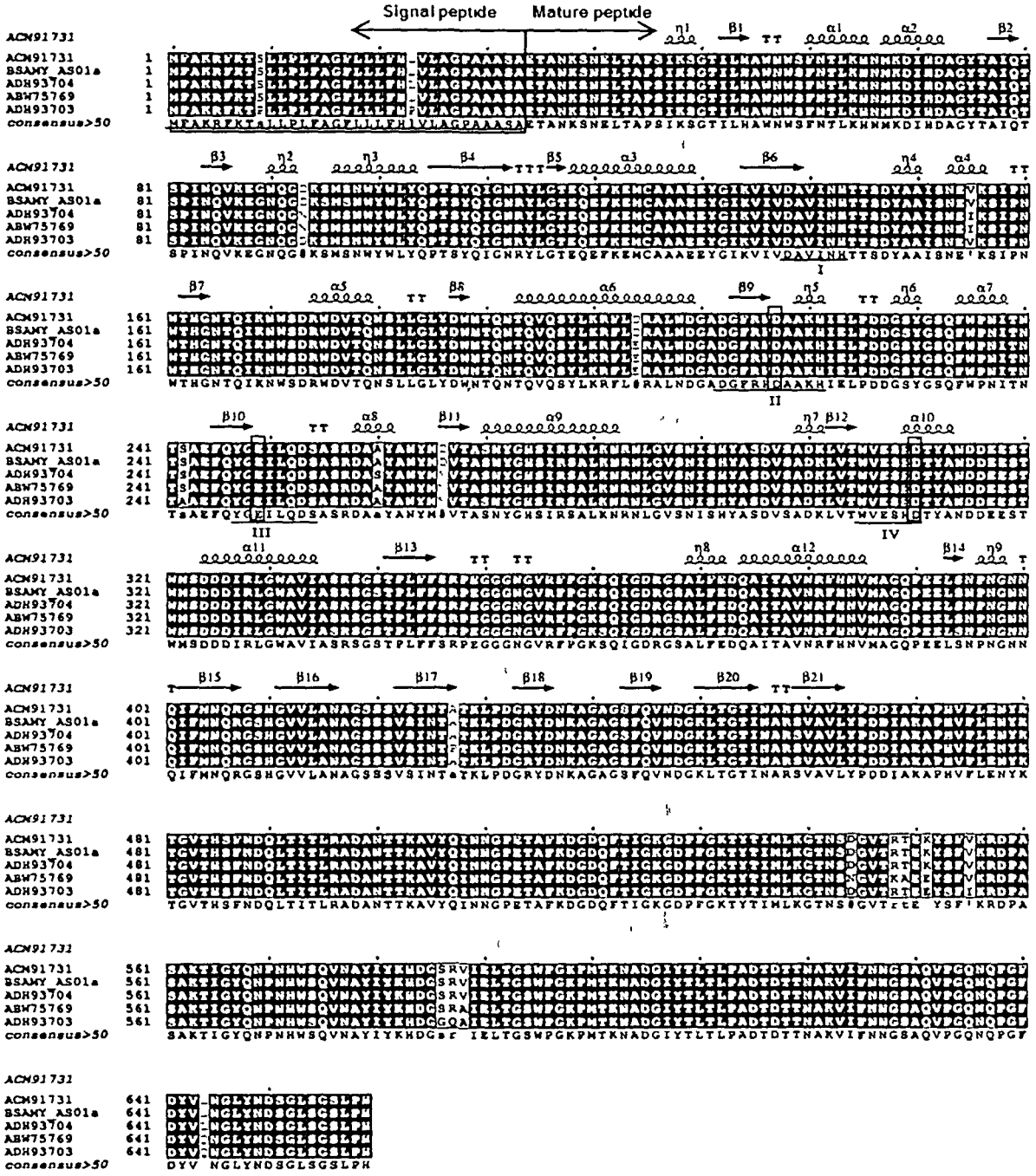

Fig 2 Multiple sequence alignment of *amyBS I* with the homologous α-amylase sequences reported in the databases The *amyBS-I* showed 99% sequence homology with *B subtilis* HLSSK-3 (ADH93704) and *B subtilis* strain 011085 (ACM91731) whereas it showed 98% sequence similarity with *B amyloliquefaciens* DL 341(ADH93703) and *B subtilis* (ABW75769) The SPS is marked underlined the four conserved regions of *amyBS I* are marked in underline with numerals and the catalytic sites residues are enclosed in rectangular boxes The conserved sequences of α-amylases were displayed as the white letters on the black background The secondary structure assignments of the AmyBS-I are indicated at the top of the alignment The TTT and TT letters represent strict alpha and beta turns respectively

molecular mass of ~70 kDa (data not shown) The mass of this protein was found to be the same as estimated from the deduced amino acid sequence of the AmyBS-I suggesting extracellular expression of the recombinant enzyme However, α-amylase assay as well as SDS-PAGE study suggested that majority of the target proteins were accumulated as inclusion bodies in *E coli* Therefore, in order to reduce the formation of inclusion bodies and efficient secretion of functionally active recombinant α-amylase into the culture medium, the *E coli* culture parameters were optimized using RSM

3 3 *Optimization of culture conditions for the extracellular expression of AmyBS-I*

It is well recognized that media components and cultivation parameters play an important role in extracellular expression of recombinant protein by *E coli* [14 15] Further, targeting recombinant protein into the periplasmic space or to the culture medium simplifies downstream processing, folding and in vivo stability, thus, enabling the cost-effective production of soluble and biologically active proteins [23] Therefore, the four most significant

Table 2
Analysis of variance (ANOVA) and regression analysis for the expression of extracellular AmyBS-I

Source	Sum of squares	Degrees of freedom	Mean squares	*F*-value	Prob (*P*)> *F*
Model	51 933 7	14	3709 55	25 14	<0 0001
Residual (error)	2213 01	15	147 53		
Lack of fit	2193 64	10	219 36	56 64	0 0002
Pure error	19 36	5	3 87		
Total	54 146 71	29			

R^2 = 0 96 Adj R^2 = 0 92 Pred R^2 = 0 79 and CV = 10 58%

parameters viz IPTG concentration, temperature, time of post-induction and EDTA concentration were optimized for the efficient extracellular expression of AmyBS-I By processing these variables, a model was obtained as shown in Eq (3) The model was evaluated by multiple regression analysis to predict the optimum cultivation conditions for optimizing the extracellular expression of AmyBS-I into the culture media All the terms regardless of their significance are included in the following equation, where Y is the response, that is, the enzyme activity (U/ml) and $C_1 - C_4$ are the actual values of the test variables

$$Y = 390\ 89 - 135\ 51C_1 - 8\ 95C_2 - 10\ 5C_3 - 23\ 36C_4 + 173\ 57C_1^2 + 0\ 64C_2^2 + 0\ 46C_3^2 + 3\ 04C_4^2 - 5\ 95C_1C_2 + 1\ 74C_1C_3 - 3\ 12C_1C_4 - 0\ 42C_2C_3 + 0\ 35C_2C_4 - 1\ 08C_3C_4 \quad (3)$$

The coefficient of the model including the significance of each coefficient was determined by *P*-values, the model terms with the *P*-value (probability > *F*) less than 0 05 are considered to be significant Results showed that C_1, C_2, C_3, C_1^2, C_2^2, C_3^2, C_4^2, C_1C_2, C_2C_3, and C_3C_4 are significant model terms The analysis of variance (ANOVA) by Fisher's statistical test was conducted for the quadratic model and the results demonstrated that the computed *F*-value for the model is 25 14 which implies that the model is significant (Table 2) There is only a 0 01% chance that a "Model *F*-Value" could occur due to noise The model's fitness accuracy can also be checked by determining the coefficient of correlation (R^2 = 0 96) It is obvious from the value of R^2 that the deduced model could not explain only 4% of the total variation (Table 2) The value of adjusted R^2 (0 92) also supported the significance of the model (Table 2)

Response surface and contour plots are graphical representations for the regression equation They investigate the interaction amongst the variables and determine the optimum levels Fig 3A–F shows the response surface curves, and contour plots for variations in extracellular AmyBS-I activity as a function of two variables at a time while the other variables were maintained at their respective zero level Figs 3A and B demonstrate that lowering the IPTG concentration as well as temperature has a positive effect on high-level secretion of AmyBS-I into the culture medium Ayadi et al [14] reported a similar phenomenon for *Paenibacillus* CGTase production in *E coli* On the other hand, increasing the EDTA concentration as well as enhancing the incubation time resulted in better expression and secretion of AmyBS-I into the culture medium (Fig 3F) This observation is in accordance with Lo et al [15] showing enhanced production of *Bacillus* CGTase in *E coli* with respect to time

By solving the regression Eq (3) using numerical method, the optimum value for each of the four test variables was found as IPTG concentration = 0 24 mM, post induction time = 26 7 h, temperature of incubation = 19 7 °C and EDTA concentration = 46 7 mM The predicted value for the extracellular AmyBS-I production at optimized conditions was calculated as 389 44 U/ml This value was in close agreement with actual experimental value of 378 24 U/ml of AmyBS-I thus justifying the suitability of RSM model applied in this study for enhancing the AmyBS-I yield The model exhibited a significant improvement in the extracellular expression of AmyBS-I (approx 7-fold) under optimized conditions as compared to its production under non-optimized conditions Our study showed that the culture conditions such as low IPTG concentration, low temperature, and increase in post induction time play a critical role in the heterologous extracellular expression of AmyBS-I All these factors keep the *E coli* under low induction level, give sufficient time to properly fold and export the AmyBS-I through the cell wall membrane into the culture medium Further, the expression and secretion of AmyBS-I in *E coli* at a low temperature (~20 °C) are unique findings of this study and hardly few reports are available showing extracellular expression of recombinant protein in *E coli* at such a low temperature without the aid of co-expression of chaperone [24] The role of EDTA in extracellular secretion of AmyBS-I may be assumed by permeabilization of the outer membrane of *E coli* [25]

3 4 Purification and biochemical characterization of AmyBS-I

The AmyBS-I was eluted from the Phenyl-sepharose column with 0% $(NH_4)_2SO_2$ salt concentration (Supplementary Fig S2A) Further fractionation of this active fraction through Sephacryl S-200 resulted in elution of active enzyme in a single peak (Supplementary Fig S2B), and proteins of this peak was found to be homogenous by SDS-PAGE (Fig 4) Under both denatured and native conditions, the enzyme yields a single band of approximately 69 0 kDa in SDS-PAGE This suggests that the α-amylase under study is monomeric in nature which is in accordance with the predicted size of the amino acids sequence (Fig 4) The purity of preparation was further re-confirmed by amylase-zymographic study where the enzyme showed a single clear zone of starch hydrolysis (Fig 4) A summary of purification of the recombinant enzyme AmyBS-I is shown in Supplementary Table S1 The AmyBS-I was purified up to 3 9-fold with 19 5% of recovery of the total enzyme activity (Supplementary Table S1) In general, molecular mass of α-amylases from bacteria particularly from *Bacillus* sp is reported in between 48 and 60 kDa [26] and there is a dearth of report on such a high molecular mass α-amylase from bacteria

Before assessing the biotechnological potential of any enzyme, characterization of its biochemical properties relevant to industrial application is most important and advantageous [27] AmyBS-I retained its activity over a broad range of pH (5 0–9 0) and temperature (40–80 C) (Supplementary Fig S3), however, the enzyme displayed optimum activity at pH 6 0 and at 70 °C, suggesting its application in starch saccharification industry The AmyBS-I also showed higher temperature optima than many of the α-amylases purified from *Bacillus* sp KSM 1378 [4], *Bacillus* sp GM 8901 [4] and *Bacillus* sp YX1 [7]

The thermo-stability study demonstrated that heating of AmyBS-I for 30 min at 70 °C had no effect on its enzyme activity However heating beyond this temperature resulted in a gradual

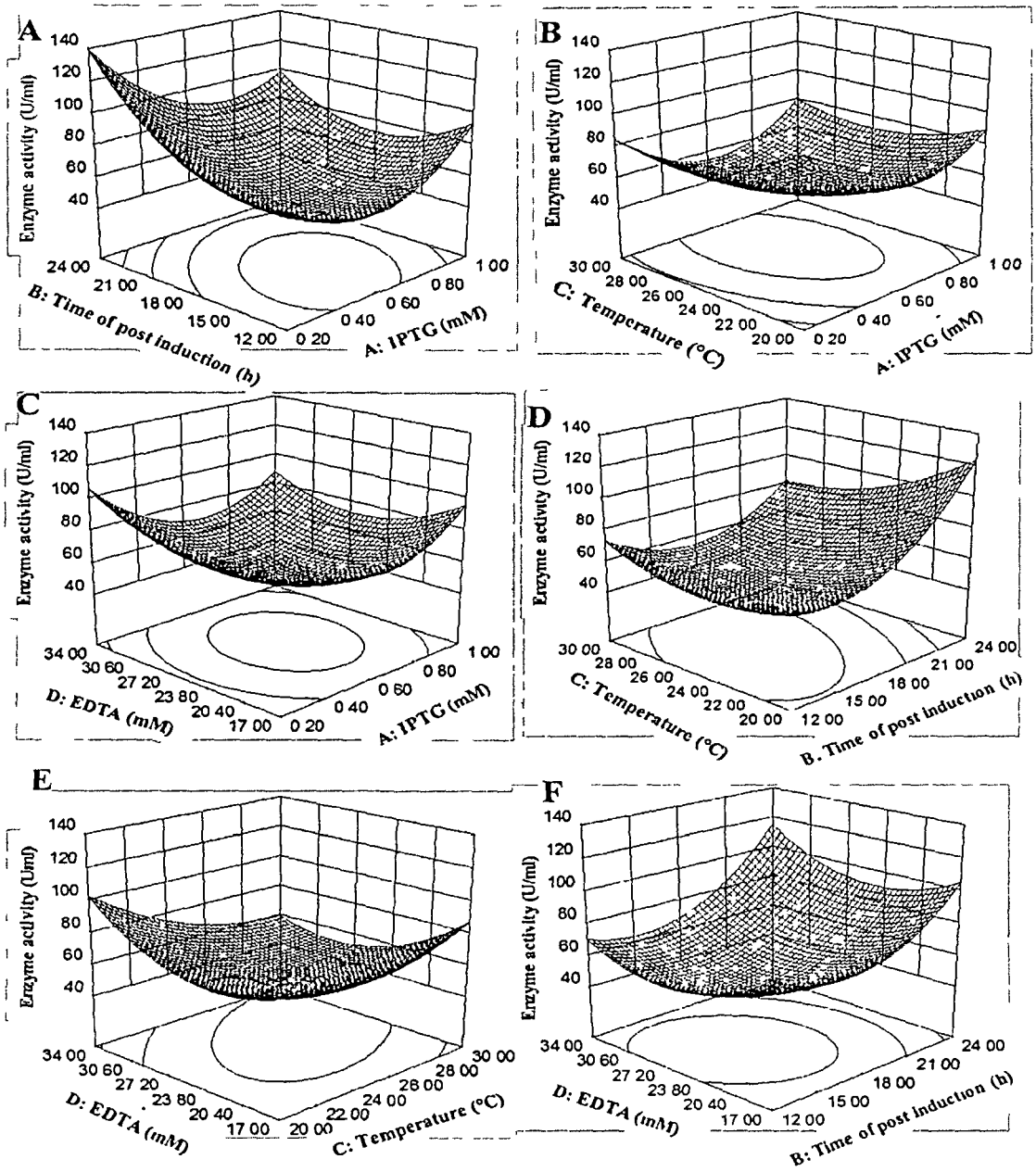

Fig 3 Response surface plots and contour plots showing interaction effect of test variables on extracellular over expression of AmyBS I in *E coli* BL21 (DE3) strain (A) IPTG concentration (mM) versus time of incubation after induction (h) (B) IPTG concentration (mM) versus temperature (°C) (C) IPTG concentration (mM) versus EDTA concentration (mM) (D) time of incubation after induction (h) versus temperature (°C) (E) temperature (°C) versus EDTA concentration (mM) and (F) time of incubation after induction (h) versus EDTA concentration (mM)

loss of enzyme activity (Supplementary Fig S4) The thermostability of the AmyBS-I was not influenced by the presence of Ca^{2+} ion (Supplementary Fig S4) which is an added advantage for application of AmyBS-I in starch saccharification process at a higher temperature because it eliminates the requirement of Ca^{2+} ion for improving the thermo-stability of α-amylases [2] Therefore application of AmyBS-I in starch processing industry may be considered as a cost-effective process

The activity of various enzymes is influenced by the presence of divalent cations and additive molecules In the present study, α-amylase activity of AmyBS-I in presence of Fe^{2+}, Cu^{2+}, Zn^{2+}, and Hg^{2+} were inhibited to 70 5%, 79 2%, 84 6% and 94 5%, respectively of its original activity The other tested divalent metal ions and EDTA did not show adverse effect on the enzyme activity of AmyBS-I In the presence of PMSF AmyBS-I lost around 22% of its original activity suggesting the presence of serine in the active site which was also confirmed by AmyBS-I sequence analysis The K_m and V_{max} values of AmyBS-I toward soluble starch were found to be 2 7 mg/ml and 454 0 μmol/min/mg, respectively The K_m value of AmyBS-I for starch hydrolysis is higher than the K_m value of alkaline α-amylase (1 9 mg/ml) purified from the same strain of *Bacillus* [2] However this K_m value is comparable with the K_m value of α-amylases from *B subtilis* (3 85 mg/ml) [26] and *Bacillus* sp TM1 (4 mg/ml) [28]

The end-products of starch hydrolysis by AmyBS-I by TLC analysis demonstrated the formation of oligosaccharide mixtures after

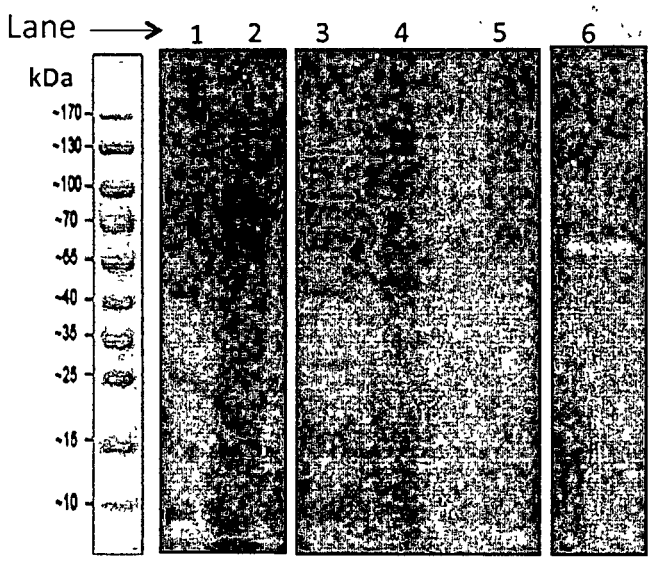

Fig. 4. SDS-PAGE analysis of AmyBS-I. Lanes 1 and 3, pre-stained protein molecular weight markers; lane 2, crude culture supernatant containing recombinant protein (30 μg); lane 4, phenyl-sepharose pooled fraction (25 μg); lane 5, purified gel filtration fraction (25 μg); and lane 6, zymogram of AmyBS-I (20 μg).

1 h of treatment; however, formations of maltose and glucose were observed after 3 h of treatment (Supplementary Fig. S5). After 12 h of treatment of soluble starch with AmyBS-I, formation of glucose (82.5%) surpassed maltose production (17.5%) (Supplementary Table S2). This result proves that the enzyme AmyBS-I is an endo-acting type α-amylase enzyme, which may be useful for the food and starch industry [2]. The biochemical properties as well as molecular mass of AmyBS-I were found to be different from the previously reported alkaline α-amylase from the same parent strain (Supplementary Table S3). These data provide convincing evidences that the recombinant enzyme (AmyBS-I) from *B. subtilis* strain AS01a is a different α-amylase than previously reported alkaline α-amylase from the same strain [2]. A bacterium can produce several isoenzymes and other metabolites to cater its requirement as well as to sustain its growth in a particular environment from where it was isolated and therefore, production of isoforms of the same enzyme is not an uncommon phenomenon.

3.5. Raw potato starch hydrolysis by AmyBS-I

The α-amylases capable of digesting various raw starches are attractive from the industrial perspective since they reduce the energy consumption as well as starches from different sources can directly be used for the hydrolysis by the same enzyme [7,18]. Further, conventional starch processing involves two enzymatic steps after starch slurry gelatinization by heating at 100–105 °C [5,18]. The first enzymatic step is the liquefaction by α-amylase at 90–95 °C and second step of starch saccharification is carried out at 60–65 °C using glucoamylse [5], thus the process involves repeated steps of cooling and heating which is costly and high energy consuming process. Since AmyBS-I can digest various raw-starches at 60 °C, therefore, application of AmyBS-I in starch saccharification process may eliminate the unnecessary repeated cooling and heating steps.

The raw starch digestibility of AmyBS-I showed that it could hydrolyze the wheat, potato and rice raw starches to 61%, 58%, and 44%, respectively after six hours of incubation at 60 °C. Moreover, the raw potato starch degradation ability of AmyBS-I suggests its potential application in potato starch hydrolysis since only a few bacterial α-amylases are reported to digest this most commonly available starch to such an extent [29]. Further, the SEM analysis of starch degradation showed that AmyBS-I, like alkaline α-amylase from *B. subtilis* AS01a [2], also formed pit and deep holes on the surface of all the tested raw starches (Fig. 5). Results of this study suggest that AmyBS-I very efficiently digests raw starch from various sources (wheat, potato, and rice) which makes this enzyme as a better candidate for its industrial application in food and fermentation industries [30]. It is noteworthy to mention that there are very few examples of α-amylases which show potency to digest raw starches from different sources [5].

3.6. Anti-staling effects of AmyBS-I on bread

Acidic and moderate thermostable amylases, which are able to produce fermentable sugars and dextrin for further use by the yeast, are applied in baking industry to improve self-life of breads [19]. Supplementation of AmyBS-I and commercial α-amylases to dough resulted in increase in self-life of bread; however, AmyBS-I supplementation resulted in a considerable higher anti-staling effect as compared to supplementation of commercial α-amylases in bread. It was also found that the AmyBS-I supplemented bread has a better loaf volume and crumb color as compared to the commercial α-amylase supplemented and control (no supplementation) breads (Fig. 6). Further, the moisture content of the fresh bread has a direct correlation with the softness of the baked products and its ideal level should be around 35–40% [19]. Lower moisture content is a desirable property to prevent the microbial growth; however, the moisture content of the bread cannot be kept less than 30% because bread having lower moisture content than this value cannot be refreshed even after heating [31]. The moisture content of AmyBS-I supplemented bread was found within the range of this ideal level and least among the tested samples which suggests adequate softness of the bread and least susceptible to the microbial attack after storage for some period of time (Table 3). Sharma and Satyanarayana [19] have also opined that the addition of amylase increases the self-life of the bread due to their anti-staling effect on bread. In addition, the AmyBS-I supplemented bread has a higher sugar content as compared to other test samples (Table 3). The higher sugar content results in improvement of the taste, crust color, and toasting quality of bread [19]. The brownness index (*BI*) of bread is an important parameter to determine its acceptability. The *BI* of AmyBS-I, and commercial amylase supplemented bread was found to be 38.2 and 37.6, respectively. For the control bread, this value was determined as 29.4 (Table 3).

The TPA evaluation of bread before and after its storage may directly be correlated with the staling rate of bread by physical examination of baked products [21]. In fact, these mechanical characteristics of TPA evaluation consisting of hardness, gumminess, cohesiveness, and springiness can be correlated well with the sensory perception of bread and can define bread quality [21]. In general, on storage of bread, its hardness and gumminess are increased whereas cohesiveness and springiness are found to decrease with time; therefore, the rate of these changes determines the quality of bread [32]. Table 4, shows that significant changes observed in all the tested parameters of bread stored for five days; except the commercial α-amylase (Himedia) supplementation to the bread did not result in a significant change ($P > 0.05$) in gumminess with respect to control. It was also observed that the bread supplemented with AmyBS-I had significant resistance to hardness and gumminess changes over the time as compared to control as well as commercial α-amylase (Himedia) supplemented bread. This result indicates that breads supplemented with AmyBS-I have adequate softness and low staling rate over time as compared to other tested samples (Table 4). Gambaro et al. [32] also reported that the

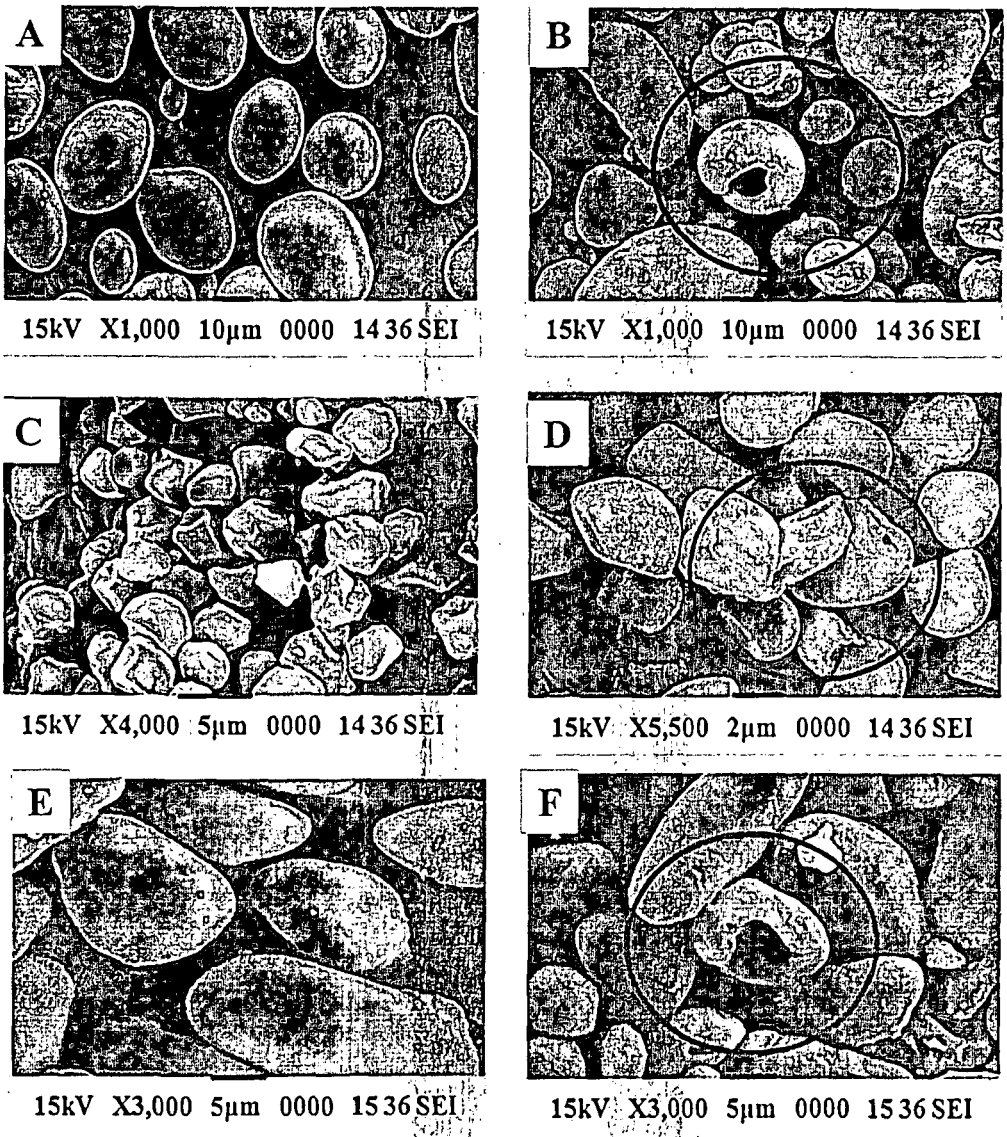

Fig. 5. SEM images of raw starch granules before and after hydrolysis with AmyBS-I for 6 h. (A) Untreated potato starch, (B) AmyBS-I treated potato starch, (C) untreated rice starch, (D) AmyBS-I treated rice starch, (E) untreated wheat starch, and (F) AmyBS-I treated wheat starch.

Table 3
A comparisons of properties of bread supplemented with commercial α-amylase and AmyBS-I. Control bread was made without supplementation of α-amylase to the dough.

Parameter	Control	Commercial α-amylase	AmyBS-I
Weight of dough (g)[a]	100 ± 5.0	100 ± 5.0	100 ± 5.0
Weight of bread (g)[a]	87.5 ± 4.4	76.5[b] ± 3.8	77[c] ± 3.8
Dough rise (cm)[a]	2.2 ± 0.1	2.9[b] ± 0.2	3.4[c,d] ± 0.2
Self-life (days)	4	5	5
Bread moisture (%)[a]	44.2 ± 2.2	39.1[b] ± 1.9	35.6[c,d] ± 1.7
Reducing sugars (mg/g of bread)[a]	37.6 ± 1.8	42.4[b] ± 2.1	44.0[c] ± 2.2
Overall acceptability[e]	++	+++	++++
Bread color[f]			
L-value	49.3	48.1	50.9
a-Value	1.2	2.5	2.9
b-Value	12.7	14.0	14.9

[a] Each value is expressed as mean ± standard dev. ($n = 3$).
[b] $P < 0.05$ between the values of control and commercial α-amylase treated bread within the same row.
[c] $P < 0.05$ between the values of control and AmyBS-I treated bread within the same row.
[d] $P < 0.05$ between the values of commercial α-amylase and AmyBS-I treated bread within the same row.
[e] Sensory evaluation (+ = average, ++ = good, +++ = very good, ++++ = the best).
[f] *L* = lightness index (0–100 = black – white), *a* = redness and greenness [(+100) – (−80) = red – green] while, *b* = yellowness and blueness [(+70) – (−80) = yellow – blue].

Table 4
Difference in TPA (between 0th day and 5thday) on storage of various bread samples supplemented with AmyBS-I and a commercial α-amylase. Values are mean ± standard deviation of triplicates data.

	Control	Bread supplemented with	
		Commercial α-amylase	AmyBS-I
Increase in hardness (*N*)	15.83 ± 0.79	4.05[a] ± 0.2	2.96[b,c] ± 0.14
Increase in gumminess (*N*)	1.7 ± 0.08	0.58[a] ± 0.029	0.45[b,c] ± 0.02
Decrease in springiness	0.12 ± 0.006	0.12 ± 0.006	0.15[b,c] ± 0.007
Decrease in cohesiveness	0.18 ± 0.009	0.12[a] ± 0.006	0.14[b,c] ± 0.007

[a] $P < 0.05$ between the values of control and commercial amylase within the same row.
[b] $P < 0.05$ between the values of control and AmyBS-I supplementation within the same row.
[c] $P < 0.05$ between the values of commercial amylase and AmyBS-I within same row.

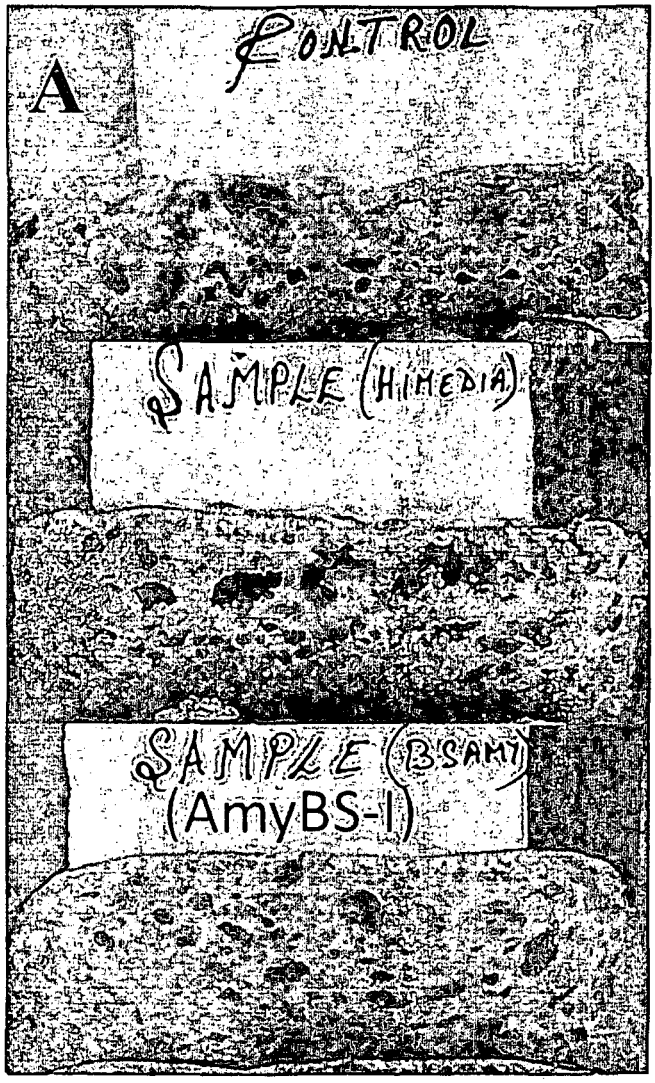

Fig. 6. Crumb structure of the loaf supplemented with AmyBS-I/commercial α-amylase/control (without enzyme).

addition of amylase retarded starch retrograding, which maintains the bread freshness for a relatively longer period.

4. Conclusions

The SPS facilitated the efficient extracellular over expression of AmyBS-I gene in *E. coli* cells. Further, the response surface optimization of culture parameters was found to be highly effective for enhancing the extracellular expression of catalytically active recombinant AmyBS-I. This suggests that this technique may be applied for the efficient extracellular expression of other recombinant proteins in *E. coli*. The biochemical properties of purified AmyBS-I suggested its candidature suitable for application in starch industry. Further, being capable of digesting raw starches from various sources, the application of AmyBS-I may reduce the production cost of starch-based foodstuffs. Additionally, due to amelioration of crumb structure and self-life of AmyBS-I supplemented bread; they may be stored for a longer period of time that is an added advantage to the baking industry.

Acknowledgements

Authors acknowledge the help extended by Dr. Naba K. Bordolai and Dr. Robin Doley of Tezpur University for technical assistance in DNA sequencing and kind donation of pET vector respectively. Authors also acknowledge Dr. Arup K. Nath of Tezpur University for careful editing of the manuscript. Mr. J.K. Roy is the recipient of Senior Research Fellowship from the Council of Scientific and Industrial Research (CSIR), New Delhi. This work was partially supported to A.K.M. by funding from "Strengthening of teaching, training and research in Universities and Colleges of North-East India" by the DBT, New Delhi and UGC-SAP (DRS-I), New Delhi. The instrument facility under DST-FIST programme of the department is duly acknowledged.

Appendix A. Supplementary data

Supplementary data associated with this article can be found, in the online version, at http://dx.doi.org/10.1016/j.molcatb.2013.07.019.

References

[1] M.J.E.C. van der Maarel, B. van der Veen, J.C.M. Uitdehaag, H. Leemhuis, L. Dijkhuizen, J. Biotechnol. 94 (2002) 137–155.
[2] J.K. Roy, S.K. Rai, A.K. Mukherjee, Int. J. Biol. Macromol. 50 (2012) 219–229.
[3] S. Sivaramakrishnan, D. Gangadharan, K.M. Nampoothiri, C.R. Soccol, A. Pandey, Food Technol. Biotechnol. 44 (2006) 173–184.
[4] R.E. Ghorbel, S. Maktouf, E.B. Massoud, S. Bejar, S.E. Chaabouni, Appl. Biochem. Biotechnol. 157 (2009) 50–60.
[5] Y. Bai, H. Huang, K. Meng, P. Shi, P. Yang, H. Luo, C. Luo, Y. Feng, W. Zhang, B. Yao, Food Chem. 131 (2012) 1473–1478.
[6] N. Goyal, J.K. Gupta, S.K. Soni, Enzyme Microb. Technol. 37 (2005) 723–734.
[7] A. Asoodeh, J. Chamani, M. Lagzian, Int. J. Biol. Macromol. 46 (2010) 289–297.
[8] S. Liu, K. Du, W. Chen, G. Liu, M. Xing, J. Ind. Microbiol. Biotechnol. 39 (2012) 1301–1307.
[9] P. Van-Solingen, D. Meijer, W.A.H. van der Kleij, C. Barnett, R. Bolle, S.D. Power, B.E. Jones, Extremophiles 5 (2001) 333–341.
[10] J.H. Choi, S.Y. Lee, Appl. Microbiol. Biotechnol. 64 (2004) 625–635.
[11] J.D. Thompson, D.G. Higgins, T.J. Gibson, Nucleic Acids Res. 22 (1994) 4673–4680.
[12] K. Das, R. Doley, A.K. Mukherjee, Appl. Biochem. Biotechnol. 40 (2004) 291–298.
[13] R.H. Myers, D.C. Montgomery, Response Surface Methodology: Process and Product Optimization using Designed Experiments, third ed., Wiley-Interscience, New York, 2002.
[14] D.Z. Ayadi, R. Kammoun, S. Jemli, S. Bejar, Biologia (Bratisl.) 66 (2011) 945–953.

[15] P K Lo O Hassan A Ahmad N M Mahadi R M Illias Enzyme Microb Technol 40 (2007) 1256–1263
[16] U Laemmli Nature 224 (1970) 680–685
[17] M Kusuda M Nagai T C Hur M Ueda T Terashita Mycoscience 44 (2003) 311–317
[18] D Mehta T Satyanarayana J Mol Catal B Enzym 85–86 (2013) 229–238
[19] A Sharma T Satyanarayana Appl Biochem Biotechnol 168 (2012) 1025–1034
[20] H Zhu F Wang W Huang J Zheng P Rayas-Duarte J Agric Food Chem 58 (2010) 1878–1883
[21] I Mnif S Besbes R Ellouze S Ellouze-Chaabouni D Ghribi Food Sci Biotechnol 21 (2012) 1105–1112
[22] M Yamabhai S Emtiat S Sukasem P Pesatcha N Jaruserance B Buranabanyat J Biotechnol 133 (2008) 50–57
[23] J J M Meirelhas D K Summers G A Monteiro Biotechnol Adv 23 (2005) 177–202
[24] G Feller O Le Bussy C Gerday Appl Environ Microbiol 64 (1998) 1163–1165
[25] R J Falconer B K O Neill A P J Middelberg Biotechnol Bioeng 53 (1997) 453–458
[26] R Gupta P Gigras H Mohapatra V K Goswami B Chauhan Process Biochem 00 (2003) 1–18
[27] S K Rai J K Roy A K Mukherjee Appl Microbiol Biotechnol 85 (2010) 1437–1450
[28] R H Sajedi H Naderi-manesh K Khajeh B Ranjbar N Ghaemi M Naderi Manesh Appl Biochem Biotechnol 119 (2004) 41–50
[29] H Li Z Chi X Wang X Duan L Ma L Gao Enzyme Microb Technol 40 (2007) 1006–1012
[30] X D Liu Y Xu Bioresour Technol 99 (2008) 4315–4320
[31] E J Pyler F J Pyler (Eds.) Baking Science and Technology vol 2 Sosland Publisher KS USA 1988 pp 815–849
[32] A Gambaro A Gimenez G Ares V Gilardi J Texture Stud 37 (2006) 300–314

Biochemical Engineering Journal 77 (2013) 220–230

Contents lists available at SciVerse ScienceDirect

Biochemical Engineering Journal

journal homepage www elsevier com/locate/bej

Regular article

Applications of a high maltose forming, thermo-stable α-amylase from an extremely alkalophilic *Bacillus licheniformis* strain AS08E in food and laundry detergent industries

Jetendra K Roy*, Ashis K. Mukherjee

Microbial Biotechnology and Protein Research Laboratory Department of Molecular Biology and Biotechnology School of Science Tezpur University Tezpur 784028 Assam, India

ARTICLE INFO

Article history
Received 24 March 2013
Received in revised form 17 May 2013
Accepted 15 June 2013
Available online xxx

Keywords
Amylase
Purification
Optimization
Starch
Alkalophilic bacteria
Maltose forming

ABSTRACT

An alkalophilic bacterial strain was isolated from the soil sample of Assam North-East India This strain was found capable of growing and producing α-amylase at extremely alkaline pH (12 5) By molecular characterization this bacterium was identified as *Bacillus licheniformis* strain AS08E Statistical optimization of media components resulted in 3-fold increase in the production of α-amylase from this bacterium From this strain a major extracellular α-amylase of ~55 kDa was purified to homogeneity with a 14 5-fold increase in its specific activity The N-terminal sequence of this enzyme showed extensive identity with α-amylases purified from thermostable bacteria The purified enzyme showed optimum activity at pH 10 0 and 80 C and demonstrated stability toward various surfactants organic solvents and commercial laundry detergents The spectroflurometric analysis suggests that the enzyme has a strong binding affinity toward soluble starch TLC analysis of starch degradation product displays this α-amylase as a high maltose-forming enzyme The future application of this enzyme in food and detergent industries is highly promising

1 Introduction

Alpha-amylase (E C 3 2 1 1) is an endo-acting enzyme that randomly hydrolyses α-(1→4) glycosidic linkages of starch macromolecules to produce dextrins, which are then gradually hydrolyzed to produce smaller oligosaccharides [1] The α-amylases can be obtained from various natural resources viz plant animal and microorganisms Nevertheless bacterial and fungal α-amylases dominate the commercial production because of their ease of manipulation cost-effectiveness and efficient production of desired characteristic enzymes [2] Amylases share about 25% of the industrial enzyme market of the world Further with the advancement of biotechnology, the application of α-amylase have been expanded to various fields such as medicinal clinical and analytical chemistry besides being widely used in starch saccharification detergent textile, food and brewing industries [2]

During the last decades, α-amylases capable of functioning at pH ≥ 8 0 and temperature ≥ 75 C have drawn attention of the scientists throughout the world for their multipurpose usage They are extensively used in starch saccharification process bio-ethanol production and in textile industries, besides being used as a detergent additive to improve the wash performance of detergents [3 4] However despite having a tremendous scope for application of this class of enzymes in commercial laundry detergent formulations limited attempts have been made so far to isolate a laundry detergent stable α-amylase [4 5] Furthermore there is also a growing demand for those α-amylases capable of producing high levels of maltose from starch owing to the fact that maltose has diverse applications in food pharmaceuticals and fine chemical industries [6]

Microbial diversity is the natural asset of any country and exploration of the biodiversity is the major dynamic force behind the expansion of biotechnological products and processes The North-eastern region of India is known as one of the mega biodiversity hot-spot zones in this earth Thus in our study, we isolated a potent bacterial strain from the soil sample of this region which was capable of secreting highly alkaline α-amylase in the culture medium at 45 °C and at a pH range of 12–13 In general 'alkalophilic bacteria grows in the pH range of 9–12 [3] but interestingly, this is the first report which shows both the growth and production of alkaline α-amylase beyond pH 12 0

The optimization of process parameters is an important prerequisite for improving the production of secondary metabolite by bacteria Therefore, development of a cost-effective production

* Corresponding author at Department of Molecular Biology and Biotechnology Tezpur University Tezpur 784028 Assam India Tel +91 9706479164 fax +91 3712 267005/3712 267006
E mail addresses jetu@tezu ernet in jetu20@gmail com (J K Roy)

1369 703X/$ - see front matter © 2013 Elsevier B V All rights reserved
http //dx doi org/10 1016/j bej 2013 06 012

Table 1
Observed and predicted values of alkaline α-amylase production by strain AS08E using Plackett–Burman design

Run order	Starch (% w/v)	Beef extract (% w/v)	Peptone (% w/v)	NaCl (% w/v)	Temp (°c)	pH (H+)	NH_4Cl (% w/v)	Glycerol (% w/v)	KNO_3 (% w/v)	Maltose (% w/v)	$CaCl_2$ (% w/v)	Enzyme activity (U/ml)	
												Observed	Predicted
1	2 0(+)	0 5(−)	1 5(+)	0 25(−)	37 0(−)	11 5(−)	0 2(+)	1 5(+)	0 2(+)	0 5(−)	0 1(+)	69 53	67 09183
2	2 0(+)	1 5(+)	0 5(−)	0 75(+)	37 0(−)	11 5(−)	0 1(−)	1 5(+)	0 2(+)	1 5(+)	0 05(−)	115 43	112 9918
3	0 5(−)	1 5(+)	1 5(+)	0 25(−)	53 0(+)	11 5(−)	0 1(−)	0 5(−)	0 2(+)	1 5(+)	0 1(+)	14 45	12 01183
4	2 0(+)	0 5(−)	1 5(+)	0 75(+)	37 0(−)	12 5(+)	0 1(−)	0 5(−)	0 1(−)	1 5(+)	0 1(+)	63 24	60 80183
5	2 0(+)	1 5(+)	0 5(−)	0 75(+)	53 0(+)	11 5(−)	0 2(+)	0 5(−)	0 1(−)	0 5(−)	0 1(+)	146 54	144 1018
6	2 0(+)	1 5(+)	1 5(+)	0 25(−)	53 0(+)	12 5(+)	0 1(−)	1 5(+)	0 1(−)	0 5(−)	0 05(−)	36 89	34 45183
7	0 5(−)	1 5(+)	1 5(+)	0 75(+)	37 0(−)	12 5(+)	0 2(+)	0 5(−)	0 2(+)	0 5(−)	0 05(−)	15 13	12 69183
8	0 5(−)	0 5(−)	1 5(+)	0 75(+)	53 0(+)	11 5(−)	0 2(+)	1 5(+)	0 1(−)	1 5(+)	0 05(−)	35 87	33 43183
9	0 5(−)	0 5(−)	0 5(−)	0 75(+)	53 0(+)	12 5(+)	0 1(−)	1 5(+)	0 2(+)	0 5(−)	0 1(+)	7 31	4 871833
10	2 0(+)	0 5(−)	0 5(−)	0 25(−)	53 0(+)	12 5(+)	0 2(+)	0 5(−)	0 2(+)	1 5(+)	0 05(−)	105 06	102 6218
11	0 5(−)	1 5(+)	0 5(−)	0 25(−)	37 0(−)	12 5(+)	0 2(+)	1 5(+)	0 1(−)	1 5(+)	0 1(+)	15 3	12 86183
12	0 5(−)	0 5(−)	0 5(−)	0 25(−)	37 0(−)	11 5(−)	0 1(−)	0 5(−)	0 1(−)	0 5(−)	0 05(−)	37 06	34 62183
13	1 25(0)	1 0(0)	1 0(0)	0 5(0)	45 0(0)	12 0(0)	0 15(0)	1 0(0)	0 15(0)	1 0(0)	0 075(0)	42 17	52 71267
14	1 25(0)	1 0(0)	1 0(0)	0 5(0)	45 0(0)	12 0(0)	0 15(0)	1 0(0)	0 15(0)	1 0(0)	0 075(0)	39 45	52 71267
15	1 25(0)	1 0(0)	1 0(0)	0 5(0)	45 0(0)	12 0(0)	0 15(0)	1 0(0)	0 15(0)	1 0(0)	0 075(0)	47 26	52 71267

R^2 = 98 33% Adj R^2 = 92 23%

medium requires proper selection of different media components followed by their optimization However, medium optimization by single dimensional search is laborious and time-consuming, especially for a large number of variables Besides, it does not ensure desirable conditions Due to aforementioned facts, statistical methodologies for media optimization are generally preferred over the strain improvement for enhancing the yield [7]

The most widely used technique for product optimization is the screening of significant factors from a large number of variables of the media components, using Plackett–Burman factorial design [8] followed by optimization of significant factors by response surface methodology [9] Therefore, the prime objective of this study was statistical optimization of process parameters for enhancing the alkaline α-amylase yield using PBD followed by RSM The other objectives were to purify and characterize a thermostable, high maltose forming alkaline α-amylase produced by this strain Subsequently, we also evaluated the biotechnological potential of the purified α-amylase for its application in laundry detergent formulations and food industry

2. Materials and methods

2 1 Materials

3 5-Dinitrosalicylic acid (DNS), soluble potato starch and all other media components were purchased from Hi-Media Laboratories (Mumbai, India) The kits (GeneJET Genomic DNA purification kit GeneJET Gel Extraction and GeneJET PCR purification kits) and other molecular biology reagents were obtained from Thermo Scientific Life Science Research (MA, USA) All other reagents of analytical grade were procured from either Merck (Mumbai India) or Hi-Media Laboratories (Mumbai, India)

2 2 Isolation and identification of alkaline α-amylase producing bacterial strain

For the screening of alkaline α-amylase producing bacteria from various soil samples of Assam, 10^{-4} dilution was plated on alkaline starch-agar plates containing fluconazole (antifungal agent) The plates were incubated for 24 h at 45 °C, and were subsequently, flooded with Gram's iodine solution (2% I_2 and 0 2% potassium iodide) The colonies with the largest halo-forming zones were selected for the further studies

Identification of this bacterium was done first by studying its morphological and physiological characteristics and secondly by sequencing of following genes gyrase subunit A (*gyrA*) RNA polymerase subunit B (*rpoB*), 16S rDNA and 16S–23S ISR region The genomic DNA of the bacteria was isolated as described by Ausubel et al [10] The PCR amplification of the above stated genes was carried out using oligonucleotide primers listed in supplementary Table S1 The amplified PCR products were purified and sequenced using automated DNA sequencer (ABI3130 Genetic Analyser, Applied Biosystems)

The sequences so obtained were aligned and verified manually using BioEdit Sequence Alignment Editor (http //www mbio ncsu edu/bioedit html) and NCBI database (http //www ncbi nlm nih gov) Evolutionary distances were calculated using the Kimura 2-parameter using MEGA 5 software [11] Phylogenetic trees were constructed by neighbor-joining method [12] and the stability of the obtained trees was assessed by using BOOTSTRAP program in sets of 1500 resampling The sequence data generated in the present study have been submitted to the GenBank databases under accession no JN118574 JN133841, JN133842 and JN133843

2 3 Selection of significant variables by Plackett–Burman design

In order to select the important media constituents for amylase production, a range of carbon–nitrogen sources and physical parameters exemplified in Table 1 were tested and identified via the Plackett–Burman design These components were chosen because of their importance in bacterial α-amylase production [2] Eleven parameters were counted in for selection with each variable representing at three levels (Table 1) Based on Plackett–Burman design, each factor was studied at two levels low level (−) and high level (+), and a center point was run to estimate the linear and curvature effects of the variables [8] The experimental design in Table 1 illustrates the name and symbol code along with the actual level of the variables The principle effect of each variable on α-amylase production was estimated based on the variation between the two level measurements [8] The impact of each variable was determined via Student's *t*-test A linear approach has been adopted for screening of significant variables

$$Y = \beta_0 + \sum \beta_i X_i \quad (i = 1, \quad , k) \tag{1}$$

where Y is the estimated target function β_0, is the model intercept, β_i, is the linear coefficient, X_i, is the level of the independent variable

Table 2
Observed and predicted values of alkaline α-amylase production by *B licheniformis* strain AS08E using RSM

Run no	Independent variables			Y response (α-amylase yield in U/ml)	
	C_1	C_2	C_3	Observed value	Predicted value
1	−1 (1 5)	−1 (0 25)	−1 (10 5)	75 14	62 37
2	1 (2 5)	−1 (0 25)	−1 (10 5)	128 18	120 26
3	−1 (1 5)	1 (0 75)	−1 (10 5)	39 61	33 44
4	1 (2 5)	1 (0 75)	−1 (10 5)	117 47	121 64
5	−1 (1 5)	−1 (0 25)	1 (12 5)	32 47	28 12
6	1 (2 5)	−1 (0 25)	1 (12 5)	84 04	90 02
7	−1 (1 5)	1 (0 75)	1 (12 5)	29 07	36 81
8	1 (2 5)	1 (0 75)	1 (12 5)	116 45	129 03
9	−α (1 16)	0 (0 5)	0 (11 5)	7 82	16 95
10	+α (2 84)	0 (0 5)	0 (11 5)	152 04	143 17
11	0 (2 0)	−α (0 08)	0 (11 5)	78 09	89 29
12	0 (2 0)	+α (0 92)	0 (11 5)	108 69	97 75
13	0 (2 0)	0 (0 5)	−α (9 8)	60 52	81 83
14	0 (2 0)	0 (0 5)	+α (13 2)	72 36	59 25
15	0 (2 0)	0 (0 5)	0 (11 5)	136 11	141 72
16	0 (2 0)	0 (0 5)	0 (11 5)	148 75	141 72
17	0 (2 0)	0 (0 5)	0 (11 5)	141 68	141 72
18	0 (2 0)	0 (0 5)	0 (11 5)	140 55	141 72
19	0 (2 0)	0 (0 5)	0 (11 5)	138 95	141 72
20	0 (2 0)	0 (0 5)	0 (11 5)	144 56	141 72

R^2 = 96 43% R^2 (adj) = 93 22%

2 4 Statistical optimization of significant variables using RSM

The next step in the formulation of the medium was to determine the optimum levels of significant variables for alkaline amylase production A central composite design (CCD) was applied for the augmentation of amylase production and to understand the effect of three significant variables (i) concentration (%, w/v) of starch (C_1) (ii) concentration (%, w/v) of peptone (C_2), and (iii) pH of the medium (C_3) A conventional level for each factor was set to zero as a coded level The three factors were studied at three levels consisting of 20 experimental runs, and were adopted to analyze the experimental data The least and extreme ranges of the variables with their values in actual and coded forms are shown in Table 2 The response value (Y) in each trial was the average of triplicate results The data obtained from RSM on alkaline amylase production were subjected to analysis of variance (ANOVA) The resultant data were fitted as a second order polynomial regression equation including single and cross effect of each variable

$$Y = a_0 + \sum_{i=1}^{3} a_i C_i + \sum_{i=1}^{3} a_{ii} C_i^2 + \sum_{i=1}^{2} \sum_{j=i+1}^{3} a_{ij} C_i C_j \quad (2)$$

where Y = predicted response (α-amylase activity in U/ml), a_0 intercept term, a_i = linear effect, a_{ii} = square effect, a_{ij} = interaction effect, and C_i and C_j = variables The above equation was used to optimize the values of independent parameters for the response The subsequent equation was used for coding the variables

$$C_i = \frac{C_i - C_0}{\Delta C_i}, \quad i = 1, 2, 3, \quad , k \quad (3)$$

Multiple regression analysis, response surface plots, and ANOVA were performed using Minitab 15 Statistical Software® (Minitab Inc , PA, USA) The statistical implication of the model equation and the model terms were evaluated via Student's *t*-test The quality of fitness of the second-order polynomial model equation was expressed via the coefficient of determination (R^2) and the adjusted R^2 The integration of different optimized variables yielding the most response was attempted to validate the model

The optimized condition achieved during RSM implementation was experimentally validated by culturing the bacterial strain in a 5 L fermenter (New Brunswick Scientific, USA) In the fermenter, 3 L of the statistically optimized media (2 40% (w/v) of starch, 0 56% (w/v) of peptone and pH 11 4 of the media) was incubated at 45 C with a constant agitation speed of 200 rpm and aeration value of 2 0 lpm α-Amylase assay was performed with the cell free supernatant (CFS) so obtained by the centrifugation post 60 h of culture incubation

2 5 Alpha-amylase assay and protein estimation

Unless stated differently, amylolytic activity was assayed by measuring the reducing sugar released by the action of the enzyme on the substrate (1% soluble starch dissolved in 50 mM Tris–Cl buffer pH 9 0) after incubating at 60 °C for 30 min [4] One unit of enzyme activity was defined as the liberation of reducing sugar equivalent to 1 μmol of D-glucose/min under the assay conditions and the specific activity of the enzyme was calculated as the enzyme activity/mg of protein The protein content of each sample was measured by Lowry's method using bovine serum albumin as a standard [13]

2 6 Isolation and purification of α-amylase

An extracellular alkaline α-amylase was purified from CFS by hydrophobic interaction of enzyme with a Phenyl-Sepharose column This was followed by fractionation of the HIC bound proteins by gel-filtration chromatography In brief, *B licheniformis* strain AS08E were cultivated in a fermenter containing 1 L of the statistically optimized media at an agitation speed of 200 rpm and aeration value of 2 0 lpm at 45 °C The samples were withdrawn after a period of 60 h of incubation (initial screening), and centrifuged at 8000 × *g* for 15 min at 4 °C Solid $(NH_4)_2SO_4$ was gradually added to 1 L CFS to attain 1 M solution and stirred slowly for an additional 30 min at 4 °C to mix uniformly This solution was then applied to a Phenyl-Sepharose column (5 mm × 20 mm) attached with AKTA FPLC Purification System (Amersham Biosciences, Uppsala, Sweden) and the column was pre-equilibrated with buffer A (50 mM K-phosphate buffer, pH 7 4 containing 1 0 M $(NH_4)_2SO_4$) The column was washed with a linear gradient of 1 0–0 0 M $(NH_4)_2SO_4$ in buffer A at flow rate of 1 ml/min and 2 0 ml fraction was collected in each tube Elution of proteins was monitored constantly at 280 nm The fractions showing maximum α-amylase activity were pooled, dialyzed, concentrated and then further fractionated using FPLC-Sephacryl S-200 gel filtration column (120 ml),

pre-equilibrated with 50 mM K-phosphate buffer (pH-7 4) Elution of proteins was carried out with the equilibration buffer at cold conditions (~10 °C) and at a flow rate of 20 ml/h One ml fraction was collected in each tube and each fraction was checked for α-amylase activity and protein content

The homogeneity as well as molecular mass of the gel-purified fraction was checked by 10% SDS-PAGE of protein(s) under both reducing and non-reducing conditions [14] For α-amylase zymography study, 1% (w/v) soluble starch was incorporated into the native PAGE prior to polymerization of the gel The purified enzyme was then used for the study of its biochemical characterization and biotechnological potential

2 7 N-terminal sequencing

The N-terminal sequence of the purified alkaline amylase was determined by transferring the purified alkaline amylase band from SDS-PAGE to a polyvinylidene difluoride membrane (PVDF) This was followed by the determination of the sequence by the Edman degradation method on an ABI Procise 494 protein sequencer (Applied Biosystems) The obtained sequence was Blastp searched using NCBI database (http //www ncbi nlm nih gov) and aligned using CLC Main Workbench 5 software (http //www clcbio com)

2 8 Biochemical characterization

The optimum pH and temperature for α-amylase activity was determined by incubating enzyme with 1% (w/v) starch dissolved in different buffers (pH ranging from 4 0 to 12 0) and at different temperatures (40–100 °C), respectively and later assayed for their α-amylase activity against the control (substrate without enzyme) For determining the heat-denaturation of catalytic activity, α-amylase solutions (1 mg/ml) were incubated at different temperatures (40–100 °C) for 60 min either in presence or in absence of 5 mM Ca^{2+}, followed by assaying the enzyme activity To investigate the effects of inhibitors metal chelator, oxidizing agent, organic solvents and surfactants on α-amylase activity treatment of enzyme with EDTA, H_2O_2, methanol, acetonitrile, SDS, Triton X-100 and Tween-80 were performed as described in our previous study [4]

2 9 Raw starch adsorbability and starch binding affinity of purified amylase

Affinity of purified amylase toward raw potato and wheat starch was studied by incubating 0 2 g of raw starch granules in 1 0 ml of phosphate buffer with 100 U of enzyme solution at 4 C for 30 min After the incubation period, the reaction mixture was centrifuged for 5000 rpm for 5 min The enzyme activity in the supernatant was determined and its adsorbability percentage [15] was calculated as given by

$$\text{Adsorption } (\%) = \frac{A-B}{A} \times 100 \quad (4)$$

where A and B represent the α-amylase activity before and after adsorption on raw starch granules, respectively

Starch binding study of the purified α-amylase was determined by monitoring the intrinsic fluorescence spectra of purified enzyme and soluble starch (dissolved in 20 mM K-phosphate buffer by slight warming) using PerkinElmer LS 55 fluorescence spectrophotometer For binding study, the enzyme sample was incubated with starch solution in a cell for 5 min at 25 °C and then excited at 295 nm Consequently, the emission spectra were registered from 300 to 500 nm The excitation and emission slit were both set to 5 nm [16] A blank was also setup under similar conditions for determining any effects of phosphate buffer solutions

2 10 Analysis of end-product of raw potato starch hydrolysis

In separate sets of experiments, α-amylase was incubated with 2% (w/v) raw potato or wheat starch (dissolved in 50 mM K-phosphate buffer, pH 7 0) at 80 °C After 3 h of incubation 50 μl of aliquots (starch-hydrolyzed products) were withdrawn from each reaction and were analyzed by silica gel TLC as described by us [4] For quantitative analysis of the product formations each spot (corresponding to the developed region of the chromatogram from different plates) from unstained plates was scraped into separate tubes and dissolved in minimum volume of water The liberated sugar from each spot was then quantified using phenol–sulphuric method as described by Dubois et al [17] We also investigated the structure of native and digested starch (enzyme treated) by scanning electron microscope (SEM) at 15 kV (JEOL model JSM-6390 LV) as described in our earlier report [4 18]

2 11 Compatibility test with various commercial laundry detergents and wash performance analysis

The stability and compatibility of alkaline α-amylase against various commercial laundry detergents available in local market such as Surf excel®, Sunlight® and Wheel® (Hindustan Unilever Ltd, India), Tide® (Procter & Gamble, India) Henko® (Henkel India Ltd), Fena Ultra® (Fena Pvt Ltd , India), Safed® (Safechem Industries Ltd , India), and Nirma® (Nirma Ltd , India) were assessed by our previously elucidated procedures [4,19] The commercial α-amylase (Hi-media Laboratories, Mumbai, India) was used for comparative study under the identical experimental conditions The relative activity of α-amylase in presence of laundry detergent was expressed in percentage activity considering the activity of control (without detergent) as 100% To test the stability of α-amylase in presence of proteases enzyme, it was incubated with proteinase K (2 U/ml) for 30 min at 37 °C and thereafter its remaining activity was determined against the control

In order to determine the efficacy of purified α-amylase as a bio-detergent additive wash performance test was evaluated by treating the chocolate stained cotton fabrics with α-amylase by following the procedure described by Roy et al [4] The test flasks were kept at 37 °C for 60 min followed by removal of the cloth pieces and their visual examination after being dried

To ascertain the desizing efficiency of alkaline α-amylase from *B licheniformis* strain AS08E, a piece of cotton fabric (5 cm × 5 cm) was starched in liquid solution and oven dried The cloth strip was then dipped into a flask containing (a) 25 ml of tap water (control), and (b) 20 ml of tap water and 5 ml of 500 U/ml of purified α-amylase The test flasks were then kept at 75 °C for 30 min followed by removal of the cloth strips After drying each cloth strip was stained with the KI_2 solution Visual examination of various pieces of dried cloth exhibited the wash performance and desizing efficiency of the purified enzymes [20]

3. Results and discussion

3 1 Screening and taxonomic identification of alkaline α-amylase producing bacteria

Screening of soil sample of Assam resulted into two distinct colonies The highest extracellular alkaline α-amylase producing strain, capable of producing a $0\,66 \pm 0\,04\,cm^2$ (data not shown) clear zone of hydrolysis around the colony, was selected for further study

The phenotypic characterization of any strain is the first step toward its identification process Some of the characteristic phenotypic features of the isolated strain AS08E revealed its identity

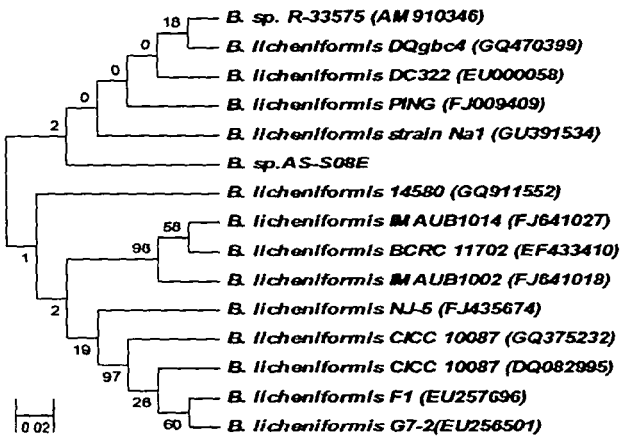

Fig 1 Phylogenetic relationships of *B licheniformis* strain AS08E and other closely related *Bacillus* species based on 16S rDNA sequencing The tree was generated using the neighbor-joining method the data set was resampled 1500 times by using the bootstrap option and percentage values are given at the nodes

with *Bacillus* group (data not shown) Nevertheless, genus *Bacillus* represents diverse genera with overlapping phenotypic characters that has prompted us for molecular characterization of the bacterium under study The 16S rDNA-based phylogenetic analysis demonstrated 97–99% sequence similarity of the strain AS08E with other species of *Bacillus* The phylogenetic tree constructed using neighbor-joining method (Fig 1) showed the detailed evolutionary relationships among strain AS08E and other closely related *Bacillus* species

In recent times, sequencing of conserved 'core genome' protein genes were used to assess phylogenies that are more determining than sequencing of 16S and 16S–23S genes alone [21] Therefore, using this approach our bacterium was identified up to species level by sequencing and phylogenetic analysis of ISR of 16S–23S rRNA (supplementary Fig S1), Rpo B (supplementary Fig S2) and gyrase A genes (supplementary Fig S3) This method offers a suitable and rapid means of providing information on the relatedness of species and strains Based on the biochemical, phenotypic and phylogenetic comparisons the bacterium was identified as *B licheniformis* strain AS08E

3 2 *Screening of significant variables using Plackett–Burman design*

The design matrix selected for the screening of significant variables, using Plackett–Burman design for alkaline α-amylase production along with corresponding responses is shown in Table 1 The adequacy of the model was assessed, and the statistically significant variables were screened via Student's *t*-test (supplementary Table S2) Significant factors with *p*-values <0 05 were selected for further optimization studies Starch with *p*-value of 0 002 was determined to be the most significant factor influencing this enzyme production, followed by peptone (0 017), and then by pH of the medium (0 021) These results are also evident from the Pareto charts for alkaline α-amylase production (Fig 2a) Fisher's test for analysis of variance shows the model *F* value is 16 10 and the coefficient of determination R^2 is 98 33% Thus, it advocates significance of the model (supplementary Table S3)

It is noteworthy that the bacterium under study could grow and produce α-amylase at highly alkaline pH (12 5), which is probably the first report on production of alkaline α-amylase by any species of *Bacillus* at such a high pH [5 22]

3 3 *Significant variables optimization using response surface methodology*

The results of the initial screening of media optimization experiment suggest the significant role-played by three factors (starch, peptone and pH of the media) in alkaline α-amylase production The experiments were conducted further using these three significant variables and were targeted toward the construction of a quadratic model consisting of twenty trials The design matrix of RSM experiments, determining the effects of three independent variables (starch, peptone, and pH of the medium) are shown in Table 2, along with the mean predicted values Multiple regression analysis was used to analyze the data and thereby derive the polynomial equation (Eq (5)) as follows

$$Y = -3358\,84 + 370\,63C_1 - 271\,01C_2 + 549\,37C_3 - 87\,26C_1^2 - 272\,91C_2^2 - 25\,17C_3^2 + 60\,63C_1C_2 + 2\,01C_1C_3 + 37\,63C_2C_3 \quad (5)$$

The adequacy of the model was checked using ANOVA which was tested using Fisher's statistical analysis (supplementary Table S4) The model *F*-value of 30 04 implies the significance of the proposed model The fitness of the model equation was further evaluated by determining the R^2 value The values of R^2 closer to 1 indicate that a major proportion of variance is accounted for by the regression model and it can predict better response [23] The observed values of R^2 (Table 2) explain that the fitted model could explain 96 43% of the total variation and hence vouch for adequacy of the model The adjusted R^2 value (93 22%) also advocates for a high significance of the model

The *p*-value suggests that among the three variables studied, C_2 (peptone concentration) and C_3 (pH of the media) showed maximum interaction between the two variables (supplementary Table S5) Among the tested variables, starch concentration and pH of the medium demonstrated a positive coefficient This suggests that an increase in the concentration of these factors might lead to enhancement of alkaline α-amylase production In contrary, the negative coefficient observed for the peptone (linear and quadratic) suggests an inverse relationship between the concentration of this complex organic source of nitrogen and the production of alkaline α-amylase Thus, lesser the concentration of peptone better is the enzyme production Our previous study has well demonstrated that the starch act as an inducer, whereas higher nitrogen content of the medium has an adverse effect on α-amylase production [4]

The three-dimensional response surface plots (Fig 2b–d) were drawn by taking two factors at a time and keeping the third factor at the minimum (zero) level It represents the regression equation and it was used to investigate the interaction amongst the variables Fig 2b depicts that lower concentration of peptone and higher concentration of starch (Fig 2c and d) could induce the optimum α-amylase production

Using the model derived from Eq (5) the predicted response for alkaline α-amylase yield was $159\,2 \times 10^3$ U/L, while the actual experimental value observed by using fermenter was $162\,9 \times 10^3$ U/L This results in three folds improvement in α-amylase production using the optimized medium Thus the validity of the model is justified The α-amylase yield reported in this study surpasses the reported values of α-amylase production by application of RSM from *Bacillus* sp [24] and *B subtilis* KCC103 [25] The alkaline α-amylase production from *B licheniformis* strain AS08E was comparable with some of the reported alkaline α-amylases production from *Bacillus* sp US 147 [5], *Bacillus* sp SMIA-2 [26] and *B licheniformis* NH1 [20]

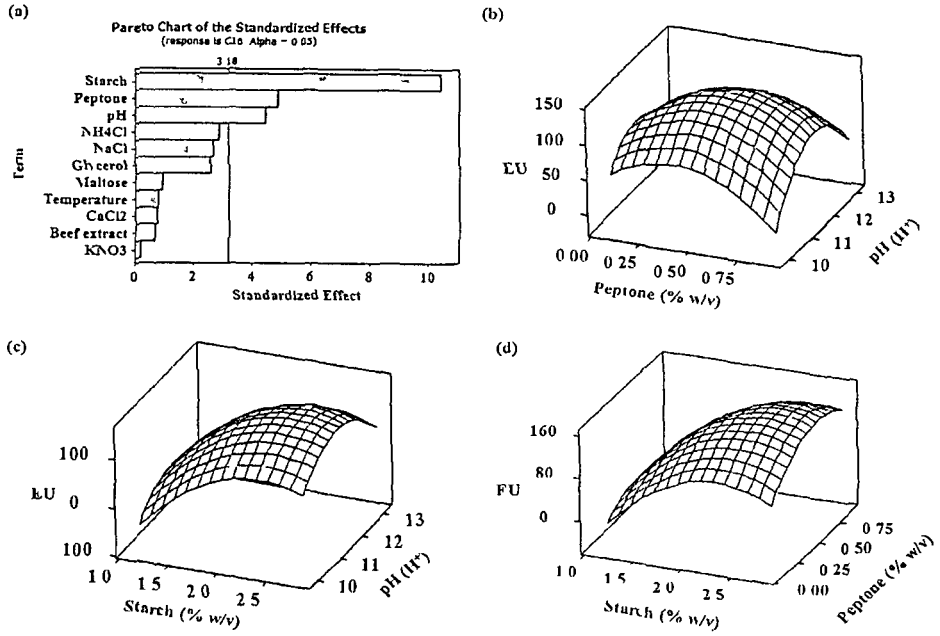

Fig 2 Pareto chart and response surface plots (RSP) for alkaline α amylase production by *B licheniformis* strain AS08E (a) Pareto chart showing the significant factors influencing the α amylase production (b) RSP between pH vs peptone (% w/v) (c) RSP between pH vs starch (% w/v) and (d) RSP between starch (% w/v) vs peptone (% w/v)

3 4 Purification and N-terminal sequencing

Alkaline α-amylase was eluted as a single peak (HIC-I) from phenyl-sepharose column with 0% salt concentration (supplementary Fig S4a) Further fractionation of this peak in gel-filtration column resulted into separation of the proteins into four peaks (supplementary Fig S4b) However the enzyme activity was confined to the third peak (GF-III) SDS-PAGE analysis of this GF-III peak showed a single band of approximately 55-kDa mass in reducing as well as non-reducing conditions (Fig 3a) suggesting monomeric nature of this enzyme This was further confirmed by amylase-zymographic study (under native condition) where it shows a single clear zone of starch hydrolysis (Fig 3a) A summary of the purification of this protein is shown in Table 3 By combination of various chromatographic techniques the alkaline α-amylase was purified up to 14 5 purification fold with a specific activity of 1043 8 U/mg The purified enzyme was named as AmyBL-I

The N-terminal amino acid sequence of *B licheniformis* strain AS08E α-amylase was found to be **ANLNGTLMQYFEWYMPNDGQ** (Fig 3b) which demonstrated 100% sequence similarity with some of the *B licheniformis* α-amylase entries in the PDB (NCBI) database The N-terminal amino acid sequence of α-amylase in the present study also demonstrated its close homology with N-terminal amino acid sequences of α-amylases isolated from thermostable bacteria (Fig 3b) This result reinforces the thermostable nature of the enzyme under study

3 5 Biochemical characterization of the purified enzyme

Biochemical characterization of any enzyme is of utmost importance before evaluating its biotechnological potential or industrial application Thus we performed the biochemical characterization of the purified alkaline α-amylase and found that it retained its activity and stability over a broad range of pH (6–12) and temperature (40–90 °C) however the enzyme displayed optimum activity at pH 10 and at 80 C The same optimum pH was obtained with the α-amylase of *Bacillus* L1711 *Bacillus* US147 [5] nevertheless α-amylase in the present study showed higher range of pH (6 0–12 0) stability as compared to the above mentioned α-amylases which vouches for its application in automatic dish-washers and laundry detergents as well as starch industry where high pH and high temperature are employed

Thermostability study demonstrated that heating the α-amylase for 60 min at 60 °C had no effect on enzyme activity However heating beyond this temperature resulted in a gradual loss of enzyme activity suggesting its moderate thermostable nature (supplementary Fig S5) Nevertheless it was also observed that the optimum temperature for enzyme activity is 80 °C which indicates that substrate (starch) act as a protective agent against the thermal denaturation of this α-amylase by forming enzyme–substrate complex which is more heat-stable than the enzyme alone [27] Further in presence of 5 mM Ca^{2+} ions the thermostability of enzyme reached up to 80 °C suggesting that it is metal dependent and requires Ca^{2+} ion for its thermostability by forming calcium–sodium–calcium triad [2] Various thermostable α-amylase enzymes have shown similar thermostability properties Such as the thermostable α-amylases isolated from *Anoxybacillus* sp show optimum activity at 60 °C [6] whereas those isolated from *B subtilis* JS-2004 [28] and *Bacillus* sp I-3 [15] show optimum activity at 70 °C but their stability reach up to 70–80 °C in presence of Ca^{2+} ions However the extracellular α-amylases from some of the bacteria such as those from *B licheni formis* CUMC 305 [29] and *B licheniformis* TCRDC-B13 [30] can reach up to 100 °C but most of them work between 60 and 80 °C and may find suitable application for the raw starch digestion in starch hydrolysis industries [11 15]

The purified alkaline α-amylase (Table 4) demonstrates significant stability in presence of metal-chelator denaturing agents oxidizing agent and surfactants which implies that it is an excel lent candidate for inclusion in laundry detergent formulations [4] However the enzyme activity was significantly effected by PMSF and 4 BPB implying a role for serine and histidine residues in the catalysis process (Table 4) Our previous study also vouched the above result [4 31] The purified α-amylase also showed

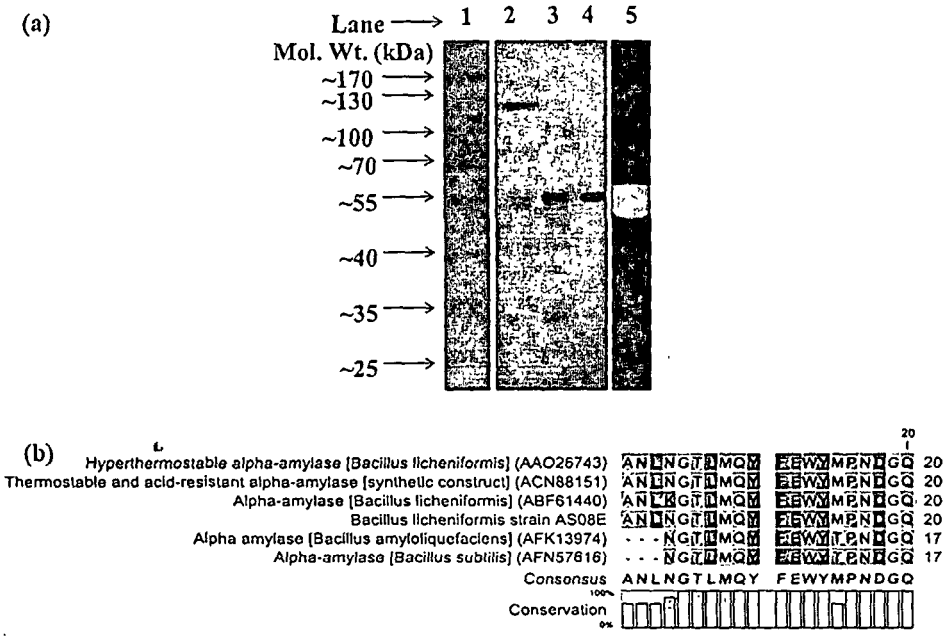

Fig. 3. (a) SDS-PAGE analysis of purified α-amylase from *B. licheniformis* strain AS08E; lane 1, protein molecular weight markers; lane 2, crude enzyme (concentrated); lane 3, HIC fraction (25 μg); lane 4, purified α-amylase (gel-filtration fraction) (15 μg); and lane 5, zymogram of purified amylase (20 μg). (b) Comparison of N-terminal amino acid sequence of α-amylase from *B. licheniformis* strain AS08E with known sequences in NCBI database.

Table 3
Summary of purification of alkaline α-amylase from *B. licheniformis* strain AS08E.

Purification step	Total protein (mg)	Total activity (U)	Specific activity (U/mg)	Purification (fold)	Enzyme yield (%)
Crude extract	2390	172,000	71.9	1	100.00
Phenyl-Sepharose	134	36,000	268.6	3.7	20.93
Sephacryl S-200	11.4	11,900	1043.8	14.5	6.9

considerable stability in presence of various organic solvents (Table 4). It bears the implication that alkaline α-amylase in the present study may be used as an additive in detergents containing organic solvents employed for washing colored stains from crocking and cutlery [5]. The purified α-amylase may also be used as model proteins for understanding the molecular basis of the alkalophilicity of the enzymes, which may be of great value in protein engineering or enzyme tailoring [32].

Table 4
Biochemical characterizations of purified α-amylase enzyme from *B. licheniformis* strain AS08E. Values are mean ± S.D. of triplicate determinations.

Effectors	Values
Control (without effectors)	100
EDTA (2 mM)	48.0 ± 2.4
PMSF (2 mM)	36.0 ± 1.8
4-BPB (2 mM)	43.0 ± 2.1
H_2O_2 (2 mM)	84.8 ± 4.2
SDS (1 mM)	88.0 ± 4.4
$CaCl_2$ (2 mM)	96.0 ± 4.8
Triton-x 100 (1%, v/v)	80.0 ± 4.0
Tween-80 (1%, v/v)	86.0 ± 4.3
Methanol (30%, v/v)	99.0 ± 4.9
Ethanol (30%, v/v)	97.0 ± 4.8
Acetonitrile (30%, v/v)	88.0 ± 4.4
Acetone (30%, v/v)	98.0 ± 4.8
Proteinase K (2 U/ml)	66.0 ± 3.3

3.6. Adsorbability and starch binding affinity of purified amylase

Adsorbability of raw starch digesting enzyme on raw starch is considered as one of the methods to determine the efficiency of the enzyme but is not an obligatory requirement [15]. Various raw starch digesting enzymes shows varied degree of raw starch adsorbability. In our study, the purified enzyme shows 95% adsorbability toward raw potato starch and 86% toward raw wheat starch. Goyal et al. [15] also observed the similar results in their studies.

The interaction effect of soluble starch on the purified enzyme (AmyBL-I) was studied by monitoring the change in the intrinsic fluorescence emissions of the enzyme with the help of fluorescence spectroscopy (Fig. 4). The maximum spectrum for the enzyme was 341 nm which suggests that the tryptophan residues is in limited contact with water and probably immobilized by bonding at the macromolecular surface [33]. While for the dissolved starch, the maximum spectra was 340 nm, which suggests that this fluorescence come from the transition from nonbonding electrons in the heteroatom (O) of the functional group (C–O–C) called ether linkage to the anti-bonding orbital sigma [34]. The fluorescence spectra of dissolved starch with enzymes showed that the enzymes have strong binding affinity toward soluble starch, as there was a clear shift in the band intensity (Fig. 4). This result also suggests that binding of starch molecules to the tryptophan residues of enzyme, protects it from quenching effects. There was also a very slight red shifting (342 nm) effect due to interaction, which may be

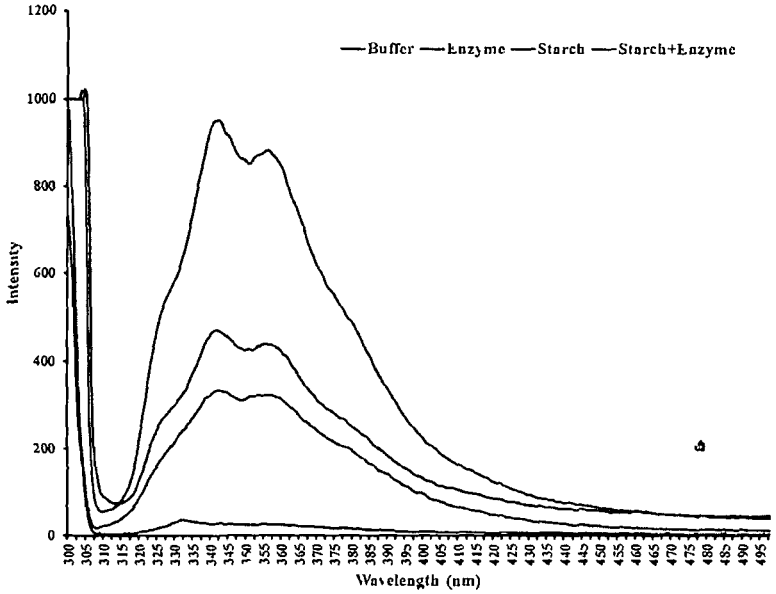

Fig 4 Fluorescence spectra of starch binding study of the purified enzyme

attributed to the maximum fluorescence emit peaks wavelength of the enzyme and the substrate [34]

3 7 *End-products of raw potato starch hydrolysis*

Maltose and maltotriose derived from starch hydrolysis are used in various fields most widely in the food industry because of their superior properties as a base material for food production and a sweetening agent [2 4] Maltose and high molecular weight oligosaccharides were detected as the main hydrolytic products post 3 h of incubation of potato and wheat starch with purified alkaline α-amylase (Fig 5a) Quantitative analysis shows that after 3 h of incubation the major products (30–40%) formed were disaccharides (maltose) followed by tri-saccharides (25–35%) and higher oligosaccharides (20–30%) While, glucose consists of only 10–15% of total product formed This study established that the enzyme is an α-amylase and suitable for the application in food processing and starch industry High maltose forming enzymes are having great demands in starch industry for their application in bio-ethanol production and baking industry [35] Further the SEM analysis also demonstrate that raw potato and wheat starches treated with purified alkaline α-amylase from *B licheniformis* strain AS08E form holes and pits (Fig 5d and e) which is in accordance with our previous finding [4]

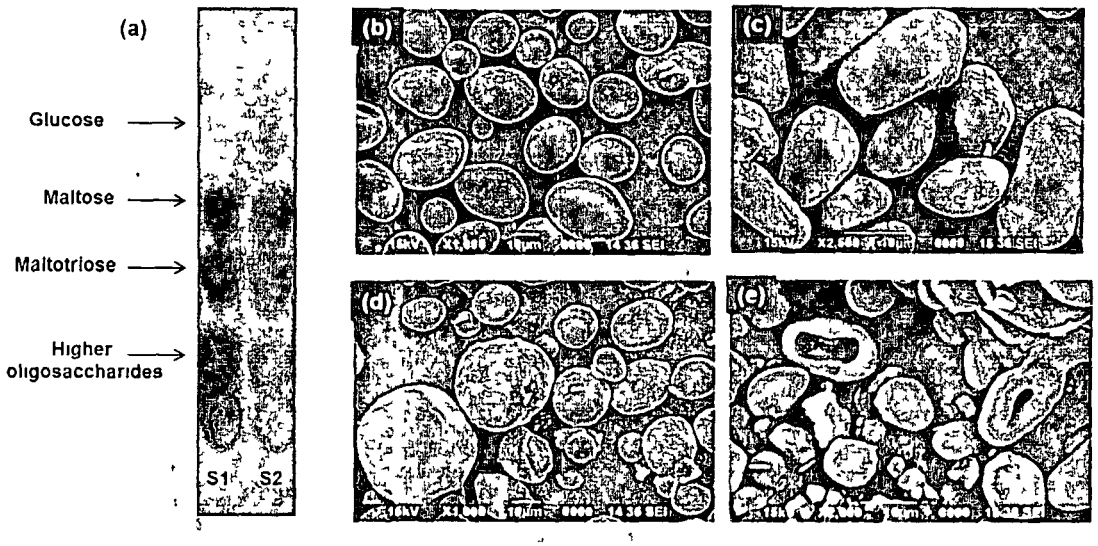

Fig 5 (a) TLC analysis of raw potato and wheat starch hydrolysis using purified alkaline α amylase from *B licheniformis* strain AS08E S1 = hydrolyzed sample of potato starch after 3 h of treatment S2 = hydrolyzed sample of wheat starch after 3 h of treatment with purified alkaline α amylase (b) SEM photograph of untreated raw potato starch (c) SEM photograph of untreated raw wheat starch (d) SEM photograph of raw potato starch treated with purified α amylase (6 h of treatment) and (e) SEM photograph of raw wheat starch treated with purified α amylase (6 h of treatment)

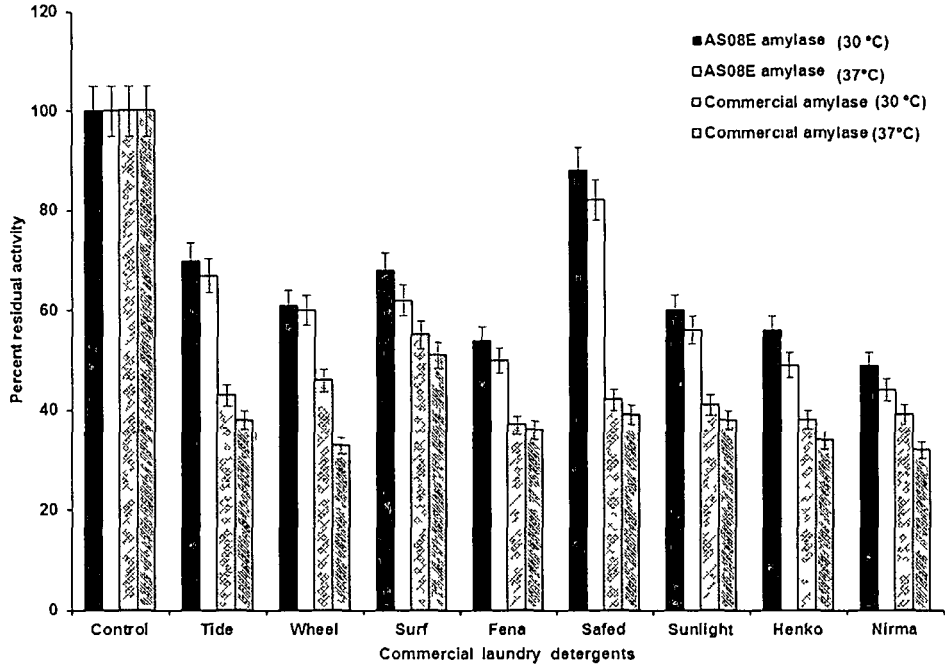

Fig 6 Detergent stability and compatibility of isolated α-amylase (0 7 mg/ml) from *B lichenıformıs* strain AS08E and commercial enzyme under the same conditions Values are mean ± S D of triplicate determinations

3 8 *Compatibility of α-amylase with commercial laundry detergents*

Powdered laundry detergents which constitute the largest part of the detergent market function at a high alkaline pH The α-amylase from *B lichenıformıs* strain AS08E exhibited a significant stability and compatibility with all the tested commercial laundry detergents (Fig 6) The purified α-amylase in the present study was found superior to the commercial α-amylase (Hi-media Laboratories Mumbai India) in laundry detergent stability study at 30 and 37 °C (Fig 6) These results clearly show that purified alkaline α-amylase might find an application in laundry detergent formulations

The partial loss of α-amylase activity in some of the laundry detergents may be attributed to inhibitory effect(s) of component(s) of these detergents for example anionic surfactants

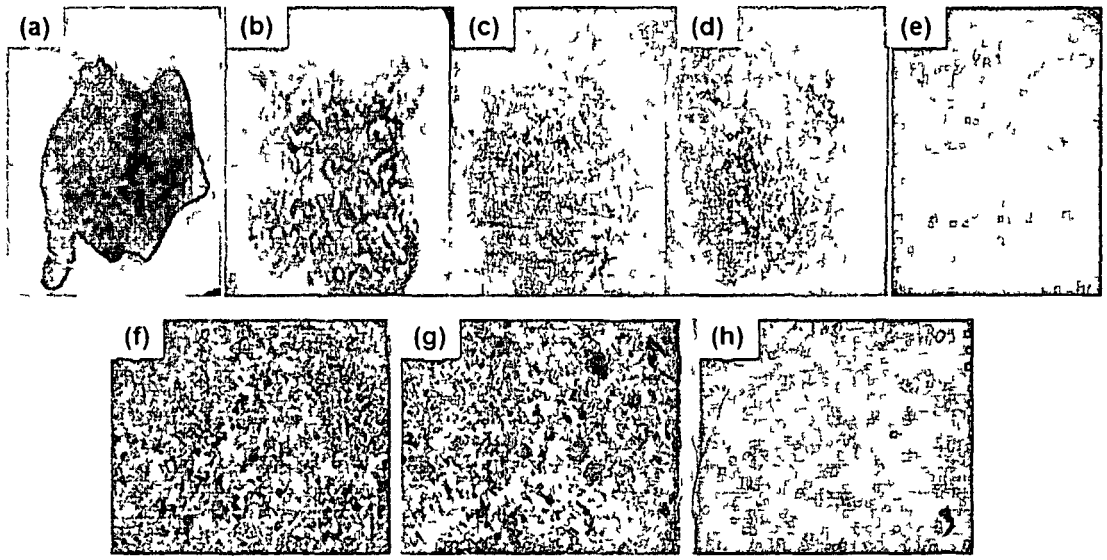

Fig 7 Wash performance and desizing analysis of purified alkaline α amylase from *B lichenıformıs* strain AS08E (a) Chocolate stain cloth (b) stained cloth washed with tap water (c) stained cloth washed with detergent solution (7 mg/ml) (d) stained cloth washed with purified alkaline α amylase (500 U/ml) (e) chocolate stained cloth washed with purified alkaline α amylase (500 U/ml) containing detergent solution (7 mg/ml) in a ratio of 1 1 (f) Starchy cloth (g) starchy cloth wash with tap water and (h) starchy cloth treated with alkaline α amylase (500 U/ml)

bleaching agents and water softening builders etc, which may influence the stability of enzyme in detergent [9 19] Further, limited proteolytic attack was observed on α-amylase activity in presence of proteinase K and was found to retain 66% of its original activity after 30 min of incubation with proteinase K at 37 °C (Table 4) This reinforces successful application of purified α-amylase in laundry detergent formulations containing protease enzymes, for improving the wash performance

3 9 *Wash performance analysis*

Fig 7a–e depicts that detergent (Safed®) supplemented with the purified α-amylase resulted in better stain removal from cotton fabrics as compared to that of detergent alone Further, Fig 7f–h shows that the purified α-amylase can also successfully remove starch from cotton fabrics, thereby, preventing the warp thread from breaking off during the weaving process [22] This reinforces the potential application of α-amylase as additives to laundry detergent formulations and for desizing activity in textile industries

4. Conclusion

Considering the ever-increasing market demand for high-maltose forming alkaline α-amylase, a three-fold increase in yield under optimized process conditions may contemplate to be a cost-effective process Furthermore, the isolated strain is probably the first example of a *Bacillus*, which can grow and produce alkaline α-amylase at highly alkaline pH (12 5) Therefore, the bacterium under study may be used as model organism for understanding the molecular basis of the alkalophilicity of various enzymes Finally, the ability of the purified enzyme to withstand higher temperature, broad range of pH and efficient digestion of raw starch suggests its biotechnological application in diverse industries

Acknowledgements

Authors acknowledge the help extended by Dr Naba K Bordoloi of MBBT Dept and Dr Lucky Dey of EFL Department, Tezpur University for the technical assistance in DNA sequencing and careful editing of the manuscript, respectively Mr J K Roy is the recipient of Senior Research Fellowship from the Council of Scientific and Industrial Research (CSIR) New Delhi This work was partially supported to A K M by funding from "Strengthening of teaching, training and research in Universities and Colleges of North-East India ' by the DBT New Delhi and UGC-SAP (DRS-I), New Delhi

Appendix A. Supplementary data

Supplementary material related to this article can be found, in the online version, at http //dx doi org/10 1016/j bej 2013 06 012

References

[1] W W Windish N S Mhatre Microbial amylases in W U Wayne (Ed) Advances in Applied Microbiology Academic Press New York 1965 pp 273–304
[2] R Gupta P Gigras H Mohapatra V K Goswami B Chauhan Microbial α-amylases a biotechnological perspective Process Biochem 00 (2003) 1–18
[3] T U Kim B G Gu J Y Jeong S M Byun Y C Shin Purification and characterization of a maltotetraose-forming alkaline α amylase from an alkalophilic *Bacillus* strain GM8901 Appl Environ Microbiol 61 (1995) 3105–3112
[4] J K Roy S K Rai A K Mukherjee Characterization and application of a detergent stable alkaline α-amylase from *Bacillus subtilis* strain AS-S01a Int J Biol Macromol 50 (2012) 219–229
[5] R E Ghorbel S Maktouf E B Massoud S Bejar S E Chaabouni New thermostable amylase from *Bacillus cohnii* US147 with a broad pH applicability Appl Biochem Biotechnol 157 (2009) 50–60
[6] Y Y Chai R N Z R A Rahman R M Illias K M Goh Cloning and characterization of two new thermostable and alkalitolerant α-amylases from the *Anoxybacillus* species that produce high levels of maltose J Ind Microbiol Biotechnol 39 (2012) 731–741
[7] Z J Xiao P H Liu J Y Qin P Xu Statistical optimization of medium components for enhanced acetoin production from molasses and soybean meal hydrolyzate Appl Microbiol Biotechnol 74 (2007) 61–68
[8] B J Naveena K Bhadriah G Reddy Selection of medium components by Plackett–Burman design for production of L(+)lactic acid by *Lactobacillus amylophilus* GV6 in SSF using wheat bran Bioresour Technol 96 (2005) 485–490
[9] S K Rai J K Roy A K Mukherjee Characterisation of a detergent-stable alkaline protease from a novel thermophilic strain *Paenibacillus tezpurensis* sp nov AS S24-II Appl Microbiol Biotechnol 85 (2010) 1437–1450
[10] F M Ausubel R Brent R E Kingston D D Moore J G Seidman J A Smith K Struhl Short Protocols in Molecular Biology John Wiley and Sons New York 1995 pp 2 12–2 14
[11] M Kimura A simple method for estimating evolutionary rate of base substitut ions through comparative studies of nucleotide sequences J Mol Evol 16 (1980) 11–120
[12] N Saitou M Nei The neighbor-joining method a new method for reconstruc ting phylogenetic trees Mol Biol Evol 4 (1987) 406–425
[13] O H Lowry N J Rosebrough A L Farr R J Randall Protein measurement with the Folin phenol reagent J Biol Chem 193 (1951) 265–275
[14] U K Laemmli Cleavage of structural proteins during the assembly of the head of bacteriophage T4 Nature 277 (1970) 680–685
[15] N Goyal J K Gupta S K Soni A novel raw starch digesting thermostable α-amylase from *Bacillus* sp 1-3 and its use in the direct hydrolysis of raw potato starch Enzyme Microb Technol 37 (2005) 723–734
[16] B Dabirmanesh S Daneshjou A A Sepahi B Ranjbar R A Khavari-nejad P Gill A Heydari K Khajeh Effect of ionic liquids on the structure stabil ity and activity of two related amylases Int J Biol Macromol 48 (2011) 93–97
[17] M Dubois K A Gilles J K. Hamilton P.A Rebers F Smith Calorimetric method for determination of sugars and related substances Anal Chem 28 (1956) 350–356
[18] T Matsubara Y B Ammar T Anindyawati S Yamamoto K Ito M Iizuka N Minamiura Degradation of raw starch granules by α-amylase purified from culture of *Aspergillus awamori* KT-11 J Biochem Mol Biol 37 (2004) 422–428
[19] A K Mukherjee M Borah S K Rai To study the influence of different components of fermentable substrates on induction of extracellular α-amylase synthesis by *Bacillus subtilis* DM-03 in solid state fermentation and exploration of feasibility for inclusion of α-amylase in laundry detergent formulations Biochem Eng J 43 (2009) 149–156
[20] N Hmidet N E Ali A Haddar S Kanoun S Alya M Nasri Alkaline proteases and thermostable α-amylase co-produced by *Bacillus licheniformis* NH1 characterization and potential application as detergent additive Biochem Eng J 47 (2009) 71–79
[21] N Parkinson V Aritua J Heeney C Cowie J Bew D Stead Phylogenetic analysis of *Xanthomonas* species by comparison of partial gyrase B gene sequences Int J Syst Evol Microbiol 57 (2007) 2881–2887
[22] P M Souza P O Magalhaes Application of microbial α-amylase in industry–a review Braz J Microbiol 41 (2010) 850–861
[23] W W Daniel A foundation for analysis in the health sciences hypothesis testing in W W Daniel (Ed) Biostatistics 7th ed Wiley New York 2000 pp 166–167
[24] G Dey A Mitra R Banerjee B R Maiti Enhanced production of amylase by optimization of nutritional constituents using response surface methodology Biochem Eng J 7 (2001) 227–231
[25] G Rajagopalan C Krishnan α Amylase production from catabolite derepressed *Bacillus subtilis* KCC103 utilizing sugarcane bagasse hydrolysate Bioresour Technol 99 (2008) 3044–3050
[26] R V Carvalho T L R Correa J Caroline L R C O Mansur M L L Martins Prop erties of an amylase from thermophilic *Bacillus* species Braz J Microbiol 39 (2008) 102–107
[27] M Michelin T M Silva V M Benassi S C Peixoto-nogueira L A B Moraes J M Leao J A. Jorge H F Terenzi M L T M Polizeli Purification and characterization of a thermostable α-amylase produced by the fungus *Paecilomyces variotii* Carbohydr Res 345 (2010) 2348–2353
[28] M Asgher M Asad S Rahman R Legge A thermostable α-amylase from a moderately thermophilic *Bacillus subtilis* strain for starch processing J Food Eng 79 (2007) 950–955
[29] T Krishnan A K Chandra Purification and characterization of α-amylase from *Bacillus licheniformis* CUMC 305 Appl Environ Microbiol 46 (1983) 430–437
[30] P Bajpai P K Bajpai High-temperature alkaline α amylase from *Bacillus licheniformis* TCRDC-B13 Biotechnol Bioeng 33 (1989) 72–78
[31] K Das R Doley A K Mukherjee Purification and biochemical characterization of a thermostable alkaliphilic extracellular α-amylase from *Bacillus subtilis* DM 03 a strain isolated from the traditional fermentated food of India Appl Biochem Biotechnol 40 (2004) 291–298
[32] S Shanmughapriya G S Kiran J Selvin R Gandhimathi T B Baskar A Manilal S Sujith Optimization production and partial characterization of an alkalophilic amylase produced by sponge associated marine bacterium *Halobacterium salinarum* MMD047 Biotechnol Bioprocess Eng 14 (2009) 67–75

[33] E.A Burstein, N S Vedenkina, M N Ivkova, Fluorescence and the location of tryptophan residues in protein molecules, Photochem Photobiol 18 (1973) 263–279
[34] H J He, R P Yu, T Zhu, Z B Gu, H Xu, Study of fluorescence spectra of starch suspension, Guang pu xue yu guang pu fen xi Guang pu 26 (2006) 1636 (PMID 17112035)
[35] J L.U M Rao, T Satyanarayana, Statistical optimization of a high maltose-forming, hyperthermostable and Ca^{2+} independent α-amylase production by an extreme thermophile *Geobacillus thermoleovorans* using response surface methodology, J Appl Microbiol 95 (2003) 712–718

International Journal of Biological Macromolecules 50 (2012) 219–229

Contents lists available at SciVerse ScienceDirect

International Journal of Biological Macromolecules

journal homepage www elsevier com/locate/ijbiomac

Characterization and application of a detergent-stable alkaline α-amylase from *Bacillus subtilis* strain AS-S01a

Jetendra K. Roy, Sudhir K. Rai, Ashis K. Mukherjee*

Microbial Biotechnology and Protein Research Laboratory Department of Molecular Biology and Biotechnology School of Science and Technology Tezpur University Tezpur 784028 Assam, India

ARTICLE INFO

Article history
Received 28 February 2011
Received in revised form 28 October 2011
Accepted 28 October 2011
Available online 6 November 2011

Keywords
Alkaline α-amylase
Bacillus
Detergent compatibility
Response surface method
Submerged fermentation

ABSTRACT

A strain AS-S01a, capable of producing high-titer alkaline α-amylase was isolated from a soil sample of Assam, India and was taxonomically identified as *Bacillus subtilis* strain AS-S01a Optimized α-amylase yield by response surface method (RSM) was obtained as 799 0 U with a specific activity of 201 0 U/mg in a process control bioreactor A 21 0 kDa alkaline α-amylase purified from this strain showed optimum activity at 55 °C and pH 9 0 and it produced high molecular weight oligosaccharides including small amount of glucose from starch as the end product The K_m and V_{max} values for this enzyme towards starch were determined as 1 9 mg/ml and 198 21 μmol/min/mg respectively The purified α-amylase retained its activity in presence of oxidant surfactants EDTA and various commercial laundry detergents thus advocating its suitability for various industrial applications

1. Introduction

α-Amylases (1,4-α-D-glucan glucanohydrolase [E C 3 2 1 1]) represent a group of extracellular starch hydrolytic enzymes which randomly cleave the 1,4-α-D-glucosidic linkages among adjacent glucose units in the linear amylose chain Currently they comprise 30% of world's enzyme consumption [1] α-Amylases are extensively used in the starch liquefaction process, which converts starch into fructose and glucose syrups [2,3] as a partial substitute of expensive malt in the brewing industry It is also used to improve flour in the baking industry as well as to produce modified starches for the paper industry [3] In addition, α-amylases with pH values higher than 8 0 have a potential application as an ingredient in automatic dishwasher and laundry detergent formulations [4]

The use of enzymes in detergents formulations known as "green chemicals in detergents" enhances the ability of the detergents to remove tough stains, making the detergent environmentally safe [5] Detergent enzymes account for about 40% of the total worldwide enzyme production and thus they represent one of the largest and most successful applications of modern industrial biotechnology [6] Amylases are second largest enzymes used in the formulation of enzymatic detergent, and about 90% of all liquid detergents contain these enzymes [7] The alkaline α-amylases are used in detergents to degrade the residues of starchy foods such as potatoes, gravies, custard, chocolate, etc [8] In fact, removal of starch from surfaces of fabrics is also important in providing a whiteness benefit, since starch tends to spread and act as a strong dirt binder in the laundry Therefore, non-degradation of adhering starch results in a less satisfactory wash [9]

Requirements for an optimally performing amylase are fairly specific for each industry, mainly concerning pH, oxidative stability chelator resistance and temperature behavior Oxidative stability of amylases is one of the most important criteria for their use especially in detergents where the washing environment is very oxidizing [9] Furthermore, the use of amylases in detergent formulations is problematic since the enzyme must offer stability and also an ideal level of activity in commercially used formulations particularly in the presence of proteases, surfactants and bleaching agents Liquid detergent formulation also faces the problem of use of amylase in liquid detergent in presence of calcium-chelating agents, known as builders The primary functions of these builders are to soften the wash water by binding and subsequently removing calcium and magnesium ions from hard water, which results in improvement of wash performance of detergents Majority of the α-amylases reported till date are calcium dependent in nature rendering them unsuitable for use in liquid detergent formulations Therefore, there is an urgent need to search for calcium-independent α-amylases for inclusion into modern liquid detergent formulations Furthermore, there is a dearth of report on thermostable, detergent and surfactant compatible and protease

* Corresponding author Present address School of Biological Sciences University of Northern Colorado Greeley CO 80639-0017 USA. Tel +91 7896003886 fax +91 3712 267005/267006
E-mail address akm@tezu ernet in (A K Mukherjee)

0141-8130/$ – see front matter © 2011 Elsevier B V All rights reserved
doi 10 1016/j ijbiomac 2011 10 026

stable α-amylase Therefore, bio-industrial sectors would welcome new potential microbial strains capable of producing high-titer α-amylases better suited for harsh industrial processes such as starch liquefaction and laundry detergent industries

The natural microorganisms have been considered as a great source of diverse enzyme production some of which may possess interesting features worthy of industrial application [10] Therefore, there is a great possibility of isolating novel and high-titer enzyme producing promising microbes by harnessing the natural environment It is worthy of attention that the North-eastern zone of India is considered as one of the mega biodiversity zones of the world, and it may harbor several novel microbial species Furthermore, the overall cost of enzyme production is one major obstacle in successful industrial application of enzymes, therefore the optimization of fermentation medium through a statistical approach, such as response surface methodology (RSM), has been well appreciated [11 12]

In the present study, we report the taxonomic identification of a high-titer and a detergent and surfactant stable alkaline α-amylase producing bacterial strain isolated from a soil sample of Assam, North-East India Additionally, the factors significantly effecting the alkaline α-amylase production in submerged fermentation condition were screened by one variable at a time Finally, the alkaline α-amylase production by this strain in submerged fermentation (SmF) was enhanced by RSM, which uses shake-flask study This was further validated by production of amylase in a process-controlled bioreactor A detergent stable alkaline α-amylase was purified from this strain, and some biochemical properties of the purified enzyme concerning its application in the detergent industry were characterized Our study suggested the potential application of this purified alkaline α-amylase for inclusion in laundry detergent formulations as well as its use in food processing industry

2. Materials and methods

2 1 Isolation of alkaline α-amylase producing bacterium and its identification

For the screening of α-amylase producing bacteria from various soil samples of Assam, 10^{-4} dilution was plated on starch-agar plates containing fluconazole (antifungal agent) Plates were incubated in inverted position at 45 °C temperature, pH 7 0 for 24 h The visible zones of hydrolysis around the bacterial colonies were measured by Gram's iodine solution (containing KI and I_2), and the colonies with large halo-forming zones were isolated Before they were used as inoculums for α-amylase production under SmF condition the bacteria were sub-cultured on nutrient-agar plates Based on the result of initial screening, a high-titer alkaline α-amylase producing strain was selected for further study

2 2 Identification of strain

Identification of the bacterium was carried out by (a) studying its phenotypic characteristics (b) gas-chromatographic (GC) analysis of cellular fatty acid methyl esters [13], and (c) by sequencing of following genes gyrase subunit A (*gyrA*) RNA polymerase subunit B (*rpoB*), 16S rRNA and 16S-23S ISR region For the sequencing analysis the genomic DNA of bacteria was isolated as described by Ausubel et al [14] PCRs were performed for 30 cycles, each consisting of a 1 min denaturation step at 94 °C, a 1 min annealing step between 45 and 55 °C, and a 2 min extension step at 72 °C The oligonucleotide primer sequences used in the studies are listed in supplementary Table S1 The PCR products were purified and directly used for the automated DNA sequencing using 3130 Genetic Analyzer (Applied Biosystem, Switzerland) The deduced sequence was subjected to BLAST search tool from the National Center of Biotechnology, Bethesda, MD (http //www ncbi nlm nih gov) in order to retrieve the homologous sequences in Genbank The above sequences can be retrieved from the GenBank using accession number FJ887877, JN118575, JN133844 and JN133845, respectively

2 3 Phylogenetic analysis

Phylogenetic analysis of genes sequences data of bacteria under study was aligned with reference sequences homology from the NCBI database using the multiple sequence alignment programme of MEGA 4 [15] Phylogenetic trees were constructed by distance matrix-based cluster algorithms viz unweighted pair group method with averages (UPGMA) neighbour-joining, maximum-likelihood, and maximum-parsimony analysis as described elsewhere [12] All ambiguous positions were removed for each sequence pair The trees were rooted using *Escherichia coli* strain K 12 MG1655 (accession no U00096) as out group The stability of trees obtained from above cluster analysis was assessed by using BOOTSTRAP program in sets of 1000 re-samplings (MEGA 4)

2 4 Screening of the influence of process parameters on α-amylase yield in SmF

To check the effects of pH and temperature on bacterial growth and alkaline α-amylase production, the bacteria were propagated at different temperatures (30–60 C), pH ranges (5 0–12 0), and for different time intervals (24–120 h) in 100 ml aliquots of M9 media at an agitation speed of 200 rpm Any one of them was used as a co-carbon source (1 0%, w/v or v/v) glycerol, glucose, galactose lactose, sucrose, maltose, starch, and cellulose One of the following at a concentration of 1 0% (w/v) served as the co-nitrogen source beef extract, yeast extract, peptone, tryptone, casein, NH_4Cl, KNO_3, NH_4NO_3, $NaNO_3$, and $(NH_4)_2SO_4$ To evaluate the impact of agitation on α-amylase production bacterial cultures (with optimized media) were placed in an incubator shaker and were agitated at 100–300 rpm range

2 5 α-Amylase assay

Unless otherwise stated, amylolytic activity of enzyme was assayed by measuring the reducing sugars released from 1 0% (w/v) of starch (dissolved in 50 mM Tris–HCl buffer pH 9 0) by the alkaline α-amylase under study at 55 °C post 30 min of incubation [16] One unit of enzyme activity was defined as the liberation of reducing sugars equivalent to 1 μmol of D-glucose liberated per min under the assay condition For determining the kinetics (K_m and V_{max} values) of enzyme catalyzed reaction, α-amylase assay was carried out by starch–iodine method [17]

2 6 Enhancement of α-amylase production in SmF using response surface methodology

The levels of the significant parameters and the interaction effects among various media constituents which influenced significantly the α-amylase production were analyzed and optimized by RSM [18] It was used to estimate main effects on response, i e the α-amylase yield Central composite design consisting of three main critical independent variables, (i) concentration (% w/v) of starch (C_1), (ii) concentration (%, w/v) of beef-extract (C_2) and pH of the medium (C_3) were chosen as the independent variables capable of influencing the alkaline α-amylase production (Y) by strain AS-S01a in SmF (Table 1) For each factor a conventional level (determined from the earlier experiment considering one variable at a time) was

Table 1
Observed responses and predicted values of alkaline α-amylase production by *B subtilis* strain AS-S01a using RSM The observed values are mean ± S D of triplicate determinations

Run no	Independent variables			Y response (alkaline α-amylase yield in U)	
	C_1	C_2	C_3	Observed value	Predicted value
1	−1(0 75)	−1(0 2)	−1(5)	234 0 ± 11 7	266 30
2	1(1 25)	−1(0 2)	−1(5)	518 5 ± 25 9	516 00
3	−1(0 75)	1(0 4)	−1(5)	286 5 ± 14 3	316 02
4	1(1 25)	1(0 4)	−1(5)	243 5 ± 12 2	256 46
5	−1(0 75)	−1(0 2)	1(7)	10 5 ± 1 0	18 16
6	1(1 25)	−1(0 2)	1(7)	525 0 ± 26 0	516 61
7	−1(0 75)	1(0 4)	1(7)	263 5 ± 13 2	287 12
8	1(1 25)	1(0 4)	1(7)	487 5 ± 24 4	476 32
9	−α(0 58)	0(0 3)	0(6)	228 5 ± 11 0	183 03
10	+α(1 42)	0(0 3)	0(6)	536 5 ± 27 0	552 09
11	0(1)	−α(0 13)	0(6)	445 0 ± 22 3	437 60
12	0(1)	+α(0 47)	0(6)	468 0 ± 23 4	445 53
13	0(1)	0(0 3)	−α(4 3)	246 0 ± 12 3	213 21
14	0(1)	0(0 3)	+α(7 7)	186 5 ± 9 3	189 42
15	0(1)	0(0 3)	0(6)	418 5 ± 20 9	452 98
16	0(1)	0(0 3)	0(6)	423 0 ± 21 1	452 98
17	0(1)	0(0 3)	0(6)	416 0 ± 21 0	452 98
18	0(1)	0(0 3)	0(6)	426 0 ± 21 0	452 98
19	0(1)	0(0 3)	0(6)	424 0 ± 21 0	452 98
20	0(1)	0(0 3)	0(6)	423 0 ± 21 0	452 98

set to zero as a coded level These three factors, each with three coded levels consisting of 20 experimental runs, were used to analyze the experimental data The experimental data was fitted as a second order polynomial regression equation including individual and cross effect of each variable

$$Y = a_0 + \sum_{i=1}^{3} a_i C_i + \sum_{i=1}^{3} a_{ii} C_i^2 + \sum_{i=1}^{2} \sum_{j=i+1}^{3} a_{ij} C_i C_j \quad (1)$$

where Y is the predicted response (total amylase activity in U/ml), a_0 is intercept term a_i is linear effect, a_{ii} is square effect, a_{ij} is interaction effect and C_i and C_j is the variables The above Eq (1) was used to optimize the values of independent parameters for the response The following equation was used for coding the variables

$$C_i = \frac{c_i - c_0}{\Delta c_i}, \quad i = 1, 2, 3, \quad , k \quad (2)$$

Multiple regression analysis, response surface plots, and analysis of variance (ANOVA) were performed using Minitab 15 Statistical Software® (Minitab Inc , PA, USA)

2 7 *Validation of results of shake-flask study in a process-controlled bioreactor*

Batch fermentation was carried out in a 5000 ml Bioflow 110 Fermenter at 45 °C in optimized medium (RSM) composed of 1 421% (w/v) of starch, 0 131% (w/v) of beef-extract and pH of the medium was adjusted to 6 1 [19] The cells were harvested at different time periods (12, 24, 30, 36, 40, 48, 60 and 72 h post-inoculation) and the cell-free clear supernatant was used to determine the α-amylase yield from strain AS-S01a

2 8 *Isolation and purification of α-amylase*

Alkaline α-amylase was purified from crude enzyme by ammonium sulphate precipitation followed by acetone precipitation, and then fractionation of precipitated proteins by gel-filtration Briefly, solid ammonium sulphate was gradually added to 1000 ml cell-free supernatant (obtained post 60 h of fermentation) to attain 50% (w/v) saturation and it was then stirred slowly for 4 h at 4 °C The precipitate was recovered by centrifugation at 8000 rpm for 15 min at 4 C and dissolved in a minimum volume of 20 mM K-phosphate buffer, pH 7 0 The above fraction was dialyzed extensively against the distilled H_2O to remove the salt and further precipitated with pre-chilled acetone (1 1 5, v/v) The solution was left at −20 C for 12 h The precipitate was recovered by centrifugation at 8000 rpm for 15 min at 4 °C and then dissolved in 1 5 ml of 20 mM K-phosphate buffer, pH 7 0 It was then loaded to Sephadex G-50 gel-filtration column (1 cm × 64 cm) previously equilibrated with the same buffer Elution was carried out with the equilibration buffer at room temperature (~23 °C) at a flow rate of 24 ml/h One ml fraction was collected in each tube and each fraction was checked for alkaline α-amylase activity and protein content

The homogeneity as well as molecular mass of the gel filtration fraction displaying highest α-amylase activity was checked by 12 5% SDS-PAGE of protein(s) under reducing as well as and non-reducing conditions [20] This purified enzyme was used for characterizing its biochemical properties and laundry detergent stability

For amylase zymography study, 1% (w/v) soluble starch was incorporated into the native PAGE before the addition of ammonium persulphate The gel was run for about 5 h at 4 C and then it was washed with buffer containing 1% (v/v) Triton-X-100 Thereafter it was reacted with a 1% (w/v) soluble starch solution [containing 0 5% (v/v) Triton-X-100 and 0 6% NaN_3] overnight at 45 °C The gel was then stained with iodine until clear band appeared

2 9 *Analysis of end-product of starch hydrolysis*

Alkaline α-amylase was incubated with 1% (w/v) starch (in 50 mM Tris–HCl buffer, pH 9 0) at 55 C The measured volume of aliquots (starch hydrolyzed products) was withdrawn at 30 and 60 min post incubation and analyzed by TLC [16] The native and degraded products of starch post treatment with α-amylase were also studied by scanning electron microscope at 15 kV (JEOL model JSM-6390 LV) as described by Matsubara et al [21]

2 10 *Biochemical characterization*

The optimum pH for α-amylase activity was determined by incubating 10 μg of enzyme with 1% (w/v) starch dissolved in different buffers (pH ranging from 6 0 to 13 0) For determining the optimum temperature, the enzyme was incubated at different

temperatures (ranging from 25 to 65 °C) at optimum pH (9 0), followed by assaying the alkaline α-amylase activity against the control (substrate without enzyme) For determining the heat-denaturation of catalytic activity, purified alkaline α-amylase (1 mg/ml) was incubated at different temperatures ranging from 35 to 95 °C for 30 min either in presence or absence of 5 mM Ca^{2+}, followed by assaying the enzyme activity The K_m and V_{max} values of the alkaline α-amylase were calculated by using a Lineweaver–Burk plot using different concentrations of starch [0 1–2% (w/v)] as substrate and by plotting the values of $1/V$ as a function of $1/S$

To investigate the effects of chemical modifications, metal-chelator, bleaching agent and surfactants on alkaline α-amylase activity, treatment of enzyme with 4-BPB PMSF, EDTA urea, SDS, $NaBO_3$, Triton X-100, Tween-20 and Tween-80 were done as previously described [16] The alkaline α-amylase activity without any chemical was considered as 100% activity and other values were compared with that.

2 11 Compatibility test with various commercial laundry detergents

To confirm the potential of alkaline α-amylase from strain AS-S01a as a laundry detergent additive, its compatibility and stability towards some commercial laundry detergents available in the local market, such as Surf excel® and Wheel® (Hindustan Lever Ltd , India), Tide® and Ariel® (Procter & Gamble India), Henko® (Henkel India Ltd), Fena Ultra® (Fena (P) Ltd , India), Safed® (Safechem Industries Ltd , India) and Ujala® (Jyothy Laboratories Ltd India) were examined by our previously elucidated procedure [22] Before alkaline α-amylase stability assay, the detergents solutions (7 mg/ml) were pre-heated at 100 °C for 60 min to destroy the endogenous enzyme activity, if any (which was reconfirmed by α-amylase assay of heated detergents solutions) The relative activity of alkaline α-amylase in the presence of laundry detergent was expressed in percentage activity considering the activity of control (without detergent) as 100% To test the stability of alkaline α-amylase in presence of proteases enzyme, the enzyme was incubated with commercial protease preparation (proteinase K) for 1 h at room temperature and thereafter, the residual activity of alkaline α-amylase was determined against the control (alkaline α-amylase without protease treatment)

2 12 Wash performance analysis

With the aim to determine the efficacy of purified alkaline α-amylase for use as a bio-detergent additive wash performance was evaluated by determining the chocolate stain releasing capacity of alkaline α-amylase under study from cotton fabrics as described by Hmidet et al [5] with the following modifications Briefly, chocolate was heated at 70 °C to liquefy it and 100 μl (10 mg/μl of total carbohydrate solution) of the liquefied chocolate was stained to cotton fabrics (5 cm × 5 cm) which was then dried overnight under hot air oven [5] To test the wash performance each piece of stained cloth was dipped in any one of the following flasks containing (a) 25 ml of tap water (control), (b) 20 ml of tap water and 5 0 ml of 500 U/ml of purified alkaline α-amylase, (c) 20 ml of tap water and 5 ml of heated detergent (7 mg/ml) and (d) 20 ml of tap water and 5 ml of heated detergent (7 mg/ml) containing 500 U/ml of purified alkaline α-amylase preparation Flasks were kept at 37 °C for 60 min followed by removal of the cloth pieces, and the leftover washes were used to determine the quantity of total carbohydrate released from chocolate stains of the cloth [19] Stain removal capabilities of the purified enzyme was examined visually by looking at the pieces of dried cloth [5] The untreated chocolate stained cloth piece was considered as a control

3. Results and discussion

3 1 Phenotypic characterization of strain

The phenotypic characterization of any strain is the first step towards its identification process The phenotypic characters of strain AS-S01a along with related species of *Bacillus* are presented in supplementary Table S1 Some of the characteristics phenotypic features like Gram stain positive, rod shaped vegetative cell, motile, oval spore, and ability to utilize citrate, starch hydrolysis, inability to produce indole from tryptophan or gas from glucose showed the close resemblance of strain AS-S01a with *B subtilis* The fact that genus *Bacillus* represents several phylogenetically diverse genera with overlapping phenotypic characters prompted chemotaxonomic and molecular characterization of the strain under study [23]

3 2 Cellular fatty acid analysis

The analysis of bacterial cellular fatty acid methyl esters (FAMEs), particularly the iso and anteiso fatty acids profile by gas chromatography (GC), is a rapid and inexpensive technique that holds great promise in microbial identification and establishing an evolutionary scheme for microorganisms [19,24] The cellular fatty acid composition of strain AS-S01a is shown in supplementary Table S2 and is compared with the reported fatty acids profile for phylogenetically related *Bacillus* species It was observed that iso-branched $C_{15\,0}$ (45 2%) represented the predominant fatty acid in strain AS-S01a followed by anteiso-branched $C_{15\,0}$ (28 3%) Interestingly, based on the cellular fatty acid composition the strain under study showed most of the characteristic features similar to that of *Bacillus alcalophilus* However the qualitative and quantitative differences in the cellular fatty acid composition of strain AS-S01a compared to phylogenetically related species of *Bacillus* such as *B subtilis* and *B alcalophilus* warrant that strain AS-S01a may not be affiliated to any recognized species of this genus and therefore it needs further characterizations by molecular approach

3 3 Phylogenetic analysis

The 16S rDNA-based phylogenetic analysis demonstrated 96 0–97 0% sequence similarity of strain AS-S01a with other species of *Bacillus* This reinforces that strain AS-S01a belongs to the genus *Bacillus* The phylogenetic tree constructed from the sequence data by neighbour-joining method (Fig 1) showed detailed evolutionary relationships among the strain AS-S01a and other closely related *Bacillus* species, and demonstrated a distinct phylogenetic position of the strain under study (Fig 1) It is noteworthy that tree topology of the strain AS-S01a as estimated from the neighbour-joining UPGMA maximum-likelihood and parsimony analysis were consistent Although the phylogenetic analysis suggested that the strain AS-S01a was a representative of the genus *Bacillus*, but it could not be identified at a species level

The sequencing of 16S rRNA gene alone may not discriminate closely related species because of the highly conserved nature of this region Therefore, additional information obtained by sequencing of the genes encoding 'core genome' of conserved proteins is further useful for taxonomic identification of the isolated strain [25] Thus, our bacterium was identified up to species level by using this approach The sequencing and phylogenetic analysis of Gyrase A gene (supplementary Fig S1) Rpo B gene (supplementary Fig S2) and ISR of 16S-23S rRNA (supplementary Fig S3) of the strain AS-S01a showed that it belong to *B subtilis* group Based on the biochemical and phenotypic characteristics,

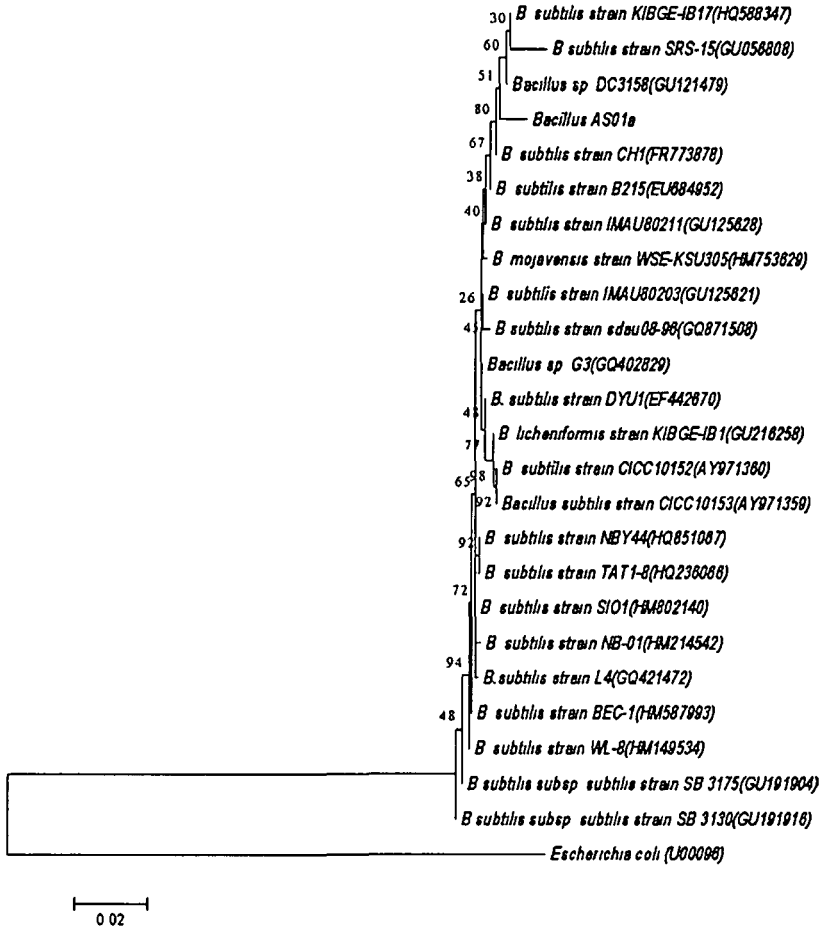

Fig 1 Phylogenetic relationships of strain AS-S01a and other closely related *Bacillus* species based on 16S rDNA sequencing The tree was generated using the neighbour-joining method and the sequence from *Escherichia coli* strain K 12 MG1655 (accession no U00096) was considered as out-group The data set was resampled 1000 times by using the bootstrap option and percentage values are given at the nodes

cellular FAMEs analysis and phylogenetic analysis, the bacterium was identified as *B subtilis* strains AS-S01a

3 4 *Screening of fermentation condition for alkaline α-amylase production*

Among the tested carbon sources, soluble starch was found to be the best carbon source for maximum growth as well as alkaline α-amylase production by the selected bacterium (Fig 2), a phenomenon that has been described for several α-amylase secreting *Bacillus* strains [16 26] When glucose was supplied as a carbon source, approx 50% of growth was observed, with a subsequent decrease in alkaline α-amylase production, showing that glucose causes a catabolic repression of carbohydrate degrading enzymes [2] Among the tested nitrogen sources, beef extract served as the best nitrogen source followed by peptone, NH_4Cl, and then KNO_3 (data not shown) These results also corroborate well with the previous reports that each bacterium has its own choice of either inorganic or organic nitrogen source for growth and α-amylase production [2,16,22]

Although *B subtilis* strain AS-S01a was able to grow and produce alkaline α-amylase enzyme over all the tested temperature, pH and rpm ranges, its optimum growth and enzyme production was observed at 45–55 °C, pH 6 0 and at an agitation speed of 150 rpm (data not shown) Alkaline α-amylase production in presence of starch was started during the exponential growth phase of the strain and it reached maximum levels (440 U/ml) during the stationary phase at 60 h (Fig 3) Beyond this period, the enzyme production was declined as the culture entered into death phase, thus giving a clear indication that alkaline α-amylase production by *B subtilis* strain AS-S01a is growth associated and is induced by the presence of its preferred substrate in the medium [27]

3 5 *Enhancement of alkaline α-amylase production in SmF*

It has been well established that medium components play an important role in enzyme production by bacteria [22] Therefore, designing an appropriate fermentation medium is of critical importance in optimizing the products yield [18 28] The conventional experimental approaches for the optimization of media components require numerous experiments to study the influence of each factor of the media on enzyme production In contrast, the statistical optimization of media components can take into account the interactions of variables in generating the process responses Since it was observed during the initial screening process that alkaline α-amylase production was highly influenced by three test variables, viz pH of the medium, concentration (%, w/v) of starch and concentration (w/v) of beef extract, therefore, these parameters were further optimized by using RSM The results of the observed and predicted values of alkaline α-amylase yield

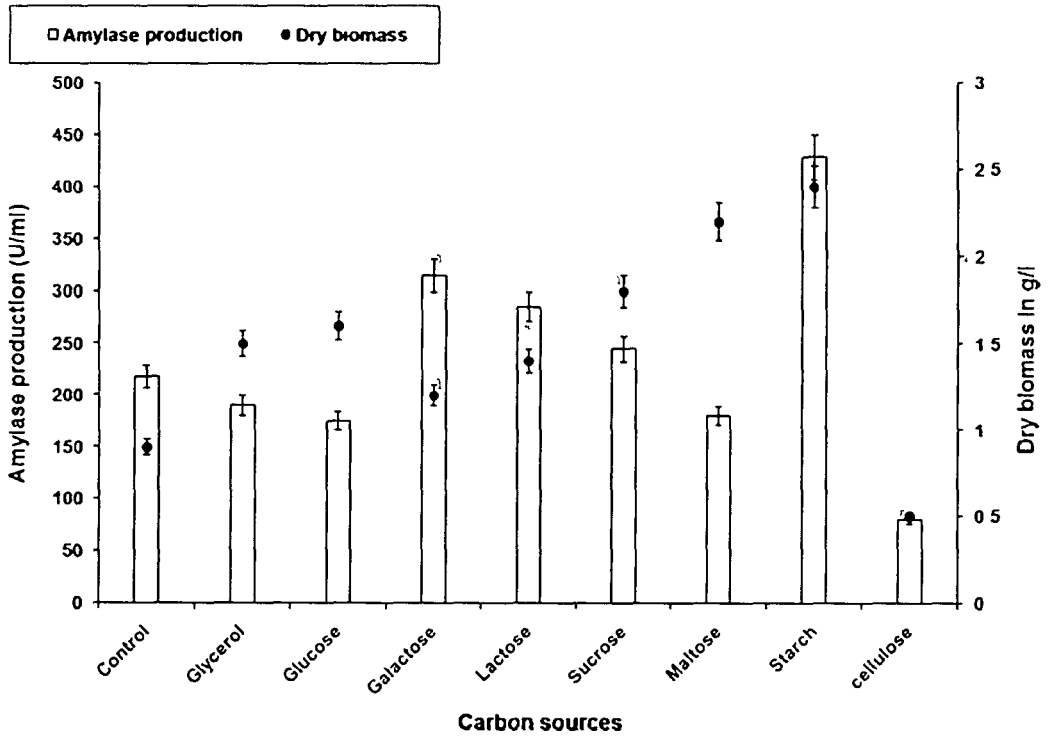

Fig 2 Influence of various sources of carbon on growth of and alkaline α-amylase production by *B subtilis* strain AS-S01a Values are mean ± S D of triplicate determinations

(response) with reference to the experiments performed according to the CCD are shown in Table 1 The parameters of Eq (1) were determined by multiple regression analysis by the application of RSM The overall second-order polynomial regression equation can be represented by Eq (3)

$$Y = -1492\,03 + 494\,04C_1 - 580\,17C_2 + 517\,54C_3 - 309\,94C_1^2 + 679\,14C_2^2 + 78\,15C_3^2 - 3092\,50C_1C_2 + 248\,75C_1C_3 + 548\,13C_2C_3 \quad (3)$$

The coefficient of the model including the significance of each coefficient was determined by *t*-test and *P* values Results showed that all the terms of the model except the linear effects of C_1 (starch content) C_2 (concentration, % w/v of beef-extract) and square effect of C_2 (concentration % w/v of beef-extract) were significant ($P < 0\,05$) The negative coefficient observed in the case of beef extract indicates that a lower concentration of it can increase the alkaline α-amylase production The analysis of variance (ANOVA) by Fisher's statistical test was conducted for the second-order response surface model and the results demonstrated that the

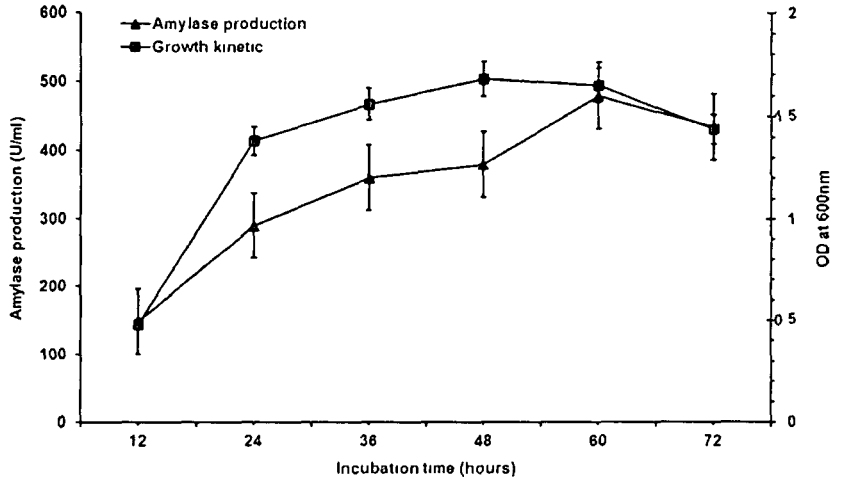

Fig 3 Kinetics of growth (■) and alkaline α-amylase production (▲) by *B subtilis* strain AS-S01a on M9 medium containing starch and beef-extract pH 6 0 Values are mean ± S D of triplicate determinations

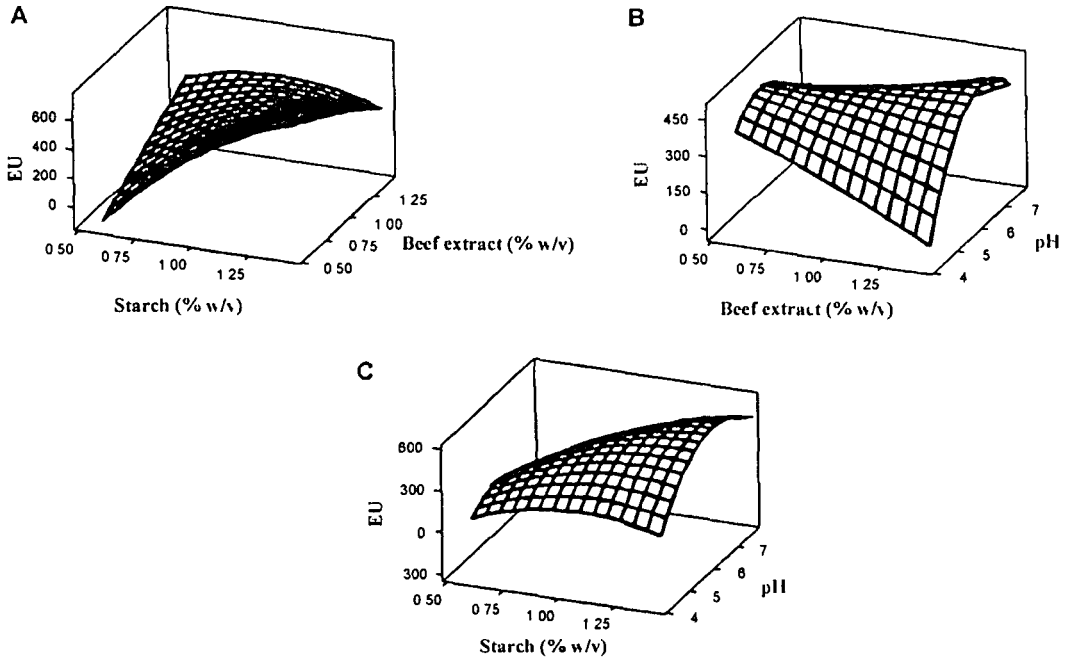

Fig 4 Response surface plots for alkaline α-amylase production by *B subtilis* strain AS-S01a The interactions between (A) pH vs starch (% w/v) (B) pH vs beef extract (% w/v) and (C) starch (% w/v) vs beef extract (% w/v)

computed *F* value for linear regression was much greater than the tabulated (*P*) > *F* value (data not shown) The R^2 and adjusted R^2 values were determined as 98 12% and 96 42%, respectively (supplementary Table S4) The significance of the quadratic model was evident from the coefficient of determination (R^2) value Nearer of values of R^2 to 1, the stronger is the model and better it predicts the response [29] The observed values of R^2 suggest that the fitted model could explain 98 12% of the total variation and hence vouches for adequacy of the model The adjusted R^2 value (96 42%) also advocates for a high significance of the model

The three-dimensional response surface plots and 2D contour plots are the graphical representations of the regression equation and used to investigate the interaction among the variables and to determine the optimum concentration of each factor for maximum yield (alkaline α-amylase production in the present study) The interactions between the variables can be implied from the shapes of the contour plots A circular counter plot shows that the interactions between the variables are negligible whereas an elliptical or saddle nature of the contour plot shows significant interaction between the corresponding variables [30] The three-dimensional response surface plots and contour plots drawn as a function of two factors at a time maintaining the third factor at the minimum (zero) level are depicted in Fig 4A–C, and in Fig 5A–C, respectively As shown in Fig 4 the lower concentration of beef-extract (Fig 4A and B) and higher concentration of starch (Fig 4A and C) could induce the optimum alkaline α-amylase production The negative coefficient observed for the beef-extract (linear and interaction effects) showed that a decrease in the concentration of beef extract can improve the alkaline α-amylase yield by *B subtilis* strain AS-S01a The contour plots (Fig 5A–C) show the significant interactions among the test variables (starch, beef-extract and pH) for alkaline α-amylase production The Fig 5A and C demonstrate that higher starch concentration enhanced the alkaline α-amylase production The pH of the medium influenced the alkaline α-amylase production in the acidic range which was less than 6 0 (Fig 5A and B)

3 6 *Validation of response surface model in a process-controlled bioreactor*

By regression Eq (3), the optimum levels of test variables for maximum alkaline α-amylase yield were predicted by using the predict programmed (Minitab 15 Statistical Software®) as 1 421% (w/v) of starch, 0 131% (w/v) of beef-extract and at 6 1 pH of the medium It is worth mentioning here that the pH of the soil sample from where the bacterium under study was isolated within the range of 6 0–6 2 and therefore it is obvious that the acidic pH favored the alkaline α-amylase production by *B subtilis* strain AS-S01a The predicted response for alkaline α-amylase yield was observed as 786 0 U, while the actual experimental value of alkaline α-amylase production in a process-controlled fermenter was obtained as 799 0 U (specific activity of 210 2 U/mg) post 72 h of incubation, which established the validity of the model It is worthy of mention here that both the initial screening experiments as well as optimization of process parameters were done in a shake-flasks culture rather than in a process control bioreactor It has several advantages, such as having a potential for large numbers of parallel fermentation, low cost vessels, vessels taking little space needing little infrastructure, and most importantly it is easy to scale up However, in general, the production of enzymes in a process control bioreactor is higher than with shake-flasks culture because in a process-controlled bioreactor the concentration of dissolved oxygen as well as the pH of the medium could be maintained at the desired level [31] This may not be possible in a shake-flask study Therefore, the final validation and subsequent alkaline α-amylase production was carried out in a process control fermenter

The alkaline α-amylase production by *B subtilis* strain AS-S01a under optimized condition in a process-controlled bioreactor was significantly higher than the reported yield of the same enzyme from the other wild-type bacteria such as *B subtilis* DM-03 [16], *Bacillus licheniformis* [32], *B subtilis* [32], *Bacillus* sp strain TSCVKK [33] This reinforces the industrial exploitation of

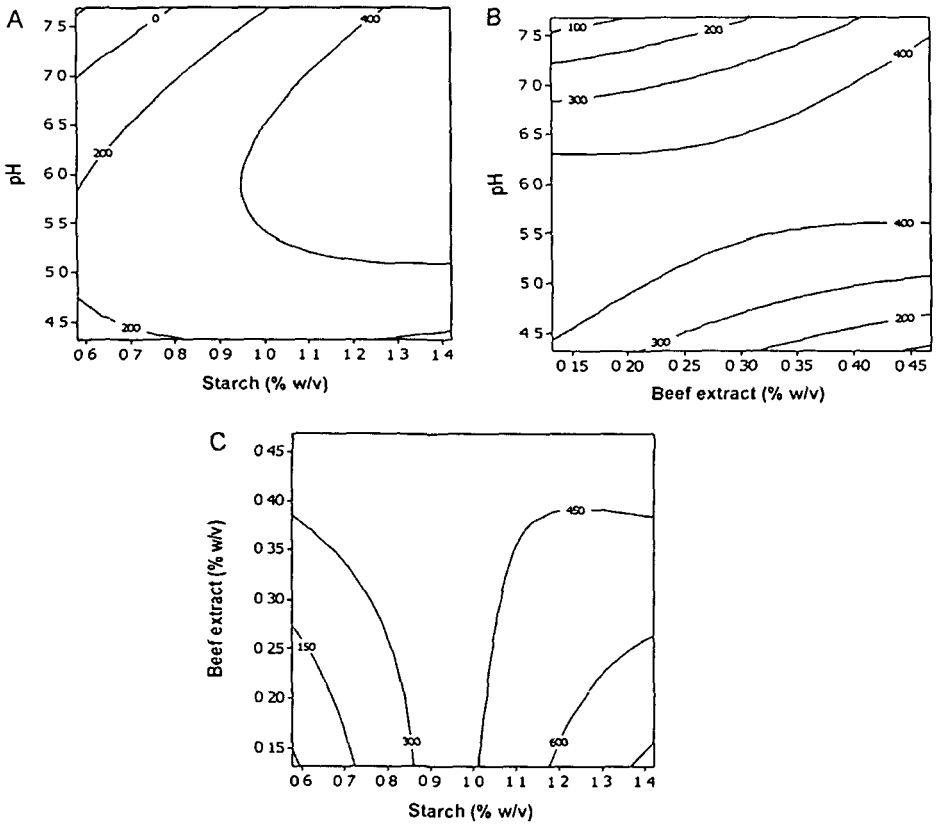

Fig 5 Contour plots showing interaction effect of test variables on alkaline α-amylase production from *Bacillus subtilis* strain AS-S01a (A) pH vs starch (% w/v) (B) pH Vs beef extract (% w/v) and (C) starch (% w/v) vs beef extract (% w/v)

selected bacterium as microbial cell factory for high-titer alkaline α-amylase production

3 7 *Purification and biochemical characterization of alkaline α-amylase*

The alkaline α-amylase enzyme was eluted from the gel-filtration column in a single peak (see supplementary Fig S4) and this peak were found to be homogenous by SDS-PAGE (Fig 6) Under both denatured (Fig 6) and native condition (data not shown) the enzyme yields a single band in SDS-PAGE showing it is monomeric in nature This was further confirmed by amylase-zymographic study where the enzyme showed a single clear zone of hydrolysis (Fig 6) The summary of purification of alkaline α-amylase from *B subtilis* strain AS-S01a is shown in Table 2 The enzyme was purified to 7 7-fold (Table 2) with a molecular mass of 21 0 kDa (Fig 6) In general molecular mass of α-amylases from bacteria particularly from *Bacillus* sp is reported between 48 and 60 kDa [2 16] and there is a dearth of report on 21 0 kDa α-amylase from bacteria

Before assessing the biotechnological potential of any enzyme, characterization of biochemical properties pertinent to industrial application is most important and advantageous The purified alkaline α-amylase retained its activity and stability over a broad range of alkaline pH (8 0–12 0) and temperature (25–65 °C), however, the enzyme displayed optimum activity at pH 9 0 and at 55 C temperature (Table 3) The same optimum pH was obtained with the amylase from *Bacillus* US147 [34], *Bacillus* sp TS-23 [34] *Halobacterium salinarum* MMD047 [35] and *Streptomyces gulbargensis* [36] but our results showed that the alkaline α-amylase in the present study has a higher range of pH (8 0–12 0) stability as compared to

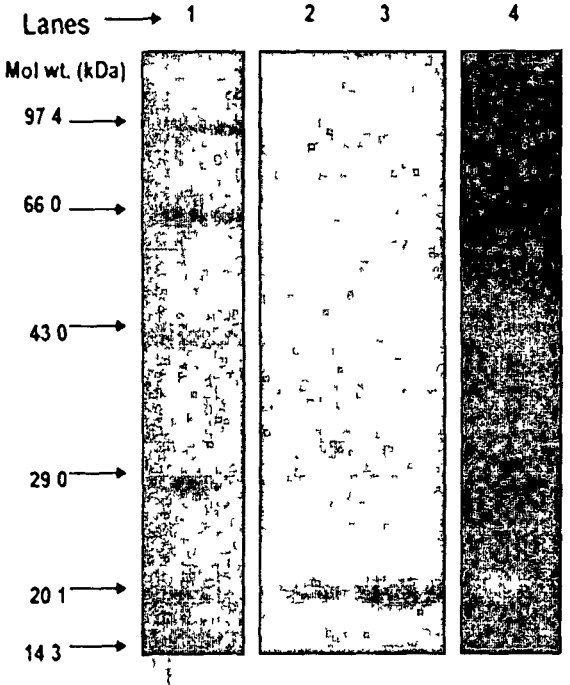

Fig 6 SDS-PAGE analysis of purified alkaline α-amylase from *B subtilis* strain AS-S01a lane 1 protein molecular weight markers lane 2 purified alkaline α amylase (gel-filtration fraction) (15 μg) lane 3 acetone precipitated fraction (25 μg) and lane 4 zymogram of purified amylase (10 μg)

Table 2
Summary of purification of an alkaline α-amylase from *B subtilis* strain AS-S01a

Purification step	Total protein (mg)	Total amylase activity (U)	Specific amylase activity (U/mg)	Purification (fold)	Enzyme recovery (%)
Crude extract	3160 0	6350000	201 0	1 0	100
$(NH_4)_2SO_4$ precipitation	160 8	425000	264 0	1 3	67
Acetone precipitation	10 2	31200	305 0	1 5	0 5
Sephadex G-50	1 3	18900	1500 0	7 5	0 3

the above mention enzymes, which suggests its application in automatic dishwashers and laundry detergents The purified alkaline α-amylase also showed a higher temperature optima than some of the reported alkaline α-amylases from other strains like *Bacillus* sp isolate L1711 [34], *S gulbargensis* [36], *H salinarum* MMD047 [35], and *Bacillus* sp NRRL B 3881 [36]

The K_m and V_{max} values for the purified enzyme, which are indicators of affinity of the enzyme towards its substrate (starch), were determined as 1 9 mg/ml and 198 21 μmol/min/mg, respectively Kinetic study showed that substrate (starch) specificity of alkaline α-amylase from *B subtilis* strain AS-S01a was higher than the reported substrate specificity of amylases isolated from other species of *Bacillus* such as *Bacillus stearothermophilus* [37] and *Geobacillus* sp [38]

Thermostability study demonstrated that heating the alkaline α-amylase for 30 min at 45–55 °C had no effect on enzyme activity, but heating beyond this temperature resulted in a gradual loss of enzyme activity, which suggested the moderate thermostable nature of this enzyme (supplementary Fig S5) The thermostability of alkaline α-amylase under study was slightly decreased in presence of Ca^{2+} ions (supplementary Fig S5) In general, bacterial α-amylases are shown to be much more thermostable in the presence of this cation [2], and few reports are available to demonstrate Ca^{2+}-independent thermostable α-amylase [39] This Ca^{2+}-independent thermostable α-amylase is an added advantage in starch saccharification process at a higher temperature because it eliminates the addition of Ca^{2+} for improving the stability of α-amylases Therefore, this can be considered as a cost-effective process [39] This property of purified α-amylase can also solve the problems that are faced by liquid detergent industries, where most of the α-amylase enzymes used lose their stability in presence of builders [40]

As shown in Table 3, the purified alkaline α-amylase demonstrated significant stability in presence of metal-chelator, denaturing agents, oxidizing agent and surfactants like EDTA (2 mM), urea (2 M), $NaBO_3$ (5 mM), SDS (1%, w/v), Triton X-100 (1%, w/v), Tween-20 (1%, w/v) and Tween-80 (1%, w/v) This property of enzyme supports its candidature for inclusion in laundry detergent formulations, which demand that added enzyme should be stable in presence of bleach surfactant and metal ions chelating agent However, the enzyme activity was significantly affected by PMSF (2 mM) and 4-bromophenacyl bromide (2 mM), thus suggesting a role for serine and histidine residues in the catalysis process (Table 3) Our previous study also demonstrated the roles of serine and histidine residues in the catalytic activity of an α-amylase from *B subtilis* DM-03 [16] Besides, this enzyme also had an added advantage as it works optimum at a temperature of 55 °C These established that the enzyme under the present study is a good contestant for the liquid detergents formulation for use in hospitals, which demands that the amylase to be used must resist the working temperature employed to clean instruments in hospitals, on average of 53 °C [7] The purified alkaline α-amylase may also be used as model proteins for understanding the molecular basis of the alkalophilicity of the enzymes, which may be of value in protein engineering [35]

Table 3
Biochemical characterization of purified alkaline α-amylase enzyme from *B subtilis* strain AS-S01a Values are mean ± S D of triplicate determinations

Parameters	Values
Optimum pH	9 0 ± 0 45
Optimum temperature (°C)	55 ± 2 75
pH stability	8 0–12 0
K_m (mg/ml)	1 9 ± 0 1
V_{max} (μmol/min/mg)	198 21 ± 4 9
Apparent molecular mass by SDS-PAGE (kDa)	21 0
End product of starch hydrolysis	High molecular oligosaccharides maltose small amount of glucose
Effectors	
Control (without effectors)	100
EDTA (2 mM)	101 0 ± 5 5
PMSF (2 mM)	38 8 ± 1 9
4 BPB (2 mM)	32 8 ± 1 6
$NaBO_3$ (5 mM)	73 2 ± 3 6
Urea (2 M)	79 6 ± 3 9
SDS (1% w/v)	103 3 ± 5 6
Triton-X 100 (1% v/v)	103 4 ± 5 2
Tween 20 (1% v/v)	105 0 ± 5 3
Tween-80 (1% v/v)	106 0 ± 5 3

3 8 End-products of starch hydrolysis

Disaccharides and oligosaccharides such as maltose and maltotriose derived from starch hydrolysis are used in various fields most widely in the food industry, because of their superior properties as a base material for food production and a sweetening agent [1 2] Furthermore, the demand for purified maltose as an ingredient of transfusion liquids has also increased, when compared with the conventionally used glucose High molecular weight oligosaccharides were detected as the main hydrolytic products post 60 min incubation of starch with purified alkaline α-amylase (supplementary Fig S6) This confirmed that the enzyme was α-amylase and a good candidate for application in the food processing industry Small amount of glucose was also liberated as a result of the action of alkaline α-amylase on starch The starch degrading property of alkaline α-amylase under study was slightly different as compared to the same property exhibited by Bsamy-1 an alkaline α-amylase purified from *B subtilis* strain DM-03 [16] The SEM photographs of starch granules before and after the degradation with purified alkaline α-amylase from *B subtilis* strain AS-S01a are depicted in Fig 7 Holes were observed in the starch granules post treatment with alkaline α-amylase and our result corroborates well with the report of Matsubara et al [21] The purified alkaline α-amylase may also be applied for the production of maltotetraose from starch for use in nutrient foods for infants and aged persons [35]

3 9 Detergent compatibility of alkaline α-amylase with commercial laundry detergents

Powdered laundry detergents which constitute the largest part of the detergent market, function at a high alkaline pH Enzymes whose activity depends on loosely bound metal ions Mg^{2+} and Ca^{2+} cannot find application in detergent formulations because many detergents contain sequestering agents like polyphosphates nitrilotriacetics acid (NTA), or zeolites The biochemical properties of alkaline α-amylase in the present study suggested that it

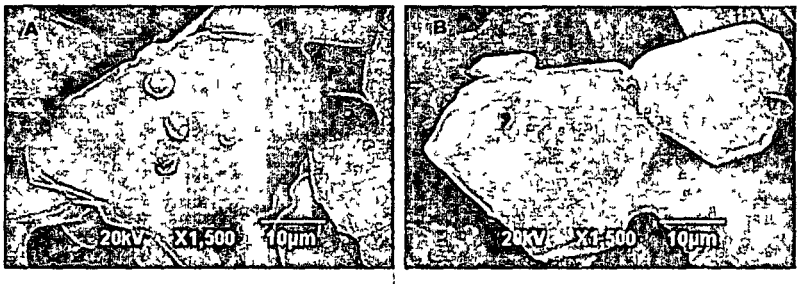

Fig 7 Scanning electron microscopic (SEM) photographs of starch granules (A) before and (B) 60 min post incubation with purified alkaline α-amylase

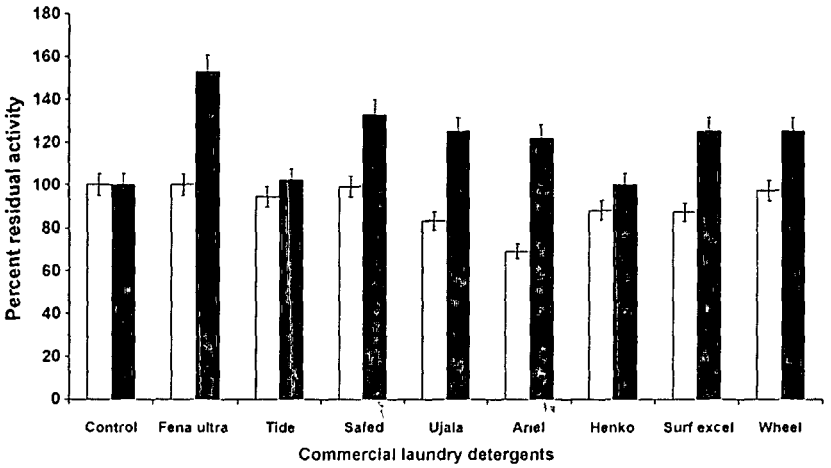

Fig 8 Detergent compatibility study of the purified alkaline α-amylase from *B subtilis* strain AS-S01a at 30 °C (□) and 37 °C (■) Values are mean ± S D of triplicate determinations

may be used as an ingredient in detergent formulations for automatic dishwashers and laundries The alkaline α-amylase from *B subtilis* strain AS-S01a exhibited a significant compatibility with all the tested commercial laundry detergents (Fig 8) The alkaline α-amylase retained 69 0–100 0% and 100 0–153 0% of its original activity in presence of tested detergents at 30 and 37 °C, respectively Increase in enzyme activity at 37 C may be attributed to the stimulatory effect of the some of the detergent components [41] Since we could not detect surface tension reducing property of the pure enzyme preparation (Rai, S K and Mukherjee, A K, unpublished observation), it ruled out the possible interference of biosurfactant produced by this bacterium, on the detergent stability of alkaline α-amylase Ideally, α-amylase or other hydrolytic enzymes to be used in detergent formulations should be effective at low levels ranging from 0 4% to 0 8% [42] The 0 7 mg/ml (0 1%) dose of alkaline α-amylase form *B subtilis* strain AS-S01a is significantly lower than the recommended level of enzyme to be added in laundry detergents for improving its wash performance

It has been reported that different ingredients of laundry detergents, such as anionic surfactants, bleaching agents and stabilizers influence the stability of added enzyme(s) in detergents [41] The partial loss of alkaline α-amylase activity in some of the laundry detergents may be attributed to inhibitory effect(s) of component(s) of these detergents In contrast, some other components of the detergent(s), for example, ethoxylated surfactants non-ionic copolymeric builders, and sucrose may have a stimulatory effect [41] on alkaline α-amylase activity from *B subtilis* strain AS-S01a as seen in some of the tested detergent(s) Furthermore, it was observed that alkaline α-amylase retained 71% of its original activity after 1 h of incubation with proteinase K at room

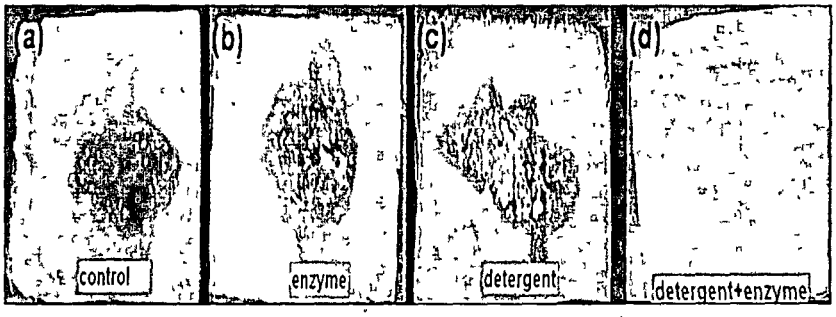

Fig 9 Wash performance analysis tests of chocolate stain cloth pieces washed with (A) control tap water (B) detergent (7 mg/ml) (C) purified alkaline α-amylase (500 U/ml) and (D) purified alkaline α-amylase amylase (500 U/ml) + detergent (7 mg/ml)

temperature (data not shown) suggesting limited proteolysis of the enzyme under study. This reinforces successful application of purified alkaline α-amylase in laundry detergent formulations containing protease enzymes, besides other enzymes, for enhancing the wash performance of the detergents

3.10 Wash performance analysis

Stain removal ability of the purified alkaline α-amylase was assessed by using chocolate-stained cotton fabrics Fig. 9 depicts that treatment of chocolate stain by detergent (Fena®) supplemented with the purified alkaline α-amylase resulted in a better stain removal from cotton fabrics as compared to stain removal by detergent or enzyme alone. The detergent supplemented with alkaline α-amylase from *B. subtilis* strain AS-S01a showed a 2.8-fold increase in carbohydrate release as compared to release of carbohydrate by detergent alone (supplementary Fig. S5).

4. Conclusions

The data lead us to assume that *B. subtilis* strain AS-S01a is a high titer alkaline α-amylase producing novel bacterium and it may be exploited industrially as a microbial cell factory for high-level of alkaline α-amylase production under statistically optimized condition. The biochemical properties of purified alkaline α-amylase as well as its detergent compatibility data evidently support that the enzyme has a potential application in the dishwasher and laundry detergent industry because this enzyme fulfills most of the requirements of the detergent industry, such as, it does not require Ca^{2+} ion for exerting its activity and it demonstrates stability in presence of protease, surfactant, oxidant and metal ions chelating agent. The enzyme is cable of functioning at a wide range of temperature, which is a pre-requisite for inclusion of alkaline α-amylase in most of the detergents including liquid detergent formulations. Furthermore, the biochemical property of the purified alkaline α-amylase from the strain under study also suggests its potential candidature for use in the food processing industries.

Acknowledgements

Authors acknowledge the help extended by Institute of Microbial Technology (IMTECH), Chandigarh for bacterial cellular fatty acid analysis, Delhi University for DNA sequencing, and Dr. G.K. Borah from Tezpur University for editing the manuscript. Mr. S.K. Rai and Mr. J.K. Roy were recipients of Senior Research Fellowship from the Council of Scientific and Industrial Research (CSIR), New Delhi and fellowship from UGC-SAP, Department of MBBT respectively. This work was partially supported to A.K.M. by funding from "Special Assistance Programme (DRS-I)" of the UGC, New Delhi and 'Strengthening of teaching, training and research in Universities and Colleges of North-East India" by the DBT, New Delhi.

Appendix A. Supplementary data

Supplementary data associated with this article can be found in the online version, at doi: 10.1016/j.ijbiomac.2011.10.026.

References

[1] M.J.E.C. van der Maarel, B. van der Veen, J.C.M. Uitdehaag, H. Leemhuis, L. Dijkhuizen, J. Biotechnol. 94 (2002) 137–155.
[2] R. Gupta, P. Gigras, H. Mohapatra, V.K. Goswami, B. Chauhan, Microbial. Process Biochem. (2003) 1–18.
[3] A. Pandey, P. Nigam, C.R. Soccol, V.T. Soccol, D. Singh, R. Mohan, Biotechnol. Appl. Biochem. 31 (2000) 135–152.
[4] T.U. Kim, B.G. Gu, J.Y. Jeong, S.M. Byun, Y.C. Shin, Appl. Environ. Microbiol. 310 (1995) 5–3112.
[5] N. Hmidet, N.E. Ali, A. Haddar, S. Kanoun, S.K. Alya, M. Nasri, Biochem. Eng. J. 47 (2009) 71–79.
[6] K. Igarashi, H. Hagihara, S. Ito, Trends Glycosci. Glycotechnol. 82 (2003) 101–114.
[7] S. Mitidieri, A.H.S. Martinelli, A. Schrank, M.H. Vainstein, Bioresour. Technol. 97 (2006) 1217–1224.
[8] P.M. Souza, P.O. Magalhaes, Braz. J. Microbiol. 41 (2010) 850–861.
[9] S. Ito, T. Kobayashi, K. Ara, K. Ozaki, S. Kawai, Y. Hatada, Extremophiles 2 (1998) 185–190.
[10] M.A. McTigue, C.T. Kelly, E.M. Doyle, W.M. Fogarty, Enzyme Microb. Technol. 17 (1995) 570–573.
[11] H.C. Chen, Food Biotechnol. 10 (1996) 13–27.
[12] S.K. Rai, J.K. Roy, A.K. Mukherjee, Appl. Microbiol. Biotechnol. 85 (2010) 1437–1450.
[13] K.K. Pandey, S. Mayilraj, T. Chakrabarti, Int. J. Syst. Evol. Microbiol. 52 (2002) 1559–1567.
[14] F.M. Ausubel, R. Brent, R.E. Kinston, D.D. Moorse, J.D. Seidman, J.A. Smith, K. Struhl, Short Protocols in Molecular Biology, John Wiley and Sons, New York, 1995, pp. 2.12–2.14.
[15] A. Tamura, Y.K. Shimizu, T. Tanaka, K. Kuroda, Y. Arakawa, K. Takahashi, S. Mishiro, K. Shimizu, M. Moriyama, Hepatol. Res. 37 (2007) 113–120.
[16] K. Das, R. Doley, A.K. Mukherjee, Appl. Biochem. Biotechnol. 40 (2004) 291–298.
[17] H. Fuwa, J. Biochem. 41 (1954) 583–603.
[18] D. Gangadharan, S. Sivaramakrishnan, K.M. Nampoothiri, R.K. Sukumaran, A. Pandey, Bioresour. Technol. 99 (2008) 4597–4602.
[19] K. Das, A.K. Mukherjee, Process Biochem. 42 (2007) 1191–1199.
[20] U.K. Laemmli, Nature 277 (1970) 680–685.
[21] T. Matsubara, Y.B. Ammar, T. Anindyawati, S. Yamamoto, K. Ito, M. Iizuka, N. Minamiura, J. Biochem. Mol. Biol. 37 (2004) 422–428.
[22] A.K. Mukherjee, M. Borah, S.K. Rai, Biochem. Eng. J. 43 (2009) 149–156.
[23] M.A.R.V. Guerra-Cantera, A.K. Raymundo, World J. Microbiol. Biotechnol. 21 (2005) 635–644.
[24] T. Kaneda, Bacteriol. Rev. 41 (1977) 391–418.
[25] N. Parkinson, V. Aritua, J. Heeney, C. Cowie, J. Bew, D. Stead, Int. J. Syst. Evol. Microbiol. 57 (2007) 2881–2887.
[26] M. Jane, D.J. Chattopadhyay, B.R. Pati, Acta Microbiol. Immunol. Hung. 45 (2) (1998) 229–237.
[27] N. Goyal, J.K. Gupta, S.K. Soni, Enzyme Microb. Technol. 37 (2005) 723–734.
[28] P.D. Haaland, Experimental Design in Biotechnology, Elsevier Science Publishing Co., New York, USA, 1990.
[29] W.W. Daniel, in: W.W. Daniel (Ed.), Biostatistics, 7th ed., John Wiley and Sons, Inc., New York, 2000, pp. 166–167.
[30] L. Yu, T. Lei, X. Rena, X. Pei, Y. Feng, Biochem. Eng. J. 39 (2008) 496–502.
[31] P. Calik, G. Calik, T.H. Ozdamar, Enzyme Microb. Technol. 23 (1998) 451–461.
[32] J. Shukla, R. Kar, World J. Microbiol. Biotechnol. 22 (2006) 417–422.
[33] K.K. Kiran, T.S. Chandra, Appl. Microbial. Biotechnol. 77 (2008) 1023–1031.
[34] R.E. Ghorbel, S. Maktouf, E.B. Massoud, S. Bejar, S.E. Chaabouni, Appl. Biochem. Biotechnol. 157 (2009) 50–60.
[35] S. Shanmughapriya, G.S. Kiran, J. Selvin, R. Gandhimathi, T.B. Baskar, A. Manilal, S. Sujith, Biotechnol. Bioprocess Eng. 14 (2009) 67–75.
[36] D.G. Syed, D. Agasar, A. Pandey, J. Ind. Microbiol. Biotechnol. 36 (2009) 189–194.
[37] M. Vihinen, P. Mantsala, Crit. Rev. Biochem. Mol. Biol. 24 (1989) 329–418.
[38] P. Dheeran, S. Kumar, Y.K. Jaiswal, D.K. Adhikari, Appl. Microbiol. Biotechnol. 86 (2010) 1857–1866.
[39] J.L.U.M. Rao, T. Satyanarayana, J. Appl. Microb. 95 (2003) 712–718.
[40] B. Khemakhem, M.B. Ali, N. Aghajari, M. Juy, R. Haser, S. Bejar, Biotechnol. Bioeng. 102 (2009) 380–389.
[41] K. Maurer, Curr. Opin. Biotechnol. 15 (2004) 330–334.
[42] C.G. Kumar, H. Takagi, Biotechnol. Adv. 17 (1999) 561–594.

Biotechnology and Bioprocess Engineering 15: 984-992 (2010)
DOI 10.1007/s12257-009-3160-7

RESEARCH PAPER

Statistical Optimization of *Bacillus alcalophilus* α-amylase Immobilization on Iron-oxide Magnetic Nanoparticles

Ashis K. Mukherjee, Tadi Satish Kumar, Sudhir K. Rai, and Jetendra K. Roy

Received: 28 December 2009 / Revised: 14 March 2010 / Accepted: 20 April 2010

Abstract We report the statistical optimization of the immobilization of alkaline α-amylase [E.C. 3.2.1.1] from *Bacillus alcalophilus* onto nano-sized supermagnetic iron-oxide nanoparticles (MNPs) for augmenting the cost effective industrial application of MNP-bound α-amylase. Both Plackett-Burman factorial design and response surface methodology (RSM) were employed to screen the influence of different parameters and the central effect of response on the α-amylase-iron oxide MNP binding process. The high coefficient of determination (R^2) and analysis of variance (ANOVA) of the quadratic model indicated the competence of the proposed model. The size of the MNPs was confirmed by X-ray diffraction and scanning electron microscope analyses in which Fourier transform infrared spectroscopy suggested immobilization of the enzyme on iron-oxide MNPs. A significant improvement (~ 26-fold) in specific activity, thermal and storage stability, and reusability of α-amylase after binding with iron-oxide MNP reinforced the improved biotechnological potential of the α-amylase iron-oxide MNP bioconjugate compared to free α-amylase. These results open new avenues for applying this MNP immobilized enzyme in different industrial sectors, notably in the paper and brewing industries.

Keywords: alkaline α-amylase, *Bacillus alcalophilus*, magnetic nanoparticles, Plackett-Burman design, response surface, starch hydrolysis

Ashis K. Mukherjee*, Tadi Satish Kumar, Sudhir K. Rai, Jetendra K. Roy
Department of Molecular Biology and Biotechnology, School of Science and Technology, Tezpur University, Tezpur 784-028, India
Tel +91-9957-184351; Fax: +91-3712-267005/267006
E-mail: akm@tezu.ernet.in

1. Introduction

Among the industrially important hydrolytic enzymes, α-amylases (*e.g.*, 1,4-α-D-glucan glucanohydrolase, [E.C. 3.2.1.1]) that catalyze the hydrolysis of starch molecules to low molecular weight diverse products such as dextrins, oligosaccharides, maltose, and glucose molecules, occupy a pivotal position. The starch hydrolytic enzymes comprise 30% of the world's enzyme consumption. With the advent of new frontiers in biotechnology, the spectrum of α-amylase application has expanded to medicinal and analytical chemistry apart from their use in automatic dish washing detergents, textile desizing, the pulp and paper industry, and in sewage treatment for reducing the disposable solid content of sludge [1,2]. While α-amylases have been used for a variety of purposes, the most important are starch liquefaction and starch modification in the paper and pulp industry. Recently, attempts have been made to directly treat raw starch with thermostable α-amylase and, therefore, there is a great industrial demand for such enzymes.

Although α-amylases can be derived from a large number of sources, the industrial demand is generally met from microbial sources. The most abundantly used bacterial α-amylases for industrial purpose are derived from the *Bacillus* species; however, the loss of enzyme activity at higher temperature, pH, and/or post storage is one of the crucial factors of great concern from an industrial perspective, [1,2]. Site-directed and enzyme evolution technologies might be the approach for improving the thermostability of enzymes; however, these are time consuming and costly. In contrast, enzyme immobilization to any solid support is an efficient and easy method to improve enzyme stability [3]. Furthermore, there are several advantages to enzyme immobilization. For example, multiple uses of a single

batch of enzyme without the enzyme contaminating the product is vital to the food and pharmaceutical industries. A large number of solid supports including nano-scaled carriers have been applied in the enzyme immobilization process [3]. However, they face several disadvantages due to the difficulty experienced in recovering and handling the nanoparticles at the industrial level. Therefore, use of magnetic nanoparticles (MNP) may be an alternative approach to simple recovery of the enzyme's post binding with MNP [4]. MNP-enzyme conjugates represent a specific class of bio-nanoparticle conjugates that are of great interest for biotechnological applications in which high catalytic specificity, prolonged reaction time, and, in some cases, the ability to recycle an expensive biocatalyst are required [5,6]. In recent years, iron-oxide MNP has received considerable attention in the fields of biotechnology and medicine due to its strong magnetism, low toxicity, and biocompatibility [7,8]. Considering the increasing industrial demand for thermostable microbial α-amylases, the present study was initiated to improve the biotechnological potential, catalytic efficiency, thermo- and storage-stability, and reusability of *Bacillus alcalophilus* α-amylase after immobilization onto iron-oxide MNP. This is the first report on the statistical optimization of bacterial α-amylase binding onto iron-oxide (Fe_3O_4) MNP.

2. Materials and Methods

2.1. Isolation and partial purification of α-amylase

Extracellular alkaline α-amylase was obtained from a thermophilic *B. alcalophilus* isolated in our laboratory (unpublished report). Alkaline α-amylase was partially purified by acetone precipitation. Briefly, twice the volume of cold acetone was added to 100 mL of cell-free culture supernatant (48 h post growth of bacteria) slowly by stirring at −70°C, and the resulting solution was left at −70°C for 1 h. The precipitate was recovered by centrifugation at 10,000 × g for 15 min at 4°C, dissolved in a minimum volume of 100 mM K-phosphate buffer, pH 7.5, and used for further experiments.

2.2. Assay of α-amylase activity

Amylolytic activity was assayed by measuring the reducing sugars released during the reaction, with starch as the substrate [9]. One unit of enzyme activity was defined as the liberation of reducing sugars equivalent to 1 μmol of D-glucose/min under the assay conditions.

2.3. Covalent coupling of α-amylase onto iron-oxide MNPs

Fe_3O_4-MNPs were prepared as described by Rossi *et al.* [10]. Initially, the binding efficiency of α-amylase onto Fe_3O_4-MNPs was evaluated by the following two methods. In the first method, 50 mg of Fe_3O_4-MNPs were re-dispersed in 100 mL of ethanol by sonication, and 70 μL of 3-(aminopropyl) triethoxy silane was added with mechanical stirring. The resulting suspension was kept overnight at room temperature. The black precipitate was separated by magnetic decantation, washed twice with 20 mL ethanol, dried in air at room temperature, and then re-suspended (by sonication) in 0.5 mL of either 20 mM K-phosphate, pH 8.0 or 20 mM Tris-HCl, pH 8.0 each containing 10% (v/v) glutaraldehyde. Partially purified α-amylase enzyme (0.5 mL of 5 mg/mL protein concentration) was added to this suspension, stirred gently, and kept overnight at 4°C for the binding reaction. The enzyme coupled MNPs were recovered from the reaction mixture by a permanent magnet, washed with distilled water, and then re-suspended in 2.0 mL of the respective buffer.

In the second method, 50 mg of Fe_3O_4-MNPs were suspended by sonication in any of the buffers (without glutaraldehyde) as mentioned under the first method. Then, 0.5 mL of freshly prepared cyanamide solution (20 mg/mL in respective buffer) was added to each of the three replicates of each of the MNP sets and sonicated for 15 minutes at room temperature. α-amylase (0.5 mL of a 5 mg/mL protein concentration solution) was added to the cyanamide-treated MNP suspension and then re-sonicated for 30 min at 4°C (ice-bath). The enzyme-bound Fe_3O_4-MNPs were separated from the reaction mixture by magnetic decantation, washed with distilled water several times until no protein was detected in the post washes, re-suspended in 2.0 mL of the respective buffer containing 0.1 M NaCl (for flocculation of MNPs), and finally stored at 4°C until used.

In each method, the amount of protein immobilized onto Fe_3O_4-MNPs was determined by measuring the total protein content [11] of the supernatant after the immobilization process as well as in the pooled post washes, and then subtracting this combined value of protein content from the protein content of the enzyme solution (5 mg/mL) used for the binding reaction.

2.4. Screenings of factors effecting enzyme-MNP coupling

Plackett-Burman factorial design, which is based on a first order polynomial model (equation 1), was employed to screen the influence of different factors, such as pH of the binding solution, amount of magnetic nanoparticles, and duration of reaction in the α-amylase Fe_3O_4-MNP binding process.

$$Y = \beta_0 + \Sigma\beta_i x_i \quad (1)$$

Where Y represents the response (specific activity of enzyme after binding with MNP), β_0 is the intercept term,

β_i is the linear coefficient, and X_i denotes the independent variable. The contribution of each factor was examined at −1 (lower level) and at +1 (higher level). A center point was identified to evaluate the linear and curvature effects of the variables [12]. Independent variables were screened in a total of eight runs including two runs at their center points. The significance of each factor was analyzed using Minitab 15 statistical software (Minitab Inc., State College, PA, USA).

2.5. Optimization of α-amylase MNP coupling using Response Surface Methodology (RSM)

RSM was used to estimate the main effects on response, i.e., the specific activity of the α-amylase coupled with Fe_3O_4-MNP. Based on the results of the Plackett-Burman Factorial design, central composite design (CCD) consisting of two factors, such as the amount of MNP used for binding (C_1) and the pH of the buffer system used (C_2) with three levels and coded values consisting of 13 experimental runs, were used to analyze the experimental data. The experimental data were fitted as a second order polynomial regression equation including individual and cross effects of each variable.

$$Y = a_0 + \sum_{i=1}^{3} a_i C_i + \sum_{i=1}^{3} a_{ii} C_i^2 + \sum_{i=1}^{2} \sum_{i=i+1}^{3} a_{ij} C_i C_j \quad (2)$$

Where, Y is the predicted response (total α-amylase activity in U/mg), a_0 is the intercept term, a_i is the linear effect, a_{ii} is the square effect, a_{ij} is the interaction effect, and C_i and C_j are variables. This equation was used to optimize the independent parameter values for the response. The following equation was used for coding the variables

$$C_i = \frac{C_i - C_0}{\Delta C_i}, \quad i = 1, 2, 3, ..., k \quad (3)$$

Where C_i is the dimensionless value of an independent variable, C_i is the real value of an independent variable, C_0 is the value of C_i at the center point, and ΔC_i is the step change. Multiple regression analysis, response surface plots, and an analysis of variance (ANOVA) were performed using statistical software (Minitab).

2.6. Characterization of the free and α-amylase immobilized MNPs

The size and morphology of the free and enzyme bound Fe_3O_4-MNPs were observed by scanning electron microscopy (SEM; JEOL model JSM-6390 LV, Peabody, MA, USA) at 80 kV. The binding of α-amylase to the MNPs was re-confirmed using a Fourier transform spectrometer (FTIR) spectrophotometer (Nicolet, model Impact-410, Madison, WI, USA), and the procedure was followed as described previously [13]. The magnetic behavior of the MNP-coupled and free enzyme was studied using a hysteresis loop tracer (Model HLT-III, Sestechno Roorkee, UK). The nanocrystallite sizes of the free and α-amylase conjugated Fe_3O_4-MNPs were also determined by X-ray diffraction (XRD) measurement on an X-ray diffractometer (Miniflex, Rigaku Corporation, Tokyo, Japan) using Cu Kr radiation (λ = 0.1542 nm). The XRD data was analyzed with X-PERT software.

2.7. Kinetic properties, thermal and storage stabilities, and reusability

The K_m and V_{max} values of the α-amylase enzyme were calculated with a Lineweaver-Burk plot using 0.5 ~ 2% (w/v) of starch as a substrate and by plotting the values of 1/V as a function of 1/S. For the heat-inactivation study, a predetermined amount of either the free α-amylase or Fe_3O_4-MNP-bound α-amylase was heated to 60°C and, after a specified period of time, the required volume was withdrawn for the enzyme assay. The percentage of residual enzyme activity remaining after heating the α-amylase (bound or free) was calculated by considering the activity of the control (without heating) as 100%.

The storage stability of MNP-bound or free α-amylase either in the presence or absence of different osmolytic stabilizers such as glycerol, erythritol, sorbitol, mannitol, sucrose, PEG, glycine, and proline was examined by assaying their residual activity after storage at 4°C for the required time period. The free or Fe_3O_4-MNP bound α-amylase was mixed with different stabilizers (10% w/v or v/v) in a 1:1 (w/v) ratio, the required volume was withdrawn at a regular time interval, and the amylolytic assay was performed as described above. The activity of free or Fe_3O_4 MNP-bound enzyme at the beginning of experiment was considered to be 100% and other values were compared with it.

2.8. Starch hydrolysis by MNP-bound α-amylase

A glass column (10.0 × 25.0 mm^2) was packed with Fe_3O_4-MNP-bound α-amylase and washed with 0.1 M Tris-HCl (pH 9.0) buffer several times. Then, 2.0 mL of 1% (w/v) starch dissolved in 0.1 M Tris-HCl buffer (pH 9.0) was transferred to the column and incubated at 45°C for different time periods. The starch-hydrolysis efficiency of MNP-bound α-amylase was compared with starch hydrolysis using free enzyme under identical conditions. Two controls were set and in one set starch was kept at 45°C without enzyme but with free Fe_3O_4-MNP particles and other set with starch alone (dissolved in 0:1 M Tris-HCl buffer pH-9.0).

Table 1. A comparison of binding efficiency of α-amylase onto iron-oxide magnetized nanoparticles (MNPs) and the increase in specific activity of the enzyme after binding to MNP using two different methods

Immobilization method	K-phosphate buffer, pH 8 0		Tris-HCl buffer, pH 8 0	
	Percent enzyme binding	Increase in specific activity (fold)*	Percent enzyme binding	Increase in specific activity (fold)*
Method I#	23 ± 1 9	3 3 ± 0 3	44 ± 1 9	14 2 ± 1 1
Method II+	34 ± 1 9	7 2 ± 0 8	69 ± 1 9	19 6 ± 1 7

*Compared to specific activity of free α-amylase
Treatment of MNP with #3-(amino propyl) triethoxy silane and +carbodiimide prior to α-amylase coupling.
Values are mean ± S D of three different experiments

3. Results and Discussion

3.1. Screening of influencing factors and statistical optimization of binding

Crude and partially purified (acetone precipitate) α-amylase showed specific activities of 57 and 170 U/mg, respectively, indicating that the enzyme was purified 2.9-fold after acetone precipitation compared to the crude enzyme The cyanamide treatment of the Fe_3O_4-MNPs (method II) prior to enzyme coupling was a better method than amino-functionalization of MNP (method I). The former method significantly enhanced binding efficiency of α-amylase and also increased the specific activity of the enzyme after immobilization onto Fe_3O_4-MNPs (Table 1). The analysis of regression coefficients and *t*-value obtained from the Placket-Burman design showed that, among the tested factors, two independent variables such as the amount of Fe_3O_4-MNP and pH of the buffer system used for the binding reaction significantly affected the α-amylase MNP coupling (data not shown). The optimum condition requirement for these two key variables in the best MNP-amylase coupling was further explored by RSM

Literature study revealed that RSM is an important statistical technique for media optimization in different fermentation procedures. In the present study, RSM was used to estimate main effects on response *i e*, the enzyme coupling to the iron-oxide MNP. The observed and predicted Y response (specific activity) values by Central Composite design are shown in Table 2. The maximum Y response was observed when 25 mg MNP was coupled with α-amylase at pH 8 0 It might be reasonable to assume that pH of the binding buffer plays an important role in the binding process by protonation and deprotonation of the charged functional groups in the enzyme molecule. The estimated regression coefficients for Y are shown in Table 3 An ANOVA and Fisher's statistical test were conducted for the second-order RSM, and the results demonstrated that the computed F value for linear regression was much greater than the tabulated (P) > F value, suggesting significance of the model (data not shown) The RSM showed that both chosen factors independently exerted their influence in both a linear and quadratic manner onto the specific activity of the MNP-coupled enzyme However, the interaction effect was not significant in the final optimized response, which was evident from the quadratic model ANOVA and from the response surface and contour plots. The sample coefficient of determination

Table 2. Observed and predicted values of Y response by response surface methodology

Run no	Independent variables		Y Response (α-amylase activity in U/mg)	
	C_1 (Amount of MNP)	C_2 (pH)	Observed	Predicted
1	25 (−1)	7 5 (−1)	3450 45	3452 41
2	25 (−1)	8 0 (0)	4433 68	4429 75
3	25 (−1)	8 5 (1)	3667 40	3669 36
4	50 (0)	7 5 (−1)	2327 87	2323 94
5	50 (0)	8 5 (1)	2544 83	2540 98
6	75 (1)	7 5 (−1)	1010 00	1011 96
7	75 (1)	8 0 (0)	1993 24	1989 31
8	75 (1)	8 5 (1)	1226 96	1228 92
9	50 (0)	8 0 (0)	3311.11	3301 29
10	50 (0)	8 0 (0)	3226 26	3301 29
11	50 (0)	8 0 (0)	3309 14	3301.29
12	50 (0)	8 0 (0)	3340.11	3301 29
13	50 (0)	8 0 (0)	3312 01	3301 29

The observed values are the mean of triplicate determinations Coded values are shown in parenthesis

Table 3. Model coefficients estimated by multiple regression analysis (model adequacy checking)

Factor	Coefficient	SE coefficient	Computed t-value	*p*-value
Constant	−218792	5034 36	−43 460	0 000
C_1	−34	10 94	−3 119	0 017
C_2	55825	1261 39	44 256	0 000
C_1^2	−0	0 03	−4 663	0 002
C_2^2	−3475	78 71	−44.154	0 000
$C_1 C_2$	0	1 31	0 000	1.000

R^2 = 99 9, R^2 (predicted) = 99 4, R^2 (adjusted) = 99 7

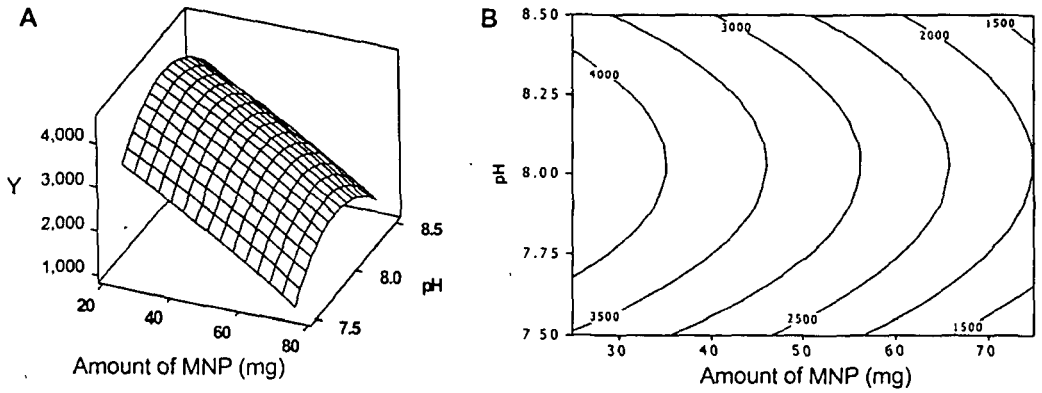

Fig. 1. Specific activity of iron-oxide magnetized nanoparticle (MNP) bound α-amylase vs. pH of the buffer system used. (A) Response surface plot and (B) contour plot.

(R^2) measures the closeness of fit of the sample regression equation to the observed value of Y [14,15]. The high R^2 value supported the significance of the model and indicated that the proposed model explained more than 99% of the specific activity sample variation of the Fe_3O_4-MNP-coupled α-amylase. The adjusted R^2, which may be smaller than the R^2 (provided that sample size is not very large), corrects the R^2 value for sample size and for the number of terms in the model. The adjusted R^2 value (99.7) in the present study advocated high significance of the model. The three-dimensional response surface plots and contour plots as a function of two factors are depicted in Figs. 1A and 1B, respectively. Further, the larger magnitude of the t-value and smallest *p*-value vouched for the significance of the corresponding coefficient of the model. The combined results reinforced that the response equation provided a suitable model for the CCD experiment.

Model validity was further confirmed using the predict program in Minitab 15 statistical software. Based on regression equation (3), the maximum Y response (4433.8 units/mg) was predicted when the binding reaction was performed with 25 mg of Fe_3O_4-MNP at pH 8.0. The actual Y value under the above mentioned conditions was obtained as 4435.1 units/mg and the difference in predicted and actual values was not significant, suggesting the validity of the model.

Enzyme-MNP coupling interactions play a vital role between organic ligands and between the amino acid side chains of proteins and their metals centers [7]. Additionally, dispersive and van der Waal's forces may be involved in the binding mechanism. It might be reasonable to assume that the covalent coupling with cyanamide resulted in inter and/or intra cross-linking of the α-amylase, which provided better stability to the enzyme tertiary structure [4,16]. Furthermore, the nature of the binding solvent, the strength and nature of the interaction with the surface, the kinetics of the spreading versus surface approach, and spatial organization of the protein itself are some of the important parameters influencing the effective binding of the enzyme with the support that preserve the biological function of the protein [17]. These may well explain the observed differences in binding with MNP as well as the increase in specific activity of α-amylase after treatment with K-phosphate or Tris-HCl buffers.

3.2. Biophysical characterization of free and enzyme bound iron-oxide MNP

The XRD pattern of the synthesized MNP revealed characteristic peaks (26.1°, 30.1°, 35.8°, 43.1°, 57.1°, and 62.6°) for maghemite, [8,18]. Using X-PERT software, the nanocrystallite size for the bare MNP was about 38.2 nm, and the α-amylase-bound MNP showed almost the same crystallite size of 38.4 nm, suggesting that nanocrystallite size was not altered even after enzyme binding. The SEM images revealed that non-functionalized MNPs existed as discrete particles with a size of about 60.0 ± 10.0 nm. However, the enzyme coupled MNPs showed agglomeration with particle sizes ranging between 200 and 500 nm (data not shown).

The FTIR spectra of the MNP and MNP bound α-amylase were measured, and the results are shown in Figs. 2A and 2B, respectively. The characteristic band of metal oxygen interaction at approximately 572.79/cm was typical for the synthesized Fe_3O_4 magnetic nanoparticles. Bands 1467.36, 1516.86, and 1629.30/cm wave numbers were assignable to the symmetric stretching of the dissociated carboxylic group originating from the amino acid, amide I and amide II, as shown in the MNP bound amylase spectra. Band shifting was observed from 1627 to 1629/cm post MNP functionalization with cyanamide and the enzyme coupling process. Band 2923.90/cm, shown in Fig. 2A disappeared in the MNP-bound α-amylase, and a

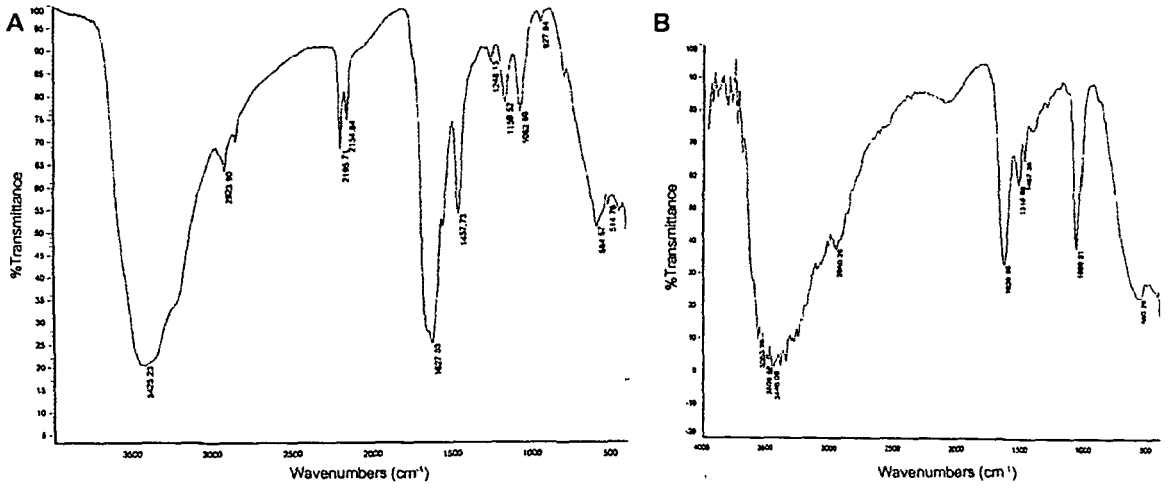

Fig. 2. Fourier transform infrared spectra of (A) bare magnetized nanoparticles (MNP) and (B) MNP-bound α-amylase.

new high intensity band at 2950.28/cm (Fig. 2B) was assigned to the C-H bond stretching vibration after treatment with cyanamide. A very broad band of O-H stretching was observed in the 3,000 ~ 3,600/cm region during MNP KOH treatment.

Measuring the magnetic properties of bare Fe_3O_4-MNP demonstrated a low-field (178 G) hysteresis loop, and the magnetization at this field remained constant for free as well as enzyme bound Fe_3O_4-nanoparticles. The saturation magnetization (μ_s), remnant magnetization (μ_r), and coercivity (H_c) values for free Fe_3O_4-MNP were 4.648 emu/cm^3, 2.703 emu/cm^3, and 9.28 G, respectively. For α-amylase conjugated Fe_3O_4-MNP, these values were 4.589 emu/cm^3, 2.711 emu/cm^3, and 9.6 G, respectively. The magnetic susceptibility of the iron-oxide MNP ($\lambda = 0.366$) remained the same both before and after enzyme immobilization.

The FTIR as well as the XRD data confirmed the binding of α-amylase onto Fe_3O_4-MNP. The washing of Fe_3O_4-MNP post binding with the enzyme ruled out the possibility of non-specific adherence of protein(s) on the surface of the nanoparticles. Moreover, the XRD study revealed no change in the nanocrystalline size of the MNP after binding with α-amylase. The agglomeration of nanoparticles after binding with α-amylase (observed from the SEM study) may have been due to the binding of several enzyme molecules onto a single Fe_3O_4-MNP. It may be that enzyme molecules formed aggregates to bind several magnetic nanoparticles. Glutaraldehyde used in the buffer systems might have resulted in enzyme cross-linking. To account for the increased activity of the MNP-amylase conjugate in this context, the possible modulation of the enzyme structural conformation upon interaction with MNP cannot be ruled out and needs further investigation. The low field hysteresis loop indicated proportionately large density, single domain, super-paramagnetic Fe_3O_4-nanoparticles. The magnetic susceptibility of the Fe_3O_4-nanoparticles indicated that immobilization of α-amylase had not altered the magnetic behavior of the Fe_3O_4-nanoparticles to a statistically significant extent.

3.3. Biochemical characterization of free and enzyme bound iron-oxide MNP

The K_m and V_{max} values are two parameters used to assess the catalytic efficiency of a given enzyme. The kinetic studies of the free and Fe_3O_4-immobilized enzyme reinforced the enhanced catalytic (starch degrading) potency of the immobilized enzyme, indicating that it is an effective application for various industrial processes. The kinetic studies showed that the K_m and V_{max} values for free α-amylase towards starch were 5.0 mg/ml and 0.21 μmol/min/mg, respectively. The same values for Fe_3O_4 MNP-bound α-amylase towards starch were 2.5 mg/mL and 0.78 μmol/min/mg, respectively. Similarly, the specific activity of free and bound α-amylase was 170 and 4435 units/mg, respectively, indicating more than a 26-fold increase in enzyme specific activity after binding to MNP. This result suggests that a very low amount of Fe_3O_4-MNP-bound α-amylase would be required compared to a free enzyme to catalyze a reaction, which favors the cost-effectiveness of the process. This is particularly important when the cost of an enzyme such as thermostable α-amylase is a defining factor in industrial product development. This higher affinity towards its substrate might be attributed to either the increase in the surface area available to the enzyme moieties resulting in a better orientation and/or a change in the conformation of catalytic site of α-amylase leading to higher catalytic efficiency [18]. This improvement in catalytic activity of α-amylase after binding Fe_3O_4-MNP was

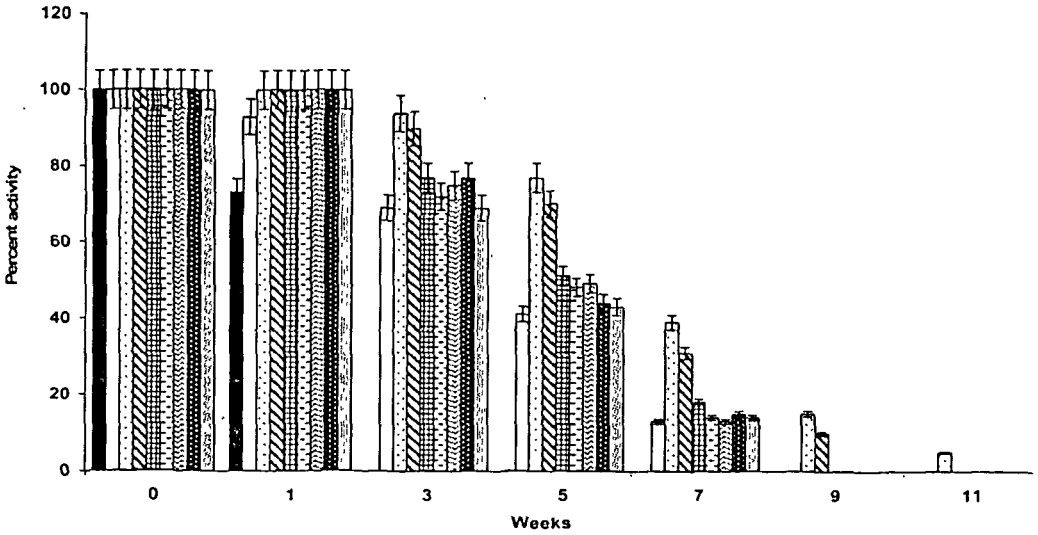

Fig. 3. Storage stability of the α-amylase iron-oxide magnetized nanoparticle (MNP) bioconjugate in the presence and absence of osmotic stabilizers. Free enzyme (■), enzyme-MNP (□), enzyme-MNP-polyethylene glycol (▒), enzyme-MNP-glycine (▨), enzyme-MNP-proline (▦), enzyme-MNP-sucrose (□), enzyme-MNP-mannitol (▨), enzyme-MNP-sorbitol (▩), and enzyme-MNP-glycerol (▒). Values are mean ± S.D. of triplicate determinations.

significantly higher than the reported enhancement of catalytic activity of other enzymes such as lipase, yeast alcohol dehydrogenase, and alkaline phosphatase immobilized onto Fe_3O_4-MNPs [5,6,18]

Thermostable α-amylases are capable of hydrolyzing raw starch to maltose and maltotriose, so the conventional gelatinization and liquefaction steps can be avoided. A thermostability study demonstrated that free α-amylase lost 15 and 35% of its original activity after heating at 60°C for 30 and 60 min, respectively. However, the Fe_3O_4-MNP-coupled enzyme retained 97 and 83% of its original activity under the identical heating conditions (data not shown). This enhanced thermostability of α-amylase after binding with Fe_3O_4-MNP may augment the industrial application of amylase-MNP bioconjugate, particularly in the food-processing industry. The anticipated increase in α-amylase stability against thermal denaturation may be due to restricted conformational mobility of the molecules post immobilization [19]. The results showed that the thermal and storage stability of α-amylase improved significantly after the immobilization process. Furthermore, the reusability data reinforced the industrial application of the α-amylase Fe_3O_4-MNP bioconjugate.

3.4. Storage stability of free and MNP-bound α-amylase and effect of osmotic stabilizers

Enhancing enzyme storage stability is highly desirable from an industrial perspective. The storage stability of free and Fe_3O_4-MNP bound α-amylase including the effects of some stabilizers is shown in Fig. 3. The free enzyme lost its activity after storage at 4°C for 3 weeks, whereas MNP-bound enzyme activity could be detected after 7 weeks of storage under identical conditions.

Stabilizers are a class of low-molecular weight, weakly charged compounds used for stabilizing proteins during storage. Their major effects are on the viscosity and surface tension of water, but they have little effect on enzyme activity [20]. Additionally, they stabilize hydration shells and protect against aggregation by increasing the molecular density of the solution without changing the dielectric constant. Among the tested stabilizers, polyethylene glycol (PEG) followed by glycine maximally enhanced the storage stability of the α-amylase Fe_3O_4-MNP conjugate. In the presence of these stabilizers, the MNP-bound α-amylase retained its activity even after 11 weeks of storage (Fig. 3). However, sucrose, mannitol, sorbitol, glycerol, and proline were not effective for maintaining the storage stability of the Fe_3O_4- immobilized enzyme after just 3 weeks. This significant improvement in storage stability in the presence of PEG and glycine may have additional advantages from an industrial perspective.

3.5. Reusability of Fe_3O_4-MNP bioconjugate and starch hydrolysis efficiency

One of the major hurdles for the cost effectiveness of any process is the inability to reuse the enzyme to catalyze a particular reaction. As shown in Fig. 4A, the activity of immobilized α-amylase started to decline marginally after five cycles of reuse, and about 29% of its initial activity was lost after ten cycles of use.

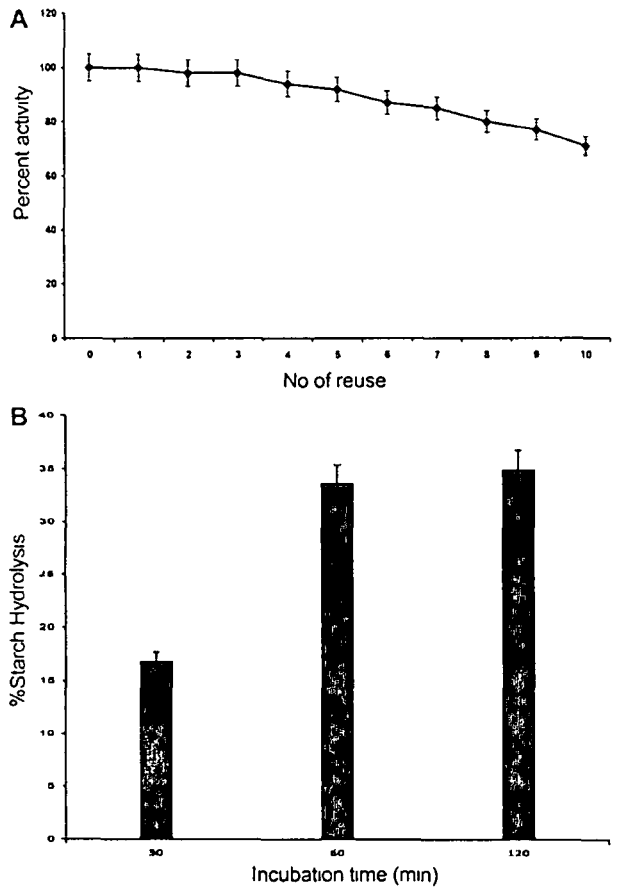

Fig 4. (A) Reusability of the α-amylase iron-oxide magnetized nanoparticle bio-conjugate for starch hydrolysis Values are mean ± S D of triplicate determinations (B) Starch hydrolysis by iron-oxide magnetized nanoparticle bound α-amylase at different time intervals Values are mean ± S D of triplicate determinations

A packed-column study showed that 60 min was the optimum time required for starch hydrolysis using the MNP bound α-amylase, beyond which no further hydrolysis ($P > 0.05$) occurred (Fig 4B) The degree of starch hydrolysis by Fe_3O_4-MNP coupled α-amylase was significantly higher ($p < 0.01$) compared to free enzyme In contrast, free MNP did not display starch hydrolysis activity, suggesting it has no role in the starch hydrolysis process Therefore, the significant starch degrading efficiency, reusability, thermostability, and storage stability of MNP bound α-amylase compared to free α-amylase reinforced the cost effective industrial applicability of the former in the starch processing and other related industries

4. Conclusion

A significant improvement in catalytic activity, thermal and storage stability, as well as reusability of α-amylase after binding with Fe_3O_4-MNP enhanced the biotechnological potential of an α-amylase Fe_3O_4-MNP bioconjugate for the starch processing industry Further, these results open new avenues of application for Fe_3O_4-MNP immobilized α-amylase as a cost-effective technology for use in different industrial sectors

Acknowledgements

The authors thank Dr G Maitra for critically reading and editing the manuscript S K R and J K R were recipients of fellowships from DBT, New Delhi, and Tezpur University, respectively

References

1 Haki, G D and S K Rakshit (2003) Developments in industrially important thermostable enzymes A review *Bioresource Technol* 89 17-34
2 Kirk, O, T V Borchert, and C C Fuglsang (2002) Industrial enzyme applications *Curr Opini Biotechnol* 13 345-351
3 Kim, S -B, D -W Lee, C -I Cheigh, E -A Choe, S -J Lee, Y -H Hong, H -J Choi, and Y -R Pyun (2006) Purification and characterization of a fibrinolytic subtilisin-like protease of *Bacillus subtilis* TP-6 from an Indonesian fermented soybean, Tempeh *J Ind Microbiol Biotechnol* 33 436-444
4 Tong, X D, B Xue, and Y Sun (2001) A novel magnetic affinity support for protein adsorption and purification *Biotechnol Prog* 17 134-139
5 Liao, M H and D H Chen (2001) Immobilization of yeast alcohol dehydrogenase on magnetic nanoparticles for improving its stability *Biotechnol Lett* 23 1723-1727
6 Saiyed, Z M, S Sharma, R Godawat, S D Telang, and C N Ramchand (2007) Activity and stability of alkaline phosphatase (ALP) immobilized onto magnetic nanoparticles (Fe_3O_4) *J Biotechnol* 131 240-244
7 Gupta, A K and M Gupta (2005) Synthesis and surface engineering of iron oxide nanoparticles for biomedical applications *Biomaterials* 26 3995-4021
8 Liang, S, Y Wang, J Yu, C Zhang, J Xia, and D Yin (2007) Surface modified superparamagnetic iron oxide nanoparticles as a new carrier for bio-magnetically targeted therapy *J Mater Sci Mater Med* 18 2297-2302
9 Das, K, R Doley, and A K Mukherjee (2004) Purification and biochemical characterization of a thermostable, alkaliphilic, extracellular a-amylase from *Bacillus subtilis* DM-03, isolated from the traditional fermented food of India *J Biotechnol Appl Biochem* 40 291-298
10 Rossi, L M, A D Quach, and Z Rosenzweig (2004) Glucose oxidase-magnetite nanoparticle bioconjugate for glucose sensing *Ana Bioanal Chem* 380 606-613
11 Lowry, O H, N J Rosebrough, A L Farr, and R J Randall (1951) Protein measurement with the folin-phenol reagent *J Biol Chem* 193 267-275
12 Plackett, R L and J P Burman (1946) The design of optimum multifactorial experiments *Biometrika* 33 305-325
13 Das, K and A K Mukherjee (2007) Comparison of lipopeptide biosurfactants production by *Bacillus subtilis* strains in submerged and solid state fermentation systems using a cheap car-

bon source Some industrial applications of biosurfactants *Proc Biochem* 42 1191-1199
14 Daniel, W W (2000) A foundation for analysis in the health sciences Hypothesis testing 7th ed , pp 166-167 In W W Daniel (eds) *Biostatistics* John Wiley and Sons, Inc , NY USA
15 Raymond, H M and D C Montgomery (2002) Response surface methodology Process and product optimization using designed experiments, 2nd ed , Wiley, NY, USA
16 Simons, B L , M C King, T Cyr, M A Hefford, and H Kaplan (2002) Covalent crosslinking of proteins without chemical reagents *Protein Sci* 11 1558-1564
17 Malmsten, M (2003) *Biopolymers at interfaces* 2nd ed , pp 184 Marcel Dekker, NY, USA
18 Huang, S -H , M -H Liao, and D -H Chen (2003) Direct binding and characterization of lipase onto magnetic nanoparticles *Biotechnol Prog* 19 1095-1100
19 Bayramoglu, G., S Kiralp, M Yilmaz, L Toppare, and M Y Arica (2008) Covalent immobilization of chloroperoxidase onto magnetic beads Catalytic properties and stability *Biochem Eng J* 38 180-188
20 Arakawa, T and S N Timasheff (1985) The stabilization of proteins by osmolytes *Biophysical J* 47 411-414